Advances in VIRUS RESEARCH

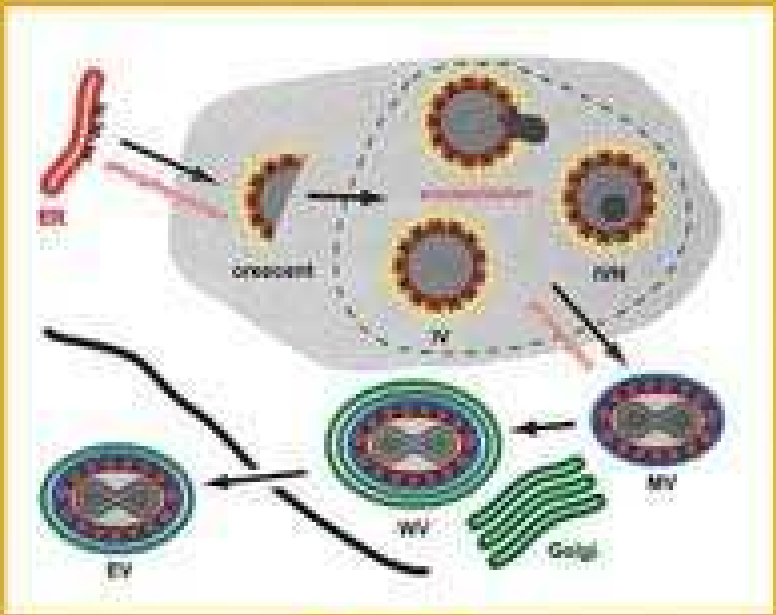

66

Edited by
Karl Maramorosch
Aaron J. Shatkin

Advances in

VIRUS RESEARCH

VOLUME 66

ADVISORY BOARD

Advances in
VIRUS RESEARCH

Edited by

KARL MARAMOROSCH
Department of Entomology
Rutgers University
New Brunswick, New Jersey

AARON J. SHATKIN
Center for Advanced Biotechnology
and Medicine
Piscataway, New Jersey

VOLUME 66

ELSEVIER

AMSTERDAM • BOSTON • HEIDELBERG • LONDON
NEW YORK • OXFORD • PARIS • SAN DIEGO
SAN FRANCISCO • SINGAPORE • SYDNEY • TOKYO
Academic Press is an imprint of Elsevier

Academic Press is an imprint of Elsevier
525 B Street, Suite 1900, San Diego, California 92101-4495, USA
84 Theobald's Road, London WC1X 8RR, UK

This book is printed on acid-free paper. ♾

For information on all Elsevier Academic Press publications
visit our Web site at www.books.elsevier.com

ISBN-13: 978-0-12-039869-0
ISBN-10: 0-12-039869-9

PRINTED IN THE UNITED STATES OF AMERICA
06 07 08 09 9 8 7 6 5 4 3 2 1

CONTENTS

Plant Signal Transduction and Defense Against Viral Pathogens

PRADEEP KACHROO, A. C. CHANDRA-SHEKARA, AND DANIEL F. KLESSIG

The Molecular Biology of Coronaviruses

PAUL S. MASTERS

Chlorella Viruses

TAKASHI YAMADA, HIDEKI ONIMATSU, AND JAMES L. VAN ETTEN

Messenger RNA Turnover and Its Regulation in Herpesviral Infection

BRITT A. GLAUNSINGER AND DONALD E. GANEM

ADVANCES IN VIRUS RESEARCH, VOL 66

SPREAD OF PLANT VIRUS DISEASE TO NEW PLANTINGS: A CASE STUDY OF RICE TUNGRO DISEASE

T. C. B. Chancellor,* J. Holt,* S. Villareal,†
E. R. Tiongco,† and J. Venn*

*Natural Resources Institute, University of Greenwich, Central Avenue
Chatham Maritime, Chatham, Kent ME4 4TB, United Kingdom
†International Rice Research Institute, P.O. Box 933
1099 Manila, Philippines

ABSTRACT

The spread of plant virus disease between fields is reviewed for several horticultural and agricultural crops. Previous studies have focused on cropping systems where there is scope for using separation in time and space to reduce the potential for virus spread between plantings. In our study, data are presented on virus disease spread between fields in an irrigated rice area in the tropics where crops are grown continuously throughout the year. An intensive survey was conducted in rice fields planted from November 1992 to October 1994 in which the occurrence of new infections of rice tungro virus disease was recorded. The effect of a number of variables on disease incidence,

0065-3527/06 $35.00
DOI: 10.1016/S0065-3527(06)66001-6

including the proximity of a field to inoculum sources, was examined using ordinal regression analysis. Primary infection showed large seasonal fluctuation. In addition, the number of leafhopper vectors had a significant effect, as did the tungro vector resistance of the rice variety grown. The distance to nearest inoculum source and the tungro incidence of this source significantly affected the level of infection occurring in a vulnerable field. The results are discussed in relation to management strategies to reduce the spread of tungro disease between fields in irrigated lowland rice cropping systems.

I. Introduction

In this chapter we begin by reviewing approaches to investigating the spread of plant virus diseases, with a particular focus on virus spread between fields. We then present a case study on rice tungro virus disease in the tropics. The aim of the research that is described was to identify risk factors associated with the spread of rice tungro virus disease to new plantings and to use the information to develop improved disease management practices.

A. Economic Importance of Plant Virus Diseases

Most economically important crop plants are prone to infection with viruses, which result in a reduction in yield or in quality (Walkey, 1985). The extent of the economic loss may vary greatly and depends on a range of factors. Although the impacts of virus diseases are seen primarily in reductions in crop yield and quality and in effects on market prices, significant economic costs also arise through the need to take preventive measures or to implement control strategies. In developing countries harmful impacts of plant virus diseases may be particularly severe because reduced crop yields can seriously affect the livelihoods of poor people and even threaten food security. The epidemic of cassava mosaic disease in Uganda in the 1990s led to starvation in some districts in the country and is estimated to have resulted in a loss of US$60 million per annum during the height of the epidemic (Thresh and Cooter, 2005).

Virus disease epidemics in perennial crops may be especially serious. As it is not usually possible to eliminate the virus infection, crops will remain diseased throughout their life. High-value trees infected with virus may have to be removed to prevent spread to neighboring healthy trees and it may take several years before replacement trees become productive. The serious economic consequences that result may be seen in the outbreaks of citrus tristeza disease, which have

occurred in the Americas (Wutscher, 1977). Crops that are propagated vegetatively present particular challenges for virus disease control as spread can occur very rapidly through infected planting material. If adequate precautions are not taken, spread of viruses through human movement of infective vegetative propagules can take place over much longer distances than would be possible through natural means (Thresh, 1986).

Oubreaks of virus diseases in annual crops can develop extremely rapidly and cause total yield loss in a particular growing season. As with vegetative propagules, transfer of infected seed can result in the introduction of virus disease to new areas. Seed-borne infection leads to early onset of disease and therefore creates the potential for significant epidemics to arise in new plantings, assuming that the virus has other modes of spread from plant to plant. However, rapid virus disease spread may also occur where there are no introduced foci of infection through infected planting material. Nonpersistent viruses that are transmitted by arthropod vectors can be spread very quickly within a crop due to the short feeding periods required for virus acquisition and inoculation. Semipersistent viruses are transmitted less rapidly than nonpersistent viruses, but they are retained for longer periods in the vector and can potentially be carried over longer distances to initiate new infections. Semipersistent viruses, such as sugar beet yellows, continue to cause serious losses in sugar beet crops in Europe and North America. Heathcote (1978) estimated that annual losses incurred by sugar beet growers due to the disease are in the region of £4.2 million.

B. Spread of Plant Virus Disease Within Plantings

Considerable attention has been devoted by plant virus epidemiologists to assessing the spread of virus diseases within crop plantings (Campbell and Madden, 1990). The analysis of patterns of diseased plants within crops can provide important information about how disease is spread. For example, where virus disease is spread by mobile arthropod vectors, a random distribution of diseased plants is consistent with the introduction of primary inoculum by viruliferous vectors (Thresh, 1976). Random distributions of virus-diseased plants may also be characteristic of seed-borne infection. By contrast, aggregation of diseased plants in close proximity to each other suggests secondary, plant-to-plant spread of disease (Madden *et al*., 1982). For virus diseases that are transmitted mechanically, this may arise through cultural practices such as weeding or through damage caused by extreme weather conditions. Secondary virus disease spread may also arise

through the movement of infective arthropod vectors, particularly for nonpersistent and semipersistent viruses.

Many statistical tools are now available to analyze spatial patterns of diseased plants in crops and in natural populations. These include quadrat-based approaches, adapted from plant ecology, and geostatistical methods, such as "kriging," which was developed for geological surveys (Gottwald *et al.*, 1996). Perhaps the most commonly used statistical tools currently used are those based on distance class methods. Distances between individuals in a plant population are measured and analyzed in programs such as 2DCLASS. This type of analysis can provide information about the size and shape of individual clusters of diseased plants, the number of clusters, and the direction between clusters (Nelson *et al.*, 1992).

C. Spread of Plant Virus Diseases Between Fields

1. Long Distance Virus Disease Spread

Most vector-borne plant virus diseases spread over relatively short distances and disease gradients from known sources of infection have been documented over meters or tens of meters (Thresh, 1976). There are pathosystems where virus spreads over considerably greater distances and these tend to be for viruses that persist for longer in the vector. The classic example is beet curly top in the USA, transmitted persistently by the leafhopper *Circulifer tenellus* (Bennett, 1971). Wind-assisted flights of *C. tenellus* from temporary weed hosts in California and neighboring states have been recorded over distances of over 398 miles (Bennett, 1967). This results in very shallow gradients of *Beet curly top virus* over hundreds of miles.

It is usually difficult to attribute virus outbreaks to specific sources of inoculum. Only rarely has it been possible to track the spread of disease from a known source over long distances. One such example is a series of experiments on a fungal pathogen, wheat stem rust, conducted in the 1950s on St. Croix in the Virgin Islands (Kingsolver *et al.*, 1984). In one experiment, five small fields of wheat were sown at successive 3.3 km intervals downwind from a 2.43 ha source of diseased wheat. The results showed that wind-borne inoculum from the disease source initiated destructive epidemics in test fields up to 15 km distant. The study was made possible because there were no natural sources of leaf or stem rust of wheat on, or upwind of, the island, and isolation from wheat-growing regions allowed the study of virulent stem rust races in the experiment.

2. Field-to-Field Spread of Virus Diseases

There are no comparable experiments for plant viruses, but there have been a few studies of virus dispersal between fields, which have led to the development of improved disease management practices. The most detailed study was carried out on the spread of lettuce mosaic disease between lettuce crops on two farms in the United Kingdom during 1947–1950 (Broadbent *et al*., 1951). Lettuce mosaic disease is seed-borne and so the production of virus-free seed is a key component of any strategy to control the disease. However, the disease is also spread nonpersistently by aphids, the most important of which is *Myzus persicae*. The aim of the studies conducted by Broadbent *et al.* (1951) was to examine the effects of isolation, field size, and crop sanitation on the spread of lettuce mosaic to newly planted lettuce fields.

Patterns of disease spread on two farms with contrasting management practices were compared. On one farm, disease spread from crop to crop was reduced by planting or drilling in large blocks, well separated from each other and by not planting a winter crop. By contrast, overwintering lettuce was present on the second farm and served as an infection source for subsequent spring sowings of the crop. Furthermore, no attempt was made on this farm to isolate successive lettuce crops and substantially higher disease incidence resulted. The authors concluded that, in addition to the use of virus-free seed, growers should cultivate lettuce fields in discrete blocks rather than allowing them to be scattered throughout the farm. They also recommended that the residues of lettuce crops should be ploughed in as soon as possible after harvest. Crop residue management is also important for other diseases. Cauliflower mosaic disease, for example, can usually be controlled by a combination of insecticides and physical isolation. However, Garrett and Mclean (1983) illustrated an unusual case of high-disease incidence in brassica fields in Australia, which was due to the presence of a nearby previously infected crop that had not been removed.

In the United Kingdom, beet yellows and beet mosaic viruses are prevalent in areas where seed crops are grown. The incidence of both diseases increases with increasing numbers of the main vector *Myzus persicae*, but there is an interesting contrast in the relationship between the two diseases and proximity to individual seed crops. Surveys revealed that there was no clear relationship between distance from a seed crop and the level of infection with *Beet yellows virus* (Watson *et al*., 1951). However, the same surveys showed that distance from the nearest seed crop had a clear effect on the prevalence of infection with *Beet mosaic virus*, although the disease was largely

restricted to fields within 100 yards of a seed crop. The difference was attributed to the differing transmission characteristics of the two diseases. Beet yellows is a persistent virus and, as aphids remain infective for longer periods, there is a greater likelihood that aphids will be carried over relatively long distances from sources of infection. By contrast, beet mosaic is a nonpersistent virus and is lost rapidly by vectors, especially during feeding.

3. Geographic Information Systems and Geostatistics

Some disease systems are highly complex and involve multiple vectors and viruses. These present particular challenges for epidemiological studies, but approaches have been developed based on the principles of landscape ecology and utilizing geographic information systems and geostatistics (Coulson, 1992). The first published example of the use of such approaches for virus diseases was the attempt to develop a regional management plan for a complex of tomato diseases in the Del Fuerte Valley in Sinaloa, Mexico (Nelson *et al*., 1994). With the exception of *Tomato mosaic virus*, each of the viruses involved is transmitted by a vector (aphid, whitefly, or thrips) and has alternative hosts among weeds and other crop plants in the area. The existence of these common characteristics provided the rationale for developing general virus risk assessments rather than focusing on individual virus diseases.

In the Sinaloa study, field surveys were used to generate risk assessments for individual fields. The risk assessments were based on data collected on the abundance of vector and virus sources within and adjacent to the fields planted with tomatoes. The fields were located on digitized topographic maps (1:50,000), and coordinates for the center of these fields were then estimated. This method was later supplemented with the use of Global Positioning System units that were able to obtain map coordinates to a resolution of about 100 m. Geostatistics were then used to analyze disease risk and disease incidence data at a regional level.

Initial findings indicated that both disease risk and incidence were spatially dependent variables with a variogram range of 20–25 km (Nelson *et al*., 1994). There was also a correlation between risk assessment scores and virus disease incidence. The management strategy adopted by the project was to apply traditional virus management techniques such as removing sources of virus and vectors and facilitating the supply of healthy seed (Barnes *et al*., 1999). These measures were focused on the areas of highest risk and led to a gradual reduction in the incidence of tomato virus diseases from a peak of over 7% in

1991–1992 to less than 1% in 1995–1996. The spatial analysis was not needed to implement the virus control measures, but provided a framework for regional cooperation and information exchange. For example, commercial growers producing tomatoes for processing used the information to avoid areas of high-virus disease incidence in previous years.

Each of the examples discussed earlier involve annual horticultural and root crops with distinct cropping seasons. Cropping patterns in time and space can be manipulated, at least to some extent, in these agricultural systems. In extensive monocultures where continuous cropping is practiced, the range of possible management interventions is necessarily more limited. In Asia, large areas of continuous rice are grown and in some low-lying locations where drainage is restricted there are no alternative cropping options for much of the year. Consequently, the impact of virus diseases in these lowland rice systems can be especially serious.

II. Rice Tungro Disease

A. The Economic Importance of Rice

Rice is the main staple food for more than half of the world's population, including seventeen countries in Asia and the Pacific. In Asia, it has been estimated that 2 billion people receive 60–70% of the calories in their daily diet from rice (FAO, 2003). There are about 840 million undernourished people worldwide, including 200 million children, and increased rice production has the potential to significantly reduce these numbers. In addition to its importance as a food source, rice provides employment in production and postharvest activities for large numbers of rural and urban dwellers. Rice-based systems include much of the biodiversity of plants, insects, and other organisms in large areas of tropical Asia. Insect pest management depends to a large extent on predation and parasitism by natural enemies that are present in these ecosystems.

B. The Economic Threat of Rice Virus Disease

In view of the crucial importance of rice to the livelihoods of people in many countries, any major biotic constraint to rice production has potentially devastating consequences. Following a large-scale expansion of irrigation schemes during the 1960s and 1970s, irrigated areas in Asia comprise about 49% of the cultivated land and account

for 72% of total production (IRRI, 1989). These areas saw the introduction of modern semidwarf high-yielding varieties, which were responsive to inorganic fertilizers and required good water management to realize their full potential. The new rice varieties were not sensitive to photoperiod and so could be planted throughout the year where conditions were suitable. These varieties also matured considerably earlier than traditional varieties and local landraces. Consequently, it was possible to plant rice continuously and to harvest up to five crops within a 2-year period. This dramatic intensification of rice production systems resulted in the large increase in yields, which came to be characterized as the "Green Revolution."

The new systems of rice cultivation led to greatly increased production but they were also vulnerable to a heightened risk of certain pests and diseases. During the 1960s a virus disease emerged as a major threat to rice production in irrigated lowland ecosystems in Asia. There were several large-scale outbreaks of rice tungro virus disease in the 1960s and 1970s. These led to severe disruption of rice production in the areas affected and resulted in significant hardship for farming families (Thresh, 1989). Further outbreaks arose in the 1980s and 1990s, but these decreased in frequency and, with one or two exceptions, tended to be confined to smaller areas. Although tungro was first described in 1965 (Rivera and Ou, 1965), it is probable that it was present in rice crops for much longer. This view is supported by the fact that there are local names for the disease in several countries in South and Southeast Asia (Thresh, 1989). Tungro disease emerged as a major problem because the new irrigated production systems created the ideal conditions for its persistence and spread.

C. Biology of Rice Tungro Disease

Tungro is associated with two leafhopper-transmitted viruses, which interact to allow disease development (Hibino, 1983). *Rice tungro spherical virus* (RTSV) is an RNA virus in the family *Sequiviridae*. RTSV can be transmitted independently by leafhopper vectors but does not cause visible symptoms or yield loss in most rice varieties. However, RTSV acts a helper virus for the transmission of a DNA/RNA pararetrovirus in the family *Caulimoviridae*. This second virus, *Rice tungro bacciliform virus* (RTBV) is responsible for the symptoms that intensify in rice plants with dual infections. Tungro symptoms vary depending on the age of the plant, the susceptibility of the variety, and the strains of the viruses (Azzam and Chancellor, 2002). Early infections in a

susceptible variety lead to severe stunting, limited tiller development, and the characteristic yellow to orange leaf discoloration.

Tungro viruses are transmitted by six leafhopper species, the most important of which is the rice green leafhopper *Nephotettix virescens* (Distant). *N. virescens* transmits tungro viruses more efficiently than the other vector species and is usually more abundant in irrigated rice fields (Hibino and Cabunagan, 1986). The viruses are transmitted in a semipersistent manner by the leafhopper vectors, which remain infective for periods up to 7 days. RTSV can be transmitted independently, whereas RTBV may only be spread after leafhoppers feed on rice plants with dual infections or when they acquire RTSV first and then RTBV (Cabauatan and Hibino, 1988). Rice plants can become infective and begin to develop symptoms within 1 week to 10 days of infection (Narayanasamy, 1972).

A wide range of nonrice plants have been reported as hosts of tungro viruses based on symptoms or on serology (Khan *et al*., 1991). However, weeds and other nonrice hosts are unlikely to be major sources of virus inoculum, with the possible exception of some wild rices in certain locations (Tiongco *et al*., 1993). Leafhopper recovery of tungro viruses from weeds to rice has not been definitively shown in controlled experiments, especially for *N. virescens*. Rice seedbeds are not generally potential sources of infection, except in areas where seedlings remain in nurseries for significantly longer than the normal period of 3 weeks (Bottenberg *et al*., 1990; Tiongco *et al*., 1993). Regrowth from rice stubbles and volunteer rice plants may act as virus sources, but in areas where tungro is endemic rice plants in standing crops are likely to be much the most potent inoculum sources.

D. Within-Field Spatial Patterns of Tungro Disease Spread

In view of the short feeding periods needed for leafhopper vectors to acquire and transmit the virus and the short latent period of infection in rice plants, the potential for rapid spread of tungro within rice crops is very high. Kondaiah *et al.* (1976) designed a circular planting technique to examine the plant-to-plant spread of tungro from a central inoculum source. Clear gradients of infection were recorded with decreasing levels of disease incidence as the distance from the source increased. Subsequent experiments conducted in the Philippines investigated the role and relative importance of tungro spread into and within rice plantings (Satapathy *et al*., 1997). The results from a series of experiments using introduced sources of inoculum showed clear spatial patterns. Even in seasons when there were several other

disease sources in the area, it was possible to detect the effects of the introduced sources through observed disease gradients (Satapathy *et al.*, 1997). This suggests that most of the disease spread was secondary, plant-to-plant spread by leafhoppers that acquired tungro viruses from sources within the plots. The experiments also showed that gradients in a resistant variety were much steeper than those in a susceptible variety, indicating the potential of resistant varieties to reduce secondary spread.

In other field trials conducted in the Philippines, seasonal patterns of leafhopper immigration and population development were examined in relation to temporal and spatial patterns of disease incidence (Chancellor *et al.*, 1996). Leafhopper immigration into rice plots occurred during the early stages of crop growth in the rainy season and also in a late-planted dry season crop. Early disease infections were randomly distributed and clusters of diseased plants emerged as tungro disease developed, indicating that secondary spread had taken place within the plantings. Although tungro disease incidence and leafhopper abundance tended to be higher during rainy seasons, there was no clear relationship between vector numbers and disease levels. The results from this and other studies indicate that leafhopper vector numbers alone are not always an accurate predictor of tungro disease risk and must be viewed in combination with the prevailing levels of inoculum (Savary *et al.*, 1993). The findings also suggested that there was limited scope for the successful deployment of control measures aimed at reducing leafhopper numbers or plant-to-plant spread within individual fields. Tungro disease can spread rapidly even when immigration rates of vectors are low and the use of insecticides to control vectors, or of roguing to remove diseased plants, are usually not efficient enough to have significant impact on the disease (Holt and Chancellor, 1996; Tiongco *et al.*, 1998).

E. Flight Characteristics of Tungro Vectors

The experiments conducted in the Philippines showed that rapid spread of tungro disease within plantings can occur when conditions are favorable. However, little information is available about tungro disease spread between plantings. The distance over which such spread occurs is important in the assessment of tungro risk and for the effective targeting of disease management strategies. Although there is evidence to suggest that leafhoppers may undertake flights of up to at least 30 km (Riley *et al.*, 1987), results from tethered flight studies suggest that only a small proportion of a given population

makes such long distance flights (Cooter *et al*., 2000). In an asynchronously planted area in Bali, Indonesia, where fields are small in size and where there are few extensive areas of rice production, most leafhopper dispersal is thought to occur over distances of up to 2 km (Suzuki, Y., personal communication). It is not clear whether leafhopper movement commonly occurs over similar distances in larger rice basins, but some circumstantial evidence is available from light trap data collected in Central Luzon in the Philippines (Loevinsohn, 1984). This suggested that the common dispersal range of tungro vectors was about 1 km.

III. Area-Wide Investigation of Rice Tungro Disease Incidence

In order to examine the main factors influencing temporal and spatial patterns of tungro disease in an endemic area, an intensive survey was conducted over a 2-year period in the Philippines. We now describe the spatial patterns of tungro disease incidence that were found in the survey area and examine the main factors that affected the risk of primary infection in a field.

A. Tungro Disease Study Site

The study site was located at 13°18′ N, 123°18′ E in a tungro-endemic area in the province of Albay, Luzon Island, Philippines where rice is grown throughout the year. Rice seedlings are raised in seedbeds and transplanted into puddled fields at 21–30 days after sowing. Irrigation water from the Kinale and San Francisco rivers is generally available throughout the year, enabling two or more rice crops to be planted annually. Some areas in the study site are poorly drained, causing problems with water control during periods of heavy rainfall that could occur between the months of June and November. The driest period is from January to April when the mean monthly rainfall is generally less than 100 mm.

B. Field Surveys

Surveys were conducted between January 1993 and December 1994 in approximately 170 fields in a contiguous area of 150 ha in the *barangays* (villages) of Kinale and Balangibang. From January to May 1993, numbers of leafhopper vectors and tungro disease incidence were recorded every 3–4 weeks in rice crops up to panicle emergence at

approximately 60 days after transplanting (DAT). The data collection was done once a week from June 1993 until the end of the survey period. The planting date for each rice crop was also recorded and the variety was determined by interviewing the farmer. Varieties with resistance to leafhoppers and which had "field" resistance to tungro disease were identified based on the classification adopted by Philippine Rice Research Institute, and all other varieties were classified as susceptible. None of the varieties grown had virus resistance.

Adults and nymphs of leafhopper vectors were estimated by ten sweeps of a 30 cm diameter sweep net. Insects were counted directly after collection in the field. Tungro incidence was assessed by counting the number of diseased hills (clump of rice plants) in five randomly selected quadrats of 100 hills in each field. A hill was considered diseased if any tiller within it showed the characteristic symptoms of yellow to orange discoloration, twisting of the leaves, and stunting of the plant (Ou, 1985). The presence of tungro was confirmed by indexing a few leaf samples with enzyme-linked immunological assay (Bajet *et al*., 1985).

C. Data Analysis

For each observation date, two categories of rice field were identified: those vulnerable to tungro infection and those that could act as infection sources. There is a delay between a plant becoming infected and the symptoms of the disease becoming clearly identifiable. Thus the incidence of new infection must be related to the presence of disease sources at an earlier time. This interval used was defined partly by the latent period of the disease, and partly by labor constraints on the survey protocol. The longest period between sampling dates was 4 weeks, but this occurred on only three occasions. Except in these cases, observations were made at least every 3 weeks throughout the study, a period which also allows time for symptoms to become apparent. Therefore, a 3-week interval was used to relate new infections to prior disease sources.

"Vulnerable" fields were defined as those which were either at growth stage tillering or booting, and which also had no symptoms of infection 3 weeks earlier (or as close to 3 weeks as observation dates allowed). Vulnerable fields thus fall into two categories, those that still do not show symptoms of infection and those that do. If a field remains uninfected and within the appropriate growth stage, it may be recorded over successive observation dates as being vulnerable and uninfected. Once a field became infected, it was no longer included

when the set of vulnerable fields was next established. Three categories of disease incidence were distinguished; fields in which the incidence of tungro was zero, $<1\%$, and $\geq 1\%$, respectively. In fields with tungro incidence $\geq 1\%$, it was possible to make a quantitative estimate of the proportion of plants infected. The occurrence of new (primary) infection in a vulnerable field was related to a number of possible explanatory variables, including the proximity of the field to potential sources of tungro infection.

An infection source was defined as a field with the rice at the tillering or booting stage and in which tungro incidence was $\geq 1\%$. Parcelliary maps at a scale of 1:2500, and which showed individual field boundaries, were obtained from the Bureau of Land and Soils. The maps were digitized using the PC ARC/INFO version 3.4.2 (Environmental Systems Research Institute Inc., New York) geographical information systems program, which allowed the coordinates of the centroid of each field to be calculated. The distances between the centroids of vulnerable fields and sources were calculated using simple geometry. Clearly, several fields could act as sources for one vulnerable field and our aim was to determine whether tungro infection in a vulnerable field was related to the proximity of sources.

Other variables of interest, which were thought likely to have an impact on primary infection, were included in the regression analysis. These were the number of vectors recorded in both the vulnerable field (at the time) and source fields (3 weeks earlier), the variety type (resistant or susceptible) of both the vulnerable field and the source fields, and the percentage disease incidence recorded in the source fields. A further factor, Period, was also included in the analysis so that the contribution of variables could be established *after* seasonal fluctuation had been accounted for. Thus, Period accounted for any differences in disease incidence that were simply due to variation between sampling periods.

D. Results

The number of fields into which rice was transplanted in different months of the year is shown for the period November 1992 to October 2004 (Fig. 1). The pattern of planting was broadly similar for leafhopper-resistant and susceptible varieties. There was a marked contrast in planting pattern between the first and second years of the study. During the initial 12-month period, substantial numbers of fields were planted in each month. There were peaks in the number of fields planted in November 1992–January 1993 and June–August 1993, corresponding to the dry

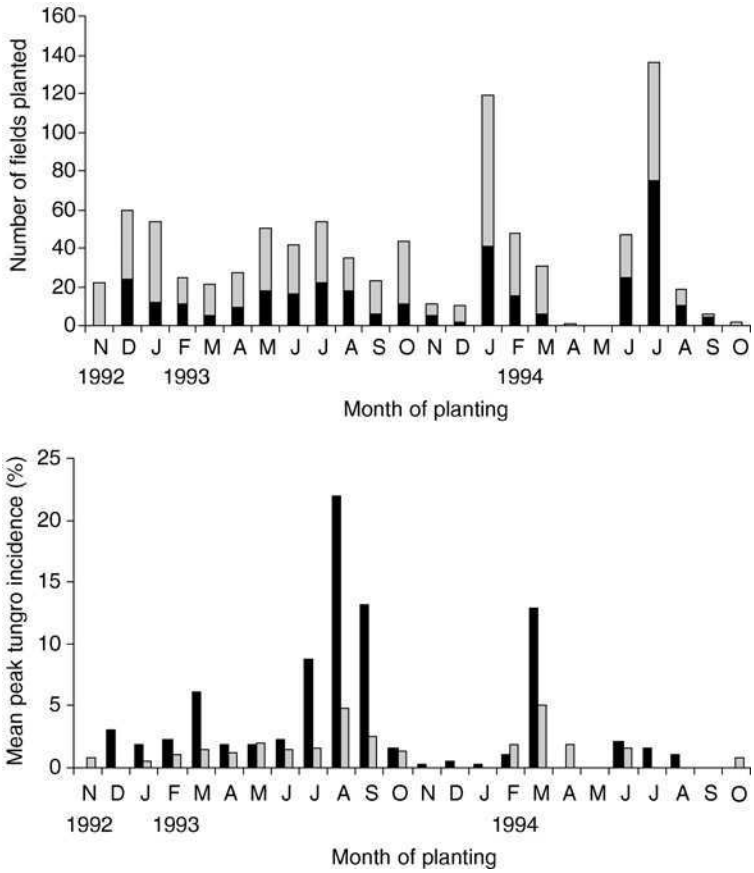

FIG 1. Frequency of planting and mean peak tungro disease incidence for rice fields with susceptible (dark shading) and resistant (light shading) varieties in Albay Province, Philippines between November 1992 and October 1994.

and wet seasons, respectively. However, there was no clear break between the two cropping seasons. By contrast, planting dates in the second year were more closely synchronized and most fields were planted in December 1993–January 1994 and in July 1994. Consequently, there was a distinct gap between the dry and wet season plantings, with only one field planted in April and none in May. As a result, there were very few fields of standing rice when the bulk of the new plantings occurred in July.

Tungro disease incidence was highest during the first year of the study. Peaks in disease incidence were generally observed during the

later plantings within the main cropping seasons: March (1993 and 1994; dry seasons) and August–September (1993; wet season). Tungro disease levels in the 1994 wet season were very low and no peak in incidence could be detected. In each year, mean peak tungro disease incidence was higher on susceptible than on resistant varieties. For example, mean peak incidence on susceptible varieties planted in August 1993 was 22%. This compares with an equivalent figure of 5% for resistant varieties. Similarly, 13% of rice hills in susceptible varieties planted in March 1994 were affected by tungro, whereas only 5% were affected on resistant varieties.

The period selected for more detailed data analysis covered the November 1992–October 1993 plantings. This period was chosen because it included the largest number of new infections and source fields. A total of eleven sample dates were examined in the analysis (Fig. 2). Periods 5 and 7 were omitted because no new infections occurred and Period 8 was omitted because there were no disease sources. There were distinct differences over time in the distribution of tungro infection in the set of vulnerable fields. The first three sample periods, corresponding to the early to middle part of the dry season, had low-disease incidence. The proportion of vulnerable fields in the

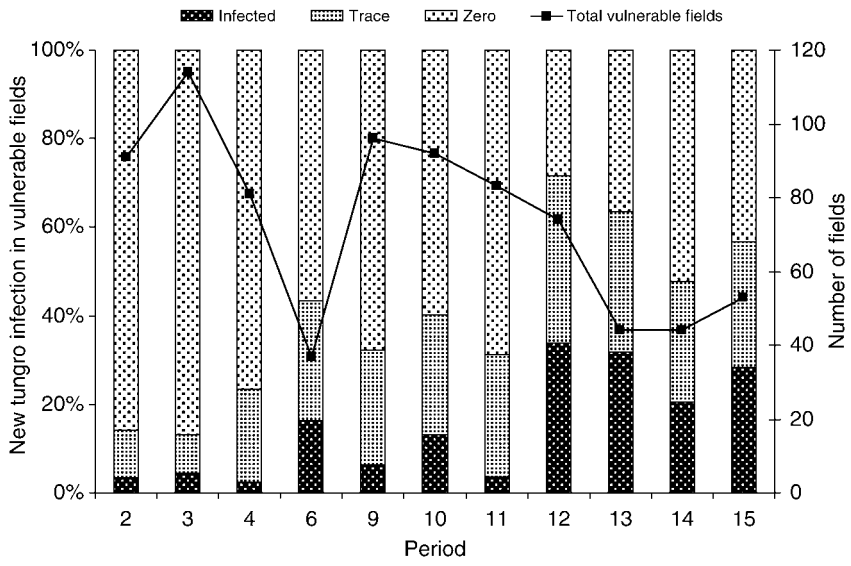

FIG 2. The percentage of fields in each infection category and the total number of fields vulnerable to new tungro infection over successive periods.

"infected" ($\geq$1% tungro incidence) and "trace" ($<$1% tungro incidence) categories increased at sample Period 6, at the end of the dry season. Infection was greatest during the final four sampling periods, which corresponded to the middle to later part of the rainy season.

The pattern of tungro infection over time was strongly associated with the average distance to an infection source (Fig. 3). The percentage of rice fields with zero infection was generally lowest during periods when the mean distance to the nearest source was shortest. There were no obvious temporal trends in the cultivation of resistant or susceptible varieties, with the percentage of susceptible varieties ranging from 27% to 37% over the 11 sampling periods. Similarly, while leafhopper vector abundance in the vulnerable fields fluctuated over time, there was no clearly discernible pattern linking it to seasonal fluctuation in infection.

In order to investigate the effect of distance to sources and other variables on the risk of a vulnerable field becoming infected, the effect of Period was first included in the regression. Other variables making an additional significant contribution to the model therefore have an effect in addition to any caused by the seasonal fluctuation. The results of the regression analysis are shown in Table I. As expected, there was

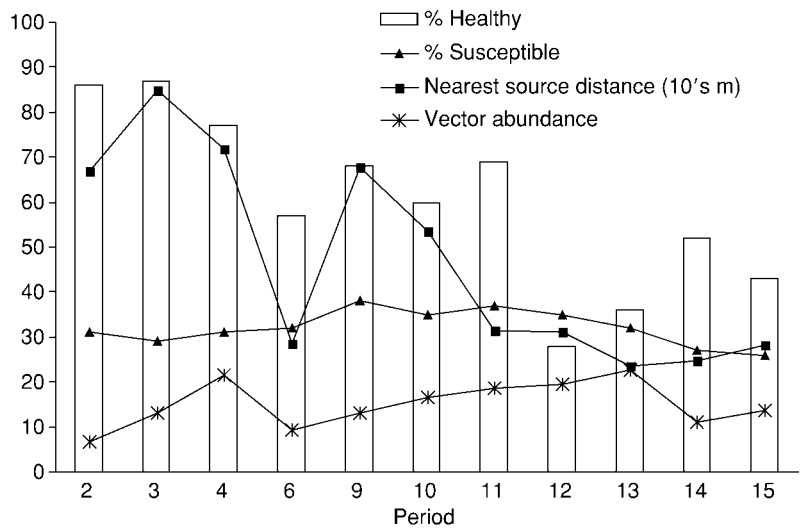

FIG 3. Period averages for tungro-vulnerable fields: the percentage healthy (i.e., showing zero tungro infection), the percentage of a susceptible variety, the distance to a tungro source, and the vector abundance.

TABLE I

ORDINAL REGRESSION MODEL FOR TUNGRO INCIDENCE CATEGORIES: ZERO, TRACE, AND INFECTED, 802 D.F., DEVIANCE RATIO 20, APPROXIMATE χ^2 $P < 0.001$

Variable	Estimate	S.E	t	$p(t)$
Period 9	0.825	0.278	2.97	0.003
Period 10	0.935	0.270	3.47	<0.001
Period 12	1.987	0.309	6.43	<0.001
Period 13	1.236	0.372	3.32	<0.001
Period 14	1.351	0.429	3.15	0.002
Period 15	1.251	0.342	3.66	<0.001
Distance to next-nearest source	−0.001731	0.000364	−4.76	<0.001
Tungro incidence in nearest source	0.0400	0.0158	2.53	0.011
Tungro-resistant variety	−0.559	0.242	2.31	0.021
Vector abundance	0.0603	0.0105	5.76	<0.001
Vector abundance in nearest source	−0.00912	0.00405	−2.25	0.025
Resistant variety × vector interaction	−0.0261	0.0117	−2.23	0.026

All significant two-way interactions and main effects are included. Interactions with period cannot be included as liaised with other variables. Parameters for factors, Period and Variety, are differences compared with the reference levels, Period 2 and tungro-susceptible variety.

a strong effect of Period with six dates contributing to the model when compared with the reference level, Period 2.

In addition to the effects of Period, five other variables made significant contributions to explaining differences in tungro infection in the set of vulnerable fields. Two variables concerned the vulnerable field itself: the variety reaction to tungro and the abundance of leaf hopper vectors. Not unexpectedly, higher tungro infection was associated with tungro-susceptible varieties ($p < 0.02$) and higher vector abundance ($p < 0.001$). The interaction between variety reaction and vector abundance was also significant, indicating that high-vector abundance had less effect when the variety concerned was resistant to tungro. This was the only interaction term that proved significant. A separate analysis showed that, for the set of vulnerable fields infected with tungro disease, in other words those in which incidence was $\geq$1% and could therefore be quantified, mean incidence was 6.17% in susceptible varieties compared with 2.42% in resistant varieties ($n = 100$, $p < 0.001$).

Three variables associated with tungro sources had a significant effect on tungro disease risk in vulnerable fields. The strongest effect

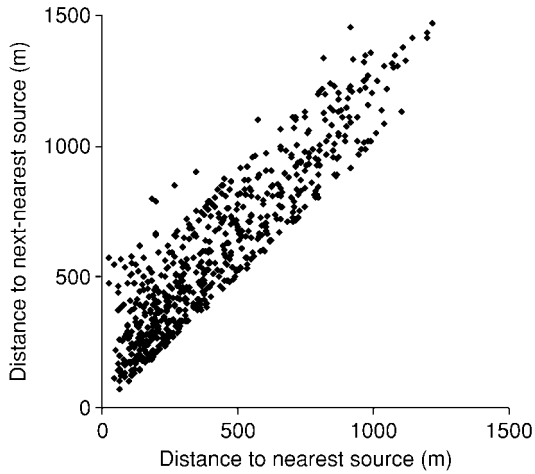

FIG 4. Distance from the vulnerable field to tungro sources are highly correlated.

was that of distance. The approach taken in the analysis to investigate the effect of tungro sources was first to include the variables relating to the nearest source, then to add those for the next nearest source. To some extent sources were correlated, for example, if the nearest source is a long distance away the next-nearest source must be at least that far. In fact, the distance to the nearest source and the next-nearest source were highly correlated (Fig. 4), and it was the distance to next-nearest source that proved to be a slightly better predictor of tungro infection in vulnerable fields than the distance to the nearest source, the two terms being interchangeable in the model. Infected fields were, on an average, significantly closer to tungro sources than fields, which remained free of tungro disease (Fig. 5).

An example of the spatial pattern of tungro is illustrated in Fig. 6, which shows the distribution of tungro incidence at two successive sampling dates. These dates correspond to Periods 11 and 12 in Fig. 2. The figure illustrates a period when tungro was increasing, and by comparison of the successive patterns it can be seen that new infections often occurred close to prior infections that act as sources. Infections that are present in the first map, but not the second, represent those fields with crops that have become too mature to be disease sources or which have been harvested.

Both tungro incidence in the nearest source and vector abundance in the nearest source made significant contributions to the model, in this case slightly better than the equivalent terms for the next-nearest

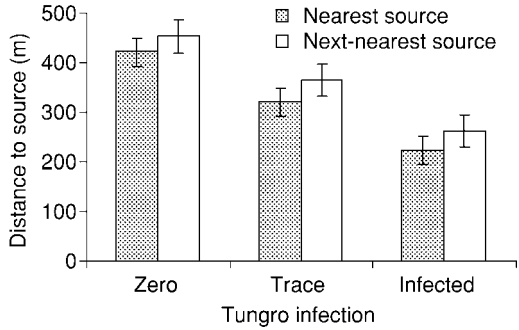

FIG 5. Average distances to sources of vulnerable fields falling in each tungro infection class.

source. Higher levels of disease in sources led to an increased risk of infection in vulnerable fields, as might be expected. For vulnerable fields with zero tungro infection, mean tungro disease incidence in both nearest and next-nearest sources was 3% (Fig. 7). By contrast, for fields with at least 1% infection, mean disease incidence in nearest and next-nearest sources was 5% and 7%, respectively.

The effect of vector abundance in sources on tungro risk in vulnerable fields is less easy to explain. The negative coefficient indicates that lesser number of vectors in the nearest source was associated with increased risk of infection. The effect was small being an order of magnitude less than the effect of vector numbers in the vulnerable field itself. Explained by the lesser differences between infection categories compared with those in the vulnerable field, the term moderates the larger effect of vector differences between the categories of vulnerable field (Fig. 8).

E. Discussions

The survey was conducted over 2 years, which differed greatly in the pattern of rice planting and in tungro disease incidence. Continuous planting during the first year was associated with relatively high levels of tungro incidence, particularly in fields planted during the middle and later periods of the rainy season. By contrast, the planting pattern was more closely synchronized during the second year, especially during the rainy season. Farmers did not make a conscious decision to reduce the temporal variability of planting times during the second year. They were forced to plant in this way due to a shortage of water caused by

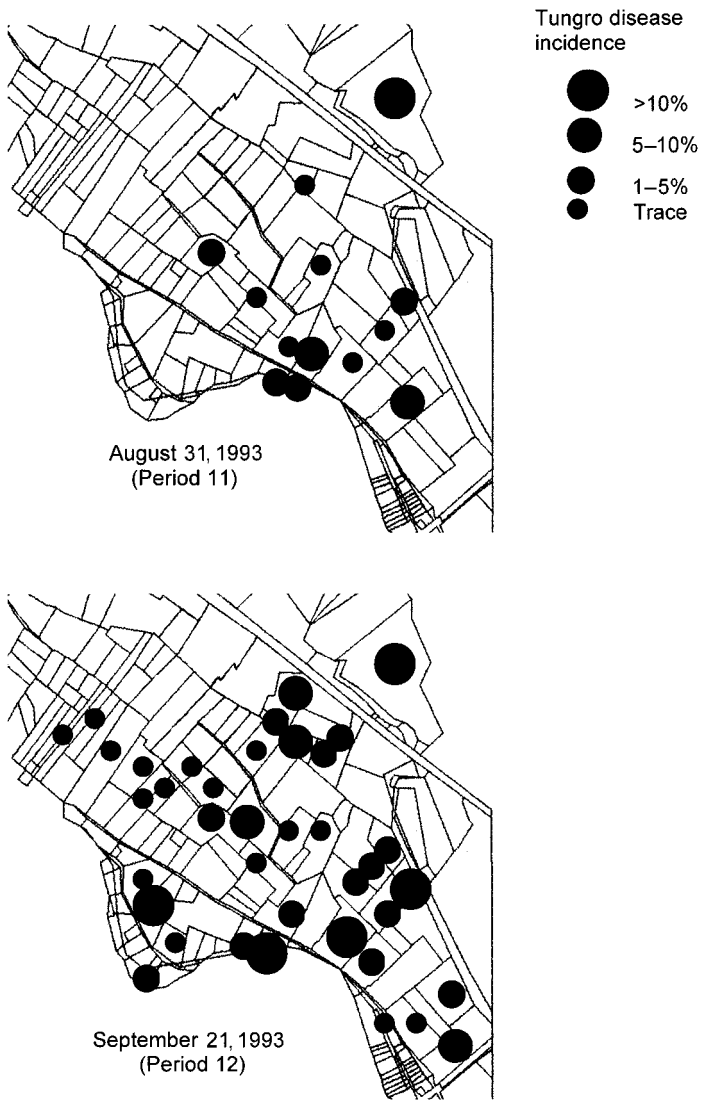

FIG 6. Maps of a section of the study area showing the change in infection pattern between two successive sampling periods.

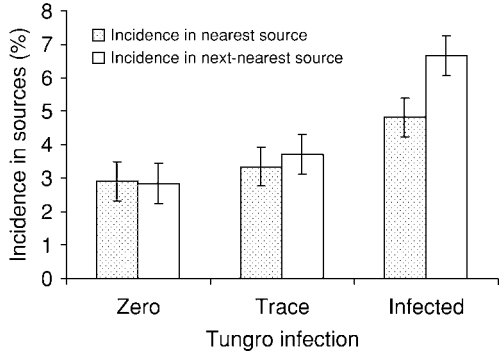

FIG 7. Average disease incidence in tungro infection sources for each category of infection of vulnerable fields.

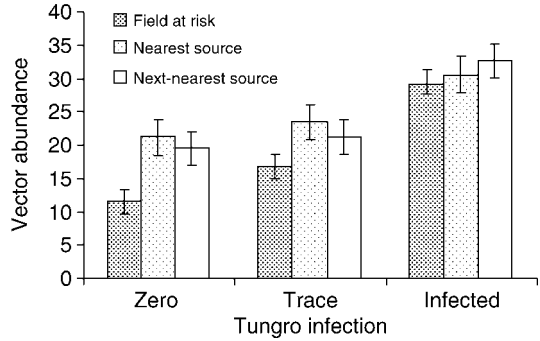

FIG 8. Average abundance of leafhopper vectors in vulnerable fields and their nearest sources, for each infection category of the vulnerable field.

repair work conducted on irrigation facilities during the months of April and May 1994. The 2-month break in planting significantly reduced the potential for tungro inoculum to be carried over from the later dry season plantings. This resulted in much lower tungro disease incidence than in the equivalent period during the previous year. The findings support results from elsewhere in the Philippines, which indicated that staggered planting contributes to increased tungro incidence (Cabunagan *et al*., 2001; Loevinsohn, 1984). In South Sulawesi, Indonesia, staggered planting was thought to be a major cause of tungro problems, and regulations were introduced to synchronize planting during periods when vector populations were relatively low (Sama *et al*., 1991).

The results of the regression analysis showed that the risk of tungro infection in a vulnerable field varied significantly at different times during the "high incidence" year that was examined. Early rice plantings tended to be largely free of tungro disease and the risk of infection increased toward the end of the dry season. As the proportion of infected fields increased, the mean distance to disease sources reduced thus increasing the potential risk to the declining number of healthy "vulnerable" fields. The risk of tungro infection was relatively high throughout most of the rainy season. Higher tungro incidence during the rainy season has been reported in several studies and is usually explained by a combination of greater leafhopper abundance or activity and a higher proportion of available fields planted to rice (Thresh, 1989). In rainy seasons, leafhopper generations generally develop quite rapidly with peak population densities occurring during the middle of the season. In dry seasons, population build-up is more gradual and peak densities are often reached when plants are at an advanced growth stage (Chancellor *et al*., 1996; Cook and Perfect, 1989).

The temporal pattern in leafhopper abundance was not related to that of disease during the period analyzed. However, vector abundance in the vulnerable field, though not in the nearest source, contributed significantly to the probability of new infection. The importance of overall number of vectors on the risk of tungro occurrence has been emphasized by Suzuki *et al*. (1997). Older crops tend to be more important sources of leafhoppers, whereas young crops may supply a greater proportion of infective leafhoppers due to the higher efficiency with which virus is recovered during feeding. Further, early season immigration of leafhoppers tends to be greatest in areas where planting dates are highly variable and there are overlapping rice crops (Widiarta *et al*., 1990).

The relationship between vector numbers and disease incidence is often complex but is largely dependent on the availability of inoculum sources. In a comparison of factors affecting tungro outbreaks in endemic and nonendemic areas in the Philippines, the occurrence of outbreaks in the nonendemic area was primarily determined by the appearance of viruliferous vectors. Overall leafhopper numbers were also important but the epidemics were essentially driven by the availability of sufficient inoculum (Savary *et al*., 1993). There were differences in the disease–vector relationships between the two endemic areas included in the study but outbreaks were less responsive to changes in inoculum. Presumably, if inoculum is not limiting, one of the basic requirements for a tungro epidemic has been fulfilled and vector abundance then has greater influence on disease development, although the outcome will depend on other factors such as the susceptibility of rice

varieties. Similar conclusions can be drawn from other studies conducted in Southeast Asia (Chancellor *et al*., 1996; Suzuki *et al*., 1992).

Our results suggest that a strategy aimed at reducing leafhopper numbers in vulnerable fields is likely to reduce the risk of tungro occurring. Insecticides have been used in attempts to prevent tungro infection from occurring (e.g., Thresh, 1989). However, insecticides are not always effective in controlling tungro, especially where leafhopper immigration pressure is high and may occur over a long period and where there is no coordination between farmers in a locality (Suzuki *et al*., 1997). Further, the threat posed to human health and the risk of initiating resurgence of other pests, principally the brown planthopper *Nilaparvata lugens* (Stål), are major constraints to insecticide use in rice (Holt *et al.*, 1996).

Rather than attempting to protect vulnerable fields, another approach might be to target the use of insecticides on source fields in an attempt to reduce the potential for disease spread to neighboring rice crops. From the 1970s, it has been a common practice in the Philippines for the Department of Agriculture to organize "mass spray" campaigns against the insect vector in response to a tungro outbreak (Warburton *et al*., 1997). Although a more broad-based approach to tungro management has evolved in recent years, spraying campaigns are still conducted in endemic areas if tungro incidence in a particular locality is perceived to be great enough to pose a threat to neighboring rice areas. Both the affected area and a buffer zone around it are usually sprayed in order to try to prevent the spread of the disease, but it is not known whether this approach has been successful. As with the use of insecticides to protect vulnerable fields, the strategy has the disadvantage of posing a threat to human health and of creating the conditions for outbreaks of other secondary pests.

The regression analysis showed that the risk of tungro infection in a vulnerable field was associated with tungro incidence in the nearest source. In "point" source experiments carried out in the Philippines, to examine the effect of sources within rice plantings, there were significant effects of source size on tungro incidence (Satapathy *et al*., 1997). The effects were less pronounced during a wet season trial when background levels of disease in the surrounding area were high. However, in a dry season trial when disease incidence was relatively low, even the effect of a single-hill central source could be detected ($p < 0.05$). Mean disease incidence in the single-hill plots was 3.3%, compared with 0.6% in the plots with no source and 11.0% in plots with a central source of 25 infected hills. The data from our survey demonstrate that a source effect operates over a larger scale between rice fields.

The strongest effect among variables associated with tungro sources was shown by the variable that was most central to the objectives of the study—distance to inoculum sources. The best-fit regression model included distance to the "next-nearest" source, but this was only marginally better than distance to the nearest source and the two variables were strongly correlated. In general, the addition to the regression of variables associated with the next-nearest source added rather little to the model, which included only those for the nearest source. It can be argued, therefore, that the nearest source contributed most of the information about source, which was relevant to explaining new infections. As discussed earlier, proximity effects in relation to infection sources have been demonstrated for *Lettuce mosaic virus* (Broadbent *et al.*, 1951) and *Beet mosaic virus* (Watson *et al.*, 1951), which are both nonpersistent aphid-borne viruses. Similarly, infection sources in neighboring fields and ditches were shown to have a strong influence on the risk of infection of tomato crops with a virus disease complex transmitted by a range of aerial vectors (Nelson *et al.*, 1994). The relatively short retention period of tungro viruses in their leafhopper vectors, and the tendency for most of the leafhoppers to make short flights (Chancellor *et al.*, 1997), probably explain the proximity effect observed in our study.

The methodology utilized in our study has enabled the magnitude of the distance effect to be quantified and the results to be used to develop practical management recommendations for farmers. The results show that the average distance to an inoculum source for vulnerable rice fields which became infected was about half that for fields in which no disease developed. Very few vulnerable fields were infected with tungro when they were located at distances of over 600 m from an inoculum source. Figure 9 illustrates that the infection risk approximately halved for every additional 200 m distance increment to the nearest source. Of course, constrained by the size of the study area, the total number of fields was fewer in the higher distance categories, but even in the highest category (>1000 m) there were 20 fields, none of which were infected. Thus, where farmers have the option of planting a resistant variety they should do so if there is a source within a few hundred meters. As the risk of infection is significantly lower at greater distances, farmers may decide to accept this risk by planting a preferred susceptible variety. The risk of infection will also be influenced by the level of tungro disease in the source field, but this may not be so easy for farmers to determine.

As expected, growing a resistant variety significantly reduced the risk of a vulnerable rice field from becoming infected. There was also a significant interaction of resistant variety and leafhopper abundance,

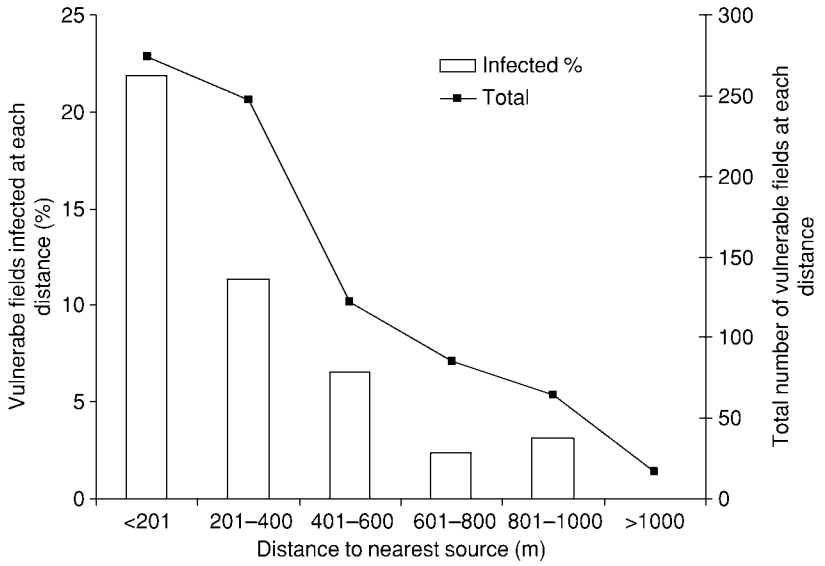

FIG 9. Probability (%) of a vulnerable field becoming infected at different distances from the nearest tungro source. The total number of fields at each distance is also shown.

indicating that the effect of vectors in increasing risk was less pronounced on resistant varieties. The varieties classified as resistant in the survey were resistant to *N. virescens* and this conferred "field resistance" to tungro, which has been shown to be effective in other locations in the Philippines (Cabunagan *et al.*, 2001). In some areas of high-tungro incidence, resistance characteristics were found to be an important criterion for varietal selection (Warburton *et al.*, 1997). However, other characteristics, such as aroma and grain quality, may be considered more important by farmers. As the adoption rate of resistant varieties is likely to be influenced by these considerations, it may be more appropriate to target the deployment of resistant varieties to the most vulnerable fields and to later plantings, which carry a higher risk. Focusing on later plantings would have the added benefit of reducing the amount of inoculum that can be carried over into the next cropping season.

In the case of the lettuce, sugar beet, and tomato crops mentioned earlier, virus disease management recommendations included greater spatial or temporal separation between fields or blocks of fields to reduce the risk of primary infection. Spatial separation is clearly not possible in an irrigated lowland rice area where rice is the dominant

crop and is grown throughout the year. Temporal separation may be achieved in areas where irrigation water is scheduled and there is evidence to suggest that the imposition of a fallow period between rice crops has contributed to a reduction in tungro incidence in some localities (Sama *et al.*, 1991; Taib, 1987). The results of our study indicate that a break between crops can reduce carryover of disease into the next season. However, modeling work suggests that there is a critical relationship between planting date variance and the length of the fallow period needed to reduce carryover of disease (Holt and Chancellor, 1997). Model outputs showed that persistence of disease within a matrix of fields was determined primarily by planting date variance. There was a threshold of planting date variance where a relatively small reduction in variance led to a large reduction in disease incidence. However, where planting date variance was relatively high the response to changes in variance was very small, and disease persisted in the system. Thus, attempts to reduce tungro incidence by manipulating planting dates are more likely to be effective in areas with moderate rather than high levels of cropping asynchrony.

Most research on the spread of virus diseases has concentrated on patterns of disease spread within fields. Such experiments can determine whether primary spread is taking place and can quantify patterns of any secondary spread that occurs. Different approaches are needed to answer questions about the spread of virus disease between fields. Surveys of the kind we carried out in Polangui are costly in time and resources. However, they do provide a means of examining the factors that affect risk of primary infection by a virus disease in space and time. The occurrence of new infections can be explicitly related to the occurrence of inoculum sources and, as we have shown for rice tungro disease, it may be possible to detect and quantify a proximity effect.

Acknowledgments

We thank the farmers who allowed us to collect data from their fields and the staff of the Department of Agriculture in Polangui, especially Mr. Ted Cypriano, who facilitated the survey activities. We also thank to Max Banasihan, Celso Lantican, Teody Gonzalez, Elmer Micosa, and Tom Llaneta, who assisted in the data collection, and to Nestor Fabellar and Mary Grace Magbanua, who prepared the digitized maps. We benefited from useful advice from Drs Paul Teng, Mike Thresh, and Anthea Cook. This document is an output of a project funded by the UK Department for International Development (DFID) for the benefit of developing countries. The views expressed are not necessarily those of the DFID (R6519 Crop Protection Programme).

References

Azzam, O., and Chancellor, T. C. B. (2002). The biology, epidemiology and management of rice tungro disease in Asia. *Plant Dis.* **86**(2)**:**88–100.

Bajet, N. B., Daquioag, R. D., and Hibino, H. (1985). Enzyme-linked immunosorbent assay to diagnose tungro. *J. Plant Prot. Trop.* **2**(2)**:**125–129.

Barnes, J. M., Trinidad-Correa, R., Orum, T. V., Felix-Gastelum, R., and Nelson, M. R. (1999). Landscape ecology as a new infrastructure for improved management of plant viruses and their insect vectors in agroecosystems. *Ecosyst. Health* **5**(1)**:**26–35.

Bennett, C. W. (1967). Epidemiology of leafhopper-transmitted viruses. *Annu. Rev. Phytopathol.* **5:**87–108.

Bennett, C. W. (1971). The curly top disease of sugar-beet and other plants. Monograph 7, American Phytopathological Society.

Bottenberg, H., Litsinger, J. A., Barrion, A. T., and Kenmore, P. E. (1990). Presence of tungro vectors and their natural enemies in different rice habitats in Malaysia. *Agric. Ecosyst. Environ.* **31:**1–15.

Broadbent, L., Tinsley, T. W., Buddin, W., and Roberts, E. T. (1951). The spread of lettuce mosaic in the field. *Ann. Appl. Biol.* **38:**689–706.

Cabauatan, P., and Hibino, H. (1988). Isolation, purification, and serology of rice tungro bacilliform and rice tungro spherical viruses. *Plant Dis.* **72:**526–528.

Cabunagan, R. C., Castilla, N., Colloquio, E. L., Tiongco, E. R., Truong, X. H., Fernandez, J., Du, M. J., Zaragosa, B., Hozak, R. R., Savary, S., and Azzam, O. (2001). Synchrony of planting and proportions of susceptible varieties affect rice tungro disease epidemics in the Philippines. *Crop Prot.* **20:**499–510.

Campbell, C. L., and Madden, L. V. (1990). "Introduction to plant disease epidemiology." John Wiley, New York.

Chancellor, T. C. B., Cook, A. G., and Heong, K. L. (1996). The within-field dynamics of rice tungro disease in relation to the abundance of its major leafhopper vectors. *Crop Prot.* **15:**439–449.

Chancellor, T. C. B., Cook, A. G., Heong, K. L., and Villareal, S. (1997). The flight activity and infectivity of the major leafhopper vectors (Hemiptera: Cicadellidae) of rice tungro viruses in an irrigated rice area in the Philippines. *Bull. Entomol. Res.* **87:**247–258.

Cook, A. G., and Perfect, T. J. (1989). Population dynamics of three leafhopper vectors of rice tungro viruses, *Nephotettix virescens* (Distant), *N. nigropictus* (Stål) and *Recilia dorsalis* (Motschulsky) (Hemiptera: Cicadellidae), in farmers' fields in the Philippines. *Bull. Entomol. Res.* **79:**437–451.

Cooter, R. J., Winder, D., and Chancellor, T. C. B. (2000). Tethered flight activity of *Nephotettix virescens* (Hemiptera: Cicadellidae) in the Philippines. *Bull. Entomol. Res.* **90:**49–55.

Coulson, R. N. (1992). Intelligent geographic information systems and integrated pest management. *Crop Prot.* **11:**507–516.

Food and Agriculture Organization of the United Nations (2003). The International Year of Rice 2004, Concept Paper.

Garrett, R. G., and McLean, G. D. (1983). The epidemiology of some aphid-borne viruses in Australia. *In* "Plant Virus Epidemiology: The Spread and Control of Insect-Borne Viruses" (R. T. Plumb and J. M. Thresh, eds.), Blackwell, London.

Gottwald, T. R., Cambra, M., Moreno, P., Camarasa, E., and Piquer, J. (1996). Spatial and temporal analyses of citrus tristeza virus in eastern Spain. *Phytopathology* **86:**45–55.

Heathcote, G. D. (1978). Review of losses caused by virus yellows in English sugar beet crops and the cost of partial control with insecticide. *Plant Pathol.* **27:**12–17.

Hibino, H. (1983). Transmission of two rice tungro-associated viruses and rice waika virus from doubly or singly infected source plants by leafhopper vectors. *Plant Dis.* **67:**774–777.

Hibino, H., and Cabunagan, R. C. (1986). Rice tungro-associated viruses and their relations to host plants and leafhopper vectors. *In* "International Symposium on Virus Diseases of Rice and Leguminous Crops in the Tropics," pp. 173–182. Tropical Agricultural Research Series no. 19, Ministry of Agriculture, Forestry and Fisheries, Japan.

Holt, J., and Chancellor, T. C. B. (1996). Simulation modelling of the spread of rice tungro disease: The potential for management by roguing. *J. Appl. Ecol.* **33:**927–936.

Holt, J., and Chancellor, T. C. B. (1997). A model of plant virus disease epidemics in asynchronously-planted cropping systems. *Plant Pathol.* **46:**490–501.

Holt, J., Chancellor, T. C. B., Reynolds, D. R., and Tiongco, E. R. (1996). Risk assessment for rice planthopper and tungro disease outbreaks. *Crop Prot.* **15:**359–368.

IRRI (1989). Annual Report. International Rice Research Institute, Los Banos, Philippines.

Khan, M. A., Hibino, H., Aguiero, V. M., and Daquioag, R. D. (1991). Rice and weed hosts of rice-tungro associated viruses and leafhopper vectors. *Plant Dis.* **75:**926–930.

Kingsolver, C. H., Peet, C. E., and Underwood, J. F. (1984). "Measurement of the epidemiologic potential of wheat stem rust: St. Croix, United States Virgin Islands, 1954–57." Pennsylvania State University, College of Agriculture, Bulletin 854.

Kondaiah, A., Rao, A. V., and Srinivasan, T. E. (1976). Factors favoring spread of rice "tungro" disease under field conditions. *Plant Dis. Rep.* **60**(9)**:**803–806.

Loevinsohn, M. E. (1984). The ecology and control of rice pests in relation to the intensity and synchrony of cultivation. PhD thesis, University of London, London, UK.

Madden, L. V., Louie, R., Abt, J. J., and Knoke, J. K. (1982). Evaluation of tests for randomness of infected plants. *Phytopathology* **72:**195–198.

Narayanasamy, P. (1972). Influence of age of the rice plant at the time of inoculation on the recovery of tungro virus by *Nephotettix impicticeps* (Isihara). *Phytopathologische Zeitschrift* **74:**109–114.

Nelson, M. R., Felix-Gastelum, R., Orum, T. V., Stowell, L. J., and Myers, D. E. (1994). Geographic information systems and geostatistics in the design and validation of regional plant virus management programs. *Phytopathology* **84:**898–905.

Nelson, S. C., Marsh, P. L., and Campbell, C. L. (1992). 2DCLASS, a two-dimensional distance class analysis software for the personal computer. *Plant Dis.* **76:**427–432.

Ou, S. H. (1985). "Rice Diseases." Commonwealth Agricultural Bureau, Wallingford.

Riley, J. R., Reynolds, D. R., and Farrow, R. (1987). The migration of *Nilaparvata lugens* (Stål) (Delphacidae) and other Hemiptera associated with rice during the dry season in the Philippines: A study using radar, visual observations, aerial netting and ground trapping. *Bull. Entomol. Res.* **77:**145–169.

Rivera, C. T., and Ou, S. H. (1965). Leafhopper transmission of 'tungro' disease of rice. *Plant Dis. Rep.* **49:**127–131.

Sama, S., Hasanuddin, A., Manwan, I., Cabunagan, R. C., and Hibino, H. (1991). Integrated management of rice tungro disease in South Sulawesi, Indonesia. *Crop Prot.* **10:**34–40.

Satapathy, M. K., Chancellor, T. C. B., Teng, P. S., Tiongco, E. R., and Thresh, J. M. (1997). Effect of introduced sources of inoculum on tungro disease spread in different rice varieties. *In* "Epidemiology and Management of Rice Tungro Disease" (T. C. B. Chancellor and J. M. Thresh, eds.), pp. 11–21. Natural Resources Institute, Chatham, UK.

Savary, S., Fabellar, N., Tiongco, E. R., and Teng, P. S. (1993). A characterization of rice tungro epidemics in the Philippines from historical survey data. *Plant Dis.* **77:**376–382.

Suzuki, Y., Astika, I. G. N., Widrawan, I. K. R., Gede, I. G. N., Raga, I. N., and Soeroto (1992). Rice tungro disease transmitted by the green leaf hopper: Its epidemiology and forecasting technology. *Jpn. Agric. Res. Q.* **26:**98–104.

Suzuki, Y., Astika, I. G. N., Widrawan, I. K. R., Gede, I. G. N., Astika, I. N. S., Suwela, I. N., Aryawan, I. G. N., and Soeroto (1997). Epidemiology-oriented forecasting of rice tungro disease in asynchronous cropping areas. *In* "Epidemiology and Management of Rice Tungro Disease" (T. C. B. Chancellor and J. M. Thresh, eds.), pp. 30–41. Natural Resources Institute, Chatham, UK.

Taib, A. B. (1987). Status of rice pests and measures of control in the double cropping area of Muda irrigation scheme, Malaysia. *Trop. Agric. Res. Ser.* **20:**107–115.

Thresh, J. M. (1976). Gradients of plant virus diseases. *Ann. Appl. Biol.* **82:**381–406.

Thresh, J. M. (1986). Plant virus dispersal. *In* "The Movement and Dispersal of Agriculturally Important Biotic Agents" (D. R. Mackenzie, G. S. Barfield, G. G. Kennedy, R. D. Berger, and D. J. Taranto, eds.), pp. 51–101. Claitor's Publishing Division, Baton Rouge, Louisiana.

Thresh, J. M. (1989). Insect-borne viruses of rice and the Green Revolution. *Trop. Pest Manage.* **35**(3)**:**264–272.

Thresh, J. M., and Cooter, R. J. (2005). Strategies for controlling cassava mosaic disease in Africa. *Plant Pathol.* **54:**587–614.

Tiongco, E. R., Flores, Z. M., Koganezawa, H., and Teng, P. S. (1993). Inoculum sources of rice tungro viruses. *Philipp. Phytopathol.* **29:**30–41.

Tiongco, E. R., Chancellor, T. C. B., Villareal, S., Magbanua, M., and Teng, P. S. (1998). Roguing as a tactical control for rice tungro virus disease. *J. Plant Prot. Trop.* **11:**45–52.

Walkey, D. G. A. (1985). "Applied plant virology." Heinemann, London.

Warburton, H., Palis, F. L., and Villareal, S. (1997). Farmers' perceptions of rice tungro disease in the Philippines. *In* "Pest Management Practices of Rice Farmers" (K. L. Heong and M. M. Escalada, eds.), pp. 129–142. International Rice Research Institute, Los Banos, Philippines.

Watson, M. A., Hull, R., Blencowe, J. W., and Hamlyn, B. M. G. (1951). The spread of beet yellows and beet mosaic viruses in the sugar-beet root crop. 1. Field observations on the virus diseases of sugar beet and their vectors *Myzus Persicae* Sulz., and *Aphis Fabae* Koch. *Ann. Appl. Biol.* **38:**743–764.

Widiarta, I. N., Suzuki, Y., Sawada, H., and Nakasuji, F. (1990). Population dynamics of the green leaf hopper, *Nephotettix virescens* Distant (Hemiptera: Cicadellidae) in synchronised and staggered transplanting areas of paddy fields in Indonesia. *Res. Popul. Ecol.* **32:**319–328.

Wutscher, H. K. (1977). Citrus tree virus and virus-like diseases. *Hortic. Sci.* **12:**478–484.

This page intentionally left blank

ADVANCES IN VIRUS RESEARCH, VOL 66

IN A NUTSHELL: STRUCTURE AND ASSEMBLY OF THE VACCINIA VIRION

Richard C. Condit,* Nissin Moussatche,*,† and Paula Traktman‡

*Department of Molecular Genetics and Microbiology
University of Florida, Gainesville, Florida 32610
†Laboratório de Biologia Molecular de Vírus, Instituto de Biofísica
Carlos Chagas Filho, CCS, UFRJ, Rio de Janeiro, RJ 21941-590, Brazil
‡Department of Microbiology and Molecular Genetics
Medical College of Wisconsin, Milwaukee, Wisconsin 53226

0065-3527/06 $35.00
DOI: 10.1016/S0065-3527(06)66002-8

Abstract

Poxviruses comprise a large family of viruses characterized by a large, linear dsDNA genome, a cytoplasmic site of replication and a complex virion morphology. The most notorious member of the poxvirus family is variola, the causative agent of smallpox. The laboratory prototype virus used for the study of poxviruses is vaccinia, the virus that was used as a live, naturally attenuated vaccine for the eradication of smallpox.

Both the morphogenesis and structure of poxvirus virions are unique among viruses. Poxvirus virions apparently lack any of the symmetry features common to other viruses such as helical or icosahedral capsids or nucleocapsids. Instead poxvirus virions appear as "brick shaped" or "ovoid" membrane-bound particles with a complex internal structure featuring a walled, biconcave core flanked by "lateral bodies." The virion assembly pathway involves a remarkable fabrication of membrane-containing crescents and immature virions, which evolve into mature virions in a process that is unparalleled in virology. As a result of significant advances in poxvirus genetics and molecular biology during the past 15 years, we can now positively identify over 70 specific gene products contained in poxvirus virions, and we can describe the effects of mutations in over 50 specific genes on poxvirus assembly. This review summarizes these advances and attempts to assemble them into a comprehensible and thoughtful picture of poxvirus structure and assembly.

I. Preface

Both the morphogenesis and structure of poxvirus virions are unique among viruses. Poxvirus virions apparently lack any of the symmetry features common to other viruses such as helical or icosahedral capsids or nucleocapsids. Instead poxvirus virions appear as "brick shaped" or

"ovoid" membrane-bound particles with a complex internal structure featuring a walled, biconcave core flanked by "lateral bodies." The virion assembly pathway involves a remarkable fabrication of membrane-containing crescents and immature virions, which evolve into mature virions in a process that is unparalleled in virology.

Poxvirus structure and assembly has been the subject of intense scrutiny since the virus was first subjected to detailed examination by electron microscopy in 1950s and 1960s, yet the most recent comprehensive reviews of the subject are at least 15 years old (Dales and Pogo, 1981; Fenner *et al*., 1989; see also Moss, 2001; Sodeik and Krijnse-Locker, 2002). During these 15 years, key advances in poxvirology have brought us to a point where a comprehensive review of virus structure and assembly is appropriate. First, advances in genome and protein sequencing now readily permit the unambiguous assignment of protein products to specific genes on the poxvirus genome (Chung *et al*., 2006; Goebel *et al*., 1990; Jensen *et al*., 1996; Takahashi *et al*., 1994). Second, advances in poxvirus genetics have yielded both well-characterized collections of temperature-sensitive mutants and techniques for targeted construction of conditional lethal mutants with alterations in specific poxvirus genes (Condit and Niles, 1990; Hassett and Condit, 1994; Lackner *et al*., 2003; Rodriguez and Smith, 1990b; Zhang and Moss, 1991a). As a result of these advances, we can now positively identify over 70 specific gene products contained in poxvirus virions, and we can describe the effects of mutations in over 50 specific genes on poxvirus assembly. This review summarizes these advances and attempts to assemble them into a comprehensible and thoughtful picture of poxvirus structure and assembly.

II. Introduction

A. Poxvirus Biology and Replication: An Overview

Poxviruses comprise a large family of viruses that infect a wide variety of vertebrate and invertebrate hosts. Members of the family *Poxviridae* are characterized by a large, linear dsDNA genome, a cytoplasmic site of replication and a complex virion morphology. The most notorious member of the poxvirus family is variola, the causative agent of smallpox. The laboratory prototype virus used for the study of poxviruses is vaccinia, the virus that was used as a live, naturally attenuated vaccine for the eradication of smallpox. Because the vast majority of genetic and biochemical studies on poxvirus structure and

morphogenesis have been performed with vaccinia, this review will confine itself exclusively to this virus. Members of the poxvirus family are sufficiently similar such that lessons learned from vaccinia can easily be applied to other poxviruses.

The vaccinia virus genome is approximately 200 kb in length and encodes approximately 200 genes (there is some strain variation in DNA size and coding capacity) (Goebel *et al*., 1990; Johnson *et al*., 1993; Lefkowitz *et al*., 2005). Because of the cytoplasmic site of virus replication, vaccinia viral mRNAs are not spliced, and therefore vaccinia genes do not contain introns, greatly simplifying interpretation of genomic sequence. Genes are closely spaced on the genome, and each gene appears to be controlled by its own transcriptional promoter. Comparison of poxvirus genomes reveals a set of 91 genes that are conserved throughout the *Chordopoxvirinae* subfamily (vertebrate poxviruses); a subset of 49 of these genes are conserved throughout the entire *Poxviridae* family (including both vertebrate and invertebrate poxviruses) (Upton *et al*., 2003). The remaining nonconserved genes, many of which are non essential for replication in cell culture, dictate individual virus characteristics of host range and pathogenicity.

Poxvirus virions exist in three infectious forms: mature virions (MV), wrapped virions (WV), and extracellular virions (EV).[1], MV, the simplest form of the virus, are membraned particles containing a biconcave, DNA-containing core flanked by lateral bodies, which fill the concavities of the core. MV are normally found exclusively inside cells and are liberated only by cell lysis. WV consist of MV which are surrounded by two additional lipid bilayers derived from trans-Golgi cisternae. WV, whose outer membranes contain characteristic viral proteins, are precursors of EV and are also found within the cell. EV consist of WV which have been exocytosed via fusion of the outermost WV membrane with the plasma membrane, leaving an MV wrapped in one additional membrane. A fraction of EV are found attached to the cell surface, while some are found free in the extracellular medium. EV are thought to be important for spread of the virus within an organism,

[1] This nomenclature follows a recent proposal by Moss (2005). Previously, MV was called intracellular mature virus (IMV), WV was called intracellular enveloped virus (IEV), and EV included both cell associated extracellular enveloped virus (CEV) and extracellular enveloped virus (EEV). In older literature, MV was called "intracellular naked virus" (INV) (Sodeik *et al*., 1993), thus MV is identical to both IMV and INV.

while MV are thought to be important for long-term stability and transmission of the virus between hosts in the environment. It should be noted, however, that the EV membrane is disrupted when EV bind to cells, enabling MV to make direct contact with the plasma membrane and enter cells (Law, M., Carter, G. C., Roberts, K. L., Hollinshead, M., and Smith, G. L., personal communication). The extra membrane composition, assembly, and transport of WV and EV have been reviewed (Smith *et al*., 2002); therefore, this review will confine itself exclusively to the structure and assembly of MV.

MV enter cells by fusion of the MV membrane with the plasma membrane of the host cell, releasing the core (and lateral bodies) into the cytoplasm and activating the virus' transcriptional program (Armstrong *et al*., 1973; Carter *et al*., 2005). The virion cores contain the full complement of virus-coded enzymes required for synthesis and modification of early mRNA, including a nine subunit RNA polymerase, a virus early transcription factor (VETF), a capping enzyme, and a poly(A) polymerase. Early genes encode enzymes required for DNA replication, and thus as early gene expression peaks, viral DNA replication ensues in cytoplasmic sites termed "factories." Early genes also encode intermediate transcription factors, and intermediate genes, in turn, encode late transcription factors, so that intermediate and late genes are expressed in succession after the prerequisite initiation of viral DNA replication. Thus, the full complement of viral genes are transcribed in a temporal cascade, with the early, intermediate and late classes being distinguished by class-specific transcriptional promoters and virally encoded transcription factors. Furthermore, only replicated genomes are competent templates for intermediate and late transcription. These two classes of genes together encode virion structural proteins, virion enzymes, and assembly factors required for assembly of new virus particles (for a review of poxvirus replication, see Moss, 2001).

B. Genetic Nomenclature

The first complete poxvirus genome sequence to be published was that of the Copenhagen strain of vaccinia virus (Goebel *et al*., 1990). With the publication of this sequence, a genetic nomenclature was adopted in which genes were named according to their position relative to the left end of individual Hind III restriction fragments of the genome and also according to their transcriptional orientation. Thus, for example, the virus DNA polymerase is encoded by gene *E9L*, the

ninth gene from the left end of the Hind III E fragment, and the gene is transcribed in a leftward direction relative to the standard orientation of the genome.

While Copenhagen was the first vaccinia strain sequenced, most of the genetic and biochemical analysis of vaccinia has been performed using the WR strain, a strain that is not identical in genetic content to Copenhagen. Initially, the Copenhagen system of nomenclature was applied to WR; however, strain variation, sequencing glitches, and the absence of complete genome sequence made this usage occasionally confusing. For example, the vaccinia strain WR genes initially dubbed *A5L* and *A8L* are orthologous to the Copenhagen genes *A4L* and *A7L*, while further to the right in the Hind III A fragment, WR genes orthologous to Copenhagen genes were given the precise Copenhagen name. Despite this initial confusion, over the years the Copenhagen nomenclature has become the most familiar among poxvirologists, and a custom has emerged which is to refer to genes in WR using the orthologous Copenhagen gene identification. Accordingly, the WR genes previously called *A5L* and *A8L* are now referred to as *A4L* and *A7L*.

More recently, faced with an explosion of poxvirus genome sequences available and the impossibility of maintaining the Copenhagen nomenclature across such a diversity of sequences, a new nomenclature has emerged in which genes are simply numbered in sequence from left to right on the genome, along with an identifier specifying the virus strain. Thus while the *E9L* gene in Copenhagen is now officially "*VV-Cop-E9L*," in WR it is "*VACWR065*."

This review deals almost exclusively with experiments done with the WR strain of vaccinia. For the sake of clarity, we have maintained the custom of referring to WR genes using the Hind III designation of the Copenhagen ortholog. Following established convention, genes are referred to using the entire designation, for example, "*E9L*" for the DNA polymerase gene, while proteins are specified by omitting the "L" or "R," for example, "E9" for the DNA polymerase enzyme. For the sake of precision, in Table I we have included a column specifying the official WR gene name for each protein.

C. Poxvirus Genetics: Special Considerations

Conditional lethal mutants have been isolated which encode alterations in over half of the essential genes in vaccinia virus. These mutants are of two different types, inducible and temperature sensitive. The two different types of mutants function by fundamentally different

TABLE I

VACCINIA VIRION PROTEINS

Gene*	WR designation	MW†	Location	Mutants‡	Comment§
D13L	*VACWR118*	62	Absent	ind, ts	Rifampicin target, IV scaffold protein
A11R	*VACWR130*	36	Absent	ind	Hydrophobic, phosphorylated (independent of F10), interacts with A32, itself
A2.5L	*VACWR121*	9	Virion enzyme	ind	Thiol oxidoreductase
A32L	*VACWR155*	31	Virion	ind	Putative ATPase, DNA encapsidation
A17L	*VACWR137*	23	Membrane	ind	TM(2), F10-dependent phosphorylation, cleaved, complex with A14, A27
A14L	*VACWR133*	10	Membrane	ind	TM(2), F10-dependent phosphorylation, dimerizes, complex with A17, A27
A13L	*VACWR132*	8	Membrane	ind, ts	TM(1), phosphorylated (independent of F10), DNA encapsidation
A9L	*VACWR128*	12	Membrane	ind	TM(1)
L1R	*VACWR088*	27	Membrane	ind	TM(1), myristylated, redox substrate
H3L	*VACWR101*	37	Membrane	ind, ko	TM(1), heparin binding
A21L	*VACWR140*	14	Membrane	ind	TM(1), redox substrate, fusion complex
L5R	*VACWR092*	15	Membrane	ind	TM(1), redox substrate, fusion complex
A28L	*VACWR151*	16	Membrane	ind, ts	TM(1), redox substrate, fusion complex
H2R	*VACWR100*	22	Membrane	ind	TM(1), redox substrate, fusion complex
G3L	*VACWR079*	13	Membrane	ts	TM(1), fusion complex
G9R	*VACWR087*	39	Membrane	ind	TM(1), myristylated, fusion complex
J5L	*VACWR097*	15	Membrane		TM(1), myristylated, fusion complex
A16L	*VACWR136*	43	Membrane	ind	TM(1), myristylated, fusion complex
I2L	*VACWR071*	8	Membrane	ind	TM(1)
D8L	*VACWR113*	35	Membrane	ko	TM(1), chondroitin binding

(*continues*)

TABLE I (*continued*)

Gene*	WR designation	MW†	Location	Mutants‡	Comment§
A27L	*VACWR150*	13	Membrane	ind, ko	No TM, complex with A17, A14, heparin binding
A26L	*VACWR149*	58	Membrane	ko	p4c, TM(?)
A14.5L	*VACWR134*	6	Membrane	ko	TM(2)
I5L	*VACWR074*	9	Membrane		TM(2)
E10R	*VACWR066*	11	Membrane enzyme	ind	Thiol oxidoreductase, no TM
G4L	*VACWR081*	14	Membrane enzyme	ind	Thiol oxidoreductase, no TM
H5R	*VACWR103*	22	Core	ts	F10, B1-dependent phosphorylation, roles in DNA replication, transcription, morphogenesis
G5R	*VACWR082*	50	Core	ind	
A30L	*VACWR153*	9	Core	ind, ts	7 complex, F10-dependent phosphorylation, partially NP40 extractable, in viroplasm, IV's
G7L	*VACWR085*	42	Core	ind, ts	7 complex, F10-dependent phosphorylation, cleaved
J1R	*VACWR093*	18	Core	ind, ts	7 complex, partially NP40 extractable
A15L	*VACWR135*	11	Core	ind	7 complex
D2L	*VACWR107*	17	Core	ind, ts	7 complex
D3R	*VACWR108*	28	Core	ts	7 complex
A10L	*VACWR129*	102	Core	ind, ts	p4a/4a, cleaved, complex A4, core wall?
I6L	*VACWR075*	43	Core	ts	Telomere binding, DNA encapsidation
I1L	*VACWR070*	36	Core	ind	DNA binding
F17R	*VACWR056*	11	Core	ind	H1 dependent, partially F10 dependent phosphorylation, DNA binding

A4L	*VACWR123*	31	Core	ind	Core wall spike protein(?), membrane associated(?), F10, H1-dependent phosphorylation, complex with A10
A3L	*VACWR122*	73	Core	ts	p4b/4b, cleaved, core wall
L4R	*VACWR091*	28	Core	ind	VP8, cleaved
E8R	*VACWR064*	32	Core	ts	TM(2), phosphorylated
E11L	*VACWR067*	15	Core	ts	
L3L	*VACWR090*	41	Core	ind	
A12L	*VACWR131*	20	Core		Cleaved
J6R	*VACWR098*	147	Core enzyme	ts	RNA polymerase subunit, rpo147
A24R	*VACWR144*	133	Core enzyme	ts	RNA polymerase subunit, rpo132
H4L	*VACWR102*	94	Core enzyme	ind, ts	RNA polymerase subunit, rap94, early gene specificity factor, required for early transcription termination
A29L	*VACWR152*	35	Core enzyme	ts	RNA polymerase subunit, rpo35
E4L	*VACWR060*	30	Core enzyme		RNA polymerase subunit, rpo30
J4R	*VACWR096*	21	Core enzyme	ts	RNA polymerase subunit, rpo22
A5R	*VACWR124*	19	Core enzyme		RNA polymerase subunit, rpo19
D7R	*VACWR112*	18	Core enzyme	ts	RNA polymerase subunit, rpo18
G5.5R	*VACWR083*	7	Core enzyme		RNA polymerase subunit, rpo7
A7L	*VACWR126*	82	Core enzyme	ind	Early gene transcription initiation factor, VETF
D6R	*VACWR111*	74	Core enzyme	ind, ts	Early gene transcription initiation factor, VETF
D1R	*VACWR106*	97	Core enzyme	ts	Capping enzyme, also early gene termination factor, intermediate gene initiation factor
D12L	*VACWR117*	33	Core enzyme	ts	Capping enzyme, also early gene termination factor, intermediate gene initiation factor

(*continues*)

TABLE I (*continued*)

Gene*	WR designation	MW†	Location	Mutants‡	Comment§
E1L	*VACWR057*	55	Core enzyme		Poly(A) polymerase catalytic subunit
J3R	*VACWR095*	39	Core enzyme	ko	Poly(A) polymerase elongation subunit, also 2′ 0 methyltransferase, transcription elongation factor
D11L	*VACWR116*	72	Core enzyme	ts	Early gene termination factor, NPH I
I8R	*VACWR077*	78	Core enzyme	ts	RNA helicase
A18R	*VACWR138*	57	Core enzyme	ts	Postreplicative transcription termination factor, RNA release factor
A22R	*VACWR142*	22	Core enzyme	ind	Holliday resolvase, concatemer resolution, palmitylprotein
H6R	*VACWR104*	37	Core enzyme	ko	Topoisomerase
K4L	*VACWR035*	49	Core enzyme	ko	DNA nicking and joining enzyme, nonessential
G1L	*VACWR078*	68	Core enzyme	ind	Metalloproteinase(?)
I7L	*VACWR076*	49	Core enzyme	ind, ts	Cysteine proteinase(?), virion protein processing
F10L	*VACWR049*	52	Core enzyme	ts, ind	Ser/Thr/Tyr kinase, 7 complex
B1R	*VACWR183*	34	Core enzyme	ts	Ser/Thr kinase, essential for DNA replication
H1L	*VACWR099*	20	Core enzyme	ind	Tyr/Ser/Thr phosphatase
O2L	*VACWR069*	12	Core enzyme	ko	Glutaredoxin, nonessential, not conserved
A45R	*VACWR171*	14	Core enzyme	ko	Inactive superoxide dismutase, nonessential

* Copenhagen designation.
† predicted, apparent MW may differ.
‡ ind, inducible; ts, temperature sensitive; ko, knockout.
§ TM, transmembrane domain, number of domains in parentheses.

mechanisms; an understanding of these mechanisms is important for proper evaluation of mutant phenotypes.

In inducible mutants, the gene in question is engineered such that its expression is controlled by the regulatory elements of a bacterial operon, commonly either lac or tet (Rodriguez and Smith, 1990a; Traktman *et al*., 2000; Zhang and Moss, 1991a). Thus, in the presence of inducer, the wild-type gene and protein in question are expressed, a permissive condition exists, and virus can be grown for study. In the absence of inducer, the gene is not expressed, a nonpermissive condition exists, and the mutant phenotype can be studied. Importantly, under nonpermissive conditions in an inducible mutant, the gene product in question is absent or present at only low levels.

In temperature-sensitive mutants, the gene in question contains a missense mutation that renders the protein product either unstable or nonfunctional at high temperature (Condit and Niles, 1990). Thus, virus is grown for study at low temperature, the permissive condition, and the mutant phenotype studied using infections at high temperature, the nonpermissive condition. In mutants where the protein in question is unstable at high temperature, the protein is effectively absent from the infection and thus mechanistically the mutant is similar to an inducible mutant. An important caveat to this statement, however, is that any residual protein is mutant in nature, whereas the residual protein present in the case of inducible mutants is wild type. For temperature-sensitive mutants in which the target protein is nonfunctional at the high temperature but nevertheless physically present, the mechanism of temperature sensitivity is significantly different than in an inducible mutant. Most temperature-sensitive mutants extant have been isolated by classical mutagenesis and random screening methods;[2], however, methods exist whereby temperature-sensitive mutants can be engineered into specific genes in a targeted fashion (DeMasi and Traktman, 2000; Grubisha and Traktman, 2003; Hassett and Condit, 1994; Hassett *et al*., 1997; Ishii and Moss, 2001; Punjabi *et al*., 2001).

[2] Temperature-sensitive mutants are referred to using either a mutant-specific designation or a generic protein-specific designation. The mutant-specific designation consists of a letter, either C, D, or E, signifying the original mutant collection, (Condit, Dales, or Ensinger) followed by "ts" and a number specific to the mutant, for example, Dts46 (Lackner *et al*., 2003). The generic, protein-specific notation consists of "ts" followed by the name of the protein, for example, tsA30.

Each mutant type has advantages and disadvantages. Advantages of inducible mutants include the relative ease with which a mutant may reliably be targeted to a specific gene and the fact that all experiments can be done at one temperature, thus avoiding the possibility of temperature-induced abnormalities in the infection. Disadvantages include the inability to use this system effectively for viral genes expressed early in infection and the inability to engender a tight phenotype for some late genes, due to some intrinsic leakiness in the system. Advantages of temperature-sensitive mutants include the ability sometimes to perform temperature shift-up and shift-down experiments to test for the requirement for a gene at different times during the life cycle and the existence of some mutants which synthesize stable but nonfunctional protein at the nonpermissive temperature. Disadvantages of temperature-sensitive mutants include the difficulty of isolating mutants in specific genes in a targeted fashion and the necessity of performing experiments at high temperature, which may induce mutant-independent abnormalities in the infection. In the end, the two types of mutants have complementary advantages and provide powerful tools for the study of gene function.

III. Vaccinia Virion Structure

A. Imaging Studies of MV Structure

Electron microscopic investigation of vaccinia virus structure has involved analysis of both whole mount preparations of purified virus and thin sections of purified virions or virus-infected cells. Each approach has strengths and limitations that are important to consider in deriving an overall model for the structure of the virus. In overall dimensions, the virion is highly asymmetric, described variously as ellipsoidal, brick shaped, or barrel shaped (see the following paragraph). As a result of this asymmetry, in most whole mount preparations of virus, the majority of particles appear to be oriented in a nonrandom fashion, presenting the broadest surface of the virion perpendicular to the electron beam, revealing clearly only the two widest dimensions. Whole mount preparations also provide detail relevant to the surface of the particle but usually reveal less information about the internal structure. By contrast, thin sections present all possible orientations and sections of the virion for viewing; however,

reconstructing an accurate three-dimensional (3D) view of a relatively complex and asymmetric structure can be daunting. While thin sections provide minimal information about the surface of the particle, they reveal significant information about internal structure.

Three studies provide estimates of the external dimensions of the virion that are consistent with historical measurements (Dales and Pogo, 1981; Fenner *et al*., 1989) and at the same time reflect some continuing uncertainty regarding the ultimate shape of the virion. Measurements of cryo-electron micrographs by Griffiths and coworkers suggest a brick- or pillow-shaped particle, with dimensions of 310 × 240 × 140 nm (Griffiths *et al*., 2001b; Roos *et al*., 1996; Sodeik and Krijnse-Locker, 2002). A study using atomic force microscopy suggests a slightly flattened ellipsoid with dimensions of 350 × 300 × 265 nm (Malkin *et al*., 2003). Lastly, recent cryo-electron tomography of the virus provides evidence that MV are barrel shaped, with dimensions of 360 × 270 × 250 nm (Cyrklaff *et al*., 2005). Malkin *et al*. (2003) note that if particles are air dried and examined by atomic force microscopy, they shrink more than twofold along the shortest axis but only slightly along the longer two axes, yielding final dimensions of approximately 330 × 260 × 125 nm, provocatively similar to the measurements reported by Griffiths and coworkers using cryo-electron microscopy (Griffiths *et al*., 2001b; Roos *et al*., 1996). In summary all three of these studies, using different approaches, suggest a flattened ellipsoid or barrel but leave some lingering uncertainty concerning the ratio of the length of the shortest axis to the longer axes.

The surface of purified MV particles, as viewed in whole mount preparations, assumes two fundamentally different appearances depending on the integrity of the particles and the method of preparation. Particles observed using negative staining, metal shadowing, freeze etch or deep etch electron microscopy, or atomic force microscopy possess randomly arranged surface ridges called "surface tubule elements" (STEs) (Fig. 1A–E) (Dales, 1962; Heuser, 2005; Malkin *et al*., 2003; Medzon and Bauer, 1970; Noyes, 1962a,b; Stern and Dales, 1976; Westwood *et al*., 1964; Wilton *et al*., 1995). This form of virus was named the "M" form by Westwood *et al*. (1964) for its *m*ulberry like appearance. Most negatively stained, purified preparations of MV also contain virions which lack obvious STEs but instead possess a clearly delineated boundary surrounding the particle (Fig. 1A). These latter forms were dubbed the "C" form by Westwood *et al*. (1964), because the boundary looks like a *c*apsule surrounding the particle.

Visualization of purified MV in whole mount using cryo-electron microscopy reveals particles that closely resemble the C form of virus, that is, lacking evidence of STEs and possessing a boundary layer or "surface domain" (Fig. 1F) (Dubochet *et al*., 1994; Griffiths *et al*., 2001b). In negatively stained preparations, treatments that are likely to disturb the integrity of the particle convert the M form of the virus to the C form (Dubochet *et al*., 1994; Westwood *et al*., 1964). Dubochet *et al*. (1994) interpreted these results to mean that the STEs are preparation artifacts induced by osmotic stress imposed during

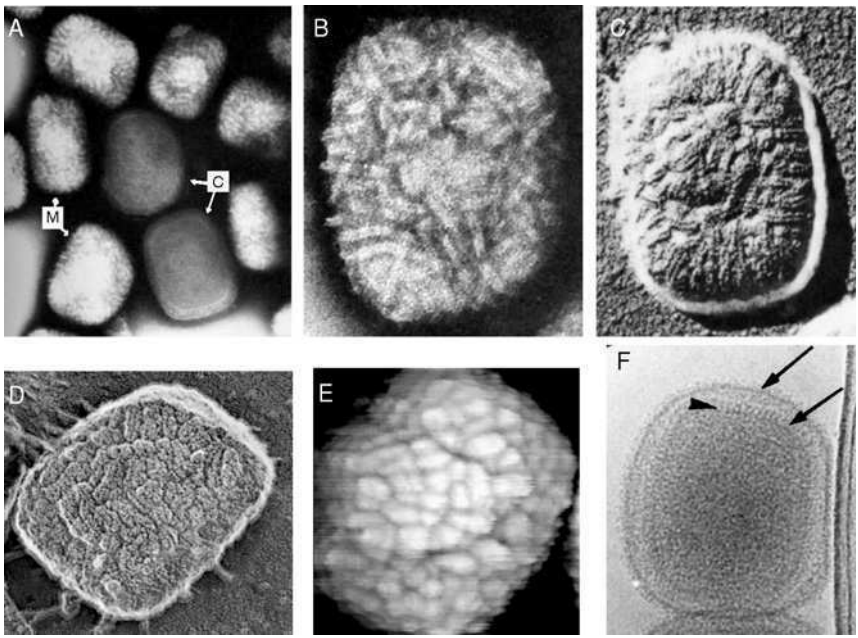

FIG 1. Vaccinia virus surface features. (A) Electron micrograph of purified virus, whole mount, negative stain. "Mulberry" (M) and "capsule" (C) forms are shown (Westwood *et al*., 1964). (B) Electron micrograph of a purified virion, whole mount, negative stain (Wilton *et al*., 1995). (C) Freeze etch electron micrograph of a purified virion (Nermut, 1973). (D) Deep etch electron micrograph of a purified virion (Heuser, 2005). (E) Atomic force micrograph of a purified virion (Malkin *et al*., 2003). (F) Cryo-electron micrograph of a whole mount preparation of purified virions (Griffiths *et al*., 2001b). Arrows denote the limits of the surface domain; arrowhead denotes the palisade layer. (A) Reprinted from Westwood *et al*. (1964) with permission. (B) Reprinted from Wilton *et al*. (1995) with permission. (C) Reprinted from Nermut (1973) with permission. (D) Reprinted from Heuser (2005) with permission. (E) Reprinted from Malkin *et al*. (2003) with permission. (F) Reprinted from Griffiths *et al*. (2001b) with permission.

negative staining and that the smooth surfaced C form of virus revealed by cryo-electron microscopy most accurately represents the surface of the virus. However, the persistence of STEs in metal shadowing, freeze etch and deep etch electron microscopy, and atomic force microscopy (Heuser, 2005; Malkin *et al*., 2003; Medzon and Bauer, 1970), plus the biochemical evidence for a structure resembling STEs (Wilton *et al*., 1995) (Sections III.C and IX.E.3) suggests that STEs are not artifactual. As originally proposed by Westwood *et al*. (1964), the C form of virus present in negatively stained preparations most likely results from penetration of stain into damaged virions, which destroys the contrast that ordinarily highlights STEs. The C form appearance of particles viewed by cryo-electron microscopy probably results from an insensitivity of cryo-electron microscopy to fine surface detail (Malkin *et al*., 2003).

Insights into the internal architecture of MV have been gained primarily through the use of thin sections, although some information can be obtained from whole mount preparations. Thin sections reveal two distinct boundaries, the membrane,[3], which surrounds the entire MV particle, and the core wall, which surrounds an internal core. Cryosections, such as that shown in Fig. 2A, offer the clearest definition of the substructure of the membrane and the core wall, each of which comprises two layers or domains. Estimates of the thicknesses of each of these domains vary, and the numbers bear significance to the biochemical makeup of each domain (discussed in Section VI.A.3) (Cyrklaff *et al*., 2005; Dubochet *et al*., 1994; Fenner *et al*., 1989; Hollinshead *et al*., 1999; Ichihashi *et al*., 1984). The outer domain of the membrane (outermost dark layer in Fig. 2A) is between 3 and 9 nm thick, the inner domain (light layer underneath the outer domain and surrounding the entire particle in Fig. 2A) 5–6 nm thick, and estimates of the thickness of the membrane in aggregate range from 10 to 20 nm. The outer core wall (dark layer surrounding the core in Fig. 2A) is clearly thicker than any of the four domains comprising

[3] Dales and coworkers proposed the term "envelope" to describe the MV outer boundary, based on its lipid content and its function analogous to envelopes of other viruses (Dales and Pogo, 1981). However, the common usage of the term envelope in referring to WV and EV (heretofore called IEV, CEV, and EEV) invites confusion over the origin, structure, and function of the MV outer boundary. We use the term "membrane" to describe the MV outer boundary; however, it is critical to understand that this two-domain structure is clearly significantly more complex than a simple single lipid membrane bilayer. Details of the substructure, lipid and protein composition of the MV membrane are provided in subsequent sections.

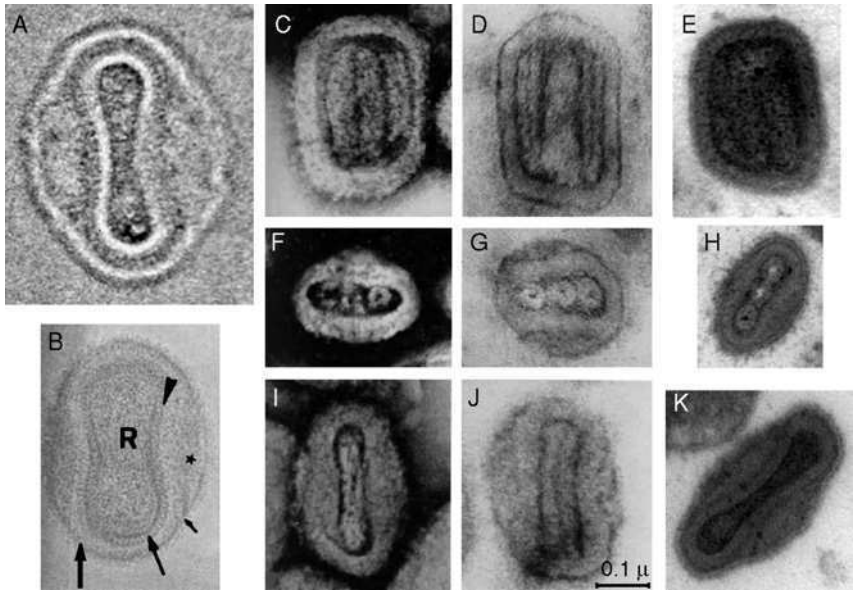

FIG 2. Vaccinia virus internal features. (A) Cryosection (Hollinshead *et al*., 1999). (B) Whole mount cryo-electron micrograph using uranyl acetate staining (Griffiths *et al*., 2001b). The authors interpreted images of isolated particles as revealing significant asymmetry in the virion structure, two lipid bilayer membranes, and infoldings of the membranes (Section VI, Fig. 8, Model 4). Hence, the "R" indicates the right hand side of the particle. The authors state that "The particle has attached to the grid support in a manner such that a classical side view is evident. The two membrane layers are indicated with large arrows, and the spikes are indicated by an arrowhead. The star indicates the projection of one of the lateral bodies that we believe is due to the overlapping of the peripheral lobes of the virus (top and bottom). The small arrow indicates an inward groove in the membrane." The image is one of the best available showing the internal structure of the virion in a whole mount preparation of virus. (C, F, and I) Three different projections of a whole mount preparation of virus, phosphotungstic acid stained (Peters and Mueller, 1963). (D, G, and J) Sections of purified virus, uranyl acetate stained, in three different perpendicular planes (Peters and Mueller, 1963). (E, H, and K) Sections of MV in three different perpendicular planes (Kato *et al*., 2004; Condit, unpublished). (E) and (H) are virions in infected cells; (K) was from a preparation of purified virus. (A) Reprinted from Hollinshead *et al*. (1999) with permission. (B) Reprinted from Griffiths *et al*. (2001b) with permission. (C, D, F, G, I, and J) Reprinted from Peters and Mueller (1963) with permission. (K) Reprinted from Kato *et al*. (2004) with permission.

the membrane and the core wall; estimates of the width of the outer core wall range from 8 to 17 nm. The outer core wall has a striated appearance and therefore has been called the "palisade layer." The inner core wall or "smooth layer" (innermost light layer in Fig. 2A), has been estimated at 5–8 nm in thickness. While biochemical evidence suggests

that the layers of the core wall are in fact biochemically distinct, the layered appearance of the membrane may simply reflect a structural asymmetry within an otherwise unitary structure. Over much of its surface, the outer core wall appears to be closely apposed to the inner domain of the membrane, as is clearly seen at the top and bottom of the particle in Fig. 2A. Appropriate sections of the particle reveal the central bilateral concavities in the core, formed by a separation of the core wall from the membrane. Filling these concavities between the core wall and the membrane are two apparently amorphous masses called "lateral bodies," as shown clearly in the particles in Fig. 2A and K.

Importantly, different sections through the virion yield very different impressions of the relationship between the core and the membrane. Figure 2C–K shows sections in all three possible spatial planes. Sections through the broadest plane (Fig. 2C–E) closely resemble whole mount cryo-EM images of purified virus or the C form of virus viewed by negative staining. Thus, the capsule of the C form and the surface domain of the cryo-EM images most likely represent the four domains of the membrane and the core wall, tightly apposed with no separation between the core wall and the membrane and no evidence of lateral bodies. While most whole mount preparations of virus seem to be nonrandomly oriented in this fashion with the broadest plane perpendicular to the electron beam, particles are occasionally oriented on their sides, revealing the biconcave shape of the core and hinting at lateral bodies (Fig. 2B) (Griffiths *et al.*, 2001b). Sections through the other two planes perpendicular to the broadest plane (Fig. 2F–K) often reveal the lateral bodies but may not if they are cut close to the ends or the sides of the particle.

The core contains a tube-like structure first detailed by Peters and Mueller (1963) (Fig. 2C–K). Images that clearly reveal the length of the tube are rare, possibly because this structure is relatively labile (Peters and Mueller, 1963) and also because sections must be cut precisely parallel to, and must bisect, the broadest plane of the virus in order to clearly visualize the tube. Images of the tube in cross section are more common, although still relatively rare (Fig. 2F–H) (Heuser, 2005).

B. Chemical Composition of MV

Whole MV particles contain approximately 3.2% (of dry weight) DNA and 5% lipid, the balance of the mass presumably being composed of protein (Zwartouw, 1964). There is general agreement that the particle does not contain significant amounts of RNA. In addition, the presence of spermine and spermidine in MV has been reported;

as described in Section VIII, these polyamines may play a role in condensation of the viral DNA (Lanzer and Holowczak, 1975).

The lipid composition of MV is generally similar to that of the host cell, with two significant differences. First, the fraction of phosphatidyl ethanolamine is about one-third less than the host cell and second, MV lipid contains approximately 25% of a biphosphatidic acid analog, acyl bis(monoacylglycero)phosphate, three to four times the amount found in host cells (Hiller *et al.*, 1981; Stern and Dales, 1974). These differences carry implications for the origin of the lipid in MV, discussed in a later section.

C. Controlled Degradation of MV

Additional detail regarding the fine structure of MV has been obtained through controlled degradation of the particle, followed by electron microscopic analysis of subparticle fractions. Easterbrook (1966) first demonstrated that treatment of MV with a neutral detergent (NP40) and a reducing agent (2-mercaptoethanol or dithiothreitol (DTT)) solubilizes the virion membrane, leaving behind an intact core with lateral bodies attached. This observation, coupled with the observation that MV can enter cells by fusion (Armstrong *et al.*, 1973; Carter *et al.*, 2005), demonstrates that the MV membrane contains a lipid bilayer, which probably corresponds to the innermost of the two visible domains comprising the MV membrane (Section III.A) (Hollinshead *et al.*, 1999). Ichihashi *et al.* (1984) observed that treatment of MV with SDS alone yielded a "ghost" particle, which remained bounded by a structure that resembles the membrane but is reduced in thickness from 20 to 5–7 nm. This finding implies that the protein component(s) of the membrane comprise an extensive disulfide bonded network (Section VI.D.2).

Careful titration of NP40 and 2-mercaptoethanol into suspensions of MV yields cores mixed with an abundance of tubular structures (Fig. 3A) (Wilton *et al.*, 1995). Wilton *et al.* (1995) equated these structures with STEs. While the isolated tubules are not identical in dimension and structure to STEs, the overall similarity in appearance is compelling. After complete solubilization of the MV membrane with saturating amounts of NP40 and 2-mercaptoethanol, the core, with lateral bodies attached, can be purified from the solubilized membrane fraction by differential centrifugation (Fig. 3B). (It is noteworthy that most investigators refer to this NP40 and 2-mercaptoethanol insoluble fraction as the "core" fraction, when it in fact contains both the virion core and the lateral bodies.) Isolated cores no longer possess concavities and reveal clearly the details of the outer palisade layer of the core wall (Fig. 3C and D)

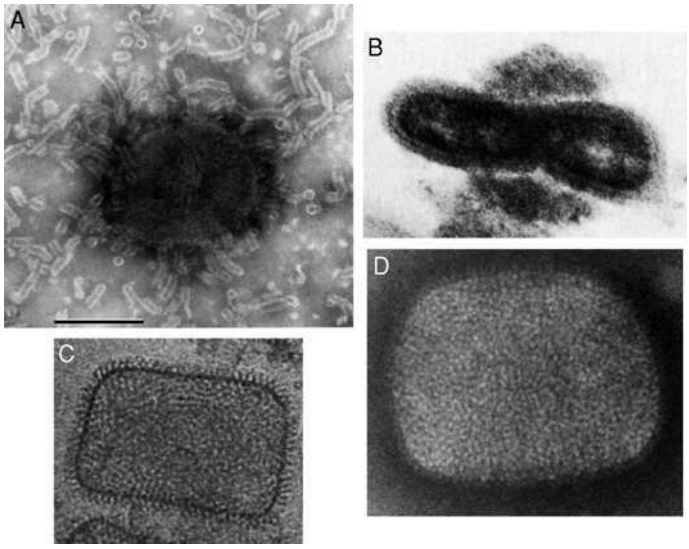

FIG 3. Vaccinia virion substructures. (A) Negatively stained preparation of MV after mild treatment with NP40 and 2-mercaptoethanol, so that surface tubule elements remain intact (Wilton *et al*., 1995). Bar, 0.2 μm. (B) Isolated core in thin section. Note lateral bodies still attached (Ichihashi *et al*., 1984). (C) Isolated core visualized by cryo-electron microscopy (Dubochet *et al*., 1994). (D) Isolated core visualized by negative staining (Wilton *et al*., 1995). (A and D) Reprinted from Wilton *et al*. (1995) with permission. (B) Reprinted from Ichihashi *et al*. (1984) with permission. (C) Reprinted from Dubochet *et al*. (1994) with permission.

(Dubochet *et al*., 1994; Easterbrook, 1966; Wilton *et al*., 1995). The palisade is composed of a lattice, sometimes hexagonal, of cylindrical pegs measuring approximately 5 nm in diameter and 10 nm in length (Dubochet *et al*., 1994; Easterbrook, 1966; Westwood *et al*., 1964). The lateral bodies and palisade layer sometimes spontaneously dissociate from a fraction of isolated cores, revealing the inner smooth layer and thus substantiating the two-layer character of the core wall. Treatment of the NP40, 2-mercaptoethanol insoluble fraction with trypsin actively removes the lateral bodies, suggesting that the lateral bodies are proteinaceous in nature (Easterbrook, 1966). Within the core resides the viral DNA genome.

D. Structure of the Genome in the Core

Investigation of the core substructure suggests that the viral genome exists in the core complexed with viral protein. Rupture of MV by various methods can release 30–40-nm diameter tubules that

possess an apparently helical substructure (Griffiths *et al.*, 2001b; Malkin *et al.*, 2003). The relationship, if any, between these tubules and the 50-nm diameter tube contained in the core (Peters and Mueller, 1963) is unclear. Treatment with protease reduces the 30-nm tubes to 16-nm fibers, also helical in substructure, which coat the viral DNA (Malkin *et al.*, 2003). Holowczak and coworkers, using various treatments with detergents and denaturing agents, isolated from MV DNA-containing substructures of varying complexity they termed "nucleoids" and "subnucleoids" (Holowczak *et al.*, 1975; Soloski and Holowczak, 1980, 1981; Soloski *et al.*, 1979; reviewed in Holowczak, 1982). Subnucleoids, the simplest of these structures, contained four proteins apparently complexed with supercoiled DNA in 30–60-nm spherical structures interconnected with DNA fibers, roughly reminiscent of a very loose nucleosome structure. In summary, these studies suggest that the vaccinia genome exists within the core complexed in an organized fashion with viral proteins. However, this conclusion is still controversial. As described later in Section VIII.B, repression or inactivation of two different proteins required for genome encapsidation leads to the production of MV that lack the viral genome. These virions contain what appears to be the full complement of viral proteins: the absence of the encapsidated genome is not accompanied by the absence of an abundant DNA-wrapping protein. It may be that association of the genome with viral proteins to form a nucleoprotein complex occurs after genome encapsidation, within the context of the nascent virion core.

E. MV Proteins

Historically, the protein composition of MV has been analyzed using three fundamentally distinct approaches. First, virion proteins have been cataloged by electrophoretic resolution of whole virions or virion subfractions (Essani and Dales, 1979; Ichihashi *et al.*, 1984; Jensen *et al.*, 1996; Sarov and Joklik, 1972; Takahashi *et al.*, 1994; Wilton *et al.*, 1995). Second, numerous proteins have been purified from MV by virtue of their enzymatic activities and subsequently characterized (Martin *et al.*, 1975; Morgan *et al.*, 1984; Niles *et al.*, 1989). Finally, antibodies have been generated for individual gene products in a targeted fashion, allowing proteins to be subsequently localized to virions by immunoblot analysis (da Fonseca *et al.*, 2000a, 2004). Early attempts at cataloging the protein content of virions by gel electrophoresis relied on apparent molecular weights as a means of identifying proteins. Because of inconsistencies in molecular weight determinations, these

studies are often difficult to compare with each other, and an unambiguous assignment of a specific protein from the older literature to a discrete vaccinia gene is prone to error. More recently, the combination of genetics and protein sequencing techniques has made possible the unambiguous correlation of genes with virion proteins. We have confined ourselves in this review exclusively to those virion proteins for which a positive gene identification has been made.

A complete list of the virion proteins for which a specific gene has been identified is given in Table I. These virion proteins can be sorted into four groups based on whether or not they are solubilized by NP40 and a reducing agent and whether or not they possess enzymatic activity: (1) proteins that are solubilized by NP40 and a reducing agent but have not been assigned an enzymatic activity are presumed to be *membrane structural proteins*; (2) proteins that are solubilized by NP40 and a reducing agent and also possess an enzymatic activity are classified as *membrane enzymes*; (3) proteins that are not solubilized by NP40 and a reducing agent and have not been assigned an enzymatic activity are presumed to be *core structural proteins*; and (4) proteins that are not solubilized by NP40 and a reducing agent and also possess an enzymatic activity are classified as *core enzymes*. For completeness, Table I also includes two proteins (D13 and A11) that affect virion morphogenesis but are not encapsidated and two proteins (A32 and A2.5) whose subvirion localization remains to be determined. The list given in Table I is undoubtedly incomplete but is probably approaching saturation. Indeed, a comprehensive catalog of specific vaccinia gene products contained in MV has been compiled based on gel-free liquid chromatography and tandem mass spectroscopy of whole virions (Chung *et al*., 2006). These new data correlate remarkably well with the data in Table I and identify an additional 10 proteins (C6, F8, F9, E6, I3, A6, A25, A31, A42, and A46), whose virion localization is currently either disputed or unconfirmed by other techniques. Because of the possibility of nonspecific association of proteins with virions (Franke and Hruby, 1987), we have not included in Table I these 10 new candidate virion proteins and have instead focused attention on proteins whose presence in the virion has been confirmed by additional experiments. A few general features of the catalog of virion proteins are highlighted here, and otherwise the details of the contributions of individual proteins to structure and morphogenesis of the virions are detailed in the remainder of the review.

To date, a total of 22 proteins have been localized to the virion membrane. Of these, 2 are enzymes associated with a virus coded redox pathway responsible for maintenance of some of the disulfide bonds in

the membrane, while the remaining 20 proteins can be thought of as structural proteins. Eighteen of the 20 structural proteins are integral membrane proteins containing at least one transmembrane domain. Interestingly, none of these proteins are glycosylated in the MV membrane, reflecting the unusual origin and structure of the membrane.

To date, 47 proteins have been localized to the virion "core," that is, the NP40, reducing agent insoluble fraction, which includes both the core and the lateral bodies. Of these 47 proteins, 19 have no known enzymatic function and are presumed to be structural proteins. Sixteen of the enzyme proteins have well-characterized roles in early viral mRNA synthesis, including initiation, elongation and termination of transcription, mRNA capping and polyadenylation. The remaining enzymes play less clearly defined roles in the viral life cycle but have in some cases been shown to interact with and/or modify both proteins and nucleic acids. It is important to note that virion enzymes may have structural as well as enzymatic roles in the virion. While attempts have been made to sublocalize proteins to core nucleoprotein, inner core wall, outer core wall, and lateral bodies (Ichihashi *et al*., 1984; Sarov and Joklik, 1972), these studies date from the pregenomic era and few if any unambiguous assignments of core proteins to core substructures have been made.

Finally, several cellular proteins have been found associated with purified particles (Castro *et al*., 2003; Chung *et al*., 2006; Jensen *et al*., 1996; Webb *et al*., 1999). It is possible that some of these proteins adhere to the MV during purification or are incorporated nonspecifically during virus maturation (Franke and Hruby, 1987). However, cyclophilin A has been clearly demonstrated to be packaged into virus cores (Castro *et al*., 2003). The role of this protein in virus formation is not known, although it could participate in the trafficking of virus proteins to the factories or in the proper folding of viral proteins during the maturation process.

F. Model for MV Structure

Based on the evidence presented previously, we have constructed a schematic 3D model of the vaccinia virion. The model is not intended to be definitive in its details, especially given the continuing uncertainty regarding dimensions of the virion and its substructures. Nevertheless, we feel that such a schematic will clarify some of the microscopic images available and the interrelationships of the virion components. For external dimensions we have used the measurements determined by Cyrklaff *et al*. (2005) using cryo-electron tomography, and for

internal dimensions we have used the measurements determined by Hollinshead *et al*. (1999) from cryosections (Fig. 2A). Thus the virus appears as a slightly flattened barrel (Fig. 4A) with overall dimensions of approximately 360 × 270 × 250 nm. The particle is encased in an outer membrane, which itself consists of two component domains. The outermost membrane domain is 9 nm thick, and the innermost membrane domain is 5 nm thick (Fig. 4C–F). The membrane clearly contains lipid; however, the details of the lipid bilayer content and structure of MV are the subject of some debate and will be therefore be discussed at length later in the review (Section VI.A). Within the membrane is the core, which is also barrel shaped but contains two indentations, one on each

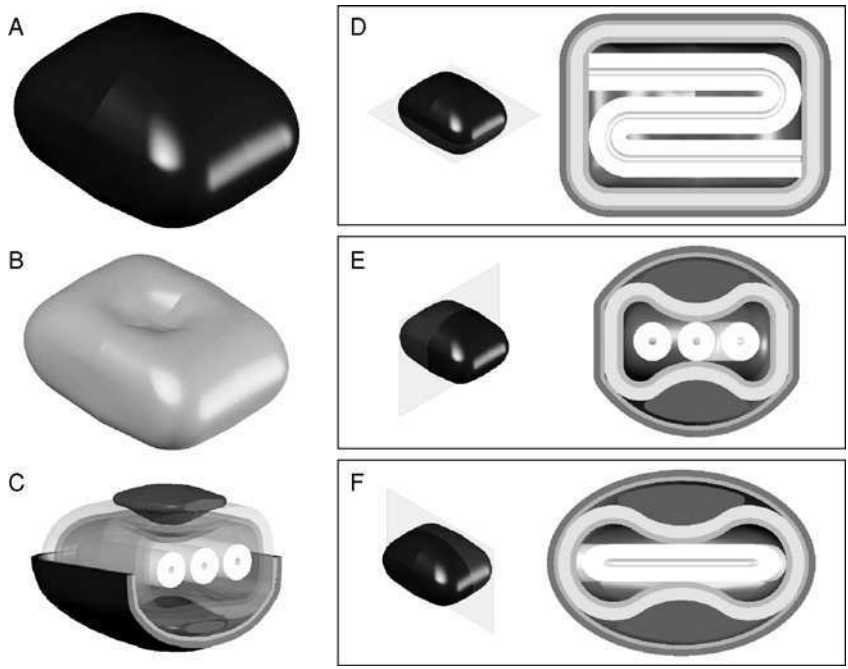

FIG 4. A model for vaccinia virion structure. (A) The intact MV. No attempt has been made to represent surface tubule elements. (B) The virion core. (C) Cutaway view. The membrane has been removed from the upper half of the virion, the near end has been removed, and the core wall has been rendered transparent, thus revealing the multiple layers, the concavities in the core, the lateral bodies, and the tubular internal structure. (D and E) Sections through the virion in three different perpendicular planes. The sections correspond to sections shown in Fig. 2. See text for details. (Model courtesy of Michel Moussatche. A dynamic 3D model is available online at http://www.vacciniamodel.com/.)

of the largest surfaces (Fig. 4B). The core is defined by a core wall, which is also composed of two layers, an outer, thicker, striated "palisade" layer 17 nm thick, and an inner smooth layer 8 nm thick (Fig. 4C–F). Filling the spaces between the core wall and the membrane that are created by the indentations in the core are "lateral bodies." Within the core is a tube-like structure, 50 nm in diameter with a 10 nm diameter core. This tube is folded upon itself into three continuous segments, with a total length of approximately 250 nm. Importantly, sections through the center of the particle in each of the three possible spatial planes yield three significantly different impressions of the overall shape and internal structure of the particle (Fig. 4D–F). For comparison, the electron micrographic images in Fig. 2C–E correspond to the model section shown in Fig. 4D; Fig. 2F–H correspond to Fig. 4E; Fig. 2I–K corresponds to Fig. 4F. A dynamic 3D rendering of the model can be found online at http://www.vacciniamodel.com/.

IV. Vaccinia Virus Morphogenesis: An Overview

The balance of this review focuses on the details of the assembly of vaccinia, with particular emphasis on lessons learned from the study of mutants affected in individual virus genes that influence virus morphogenesis. To establish a context for this discussion, we offer here a bird's-eye view of the entire assembly process.

The temporal sequence of events comprising vaccinia assembly was first deciphered experimentally by electron microscopic examination of cultured cells synchronously infected with virus (Dales, 1963; Dales and Siminovitch, 1961). At very early times following uptake of virus and dissolution of the core particle, infection-specific cytoplasmic domains are observed that are uniform in density, contain few if any cellular organelles, and are sometimes surrounded by ER derived cisternae (Fig. 5A and B) (Tolonen *et al.*, 2001). These domains represent sites of viral DNA replication, sometimes called "factories," "viral factories," or "DNA factories," and they increase in size with time. The earliest evidence of virus assembly is the appearance within factories of rigid crescent-shaped structures, cupules in three dimensions, 10–15 nm in thickness (Figs. 5C and 6). In most electron micrographs crescents comprise two distinct layers, an inner, smooth layer that at high resolution in fixed embedded sections has the trilamellar appearance of a lipid bilayer and an outer layer composed of regularly spaced projections termed "spicules" (Dales and Mosbach, 1968; Risco *et al.*, 2002). It is universally accepted that crescents contain at least one

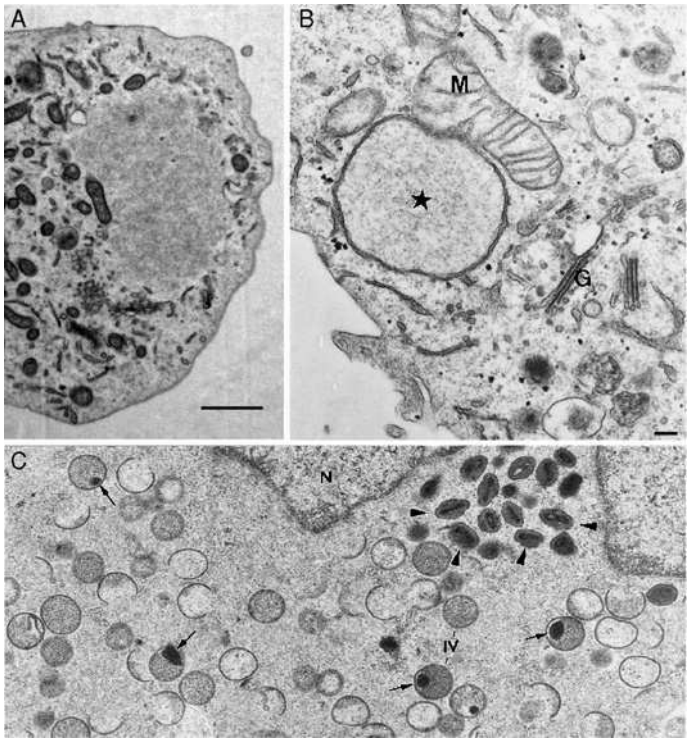

FIG 5. Vaccinia factories. (A) An early factory, 4 hpi. The factory is represented by the central cleared area surrounded by cytoplasmic organelles. Bar, 1 μm. (Kato and Condit, unpublished) (B) A factory 2 h, 45 min pi (Tolonen *et al.*, 2001). The star indicates the factory. G, Golgi stack. M, mitochondria. Bar, 0.2 μm. (C) A factory late during infection (Rodriguez *et al.*, 1998). N, nucleus. IV, immature virions. Arrows indicate IVN. Arrowheads indicate MV. Note that the MV are removed from the factory. (B) Reprinted from Tolonen *et al.* (2001) with permission. (C) Reprinted from Rodriguez *et al.* (1998) with permission.

lipid bilayer, although the precise membrane makeup of crescents has been the subject of some debate, discussed in more detail in Section VI.A. Crescents apparently grow in length while maintaining the same curvature until they become closed circles, spheres in three dimensions, called immature virions (IV) (Figs. 5C and 6). IV are approximately 350 nm in diameter and are filled with "viroplasm," material that is uniform in density but discernibly more electron dense than the surrounding factory. Viroplasm appears not only in IV but it also often appears to fill the concavities defined by crescents. Viroplasm is also often present as relatively large sub domains, "virosomes," within the surrounding factory, sometimes unbounded, sometimes surrounded

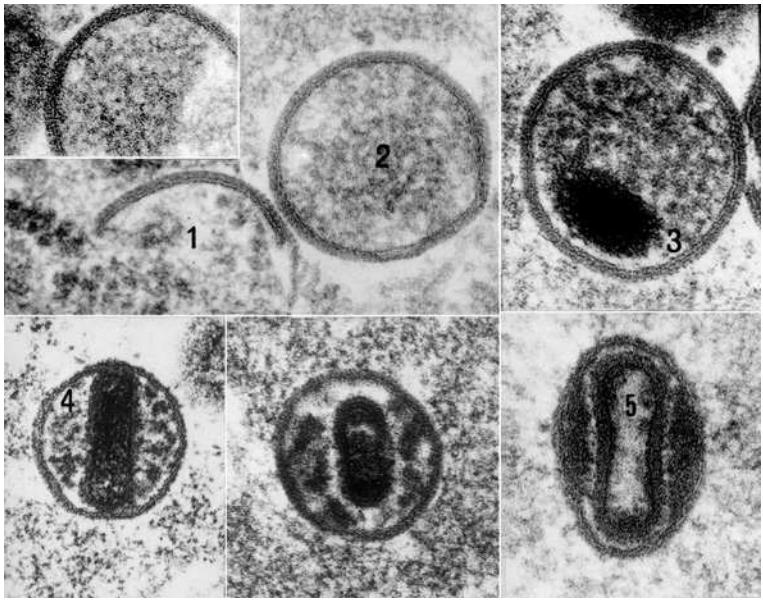

FIG 6. Vaccinia morphogenesis intermediates. (1) Crescents. (2) IV. (3) IVN. (4) Structures intermediate between IV and MV. (5) MV. Reprinted from Moss (2001) with permission.

by multiple crescents that appear to "bite off" portions of viroplasm. Appearing at approximately the same time as IV are IV which contain an electron dense, round or ovoid subdomain called a "nucleoid" (Figs. 5C and 6). We refer to IVs that contain nucleoids as "IVN." Nucleoids contain DNA (Dales, 1963; Ericsson *et al.*, 1995). Nucleoid material is frequently observed spanning a small gap in a nearly complete IV, so that it lies partially inside and partially outside of the particle (Morgan, 1976a). Under some conditions, larger inclusions of DNA-containing nucleoid material are found within factories, and may appear as either large, spherical, granular inclusions or alternatively paracrystalline arrays. Importantly, serial sections reveal that most if not all IVs contain nucleoids, so that in fact in a normal infection, there may be no real distinction between IVs and IVNs, rather, an IV is merely an IVN that has been sectioned through a plane that does not include the nucleoid (Morgan *et al.*, 1955). Following the appearance of IVNs, MV appear (Figs. 5C and 6). Proteolytic cleavage of several virion protein precursors to a mature form accompanies, and in fact is required for, morphogenesis from IVN to MV (Ansarah-Sobrinho and Moss, 2004b; Katz and Moss, 1970b). The majority of MV are found outside factories and may exist in clusters either at the periphery of a factory or apparently separated by a

significant distance from the nearest factory. Particles which have a structure that appears to be intermediate between IVN and MV have been described, but they are rare, suggesting that the transition from IV to MV is a rapid and concerted process (Fig. 6).

For the purposes of this review, we have artificially divided vaccinia morphogenesis into stages, including formation of factories, crescents, IV, IVN, and MV. A summary of the entire process is shown in Fig. 7. We now consider the details of each of these stages separately. Critical to the understanding of the assembly process is the phenotypic analysis of infections performed with conditional lethal mutants; a complete list of the currently available mutants affected in genes that encode proteins required for virion morphogenesis or infectivity is shown in Table II.

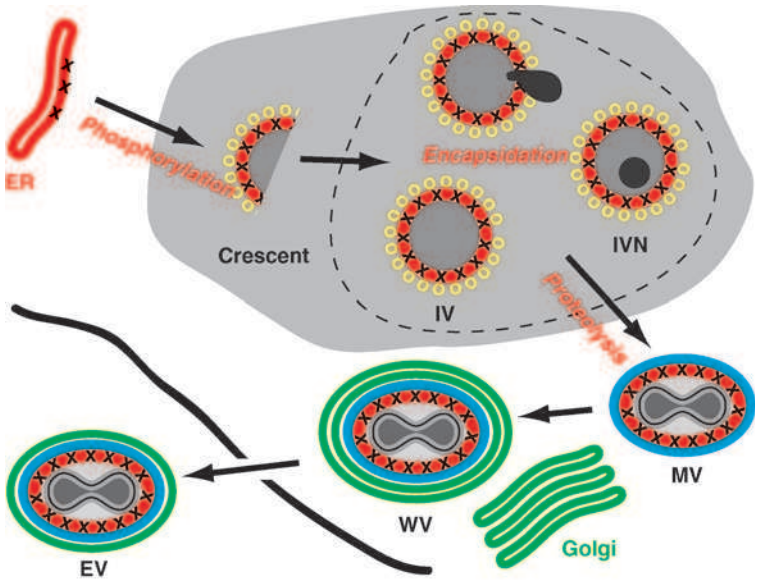

FIG 7. Vaccinia morphogenesis summary. Following the arrows in sequence from the upper left corner: Several integral viral membrane proteins (black Xs) are made in the ER (red lines) and transported to viral factories (gray area) along with ER derived lipid to be assembled into crescents which contain a lipid bilayer (red line) and the membrane proteins, scaffolded on a honeycomb structure composed of the D13 protein (yellow circles). Crescent formation is controlled by phosphorylation. The crescents mature to IV and IVN, accompanied by encapsidation of the genome. The dotted line surrounding IV, IVN, and encapsidation signifies that the order of these events is uncertain. Metamorphosis to MV is accompanied by loss of the D13 scaffold, proteolysis, further addition of membrane proteins (blue line) and movement of particles outside of factories. MV acquire Golgi derived membranes (green lines) to become WV and are exocytosed through the plasma membrane (black line) to become EV.

TABLE II
VACCINIA MORPHOGENESIS GENETICS

Gene	Identity	Location	Phenotype*								Notes on phenotype
			Mutants	Cres	IV	MV	EV	Telo	Cleave	DNA	
J4R	rpo22	Core	ts	–	–	–					Factories only
J6R	rpo147	Core	ts	–	–	–					Factories only
F10L	Kinase, 7 complex	Core	ts, ind	–	–	–	–		–		Factories only
H5R		Core	ts	–	–	–	–	+	–		Curdled virosomes or DNA
G5R		Core	ts	–	–	–	–	+	–		Curdled virosomes
A11R		Absent	ind	–	–	–			–		Some normal and aberrant virosomes
A17L	A17-A24-A27 complex	Membrane	ind	–	–	–	–		–		Virosomes, vesicles
A14L	A17-A24-A27 complex	Membrane	ind, ts	–	–	–	–		–		Virosomes, vesicles
D13L	IV scaffold protein	Absent	ind, ts	–	–	–	–		–		Aberrant crescents, rif resistance locus
A30L	7 complex	Membrane/ core	ind, ts	+	–	–	–		–		Empty IV
G7L	7 complex	Core	ind, ts	+	–	–	–				Virosomes + crescents (ts), or empty IV (ind)
J1R	7 complex	Membrane/ core	ind, ts	+	–	–	–	+	–		Aberrant, partial, empty IV
A15L	7 complex	Core	ind	+	–	–	–		–		Empty IV
D2L	7 complex	Core	ind, ts	+	–	–	–		–		Empty IV
D3R	7 complex	Core	ts	+	–	–	–		–		Empty IV

A10L	p4a	Core	ind, ts	+	−	−	−		−		Aberrant, empty IV's, DNA nucleoid aggregates
A13L		Membrane	ind, ts	+	+	−		+	−		No IVN, membraned DNA crystalloids
A32L	NTP motif	Virion	ind	+	+	−	+	+	−	−	Dense spherical particles lacking DNA
I6L	Telomere binding	Core	ts	+	+	−	−	+	−	−	Dense spherical particles lacking DNA
A22R	Holliday resolvase	Core	ind	+	+	−	−	−	−		Dense spherical particles
A7L	VETF	Core	ind	+	+	−	−			+	IVN, dense spherical particles, viroplasm
D6R	VETF	Core	ind, ts	+	+	−	−				IVN, dense spherical particles, viroplasm
I1L	DNA binding protein	Core	ind	+	+	−	−	+	−		IVN, DNA crystalliods
F17R	11k	Core	ind	+	+	−	−	+	−		Some aberrant, unstable IV
A4L		Membrane/ core	ind	+	+	−	−	+	−	+	IVN
A3L	p4b	Core	ts	+	+	−	+	+	+	+	Aberrant MV
G1L	Metallo-proteinase(?)	Core	ind	+	+	−	+		+	+	Aberrant MV
I7L	Cysteine proteinase(?)	Core	ind, ts	+	+	−	+		−	+	Aberrant MV
A9L		Membrane	ind	+	+	−	−		−		Some aberrant IV
L1R	Myristylated protein	Membrane	ind	+	+	−	−		−		Unstable IV, IVN
H3L	Heparin binding	Membrane	ind, ko	+	+	−	−		−		Some MV, defective, viroplasm

(*continues*)

TABLE II (*continued*)

Gene	Identity	Location	Phenotype*								Notes on phenotype
			Mutants	Cres	IV	MV	EV	Telo	Cleave	DNA	
E10R	Thiol oxidoreductase	Membrane	ind	+	+	−	−		−		
G4L	Thiol oxidoreductase	Membrane	ind	+	+	−	−		−		
A2.5L	Thiol oxidoreductase	Virion	ind	+	+	−	−				
H4L	rap94	Core	ind, ts	+	+	+					Noninfectious MV, transcription enzymes missing
I8R	RNA helicase	Core	ts	+	+	+			+		Transcription defective MV
H6R	Topoisomerase	Core	ko	+	+	+		+			MV show reduced infectivity, reduced early txn
L4R	VP8	Core	ind	+	+	+	+	+	+		Noninfectious, unstable, transcription defective MV
H1L	Phosphatase	Core	ind	+	+	+					Noninfectious, transcription defective MV
E8R		Core	ts	+	+	+	+				Noninfectious, transcription defective MV
L3L		Core	ind	+	+	+	+		+	+	Noninfectious, transcription defective MV
L5R		Membrane	ind	+	+	+	+				Noninfectious MV, fusion/entry defective

A21L		Membrane	ind	+	+	+	+		+	Noninfectious MV, fusion/entry defective
A28L		Membrane	ind, ts	+	+	+		+		Noninfectious MV, fusion/entry defective
H2R		Membrane	ind	+	+	+	+			Noninfectious MV, fusion/entry defective
A16L		Membrane	ind	+	+	+	+			Noninfectious MV, fusion/entry defective
G3L		Membrane	ts	+	+	+	+			Noninfectious MV
I2L		Membrane	ind	+	+	+			+	Noninfectious MV, fusion/entry defective
D8L		Membrane	ko	+	+	+				Reduced infectivity MV, cell binding
A27L	A17-A14-A27 complex	Membrane	ind, ko	+	+	+	-			Infectious MV, defective in EV formation
A26L	p4c	Membrane	ko	+	+	+	+			Infectious MV; empty ATI
A14.5L		Membrane	ko	+	+	+				Infectious MV, attenuated in animals
E11L		Core	ts	+	+	+				
A45R	Inactive SOD	Core	ko	+	+	+	+			Nonessential
K4L	Nicking/joining enzyme	Core	ko	+	+	+	+			Nonessential

[*] Mutant designations: ind, inducible; ts, temperature sensitive; ko, knockout; Cres, crescents; Telo, telomere resolution; Cleave, virion protein proteolyzed; DNA, purified particles contain DNA; +, normal structure formed; −, normal structure not formed; blank, not reported.

V. Formation of Factories

Early studies by Cairns (1960) demonstrated that the number of factories observed early during vaccinia infection was proportional to the multiplicity of infection and concluded that each factory observed arose from a single infecting particle. Factories represent sites of viral DNA replication: factories become labeled with DNA precursors as assessed by EM autoradiography, factory formation is absent or severely restricted following infection with mutants defective in DNA replication, and infection with mutants that are DNA replication competent but defective in late viral protein synthesis results in formation of large factories that are lacking in crescents or any other evidence of virus morphogenesis (Cairns, 1960; Hooda-Dhingra *et al.*, 1989).[4], Most reports described early factories as unbounded in the cytoplasm (Fig. 5A) (Dales and Kajioka, 1964); however, recent reports suggest that at early times, before the appearance of any specific viral structures, factories are transiently surrounded by cellular ER-derived membrane cisternae (Fig. 5B) (Doglio *et al.*, 2002; Tolonen *et al.*, 2001; Traktman, unpublished).

VI. Crescent Formation

A. One Membrane or More?

The earliest detailed descriptions of the substructure of vaccinia viral crescents concluded that they consisted of a single lipid bilayer coated on its outer surface with a layer of spicules, which conferred the rigid arched shape to the crescents. Furthermore, these studies concluded that the lipid bilayer of the crescent formed within factories without any direct connection to other existing cellular membranes (Fig. 8, Model 1) (Dales and Mosbach, 1968). This *de novo* formation model, although unique in biology, nevertheless stood as the accepted model until it was challenged in 1993 by Griffiths and coworkers (Sodeik *et al.*, 1993). Central to this challenge was the commonly held

[4] A significant body of literature has made use of inhibitors of DNA replication to study morphogenesis. For example, hydroxyurea has been used to segregate early and late stages of morphogenesis (Morgan, 1976a; Pogo and Dales, 1971). It is now clear that in the absence of DNA replication, factory formation and therefore morphogenesis is inhibited. It seems probable that in reports where factory formation and some morphogenesis were observed in the presence of DNA replication inhibitors, the inhibitors were used under conditions that were not completely inhibitory, and thus some DNA replication and late viral protein synthesis occurred. These studies should be interpreted with this caveat in mind.

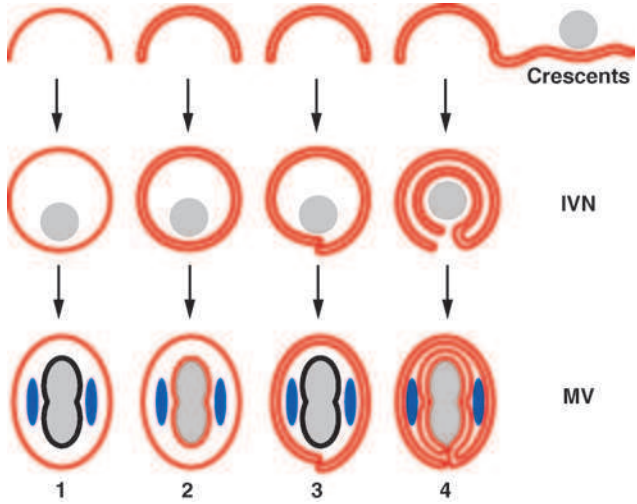

FIG 8. Models for membrane processing during vaccinia morphogenesis. In each case, a single solid red line represents a single lipid bilayer. DNA/nucleoid material is represented in gray; lateral bodies are represented in blue. Four models are shown in four columns. Each row represents and compares a discrete state of morphogenesis, with the top row representing crescents, the middle row representing immature virions with nucleoids (IVN) and the bottom row representing mature virions (MV). Model 1: Crescents and IVN contain a single lipid bilayer, which becomes a single lipid bilayer of the structure surrounding MV (Dales and Mosbach, 1968; Hollinshead *et al.*, 1999). In this case the core wall does not contain lipid and is therefore represented in black. Model 2: Crescents are derived from cisternae and comprise two tightly apposed lipid bilayers. The ends of cisternae fuse or are sealed to form IVN containing two tightly apposed bilayers. During MV formation from IVN, the inner bilayer separates from the outer bilayer so that the inner bilayer becomes a component of the core wall while the outer bilayer remains as a component of the MV membrane (Sodeik *et al.*, 1993). Model 3: Crescent and IVN formation is similar to Model 2; however, the cisternae do not fuse but are "sealed." During morphogenesis to MV the two bilayers do not separate, and thus the MV membrane contains two tightly apposed bilayers (Roos *et al.*, 1996). As in Model 1, the core wall does not contain lipid and is therefore represented in black. Model 4: Crescents are derived from cisternae as in Models 2 and 3; emphasis is placed on the continuity of the rigid crescent domain of this cisternae with extensive flaccid cisternal domains. DNA in a prenucleoid structure is associated with the flaccid cisternal domain. IVN is formed by the infolding of the flaccid domain within the rigid crescent domain. The cisterna of IVN are sealed so that the resulting MV contains four lipid bilayers, two forming the virion envelope and two forming the core wall (Griffiths *et al.*, 2001a; Sodeik and Krijnse-Locker, 2002).

view that all cellular membranes are derived from preexisting organelles (Palade, 1983). Sodeik *et al.* (1993) proposed that crescents in fact were derived from preexisting cisternae of the cellular secretory machinery, which had collapsed on themselves through the action of

virus proteins. Crescents formed in this manner would consist of two tightly apposed bilayers rather than a single bilayer (Fig. 8, Model 2). (Crescents would therefore be analogous to the membranes involved in the development of spherical autophagosomes, which are delimited by a double bilayer [Reggiori and Klionsky, 2005].) Investigations into the consequences of this cisternae-based model for crescent formation ultimately resulted in three different new models for IV and MV formation, shown in Fig. 8, Models 2–4. In the balance of this section, we describe and evaluate these models.

Model 1. Single membrane bilayer (Dales and Mosbach, 1968). As described previously, this model states that crescents arise *de novo*, that is, without apparent continuity with other preexisting membrane organelles, and that crescents contain a single lipid bilayer coated on its outer surface with a layer of spicules. During morphogenesis from IVN to MV, the spicules are lost, the surface undergoes some additional modifications, and the contents of IVN are reorganized to yield the core and lateral bodies (Essani *et al*., 1982; Stern and Dales, 1976). In this model, the core is not surrounded by a lipid membrane (Wilton *et al*., 1995). The primary objections to this model are that it seems to violate a principle which dictates that all membranes in the cell are derived from preexisting organelles and that at the edges of a crescent, the hydrophobic core of the bilayer is left exposed to the cytoplasm, a theoretically unstable condition. The model is supported by the fact that it is consistent with some existing microscopic data and that it yields a single membraned MV that can enter cells by a simple fusion event at the plasma membrane.

Model 2. Double membrane bilayer; membrane bound core (Sodeik *et al*., 1993). As described previously, this model states that crescents actually contain two tightly apposed lipid bilayers, formed by collapse of preexisting cellular membrane cisternae, modified by virus proteins. The model states further that during morphogenesis from IVN to MV, the two membranes separate and the innermost membrane collapses around the core, so that both the MV surface and the core are each now bounded by a single lipid bilayer. The primary theoretical objections to this model are that it introduces a problem of how the material making up the lateral bodies is transported across the innermost membrane during morphogenesis from IV to MV and that it would result in delivery of a membrane-bound core to the cytoplasm if MV were to enter cells by a simple fusion event at the plasma membrane. The model is supported by numerous electron micrographs which seem to show continuity between crescents and cisternae (Ericsson *et al*., 1997; Sodeik *et al*., 1993, 1994), and by electron microscopic images of MV

which seem to show a membrane surrounding the core (Cyrklaff *et al*., 2005; Sodeik *et al*., 1993).

Model 3. Double membrane bilayer; naked core (Roos *et al*., 1996). This model also proposes that crescents are composed of two tightly apposed lipid bilayers; however, it differs from Model 2 with respect to the fate of the innermost bilayer during the morphogenesis from IV to MV. Specifically, Model 3 states that the two bilayers do not separate during MV morphogenesis, so that the resulting MV contains two tightly apposed bilayers on its surface, and the core is not bound by a membrane. The model also states that the membranes surrounding the particle are not fused but rather joined in an overlap by a proteinaceous plug. Relative to Model 2, this model resolves the theoretical problem of transport of material across the innermost membrane during formation of lateral bodies but complicates further the problem of virus entry; in this case, a simple fusion event between the virion and the plasma membrane would leave the entire contents of the particle outside of the cell. In support of this model are the same micrographs that seem to show continuity between crescents and cisternae (Ericsson *et al*., 1997; Sodeik *et al*., 1993, 1994), coupled with experiments that indicate that core surface antigens are exposed when MV are disrupted with a reducing agent (Roos *et al*., 1996).

Model 4. Folded cisternae (Griffiths *et al*., 2001a; Rodriguez *et al*., 2006). In this model collapsed cisternae evolve distinct virus-specific domains, including a rigid crescent domain that is continuous with a DNA binding domain. IV and MV are formed by folding of these domains upon themselves, resulting in a particle which now contains, in effect, four lipid bilayers, two on the surface of MV and two surrounding the core. Like Model 3, Model 4 proposes that the membranes are not fused but rather joined in an overlap by a proteinaceous plug. Like Model 3, this model resolves the theoretical problem of transport of material across the innermost membrane during formation of lateral bodies, but leaves the same problem of virus entry described previously for Model 3. The model is supported by electron micrographs which seem to show the continuity of the cisternal domains, and by electron micrographs of isolated MV which are interpreted to reveal a complexity consistent with the model (Griffiths *et al*., 2001a,b).

The distinction among these four models is embodied by four questions relating to crescent, IV and MV structure and assembly: (1) Do the crescents contain two membranes? (2) Are the crescents continuous with cisternae, and is this continuity theoretically necessary? (3) Are nucleoids or cores bounded by membranes? (4) How does the virus enter cells? Each of these questions is addressed separately below.

1. Do Crescents Contain Two Membranes?

The structure of viral crescents has been investigated by various methods of electron microscopy, with conflicting interpretations of the results. The overall thickness of crescents including the inner smooth later and the outer "spicule" layer is 10–15 nm, at least enough to accommodate two tightly apposed bilayers. Occasional micrographs show that these layers are physically distinct in that they sometimes appear separated (Dales and Mosbach, 1968; Essani *et al.*, 1982; Hollinshead *et al.*, 1999; Sodeik *et al.*, 1993). Some investigators interpret the outermost layer to be devoid of lipid membrane and conclude that crescents contain only one membrane corresponding to the innermost layer (Dales and Mosbach, 1968; Essani *et al.*, 1982; Hollinshead *et al.*, 1999). Other investigators conclude that both layers represent lipid bilayers and that the spicules can obscure the outermost lipid bilayer in conventional electron micrographs (Risco *et al.*, 2002; Sodeik *et al.*, 1993). Freeze fracture of multiply membraned organelles often clearly reveals the individual membranes as steps in the fracture pattern. While one freeze fracture study of vaccinia IVs suggests a double membraned particle (Risco *et al.*, 2002), most freeze fracture studies fail to reveal evidence of more than one membrane in IV (Heuser, 2005).

Electron microscopy of IVs formed after reversal of a rifampicin block provides unique insight into the formation of crescents. As detailed in Section VI.E, it is now clearly established that the major component of the spicule layer is a lattice of the D13 protein. In the presence of the antibiotic rifampicin, the association of D13 protein with viral membranes is prevented, so that flaccid viral membranes accumulate at the periphery of virosomes while D13 protein accumulates within viroplasmic inclusions distant from the membranes. While some investigators describe only single lipid bilayers accumulating in the presence of rifampicin (Grimley *et al.*, 1970), others describe both single membranes and cisternae (Sodeik *et al.*, 1994), or "dense membranes (around 18 nm thick), twisted double membranes with vesicular ends, and tubular elements (30 nm thick), some of them with vesicles at one end" (Risco *et al.*, 2002). Removal of rifampicin results in formation of rigid crescents within minutes, presumably via association of accumulated D13 with viral membranes. Under conditions of rifampicin reversal, multiple crescents can form on one continuous membrane, providing a direct comparison of crescents with spicule-free viral membranes. Under these circumstances, clear images have been obtained which suggest that the crescent membrane is a single lipid bilayer and that the spicule layer is attached in patches along this unit membrane (Fig. 9) (Grimley *et al.*, 1970).

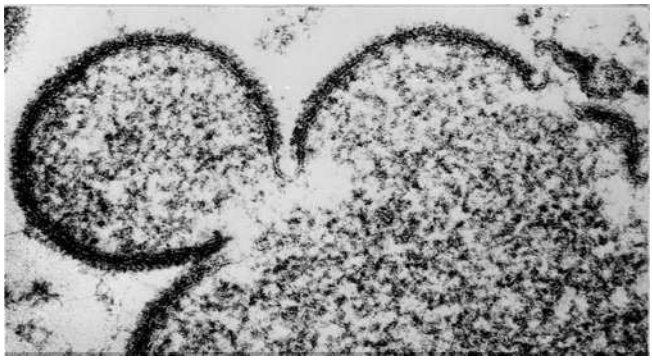

FIG 9. Evidence that crescents contain a single lipid bilayer. Electron micrograph of an infected cell 10 min following reversal of a rifampicin block (Grimley *et al*., 1970). Two crescents are connected by a continuous membrane, which has the dimensions and appearance of a single lipid bilayer. Reprinted from Grimley *et al*. (1970) with permission.

In summary, while electron micrographs are subject to different interpretations, the bulk of the evidence, in particular from freeze fracture microscopy and rifampicin reversal, favors the model that crescents contain a single lipid bilayer formed beneath a scaffold composed predominantly of D13 protein.

2. Are the Crescents Continuous with Cisternae, and is this Continuity Theoretically Necessary?

Much has been made of the use of the term *de novo* to describe vaccinia viral membrane biogenesis. To some the appearance of membranes without continuity with other intracellular membranes is a heretical violation of biological principle, while to others it is simply another amusing example of the inventiveness of nature. Numerous electron micrographic studies have drawn conclusions on either side of this debate. On the one hand, for example, serial sections of crescents have been published which show no continuity between crescents and other membranes, and in the same study tilt series electron micrographs reveal that crescents which are in fact not continuous with cisternae, may appear to be in continuity when viewed at an appropriate angle, raising the possibility of artifact (Hollinshead *et al*., 1999). On the other hand, numerous, highly convincing electron micrographs exist which seem to show crescents in continuity with membranes or cisternae, or crescents with membranous extensions or loops at the ends (Ericsson *et al*., 1997; Griffiths *et al*., 2001a; Risco *et al*., 2002; Sodeik *et al*., 1993, 1994). In fact, the *de novo* argument may be irrelevant. Based on evidence cited in Section VI.B, a reasonable model for viral

membrane biogenesis is that lipid is delivered to factories from the ER as vesicles complexed with viral protein and that crescents may form and grow via addition of lipid and viral protein from these vesicles. Assuming the vesicles are relatively small and short lived, any number of structures may be visible in viral factories, including vesicles, tubules, crescents with no apparent continuity with other membranes, or crescents with long, short, or looped extensions at their ends. Furthermore, all these structures may be subject to variation in sample preparation and interpretation. Formation of a crescent, which contains a double bilayer, would be the obvious outcome of vesicle fusion. However, if crescents contain a single bilayer, then some mechanism must exist for building a single bilayer from a vesicle, tubule, or cisterna, and some "capping" mechanism must exist to sequester the hydrophobic core of the single membrane bilayer from the aqueous environment of the cytoplasm. Heuser (2005) suggests one possible mechanism for formation of a single bilayer from virtually any other membrane, based on a current "T junction" model for lipid droplet formation (Fig. 10). Capping of the crescent ends might be accomplished by a novel, yet to be discovered viral gene product. Alternatively, the lateral edges of the crescent membrane may contain phospholipids which assume a curved, micellar formation rather than a true lipid bilayer, such that only polar head groups are in contact with the cytoplasm.

In summary, it is possible that growing crescents may appear either continuous or discontinuous with other membranes; however, the presence of absence of such continuities does not necessarily dictate whether the crescent and IV membrane is a single bilayer or two tightly apposed bilayers.

3. Are Nucleoids or Cores Bounded by Membranes?

As described previously, two of the double membrane models require that the core be surrounded by at least one membrane; therefore, the question of whether or not the core is bounded by a membrane is relevant to distinguish between one and two membrane models for crescent and IV assembly. In common with other aspects of the debate, much of this discussion rests on electron microscopic data, which is subject to varied interpretation. For example, in cryo-electron micrographs, the inner layer of the core wall appears electron lucent or "white," consistent with a lipid bilayer (Fig. 2A). While some authors interpret this layer as lipid (Cyrklaff *et al.*, 2005; Sodeik *et al.*, 1993), others conclude that its dimensions are inconsistent with a lipid bilayer (Hollinshead *et al.*, 1999). Similarly, while some images are interpreted to reveal a complex folding of membranes in developing

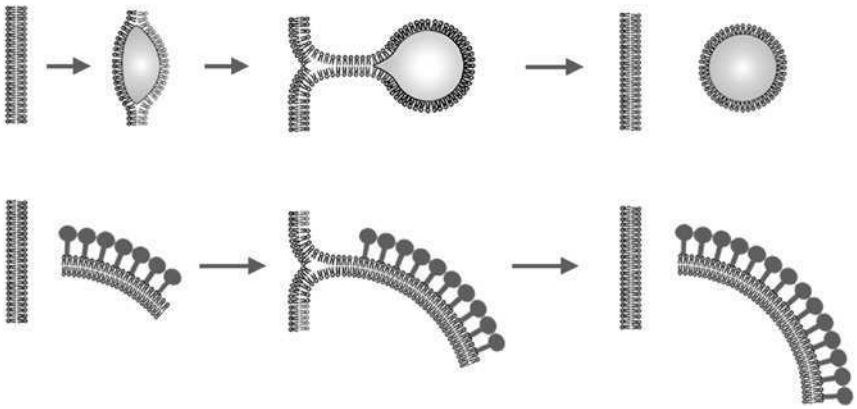

FIG 10. Model for poxvirus membrane growth. (Top) Model for lipid droplet formation from ER. (Bottom) Model for vaccinia crescent formation based on the lipid droplet formation model (Heuser, 2005). A crescent membrane, represented by a bilayer studded with lollipops, is extruded in a T junction from another bilayer, which could be part of any membrane structure. The lollipops represent a viral protein that directs the process. Reprinted from Heuser (2005) with permission.

or mature particles consistent with the folded cisternae model (Model 4) (Griffiths *et al*., 2001a,b; Sodeik *et al*., 1993), numerous other images show no evidence of membrane boundaries within IV, IVN, or MV and no surface folds or continuity between internal and external boundaries in MV (Dales and Mosbach, 1968; Dales and Siminovitch, 1961; Essani *et al*., 1982; Heuser, 2005; Hollinshead *et al*., 1999; Mohandas and Dales, 1995; Morgan, 1976a,b; Risco *et al*., 2002). Perhaps the most compelling data relevant to the lipid content of cores consists of examination of isolated cores. As described previously, cores are typically isolated by dissociating the MV membrane with a neutral detergent (NP40) and DTT. This treatment completely dissolves the MV membrane and should therefore extract any lipid from the cores, and yet the structure of the isolated core remains essentially the same as the core found in intact MV (Dubochet *et al*., 1994; Easterbrook, 1966; Ichihashi *et al*., 1984; Wilton *et al*., 1995). Isolated cores lose the concavities present in mature MV and assume a more regular barrel shape but nevertheless maintain a bilaminar structure with an inner, smooth layer and an outer palisade layer, virtually identical to the core present in mature MV. If the core were to be encased in one or two lipid bilayers, then this lipid would have to be resistant to detergent extraction sufficient to dissolve the membrane, or the lipid would have to contribute very little to the structure of the core, so that its absence

would not affect the gross structure of the core. Both of these latter possibilities seem unlikely.

In summary, the weight of the evidence seems to favor the conclusion that the core is not bounded by a lipid bilayer.

4. How Does the Virus Enter Cells?

As noted previously, any of the two membrane models present problems for entry of virus into cells. If Model 2 were correct, a simple fusion of the outermost viral membrane with the plasma membrane would deliver a membraned subparticle to the cell cytoplasm, which would then require further uncoating. If Model 3 or 4 were correct, then fusion of the outermost lipid bilayer of MV with the plasma membrane would leave the entire contents of the particle outside of the cell. While novel models for entry of a multiply membraned particle have been proposed, backed by some electron microscopy (Griffiths *et al*., 2001a; Locker *et al*., 2000; Pedersen *et al*., 2000), the best evidence to date shows that MV enters cells by a simple fusion event between the virus membrane and the plasma membrane, releasing the core and lateral bodies into the cell cytoplasm (Carter *et al*., 2005). Therefore, the mechanism of entry of the virus particle favors the single membrane model (Model 1) for vaccinia crescent, IV, and MV formation.

In summary, while no single experiment necessarily provides an incontrovertible distinction among the models proposed for the membrane structure of maturing and mature vaccinia virus, taken together the data strongly favor the original one membrane model. This leaves open several interesting issues to be resolved, foremost being the mechanism by which a single bilayer may be fabricated and stabilized using virus-modified cellular precursors in the viroplasm. For the balance of this review, we will use the single membrane model in discussing vaccinia structure and assembly.

B. Source of the Virion Membrane

Few topics in vaccinia morphogenesis have been as controversial as the source of the virion membrane (Sodeik and Krijnse-Locker, 2002). As described previously, *de novo* biogenesis was initially favored, first because no ultrastructural continuity with intracellular membranes could be observed and second, because the lipid content of the virion membrane was distinct from known cellular membranes (Dales and Mosbach, 1968). However, no plausible mechanism for the *de novo* assembly of a membrane within the cytosol has been proposed. The second model for membrane biogenesis was diversion of membranes

from a component of the secretory apparatus. Although none of the membrane proteins within MV were glycosylated, it was assumed that they were synthesized in the ER. This assumption followed first from the findings that several of the major membrane proteins (A14, A17) (Section VI.D) could be cotranslationally inserted into microsomal membranes *in vitro*, and second from ultrastructural observations. Indeed, the ultrastructural observations initially seemed to support a colocalization of the A17 and A14 proteins with the cellular Rab1 protein, which was thought to be a specific marker of the ER/Golgi intermediate compartment (ERGIC) (Sodeik *et al*., 1993). Thus, derivation of the virion membrane from the ERGIC was assumed for a number of years. However, experiments involving pharmacological inhibitors (brefeldin A, nordihydroguiaretic acid) or dominant negative variants of cellular proteins (Sar1p) have argued against the role of either the COPI or COPII trafficking pathways in MV biogenesis (Husain and Moss, 2003; Ulaeto *et al*., 1995; Traktman, unpublished). These two vesicular trafficking pathways are the crux of the ERGIC system. Consequently, it seems more likely that a specialized compartment of the ER is the initial source of the virion membrane. Consistent with this idea, H89, a known inhibitor of ER exit site formation, and cerulenin, an inhibitor of *de novo* lipid biosynthesis, have been shown to block the recovery of virion morphogenesis in cultures released from an early morphogenesis block (Punjabi and Traktman, 2005).

If the MV membrane were composed of two lipid bilayers, it would be relatively straightforward to envision how vesicular elements could fuse to form growing crescents and remain stable in the cytoplasm. However, diversion of a single lipid bilayer from the ER in order to form nascent crescents, stabilization of the exposed fatty acid chains in these crescents within the cytoplasm, and enlargement of these crescents to form the IV membrane, remains a conundrum. Lipid synthesis is normally centered in the smooth endoplasmic reticulum, and in recent studies delivery of lipids to existing organelles have been focused on the subcellular compartments, plasma membrane associated membranes (PAM), and mitochondrial associated membranes (MAM) (Gaigg *et al*., 1995; Pichler *et al*., 2001). Gaining an understanding of how the virus accomplishes membrane biogenesis will be a fascinating challenge.

C. Regulatory Proteins in Viral Membrane Formation

The mechanism by which crescents form remains largely unknown. However, cumulative genetic data implicate four viral proteins in

regulating the earliest steps of this process. These are encoded by the *F10L*, *H5R*, *G5R*, and *A11R* genes.

1. F10

The F10 protein was first identified as the major protein kinase encapsidated in the virion core (VPK2) (Lin and Broyles, 1994). Recombinant F10 has enzymatic activity *in vitro*, indicating that the protein possesses intrinsic kinase activity and does not need additional protein cofactors (Lin and Broyles, 1994; Traktman *et al*., 1995; Wang and Shuman, 1995). The predicted amino acid sequence of F10 retains some of the conserved sequence motifs associated with ATP binding or phosphotransfer, but other motifs cannot be recognized due to the divergence of the F10 sequence from that of the majority of protein kinases. F10 has been shown to direct phosphorylation of serine, threonine and tyrosine residues, indicating that it is a dual specificity kinase (DSP) (Derrien *et al*., 1999). The 50-kDa protein is expressed late during infection and undergoes autophosphorylation but does not appear to be proteolytically processed despite having the canonical AG↓X motif associated with the virally encoded proteolytic processing machinery (Section IX.C) (Punjabi and Traktman, 2005). F10 is known to be part of a seven-protein complex implicated in the filling of growing crescents with viroplasmic proteins (Section VII.A), but it has also been shown to be tightly associated with membranes during infection and to bind to some lipid species (phosphoinositide phosphates) *in vitro* (Punjabi and Traktman, 2005; Szajner *et al*., 2004a). F10 is itself encapsidated in nascent virions, with an average abundance of ~300 copies/core.

The importance of F10 during infection was foreshadowed by the inability of investigators to generate a viable virus in which the *F10L* gene had been deleted. Subsequent studies identified four temperature-sensitive mutants as encoding mutant alleles of *F10L*; cells infected with these viruses show a profound defect in virion morphogenesis at the nonpermissive temperature (Traktman *et al*., 1995; Wang and Shuman, 1995). This phenotype has been recapitulated by engineering viruses in which F10 expression is dependent on inclusion of IPTG or tetracycline in the culture medium (Punjabi and Traktman, 2005; Szajner *et al*., 2004b). The latter studies also confirmed that expression of a catalytically active F10 protein is essential for virus morphogenesis. The first arrest observed on inactivation of F10 occurs prior to the formation of any signs of membrane biogenesis. Although the late viral proteins accumulate normally and factories are formed, virosomes are either absent or malformed, and no crescents,

IV, IVN, or MV are observed (Fig. 11A). Under these circumstances, there is also no phosphorylation of the major membrane proteins A14 or A17 (Section VI.D). When cells infected with tsF10 mutants under nonpermissive conditions were shifted to the permissive temperature at 12 hour postinfection (hpi), membrane biogenesis resumed, and crescents were observed within 45 min. Execution point studies have shown that the F10 kinase is also required for later steps in morphogenesis; under certain experimental protocols, tsF10-infected cells show a defect in crescent filling that it is nearly indistinguishable from that observed when other proteins found within the seven-protein complex are repressed or inactivated (Section VII.A). Identification of viral and cellular proteins whose phosphorylation by F10 is important in morphogenesis is an area of intense interest. Although the phosphorylation of a number of viral proteins either fails to occur during nonpermissive infections with tsF10 mutants (e.g., A14, A17, A30, G7) or is diminished (H5, F17), the phosphorylation of at least some of these proteins has been shown to be blocked when morphogenesis is arrested by other means. Thus, it is not clear which phosphorylation events are directly mediated by F10, and which may be mediated by other viral or cellular kinases in the context of productive morphogenesis. Phosphorylation of at least H5 and A30 has been verified *in vitro*.

In summary, studies with mutants in *F10L* suggest that virus-mediated phosphorylation plays a critical role throughout MV assembly, starting from the very earliest events in virus membrane formation. It is important to reiterate that there is no evidence of membrane diversion or remodeling when F10 is repressed or inactivated.

2. H5

The H5 protein has a predicted MW of 22 kDa but has an electrophoretic mobility consistent with a MW of 35 kDa, due to a proline-rich domain within the N-terminus (Gordon *et al*., 1991). The protein is expressed constitutively and is encapsidated at ~2500 copies/core (Traktman, unpublished). Some of the early literature on the H5 protein is misleading because an antiserum purported to show specificity for H5 was in fact quite reactive against the comigrating H3 protein. The bona fide role of H5 during the viral life cycle has been confusing because genetic and biochemical studies have implicated H5 in several processes. The protein has an amphipathic helix and is phosphorylated *in vivo*; H5 can be phosphorylated by both vaccinia-encoded kinases (B1 and F10) as well as by cellular kinases (Beaud and Beaud, 2000; Beaud *et al*., 1995; Brown *et al*., 2000; Traktman, unpublished).

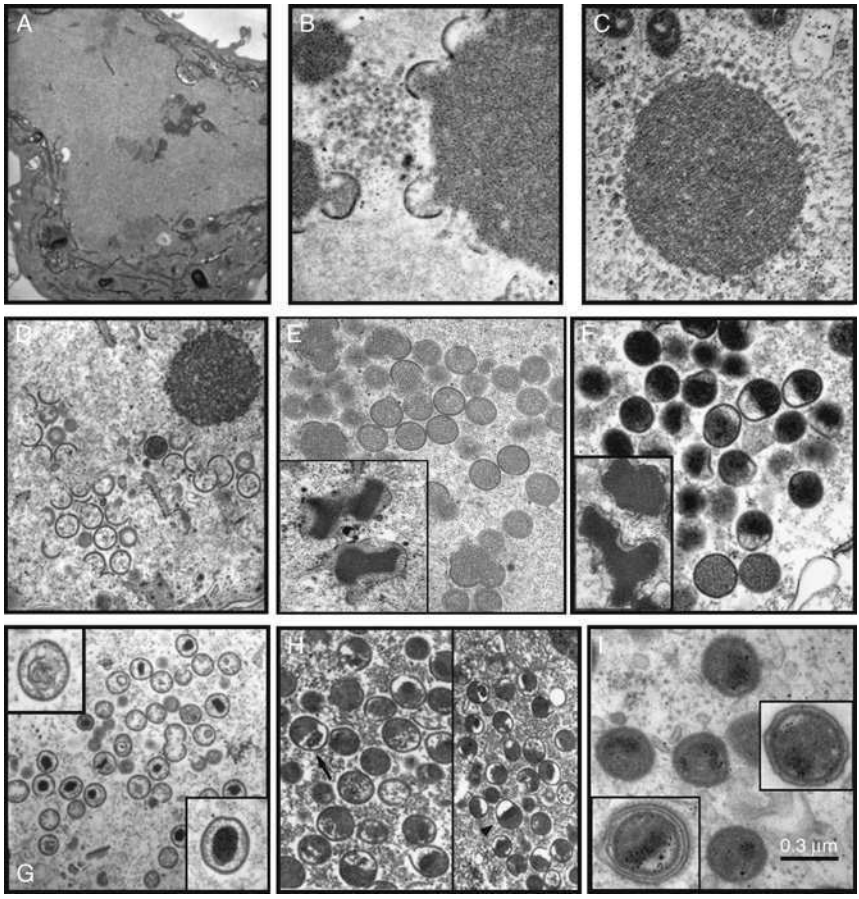

FIG 11. Representative morphogenesis arrests seen during nonpermissive infections with mutants affected in genes involved in MV formation. (A–C) Mutants affecting membrane formation. (D–F) Mutants affecting IV formation and encapsidation. (G–I) Mutants affecting core formation. (A) Formation of factories, but no virosomes and no evidence of morphogenesis: tsF10 mutant (Traktman *et al*., 1995); (B) accumulation of virosomes, membrane vesicles, and a few aberrant crescents: inducible A14 mutant (Traktman *et al*., 2000); (C) formation of virosomes and accumulation of membrane vesicles: inducible A17 mutant (Punjabi, Mercer, and Traktman, unpublished); (D) accumulation of empty IV and virosomes: tsG7 mutant (2nd arrest) (Mercer and Traktman, 2005); (E) formation of IV and DNA crystalloids due to arrest prior to genome encapsidation: inducible A13 mutant (Unger and Traktman, 2004); (F) accumulation of IV, DNA crystalloids and aberrant MV due to lack of genome encapsidation: tsI6 mutant (Grubisha and Traktman, 2003); (G) accumulation of aberrant IV due to absence of nucleoid and/or core formation: inducible F17 mutant (Mercer and Traktman, unpublished); (H) accumulation of IV and aberrant particles due to lack of core formation; tsI7

An interaction between H5 and A20, a stoichiometric component of the processive DNA polymerase, has been found by yeast two hybrid analysis, thus implicating H5 in DNA replication (Ishii and Moss, 2002; McCraith *et al*., 2000). Consistent with this finding, one of the temperature-sensitive mutants from the Dales collection, which has been the subject of recent systematic analysis, has been shown to have a lesion within the *H5* gene, and preliminary analysis of this mutant reveals a defect in DNA replication (D'Costa, Prins, and Condit, unpublished; Lackner *et al*., 2003). Two lines of evidence also implicate H5 in the process of viral transcription: H5 stimulates late gene transcription *in vitro*, and H5 has been shown to interact with proteins which regulate late gene transcription (G2, G8, A2) (Black *et al*., 1998; Dellis *et al*., 2004; Kovacs and Moss, 1996). However, a different temperature-sensitive mutant, generated by targeted alanine-scanning mutagenesis of the *H5R* gene, implicates H5 in virus assembly. This mutant, which has a dominant phenotype, is unimpaired in its ability to direct viral gene expression but shows a profound defect in virion morphogenesis (DeMasi and Traktman, 2000). The phenotype is quite similar to that seen in tsF10 mutants: virosomes are either absent or malformed, and no signs of membrane biogenesis are seen. Whether H5 plays a direct role in morphogenesis, or whether the mutant H5 protein somehow sequesters F10 and hence arrests morphogenesis, is not known. Because H5 is so abundant, it is also possible that it serves as a scaffold for transcription, replication, and virion assembly, thus accounting for the apparent diversity of roles for the H5 protein during infection.

3. G5

The 50-kDa G5 protein is expressed at early times postinfection and is encapsidated in the virion core, although the abundance of the protein within virions has not been reported (da Fonseca *et al*., 2004). The essentiality of the *G5R* gene is suggested by its conservation

mutant (Kane and Shuman, 1993); (I) accumulation of aberrant MV due to defect in core wall formation: tsA3 mutant (insets are wrapped aberrant MV [lower left] and extracellular aberrant MV [mid right]) (Kato *et al*., 2004). (A) Reprinted from Traktman *et al*. (1995) with permission. (B) Reprinted from Traktman *et al*. (2000) with permission. (D) Reprinted from Mercer and Traktman (2005) with permission. (E) Reprinted from Unger and Traktman (2004) with permission. (F) Reprinted from Grubisha and Traktman (2003) with permission. (H) Reprinted from Kane and Shuman (1993) with permission. (I) Reprinted from Kato *et al*. (2004) with permission.

within most if not all poxviral genomes; attempts to isolate a virus deleted for the *G5R* ORF have been unsuccessful. Temperature-sensitive mutants carrying *G5R* lesions were isolated by targeted alanine scanning mutagenesis, and phenotypic analysis of two such mutants revealed a role for *G5R* in the earliest stages of virion morphogenesis (da Fonseca *et al*., 2004). As was seen in tsF10 and tsH5 infections, factories were formed during tsG5 infections; however, electron-dense virosomes were either absent or malformed, and, most importantly, no signs of membrane biogenesis were seen.

4. A11

The 40-kDa A11 protein is expressed at late times postinfection and is phosphorylated in an F10-independent manner (Resch *et al*., 2005). An inducible recombinant in which A11 expression is dependent on inclusion of IPTG in the culture medium has been generated; repression of *A11R* transcription has a profound impact on virus production and leads to an early arrest in virion morphogenesis. This is a striking observation, since A11 itself does not appear to be encapsidated and is therefore the first nonstructural protein to be identified as playing an essential role in the biogenesis of the virion membrane. In the absence of A11, factories were formed; however, no crescents, IV, IVN, or MV were seen. Electron-dense virosomes were observed, as were unusual areas of intermediate electron-density that were associated with membranous structures containing markers of the endoplasmic reticulum. These areas of intermediate density also contained the D13 crescent scaffold protein (Section VI.E).

D. Membrane Proteins Essential for Membrane Biogenesis: A14 and A17

The proteins encoded by the *A14L* and *A17L* genes are abundant components of the MV membrane, and both are essential for its biogenesis.

1. A17

The 203-aa A17 protein is expressed at late times of infection. The protein has been shown to undergo cotranslational insertion into microsomal membranes *in vitro* and to associate with ER membranes *in vivo* (Krijnse-Locker *et al*., 1996). In the context of its association with microsomal membranes, A17 spans the membrane twice, with

the N- and C-termini extending into the solution and an internal hydrophilic loop extending into the lumenal space (Fig. 12) (Betakova *et al*., 1999a). An intramolecular disulfide bond is formed within this central loop (Betakova and Moss, 2000). A fraction of A17 proteins appear to form intermolecular disulfide bonds through a Cys residue found in the cytosolic C-terminal tail.

The N- and C-termini of A17 are modified by proteolytic cleavage events, which occur at AG16↓A and AG185↓A motifs (Section IX.C) (Fig. 13). These cleavages occur earlier than those associated with maturation of the major core proteins and do not depend on the IV to MV transition, since they occur in rifampicin-arrested cultures in which morphogenesis is blocked prior to IV formation (Section VI.E). However, during the normal morphogenetic pathway, immunoEM analysis suggests that loss of the C-terminal tail, at least, occurs largely after IV are formed. The N-terminal hydrophilic tail of the mature form of A17 (aa 17–60) is accessible to antibodies and to protease in intact MV, confirming the surface localization of the protein; the hydrophilic tail at the C-terminus is only predicted to be 23 aa long after proteolytic cleavage, which may limit its accessibility to these reagents (Betakova *et al*., 1999b; Wallengren *et al*., 2001).

A17 also undergoes phosphorylation on Ser, Thr, and Tyr residues in an F10-dependent manner (Betakova *et al*., 1999b; Derrien *et al*., 1999). Phosphorylation of A17 fails to occur if morphogenesis is arrested prior to normal crescent formation. Tyr phosphorylation has been shown to occur on Tyr203, the terminal amino acid in the protein; conflicting results obtained with different pTyr antibodies has obscured the question of whether other Tyr residues also undergo modification. The Ser/Thr phosphorylation appears to occur solely in the C-terminal hydrophilic tail of the protein that is removed during morphogenesis.

Inducible recombinants in which A17 expression is dependent on inclusion of IPTG in the culture medium have been generated; A17 is essential for virion production (Rodriguez *et al*., 1995, 1996; Wolffe *et al*., 1996). In the absence of A17, vast numbers of membrane vesicles accumulate at the periphery of electron dense virosomes (Fig. 11C). Thus, A17 does not appear to be essential for the F10-dependent process of membrane diversion but is essential for crescent formation. The A17 protein has been shown by coimmunoprecipitation analysis to interact with the A14 protein during productive membrane biogenesis (Betakova *et al*., 1999b; Mercer and Traktman, 2003; Rodriguez *et al*., 1997); this interaction is mediated by the N-terminus of A17 (Unger, Mercer, and Traktman, submitted for publication).

External
Internal
A14
A17
A13
A9
L1
H3
D8
a.a.
90
203
70
108
250
324
308
External
Internal
G3
A21
L5
J5
A28
H2
G9
A16
I2
A14.5
I5
a.a.
111
117
128
133
146
169
309
378
78
53
79

2. A14

The 90-aa A14 protein, which interacts with the A17 protein, is another major component of the MV membrane. A14 undergoes cotranslational insertion into microsomal membranes *in vitro* and has been shown to associate with ER membranes *in vivo* (Rodriguez *et al*., 1997; Salmons *et al*., 1997). The protein appears to span the membrane twice, assuming a topology in which the N- and C-terminal tails are lumenal and the central hydrophilic loop is exposed (Fig. 12). The C-terminal tail contains an N83HS motif, which is readily glycosylated *in vitro* but poorly glycosylated *in vivo* during wt infections (Mercer and Traktman, 2003). Moreover, none of the glycosylated A14 protein appears to be encapsidated, suggesting that interactions of A14 with other viral proteins, or further posttranslational modifications (see later) may prevent glycosylation of A14. Alternatively, the majority of A14 may be synthesized in, or rapidly diverted to, a membrane domain that does not support glycosylation. This latter hypothesis is supported by observations that the fraction of A14 that undergoes glycosylation is significantly higher when membrane biogenesis is prevented at an early stage by repression or inactivation of F10, H5, A17, or G7.

A14 undergoes F10-dependent phosphorylation on Ser85, which is also part of the glycosylation motif discussed previously (Mercer and Traktman, 2003). Disruption of the glycosylation motif increases the level of A14 phosphorylation, suggesting that the two posttranslational modification systems are competing for access to the protein. Finally, the vast majority of A14 dimerizes by forming intermolecular disulfide bonds through Cys71. A mutant allele of A14 in which Cys71 has been altered to Ser is viable, although viral yields are reduced approximately fivefold. Virions containing this altered A14

FIG 12. Schematic view of integral MV membrane proteins. The overall topology of known transmembrane proteins contained within the MV membrane is shown; external and internal refers to the orientation within MV. A14 and A17 are essential for biogenesis; A13, A9, and L1 are required for virion maturation; H3 stimulates virion maturation and, along with D8, binds to glycosaminoglycans on the surface of target cells; G3, A21, L5, J5, A28, H2, G9, and A16 comprise an eight-member fusion/entry complex; 12 is also required for virion entry; A14.5 affects virulence in mice, and the function of I5 has not been determined. The number of amino acid residues is shown beneath each protein. Sites of phosphorylation, P0 myristylation (chemical structure), proteolytic cleavage (dotted line), and disulfide bond formation (-S-) are shown. The symbol shown adjacent to the H2 and A16 proteins ✦ indicaes that, although these proteins are known to contain intramolecular disulfide bonds, the number and position of these linkages are not known.

protein are exquisitely sensitive to nonionic detergents. Under conditions in which wt virions remain intact and infectious, NP40 treatment of these A14-Cys71 virions leads to the extraction of both A14 and A17 and causes a 1000-fold decrease in specific infectivity. These findings support a model in which dimerized A14, interacting noncovalently with A17, forms a lattice within the MV membrane that sustains virion integrity, consistent with previous results from controlled degradation of MV described in Section III.C.

Recombinant viruses in which expression of A14 is dependent on inclusion of either IPTG or tetracycline in the culture medium have been generated; expression of A14 is essential for virion production (Rodriguez *et al*., 1998; Traktman *et al*., 2000). In the absence of A14, vast numbers of vesicles (and/or tubules) accumulate within the cytoplasm (Fig. 11B). Some aberrant crescents are seen which are adjacent to, but fail to make contact with, electron-dense virosomes that accumulate in factories. Importantly, the vesicles formed in the absence of A14 contain A17 and another membrane protein, D8, while the virosomes formed contain the core proteins L4 and F17 (Traktman *et al*., 2000). Thus, the A14 mutant phenotype is similar but not identical to that seen upon repression of A17. Most importantly, the presence of both of A14 and A17 is required to form bona fide crescents, which can progress to form the IV membrane. Whether the vesicles seen upon their repression represent stalled intermediates, or aberrant structures formed by the collapse of unstable membranes, has not been determined. This is a question of considerable relevance to a fuller appreciation of the mechanism of IV membrane biogenesis.

Transient complementation has been used to probe which features of the A14 protein are essential for membrane biogenesis. Sequences that flank the first transmembrane domain, and those within the external, hydrophilic loop are most sensitive to mutation. The latter region has been found to interact with the N-terminus of A17 *in vitro*; moreover, mutations that disrupt complementation activity *in vivo* disrupt interaction *in vitro* (Unger, Mercer, and Traktman, submitted for publication).

In summary, the A17 and A14 membrane proteins are critical players in diversion of ER membranes to viral factories and formation of the viral membrane. The proteins are synthesized in the ER and trafficked to viral factories to form membrane-containing crescents. Within crescents and the mature virion membrane, A14 and A17 appear to form a lattice that is stabilized by disulfide bonds, probably contributing to the sensitivity of the virion membrane to reducing agents. Finally, the A14–A17 lattice serves as an anchor within the

viral membrane to which several other proteins important in virion structure and morphogenesis attach (see in a later section).

E. D13: The Crescent Scaffold Protein

The "spicule" layer that comprises the convex surface of crescents, IV and IVN was first described in detail by Dales and Mosbach (1968). Based on studies with metabolic inhibitors that partially disrupted crescent formation these authors concluded that the spicule layer conferred curvature and rigidity to the crescents. This conclusion was confirmed and extended through studies with the antibiotic inhibitor rifampicin. Rifampicin, better known as an inhibitor of prokaryotic transcription, inhibits vaccinia virus morphogenesis (Grimley *et al*., 1970; Moss *et al*., 1969a,b; Nagayama *et al*., 1970). In the presence of this drug, irregularly shaped membranes that lack a spicule layer accumulate around areas of electron-dense viroplasm. These membranes can be labeled with anti-A17 antibody using immune electron microscopy, confirming a relatedness to virus crescent membranes (Wolffe *et al*., 1996). Inhibition with rifampicin is rapidly reversible; normal crescents form within minutes after the removal of drug.

Several lines of evidence demonstrate that the spicule protein is the product of gene *D13L*. First, immune electron microscopy shows that in a normal infection, antibody specific for the D13 protein decorates crescents and IV (Miner and Hruby, 1989; Mohandas and Dales, 1995; Sodeik *et al*., 1994; Szajner *et al*., 2005). In the presence of rifampicin, virus membranes do not label with D13 antibody, and instead D13 antigen accumulates in inclusions within factories, removed from membranes. When the rifampicin block is reversed, newly formed crescents are now labeled with D13 antibody and the D13 inclusions disappear. Second, mutations that confer resistance to rifampicin map to the *D13L* gene (Baldick and Moss, 1987; Tartaglia and Paoletti, 1985). Third, conditional lethal mutations in the *D13L* gene display a phenotype identical to the effects of rifampicin (Lackner *et al*., 2003; Stern *et al*., 1977; Zhang and Moss, 1992).

Experiments demonstrate that the "spicule" layer is in fact a spherical honeycomb lattice composed of D13 trimers (Heuser, 2005; Szajner *et al*., 2005). The D13 protein itself can associate with two integral virus membrane proteins, A17 and H3, thus providing a mechanism for scaffolding of the virus membrane onto the D13 lattice. As discussed in Section IX.E.1, D13 is lost from virions during maturation from IVN to MV (Essani *et al*., 1982; Mohandas and Dales, 1995; Sodeik *et al*., 1994); how the completion of the IV membrane sends a

signal that activates dissolution of the D13 lattice, and how this lattice is dismantled, are intriguing questions that remain to be answered.

In summary, the "spicule" layer that appears on the convex surface of crescents and the outside of IV and IVN is a temporary scaffold for assembly of the virus membrane and is composed primarily of a honeycomb lattice built from D13 protein trimers. It follows that the curvature of the IV membrane, and therefore the final size of IV, is largely determined by the structure of the D13 lattice. Parallels between the D13 lattice and the clathrin coats of endocytic vesicles are evident.

VII. Immature Virion Formation: A Complex Process

Mutants in seven different vaccinia genes produce a similar phenotype which suggests a role for the gene products in the association of viral crescents with viroplasm. One of these seven proteins, A10 or 4a, is one of the most abundant virion core proteins. The other six proteins, A15, A30, D2, D3, G7, and J1, are found in a seven-protein complex along with the F10 protein kinase, which, as described previously, phosphorylates several membrane and core proteins and plays a critical role throughout virus assembly. The role of each of these proteins in IV formation is summarized in the following sections.

A. Seven-Protein Complex

As membrane crescents appear, they are often seen at the periphery of electron-dense regions of viroplasm, which is known to contain viral proteins destined for encapsidation into the virion core. It is not known what protein–protein or protein–lipid interactions are involved in mediating the association of viroplasm with growing crescents: there are no known interactions of individual membrane proteins with core proteins. However, a group of seven core proteins, F10, A30, G7, J1, D2, D3, and A15, has been shown to form a multimeric complex, and in some cases the proteins are mutually dependent on one another for stability (Szajner *et al.*, 2004a). Several members of the complex are phosphorylated *in vivo* in an F10-dependent manner. The stoichiometry of the individual components within the complex has not been determined. In addition to being physically linked, these proteins show a genetic interaction, since comparable phenotypes are observed upon mutation or repression of individual members of the complex. As detailed in a later section, the phenotypes suggest a role for these proteins in the association of viroplasm with crescents.

1. F10

F10 has been described previously in significant detail (Section VI.C.1). With regard to its involvement as a member of the seven-protein complex which mediates the association of viroplasm with growing crescents, it is worth recalling the fact that F10 has been shown to be tightly associated with membranes *in vivo* (Punjabi and Traktman, 2005). Direct evidence for the functional involvement of F10 in the association of viroplasm with crescents was obtained from ultrastructural analyses of tsF10 infections that were initiated at the permissive temperature in the presence of rifampicin, and then shifted to the nonpermissive in the absence of rifampicin at 12 hpi. The phenotype seen here was nearly identical to that observed upon disruption of A30 or G7 expression (see later). Indeed, the phosphorylation of A30 and G7 is dependent on F10 *in vivo* and also appears to be dependent on the assembly of the multimeric complex and the normal progression of morphogenesis (Mercer and Traktman, 2005; Szajner *et al*., 2004c). It seems likely that F10 mediates phosphorylation of these proteins in a context-dependent manner.

2. A30

Disruption of the *A30L* gene was shown to lead to a phenotype in which the association of nascent membranes with viroplasm was disrupted. This disruption led to the appearance of large virosomes and "empty" IV and/or pseudo-IV with multiple membrane wrappings. This phenotype was observed when an inducible recombinant was generated permitting the repression of A30, or when a temperature-sensitive mutant, Dts46, was analyzed at the nonpermissive temperature (Szajner *et al*., 2001a,b). The tsA30 protein is extremely thermolabile: effectively, at the nonpermissive temperature, repression of the A30 protein is mimicked. A30 is a 9-kDa protein that is found in viroplasm and encapsidated within virions; fractionation studies have demonstrated that A30 is loosely associated with the virion core. A30 is phosphorylated on Ser residues *in vivo* in an F10-dependent manner, and it has been shown to be a direct substrate of F10 *in vitro*. A30 has been shown to interact directly with the G7 protein (discussed in a later section), and these proteins appear to depend on one another for their mutual stability.

3. G7

G7 was first implicated in virion morphogenesis because of its association with the A30 protein (Szajner *et al*., 2003). The 42-kDa G7 protein is expressed at late times postinfection, encapsidated into

virion cores, and processed by proteolytic cleavage at two AG↓X motifs during virion maturation (Fig. 13). The G7 protein is phosphorylated *in vivo* in an F10-dependent manner, but F10 does not appear to phosphorylate G7 *in vitro*, either when presented alone or in the presence of its binding partner A30 (Mercer and Traktman, 2005; Szajner *et al*., 2004c). The function of G7 *in vivo* has been addressed both by the generation of an inducible recombinant in which G7 expression is IPTG-dependent and by characterization of Cts11, which encodes a defective G7 protein (Mercer and Traktman, 2005; Szajner *et al*., 2003). These two approaches have yielded somewhat different answers regarding G7's function, as detailed below.

During infections with Cts11, virosomes accumulate as do short membrane crescents that are embedded within a distinct matrix of medium electron density. Both the G7 and A30 proteins are stable during these infections, permitting the examination of the impact of a specific loss of G7 function. When various G7 and A30 proteins were synthesized *in vitro* and subjected to coimmunoprecipitation protocols, the tsG7 protein had lost the ability to interact with A30. When Cts11

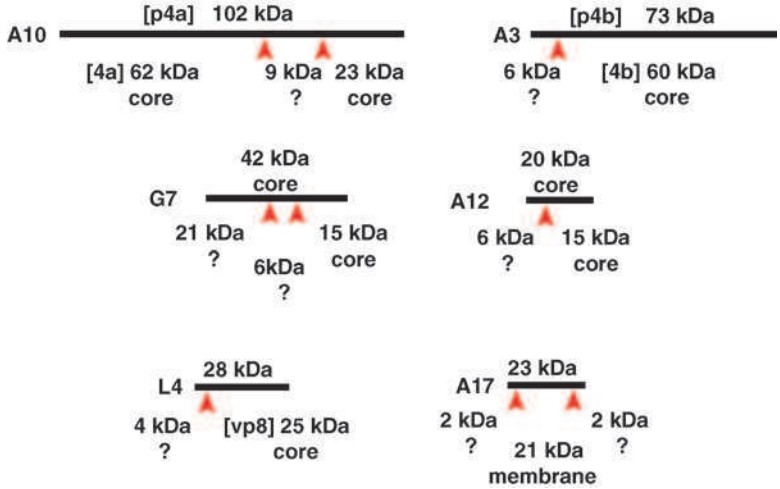

FIG 13. Proteolysis of vaccinia core and membrane proteins. The proteolysis of five core proteins (A10, A3, G7, A12, and L4) and one membrane protein (A17) is shown. Black lines represent the length of the precursor polypeptide, drawn to scale. Red arrowheads represent known cleavage sites. Information concerning the precursor (MW, any pseudonyms in brackets, and localization if relevant) is given above each line. Information concerning each product (MW, pseudonyms in brackets, localization if known) is given below each line. ? = fate of the product is unknown.

infections were performed at permissive temperature in the presence of rifampicin for 12 h and then removed from the rifampicin block and shifted to the nonpermissive temperature, the phenotype observed mimicked what had been observed on repression of A30 (Fig. 11D). This phenotype, characterized by the accumulation of empty IV, is also observed when G7 is repressed. Interestingly, tsG7 mutants are noncomplementing with tsA30 mutants, providing additional genetic evidence for an interaction between G7 and A30 (Lackner *et al*., 2003). In summary, G7 appears to play crucial roles at two stages of morphogenesis (Mercer and Traktman, 2005). First, G7 is required for the movement of crescents to the periphery of virosomes, where they enlarge; later, G7 is required for the filling of the crescents with viroplasmic material. The small amount of wt G7 that is likely to accumulate when infections with the inducible recombinant are performed in the absence of the IPTG inducer may be sufficient for the initial G7-dependent step, whereas the tsG7 protein must be unable to mediate this effect.

4. J1

The 21-kDa J1 protein is expressed at late times and encapsidated; like A30, although J1 is associated with virion cores, a fraction of the protein can be extracted with nonionic detergents. Purified J1 has been shown to form oligomers (Chiu *et al*., 2005), and interactions between the N- and C-termini of J1 have been observed in yeast two-hybrid analyses. The role of J1 *in vivo* has been analyzed using both an inducible recombinant in which J1 expression is IPTG-dependent and through the analysis of Cts45, which encodes a mutant J1 protein (Chiu and Chang, 2002; Chiu *et al*., 2005). Repression or inactivation of J1 phenocopies the repression of A30 or G7, and indeed both A30 and G7 become unstable in the absence of J1 at 40°C. J1 is part of the seven-protein complex involved in viroplasm/membrane association, although the proteins with which J1 associates directly have not been identified (Szajner *et al*., 2004a). The tsJ1 protein remains stable at the nonpermissive temperature but does not associate with the multiprotein complex.

5. A15

The 10-kDa A15 protein was shown to be a component of the seven-protein complex by mass spectroscopy (Szajner *et al*., 2004a). This protein is expressed at late times postinfection and encapsidated in the virion core. An inducible recombinant in which A15 expression is IPTG-dependent has been generated; in the absence of A15, the characteristic accumulation of empty IV was observed (Szajner *et al*., 2004a).

6. D2

D2 was identified as being a component of the seven-protein complex by mass spectroscopy (Szajner *et al.*, 2004a). The 16.9-kDa D2 protein had been known to be a component of the virion core (Dyster and Niles, 1991). The temperature sensitivity of the Ets52 mutant is due to a mutation in D2 that renders the protein extremely thermolabile; at the nonpermissive temperature, few signs of morphogenesis are seen. Crescents and empty IV are observed only occasionally. The phenotype is similar to that seen for the leakier tsF10 mutants (Traktman *et al.*, 1995; Wang and Shuman, 1995). An inducible recombinant has been generated in which expression of D2 is dependent on IPTG. Even in the presence of IPTG, the virus forms small plaques, suggesting that the epitope tag appended to D2 is deleterious. Nevertheless, repression of D2 does severely impair virion maturation, leading to an accumulation of empty IV (Szajner *et al.*, 2004a).

7. D3

The 27-kDa D3 protein is also a component of the virion core and seven-protein complex (Dyster and Niles, 1991; Szajner *et al.*, 2004a). The phenotype of Cts35, which encodes a defective D3 protein that is extremely thermolabile, is virtually indistinguishable from that seen for tsD2. Consistent with their presence in the seven-protein complex, stability of the D2 and D3 proteins is mutually interdependent: both D3 and D2 are destabilized during tsD3 and tsD2 infections.

B. A10: p4a / 4a

The *A10L* gene encodes the virion precursor protein p4a (Wittek *et al.*, 1984). During morphogenesis from IV to MV, p4a is processed by two proteolytic cleavages into an N-terminal 62-kDa polypeptide, an internal 9-kDa polypeptide, and a C-terminal 23-kDa polypeptide (Fig. 13) (Vanslyke *et al.*, 1991b). Both the 62- and the 23-kDa polypeptides are packaged into virions; the fate of the 9-kDa polypeptide is unknown (Vanslyke and Hruby, 1994; Vanslyke *et al.*, 1991b). The 62-kDa polypeptide is also commonly called 4a. 4a localizes to the virion core (Sarov and Joklik, 1972); Ichihashi *et al.* (1984) suggest that in fact it is a component of the outer core wall. 4a comprises an impressive 14% of the mass of the mature virion, or 28% of the mass of the virion core (Sarov and Joklik, 1972). Thus, p4a and its proteolytic products are major determinants of vaccinia virion structure.

A10 function has been examined using an inducible recombinant in which A10 expression is IPTG-dependent. In the absence of

inducer, normal crescents are seen, but the IV that form are aberrant (Heljasvaara *et al*., 2001). Many of the abnormal IV particles appear empty, but others contain dense patches of DNA-containing material. DNA aggregates also accumulate in the cytoplasm. The membranes surrounding the IV are normal in appearance and contain the A14 and A17 membrane proteins as well as the D13 scaffold protein, as judged by immunoelectron microscopy. Thus, A10 appears to be dispensable for the formation of the IV membrane but is required for the proper organization and packaging of the viroplasmic matrix that is normally included in IV. The phenotype observed on repression of A10 mimics to a great degree the phenotype of mutants affected in components of the seven-protein complex described previously.

The A10 precursor and the 60-kDa cleavage product form stable complexes with another abundant virion core protein, A4 (Risco *et al*., 1999). The implications of this interaction are discussed in Section IX.B.3 along with the role of A4 in MV formation.

VIII. IV→IVN Transition: Genome Encapsidation

The process of viral DNA replication produces progeny genomes that will be encapsidated into nascent virions. Concatemeric intermediates are formed during the replication process, and these are processed to monomeric genomes by a virally encoded resolvase (Garcia *et al*., 2000) (Section VIII.B.3). Genome maturation occurs normally when virion morphogenesis is blocked in the very earliest stages of morphogenesis, for example, in H5, G5, and J1 mutant infections (Table II), indicating that this maturation is a prerequisite for, but is not coupled to, genome encapsidation (Chiu and Chang, 2002; da Fonseca *et al*., 2004; DeMasi and Traktman, 2000). Much remains to be discovered about the encpasidation of the viral genome, although it appears to be distinct from the process described previously for the filling of maturing crescents with viroplasmic proteins destined to form the virion core. One of the unresolved questions is whether genome entry precedes closure of the IV membrane. Serial section analysis shows that most fully closed IV do indeed have nucleoids (Morgan *et al*., 1955), suggesting that genome encapsidation is likely to occur prior to the closure of the IV (Morgan, 1976a,b). If this model is not correct, then the encapsidation machinery must either pass through a proteinaceous plug that has been proposed to mark the site of IV membrane closure, or it must pass through the IV membrane itself. Some investigators have proposed that genome entry causes membrane invagination, leading to the

presence of a membrane around the nucleoid and, consequently, the core. However, this model is not widely accepted (Section VI.A) (Fig. 8).

It is not known exactly how replicated genomes are distributed throughout the cytoplasm, although sites of replication have been visualized by autoradiography or with antisera directed against BrdU, DNA, or the single-stranded binding protein, I3. When morphogenesis is arrested prior to the appearance of IVN, DNA crystalloids accumulate in the cytoplasm (Ericsson *et al*., 1995; Grimley *et al*., 1970; Grubisha and Traktman, 2003; Unger and Traktman, 2004). These crystalloids are often surrounded by membranes, consistent with the proposal that DNA replication occurs within ER-delimited domains of the cytoplasm (Schramm and Locker, 2005; Tolonen *et al*., 2001) (Section V) (Fig. 5).

The literature contains a number of ultrastructural images that have been interpreted as representing the ongoing process of DNA encapsidation (Morgan, 1976a,b). Although this process is commonly referred to as encapsidation of the viral "nucleoprotein," there is in fact nothing known about how the genome is condensed and whether it is indeed bound to proteins. As described later, when either of the two proteins that have been specifically associated with genome encapsidation are repressed or inactivated, no other proteins appear to be missing from the virions (Cassetti *et al*., 1998; Grubisha and Traktman, 2003). These data do not support a model in which the genome is assembled into a conventional nucleoprotein complex. In fact, it may be that condensation of the genome is effected by interactions with polyamines; encapsidation of spermidine has been reported (Lanzer and Holowczak, 1975; Saminathan *et al*., 2002). In any case, the genome has a predicted dimension of 2 nm $\times$ 68 μm, which must fit into the viral core. The approximate dimensions of the nucleoid, as observed in ultra thin sections, are 0.1 $\times$ 0.15 μm, indicating that the genome must undergo massive condensation before encapsidation.

To date, four viral proteins have been implicated in maturation and processing of the viral genome. These include the core proteins A22 (a Holliday resolvase), I6 and A32, and the membrane protein A13.

A. Membrane Proteins

1. A13

The 70-amino acid A13 protein has a hydrophobic N-terminus, which is predicted to be the membrane-spanning domain; indeed A13 undergoes cotranslational insertion into microsomal membranes *in vitro* (Salmons *et al*., 1997) and is a component of the virion

membrane (Fig. 12). The hydrophilic tail of A13 undergoes phosphorylation *in vivo* on Ser residues; mutation of Ser40→Ala prevents phosphorylation (Unger and Traktman, 2004). This modification appears to be independent of the F10 kinase; Ser40 is found within the motif NSPPP, which is predicted to be a high-affinity site for the cellular kinase ERK. The function of A13 has been elucidated both by the analysis of a TET-inducible recombinant and a temperature-sensitive mutant (Cts40) (Unger and Traktman, 2004); the A13 protein in Cts40 has a Thr48→Ile substitution and is thermostable but apparently inactive. When A13 is inactivated, a morphogenesis arrest is seen; IV are formed, but IVN are rare and MV are not seen (Fig. 11E). Numerous DNA crystalloids, which appear to be surrounded by membranes, accumulate in the cytoplasm. Thus, A13 appears to be essential for the encapsidation of DNA into IV and the subsequent maturation of IV→IVN→MV.

B. Core Proteins

1. A32

Bioinformatic analysis was first used to identify the A32 protein as a putative ATPase with limited homology to the encapsidation proteins encoded by bacteriophages and adenovirus (Koonin *et al.*, 1993). The 34-kDa protein is expressed at late times postinfection and is encapsidated; to date, there has been no experimental data confirming that the protein indeed possesses the predicted ATPase activity. An inducible recombinant in which expression of A32 is IPTG-dependent has been generated; in the absence of A32, the production of infectious virus is severely diminished (Cassetti *et al.*, 1998). Morphogenesis appears normal through the IV stage, but then aberrant forms are seen. Spherical virions that appear dense or half-dense/half-empty are numerous, as are cytoplasmic DNA crystalloids. The aberrant virions have been purified and shown to contain the full-protein complement but to be devoid of viral DNA.

2. I6

The 44-kDa I6 protein was identified as binding with great specificity and stability to the telomeric hairpins of the viral genome (Demasi *et al.*, 2001b). The telomere–I6 interaction was shown to be dependent on the presence of the extrahelical bases, which are so characteristic of the viral telomeres. Very low levels of I6 are made at early times postinfection; the majority of the protein is synthesized after the onset of DNA replication. An average of ~35 copies of I6 is encapsidated in the virion core. A series of mutants with lesions in the *I6L* gene have been

generated by clustered charge-to-alanine mutagenesis, and one of these has a tight temperature-sensitive phenotype (Grubisha and Traktman, 2003). At the nonpermissive temperature, the phenotype observed is almost indistinguishable from that seen on repression of A32: IV appear normal, cytoplasmic DNA crystalloids are abundant, and aberrant, spherical virions are produced that contain the full-protein complement but no viral DNA (Fig. 11F). A32 remains stable during these infections and is encapsidated into the aberrant virions, indicating that its encapsidation is independent of DNA encapsidation and I6 function. Conversely, no I6 is encapsidated into A32-deficient virions.

These cumulative data support a model in which the presence of A32 within virions enables the encapsidation of a DNA genome on which I6 protein is bound to the telomeric hairpins. As described previously, repression of certain membrane proteins, such as A13, leads to the accumulation of IV and DNA crystalloids; it is possible that the presence of these proteins in the membrane is also important for A32 and/or I6-DNA encapsidation.

3. A22, a Holliday Resolvase

As described previously, concatemeric replication intermediates are processed to mature genomes by a virally encoded Holliday junction resolvase, the A22 protein (Garcia *et al*., 2000). The product of the *A22R* gene is a palmityl protein that is expressed late during virus infection and packaged into the virion core (Garcia and Moss, 2001; Grosenbach *et al*., 2000). Analysis of an inducible mutant demonstrates that in the absence of A22, concatemer resolution is defective, and virion morphogenesis is arrested at an intermediate stage (Garcia and Moss, 2001). In these A22-deficient infections, MV formation is inhibited and IV accumulate, a very few of which have nucleoids. In addition, there is an accumulation of dense spherical particles similar to those seen in other encapsidation defective mutants. Thus, while genome maturation can proceed in the absence of virion morphogenesis, the converse is not true. If concatemer resolution is inhibited, virion morphogenesis is arrested and the nature of the intermediate particles that accumulate suggests that the defect lies in DNA packaging.

IX. MV Formation

Perhaps the most striking event during morphogenesis of vaccinia is the transition from IVN to MV. The precise protein composition of immature particles is difficult to assess because normal IV and IVN

are difficult to isolate in sufficient quantity or purity to permit rigorous biochemical study (Vanslyke *et al*., 1993). Nevertheless, as detailed later, a synthesis of the evidence to date suggests that IVN contain the full complement of proteins contained in MV, with the exception of a few membrane proteins that are added during the IV/IVN to MV transition. Furthermore, since both the IV membrane and the MV membrane contain the major viral membrane proteins A14 and A17, the membrane of IVN is the precursor for the MV membrane (Griffiths *et al*., 2001a; Rodriguez *et al*., 1997; Traktman *et al*., 2000). Thus the IV/IVN to MV transition involves a rearrangement of the contents of IVN to form a distinct core and lateral bodies, and in the process the particle is transformed from a spherical to a barrel shape. Indicative of the complexity of this process, a significant majority of virus mutants that affect virion morphogenesis affect the IV/IVN to MV transition. These mutants fall into two general classes: those that fail to assemble morphologically normal looking MV particles and those that assemble normal looking MV particles, which are nevertheless not infectious. Analysis of these mutants informs us that the IV/IVN to MV transition involves or requires: (1) assembly of the transcription apparatus within the core, (2) restructuring of the particle surface, including loss of the D13 protein, formation of numerous disulfide bond linkages by the virally encoded redox system and addition of several additional surface proteins, (3) proteolysis of several virion protein precursors and formation of an enzymatically active core, in part through the action of the viral phosphatase, and (4) movement of the finished MV from viroplasm to the periphery of the cell. Each of these events is discussed in more detail in later sections.

A. Assembly of the Transcription Apparatus Within the Core

The phenotype of virus mutants affecting two different virus coded transcription factors, VETF and rap94, reveals an intriguing relationship between assembly of the early transcription machinery within the virion core and formation of MV. Vaccinia RNA polymerase exists in two different forms, one that contains the subunit rap94 (the product of the *H4L* gene), and one that lacks rap94 (Broyles, 2003). The rap94-containing enzyme transcribes early viral genes exclusively, while RNA polymerase lacking rap94 transcribes exclusively intermediate and late genes. VETF, composed of the D6 and A7 proteins, binds specifically to early virus promoters and is required for early gene transcription *in vitro* (Broyles, 2003). Thus, specificity of the RNA polymerase for early promoters is thought to result from a specific

interaction between rap94 and VETF, although such an association has never been proven directly.

1. D6 and A7: VETF

Genetic analysis of VETF is facilitated by the existence of inducible recombinants and temperature-sensitive mutants. There exist multiple temperature-sensitive mutants with lesions in the *D6R* gene, and inducible recombinants have been generated which allow IPTG-dependent expression of both subunits of VETF, D6 and A7 (Christen *et al*., 1992; Hu *et al*., 1996, 1998). Ultrastructural analysis of cells infected with the temperature-sensitive mutants has not been reported, but such studies have been published for the inducible recombinants. When either VETF subunit is repressed, a "normal" gene expression phenotype is observed; that is, all three classes of viral proteins, early, intermediate, and late, are synthesized in normal amounts and with normal kinetics.[5], However, electron microscopic analysis of the mutant infections reveals a block in morphogenesis at the IV/IVN stage. MV are either absent (D6) or significantly reduced in number (A7) in the mutant infections. Instead, an abundance of morphologically normal IV and IVN accumulate and occasional abnormal, dense, spherical particles are seen in viral factories. Confocal microscopy of A7-deficient infections stained for DNA and a virion membrane protein suggests that at least a fraction of the immature particles

[5] A general and seemingly peculiar feature of mutants in vaccinia genes affecting virion transcription enzymes is that they confer a phenotype that is expressed late rather than early during infection. Offhand, one might expect a mutation in a virion transcription enzyme, in particular a temperature-sensitive mutant, to affect early viral transcription and thus disrupt the infection at an early stage. However, all mutants in transcription enzymes reported to date proceed through the early phase of infection normally and display a phenotype that impacts the late phase of infection. In the case of inducible mutants, this phenomenon is not difficult to understand. The inducible mutant must be grown under permissive conditions in order to study the phenotype under nonpermissive conditions. During growth under permissive conditions, the wild type gene product is synthesized and packaged into virions, which are therefore competent for early transcription under nonpermissive conditions. The nonpermissive infection therefore only tests for any requirement for the protein during the later phases of infection. In the case of temperature-sensitive mutations the same phenomenon is observed; however, in this case the virions synthesized under permissive conditions package mutant enzyme. One must therefore argue that the mutant proteins are not thermolabile in virions, but rather that they are temperature sensitive for synthesis, that is, newly synthesized mutant protein is either rapidly degraded or cannot form an active conformation at the nonpermissive temperature, and thus the phenotype observed represents the requirement for newly synthesized enzyme late during infection (Hooda-Dhingra *et al*., 1989).

contain DNA. Both mutants also accumulate abnormally large masses of viroplasm within viral factories. The protein composition of the accumulated IV and IVN is unknown. Thus in the absence of VETF, virus assembly arrests at the IV/INV stage, implying a pivotal role for VETF in formation of the viral core and transition from IVN to MV.

2. H4: rap94

Genetic analysis of the *H4L* gene, which encodes rap94, is also enabled by the existence of both inducible and temperature-sensitive mutants affected in this gene (Kane and Shuman, 1992; Zhang *et al*., 1994). As was described for the VETF mutants, inactivation or repression of rap94 does not impair the profile of viral gene expression. Unlike the VETF mutants however, both the temperature sensitive and the inducible mutants in rap94 assemble particles that are morphologically indistinguishable from wt MV as judged by electron microscopy. These MV made under nonpermissive conditions are deficient in their ability to direct *in situ* transcription *in vitro*. Moreover, they lack not only rap94 as expected but also specifically lack all of the major known or suspected enzymes involved in early viral transcription, including the viral RNA polymerase, the capping enzyme/termination factor, the poly(A) polymerase large subunit, DNA-dependent ATPase I, RNA helicase, and topoisomerase. These abnormal MV contain normal amounts of VETF. These results are interpreted to mean that a presumed rap94–VETF interaction seeds assembly of a transcription complex onto the viral genome and thus coordinates packaging of the transcription machinery during virus assembly. Notably, the result also implies that the morphological transformation from IV to MV, including formation of the core and lateral bodies, occurs independently of the assembly of the transcription apparatus within the core.

Together, studies with mutants in VETF and rap94 suggest that the early viral transcription factor VETF, perhaps in conjunction with or through interaction with other DNA binding or structural proteins, plays a critical role in the morphological transition from IVN to MV, and also, perhaps through an interaction with rap94, plays a critical role in recruitment and assembly of a transcription complex in the developing virion. The recruitment and assembly of the transcription complex itself, however, is not a prerequisite for virion maturation, in that normal appearing MV can be assembled in the absence of the transcription complex. Finally, it is worth recalling that encapsidation of VETF and the early transcriptional machinery does not appear to require their association with the viral genome, since DNA-deficient

particles assembled in the absence of the A32 protein do contain the early transcriptional machinery (Cassetti *et al.*, 1998).

B. Core Proteins Involved in the IV to MV Transition

A number of core proteins are required for virion maturation, as revealed by the phenotypes exhibited by temperature-sensitive mutants that encode mutant forms of these proteins, or inducible recombinants which allow the expression of the proteins of interest to be experimentally repressed. In some cases, repression or inactivation of the protein simply arrests morphogenesis at the IV or IVN stage; in other cases, aberrant particles are seen. Since not all publications are equally thorough in their ultrastructural analysis, implication of a given protein in a precise step of virion assembly is not always possible. It would appear that when the D13 scaffold remains intact, there is an accumulation of IV and/or IVN. In contrast, when the D13 scaffold is removed, then further virion maturation is attempted unsuccessfully, leading to the production of aberrant particles.

1. I1

The 36-kDa I1 protein is expressed at late times postinfection and encapsidated into virion cores (~700 copies/virion) (Klemperer *et al.*, 1997). The protein has nonspecific DNA binding activity but shows some preference for binding to the viral telomeres (Demasi *et al.*, 2001a; Klemperer *et al.*, 1997). An inducible recombinant in which I1 expression is IPTG-dependent has been generated; upon the repression of I1, morphogenesis arrests with the accumulation of numerous IV. IVN were also seen, although some DNA crystalloids were observed in the cytoplasm (Klemperer *et al.*, 1997). The I1 protein is highly conserved among poxviral genomes, in keeping with its essentiality for virion maturation.

2. F17

The 11-kDa F17 protein is expressed at late times postinfection and is one of the major components of the core; ~27,000 copies of the protein are encapsidated per virion. This protein was initially referred to as p11 or VP11 (Kao and Bauer, 1987; Kao *et al.*, 1981; Nowakowski *et al.*, 1978a,b). The protein is phosphorylated *in vivo* on Ser residues; phosphorylation is only minimally dependent on the F10 kinase but is modulated by expression of the viral H1 phosphatase. It is likely that the protein is phosphorylated on two PSSP motifs which are target sites for cellular proline-directed kinases such as ERK1 and CDK1 (Reddy, unpublished; Traktman, unpublished). The F17 protein is

quite basic and was originally described as a DNA-binding protein that could coat DNA stoichiometrically. However, normal amounts of F17 are encapsidated even when the genomic DNA is not, suggesting that F17 is certainly not a classical "nucleoprotein" in the sense that was originally proposed (Cassetti *et al*., 1998; Grubisha and Traktman, 2003). An inducible recombinant has been generated in which expression of the *F17R* gene is IPTG-dependent; in the absence of F17, morphogenesis arrests with the appearance of aberrant IV (Fig. 11G) (Zhang and Moss, 1991a,b). In some of these particles, there is an internal nucleoid that resembles the DNA crystalloids described earlier. In other cases, the IV appear almost empty or contain small patches of condensed material and/or membrane. Because DNA crystalloids do not accumulate in the cytoplasm, however (Traktman, unpublished), it is likely that the absence of F17 does not impair genome encapsidation per se but impairs nucleoid formation and disrupts the internal organization of the IV. These aberrant IV do not form a light scattering band upon sucrose gradient ultracentrifugation, indicating that they may be unstable.

3. A4

The *A4L* gene encodes a 39-kDa protein that is expressed late and encapsidated into the virion. This protein was first identified as an immunodominant antigen and was referred to as p39 (Cudmore *et al*., 1996; Demkowicz *et al*., 1992; Maa and Esteban, 1987; Roos *et al*., 1996). A4 appears to be phosphorylated *in vivo* and is a substrate for the F10 kinase *in vitro*; A4 phosphorylation appears to be modulated by the expression of the viral H1 phosphatase (Traktman, unpublished). Immunoelectron microscopy has revealed that antibodies to A4 decorate the interior of IV but not the nucleoid, and within MV, appear to localize to a region between the core and membrane. On extraction of purified MV with neutral detergent and DTT, A4 partitions into both the core (insoluble) and the membrane (soluble) fractions. Consistent with these results, anti-A4 stains the surface of isolated cores, leading Roos *et al*. (1996) and Cudmore *et al*. (1996) to conclude that A4 comprises, at least in part, the "spike" or palisade layer of the outer core wall. The A4 protein forms a complex with both the A10 precursor protein, p4a, and the 62-kDa proteolysis product, 4a (Risco *et al*., 1999). Nevertheless, inducible A10 mutants present a significantly different phenotype than A4 mutants. A10 mutants are defective in the association of viroplasm with crescents that is required to form IV (Section VII.B). In contrast, A4 mutants are defective in formation of MV but form both normal IV and IVN; some abnormal

structures consisting of IV which appear to be surrounded by an additional membrane are also seen (Williams *et al.*, 1999). In this case the authors were able to purify virions from the A4-deficient infections. The mutant particles were seemingly normal in protein content, although they contained slightly more unprocessed A10 protein, consistent with an assembly block at the IV/IVN to MV transition. Thus, A4 appears to be necessary for core assembly during the IV to MV transition.

4. A3

The *A3L* gene encodes the p4b/4b protein, a major component of the virion core that undergoes proteolytic processing during the IV to MV transition. The 73-kDa precursor is cleaved to a mature protein of 60 kDa, called 4b (Fig. 13), which accounts for 11% of the dry mass of the virion (Sarov and Joklik, 1972). Several independent studies localize 4b to the core wall (Ichihashi *et al.*, 1984; Sarov and Joklik, 1972; Wilton *et al.*, 1995). Analysis of temperature-sensitive mutants that encode defective A3 proteins (Cts8, Cts26) has revealed that A3 is essential for the formation of a structurally normal core (Kato *et al.*, 2004). Under nonpermissive conditions, tsA3 mutants form normal IV and IVN but do not form normal MV. Instead, spherical or irregularly shaped particles are formed which accumulate at a distance from viral factories and can be wrapped in Golgi-derived membranes and released by exocytosis, as if they were normal MV (Fig. 11I). The aberrant tsA3 particles can be purified for analysis; they contain the normal complement of virion proteins and DNA; however, their internal structures are malformed relative to wild-type MV. In the tsA3 mutants, mutant 4b protein is made, processed, and packaged in normal amounts in aberrant virions, suggesting that aberrant particles observed in tsA3 mutants result from the inability of the mutant 4b protein to function in formation of a normal core wall. Importantly, the aberrant A3 mutant particles are defective in virion transcription despite containing viral DNA and an active transcriptional apparatus, demonstrating that proper core formation is required for transcription *in situ*.

C. Proteolysis of Virion Protein Precursors; Involvement of Genes I7L *and* G1L

An important role for proteolytic processing in virion maturation is a common theme in numerous systems, and vaccinia is no exception (Hellen and Wimmer, 1992). Early studies revealed that the major structural protein 4a, the product of the *A10L* gene, is derived from the p4a precursor by proteolytic processing during the late stages of

virion assembly (Katz and Moss, 1970a,b). Subsequent studies have shown that in addition to A10 (p4a/4a), the virion core proteins A3 (p4b/4b), L4 (VP8), A12, and G7, and the membrane protein A17 are also derived via proteolytic processing of precursor polypeptides (Betakova *et al*., 1999b; Mercer and Traktman, 2005; Rodriguez *et al*., 1997; Rosel and Moss, 1985; Sarov and Joklik, 1972; Szajner *et al*., 2003; Takahashi *et al*., 1994; Vanslyke *et al*., 1991a,b; Weir and Moss, 1985; Whitehead and Hruby, 1994b; Yang *et al*., 1988). The processing of each of the proteolyzed virion proteins is understood in significant detail, as summarized in Fig. 13.

Alignment of all of the known cleavage sites for proteolytically processed vaccinia proteins yields the consensus sequence AG↓X, where cleavage occurs between the G and the X (Vanslyke *et al*., 1991b). A survey of the vaccinia genome reveals 82 potential AG↓X cleavage sites, although it has been shown experimentally that not all of these sites are cleaved (Whitehead and Hruby, 1994b). Nevertheless, given the abundance of potential cleavage sites, it seems likely that additional targets for morphogenesis-associated proteolysis will be discovered.

Vaccinia contains two genes, *I7L* and *G1L*, which encode proteins with significant homology to known proteases. The G1 protein, a component of the virion core, contains the motif HXXEH that is common to a subset of metalloproteases (Ansarah-Sobrinho and Moss, 2004a; Hedengren-Olcott *et al*., 2004; Whitehead and Hruby, 1994a). In transient infection–transfection assays, the *G1* gene product can cleave the L4 precursor protein in a manner that depends on an intact HXXEH motif. G1-dependent cleavage of L4 does occur at an AG↓X motif, although cleavage occurs at a cryptic AG↓S site rather that the natural AG↓A site (Whitehead and Hruby, 1994a). An inducible recombinant in which expression of G1 can be experimentally regulated has been constructed; repression of G1 blocks the production of infectious virus at the IV to MV transition (see later) (Ansarah-Sobrinho and Moss, 2004a). This phenotype cannot be complemented by expression of a *G1L* allele containing mutations in the HXXEH motif, implying that the predicted metalloprotease activity of G1 is essential for virus growth. However, although normal MV do not form when G1 is repressed, cleavage of the A3, A10, L4, G7, and A17 precursors occurs normally, showing that the G1 protein is not required for their proteolytic maturation. Thus, although G1 is clearly required for virion maturation, its role as a protease remains unresolved.

The I7 protein, which is also a component of the virion core, has homology to known cysteine proteinases encoded by African swine fever virus and yeast (Andres *et al*., 2001; Kane and Shuman, 1993;

Li and Hochstrasser, 1999). Nonpermissive infections performed with temperature-sensitive mutants or an inducible recombinant affected in the *I7L* gene are characterized by defective processing of the A3, A10, L4, and A17 precursors. Neither this proteolysis defect nor the accompanying morphogenesis arrest at the IV to MV transition can be complemented by mutants containing alterations in residues predicted to comprise the active site of the I7 protease (Ansarah-Sobrinho and Moss, 2004b; Byrd *et al*., 2002, 2003; Ericsson *et al*., 1995). Direct biochemical evidence that purified I7 protein can cleave appropriate substrates *in vitro* is still lacking, and it is therefore formally possible that the impact of repression or inactivation of I7 on proteolysis *in vivo* is indirect. Nevertheless, it seems highly probable that the I7 cysteine protease is directly responsible for processing most or all of the viral proteins known to undergo morphogenesis-associated proteolysis.

Proteolysis of the virion core proteins, but not the A17 membrane protein, is coupled to and probably required for maturation of IV/IVN to MV. Rifampicin treatment prevents proteolysis of core proteins but not the A17 membrane protein, suggesting that membrane protein maturation is an early event in virus assembly while core protein proteolysis is a late event (Betakova *et al*., 1999b; Katz and Moss, 1970a; Rodriguez *et al*., 1993). Inspection of Table II reveals that where tested, all mutants that are blocked in the IV/IVN to MV transition are also blocked in core protein proteolysis, with two notable exceptions, namely G1 mutants and A3 mutants, discussed later. Conversely, all mutants that accumulate morphologically normal MV show normal proteolysis of core proteins. Thus, there exists a correlation between proteolysis and the IV/IVN to MV transition. The core protein precursors are almost certainly contained within completed IVN prior to the conversion to MV. Because IV and IVN appear to be unstable in the standard hypotonic buffers used for virus purifications, the precise protein composition of immature virions is difficult to assess (Hu *et al*., 1996; Klemperer *et al*., 1997; Ravanello and Hruby, 1994b; Vanslyke *et al*., 1993). Nevertheless, the presence of the A3, A10, L4, and G7 proteins, or more likely their precursors, within IV/IVN has been demonstrated by immunoelectron microscopy (Szajner *et al*., 2003; Vanslyke and Hruby, 1994). Importantly, mutation of the I7 protease not only prevents proteolysis of core proteins but also prevents formation of MV (Ansarah-Sobrinho and Moss, 2004b; Byrd and Hruby, 2005; Ericsson *et al*., 1995; Kane and Shuman, 1993) (Fig. 11H). Instead, IV and IVN accumulate, and in addition dense, spherical aberrant particles (not visible in Fig. 11H) are formed (Ansarah-Sobrinho and Moss, 2004b; Ericsson *et al*., 1995).

The aberrant particles contain viral DNA and are identical to MV in protein composition, with the exception that the normally processed core proteins remain in their precursor form. The aberrant I7 particles also become wrapped to form aberrant WV and EV, suggesting that the membrane has been properly restructured (Section IX.E). In sum, the data indicate that proteolysis of one or more core proteins is required for morphogenesis from IVN to MV, although the presence of the I7 protein itself may also be required for the internal restructuring of the virion. The phenotype of I7 mutants also suggests that core formation and restructuring of the particle surface can occur independently of each other.

The phenotypes of A3 mutants (described previously in Section IX.B.4) and G1 mutants provide interesting exceptions to the correlation between proteolysis of core proteins and the IV/IVN to MV transition. These mutants display a phenotype that is virtually identical to the phenotype of mutants affected in the I7 cysteine proteinase: accumulation of IV and IVN, inhibition of MV formation, and accumulation of dense, spherical, or abnormally shaped particles that are indistinguishable from MV in protein and DNA content and are wrapped to form aberrant WV and released by exocytosis to form aberrant EV (Fig. 11I) (Ansarah-Sobrinho and Moss, 2004a; Hedengren-Olcott *et al*., 2004; Kato *et al*., 2004). However, the core proteins contained in the aberrant virions that form when A3 or G1 are mutated have been proteolytically processed to the mature forms. In the case of the A3 mutant, the mutant phenotype likely results directly from an inability of the mutant A3 protein to form a good core wall (Section IX.B.4). The similarity between the I7 and A3 mutant phenotypes therefore suggests that failure to process the core proteins has a significant impact on formation of the core wall. The similarity of the G1 metalloprotease mutant phenotype to the I7 cysteine protease mutant phenotype is provocative, in that it suggests that the G1 protein does indeed act as a protease during infection, targeting substrates whose processing is also critical for core formation and the IV/IVN to MV transition.

D. Membrane Proteins Involved in the IV to MV Transition

There are a number of additional membrane proteins that are dispensable for formation of the IV membrane but play key roles in the IV→MV transition. How and when these proteins are added to the membrane, and how they assist in genome encapsidation and/or core formation, is a question of significant interest.

1. A9

The 12-kDa A9 protein is expressed at late times of infection and incorporated into the virion membrane (Yeh *et al.*, 2000). It is oriented with its C-terminus exposed on the surface of the virion and it appears to be present in both IV and MV (Fig. 12). The predicted transmembrane domain is located in the middle of the protein; although the N-terminus of the protein contains a predicted signal sequence, cotranslational insertion of A9 into membranes has not been documented. An inducible recombinant in which A9 expression is IPTG-dependent has been generated, and A9 has been shown to be essential for virion production. In the absence of A9, IV are formed, as well as aberrant IV that appear to be "empty" or only partially filled with viroplasmic material (Yeh *et al.*, 2000).

2. L1

The L1 protein is a myristylated component of the virion membrane; a C-terminal hydrophobic domain is responsible for anchoring the protein in the membrane, although the timing and mode of insertion are not known (Fig. 12) (Franke *et al.*, 1990; Ravanello and Hruby, 1994a). L1 was recognized early on as containing immunodominant epitopes, and antisera to the L1 protein have potent neutralizing activity (Wolffe *et al.*, 1995). The ectodomain of the L1 protein contains three intramolecular disulfide bonds that are formed by the vaccinia-encoded cytoplasmic thiol oxyreductase (Section IX.E.2) (Senkevich *et al.*, 2002a); the crystal structure of the ectodomain of L1 has been solved (Su *et al.*, 2005). An inducible recombinant in which expression of the *L1R* gene is IPTG-dependent has been generated (Ravanello and Hruby, 1994b). L1 is essential for virion production; in the absence of L1, crescents are numerous and IV do form, but maturation of IV to MV does not occur. This defect can be complemented in trans by expression of wt L1, but expression of a derivative lacking the target site for myristylation, Gly2, fails to complement. Likewise, complementation is lost when the Cys residues implicated in disulfide bond formation are altered (Blouch *et al.*, 2005).

3. H3

The *H3L* gene encodes an immunodominant protein which is exposed on the surface of MV (Chertov *et al.*, 1991; Zinoviev *et al.*, 1994). Expressed at late times postinfection, the H3 protein has a C-terminal hydrophobic tail which mediates posttranslational insertion of H3 into membranes; immunoelectron microscopy suggests that

H3 is not present in membrane crescents but associates with virion membranes during IV maturation (Fig. 12) (Section IX.E) (da Fonseca *et al*., 2000a). Antisera generated against H3 have been shown to neutralize viral infectivity (Lin *et al*., 2000). A soluble form of H3 binds to heparin sulfate on the cell surface, and indeed this protein competes with virions when present during adsorption (Lin *et al*., 2000). Together, these data support the conclusion that H3 may mediate initial, low-affinity interactions between MV and the cell surface.

The *H3L* gene is not essential in tissue culture, since deletion mutants in which *H3L* has been insertionally inactivated are viable (da Fonseca *et al*., 2000b; Lin *et al*., 2000). To aid in the analysis of the function of H3, an inducible recombinant in which H3 expression is IPTG-dependent has also been constructed (da Fonseca *et al*., 2000b). Deletion or repression of H3 causes a distinct phenotype: plaque size is diminished, and viral yields are reduced by approximately 10-fold. Electron microscopic analysis revealed that, in the absence of H3, production of MV is reduced, and virosomes, crescents, and IV accumulate to higher than normal levels. The absence of H3 does not prevent the incorporation of L1 (see in an earlier section) or D8 (another membrane protein associated with binding to chondroitin sulfate) into virion membranes. In sum, H3 appears to enhance the efficiency of the IV→MV transition, as well as mediating interactions between virions and heparin sulfate moieties found on the surface of target cells.

E. Restructuring the Particle Surface

1. Loss of D13

As described previously, IV and IVN are coated on their outer surface with a "spicule layer" composed of a honeycomb lattice of the D13 protein (Section VI.E) (Dales and Mosbach, 1968; Szajner *et al*., 2005). Electron microscopic observations led Dales and coworkers to conclude that during the transition from IVN to MV, the spicule layer was lost and replaced by a morphologically distinct structure, "surface tubule elements" (Dales and Pogo, 1981). Although low levels of the D13 protein have been found within purified MV by immunoblot analysis and mass spectroscopy (Chung *et al*., 2006; Miner and Hruby, 1989), this association is probably fortuitous (Franke and Hruby, 1987); immunoelectron microscopy reveals that anti-D13 antibodies decorate IV but not MV within infected cells (Mohandas and Dales, 1995; Sodeik *et al*., 1994). It is now accepted that, during the transition from

IV to MV, the D13 spicules are indeed lost from the maturing virus particles. Understanding the signal that initiates this disassociation will be of significant interest.

2. Disulfide Bond Formation

Numerous vaccinia virion structural proteins contain intra or intermolecular disulfide bonds. These include the core proteins A4, L4, and A10 (4a), and the membrane proteins A14, A17, A27, D8, L1, A28, A21, L5, and H2 (Ichihashi and Oie, 1996; Ichihashi *et al*., 1984; Locker and Griffiths, 1999; Oie and Ichihashi, 1981; Rodriguez *et al*., 1987, 1993; Senkevich and Moss, 2005; Senkevich *et al*., 2000b, 2004a; Townsley *et al*., 2005a,b; Senkevich, T. G., personal communication; Wolffe *et al*., 1995). Disulfide bond formation in a subset of the membrane proteins, L1, A28, A21, L5, and H2, is controlled by a virally encoded redox system, and disruption of this redox system disrupts virus morphogenesis, as described in the following paragraphs.

The vaccinia coded redox system was uncovered through investigation of vaccinia genes which are conserved throughout poxviruses and which also contained sequence motifs suggestive of redox capability (Senkevich *et al*., 2000a,b; White *et al*., 2000). The complete pathway consists of the E10, A2.5, and G4 proteins, which interact with each other to catalyze a cascade of disulfide oxidation–reduction reactions shown in Fig. 14, sequentially oxidizing and reducing intramolecular disulfide bonds within each enzyme and ultimately resulting in formation of intramolecular disulfide bonds in a number of target proteins (Senkevich *et al*., 2002a). All three redox enzymes are associated with the virion; E10 and G4 both seem to be concentrated in the virion membrane. The target proteins include L1, F9, A28, A21, L5, and H2 (Senkevich *et al*., 2000b, 2004a; Townsley *et al*., 2005a,b). L1 is described in Section IX.D.2, and A28, A21, L5, and H2, all components of

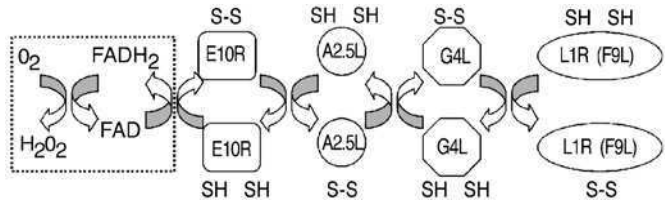

FIG 14. Vaccinia virus disulfide bond formation pathway. The coupled thiol-disulfide exchange reactions from E10R to the substrate proteins L1R and F9L are depicted. Electron transfers to FAD and oxygen indicated in the dashed rectangle are hypothetical (Senkevich *et al*., 2002a). Reprinted from Senkevich *et al*. (2002a) with permission.

a membrane-anchored complex controlling virus entry, are discussed in Section IX.G.3. The F9 protein shows significant homology to L1, containing the same six conserved cysteines, although the role of F9 in infection is currently unknown (Senkevich *et al*., 2000b).

Repression of any of the three enzymes of the redox pathway, E10, A2.5, or G4, interrupts virion morphogenesis at the IVN to MV transition (Ravanello and Hruby, 1994b; Senkevich *et al*., 2000a, 2002b; White *et al*., 2000). Specifically, in these mutants, MV are significantly decreased in number or absent from infection while IV accumulate. This does not imply that the redox pathway is active specifically during the IVN to MV transition; on the contrary, the redox substrates L1 and F9 are oxidized when morphogenesis is blocked at earlier stages by repression of the A17 membrane protein or treatment with rifampicin (Senkevich *et al*., 2000b). However, the fact that redox pathway mutants and L1 mutants (Section IX.D.2) produce the same phenotype suggests that the phenotype of the redox pathway mutants is, at least in part, a manifestation of their inability to oxidize the L1 disulfide bonds, thereby presumably rendering L1 nonfunctional (Blouch *et al*., 2005).

3. Addition of New Surface Proteins

In 1962, in a brief, prescient, and elegant report, Morgan and coworkers showed that when ferritin-labeled antibodies prepared from rabbits immunized with vaccinia virus were used in immunoelectron microscopic examination of vaccinia-infected cells, MV were stained but IV were not stained. The authors concluded "that maturation of vaccinia virus into the stable, infectious form is accompanied not only by an alteration in structure but also by the acquisition of a surface coating of antigen not present on the immature particles" (Morgan *et al*., 1962). Forty-four years later, we understand with some precision the nature of a few of these modifications. Specifically, immunoelectron microscopy of infected cells demonstrates that antibody against either of the surface proteins A27 (Section X) or H3 shows significantly more staining of MV than IV, suggesting that both proteins are added to particles during the IV to MV transition (da Fonseca *et al*., 2000a; Sodeik *et al*., 1995). As described previously (Section IX.D.3), H3 is a transmembrane protein that undergoes posttranslational insertion into virion membranes. In contrast, the peripheral protein A27 is anchored to the viral membrane via its interactions with the A17 transmembrane protein. A27 is not required for MV formation but rather for wrapping of MV with Golgi membranes to form WV. Thus, surface proteins can be incorporated during the later stages of virion

maturation by distinct mechanisms. We speculate that these additions occur after the departure of the D13 lattice from the IV membrane. Other candidates for surface proteins added during the IV to MV transition include the L1 protein (Section IX.D.2). Immunoelectron microscopy of virus infected cells using anti-L1 antibody shows a higher density of L1 staining in regions containing MV than regions containing IV (Wolffe *et al*., 1995). As described previously, L1 is required for the IV to MV transition, a process that is also stimulated by H3. It seems likely that additional surface modifications during the IV to MV transition will be revealed in the future.

Dales and coworkers have suggested that the spicule layer surrounding IV, now known to be composed of D13 protein, is replaced by the STEs appearing on MV, raising the question of the relationship between STE and the proteins added late during MV maturation (Essani *et al*., 1982; Stern and Dales, 1976). Wilton *et al*. (1995) examined the protein composition of isolated STE, and while they did not unambiguously identify each of the STE proteins, the results suggest that STE contain a mixture of proteins that appear in the crescents and MV membrane both early and late during morphogenesis, such as A17 and H3. Thus while the removal of D13 from IV and addition of several immunodominant MV membrane antigens to the developing MV may restructure the particle surface, it is likely that STE represent a complex of several of the full complement of MV membrane proteins, rather than exclusively proteins added after the removal of D13.

F. Core Proteins that are not Essential for Virion Morphogenesis but are Required for Transcriptional Competence of the Virion Core

Mutation of the genes encoding certain core proteins results, under nonpermissive conditions, in the formation of MV that are normal in appearance but not infectious. Two of these proteins, the I8 RNA helicase and the H6 topoisomerase, are virion enzymes. The phenotypes of I8 and H6 mutants are similar: permeabilized virions purified from nonpermissive infections display defects in early transcription. These data imply that the RNA helicase and DNA topoisomerase are both required to deal with the topological constraints associated with the virion transcription reaction (da Fonseca and Moss, 2003; Gross and Shuman, 1996). There also exist at least four virion proteins that are not thought to function in transcription per se but rather seem to affect the assembly of a core that is competent for *in situ* transcription. These include L4, L3, H1, and E8, described in more detail in the following sections.

1. L4

The *L4R* gene encodes a 29-kDa protein that is proteolytically processed to the mature 25-kDa form during the IV to MV transition (Fig. 13). L4 was originally referred to as VP8 and has been shown to have both DNA and RNA binding activity (Bayliss and Smith, 1997; Yang and Bauer, 1988; Yang *et al*., 1988). An inducible recombinant has been generated in which L4 expression is IPTG-dependent (Wilcock and Smith, 1994, 1996). When L4 is repressed, formation of both IV and MV is observed by electron microscopy. The IV, however, appear slightly abnormal: they possess a space between the viroplasm and the inner surface of the membrane, as if bonding of the viroplasm to the membrane is weaker than normal. L4-deficient MV contain an otherwise normal complement of virion proteins, but they are defective in transcription as judged by both *in vivo* and *in vitro* assays, and hence they are not infectious. Furthermore, when these virions are extracted with deoxycholate to solubilize virion enzymes, more proteins appear to be more easily released than when L4-containing virions are examined in parallel. Thus, the internal structure of MV assembled in the absence of L4 appears to be somewhat fragile. These findings suggest that L4 plays a structural role in the assembly of a transcriptionally-competent core; in this regard, it is worth noting that L4 was originally reported to be encapsidated at ~7000 copies/virion.

2. L3

The *L3L* gene encodes a highly conserved 41-kDa protein that is packaged into virion cores. Repression of L3 expression results in the assembly of MV that are ultrastructurally normal in appearance but are reduced in infectivity (Resch and Moss, 2005). L3-deficient virions contain the normal complement of active transcription enzymes, but they are nevertheless defective for transcription *in situ*. Consistent with these observations, the L3-deficient MV can bind and enter cells, however, only very small amounts of early viral mRNA are synthesized. Thus, similar to L4 (above) and E8 (below), L3 deficiency may produce a subtle defect in MV structure that ultimately impacts on the transcriptional competency of the mutant virions.

3. H1

The *H1L* gene encodes a dual specificity protein phosphatase. This 20-kDa protein is encapsidated at ~200 copies/virion (Guan *et al*., 1991; Liu *et al*., 1995). It is known to regulate the phosphorylation status of a number of viral and cellular proteins *in vivo* and has

been shown to dephosphorylate A17, A14, and F17 *in vitro*. An inducible recombinant has been generated in which H1 expression is TET-dependent. In the absence of H1, F17, A14, and A17 are hyperphosphorylated. Moreover, the virions purified from H1-deficient infections show a phenotype much like that engendered by repression of L4: the cores show a reduced stability and are transcriptionally incompetent. Hence, H1 is not required for morphogenesis per se but rather affects the assembly of a transcriptionally competent core and hence is required for virion infectivity.

4. E8

E8 initially drew attention during a search for proteins which might associate with the ER membranes surrounding virus factories early during infection (Doglio *et al.*, 2002; Schramm and Locker, 2005; Tolonen *et al.*, 2001). The E8 amino acid sequence predicts the presence of two possible transmembrane domains, and both immunoelectron microscopy and immunofluroescence suggests an association with viral and cellular membranes during infection. These observations led Locker and coworkers to propose a role for E8 in mediating the assembly of ER-delimited cytoplasmic domains within which viral replication would occur (Schramm and Locker, 2005) (Fig. 5) (Section V). However, other observations seem inconsistent with this model. First, the E8 protein clearly partitions to the virion core on extraction with NP40 and DTT. Second, while Locker and coworkers reported that E8 was expressed early during infection, more recent experiments demonstrate that *E8R* is a late gene, making it unlikely that the protein plays a role early during infection (Kato, Condit, and Moussatche, unpublished; Nichols and Traktman, unpublished). Lastly, infections with a temperature-sensitive mutant containing a lesion in the *E8R* gene result in the assembly of morphologically normal MV, WV, and EV; the MV that form show a defect in transcription *in situ* and a significant reduction in infectivity (Kato, Condit, and Moussatche, unpublished). Thus, in many respects E8 behaves like a structural protein that contributes to the assembly of a transcriptionally active core, similar to L4, L3, or H1.

G. Membrane Proteins Affecting Virus Binding, Entry, and Fusion

Several additional MV membrane proteins have been identified which, when mutated, result in formation of MV that are morphologically normal in appearance. Ten of these proteins have roles in virus entry and/or fusion as detailed in the following section.

1. Entry/Fusion Complex

A complex of eight interacting proteins has been described, which is anchored in the virion membrane and whose components appear to mediate fusion of the virion membrane with the plasma membrane during virus entry (Ojeda *et al.*, 2006; Senkevich and Moss, 2005; Senkevich *et al.*, 2004b, 2005; Townsley *et al.*, 2005a,b). The complex contains the proteins A21, L5, A28, H2, G3, G9, A16, and J5. At least four of the proteins contain intramolecular disulfide bonds catalyzed by the virus coded redox system (Section IX.E.2), and three are myristylated. Inducible mutants have been constructed for five of the genes encoding fusion complex proteins, and in all cases the mutants produce MV that are morphologically normal and transcriptionally active and which can undergo wrapping and export from cells as EV. These mutant MV can bind to cells but are defective in penetration. Repression of individual components of the complex does not appear to block the insertion of the remaining proteins into the virion membrane, although it does disrupt their ability to mediate virion entry. In sum, the membrane fusion complex is dispensable for virion morphogenesis but essential for virion entry.

2. I2

The *I2L* gene encodes a 78-amino acid protein with a hydrophobic C-terminus predicted to serve as a transmembrane anchor. Indeed (Nichols, Stanitsa, Traktman, submitted for publication), I2L is expressed late, behaves as an integral membrane protein, and is encapsidated into the virion membrane. I2 appears to be an essential protein, and an inducible recombinant in which I2 expression is TET dependent has been generated. In the absence of I2, the viral life cycle progresses normally, but the MV that are produced show an ~400-fold reduction in specific infectivity. These virions are transcriptionally competent and can bind to target cells but are defective in fusion-mediated entry. Interactions between I2 and the entry complex described previously have not been investigated.

3. D8

The D8 protein is expressed late and incorporated into the virion membrane; the transmembrane domain is found at the N-terminus of the protein, and the C-terminus is exposed on the surface of the virions (Niles and Seto, 1988). D8 is one of three proteins, including A27 and H3, which bind cell surface glycosaminoglycans and are therefore

implicated in initial events that facilitate the binding of virus to cells (Chung *et al.*, 1998; Hsiao *et al.*, 1998, 1999; Lin *et al.*, 2000). A soluble form of D8 has been shown to bind to chondroitin sulfate on the cell surface and to compete with virions for binding to the cell (Hsiao *et al.*, 1999). Viruses in which D8 has been insertionally inactivated are viable and direct normal morphogenesis; however, the virions that are produced show a 10-fold reduction in specific infectivity due to an impaired ability to bind to target cells.

X. Transport, Occlusion, and Secondary Wrapping of MV

As noted previously (Section III), most MV localize in clusters within the cytoplasm that are distal from the virus factories in which IV and IVN are assembled. Treatment of infected cells with drugs that inhibit microtubule formation prevents this characteristic trafficking, implying that MV dissemination is a microtubule-mediated process (Sanderson *et al.*, 2000). The mechanism by which MV interacts with microtubules has been investigated but remains unresolved (Sanderson *et al.*, 2000; Ward, 2005).

While the majority of MV remain intracellular and represent a functional end stage to virus assembly, a fraction of MV may undergo further processing to be either exported as EV or embedded within A-type inclusions (ATIs). Two MV membrane proteins are implicated in these processes, A27 and A26.

A. A27

A27 is unusual among MV membrane proteins in that it does not contain a transmembrane domain. Instead, the A27 protein forms a disulfide-bonded trimer, which is anchored to the MV membrane via a strong interaction with the integral A17 membrane protein (Lai *et al.*, 1990; Rodriguez *et al.*, 1987, 1993). A27 is an immunodominant antigen, and anti-A27 antibodies possess virus neutralizing activity (Rodriguez *et al.*, 1985). As described previously, A27 is added to virus particles late during maturation; it appears on MV but not IV (Section IX.E.3). When A27 is repressed, morphologically normal MV form that are fully infectious, although they are unable to undergo secondary wrapping by Golgi-derived membranes to form WV and, ultimately, to be released by exocytosis as EV (Rodriguez and Smith, 1990b; Ward, 2005). The A27 protein has also been implicated in attachment of virus to cells and in intracellular transport of MV (Chung *et al.*, 1998; Sanderson *et al.*, 2000).

B. A26

ATIs are large, cytoplasmic, electron-dense regions within which numerous MV are embedded (McKelvey *et al*., 2002). Formation of ATIs requires two viral genes, the *ATI* gene and the *A26L* gene. The *ATI* gene encodes the protein that forms the inclusion; the *ATI* gene is not essential, and indeed the WR strain of vaccinia does not express an intact ATI protein and hence does not form inclusions. The *A26L* gene, on the other hand, encodes an MV membrane protein, initially named p4c, which controls whether or not MV become embedded in inclusions. A26 is nonessential: if the *p4c* gene is inactivated, infectious MV, WV, and EV are produced. However, any inclusions that are formed do not contain embedded virus (McKelvey *et al*., 2002). The A26 protein is present on the surface of MV but not EEV, and it is therefore possible that the presence or absence of p4c in the virion membrane may influence whether MV undergo secondary wrapping to become WV and EV, or whether they remain unwrapped in the cytoplasm (Ulaeto *et al*., 1996). It is not yet known how A26 associates with the MV membrane; although some computer algorithms have predicted the presence of a transmembrane region, others do not, and the protein does not contain any regions of significant hydrophobicity. However, the A26 protein does contain a C-terminal region that is 44% identical to the region of the A27 protein that interacts with the membrane-bound A17 protein (see earlier). This observation raises the interesting possibility that A26 and A27 may compete for binding to A17 and thus determine the balance between MV that remain unwrapped and those that continue on to form WV and EV.

XI. Virion Proteins of Unknown Function

Four additional virion proteins of unknown function have been discussed in the literature: the E11 and A12 core proteins and the I5 and A14.5 membrane proteins (Fig. 12). Little is known about E11 except that temperature-sensitive mutants with lesions in this gene produce noninfectious virions at the nonpermissive temperature (Wang and Shuman, 1996). An inducible recombinant in which expression of A14.5 is IPTG-dependent has been generated; repression of this protein has no impact on the viral life cycle in culture but leads to an attenuated phenotype in mice (Betakova *et al*., 2000). I5 (VP13) and A12 were identified during proteomic analyses of the vaccinia virion (Chung *et al*., 2006; Takahashi *et al*., 1994). No function has been ascribed to

either protein as neither gene has been subjected to genetic analysis, although both genes are highly conserved among poxviral genomes and as such the proteins are likely to play significant roles(s) during some facet of the viral life cycle. Encapsidation of I5 into the virion membrane has been verified by analysis of a virus encoding an epitope-tagged I5 allele at the endogenous locus (Nichols, Stanitsa, and Traktman, unpublished). The A12 core protein undergoes proteolytic maturation during virion morphogenesis (Whitehead and Hruby, 1994b).

XII. Summary and Perspectives

Investigation into poxvirus structure and assembly is now at a technical and conceptual crossroads. Identification of proteins in the virion and basic characterization of mutants affecting assembly is approaching saturation. A detailed picture of the contribution of individual genes to the structure and stepwise assembly of the virion is therefore beginning to emerge. The genetic, biochemical and cell biological tools are in place to bring this task to completion. Fascinating and significant questions remain to be answered, including:

A. What are the precise localizations within the virion of each of the encapsidated proteins? What is the composition and structure of the tube-like structure within the core? What proteins make up the individual layers of the core wall? What proteins are contained in the lateral bodies and what are their functions? What are the structural relationships among the proteins in the membrane and how does this contribute to the bilaminar appearance of this structure?

B. What is the initial source of the membrane used to form crescents, how is the single bilayer of the crescents and IV assembled and stabilized in the virus factories, and what are the contributions of cellular components and individual viral proteins to this process?

C. How are viral factories organized so that assembly components are delivered to maturing virions in an organized fashion?

D. What are the details of the molecular interactions that bind crescents to viroplasm, and how does this relate to the ultimate maturation of the virion core?

E. What is the precise mechanism of DNA encapsidation into virions?

F. What triggers the transition from IVN to MV, and how are the various events in this transition co-coordinated, including loss of D13, restructuring of the virion surface, proteolysis of structural proteins,

maturation of the core, and migration of maturing virions from factories to the periphery of the cell?

A thorough understanding of poxvirus morphogenesis will provide invaluable insights into this complex and biomedically significant virus. Moreover, these studies should lead to the elucidation and discovery of cell biological strategies that have deep relevance to such diverse processes as organelle biogenesis, intracellular protein trafficking, and membrane remodeling.

Acknowledgments

We thank Bernie Moss and John Heuser for helpful discussions while the manuscript was being written. We thank Bernie Moss and Wen Chang for communicating data in advance of publication. We thank Jason Mercer for help in figure preparation. We thank Michel Moussatche for his expert rendering of the vaccinia virion model. Work described herein was supported by a grant to RCC from the NIH (5R01-AI055560) and by grants to PT from the NIH (9R01 AI 063620-11) and the GLRCE (sub-contract, 1-U54-AI057153).

References

Andres, G., Alejo, A., Simon-Mateo, C., and Salas, M. L. (2001). African swine fever virus protease, a new viral member of the SUMO-1-specific protease family. *J. Biol. Chem.* **276:**780–787.

Ansarah-Sobrinho, C., and Moss, B. (2004a). Vaccinia virus G1 protein, a predicted metalloprotease, is essential for morphogenesis of infectious virions but not for cleavage of major core proteins. *J. Virol.* **78:**6855–6863.

Ansarah-Sobrinho, C., and Moss, B. (2004b). Role of the I7 protein in proteolytic processing of vaccinia virus membrane and core components. *J. Virol.* **78:**6335–6343.

Armstrong, J. A., Metz, D. H., and Young, M. R. (1973). The mode of entry of vaccinia virus into L cells. *J. Gen. Virol.* **21:**533–537.

Baldick, C. J., Jr., and Moss, B. (1987). Resistance of vaccinia virus to rifampicin conferred by a single nucleotide substitution near the predicted NH2 terminus of a gene encoding an Mr 62,000 polypeptide. *Virology* **156:**138–145.

Bayliss, C. D., and Smith, G. L. (1997). Vaccinia virion protein VP8, the 25 kDa product of the L4R gene, binds single-stranded DNA and RNA with similar affinity. *Nucleic Acids Res.* **25:**3984–3990.

Beaud, G., and Beaud, R. (2000). Temperature-dependent phosphorylation state of the H5R protein synthesised at the early stage of infection in cells infected with vaccinia virus ts mutants of the B1R and F10L protein kinases. *Intervirology* **43:**67–70.

Beaud, G., Beaud, R., and Leader, D. P. (1995). Vaccinia virus gene H5R encodes a protein that is phosphorylated by the multisubstrate vaccinia virus B1R protein kinase. *J. Virol.* **69:**1819–1826.

Betakova, T., and Moss, B. (2000). Disulfide bonds and membrane topology of the vaccinia virus A17L envelope protein. *J. Virol.* **74:**2438–2442.

Betakova, T., Wolffe, E. J., and Moss, B. (1999a). Membrane topology of the vaccinia virus A17L envelope protein. *Virology* **261:**347–356.

Betakova, T., Wolffe, E. J., and Moss, B. (1999b). Regulation of vaccinia virus morphogenesis: Phosphorylation of the A14L and A17L membrane proteins and C-terminal truncation of the A17L protein are dependent on the F10L kinase. *J. Virol.* **73:**3534–3543.

Betakova, T., Wolffe, E. J., and Moss, B. (2000). The vaccinia virus A14.5L gene encodes a hydrophobic 53-amino-acid virion membrane protein that enhances virulence in mice and is conserved among vertebrate poxviruses. *J. Virol.* **74:**4085–4092.

Black, E. P., Moussatche, N., and Condit, R. C. (1998). Characterization of the interactions among vaccinia virus transcription factors G2R, A18R, and H5R. *Virology* **245:**313–322.

Blouch, R. E., Byrd, C. M., and Hruby, D. E. (2005). Importance of disulphide bonds for vaccinia virus L1R protein function. *Virology J.* **2:**91.

Brown, N. G., Nick, M. D., Beaud, G., Hardie, G., and Leader, D. P. (2000). Identification of sites phosphorylated by the vaccinia virus B1R kinase in viral protein H5R. *BMC Biochem.* **1:**2.

Broyles, S. S. (2003). Vaccinia virus transcription. *J. Gen. Virol.*(on line. 2003).

Byrd, C. M., Bolken, T. C., and Hruby, D. E. (2002). The vaccinia virus I7L gene product is the core protein proteinase. *J. Virol.* **76:**8973–8976.

Byrd, C. M., Bolken, T. C., and Hruby, D. E. (2003). Molecular dissection of the vaccinia virus I7L core protein proteinase. *J. Virol.* **77:**11279–11283.

Byrd, C. M., and Hruby, D. E. (2005). A conditional-lethal vaccinia virus mutant demonstrates that the I7L gene product is required for virion morphogenesis. *Virology J.* **2:**4.

Cairns, J. (1960). The initiation of vaccinia infection. *Virology* **11:**603–623.

Carter, G. C., Law, M., Hollinshead, M., and Smith, G. L. (2005). Entry of the vaccinia virus intracellular mature virion and its interactions with glycosaminoglycans. *J. Gen. Virol.* **86:**1279–1290.

Cassetti, M. C., Merchlinsky, M., Wolffe, E. J., Weisberg, A. S., and Moss, B. (1998). DNA packaging mutant: Repression of the vaccinia virus A32 gene results in noninfectious, DNA-deficient, spherical, enveloped particles. *J. Virol.* **72:**5769–5780.

Castro, A. P., Carvalho, T. M., Moussatche, N., and Damaso, C. R. (2003). Redistribution of cyclophilin A to viral factories during vaccinia virus infection and its incorporation into mature particles. *J. Virol.* **77:**9052–9068.

Chertov, O. Y., Telezhinskaya, I. N., Zaitseva, E. V., Golubeva, T. B., Zinov'ev, V. V., Ovechkina, L. G., Mazkova, L. B., and Malygin, E. G. (1991). Amino acid sequence determination of vaccinia virus immunodominant protein p35 and identification of the gene. *Biomed. Sci.* **2:**151–154.

Chiu, W. L., and Chang, W. (2002). Vaccinia virus J1R protein: A viral membrane protein that is essential for virion morphogenesis. *J. Virol.* **76:**9575–9587.

Chiu, W. L., Szajner, P., Moss, B., and Chang, W. (2005). Effects of a temperature sensitivity mutation in the J1R protein component of a complex required for vaccinia virus assembly. *J. Virol.* **79:**8046–8056.

Christen, L., Higman, M. A., and Niles, E. G. (1992). Phenotypic characterization of three temperature-sensitive mutations in the vaccinia virus early gene transcription initiation factor. *J. Gen. Virol.* **73**(Pt. 12)**:**3155–3167.

Chung, C. S., Hsiao, J. C., Chang, Y. S., and Chang, W. (1998). A27L protein mediates vaccinia virus interaction with cell surface heparan sulfate. *J. Virol.* **72:**1577–1585.

Chung, C. S., Chen, C. H., Ho, M. Y., Hwang, C. Y., Liao, C. L., and Chang, W. (2006). Vaccinia virus proteome: Identification of proteins in vaccinia virus intracellular mature virion particles. *J. Virol.* **80:** 2127–2140.

Condit, R. C., and Niles, E. G. (1990). Orthopoxvirus genetics. *Curr. Top. Microbiol. Immunol.* **163:**1–39.

Cudmore, S., Blasco, R., Vincentelli, R., Esteban, M., Sodeik, B., Griffiths, G., and Krijnse, L. J. (1996). A vaccinia virus core protein, p39, is membrane associated. *J. Virol.* **70:**6909–6921.

Cyrklaff, M., Risco, C., Fernandez, J. J., Jimenez, M. V., Esteban, M., Baumeister, W., and Carrascosa, J. L. (2005). Cryo-electron tomography of vaccinia virus. *Proc. Natl. Acad. Sci. USA* **102:**2772–2777.

da Fonseca, F., and Moss, B. (2003). Poxvirus DNA topoisomerase knockout mutant exhibits decreased infectivity associated with reduced early transcription. *Proc. Natl. Acad. Sci. USA* **100:**11291–11296.

da Fonseca, F. G., Wolffe, E. J., Weisberg, A., and Moss, B. (2000a). Characterization of the vaccinia virus H3L envelope protein: Topology and posttranslational membrane insertion via the C-terminal hydrophobic tail. *J. Virol.* **74:**7508–7517.

da Fonseca, F. G., Wolffe, E. J., Weisberg, A., and Moss, B. (2000b). Effects of deletion or stringent repression of the H3L envelope gene on vaccinia virus replication. *J. Virol.* **74:**7518–7528.

da Fonseca, F. G., Weisberg, A. S., Caeiro, M. F., and Moss, B. (2004). Vaccinia virus mutants with alanine substitutions in the conserved G5R gene fail to initiate morphogenesis at the nonpermissive temperature. *J. Virol.* **78:**10238–10248.

Dales, S. (1962). An electron microscope study of the early association between two mammalian viruses and their hosts. *J. Cell Biol.* **13:**303–322.

Dales, S. (1963). The uptake and development of vaccinia virus in strain L cells followed with labeled viral deoxyribonucleic acid. *J. Cell Biol.* **18:**51–72.

Dales, S., and Kajioka, R. (1964). The cycle of multiplication of vaccinia virus in Earle's strain L cells. I. Uptake and penetration. *Virology* **24:**278–294.

Dales, S., and Mosbach, E. H. (1968). Vaccinia as a model for membrane biogenesis. *Virology* **35:**564–583.

Dales, S., and Pogo, B. G. (1981). Biology of poxviruses. *Virol. Monogr.* **18:**1–109.

Dales, S., and Siminovitch, L. (1961). The development of vaccinia virus in Earle's L strain cells as examined by electron microscopy. *J. Biophys. Biochem. Cytol.* **10:**475–503.

Dellis, S., Strickland, K. C., McCrary, W. J., Patel, A., Stocum, E., and Wright, C. F. (2004). Protein interactions among the vaccinia virus late transcription factors. *Virology* **329:**328–336.

Demasi, J., and Traktman, P. (2000). Clustered charge-to-alanine mutagenesis of the vaccinia virus H5 gene: Isolation of a dominant, temperature-sensitive mutant with a profound defect in morphogenesis. *J. Virol.* **74:**2393–2405.

Demasi, J., Du, S., Lennon, D., and Traktman, P. (2001a). Vaccinia virus telomeres: Interaction with the viral I1, I6, and K4 proteins. *J. Virol.* **75:**10090–10105.

Demasi, J., Du, S., Lennon, D., and Traktman, P. (2001b). Vaccinia virus telomeres: Interaction with the viral I1, I6, and K4 proteins. *J. Virol.* **75:**10090–10105.

Demkowicz, W. E., Maa, J. S., and Esteban, M. (1992). Identification and characterization of vaccinia virus genes encoding proteins that are highly antigenic in animals and are immunodominant in vaccinated humans. *J. Virol.* **66:**386–398.

Derrien, M., Punjabi, A., Khanna, M., Grubisha, O., and Traktman, P. (1999). Tyrosine phosphorylation of A17 during vaccinia virus infection: Involvement of the H1 phosphatase and the F10 kinase. *J. Virol.* **73:**7287–7296.

Doglio, L., De, M. A., Schleich, S., Roos, N., and Krijnse, L. J. (2002). The vaccinia virus E8R gene product: A viral membrane protein that is made early in infection and packaged into the virions' core. *J. Virol.* **76:**9773–9786.

Dubochet, J., Adrian, M., Richter, K., Garces, J., and Wittek, R. (1994). Structure of intracellular mature vaccinia virus observed by cryoelectron microscopy. *J. Virol.* **68:**1935–1941.

Dyster, L. M., and Niles, E. G. (1991). Genetic and biochemical characterization of vaccinia virus genes D2L and D3R which encode virion structural proteins. *Virology* **182:**455–467.

Easterbrook, K. B. (1966). Controlled degradation of vaccinia virions *in vitro*: An electron microscopic study. *J. Ultrastruct. Res.* **14:**484–496.

Ericsson, M., Cudmore, S., Shuman, S., Condit, R. C., Griffiths, G., and Locker, J. K. (1995). Characterization of ts 16, a temperature-sensitive mutant of vaccinia virus. *J. Virol.* **69:**7072–7086.

Ericsson, M., Sodeik, B., Locker, J. K., and Griffiths, G. (1997). *In vitro* reconstitution of an intermediate assembly stage of vaccinia virus. *Virology* **235:**218–227.

Essani, K., and Dales, S. (1979). Biogenesis of vaccinia: Evidence for more than 100 polypeptides in the virion. *Virology* **95:**385–394.

Essani, K., Dugre, R., and Dales, S. (1982). Biogenesis of vaccinia: Involvement of spicules of the envelope during virion assembly examined by means of conditional lethal mutants and serology. *Virology* **118:**279–292.

Fenner, F., Wittek, R., and Dumbell, K. R. (1989). "The orthopoxviruses." Academic Press, San Diego.

Franke, C. A., and Hruby, D. E. (1987). Association of non-viral proteins with recombinant vaccinia virus virions. *Arch. Virol.* **94:**347–351.

Franke, C. A., Wilson, E. M., and Hruby, D. E. (1990). Use of a cell-free system to identify the vaccinia virus L1R gene product as the major late myristylated virion protein M25. *J. Virol.* **64:**5988–5996.

Gaigg, B., Simbeni, R., Hrastnik, C., Paltauf, F., and Daum, G. (1995). Characterization of a microsomal subfraction associated with mitochondria of the yeast, *Saccharomyces cerevisiae*. Involvement in synthesis and import of phospholipids into mitochondria. *Biochim. Biophys. Acta* **1234:**214–220.

Garcia, A. D., and Moss, B. (2001). Repression of vaccinia virus holliday junction resolvase inhibits processing of viral DNA into unit-length genomes. *J. Virol.* **75:**6460–6471.

Garcia, A. D., Aravind, L., Koonin, E. V., and Moss, B. (2000). Bacterial-type DNA holliday junction resolvases in eukaryotic viruses. *Proc. Natl. Acad. Sci. USA* **97:**8926–8931.

Goebel, S. J., Johnson, G. P., Perkus, M. E., Davis, S. W., Winslow, J. P., and Paoletti, E. (1990). The complete DNA sequence of vaccinia virus. *Virology* **179:**247–263.

Gordon, J., Mohandas, A., Wilton, S., and Dales, S. (1991). A prominent antigenic surface polypeptide involved in the biogenesis and function of the vaccinia virus envelope. *Virology* **181:**671–686.

Griffiths, G., Roos, N., Schleich, S., and Locker, J. K. (2001a). Structure and assembly of intracellular mature vaccinia virus: Thin-section analyses. *J. Virol.* **75:**11056–11070.

Griffiths, G., Wepf, R., Wendt, T., Locker, J. K., Cyrklaff, M., and Roos, N. (2001b). Structure and assembly of intracellular mature vaccinia virus: Isolated-particle analysis. *J. Virol.* **75:**11034–11055.

Grimley, P. M., Rosenblum, E. N., Mims, S. J., and Moss, B. (1970). Interruption by Rifampin of an early stage in vaccinia virus morphogenesis: Accumulation of membranes which are precursors of virus envelopes. *J. Virol.* **6:**519–533.

Grosenbach, D. W., Hansen, S. G., and Hruby, D. E. (2000). Identification and analysis of vaccinia virus palmitylproteins. *Virology* **275:**193–206.

Gross, C. H., and Shuman, S. (1996). Vaccinia virions lacking the RNA helicase nucleoside triphosphate phosphohydrolase II are defective in early transcription. *J. Virol.* **70:**8549–8557.

Grubisha, O., and Traktman, P. (2003). Genetic analysis of the vaccinia virus I6 telomere-binding protein uncovers a key role in genome encapsidation. *J. Virol.* **77:**10929–10942.

Guan, K. L., Broyles, S. S., and Dixon, J. E. (1991). A Tyr/Ser protein phosphatase encoded by vaccinia virus. *Nature* **350:**359–362.

Hassett, D. E., and Condit, R. C. (1994). Targeted construction of temperature-sensitive mutations in vaccinia virus by replacing clustered charged residues with alanine. *Proc. Natl. Acad. Sci. USA* **91:**4554–4558.

Hassett, D. E., Lewis, J. I., Xing, X., DeLange, L., and Condit, R. C. (1997). Analysis of a temperature-sensitive vaccinia virus mutant in the viral mRNA capping enzyme isolated by clustered charge-to-alanine mutagenesis and transient dominant selection. *Virology* **238:**391–409.

Hedengren-Olcott, M., Byrd, C. M., Watson, J., and Hruby, D. E. (2004). The vaccinia virus G1L putative metalloproteinase is essential for viral replication *in vivo*. *J. Virol.* **78:**9947–9953.

Heljasvaara, R., Rodriguez, D., Risco, C., Carrascosa, J. L., Esteban, M., and Rodriguez, J. R. (2001). The major core protein P4a (A10L gene) of vaccinia virus is essential for correct assembly of viral DNA into the nucleoprotein complex to form immature viral particles. *J. Virol.* **75:**5778–5795.

Hellen, C. U., and Wimmer, E. (1992). The role of proteolytic processing in the morphogenesis of virus particles. *Experientia* **48:**201–215.

Heuser, J. (2005). Deep-etch EM reveals that the early poxvirus envelope is a single membrane bilayer stabilized by a geodetic "honeycomb" surface coat. *J. Cell Biol.* **169:**269–283.

Hiller, G., Eibl, H., and Weber, K. (1981). Acyl bis(monoacylglycero)phosphate, assumed to be a marker for lysosomes, is a major phospholipid of vaccinia virions. *Virology* **113:**761–764.

Hollinshead, M., Vanderplasschen, A., Smith, G. L., and Vaux, D. J. (1999). Vaccinia virus intracellular mature virions contain only one lipid membrane. *J. Virol.* **73:**1503–1517.

Holowczak, J. A. (1982). Poxvirus DNA. *Curr. Top. Microbiol. Immunol.* **97:**27–79.

Holowczak, J. A., Thomas, V. I., and Flores, L. (1975). Isolation and characterization of vaccinia virus "nucleoids." *Virology* **67:**506–519.

Hooda-Dhingra, U., Thompson, C. L., and Condit, R. C. (1989). Detailed phenotypic characterization of five temperature-sensitive mutants in the 22- and 147-kilodalton subunits of vaccinia virus DNA-dependent RNA polymerase. *J. Virol.* **63:**714–729.

Hsiao, J. C., Chung, C. S., and Chang, W. (1998). Cell surface proteoglycans are necessary for A27L protein-mediated cell fusion: Identification of the N-terminal region of A27L protein as the glycosaminoglycan-binding domain. *J. Virol.* **72:**8374–8379.

Hsiao, J. C., Chung, C. S., and Chang, W. (1999). Vaccinia virus envelope D8L protein binds to cell surface chondroitin sulfate and mediates the adsorption of intracellular mature virions to cells. *J. Virol.* **73:**8750–8761.

Hu, X., Carroll, L. J., Wolffe, E. J., and Moss, B. (1996). *De novo* synthesis of the early transcription factor 70-kilodalton subunit is required for morphogenesis of vaccinia virions. *J. Virol.* **70:**7669–7677.

Hu, X., Wolffe, E. J., Weisberg, A. S., Carroll, L. J., and Moss, B. (1998). Repression of the A8L gene, encoding the early transcription factor 82-kilodalton subunit, inhibits morphogenesis of vaccinia virions. *J. Virol.* **72:**104–112.

Husain, M., and Moss, B. (2003). Evidence against an essential role of COPII-mediated cargo transport to the endoplasmic reticulum-Golgi intermediate compartment in the formation of the primary membrane of vaccinia virus. *J. Virol.* **77:**11754–11766.

Ichihashi, Y., and Oie, M. (1996). Neutralizing epitope on penetration protein of vaccinia virus. *Virology* **220:**491–494.

Ichihashi, Y., Oie, M., and Tsuruhara, T. (1984). Location of DNA-binding proteins and disulfide-linked proteins in vaccinia virus structural elements. *J. Virol.* **50:**929–938.

Ishii, K., and Moss, B. (2001). Role of vaccinia virus A20R protein in DNA replication: Construction and characterization of temperature-sensitive mutants. *J. Virol.* **75:**1656–1663.

Ishii, K., and Moss, B. (2002). Mapping interaction sites of the A20R protein component of the vaccinia virus DNA replication complex. *Virology* **303:**232–239.

Jensen, O. N., Houthaeve, T., Shevchenko, A., Cudmore, S., Ashford, T., Mann, M., Griffiths, G., and Krijnse, L. J. (1996). Identification of the major membrane and core proteins of vaccinia virus by two-dimensional electrophoresis. *J. Virol.* **70:**7485–7497.

Johnson, G. P., Goebel, S. J., and Paoletti, E. (1993). An update on the vaccinia virus genome. *Virology* **196:**381–401.

Kane, E. M., and Shuman, S. (1992). Temperature-sensitive mutations in the vaccinia virus H4 gene encoding a component of the virion RNA polymerase. *J. Virol.* **66:**5752–5762.

Kane, E. M., and Shuman, S. (1993). Vaccinia virus morphogenesis is blocked by a temperature-sensitive mutation in the I7 gene that encodes a virion component. *J. Virol.* **67:**2689–2698.

Kao, S. Y., and Bauer, W. R. (1987). Biosynthesis and phosphorylation of vaccinia virus structural protein VP11. *Virology* **159:**399–407.

Kao, S. Y., Ressner, E., Kates, J., and Bauer, W. R. (1981). Purification and characterization of a superhelix binding protein from vaccinia virus. *Virology* **111:**500–508.

Kato, S. E., Strahl, A. L., Moussatche, N., and Condit, R. C. (2004). Temperature-sensitive mutants in the vaccinia virus 4b virion structural protein assemble malformed, transcriptionally inactive intracellular mature virions. *Virology* **330:**127–146.

Katz, E., and Moss, B. (1970a). Formation of a vaccinia virus structural polypeptide from a higher molecular weight precursor: Inhibition by rifampicin. *Proc. Natl. Acad. Sci. USA* **66:**677–684.

Katz, E., and Moss, B. (1970b). Vaccinia virus structural polypeptide derived from a high-molecular-weight precursor: Formation and integration into virus particles. *J. Virol.* **6:**717–726.

Klemperer, N., Ward, J., Evans, E., and Traktman, P. (1997). The vaccinia virus I1 protein is essential for the assembly of mature virions. *J. Virol.* **71:**9285–9294.

Koonin, E. V., Senkevich, T. G., and Chernos, V. I. (1993). Gene A32 product of vaccinia virus may be an ATPase involved in viral DNA packaging as indicated by sequence comparisons with other putative viral ATPases. *Virus Genes* **7:**89–94.

Kovacs, G. R., and Moss, B. (1996). The vaccinia virus H5R gene encodes late gene transcription factor 4: Purification, cloning, and overexpression. *J. Virol.* **70:**6796–6802.

Krijnse-Locker, J., Schleich, S., Rodriguez, D., Goud, B., Snijder, E. J., and Griffiths, G. (1996). The role of a 21-kDa viral membrane protein in the assembly of vaccinia virus from the intermediate compartment. *J. Biol. Chem.* **271:**14950–14958.

Lackner, C. A., D'Costa, S. M., Buck, C., and Condit, R. C. (2003). Complementation analysis of the Dales collection of vaccinia virus temperature-sensitive mutants. *Virology* **305:**240–259.

Lai, C. F., Gong, S. C., and Esteban, M. (1990). Structural and functional properties of the 14-kDa envelope protein of vaccinia virus synthesized in *Escherichia coli*. *J. Biol. Chem.* **265:**22174–22180.

Lanzer, W., and Holowczak, J. A. (1975). Polyamines in vaccinia virions and polypeptides released from viral cores by acid extraction. *J. Virol.* **16:**1254–1264.

Law, M., Carter, G. C., Roberts, K. L., Hollinshead, M., and Smith, G. L. (2006). Ligand-induced and nonfusogenic dissolution of a viral membrane. *Proc. Natl. Acad. Sci.* **103:**5989–5994.

Lefkowitz, E. J., Upton, C., Changayil, S. S., Buck, C., Traktman, P., and Buller, R. M. (2005). Poxvirus bioinformatics resource center: A comprehensive poxviridae informational and analytical resource. *Nucleic Acids Res.* **33:**D311–D316.

Li, S. J., and Hochstrasser, M. (1999). A new protease required for cell-cycle progression in yeast. *Nature* **398:**246–251.

Lin, C. L., Chung, C. S., Heine, H. G., and Chang, W. (2000). Vaccinia virus envelope H3L protein binds to cell surface heparan sulfate and is important for intracellular mature virion morphogenesis and virus infection *in vitro* and *in vivo*. *J. Virol.* **74:**3353–3365.

Lin, S., and Broyles, S. S. (1994). Vaccinia protein kinase 2: A second essential serine/threonine protein kinase encoded by vaccinia virus. *Proc. Natl. Acad. Sci. USA* **91:**7653–7657.

Liu, K., Lemon, B., and Traktman, P. (1995). The dual-specificity phosphatase encoded by vaccinia virus, VH1, is essential for viral transcription *in vivo* and *in vitro*. *J. Virol.* **69:**7823–7834.

Locker, J. K., and Griffiths, G. (1999). An unconventional role for cytoplasmic disulfide bonds in vaccinia virus proteins. *J. Cell Biol.* **144:**267–279.

Locker, J. K., Kuehn, A., Schleich, S., Rutter, G., Hohenberg, H., Wepf, R., and Griffiths, G. (2000). Entry of the two infectious forms of vaccinia virus at the plasma membane is signaling-dependent for the IMV but not the EEV. *Mol. Biol. Cell* **11:**2497–2511.

Maa, J. S., and Esteban, M. (1987). Structural and functional studies of a 39,000-Mr immunodominant protein of vaccinia virus. *J. Virol.* **61:**3910–3919.

Malkin, A. J., McPherson, A., and Gershon, P. D. (2003). Structure of intracellular mature vaccinia virus visualized by in situ atomic force microscopy. *J. Virol.* **77:**6332–6340.

Martin, S. A., Paoletti, E., and Moss, B. (1975). Purification of mRNA guanylyltransferase and mRNA (guanine-7-) methyltransferase from vaccinia virions. *J. Biol. Chem.* **250:**9322–9329.

McCraith, S., Holtzman, T., Moss, B., and Fields, S. (2000). Genome-wide analysis of vaccinia virus protein-protein interactions. *Proc. Natl. Acad. Sci. USA* **97:**4879–4884.

McKelvey, T. A., Andrews, S. C., Miller, S. E., Ray, C. A., and Pickup, D. J. (2002). Identification of the orthopoxvirus p4c gene, which encodes a structural protein that directs intracellular mature virus particles into A-type inclusions. *J. Virol.* **76:**11216–11225.

Medzon, E. L., and Bauer, H. (1970). Structural features of vaccinia virus revealed by negative staining, sectioning, and freeze-etching. *Virology* **40:**860–867.

Mercer, J., and Traktman, P. (2003). Investigation of structural and functional motifs within the vaccinia virus A14 phosphoprotein, an essential component of the virion membrane. *J. Virol.* **77:**8857–8871.

Mercer, J., and Traktman, P. (2005). Genetic and cell biological characterization of the vaccinia virus A30 and G7 phosphoproteins. *J. Virol.* **79:**7146–7161.

Miner, J. N., and Hruby, D. E. (1989). Rifampicin prevents virosome localization of L65, an essential vaccinia virus polypeptide. *Virology* **170:**227–237.

Mohandas, A. R., and Dales, S. (1995). Involvement of spicules in the formation of vaccinia virus envelopes elucidated by a conditional lethal mutant. *Virology* **214:**494–502.

Morgan, C. (1976a). The insertion of DNA into vaccinia virus. *Science* **193:**591–592.

Morgan, C. (1976b). Vaccinia virus reexamined: Development and release. *Virology* **73:**43–58.

Morgan, C., Ellison, S. A., Rose, H. M., and Moore, D. H. (1955). Serial sections of vaccinia virus examined at one stage of development in the electron microscope. *Exp. Cell Res.* **9:**572–578.

Morgan, C., Rose, H. M., and Rifkind, R. A. (1962). Use of ferritin-conjugated antibodies in electron microscopic studies of influenza and vaccinia viruses. *Cold Spring Harb. Symp. Quant. Biol.* **27:**57–65.

Morgan, J. R., Cohen, L. K., and Roberts, B. E. (1984). Identification of the DNA sequences encoding the large subunit of the mRNA-capping enzyme of vaccinia virus. *J. Virol.* **52:**206–214.

Moss, B. (2001). Poxviridae: The viruses and their replication. *In* "Fields Virology" (D. M. Knipe and P. M. Howley, eds.), pp. 2849–2884. Lippincott Williams & Wilkins, Philadelphia.

Moss, B. (2006). Poxvirus entry and membrane fusion. *Virology* **344:**48–54.

Moss, B., Katz, E., and Rosenblum, E. N. (1969a). Vaccinia virus directed RNA and protein synthesis in the presence of rifampicin. *Biochem. Biophys. Res. Commun.* **36:**858–865.

Moss, B., Rosenblum, E. N., Katz, E., and Grimley, P. M. (1969b). Rifampicin: A specific inhibitor of vaccinia virus assembly. *Nature* **224:**1280–1284.

Nagayama, A., Pogo, B. G., and Dales, S. (1970). Biogenesis of vaccinia: Separation of early stages from maturation by means of rifampicin. *Virology* **40:**1039–1051.

Nermut, M. V. (1973). Freeze-drying and freeze-etching of viruses. *In* "Freeze-Etching Techniques and Applications" (E. L. Benedetti and P. Favard, eds.), pp. 135–150. Societe Francaise de Microscopie Electronique, Paris.

Niles, E. G., and Seto, J. (1988). Vaccinia virus gene D8 encodes a virion transmembrane protein. *J. Virol.* **62:**3772–3778.

Niles, E. G., Lee-Chen, G. J., Shuman, S., Moss, B., and Broyles, S. S. (1989). Vaccinia virus gene D12L encodes the small subunit of the viral mRNA capping enzyme. *Virology* **172:**513–522.

Nowakowski, M., Bauer, W., and Kates, J. (1978a). Characterization of a DNA-binding phosphoprotein from vaccinia virus replication complex. *Virology* **86:**217–225.

Nowakowski, M., Kates, J., and Bauer, W. (1978b). Isolation of two DNA-binding proteins from the intracellular replication complex of vaccinia virus. *Virology* **84:**260–267.

Noyes, W. F. (1962a). Further studies on the structure of vaccinia virus. *Virology* **18:**511–516.

Noyes, W. F. (1962b). The surface fine structure of vaccinia virus. *Virology* **17:**282–287.

Oie, M., and Ichihashi, Y. (1981). Characterization of vaccinia polypeptides. *Virology* **113:**263–276.

Ojeda, S., Senkevich, T. G., and Moss, B. (2006). Entry of vaccinia virus and cell-cell fusion require a highly conserved cysteine-rich membrane protein encoded by the A16L gene. *J. Virol.* **80:**51–61.

Palade, G. E. (1983). Membrane biogenesis: An overview. *Methods Enzymol.* **96:**xxix–xxLv.

Pedersen, K., Snijder, E. J., Schleich, S., Roos, N., Griffiths, G., and Locker, J. K. (2000). Characterization of vaccinia virus intracellular cores: Implications for viral uncoating and core structure. *J. Virol.* **74:**3525–3536.

Peters, D., and Mueller, G. (1963). The fine structure of the DNA-containing core of vaccinia virus. *Virology* **21:**267–269.

Pichler, H., Gaigg, B., Hrastnik, C., Achleitner, G., Kohlwein, S. D., Zellnig, G., Perktold, A., and Daum, G. (2001). A subfraction of the yeast endoplasmic reticulum associates with the plasma membrane and has a high capacity to synthesize lipids. *Eur. J. Biochem.* **268:**2351–2361.

Pogo, B. G., and Dales, S. (1971). Biogenesis of vaccinia: Separation of early stages from maturation by means of hydroxyurea. *Virology* **43:**144–151.

Punjabi, A., and Traktman, P. (2005). Cell biological and functional characterization of the vaccinia virus f10 kinase: Implications for the mechanism of virion morphogenesis. *J. Virol.* **79:**2171–2190.

Punjabi, A., Boyle, K., DeMasi, J., Grubisha, O., Unger, B., Khanna, M., and Traktman, P. (2001). Clustered charge-to-alanine mutagenesis of the vaccinia virus A20 gene: Temperature-sensitive mutants have a DNA-minus phenotype and are defective in the production of processive DNA polymerase activity. *J. Virol.* **75:**12308–12318.

Ravanello, M. P., and Hruby, D. E. (1994a). Characterization of the vaccinia virus L1R myristylprotein as a component of the intracellular virion envelope. *J. Gen. Virol.* **75** (Pt. 6)**:**1479–1483.

Ravanello, M. P., and Hruby, D. E. (1994b). Conditional lethal expression of the vaccinia virus L1R myristylated protein reveals a role in virion assembly. *J. Virol.* **68:**6401–6410.

Reggiori, F., and Klionsky, D. J. (2005). Autophagosomes: Biogenesis from scratch? *Curr. Opin. Cell Biol.* **17:**415–422.

Resch, W., and Moss, B. (2005). The conserved poxvirus L3 virion protein is required for transcription of vaccinia virus early genes. *J. Virol.* **79:**14719–14729.

Resch, W., Weisberg, A. S., and Moss, B. (2005). Vaccinia virus nonstructural protein encoded by the A11R gene is required for formation of the virion membrane. *J. Virol.* **79:**6598–6609.

Risco, C., Rodriguez, J. R., Demkowicz, W., Heljasvaara, R., Carrascosa, J. L., Esteban, M., and Rodriguez, D. (1999). The vaccinia virus 39-kDa protein forms a stable complex with the p4a/4a major core protein early in morphogenesis. *Virology* **265:**375–386.

Risco, C., Rodriguez, J. R., Lopez-Iglesias, C., Carrascosa, J. L., Esteban, M., and Rodriguez, D. (2002). Endoplasmic reticulum-Golgi intermediate compartment membranes and vimentin filaments participate in vaccinia virus assembly. *J. Virol.* **76:**1839–1855.

Rodriguez, D., Rodriguez, J. R., and Esteban, M. (1993). The vaccinia virus 14-kilodalton fusion protein forms a stable complex with the processed protein encoded by the vaccinia virus A17L gene. *J. Virol.* **67:**3435–3440.

Rodriguez, D., Esteban, M., and Rodriguez, J. R. (1995). Vaccinia virus A17L gene product is essential for an early step in virion morphogenesis. *J. Virol.* **69:**4640–4648.

Rodriguez, D., Risco, C., Rodriguez, J. R., Carrascosa, J. L., and Esteban, M. (1996). Inducible expression of the vaccinia virus A17L gene provides a synchronized system to monitor sorting of viral proteins during morphogenesis. *J. Virol.* **70:**7641–7653.

Rodriguez, D., Barcena, M., Mobius, W., Schleich, S., Esteban, M., Geerts, W. J. C., Koster, A. J., Griffiths, G., and Locker, J. K. (2006). A vaccinia virus lacking A10L: Viral core proteins accumulate on structures derived from the endoplasmic reticulum. *Cellular Microbiology* **8:**427–437.

Rodriguez, J. F., and Smith, G. L. (1990a). Inducible gene expression from vaccinia virus vectors. *Virology* **177:**239–250.

Rodriguez, J. F., and Smith, G. L. (1990b). IPTG-dependent vaccinia virus: Identification of a virus protein enabling virion envelopment by Golgi membrane and egress. *Nucleic Acids Res.* **18:**5347–5351.

Rodriguez, J. F., Janeczko, R., and Esteban, M. (1985). Isolation and characterization of neutralizing monoclonal antibodies to vaccinia virus. *J. Virol.* **56:**482–488.

Rodriguez, J. F., Paez, E., and Esteban, M. (1987). A 14,000-Mr envelope protein of vaccinia virus is involved in cell fusion and forms covalently linked trimers. *J. Virol.* **61:**395–404.

Rodriguez, J. R., Risco, C., Carrascosa, J. L., Esteban, M., and Rodriguez, D. (1997). Characterization of early stages in vaccinia virus membrane biogenesis: Implications of the 21-kilodalton protein and a newly identified 15-kilodalton envelope protein. *J. Virol.* **71:**1821–1833.

Rodriguez, J. R., Risco, C., Carrascosa, J. L., Esteban, M., and Rodriguez, D. (1998). Vaccinia virus 15-kilodalton (A14L) protein is essential for assembly and attachment of viral crescents to virosomes. *J. Virol.* **72:**1287–1296.

Roos, N., Cyrklaff, M., Cudmore, S., Blasco, R., Krijnse-Locker, J., and Griffiths, G. (1996). A novel immunogold cryoelectron microscopic approach to investigate the structure of the intracellular and extracellular forms of vaccinia virus. *EMBO J.* **15:**2343–2355.

Rosel, J., and Moss, B. (1985). Transcriptional and translational mapping and nucleotide sequence analysis of a vaccinia virus gene encoding the precursor of the major core polypeptide 4b. *J. Virol.* **56:**830–838.

Salmons, T., Kuhn, A., Wylie, F., Schleich, S., Rodriguez, J. R., Rodriguez, D., Esteban, M., Griffiths, G., and Locker, J. K. (1997). Vaccinia virus membrane proteins p8 and p16 are cotranslationally inserted into the rough endoplasmic reticulum and retained in the intermediate compartment. *J. Virol.* **71:**7404–7420.

Saminathan, M., Thomas, T., Shirahata, A., Pillai, C. K., and Thomas, T. J. (2002). Polyamine structural effects on the induction and stabilization of liquid crystalline DNA: Potential applications to DNA packaging, gene therapy and polyamine therapeutics. *Nucleic Acids Res.* **30:**3722–3731.

Sanderson, C. M., Hollinshead, M., and Smith, G. L. (2000). The vaccinia virus A27L protein is needed for the microtubule-dependent transport of intracellular mature virus particles. *J. Gen. Virol.* **81**(Pt. 1)**:**47–58.

Sarov, I., and Joklik, W. K. (1972). Studies on the nature and location of the capsid polypeptides of vaccinia virions. *Virology* **50:**579–592.

Schramm, B., and Locker, J. K. (2005). Cytoplasmic organization of POXvirus DNA replication. *Traffic* **6:**839–846.

Senkevich, T. G., and Moss, B. (2005). Vaccinia virus H2 protein is an essential component of a complex involved in virus entry and cell-cell fusion. *J. Virol.* **79:**4744–4754.

Senkevich, T. G., Weisberg, A. S., and Moss, B. (2000a). Vaccinia virus E10R protein is associated with the membranes of intracellular mature virions and has a role in morphogenesis. *Virology* **278:**244–252.

Senkevich, T. G., White, C. L., Koonin, E. V., and Moss, B. (2000b). A viral member of the ERV1/ALR protein family participates in a cytoplasmic pathway of disulfide bond formation. *Proc. Natl. Acad. Sci. USA* **97:**12068–12073.

Senkevich, T. G., White, C. L., Koonin, E. V., and Moss, B. (2002a). Complete pathway for protein disulfide bond formation encoded by poxviruses. *Proc. Natl. Acad. Sci. USA* **99:**6667–6672.

Senkevich, T. G., White, C. L., Weisberg, A., Granek, J. A., Wolffe, E. J., Koonin, E. V., and Moss, B. (2002b). Expression of the vaccinia virus A2.5L redox protein is required for virion morphogenesis. *Virology* **300:**296–303.

Senkevich, T. G., Ward, B. M., and Moss, B. (2004a). Vaccinia virus A28L gene encodes an essential protein component of the virion membrane with intramolecular disulfide bonds formed by the viral cytoplasmic redox pathway. *J. Virol.* **78:**2348–2356.

Senkevich, T. G., Ward, B. M., and Moss, B. (2004b). Vaccinia virus entry into cells is dependent on a virion surface protein encoded by the A28L gene. *J. Virol.* **78:**2357–2366.

Senkevich, T. G., Ojeda, S., Townsley, A. C., Nelson, G. E., and Moss, B. (2005). Poxvirus multiprotein entry-fusion complex. *Proc. Natl. Acad. Sci. USA* **102:**18572–18577.

Smith, G. L., Vanderplasschen, A., and Law, M. (2002). The formation and function of extracellular enveloped vaccinia virus. *J. Gen. Virol.* **83:**2915–2931.

Sodeik, B., and Krijnse-Locker, J. (2002). Assembly of vaccinia virus revisited: *De novo* membrane synthesis or acquisition from the host? *Trends Microbiol.* **10:**15–24.

Sodeik, B., Doms, R. W., Ericsson, M., Hiller, G., Machamer, C. E., van't, G., vanMeer, H. W., Moss, B., and Griffiths, G. (1993). Assembly of vaccinia virus: Role of the intermediate compartment between the endoplasmic reticulum and the Golgi stacks. *J. Cell Biol.* **121:**521–541.

Sodeik, B., Griffiths, G., Ericsson, M., Moss, B., and Doms, R. W. (1994). Assembly of vaccinia virus: Effects of rifampin on the intracellular distribution of viral protein p65. *J. Virol.* **68:**1103–1114.

Sodeik, B., Cudmore, S., Ericsson, M., Esteban, M., Niles, E. G., and Griffiths, G. (1995). Assembly of vaccinia virus: Incorporation of p14 and p32 into the membrane of the intracellular mature virus. *J. Virol.* **69:**3560–3574.

Soloski, M., and Holowczak, J. A. (1980). Preparation of subviral particles from vaccinia virions irradiated with ultraviolet light. *J. Virol. Methods* **1:**185–195.

Soloski, M. J., and Holowczak, J. A. (1981). Characterization of supercoiled nucleoprotein complexes released from detergent-treated vaccinia virions. *J. Virol.* **37:**770–783.

Soloski, M. J., Cabrera, C. V., Esteban, M., and Holowczak, J. A. (1979). Studies concerning the structure and organization of the vaccinia virus nucleoid. I. Isolation and characterization of subviral particles prepared by treating virions with guanidine-HCL, nonidet-P40, and 2-mercaptoethanol. *Virology* **99:**209–217.

Stern, W., and Dales, S. (1974). Biogenesis of vaccinia: Concerning the origin of the envelope phospholipids. *Virology* **62:**293–306.

Stern, W., and Dales, S. (1976). Biogenesis of vaccinia: Isolation and characterization of a surface component that elicits antibody suppressing infectivity and cell-cell fusion. *Virology* **75:**232–241.

Stern, W., Pogo, B. G., and Dales, S. (1977). Biogenesis of poxviruses: Analysis of the morphogenetic sequence using a conditional lethal mutant defective in envelope self-assembly. *Proc. Natl. Acad. Sci. USA* **74:**2162–2166.

Su, H. P., Garman, S. C., Allison, T. J., Fogg, C., Moss, B., and Garboczi, D. N. (2005). The 1.51-angstrom structure of the poxvirus L1 protein, a target of potent neutralizing antibodies. *Proc. Natl. Acad. Sci. USA* **102:**4240–4245.

Szajner, P., Weisberg, A. S., and Moss, B. (2001a). Unique temperature-sensitive defect in vaccinia virus morphogenesis maps to a single nucleotide substitution in the A30L gene. *J. Virol.* **75:**11222–11226.

Szajner, P., Weisberg, A. S., Wolffe, E. J., and Moss, B. (2001b). Vaccinia virus a30l protein is required for association of viral membranes with dense viroplasm to form immature virions. *J. Virol.* **75:**5752–5761.

Szajner, P., Jaffe, H., Weisberg, A. S., and Moss, B. (2003). Vaccinia virus G7L protein Interacts with the A30L protein and is required for association of viral membranes with dense viroplasm to form immature virions. *J. Virol.* **77:**3418–3429.

Szajner, P., Jaffe, H., Weisberg, A. S., and Moss, B. (2004a). A complex of seven vaccinia virus proteins conserved in all chordopoxviruses is required for the association of membranes and viroplasm to form immature virions. *Virology* **330:**447–459.

Szajner, P., Weisberg, A. S., and Moss, B. (2004b). Evidence for an essential catalytic role of the F10 protein kinase in vaccinia virus morphogenesis. *J. Virol.* **78:**257–265.

Szajner, P., Weisberg, A. S., and Moss, B. (2004c). Physical and functional interactions between vaccinia virus F10 protein kinase and virion assembly proteins A30 and G7. *J. Virol.* **78:**266–274.

Szajner, P., Weisberg, A. S., Lebowitz, J., Heuser, J., and Moss, B. (2005). External scaffold of spherical immature poxvirus particles is made of protein trimers forming a honeycomb lattice. *J. Cell Biol.* **170:**971–981.

Takahashi, T., Oie, M., and Ichihashi, Y. (1994). N-terminal amino acid sequences of vaccinia virus structural proteins. *Virology* **202:**844–852.

Tartaglia, J., and Paoletti, E. (1985). Physical mapping and DNA sequence analysis of the rifampicin resistance locus in vaccinia virus. *Virology* **147:**394–404.

Tolonen, N., Doglio, L., Schleich, S., and Krijnse, L. J. (2001). Vaccinia virus DNA replication occurs in endoplasmic reticulum-enclosed cytoplasmic mini-nuclei. *Mol. Biol. Cell* **12:**2031–2046.

Townsley, A. C., Senkevich, T. G., and Moss, B. (2005a). The product of the vaccinia virus L5R gene is a fourth membrane protein encoded by all poxviruses that is required for cell entry and cell-cell fusion. *J. Virol.* **79:**10988–10998.

Townsley, A. C., Senkevich, T. G., and Moss, B. (2005b). Vaccinia virus a21 virion membrane protein is required for cell entry and fusion. *J. Virol.* **79:**9458–9469.

Traktman, P., Caligiuri, A., Jesty, S. A., Liu, K., and Sankar, U. (1995). Temperature-sensitive mutants with lesions in the vaccinia virus F10 kinase undergo arrest at the earliest stage of virion morphogenesis. *J. Virol.* **69:**6581–6587.

Traktman, P., Liu, K., DeMasi, J., Rollins, R., Jesty, S., and Unger, B. (2000). Elucidating the essential role of the A14 phosphoprotein in vaccinia virus morphogenesis: Construction and characterization of a tetracycline-inducible recombinant. *J. Virol.* **74:**3682–3695.

Ulaeto, D., Grosenbach, D., and Hruby, D. E. (1995). Brefeldin A inhibits vaccinia virus envelopment but does not prevent normal processing and localization of the putative envelopment receptor P37. *J. Gen. Virol.* **76**(Pt. 1)**:**103–111.

Ulaeto, D., Grosenbach, D., and Hruby, D. E. (1996). The vaccinia virus 4c and A-type inclusion proteins are specific markers for the intracellular mature virus particle. *J. Virol.* **70:**3372–3377.

Unger, B., and Traktman, P. (2004). Vaccinia virus morphogenesis: A13 phosphoprotein is required for assembly of mature virions. *J. Virol.* **78:**8885–8901.

Upton, C., Slack, S., Hunter, A. L., Ehlers, A., and Roper, R. L. (2003). Poxvirus orthologous clusters: Toward defining the minimum essential poxvirus genome. *J. Virol.* **77:**7590–7600.

Vanslyke, J. K., and Hruby, D. E. (1994). Immunolocalization of vaccinia virus structural proteins during virion formation. *Virology* **198:**624–635.

Vanslyke, J. K., Franke, C. A., and Hruby, D. E. (1991a). Proteolytic maturation of vaccinia virus core proteins: Identification of a conserved motif at the N termini of the 4b and 25K virion proteins. *J. Gen. Virol.* **72**(Pt. 2)**:**411–416.

Vanslyke, J. K., Whitehead, S. S., Wilson, E. M., and Hruby, D. E. (1991b). The multistep proteolytic maturation pathway utilized by vaccinia virus P4a protein: A degenerate conserved cleavage motif within core proteins. *Virology* **183:**467–478.

Vanslyke, J. K., Lee, P., Wilson, E. M., and Hruby, D. E. (1993). Isolation and analysis of vaccinia virus previrions. *Virus Genes* **7:**311–324.

Wallengren, K., Risco, C., Krijnse-Locker, J., Esteban, M., and Rodriguez, D. (2001). The A17L gene product of vaccinia virus is exposed on the surface of IMV. *Virology* **290:**143–152.

Wang, S., and Shuman, S. (1995). Vaccinia virus morphogenesis is blocked by temperature-sensitive mutations in the F10 gene, which encodes protein kinase 2. *J. Virol.* **69:**6376–6388.

Wang, S. P., and Shuman, S. (1996). A temperature-sensitive mutation of the vaccinia virus E11 gene encoding a 15-kDa virion component. *Virology* **216:**252–257.

Ward, B. M. (2005). Visualization and characterization of the intracellular movement of vaccinia virus intracellular mature virions. *J. Virol.* **79:**4755–4763.

Webb, J. H., Mayer, R. J., and Dixon, L. K. (1999). A lipid modified ubiquitin is packaged into particles of several enveloped viruses. *FEBS Lett.* **444:**136–139.

Weir, J. P., and Moss, B. (1985). Use of a bacterial expression vector to identify the gene encoding a major core protein of vaccinia virus. *J. Virol.* **56:**534–540.

Westwood, J. C., Harris, W. J., Zwartouw, H. T., Titmuss, D. H., and Appleyard, G. (1964). Studies on the structure of vaccinia virus. *J. Gen. Microbiol.* **34:**67–78.

White, C. L., Weisberg, A. S., and Moss, B. (2000). A glutaredoxin, encoded by the G4L gene of vaccinia virus, is essential for virion morphogenesis. *J. Virol.* **74:**9175–9183.

Whitehead, S. S., and Hruby, D. E. (1994a). A transcriptionally controlled trans-processing assay: Putative identification of a vaccinia virus-encoded proteinase which cleaves precursor protein P25K. *J. Virol.* **68:**7603–7608.

Whitehead, S. S., and Hruby, D. E. (1994b). Differential utilization of a conserved motif for the proteolytic maturation of vaccinia virus proteins. *Virology* **200:**154–161.

Wilcock, D., and Smith, G. L. (1994). Vaccinia virus core protein VP8 is required for virus infectivity, but not for core protein processing or for INV and EEV formation. *Virology* **202:**294–304.

Wilcock, D., and Smith, G. L. (1996). Vaccinia virions lacking core protein VP8 are deficient in early transcription. *J. Virol.* **70:**934–943.

Williams, O., Wolffe, E. J., Weisberg, A. S., and Merchlinsky, M. (1999). Vaccinia virus WR gene A5L is required for morphogenesis of mature virions. *J. Virol.* **73:**4590–4599.

Wilton, S., Mohandas, A. R., and Dales, S. (1995). Organization of the vaccinia envelope and relationship to the structure of intracellular mature virions. *Virology* **214:**503–511.

Wittek, R., Richner, B., and Hiller, G. (1984). Mapping of the genes coding for the two major vaccinia virus core polypeptides. *Nucleic Acids Res.* **12:**4835–4848.

Wolffe, E. J., Vijaya, S., and Moss, B. (1995). A myristylated membrane protein encoded by the vaccinia virus L1R open reading frame is the target of potent neutralizing monoclonal antibodies. *Virology* **211:**53–63.

Wolffe, E. J., Moore, D. M., Peters, P. J., and Moss, B. (1996). Vaccinia virus A17L open reading frame encodes an essential component of nascent viral membranes that is required to initiate morphogenesis. *J. Virol.* **70:**2797–2808.

Yang, W. P., and Bauer, W. R. (1988). Purification and characterization of vaccinia virus structural protein VP8. *Virology* **167:**578–584.

Yang, W. P., Kao, S. Y., and Bauer, W. R. (1988). Biosynthesis and post-translational cleavage of vaccinia virus structural protein VP8. *Virology* **167:**585–590.

Yeh, W. W., Moss, B., and Wolffe, E. J. (2000). The vaccinia virus A9L gene encodes a membrane protein required for an early step in virion morphogenesis. *J. Virol.* **74:**9701–9711.

Zhang, Y., and Moss, B. (1992). Immature viral envelope formation is interrupted at the same stage by lac operator-mediated repression of the vaccinia virus D13L gene and by the drug rifampicin. *Virology* **187:**643–653.

Zhang, Y. F., and Moss, B. (1991a). Inducer-dependent conditional-lethal mutant animal viruses. *Proc. Natl. Acad. Sci. USA* **88:**1511–1515.

Zhang, Y. F., and Moss, B. (1991b). Vaccinia virus morphogenesis is interrupted when expression of the gene encoding an 11-kilodalton phosphorylated protein is prevented by the *Escherichia coli* lac repressor. *J. Virol.* **65:**6101–6110.

Zhang, Y., Ahn, B. Y., and Moss, B. (1994). Targeting of a multicomponent transcription apparatus into assembling vaccinia virus particles requires RAP94, an RNA polymerase-associated protein. *J. Virol.* **68:**1360–1370.

Zinoviev, V. V., Tchikaev, N. A., Chertov, O. Y., and Malygin, E. G. (1994). Identification of the gene encoding vaccinia virus immunodominant protein p35. *Gene* **147:**209–214.

Zwartouw, H. T. (1964). The chemical composition of vaccinia virus. *J. Gen. Microbiol.* **34:**115–123.

ADVANCES IN VIRUS RESEARCH, VOL 66

HUMAN PAPILLOMAVIRUSES AND CERVICAL CANCER

Daniel DiMaio*† and John B. Liao‡

*Department of Genetics, Yale University School of Medicine
New Haven, Connecticut 06510
†Department of Therapeutic Radiology, Yale University School of Medicine
New Haven, Connecticut 06510
‡Department of Obstetrics, Gynecology, and Reproductive Sciences
Yale University School of Medicine, New Haven, Connecticut 06510

Abstract

Carcinoma of the uterine cervix, a leading cause of cancer death in women worldwide, is initiated by infection with high-risk types of human papillomaviruses (HPVs). This review summarizes laboratory studies over the past 20 years that have elucidated the major features of the HPV life cycle, identified the functions of the viral proteins, and clarified the consequences of HPV infection for their host cells. This information has allowed the development of various strategies to prevent or treat infections, including prophylactic vaccination with virus-like particles, therapeutic vaccination against viral proteins expressed in cancer cells, and antiviral approaches to inhibit virus replication, spread, or pathogenesis. These strategies have the potential to cause a dramatic reduction in the incidence of cervical carcinoma and serve as the prototype for comprehensive efforts to combat virus-induced tumors.

I. Introduction

The study of tumor viruses has provided many insights into fundamental cellular processes such as cell cycle control, signal transduction,

0065-3527/06 $35.00
DOI: 10.1016/S0065-3527(06)66003-X

proliferation, apoptosis, and senescence. Increased understanding of human tumor viruses has also suggested new approaches to prevent or treat cancer. Approximately, 15% of all cancer deaths worldwide are caused by cancers initiated by human tumor viruses, with a particularly high burden in the developing world (Parkin *et al*., 2001). However, only a small fraction of people infected with tumor viruses develop cancer, and cancer typically arises many years after the initial infection. The recognition that a cancer has a viral etiology and the identification of the responsible virus suggest various strategies to inhibit cancer formation, including vaccination to prevent infection. The persistence of viral genes and gene products in cancer cells raises the possibility that antiviral approaches will be useful in preventing and treating cancer, even in its late stages. This review illustrates a number of these principles with regard to one of the best understood human tumor viruses, the human papillomaviruses (HPVs), and carcinoma of the uterine cervix.

II. Life Cycle of the Papillomaviruses

Papillomaviruses are small, nonenveloped DNA viruses that have been isolated from numerous vertebrate species, including humans. The viral genome is a double-stranded circular DNA molecule approximately 8000 base pairs in length that encodes no more than ten proteins. There are two clusters of viral genes, the early and the late genes, both of which are transcribed from the same DNA strand (Engel *et al*., 1983). The early region encodes genes primarily involved in viral DNA replication and cell transformation, and the late genes encode the structural proteins of the virus particle. A segment of DNA upstream of the early genes is devoid of protein coding sequences and contains the origin of viral DNA replication and transcriptional regulatory elements (Chong *et al*., 1991). Transcriptional control is complex, involving multiple promoters and enhancers, two major polyadenylation sites, and an array of alternatively spliced mRNAs (Bernard, 2002). Proper transcription of the viral genome depends on the differentiation state of the host epithelial cell and on cellular transcription factors and polymerases, as well as the splicing and other RNA processing machinery (Bernard, 2002; Longworth and Laimins, 2004).

Studies of the HPV life cycle have been hindered by the inability of papillomaviruses to undergo high-level replication in the laboratory. Nevertheless, certain aspects of the virus life cycle can be studied in animals and in various cultured cell systems, including organotypic epithelial cell systems that mimic the tissue architecture of the normal

host cells and support limited viral replication (Asselineau and Prunieras, 1984; Brandsma and Xiao, 1993; Brandsma *et al*., 1991; Dollard *et al*., 1992; Frattini *et al*., 1996; Meyers *et al*., 1992, 1997). Productive papillomavirus replication in natural settings takes place exclusively in stratified squamous epithelia, such as the epidermis or mucous membranes, tissues that are replenished by periodic replication of basal cells apposed to the basement membrane. HPV infection is thought to be initiated by inoculation of the virus into basal epithelial cells through wounds or abrasions, and cell binding and entry is mediated by a poorly characterized cellular receptor that is probably a heparin sulfate proteoglycan (Giroglou *et al*., 2001; Joyce *et al*., 1999; Shafti-Keramat *et al*., 2003). In uninfected tissue, as daughter cells migrate away from the basement membrane toward the surface of the epithelium, they cease proliferation and undergo a process of terminal differentiation until they eventually die and slough off from the surface of the tissue. Productive papillomavirus infection disrupts normal epithelial differentiation (McCance *et al*., 1988) and causes epithelial hyperplasia and the formation of benign epithelial tumors known as warts (or papillomas or condylomas, depending on the anatomic site of the lesion).

Like other small DNA viruses, HPVs utilize the host-cell DNA replication machinery to establish an environment able to support viral DNA replication and to carry out DNA synthesis. However, once epithelial cells exit the basal layer, they also normally exit the cell cycle. Therefore, the virus has to maintain the suprabasal cells in a state competent for DNA replication. This is primarily the task of the HPV E7 protein (Cheng *et al*., 1995; Foster and Galloway, 1996). The E7 protein binds to and destabilizes the cellular retinoblastoma (Rb) tumor suppressor protein and members of the Rb family, thereby displacing E2F transcription factors, which then stimulate expression of genes required for cellular (and viral) DNA synthesis and cell cycle progression (Boyer *et al*., 1996; Chellappan *et al*., 1992; Dyson *et al*., 1989; Gonzalez *et al*., 2001; Munger *et al*., 1989b). The E7 protein also inhibits the action of cyclin-dependent kinase inhibitors and interacts with cyclin–cdk complexes and other cellular proteins to stimulate cell cycle progression (Funk *et al*., 1997; Jones *et al*., 1997; McIntyre *et al*., 1996; Noya *et al*., 2001; Tommasino *et al*., 1993; Zerfass-Thome *et al*., 1996). In addition, the HPV E6 protein perturbs cell cycle control by binding to the p53 tumor suppressor and targeting it for accelerated ubiquitin-mediated degradation (Scheffner *et al*., 1990, 1993; Werness *et al*., 1990). In combination, these E6 and E7 activities generate host cells that can support viral DNA replication. Thus, both E6

and E7 are essential for the productive viral life cycle (Brandsma *et al.*, 1991; Flores *et al.*, 2000; McLaughlin-Drubin *et al.*, 2005; Wu *et al.*, 1994).

Viral DNA replication is primarily mediated by the papillomavirus E1 and E2 proteins working in concert with cellular DNA polymerases and auxiliary replication proteins (Conger *et al.*, 1999; Loo and Melendy, 2004; Masterson *et al.*, 1998; Park *et al.*, 1994; Piirsoo *et al.*, 1996; Ustav and Stenlund, 1991). The E1 and E2 proteins both bind specifically to the origin of viral DNA replication (*ori*) upstream of the *E6* gene (Androphy *et al.*, 1987; Holt *et al.*, 1994; Spalholz *et al.*, 1987; Ustav *et al.*, 1993; Wilson and Ludes-Meyers, 1991). The E1 protein, an ATP-dependent helicase, is the only viral coded enzyme (Sedman and Stenlund, 1998; Seo *et al.*, 1993; Yang *et al.*, 1993). It plays essential roles in papillomavirus DNA replication by melting *ori* as well as unwinding the parental DNA strands in advance of the replication fork (Chen and Stenlund, 2002; Gillette *et al.*, 1994; Sanders and Stenlund, 1998; Sedman and Stenlund, 1998). The participation of the E1 protein in viral DNA replication is assisted by the E2 protein, which forms a complex with the E1 protein and enables its high-affinity, high-specificity binding to *ori* (Frattini and Laimins, 1994; Mohr *et al.*, 1990; Sedman and Stenlund, 1995; Yang *et al.*, 1991). Proteins and small molecules have been described that inhibit E1 helicase activity, impair complex formation between the E1 and E2 proteins, or block E1 or E2 DNA binding (Deng *et al.*, 2004; Faucher *et al.*, 2004; Hartley and Alexander, 2002; Kasukawa *et al.*, 1998; White *et al.*, 2003). In some cases, these agents interfere with HPV DNA replication in cultured cells and may form the basis of future antiviral approaches.

The viral genome replicates at a low level in the nuclei of the infected cells in the basal layer, but no progeny virus is produced in these cells. In order for productive infection to take place, the viral DNA must replicate to a high-copy number in differentiating cells that have migrated away from the basal layer (Bedell *et al.*, 1991; Longworth and Laimins, 2004). This high-level DNA replication may involve a switch to a rolling circle mode of viral DNA replication (Flores and Lambert, 1997), but the biochemical mechanism responsible for this switch is unknown.

The E2 protein also plays an important role in segregation of viral DNA plasmids as cells divide (Ilves *et al.*, 1999; Lehman and Botchan, 1998). By simultaneously binding to viral genomes and cellular chromatin-associated proteins, such as Brd4, during mitosis, the E2 protein can "piggy-back" on cellular chromosomes to ensure proper segregation of the viral DNA into daughter cells upon cell division

(Bastien and McBride, 2000; Baxter *et al.*, 2005; Skiadopoulos and McBride, 1998; Van Tine *et al.*, 2004a; You *et al.*, 2004). As discussed in a later section, the E2 protein is also involved in transcriptional control (Hawley-Nelson *et al.*, 1988; Spalholz *et al.*, 1985). Genetic studies indicate that the E6 and E7 proteins also play a role in stable maintenance of HPV plasmid DNA (Park and Androphy, 2002; Thomas *et al.*, 1999).

HPV late mRNAs and capsid proteins are produced only in highly differentiated cells in the superficial layers of the epithelium. In these cells, mRNAs that encode abundant quantities of the L1 major capsid protein, as well as the L2 minor capsid protein, accumulate through a variety of mechanisms including activation of promoters, bypass of the early polyadenylation signal, and use of novel mRNA splicing patterns (Barksdale and Baker, 1993, 1995; Collier *et al.*, 2002; Cumming *et al.*, 2002; Kennedy *et al.*, 1991; Klumpp and Laimins, 1999; Oberg *et al.*, 2003; Ozbun and Meyers, 1998; Terhune *et al.*, 1999; Zhao *et al.*, 2004). The L1 and L2 proteins are transported into the nucleus where they assemble into virus particles and package replicated viral DNA.

Two other papillomavirus proteins play roles in the virus life cycle. The E5 protein is a very short, transmembrane protein encoded at the 3′ end of the early region of many papillomavirus types. The E5 protein from bovine papillomavirus type 1 causes tumorigenic transformation of cultured fibroblasts by inducing ligand-independent activation of the platelet-derived growth factor β receptor (DiMaio *et al.*, 2000; Petti *et al.*, 1991), but the role of the E5 protein in the normal life cycle of bovine papillomavirus is not known. The E5 proteins of the HPVs are also required for optimal productive infection (Fehrmann *et al.*, 2003; Genther *et al.*, 2003). This requirement may involve interaction of the E5 protein with the epidermal growth factor receptor or the vacuolar H^+-ATPase (Conrad *et al.*, 1993; Genther Williams *et al.*, 2005; Hwang *et al.*, 1995; Schapiro *et al.*, 2000; Straight *et al.*, 1993, 1995; Zhang *et al.*, 2005). The E4 protein is encoded by a gene in the early region that entirely overlaps the *E2* gene in an alternative translational reading frame. Nevertheless, the E4 protein is abundantly expressed during the late stages of the HPV life cycle and may facilitate release of mature virus from cells (Brown *et al.*, 2005; Doorbar *et al.*, 1991; Nakahara *et al.*, 2005; Peh *et al.*, 2004; Wilson *et al.*, 2005).

III. Evidence for an Essential Role of HPV in Cervical Carcinoma

Papillomaviruses have long been known to cause benign epithelial warts, but the role of HPVs in malignant disease has been elucidated

only within the last 25 years. The association with HPV infection is strongest for cervical carcinoma, a leading cause of cancer death in women in the developing world. HPV infection is also strongly associated with other anogenital cancers, approximately 20% of oropharyngeal cancers, and some nonmelanoma skin cancers (Gillison, 2004; Parkin *et al*., 2001). The first hint that cervical cancer had an infectious component was the observation in 1842 that uterine (presumably cervical) cancer developed in married women in Florence, Italy, but was rare in celibate nuns who lived in convents outside of the city (Scotto and Bailar III, 1969). In retrospect, this pattern reflected the existence of a sexually transmitted agent. Over the next 140 years, the notion that an infectious agent initiated cervical carcinogenesis gained credence, but the identity of the agent and the carcinogenic mechanism remained unknown. For some time, herpes simplex virus type 2 was proposed as a causative agent for cervical carcinoma, but this hypothesis has now been discarded (Vonka *et al*., 1984, 1987). The molecular cloning and sequencing of HPV genomes from various types of papillomas in the early 1980s revealed a remarkable multiplicity of related but distinct HPV genotypes. Seminal studies by Harald zur Hausen and others identified several HPV DNA types in genital warts, cervical cancer biopsies, and cervical cancer cell lines (Boshart *et al*., 1984; de Villiers *et al*., 1981; Durst *et al*., 1983; Gissmann *et al*., 1983; McCance *et al*., 1985; zur Hausen *et al*., 1981). The HPV DNA types that are preferentially present in cervical carcinomas are referred to as high-risk HPV types and include HPV16, which is present in approximately 50% of all cervical cancers worldwide, and HPV18, found in another approximately 15%. Later comprehensive PCR-based studies revealed the presence of high-risk HPV DNA in virtually all cervical cancers worldwide (Bosch *et al*., 2002; Walboomers *et al*., 1999). The same high-risk DNA types are also present in HPV-associated cancers of other mucosal sites (Gillison, 2004).

There are numerous lines of evidence that the high-risk HPV types play an essential etiologic role in cervical cancer. As noted earlier, virtually all cervical cancers contain high-risk HPV DNA, whereas other genital HPV types (the low-risk HPV) typically are absent (Walboomers *et al*., 1999). Second, extensive epidemiological studies revealed that persistent infection with a high-risk HPV type confers a dramatically elevated risk of cervical neoplasia (Bosch *et al*., 2002; Hildesheim *et al*., 1994; Ho *et al*., 1998; Koutsky *et al*., 1992; Schlecht *et al*., 2001; Wallin *et al*., 1999). Although the high-risk HPV types display worldwide distribution, some HPV16 and HP18 subtypes appear to display increased oncogenic potential compared to the

prototype strains (Berumen *et al*., 2001; Villa *et al*., 2000; Xi *et al*., 1997). Third, high-risk HPVs express oncogene products that interact with known cellular growth-regulatory components, including Rb and p53, and induce measures of oncogenic transformation in cultured human cells (Bedell *et al*., 1989; Durst *et al*., 1987; Dyson *et al*., 1989; Halbert *et al*., 1991; Hawley-Nelson *et al*., 1989; Hudson *et al*., 1990; Munger *et al*., 1989a; Pirisi *et al*., 1987; Werness *et al*., 1990). Inactivation of p53 and Rb pathways commonly occurs in sporadically arising tumors as well. Fourth, these viral oncogene products are continuously expressed in cervical cancer cells, even many years after the cancer develops, and are required for the proliferation and survival of cervical cancer cell lines (Francis *et al*., 2000; Hwang *et al*., 1993; Schwarz *et al*., 1985; von Knebel Doeberitz *et al*., 1988; Yee *et al*., 1985). Fifth, transgenic mice expressing high-risk HPV oncogenes develop carcinomas, including cervical cancer in mice treated with estrogen (Arbeit *et al*., 1994, 1996; Brake and Lambert, 2005; Lambert *et al*., 1993). Finally, vaccination that prevents persistent high-risk HPV infection prevents the development of precancerous cervical changes in women (Harper *et al*., 2004; Koutsky *et al*., 2002; Villa *et al*., 2005). In aggregate, these results provide compelling evidence that cervical carcinogenesis is initiated by high-risk HPV infection.

IV. Pathogenesis of Cervical Carcinoma

Most cervical carcinomas develop in the transformation zone of the cervix, where the columnar epithelium of the endocervix merges with the stratified squamous epithelium of the exocervix. High-risk HPV infection of this tissue causes flat cervical warts, which are usually asymptomatic and often regress spontaneously (Hildesheim *et al*., 1994). However, a fraction of these infections generate a series of increasingly dysplastic cell populations (denoted as cervical intraepithelial neoplasia [CIN]) that can culminate in carcinoma-*in situ* (Koutsky *et al*., 1992). Cervical carcinoma-*in situ* can be readily treated locally, but untreated lesions can progress to invasive cervical cancer for which there is limited treatment success. Invasive disease occurs in only a small minority of women infected with high-risk HPV, and the time between initial infection and cancer is typically $\geq$10 years (Goldie *et al*., 2003). This protracted natural history combined with the accessibility of the cervix for cell sampling is responsible for the success of Pap smear screening programs, which identify women with

HPV-induced precancerous changes at relatively early, treatable stages of their disease. These screening programs caused a dramatic decline in the incidence of cervical cancer in the developed world and represent a triumph of public health intervention (Dorn and Cutler, 1959; Gustafsson *et al*., 1997; Johannesson *et al*., 1978). The absence of robust screening programs in resource-poor areas is in large part responsible for the high incidence of cervical cancer in much of the developing world, although other factors, such as host genotype or high frequency of HPV variants with increased oncogenicity, may also play a role (Berumen *et al*., 2001). The addition of HPV DNA typing to other methods of evaluation including standard cytologic analysis of cervical cells will presumably improve the diagnosis and management of cervical disease (Goldie *et al*., 2005; Schiffman *et al*., 2005b).

During carcinogenic progression of cervical lesions, HPV DNA often integrates into cellular chromosomes, an event which can disrupt the *E1* and *E2* genes, preventing vegetative viral DNA replication and stimulating cell growth (Cullen *et al*., 1991; Hopman *et al*., 2004; Jeon *et al*., 1995; Schneider-Maunoury *et al*., 1987). Although the E2 protein is an essential replication factor, it can also function as a transcriptional repressor of the viral major early promoter (Bernard *et al*., 1989; Bouvard *et al*., 1994; Dostatni *et al*., 1991; Steger and Corbach, 1997; Thierry and Yaniv, 1987). Accordingly, loss of E2 function as a consequence of viral DNA integration relieves repression of the *E6* and *E7* oncogenes, and confers a growth advantage on these cells. The biological relevance of this mechanism is supported by the finding that E2 proteins from HPV16 strains with increased oncogenicity display reduced repressor activity (Berumen *et al*., 2001; Ordonez *et al*., 2004). In addition, in some situations the E2 protein can induce apoptosis, providing additional selective pressure for loss of E2 during malignant progression (Demeret *et al*., 2003; Desaintes *et al*., 1997; Sanchez-Perez *et al*., 1997; Webster *et al*., 2000). The E2 protein also binds to a number of cellular proteins (e.g., Massimi *et al*., 1999), so loss of E2 could have pleiotropic effects on cell function. Although there are frequently multiple sites of tandemly integrated HPV DNA in cervical cancer cells, typically only one copy of the viral genome is transcriptionally active (Van Tine *et al*., 2004b). This active copy expresses E6/E7 coding sequences fused to downstream cellular sequences, which may stabilize these mRNAs and further elevate E6/E7 levels (Jeon *et al*., 1995). In the absence of integration, E6/E7 expression can be increased by other mechanisms, such as mutations in the major viral promoter that interfere with binding of the E2

protein or cellular transcriptional repressors such as YY1 (Dong *et al*., 1994; May *et al*., 1994; Rose *et al*., 1998).

The E5 protein, the other oncogene product encoded by high-risk HPV, is expressed in some but not all cervical cancers (Chang *et al*., 2001; Hsieh *et al*., 2000). Phylogenetic comparison of the *E5* genes from various genital HPV types revealed a correlation between the E5 sequence and carcinogenic potential, suggesting that the E5 protein plays a role in carcinogenesis (Bravo and Alonso, 2004; Schiffman *et al*., 2005a).

The stepwise progression of natural lesions is mirrored by the behavior of cells transfected with high-risk HPV DNA. Primary human cervical and foreskin keratinocytes, which normally undergo a limited number of cell divisions in culture, can be efficiently immortalized by coexpression of the *E6* and *E7* genes from the high-risk HPV types (Bedell *et al*., 1989; Durst *et al*., 1987; Halbert *et al*., 1991; Hawley-Nelson *et al*., 1989; Hudson *et al*., 1990; Kaur and McDougall, 1989; Munger *et al*., 1989a; Pirisi *et al*., 1987; Woodworth *et al*., 1988). In addition, the E6 protein stimulates the expression of telomerase, an RNA-dependent DNA polymerase that maintains the ends of chromosomes in proliferating somatic cells (Gewin and Galloway, 2001; Klingelhutz *et al*., 1996; Oh *et al*., 2001; Veldman *et al*., 2001). The ability of E6 and E7 proteins to interfere with p53 and Rb function and to influence telomerase activity is presumably the basis for their immortalizing activity (Kiyono *et al*., 1998), because these same pathways are often affected during non-HPV immortalization (Vaziri and Benchimol, 1999). The E6 and E7 proteins also bind to other cellular targets, which may contribute to their carcinogenic effects (Antinore *et al*., 1996; Bernat *et al*., 2003; Bischof *et al*., 2005; Brehm *et al*., 1999; Luscher-Firzlaff *et al*., 1999). Notably, the high-risk E6 proteins bind to a number of PDZ domain-containing proteins, including some with presumed tumor suppressor activity (Gardiol *et al*., 1999; Glaunsinger *et al*., 2000; Lee and Laimins, 2004; Lee *et al*., 2000; Nakagawa and Huibregtse, 2000; Nguyen *et al*., 2003). The *E6* and *E7* genes from the low-risk genital HPV types do not display immortalization activity and show impaired interaction with cellular targets, demonstrating that these *in vitro* assays reflect the oncogenic potential of the various HPV types in people (Gage *et al*., 1990; Heck *et al*., 1992; Schlegel *et al*., 1988; Woodworth *et al*., 1989).

Even though HPV-immortalized keratinocytes express the viral oncogenes, these cells are not initially tumorigenic in experimental animals. However, continued passage of these cells results in the emergence of cells that can form tumors in animals, most likely

due to genetic instability resulting from the sustained action of the viral oncogenes (Durst *et al*., 1983, 1987; Kaur and McDougall, 1989; Pecoraro *et al*., 1991; Pirisi *et al*., 1987, 1988; Woodworth *et al*., 1988). The E5, E6, and E7 proteins from high-risk HPV eliminate various checkpoint control processes, permitting cells to replicate despite DNA damage and thereby accumulate mutations (Havre *et al*., 1995; Hickman *et al*., 1994; Jones and Munger, 1997; Kessis *et al*., 1993; Pan and Griep, 1994; Slebos *et al*., 1994, 1995; Song *et al*., 1998; Thomas and Laimins, 1998; White *et al*., 1994; Zhang *et al*., 2002). In addition, HPV16-immortalized keratinocytes display impaired DNA repair following UV-irradiation (Rey *et al*., 1999), and the E6 protein can directly interfere with DNA repair enzymes (Iftner *et al*., 2002; Srivenugopal and Ali-Osman, 2002). Finally, the E7 proteins perturb mitotic centrosomes, which in turn can result in structural and numerical chromosome abnormalities (Duensing *et al*., 2001a,b), and high-risk HPV E2 proteins can also cause genomic instability (Bellanger *et al*., 2005). As a consequence of these effects, genetic instability and chromosomal abnormalities are hallmarks of HPV-immortalized keratinocytes (Montgomery *et al*., 1995; Oda *et al*., 1996; Shin *et al*., 1996; Solinas-Toldo *et al*., 1997; Steenbergen *et al*., 1998). Some of the resulting mutations may activate cellular oncogenes, inactivate tumor suppressor genes, and disrupt various intracellular control mechanisms, thereby facilitating the acquisition of the tumorigenic phenotype (zur Hausen, 2000). Similar genetic events appear to take place in cervical cells undergoing malignant progression in women persistently infected with high-risk HPV (Duensing and Munger, 2004; Heselmeyer *et al*., 1997; Hopman *et al*., 2004; Kisseljov *et al*., 1996; Matthews *et al*., 2000; Sherwood *et al*., 2000).

Because HPV oncogene products function by modulating the activity and levels of cellular proteins, it is possible that the host cell genotype will directly influence HPV oncogene activity and cancer susceptibility. It has been reported that certain normal p53 variants are relatively resistant to E6-induced degradation, and that women harboring these variants have a reduced risk of developing cervical carcinoma (Storey *et al*., 1998). However, this finding is controversial, perhaps because of technical differences in sample acquisition and analysis (Madeleine *et al*., 2000; Makni *et al*., 2000).

V. Prophylactic Vaccination Against High-Risk HPV Infection

Because HPV is a causative agent for cervical carcinoma, it may be possible to prevent this cancer with vaccines that block infection (Lowy *et al*., 1994; Stanley, 2002). As noted earlier, the L1 protein is the major constituent of the virus particle. Recombinant L1 protein expressed in various cell types assembles into particles that resemble authentic virus particles recovered from natural lesions (Hagensee *et al*., 1993; Hofmann *et al*., 1995; Kirnbauer *et al*., 1992, 1993; Rose *et al*., 1993; Zhou *et al*., 1991). Unlike authentic virions, however, these virus-like particles (VLPs) do not contain viral DNA and hence are not pathogenic. Inoculation of various animal papillomavirus VLPs into experimental animals resulted in the efficient production of antibodies that recognized conformation-specific epitopes on authentic virions and neutralized their infectivity, thereby protecting the animals from infection after virus challenge (Breitburd *et al*., 1995; Christensen *et al*., 1996; De Bruijn *et al*., 1998; Kirnbauer *et al*., 1992, 1996; Nardelli-Haefliger *et al*., 1997; Rose *et al*., 1994; Suzich *et al*., 1995). On the basis of these results, VLPs composed of the HPV16 or the HPV18 L1 protein have been formulated into prophylactic vaccines and tested in female human volunteers. These studies demonstrated that repeated intramuscular injection of HPV VLPs generates high-titer neutralizing antibodies in humans and prevents persistent infection by the HPV type(s) in the vaccine (Harper *et al*., 2004; Harro *et al*., 2001; Koutsky *et al*., 2002; Villa *et al*., 2005). These vaccines caused a marked reduction in the incidence of type-specific CIN, the precursor lesion to cervical carcinoma. These studies strongly suggest that prophylactic vaccination against high-risk HPV types will prevent a substantial number of cervical carcinoma cases, although it will take many years to see a reduction in cancer incidence because there is a large pool of unvaccinated women who have already entered the protracted course of cervical carcinogenesis (Goldie *et al*., 2003). Nevertheless, adoption of prophylactic vaccination will cause an immediate reduction in the number of abnormal Pap smears, with resulting financial savings in patient management (Kulasingam and Myers, 2003). Prophylactic HPV vaccines will presumably also reduce the incidence of other HPV-associated anogenital and oropharyngeal cancers.

Despite the very promising activity of VLP vaccines in the published clinical trials, there are numerous issues that have to be addressed before prophylactic HPV vaccines find widespread use. First, VLP L1 vaccines are type-specific, that is, they will only protect against the

virus type in the vaccine and possibly closely related types. In clinical trials, women developed CIN containing high-risk HPV types not included in the vaccine (Harper *et al*., 2004). At the moment, the vaccines in development contain HPV16 and HPV18 VLPs, the two most common high-risk types, which in aggregate account for approximately two-thirds of cervical carcinoma. Some vaccine formulations also include HPV6 and HPV11, and so may also prevent anogenital warts caused by these low-risk types. However, women exposed to most other high-risk types will not be protected unless additional HPV types are included in the vaccine or strategies are developed to generate cross-reactive antibodies. Second, VLPs are relatively expensive to produce, distribute, and administer. This may preclude widespread use in the developing world, where the vast majority of cervical cancers occur. Thus, efforts are underway to develop less expensive vaccines such as ones that do not require intact VLPs, cold storage, needle injection, or multiple doses (Ohlschlager *et al*., 2003; Yuan *et al*., 2001). Third, it is not known how long protection will last, what the optimal age for vaccination is, and whether or not booster inoculations are required. Fourth, for maximal effect, girls should be vaccinated before they initiate sexual activity, but social, political, or religious considerations may impede the acceptance of vaccinating girls to prevent what may be characterized as a sexually transmitted disease. It is also possible that the availability of the vaccine will deter women from Pap smear screening. This is a potentially serious concern because there will be no protection against high-risk types not in the vaccine. The vaccine may also deter pharmaceutical companies from aggressively pursuing anti-HPV drugs. Finally, prophylactic vaccines will be of limited utility to women who are already persistently infected with high-risk HPV or whose infected cells have undergone preneoplastic changes. In these women, the presence of infectious virus and the infection of additional cells is presumably no longer required for carcinogenic progression. Nevertheless, even in infected women, prophylactic vaccination may provide some benefit by inhibiting the autoinfection of neighboring cells or by reducing virus load and hence transmission to new hosts.

VI. Therapeutic Vaccination Against Cervical Carcinoma

Most women infected with a high-risk HPV type do not develop cervical cancer, and the incidence of cervical cancer is increased in immunosuppressed women, including those with AIDS (Franceschi

et al., 1998; Frisch *et al*., 2000; Goldie *et al*., 2003; Halpert *et al*., 1986; Palefsky and Holly, 2003; Petry *et al*., 1994; Serraino *et al*., 1999). These findings suggest that cell-mediated immunity plays a major role in clearing cervical HPV infections and controlling precancerous lesions. In addition, studies in women with cervical neoplasia demonstrated the existence of E6- and E7-specific T cells in these patients, but the role of these cells in tumor surveillance is unclear (Bontkes *et al*., 2000; Eiben *et al*., 2002; Evans *et al*., 1997; Kadish *et al*., 1997, 2002; Steele *et al*., 2005). Nevertheless, measures that stimulate cellular immunity to HPV proteins may be therapeutically useful. Accordingly, an alternative vaccine strategy called therapeutic vaccination is also under development, with the goal of treating preneoplastic lesions or even advanced cancer by generating cytotoxic T lymphocytes (CTLs) that destroy cervical cancer and precancer cells, which express the HPV E6 and E7 proteins (Ressing *et al*., 1996; Stanley, 2002). Although these proteins function in the nucleus, proteolytic fragments are displayed at the surface of infected cells in association with major histocompatibility complex molecules, where they can serve as immune targets. Furthermore, as described in the next section, continuous expression of these viral proteins is required for the sustained survival and proliferation of the cancer cells, so the cells are unlikely to escape the immune response simply by losing expression of the viral proteins.

In mouse models, various therapeutic vaccination strategies can elicit a cytolytic $CD8^+$ T cell response directed against high-risk HPV E7 and/or E6 proteins, resulting in impaired growth or elimination of transplantable tumors expressing these viral antigens (Baldwin *et al*., 2003; Borysiewicz *et al*., 1996; Chu *et al*., 2000; Feltkamp *et al*., 1993; Hariharan *et al*., 1998; Lin *et al*., 1996; Velders *et al*., 2001). However, so far this approach has shown less impressive results in human trials against CIN and cervical carcinoma (Borysiewicz *et al*., 1996; Muderspach *et al*., 2000; van Driel *et al*., 1999). It is possible that cervical cancer cells may not be good targets for CTL killing because they express low levels of required major histocompatibility complex class I molecules (Bontkes *et al*., 1998; Connor and Stern, 1990; Koopman *et al*., 2000). In addition, the concentration of the viral proteins in human cancer cells may not be sufficient to elicit a robust immune response (Azoury-Ziadeh *et al*., 2001), or the viral proteins may induce a state of T-cell tolerance (Borchers *et al*., 1999). There are numerous reports that papillomavirus E5, E6, and E7 proteins can impair antigen presentation and other aspects of the innate or acquired immune response (Ashrafi *et al*., 2002, 2005; Barnard and McMillan, 1999; Lee *et al*., 2001; Marchetti *et al*., 2002; Park *et al*.,

2000; Perea *et al*., 2000; Ronco *et al*., 1998; Zhang *et al*., 2003). Moreover, skin transplantation studies in E7 transgenic mice suggest that epithelial cells expressing the E7 protein are not good targets for cytotoxic T cells in the absence of other immune stimulation (Dunn *et al*., 1997; Melero *et al*., 1997). Approaches to overcome these obstacles are likely to be required before therapeutic vaccination is successful.

Unlike prophylactic vaccination, which would strive to achieve full coverage of susceptible populations, therapeutic vaccines would be reserved for people who already have persistent HPV infections or cancer. This consideration will influence the testing, cost, and distribution of therapeutic vaccines. Attempts are also underway to develop combined prophylactic/therapeutic chimeric VLP vaccines that simultaneously raise neutralizing antibodies to L1 and CTLs to E6 or E7 (Greenstone *et al*., 1998; Kaufmann *et al*., 2001).

VII. Prospects for Antiviral Treatments of Cervical Carcinoma

The sustained expression of HPV oncogene products in cervical cancer cells suggests that these viral proteins may be required for the survival and proliferation of the cells. To test this possibility, a number of approaches have been used to inhibit the expression or activity of the E6 or E7 proteins in cervical cancer cell lines, including approaches that reduce the amount of viral RNA in cells or, less commonly, that interfere with the action of the viral proteins. Antisense RNA, RNA interference, or ribozymes have been used to degrade viral RNA, and transcriptional repressors have been used to inhibit transcription of the viral genes. Small proteins that bind and inhibit the E6 or E7 proteins have also been used. These experiments showed that inhibition of HPV function by a variety of methods caused either growth arrest or apoptosis in cervical carcinoma cell lines (Alvarez-Salas *et al*., 2003; Steele *et al*., 1992; Storey *et al*., 1991; von Knebel Doeberitz *et al*., 1988). The most dramatic effects were obtained after introduction of the bovine papillomavirus E2 transcription factor, which binds to the E6/E7 promoter in the integrated HPV genome and efficiently represses expression of the viral oncogenes (Desaintes *et al*., 1997; Dowhanick *et al*., 1995; Hwang *et al*., 1993). E6/E7 repression results in the reactivation of the Rb and p53 tumor suppressor pathways and in the rapid acquisition of a growth arrested state that closely resembles replicative senescence achieved by primary cells after they have

reached the end of their normal lifespan during serial passage in culture (Francis *et al*., 2000; Goodwin and DiMaio, 2000; Goodwin *et al*., 2000; Hwang *et al*., 1996; Wells *et al*., 2000; Wu *et al*., 2000). Further genetic analysis indicated that E6 expression is continuously required for p53 inactivation in cervical cancer cell lines, and that E7 expression is continuously required for Rb inactivation (DeFilippis *et al*., 2003). Several experiments indicated that Rb activation is primarily responsible for induced senescence following E7 repression (DeFilippis *et al*., 2003; Psyrri *et al*., 2004; Wells *et al*., 2000).

The continuous requirement for viral protein function in cervical cancer cells implies that the cellular mutations that accumulate during carcinogenic progression are not sufficient to maintain these cells in a proliferative state and suggests that agents that interfere with the expression of the HPV genome or block the interaction of E6 or E7 with their cellular targets may restore tumor suppressor function and inhibit the growth or survival of the cells (Sterlinko Grm and Banks, 2004). Because E7 has proapoptotic activity that can be blocked by the E6 protein (Pan and Griep, 1994; Stoppler *et al*., 1998), interventions that specifically block E6 function may be particularly useful by inducing apoptosis triggered by ongoing E7 expression (Butz *et al*., 2000, 2003; Horner *et al*., 2004). Agents that inhibit the function of E1 or E2 are not likely to be useful in most cases of cancer because these proteins are often lost in the cancers and the integrated viral DNA replicates passively in the cellular chromosomes. The absence of viral genomes and proteins from uninfected normal cells suggests that it will be possible to develop highly specific antiviral agents with relatively minor side effects.

VIII. Conclusions and Prospects

Epidemiological, laboratory, and clinical studies have established that high-risk HPVs play an obligatory role in the genesis of cervical carcinoma. Molecular and cell biological studies have revealed the basic features of the viral life cycle and provided detailed understanding of the effects of viral proteins on virus propagation and on the cellular phenotype. These advances have provided the information necessary to develop several promising strategies to combat papillomavirus infection or treat HPV-associated cancer. We can envision a future where most cases of cervical carcinoma are prevented by prophylactic vaccination, screening and early intervention, or successfully treated by thera-

peutic vaccination or nontoxic antiviral agents (Schiffman and Castle, 2005). This optimistic scenario is a direct outcome of our understanding of the basic virology of cervical carcinogenesis.

Acknowledgments

We thank Paul Lambert and members of the DiMaio laboratory for critical reading of this manuscript. J. B. L. was supported by a Reproductive Scientist Development Award from the NICHD (HD00849) and the Berlex Foundation. Research in the DiMaio laboratory was supported by grants from the National Cancer Institute (CA16038 and CA37157).

References

Alvarez-Salas, L. M., Benitez-Hess, M. L., and DiPaolo, J. A. (2003). Advances in the development of ribozymes and antisense oligodeoxynucleotides as antiviral agents for human papillomaviruses. *Antivir. Ther.* **8:**265–278.

Androphy, E. J., Lowy, D. R., and Schiller, J. T. (1987). Bovine papillomavirus E2 trans-activating gene product binds to specific sites in papillomavirus DNA. *Nature* **325:**70–73.

Antinore, M. J., Birrer, M. J., Patel, D., Nader, L., and McCance, D. J. (1996). The human papillomavirus type 16 E7 gene product interacts with and trans-activates the AP1 family of transcription factors. *EMBO J.* **15:**1950–1960.

Arbeit, J. M., Munger, K., Howley, P. M., and Hanahan, D. (1994). Progressive squamous epithelial neoplasia in K14-human papillomavirus type 16 transgenic mice. *J. Virol.* **68:**4358–4368.

Arbeit, J. M., Howley, P. M., and Hanahan, D. (1996). Chronic estrogen-induced cervical and vaginal squamous carcinogenesis in human papillomavirus type 16 transgenic mice. *Proc. Natl. Acad. Sci. USA* **93:**2930–2935.

Ashrafi, G. H., Tsirimonaki, E., Marchetti, B., O'Brien, P. M., Sibbet, G. J., Andrew, L., and Campo, M. S. (2002). Down-regulation of MHC class I by bovine papillomavirus E5 oncoproteins. *Oncogene* **21:**248–259.

Ashrafi, G. H., Haghshenas, M. R., Marchetti, B., O'Brien, P. M., and Campo, M. S. (2005). E5 protein of human papillomavirus type 16 selectively downregulates surface HLA class I. *Int. J. Cancer* **113:**276–283.

Asselineau, D., and Prunieras, M. (1984). Reconstruction of "simplified" skin: Control of fabrication *Br. J. Dermatol.* **111:**219–222.

Azoury-Ziadeh, R., Herd, K., Fernando, G. J. P., Lambert, P., Frazer, I. H., and Tindle, R. W. (2001). Low level expression of human papillomavirus type 16 (HPV16) E6 in squamous epithelium does not elicit E6 specific B- or T-helper immunological responses, or influence the outcome of immunisation with E6 protein. *Virus Res.* **73:**189–199.

Baldwin, P. J., van der Burg, S. H., Boswell, C. M., Offringa, R., Hickling, J. K., Dobson, J., Roberts, J. S., Latimer, J. A., Moseley, R. P., Coleman, N., Stanley, M. A., and Sterling, J. C. (2003). Vaccinia-expressed human papillomavirus 16 and 18 E6 and

E7 as a therapeutic vaccination for vulval and vaginal intraepithelial neoplasia. *Clin. Cancer Res.* **9:**5205–5213.

Barksdale, S., and Baker, C. C. (1995). Differentiation-specific alternative splicing of bovine papillomavirus late mRNAs. *J. Virol.* **69:**6553–6556.

Barksdale, S. K., and Baker, C. C. (1993). Differentiation-specific expression from the bovine papillomavirus type 1 P2443 and late promoters. *J. Virol.* **67:**5605–5616.

Barnard, P., and McMillan, N. A. (1999). The human papillomavirus E7 oncoprotein abrogates signaling mediated by interferon-alpha. *Virology* **259:**305–313.

Bastien, N., and McBride, A. A. (2000). Interaction of the papillomavirus E2 protein with mitotic chromosomes. *Virology* **270:**124–134.

Baxter, M. K., McPhillips, M. G., Ozato, K., and McBride, A. A. (2005). The mitotic chromosome binding activity of the papillomavirus E2 protein correlates with interaction with the cellular chromosomal protein. *J. Virol.* **79:**4806–4818.

Bedell, M. A., Jones, K. H., Grossman, S. R., and Laimins, L. A. (1989). Identification of human papillomavirus type 18 transforming genes in immortalized and primary cells. *J. Virol.* **63:**1247–1255.

Bedell, M. A., Hudson, J. B., Golub, T. R., Turyk, M. E., Hosken, M., Wilbanks, G. D., and Laimins, L. A. (1991). Amplification of human papillomavirus genomes *in vitro* is dependent on epithelial differentiation. *J. Virol.* **65:**2254–2260.

Bellanger, S., Blachon, S., Mechali, F., Bonne-Andrea, C., and Thierry, F. (2005). High-risk but not low-risk HPV E2 proteins bind to the APC activators Cdh1 and Cdc20 and cause genomic instability. *Cell Cycle* **4:**1608–1615.

Bernard, B. A., Bailly, C., Lenoir, M. C., Darmo, M., Thierry, F., and Yaniv, M. (1989). The human papillomavirus type 18 (HPV18) E2 gene product is a repressor of the HPV18 regulatory region in human keratinoctyes. *J. Virol.* **63:**4317–4324.

Bernard, H. U. (2002). Gene expression of genital human papillomaviruses and considerations on potential antiviral approaches. *Antivir. Ther.* **7:**219–237.

Bernat, A., Avvakumov, N., Mymryk, J. S., and Banks, L. (2003). Interaction between the HPV E7 oncoprotein and the transcriptional coactivator p300. *Oncogene* **22:**7871–7881.

Berumen, J., Ordonez, R. M., Lazcano, E., Salmeron, J., Galvan, S. C., Estrada, R. A., Yunes, E., Garcia-Carranca, A., Gonzalez-Lira, G., and Madrigal-de la Campa, A. (2001). Asian-American variants of human papillomavirus 16 and risk for cervical cancer: A case-control study. *J. Natl. Cancer Inst.* **93:**1325–1330.

Bischof, O., Nacerddine, K., and Dejean, A. (2005). Human papillomavirus oncoprotein E7 targets the promyelocytic leukemia protein and circumvents cellular senescence via the Rb and p53 tumor suppressor pathways. *Mol. Cell. Biol.* **25:**1013–1024.

Bontkes, H. J., Waqlboomers, J. M., Meijer, C. J., Helmerhorst, T. J., and Stern, P. L. (1998). Specific HLA class I down-regulation is an early event in cervical dysplasia associated with clinical progression. *Lancet* **351:**187–188.

Bontkes, H. J., de Gruijl, T. D., van den Muysenberg, A. J., Verheijen, R. H., Stukart, M. J., Meijer, C. J., Scheper, R. J., Stacey, S. N., Duggan-Keen, M. F., Stern, P. L., Man, S., Borysiewicz, L. K., *et al.* (2000). Human papillomavirus type 16 E6/E7-specific cytotoxic T lymphocytes in women with cervical neoplasia. *Int. J. Cancer* **88:**92–98.

Borchers, A., Braspenning, J., Meijer, J., Osen, W., Gissmann, L., and Jochumus, I. (1999). E7-specific cytotoxic T cell tolerance in HPV-transgenic mice. *Arch. Virol.* **144:**1539–1556.

Borysiewicz, L. K., Fiander, A., Nimako, M., Man, S., Wilkinson, G. W., Westmoreland, D., Evans, A. S., Adams, M., Stacey, S. N., Boursnell, M. E., Rutherford, E., Hickling, J. K., *et al.* (1996). A recombinant vaccinia virus encoding human papillomavirus types

16 and 18, E6 and E7 proteins as immunotherapy for cervical cancer. *Lancet* **347:**1523–1527.

Bosch, F. X., Lorincz, A., Munoz, N., Meijer, C. J., and Shah, K. V. (2002). The causal relation between human papillomavirus and cervical cancer. *J. Clin. Pathol.* **55:**244–265.

Boshart, M., Gissmann, L., Ikenberg, H., Kleinheinz, A., Scheurlen, W., and zur Hausen, H. (1984). A new type of papillomavirus DNA, its presence in genital cancer biopsies and in cell lines derived from cervical cancer. *EMBO J.* **3:**1151–1157.

Bouvard, V., Storey, A., Pim, D., and Banks, L. (1994). Characterization of the human papillomavirus E2 protein: Evidence of trans-activation and trans-repression in cervical keratinocytes. *EMBO J.* **13:**5451–5459.

Boyer, S. N., Wazer, D. E., and Band, V. (1996). E7 protein of human papilloma virus-16 induces degradation of retinoblastoma protein through the ubiquitin-proteasome pathway. *Cancer Res.* **56:**4620–4624.

Brake, T., and Lambert, P. F. (2005). Estrogen contributes to the onset, persistence, and malignant progression of cervical cancer in a human papillomavirus-transgenic mouse model. *Proc. Natl. Acad. Sci. USA* **102:**2490–2495.

Brandsma, J. L., and Xiao, W. (1993). Infectious virus replication in papillomas induced by molecularly cloned cottontail rabbit papillomavirus DNA. *J. Virol.* **67:**567–571.

Brandsma, J. L., Yang, Z. H., Barthold, S. W., and Johnson, E. A. (1991). Use of a rapid, efficient inoculation method to induce papillomas by cottontail rabbit papillomavirus DNA shows that the E7 gene is required. *Proc. Natl. Acad. Sci. USA* **88:**4816–4820.

Bravo, J. G., and Alonso, A. (2004). Mucosal human papillomaviruses encode four different E5 proteins whose chemistry and phylogeny correlate with malignant or benign growth. *J. Virol.* **78:**13613–13626.

Brehm, A., Nielsen, S. J., Miska, E. A., McCance, D. J., Reid, J. L., Bannister, A. J., and Kouzarides, T. (1999). The E7 oncoprotein associates with Mi2 and histone deacetylase activity to promote cell growth. *EMBO J.* **18:**2449–2458.

Breitburd, F., Kirnbauer, R., Hubbert, N. L., Nonnenmacher, B., Trin-Dinh-Desmarquet, C., Orth, G., Schiller, J. T., and Lowy, D. R. (1995). Immunization with virus-like particles from cottontail rabbit papillomavirus (CRPV) can protect against experimental CRPV infection. *J. Virol.* **69:**3959–3963.

Brown, D. R., Kitchin, D., Qadadri, B., Batteiger, T., and Ermel, A. (2005). The human papillomavirus type 11 E1;E4 protein is a transglutaminase 3 substrate and induces abnormalities of the cornified cell envelope. *Virology* **345:**290–298.

Butz, K., Denk, C., Ullmann, A., Scheffner, M., and Hoppe-Seyler, F. (2000). Induction of apoptosis in human papillomavirus-positive cancer cells by peptide aptamers targeting the viral E6 oncoprotein. *Proc. Natl. Acad. Sci. USA* **97:**6693–6697.

Butz, K., Ristriani, T., Hengstermann, A., Denk, C., Scheffner, M., and Hoppe-Seyler, F. (2003). siRNA targeting of the viral E6 oncogene efficiently kills human papillomavirus-positive cancer cells. *Oncogene* **22:**5938–5945.

Chang, J. L., Tsao, Y. P., Liu, D. W., Huang, S. J., Lee, W. H., and Chen, S. L. (2001). The expression of HPV-16 E5 protein in squamous neoplastic changes in the uterine cervix. *J. Biomed. Sci.* **8:**206–213.

Chellappan, S., Kraus, V. B., Kroger, B., Munger, K., Howley, P. M., Phelps, W. C., and Nevins, J. R. (1992). Adenovirus E1A, simian virus 40 tumor antigen, and human papillomavirus E7 protein share the capacity to disrupt the interaction between transcription factor E2F and the retinoblastoma gene product. *Proc. Natl. Acad. Sci. USA* **89:**4549–4553.

Chen, G., and Stenlund, A. (2002). Sequential and ordered assembly of E1 initiator complexes on the papillomavirus origin of DNA replication generates progressive structural changes related to melting. *Mol. Cell. Biol.* **22:**7712–7720.

Cheng, S., Schmidt-Grimminger, D. C., Murant, T., Broker, T. R., and Chow, L. T. (1995). Differentiation-dependent up-regulation of the human papillomavirus E7 gene reactivates cellular DNA replication in suprabasal differentiated keratinocytes. *Genes Dev.* **9:**2335–2349.

Chong, T., Apt, D., Gloss, B., Isa, M., and Bernard, H. U. (1991). The enhancer of human papillomavirus type 16: Binding sites for the ubiquitous transcription factors oct-1, NFA, TEF-2, NF1, and AP-1 participate in epithelial cell-specific transcription. *Virology* **65:**5933–5943.

Christensen, N. D., Reed, C. A., Cladel, N. M., Han, R., and Kreider, J. W. (1996). Immunization with viruslike particles induces long-term protection of rabbits against challenge with cottontail rabbit papillomavirus. *J. Virol.* **70:**960–965.

Chu, N. R., Wu, H. B., Wu, T., Boux, L. J., Siegel, M. I., and Mizzen, L. A. (2000). Immunotherapy of a human papillomavirus (HPV) type 16 E7-expressing tumour by administration of fusion protein comprising *Mycobacterium bovis* bacille Calmette-Guerin (BCG) hsp65 and HPV16 E7. *Clin. Exp. Immunol.* **121:**216–225.

Collier, B., Oberg, D., Zhao, X., and Schwartz, S. (2002). Specific inactivation of inhibitory sequences in the 5′ end of the human papillomavirus type 16 L1 open reading frame results in production of high levels of L1 protein in human epithelial cells. *J. Virol.* **76:**2739–2752.

Conger, K. L., Liu, J. S., Kuo, S. R., Chow, L. T., and Wang, T. S. (1999). Human papillomavirus DNA replication. Interactions between the viral E1 protein and two subunits of human DNA polymerase alpha/primase. *J. Biol. Chem.* **274:**2696–2705.

Connor, M. E., and Stern, P. L. (1990). Loss of MHC class-I expression in cervical carcinomas. *Int. J. Cancer* **46:**1029–1034.

Conrad, M., Bubb, V. J., and Schlegel, R. (1993). The human papillomavirus type 6 and 16 E5 proteins are membrane-associated proteins which associate with the 16-kilodalton pore-forming protein. *J. Virol.* **67:**6170–6178.

Cullen, A. P., Reid, R., Campion, M., and Lorincz, A. T. (1991). Analysis of the physical state of different human papillomavirus DNAs in intraepithelial and invasive cervical neoplasm. *J. Virol.* **65:**606–612.

Cumming, S. A., Repellin, C. E., McPhillips, M., Radford, J. C., Clements, J. B., and Graham, S. V. (2002). The human papillomavirus type 31 late 3′ untranslated region contains a complex regulatory element. *J. Virol.* **76:**5993–6003.

De Bruijn, M. L. H., Greenstone, H. L., Vermeulen, H., Melief, C. J. M., Lowy, D. R., Schiller, J. T., and Kast, W. M. (1998). L1-specific protection from tumor challenge elicited by HPV16 virus-like particles. *Virology* **250:**371–376.

de Villiers, E.-M., Gissmann, L., and zur Hausen, H. (1981). Molecular cloning of viral DNA from human genital warts. *J. Virol.* **40:**932–935.

DeFilippis, R. A., Goodwin, E. C., Wu, L., and DiMaio, D. (2003). Endogenous human papillomavirus E6 and E7 proteins differentially regulate proliferation, senescence, and apoptisis in HeLa cervical carcinoma cells. *J. Virol.* **77:**1551–1563.

Demeret, C., Garcia-Carranca, A., and Thierry, F. (2003). Transcription-independent triggering of the extrinsic pathway of apoptosis by human papillomavirus 18 E2 protein. *Oncogene* **16:**168–175.

Deng, S. J., Pearce, K. H., Dixon, E. P., Hartley, K. A., Stanley, T. B., Lobe, D. C., Garvey, E. P., Kost, T. A., Petty, R. L., Rocque, W. J., Alexander, K. A., and Underwood, M. R. (2004). Identification of peptides that inhibit the DNA binding, trans-activator, and

DNA replication functions of the human papillomavirus type 11 E2 protein. *J. Virol.* **78:**2637–2641.

Desaintes, C., Demeret, C., Goyat, S., Yaniv, M., and Thierry, F. (1997). Expression of the papillomavirus E2 protein in HeLa cells leads to apoptosis. *EMBO J.* **16:**504–514.

DiMaio, D., Lai, C. C., and Mattoon, D. (2000). The platelet-derived growth factor β receptor as a target of the bovine papillomavirus E5 protein. *Cytokine Growth Factor Rev.* **11:**283–293.

Dollard, S. C., Wilson, J. L., Demeter, L. M., Bonnez, W., Reichman, R. C., Broker, T. R., and Chow, L. T. (1992). Production of human papillomavirus and modulation of the infectious program in epithelial raft cultures. *Genes Dev.* **6:**1131–1142.

Dong, X. P., Stubenrauch, F., Beyer-Finkler, E., and Pfister, H. (1994). Prevalence of deletions of YY1-binding sites in episomal HPV 16 DNA from cervical cancers. *Int. J. Cancer* **58:**803–808.

Doorbar, J., Ely, S., Sterling, J., McLean, C., and Crawford, L. (1991). Specific interaction between HPV-16 E1-E4 and cytokeratins results in collapse of the epithelial cell intermediate filament network. *Nature* **352:**824–827.

Dorn, H. F., and Cutler, S. J. (1959). Morbility from cancer in the United States: Parts I and II. Publ. Health M. No. 56, US Dept. of HEW, Washington, DC.

Dostatni, N., Lambert, P. F., Sousa, R., Ham, J., Howley, P. M., and Yaniv, M. (1991). The functional BPV-1 E2 trans-activating protein can act as a repressor by preventing formation of the initiation complex. *Genes Dev.* **5:**1657–1671.

Dowhanick, J. J., McBride, A. A., and Howley, P. M. (1995). Suppression of cellular proliferation by the papillomavirus E2 protein. *J. Virol.* **69:**7791–7799.

Duensing, S., and Munger, K. (2004). Mechanisms of genomic instability in human cancer: Insights from studies with human papillomavirus oncoproteins. *Int. J. Cancer* **109:**157–162.

Duensing, S., Duensing, A., Crum, C. P., and Munger, K. (2001a). Human papillomavirus type 16 E7 oncoprotein-induced abnormal centrosome synthesis is an early event in the evolving malignant phenotype. *Cancer Res.* **61:**2356–2360.

Duensing, S., Duensing, A., Flores, E. R., Do, A., Lambert, P. F., and Munger, K. (2001b). Centrosome abnormalities and genomic instability by episomal expression of human papillomavirus type 16 in raft cultures of human keratinocytes. *J. Virol.* **75:**7712–7716.

Dunn, L. A., Evander, M., Tindle, R. W., Bulloch, A. L., de Kluyver, R. L., Fernando, G. J., Lambert, P. F., and Frazer, I. H. (1997). Presentation of the HPV16E7 protein by skin grafts is insufficient to allow graft rejection in an E7-primed animal. *Virology* **235:**94–103.

Durst, M., Gissmann, L., Ikenberg, H., and zur Hausen, H. (1983). A papillomavirus DNA from a cervical carcinoma and its prevalence in cancer biopsy samples from different geographic regions. *Proc. Natl. Acad. Sci. USA* **80:**3812–3815.

Durst, M., Dzarlieva-Petrusevska, R. T., Boukamp, P., Fusenig, N. E., and Gissmann, L. (1987). Molecular and cytogenetic analysis of immortalized human primary keratinocytes obtained after transfection with human papillomavirus type 16 DNA. *Oncogene* **1:**251–256.

Dyson, N., Howley, P. M., Munger, K., and Harlow, E. (1989). The human papilloma virus-16 E7 oncoprotein is able to bind to the retinoblastoma gene product. *Science* **243:**934–937.

Eiben, G. L., Velders, M. P., and Kast, W. M. (2002). The cell-mediated immune response to human papillomavirus-induced cervical cancer: Implications for immunotherapy. *Adv. Cancer Res.* **86:**113–148.

Engel, L. W., Heilman, C. A., and Howley, P. M. (1983). Transcriptional organization of bovine papillomavirus type 1. *J. Virol.* **47:**516–528.

Evans, E. M., Man, S., Evans, A. S., and Borysiewicz, L. K. (1997). Infiltration of cervical cancer tissue with human papillomavirus-specific cytotoxic T-lymphocytes. *Cancer Res.* **57:**2943–2950.

Faucher, A. M., White, P. W., Brochu, C., Grand-Maitre, C., Rancourt, J., and Fazal, G. (2004). Discovery of small-molecule inhibitors of the ATPase activity of human papillomavirus E1 helicase. *J. Med. Chem.* **47:**18–21.

Fehrmann, F., Klumpp, D. J., and Laimins, L. A. (2003). Human papillomavirus type 31 E5 protein supports cell cycle progression and activates late viral functions upon epithelial differentiation. *J. Virol.* **77:**2819–2831.

Feltkamp, M. C., Smits, H. L., Vierboom, M. P., Minnaar, R. P., de Jongh, B. M., Drijfhout, J. W., ter Schegget, J., Melief, C. J., and Kast, W. M. (1993). Vaccination with cytotoxic T lymphocyte epitope-containing peptide protects against a tumor induced by human papillomavirus type 16-transformed cells. *Eur. J. Immunol.* **23:**2242–2249.

Flores, E. R., and Lambert, P. F. (1997). Evidence for a switch in the mode of human papillomavirus type 16 DNA replication during the viral life cycle. *J. Virol.* **71:**7167–7179.

Flores, E. R., Allen-Hoffmann, B. L., Lee, D., and Lambert, P. F. (2000). The human papillomavirus type 16 E7 oncogene is required for the productive stage of the viral life cycle. *J. Virol.* **74:**6622–6631.

Foster, S. A., and Galloway, D. A. (1996). Human papillomavirus type 16 E7 alleviates a proliferation block in early passage human mammary epithelial cells. *Oncogene* **12:**1773–1779.

Franceschi, S., Dal Maso, L., Arniani, S., Crosignani, P., Vercelli, M., Simonato, L., Falcini, F., Zanetti, R., Barchielli, A., Serraino, D., and Rezza, G. (1998). Risk of cancer other than Kaposi's sarcoma and non-Hodgkin's lymphoma in persons with AIDS in Italy. Cancer and AIDS Registry Linkage Study. *Br. J. Cancer* **78:**966–970.

Francis, D. A., Schmid, S. I., and Howley, P. M. (2000). Repression of the integrated papillomavirus E6/E7 promoter is required for growth suppression of cervical cancer cells. *J. Virol.* **74:**2679–2686.

Frattini, M. G., and Laimins, L. A. (1994). Binding of the human papillomavirus E1 origin-recognition protein is regulated through complex formation with the E2 enhancer-binding protein. *Proc. Natl. Acad. Sci. USA* **91:**12398–12402.

Frattini, M. G., Lim, H. B., and Laimins, L. A. (1996). *In vitro* synthesis of oncogenic human papillomaviruses requires episomal genomes for differentiation-dependent late expression. *Proc. Natl. Acad. Sci. USA* **93:**3062–3067.

Frisch, M., Biggar, R. J., and Goedert, J. J. (2000). Human papillomavirus-associated cancers in patients with human immunodeficiency virus infection and acquired immunodeficiency syndrome. *J. Natl. Cancer Inst.* **92:**1500–1510.

Funk, J. O., Waga, S., Harry, J. B., Espling, E., Stillman, B., and Galloway, D. A. (1997). Inhibition of CDK activity and PCNA-dependent DNA replication by p21 is blocked by interaction with the HPV-16 E7 oncoprotein. *Genes Dev.* **11:**2090–2100.

Gage, J. R., Meyers, C., and Wettstein, F. O. (1990). The E7 proteins of the nononcogenic human papillomavirus type 6b (HPV-6b) and of the oncogenic HPV-16 differ in retinoblastoma protein binding and other properties. *J. Virol.* **64:**723–730.

Gardiol, D., Kuhne, C., Glaunsinger, B., Lee, S. S., Javier, R., and Banks, L. (1999). Oncogenic human papillomavirus E6 proteins target the discs large tumour suppressor for proteasome-mediated degradation. *Oncogene* **18:**5487–5496.

Genther, S. M., Sterling, S., Duensing, S., Munger, K., Sattler, C., and Lambert, P. F. (2003). Quantitative role of the human papillomavirus type 16 E5 gene during the productive stage of the viral life cycle. *J. Virol.* **77:**2832–2842.

Genther-Williams, S. M., Disbrow, G. L., Schlegel, R., Lee, D., Threadgill, D. W., and Lambert, P. F. (2005). Requirement of epidermal growth factor receptor for hyperplasia induced by E5, a high-risk human papillomavirus oncogene. *Cancer Res.* **65:**6534–6542.

Gewin, L., and Galloway, D. A. (2001). E box-dependent activation of telomerase by human papillomavirus type 16 E6 does not require induction of c-myc. *J. Virol.* **75:**7198–7201.

Gillette, T. G., Lusky, M., and Borowiec, J. A. (1994). Induction of structural changes in the bovine papillomavirus type 1 origin of replication by the viral E1 and E2 proteins. *Proc. Natl. Acad. Sci. USA* **91:**8846–8850.

Gillison, M. L. (2004). Human papillomavirus-associated head and neck cancer is a distinct epidemiologic, clinical, and molecular entity. *Semin. Oncol.* **31:**744–754.

Giroglou, T., Florin, L., Schafer, F., Streeck, R. F., and Sapp, M. (2001). Human papillomavirus infection requires cell surface heparan sulfate. *J. Virol.* **75:**1565–1570.

Gissmann, L., Wolnik, L., Ikenberg, H., Koldovsky, U., Schnurch, H. G., and zur Hausen, H. (1983). Human papillomavirus types 6 and 11 DNA sequences in genital and laryngeal papillomas and in some cervical cancers. *Proc. Natl. Acad. Sci. USA* **80:**560–563.

Glaunsinger, B. A., Lee, S. S., Thomas, M., Banks, L., and Javier, R. (2000). Interactions of the PDZ-protein MAGI-1 with adenovirus E4-ORF1 and high-risk papillomavirus E6 oncoproteins. *Oncogene* **19:**5270–5280.

Goldie, S. J., Grima, D., Kohli, M., Wright, T. C., Weinstein, M., and Franco, E. (2003). A comprehensive natural history model of HPV infection and cervical cancer to estimate the clinical impact of a prophylactic HPV-16/18 vaccine. *Int. J. Cancer* **106:**896–904.

Goldie, S. J., Gaffikin, L., Goldhaber-Fiebert, J. D., Gordillo-Tobar, A., Levin, C., Mahe, C., and Wright, T. C. (2005). Cost-effectiveness of cervical-cancer screening in five developing countries. *N. Engl. J. Med.* **353:**2158–2168.

Gonzalez, S. L., Stremlau, M., He, X., Basile, J. R., and Munger, K. (2001). Degradation of the retinoblastoma tumor suppressor by the human papillomavirus type 16 E7 oncoprotein is important for functional inactivation and is separable from proteasomal degradation of E7. *J. Virol.* **75:**7583–7591.

Goodwin, E. C., and DiMaio, D. (2000). Repression of human papillomavirus oncogenes in HeLa cervical carcinoma cells causes the orderly reactivation of dormant tumor suppressor pathways. *Proc. Natl. Acad. Sci. USA* **97:**12513–12518.

Goodwin, E. C., Yang, E., Lee, C. J., Lee, H. W., DiMaio, D., and Hwang, E. S. (2000). Rapid induction of senescence in human cervical carcinoma cells. *Proc. Natl. Acad. Sci. USA* **97:**10978–10983.

Greenstone, H. L., Nieland, J. D., de Visser, K. E., De Bruijn, M. L. H., Kirnbauer, R., Roden, R. B. S., Lowy, D. R., Kast, W. M., and Schiller, J. T. (1998). Chimeric papillomavirus virus-like particles elicit antitumor immunity against the E7 oncoprotein in an HPV16 tumor model. *Proc. Natl. Acad. Sci. USA* **95:**1800–1805.

Gustafsson, L., Ponten, J., Zack, M., and Adami, H.-O. (1997). International incidence rates of invasive cervical cancer after introduction of cytological screening. *Cancer Cause Control* **8:**755–763.

Hagensee, M. E., Yaegashi, N., and Galloway, D. A. (1993). Self-assembly of human papillomavirus type 1 capsids by expression of the L1 protein alone or by coexpression of the L1 and L2 capsid proteins. *J. Virol.* **67:**315–322.

Halbert, C. L., Demeres, W., and Galloway, D. A. (1991). The E7 gene of human papillomavirus type 16 is sufficient for immortalization of human epithelial cells. *J. Virol.* **65:**473–478.

Halpert, R., Fruchter, R. G., Sedlis, A., Butt, K., Boyce, J. G., and Sillman, F. H. (1986). Human papillomavirus and lower genital neoplasia in renal transplant patients. *Obstet. Gynecol.* **68:**251–258.

Hariharan, K., Braslawsky, G., Barnett, R. S., Berquist, L. G., Huynh, T., Hanna, N., and Black, A. (1998). Tumor regression in mice following vaccination with human papillomavirus E7 recombinant protein in PROVAX. *Int. J. Oncol.* **12:**1229–1235.

Harper, D. M., Franco, E. L., Wheeler, C., Ferris, D. G., Jenkins, D., Schuind, A., Zahaf, T., Innis, B., Naud, P., De Carvalho, N. S., Roteli-Martins, C. M., Teixeira, J., *et al.* (2004). Efficacy of a bivalent L1 virus-like particle vaccine in prevention of infection with human papillomavirus types 16 and 18 in young women: A randomised controlled trial. *Lancet* **364:**1757–1765.

Harro, C. D., Pang, Y. Y., Roden, R. B., Hildesheim, A., Wang, Z., Reynolds, M. J., Mast, T. C., Robinson, R., Murphy, B. R., Karron, R. A., Dillner, J., Schiller, J. T., *et al.* (2001). Safety and immunogenicity trial in adult volunteers of a human papillomavirus 16 L1 virus-like particle vaccine. *J. Natl. Cancer Inst.* **93:**284–292.

Hartley, K. A., and Alexander, K. A. (2002). Human TATA binding protein inhibits human papillomavirus type 11 DNA replication by antagonizing E1-E2 protein complex formation on the viral origin of replication. *J. Virol.* **76:**5014–5023.

Havre, P. A., Yuan, J., Hedrick, L., Cho, K. R., and Glazer, P. M. (1995). p53 inactivation by HPV16 E6 results in increased mutagenesis in human cells. *Cancer Res.* **55:**4420–4424.

Hawley-Nelson, P., Androphy, E. J., Lowy, D. R., and Schiller, J. T. (1988). The specific DNA recognition sequence of the bovine papillomavirus E2 protein is an E2-dependent enhancer. *EMBO J.* **7:**525–531.

Hawley-Nelson, P., Vousden, K. H., Hubbert, N. L., Lowy, D. R., and Schiller, J. T. (1989). HPV16 E6 and E7 proteins cooperate to immortalize human foreskin keratinocytes. *EMBO J.* **8:**3905–3910.

Heck, D. V., Yee, C. L., Howley, P. M., and Munger, K. (1992). Efficiency of binding the retinoblastoma protein correlates with the transforming capacity of the E7 oncoproteins of the human papillomaviruses. *Proc. Natl. Acad. Sci. USA* **89:**4442–4446.

Heselmeyer, K., Macville, M., Schrock, E., Blegen, H., Hellstrom, A. C., Shah, K., Auer, G., and Ried, T. (1997). Advanced-stage cervical carcinomas are defined by a recurrent pattern of chromosomal aberrations revealing high genetic instability and a consistent gain of chromosome arm 3q. *Genes Chromosomes Cancer* **19:**233–240.

Hickman, E. S., Picksley, S. M., and Vousden, K. H. (1994). Cells expressing HPV16 E7 continue cell cycle progression following DNA damage induced p53 activation. *Oncogene* **9:**2177–2181.

Hildesheim, A., Schiffman, M. H., Gravitt, P. E., Glass, A. G., Greer, C. E., Zhang, T., Scott, D. R., Rush, B. B., Lawler, P., and Sherman, M. E. (1994). Persistence of type-specific human papillomavirus infection among cytologically normal women. *J. Infect. Dis.* **169:**235–240.

Ho, G. Y., Bierman, R., Beardsley, L., Chang, C. J., and Burk, R. D. (1998). Natural history of cervicovaginal papillomavirus infection in young women. *N. Engl. J. Med.* **338:**423–428.

Hofmann, K., Cook, J., Joyce, J., Brown, D., Schultz, L., George, H., Rosolowsky, M., Fife, K., and Jansen, K. (1995). Sequence determination of human papillomavirus 6a and assembly of virus-like particles in *Saccharomyces cerevisiae*. *Virology* **209:**506–518.

Holt, S. E., Schuller, G., and Wilson, V. G. (1994). DNA binding specificity of the bovine papillomavirus E1 protein is determined by sequences contained within an 18-base-pair inverted repeat element at the origin of replication. *J. Virol.* **68:**1094–1102.

Hopman, A. H. N., Smedts, F., Dignef, W., Ummelen, M., Sonke, G., Mravunac, M., Vooijs, G. P., Speel, E. J., and Ramaekers, F. C. (2004). Transition of high-grade cervical intraepithelial neoplasia to micro-invasive carcinoma is characterized by integration of HPV 16/18 and numerical chromosome abnormalities. *J. Pathol.* **202:**23–33.

Horner, S. M., DeFilippis, R. A., Manuelidis, L., and DiMaio, D. (2004). Repression of the human papillomavirus E6 gene initiates p53-dependent, telomerase-independent senescence and apoptosis in HeLa cervical carcinoma cells. *J. Virol.* **78:**4063–4073.

Hsieh, C. H., Tsao, Y. P., Wang, C. H., Han, C. P., Chang, J. L., Lee, J. Y., and Chen, S. L. (2000). Sequence variants and functional analysis of human papillomavirus type 16 E5 gene in clinical specimens. *Arch. Virol.* **145:**2273–2284.

Hudson, J. B., Bedell, M. A., McCance, D. J., and Laimins, L. A. (1990). Immortalization and altered differentiation of human keratinocytes in vitro by the E6 and E7 open reading frames of human papillomavirus type 18. *J. Virol.* **64:**519–526.

Hwang, E.-S., Riese, II, D. J., Settleman, J., Nilson, L. A., Honig, J., Flynn, S., and DiMaio, D. (1993). Inhibition of cervical carcinoma cell line proliferation by the introduction of a bovine papillomavirus regulatory gene. *J. Virol.* **67:**3720–3729.

Hwang, E.-S., Nottoli, T., and DiMaio, D. (1995). The HPV16 E5 protein: Expression, detection, and stable complex formation with transmembrane proteins in COS cells. *Virology* **211:**227–233.

Hwang, E.-S., Naeger, L. K., and DiMaio, D. (1996). Activation of the endogenous p53 growth inhibitory pathway in HeLa cervical carcinoma cells by expression of the bovine papillomavirus E2 gene. *Oncogene* **12:**795–803.

Iftner, T., Elbel, M., Schopp, B., Hiller, T., Loizou, J. I., Caldecott, K. W., and Stubenrauch, F. (2002). Interference of papillomavirus E6 protein with single-strand break repair by interaction with XRCC1. *EMBO J.* **21:**4741–4748.

Ilves, I., Kivi, S., and Ustav, M. (1999). Long-term episomal maintenance of bovine papillomavirus type 1 plasmids is determined by attachment to host chromosomes, which is mediated by the viral E2 protein and its binding sites. *J. Virol.* **73:**4404–4412.

Jeon, S., Allen, H. B., and Lambert, P. F. (1995). Integration of human papillomavirus type 16 into the human genome correlates with a selective growth advantage of cells. *J. Virol.* **69:**2989–2997.

Johannesson, G., Geirsson, G., and Day, N. (1978). The effect of mass screening in Iceland, 1965–74, on the incidence and mortality of cervical carcinoma. *Int. J. Cancer* **21:**418–425.

Jones, D. L., and Munger, K. (1997). Analysis of the p53-mediated G1 growth arrest pathway in cells expressing the human papillomavirus type 16 E7 oncoprotein. *J. Virol.* **71:**2905–2912.

Jones, D. L., Alani, R. M., and Munger, K. (1997). The human papillomavirus E7 oncoprotein can uncouple cellular differentiation and proliferation in human keratinocytes by abrogating $p21^{Cip1}$-mediated inhibition of cdk2. *Genes Dev.* **11:**2101–2111.

Joyce, J. G., Tung, J. S., Przysiecki, C. T., Cook, J. C., Lehman, E. D., Sands, J. A., Jansen, K. U., and Keller, P. M. (1999). The L1 major capsid protein of human papillomavirus type 11 recombinant virus-like particles interacts with heparin and cell-surface glycosaminoglycans on human keratinocytes. *J. Biol. Chem.* **274:**5810–5822.

Kadish, A. S., Ho, G. Y., Burk, R. D., Wang, Y., Romney, S. L., Ledwidge, R., and Angeletti, R. H. (1997). Lymphoproliferative responses to human papillomavirus (HPV) type 16 proteins E6 and E7: Outcome of HPV infection and associated neoplasia. *J. Natl. Cancer Inst.* **89:**1285–1293.

Kadish, A. S., Timmins, P., Wang, Y., Ho, G. Y., Burk, R. D., Ketz, J., He, W., Romney, S. L., Johnson, A., Angeletti, R., and Abadi, M. (2002). Regression of cervical intraepithelial neoplasia and loss of human papillomavirus (HPV) infection is associated with cell-mediated immune responses to an HPV type 16 E7 peptide. *Cancer Epidemiol. Biomarkers Prev.* **11:**483–488.

Kasukawa, H., Howley, P. M., and Benson, J. D. (1998). A fifteen-amino-acid peptide inhibits human papillomavirus E1-E2 interaction and human papillomavirus DNA replication *in vitro*. *J. Virol.* **72:**8166–8173.

Kaufmann, A. M., Nieland, J. D., Schinz, M., Nonn, M., Gabelsberger, J., Meissner, H., Muller, R. T., Jochmus, I., Gissmann, L., Schneider, A., and Durst, M. (2001). HPV16 L1E7 chimeric virus-like particles induce specific HLA-restricted T cells in humans after *in vitro* vaccination. *Int. J. Cancer* **92:**285–293.

Kaur, P., and McDougall, J. K. (1989). HPV-18 immortalization of human keratinocytes. *Virology* **173:**302–310.

Kennedy, I. M., Haddow, J. K., and Clements, J. B. (1991). A negative regulatory element in the human papillomavirus type 16 genome acts at the level of late mRNA stability. *J. Virol.* **65:**2093–2097.

Kessis, T. D., Slebos, R. J. C., Nelson, W. G., Kastan, M. B., Plunkett, B. S., Han, S. M., Lorincz, A. T., Hedrick, L., and Cho, K. R. (1993). Human papillomavirus 16 E6 expression disrupts the p53-mediated cellular response to DNA damage. *Proc. Natl. Acad. Sci. USA* **90:**3988–3992.

Kirnbauer, R., Booy, F., Cheng, N., Lowy, D. R., and Schiller, J. T. (1992). Papillomavirus L1 major capsid protein self-assembles into virus-like particles that are highly immunogenic. *Proc. Natl. Acad. Sci. USA* **89:**12180–12184.

Kirnbauer, R., Taub, J., Greenstone, H., Roden, R. B. S., Durst, M., Gissmann, L., Lowy, D. R., and Schiller, J. T. (1993). Efficient self-assembly of human papillomavirus type 16 L1 and L1-L2 into virus-like particles. *J. Virol.* **67:**6929–6936.

Kirnbauer, R., Chandrachud, L., O'Neil, B., Wagner, E., Grindlay, G., Armstrong, A., McGarvie, G., Schiller, J., Lowy, D., and Campo, M. (1996). Virus-like particles of bovine papillomavirus type 4 in prophylactic and therapeutic immunization. *Virology* **219:**37–44.

Kisseljov, F., Semionova, L., Samoylova, E., Mazurenko, N., Komissarova, E., Zourbitskaya, V., Gritzko, T., Kozachenko, V., Netchushkin, M., Petrov, S., Smirnov, A., and Alonso, A. (1996). Instability of chromosome 6 microsatellite repeats in human cervical tumors carrying papillomavirus sequences. *Int. J. Cancer* **69:**484–487.

Kiyono, T., Foster, S. A., Koop, J. I., McDougall, J. K., Galloway, D. A., and Klingelhutz, A. J. (1998). Both Rb/p16INK4a inactivation and telomerase activity are required to immortalize human epithelial cells. *Nature* **396:**84–88.

Klingelhutz, A. J., Foster, S. A., and McDougall, J. K. (1996). Telomerase activation by the E6 gene product of human papillomavirus type 16. *Nature* **380:**79–82.

Klumpp, D. J., and Laimins, L. A. (1999). Differentiation-induced changes in promoter usage for transcripts encoding the human papillomavirus type 31 replication protein E1. *Virology* **257:**239–246.

Koopman, L. A., Corver, W. E., van der Slik, A. R., Giphart, M. J., and Fleuren, G. J. (2000). Multiple genetic alterations cause frequent and heterogeneous human histocompatibility leukocyte antigen class I loss in cervical cancer. *J. Exp. Med.* **191:**961–976.

Koutsky, L. A., Holmes, K. K., Critchlow, C., Stevens, C. E., Paavonen, J., Beckmann, A. M., DeRouen, T. A., Galloway, D. A., Vernon, D., and Kiviat, N. B. (1992). A cohort study of the risk of cervical intraepithelial neoplasia grade 2 or 3 in relation to papillomavirus infection. *N. Engl. J. Med.* **327:**1272–1278.

Koutsky, L. A., Ault, K. A., Wheeler, C. M., Brown, D. R., Barr, E., Alvarez, F. B., Chicchierini, L. M., and Jansen, K. U. (2002). A controlled trial of a human papillomavirus type 16 vaccine. *N. Engl. J. Med.* **347:**1645–1651.

Kulasingam, S. L., and Myers, E. R. (2003). Potential health and economic impact of adding a human papillomavirus vaccine to screening programs. *JAMA* **290:**781–789.

Lambert, P. F., Pan, H., Pitot, H., Liem, A., Jackson, M., and Griep, A. (1993). Epidermal cancer associated with expression of human papillomavirus type 16 E6 and E7 oncogenes in the skin of transgenic mice. *Proc. Natl. Acad. Sci. USA* **90:**5583–5587.

Lee, C., and Laimins, L. A. (2004). Role of the PDZ domain-binding motif of the oncoprotein E6 in the pathogenesis of human papillomavirus type 31. *J. Virol.* **78:**12366–12377.

Lee, S. J., Cho, Y. S., Cho, M. C., Shim, J. H., Lee, K. A., Ko, K. K., Choe, Y. K., Park, S. N., Hoshino, T., Kim, S., Dinarello, C. A., and Yoon, D. Y. (2001). Both E6 and E7 oncoproteins of human papillomavirus 16 inhibit IL-18-induced IFN-gamma production in human peripheral blood mononuclear and NK cells. *J. Immunol.* **167:**497–504.

Lee, S. S., Glaunsinger, B., Mantovani, F., Banks, L., and Javier, R. T. (2000). Multi-PDZ domain protein MUPP1 is a cellular target for both adenovirus E4-ORF1 and high-risk papillomavirus type 18 E6 oncoproteins. *J. Virol.* **74:**9680–9693.

Lehman, C. W., and Botchan, M. R. (1998). Segregation of viral plasmids depends on tethering to chromosomes and is regulated by phosphorylation. *Proc. Natl. Acad. Sci. USA* **95:**4338–4343.

Lin, K. Y., Guarnieri, F. G., Staveley-O'Carroll, K. F., Levitsky, H. I., August, J. T., Pardoll, D. M., and Wu, T. C. (1996). Treatment of established tumors with a novel vaccine that enhances major histocompatibility class II presentation of tumor antigen. *Cancer Res.* **56:**21–26.

Longworth, M. S., and Laimins, L. A. (2004). Pathogenesis of human papillomaviruses in differentiating epithelia. *Microbiol. Mol. Biol. Rev.* **68:**362–372.

Loo, Y. M., and Melendy, T. (2004). Recruitment of replication protein A by the papillomavirus E1 protein and modulation by single-stranded DNA. *J. Virol.* **78:**1605–1615.

Lowy, D. R., Kirnbauer, R., and Schiller, J. T. (1994). Genital human papillomavirus infection. *Proc. Natl. Acad. Sci. USA* **91:**2436–2440.

Luscher-Firzlaff, J. M., Westendorf, J. M., Zwicker, J., Burkhardt, H., Henriksson, M., Muller, R., Pirollet, F., and Luscher, B. (1999). Interaction of the fork head domain transcription factor MPP2 with the human papilloma virus 16 E7 protein: Enhancement of transformation and transactivation. *Oncogene* **18:**5620–5630.

Madeleine, M. M., Shera, K., Schwartz, S. M., Daling, J. R., Galloway, D. A., Wipf, G. C., Carter, J. J., McKnight, B., and McDougall, J. K. (2000). The p53 Arg72Pro polymorphism, human papillomavirus, and invasive squamous cell cervical cancer. *Cancer Epidemiol. Biomarkers Prev.* **9:**225–227.

Makni, H., Franco, E. L., Kaiano, J., Villa, L. L., Labrecque, S., Dudley, R., Storey, A., and Matlashewski, G. (2000). P53 polymorphism in codon 72 and risk of human papillomavirus induced cervical cancer: Effect of inter-laboratory variation. *Int. J. Cancer* **87:**528–533.

Marchetti, B., Ashrafi, G. H., Tsirimonaki, E., O'Brien, P. M., and Campo, M. S. (2002). The bovine papillomavirus oncoprotein E5 retains MHC class I molecules in the Golgi apparatus and prevents their transport to the cell surface. *Oncogene* **21:**7808–7816.

Massimi, P., Pim, D., Bertoli, C., Bouvard, V., and Banks, L. (1999). Interaction between the HPV-16 E2 transcriptional activator and p53. *Oncogene* **18:**7748–7754.

Masterson, P. J., Stanley, M. A., Lewis, A. P., and Romanos, M. A. (1998). A C-terminal helicase domain of the human papillomavirus E1 protein binds E2 and the DNA polymerase alpha-primase p68 subunit. *J. Virol.* **72:**7407–7419.

Matthews, C. P., Shera, K. A., and McDougall, J. K. (2000). Genomic changes and HPV type in cervical carcinoma. *P. Soc. Exp. Biol. Med.* **223:**316–321.

May, M., Dong, X. P., Beyer-Finkler, E., Stubenrauch, F., Fuchs, P. G., and Pfister, H. (1994). The E6/E7 promoter of extrachromosomal HPV16 DNA in cervical cancers escapes from cellular repression by mutation of target sequences for YY1. *EMBO J.* **13:**1460–1466.

McCance, D. J., Campion, M. J., Clarkson, P. K., Chesters, P. M., Jenkins, D., and Singer, A. (1985). Prevalence of human papillomavirus type 16 DNA sequences in cervical intraepithelial neoplasia and invasive carcinoma of the cervix. *Br. J. Obstet. Gynaecol.* **92:**1101–1105.

McCance, D. J., Kopan, R., Fuchs, E., and Laimins, L. A. (1988). Human papillomavirus type 16 alters human epithelial cell differentiation *in vitro*. *Proc. Natl. Acad. Sci. USA* **85:**7169–7173.

McIntyre, M. C., Ruesch, M. N., and Laimins, L. A. (1996). Human papillomavirus E7 oncoproteins bind a single form of cyclin E in a complex with cdk2 and p107. *Virology* **215:**73–82.

McLaughlin-Drubin, M. E., Bromberg-White, J. L., and Meyers, C. (2005). The role of the human papillomavirus type 18 E7 oncoprotein during the complete viral life cycle. *Virology* **338:**61–68.

Melero, I., Singhal, M. C., McGowan, P., Haugen, H. S., Blake, J., Hellstrom, K. E., Yang, G., Clegg, C. H., and Chen, L. (1997). Immunological ignorance of an E7-encoded cytolytic T-lymphocyte epitope in transgenic mice expressing the E7 and E6 oncogenes of human papillomavirus type 16. *J. Virol.* **71:**3998–4004.

Meyers, C., Frattini, M. G., Hudson, J. B., and Laimins, L. A. (1992). Biosynthesis of human papillomavirus from a continuous cell line upon epithelial differentiation. *Science* **257:**971–973.

Meyers, C., Mayer, T. J., and Ozbun, M. A. (1997). Synthesis of infectious human papillomavirus type 18 in differentiating epithelium transfected with viral DNA. *J. Virol.* **71:**7381–7386.

Mohr, I. J., Clark, R., Sun, S., Androphy, E. J., MacPherson, P., and Botchan, M. R. (1990). Targeting the E1 replication protein to the papillomavirus origin of replication by complex formation with the E2 transactivator. *Science* **250:**1694–1699.

Montgomery, K. D., Tedford, K. L., and McDougall, J. K. (1995). Genetic instability of chromosome 3 in HPV-immortalized and tumorigenic human keratinocytes. *Genes Chromosomes Cancer* **14:**97–105.

Muderspach, L., Wilczynski, S., Roman, L., Bade, L., Felix, J., Small, L. A., Kast, W. M., Fascio, G., Marty, V., and Weber, J. (2000). A phase I trial of a human papillomavirus (HPV) peptide vaccine for women with high-grade cervical and vulvar intraepithelial neoplasia who are HPV 16 positive. *Clin. Cancer Res.* **6:**3406–3416.

Munger, K., Phelps, W. C., Bubb, V., Howley, P. M., and Schlegel, R. (1989a). The E6 and E7 genes of the human papillomavirus type 16 together are necessary and sufficient for transformation of primary human keratinocytes. *J. Virol.* **63:**4417–4421.

Munger, K., Werness, B. A., Dyson, N., Phelps, W. C., Harlow, E., and Howley, P. M. (1989b). Complex formation of human papillomavirus E7 proteins with the retinoblastoma tumor suppressor gene product. *EMBO J.* **8:**4099–4105.

Nakagawa, S., and Huibregtse, J. M. (2000). Human scribble (Vartul) is targeted for ubiquitin-mediated degradation by the high-risk papillomavirus E6 proteins and the E6AP ubiquitin-protein ligase. *Mol. Cell. Biol.* **20:**8244–8253.

Nakahara, T., Peh, W. L., Doorbar, J., Lee, D., and Lambert, P. F. (2005). Human papillomavirus type 16 E1^E4 contributes to multiple facets of the papillomavirus life cycle. *J. Virol.* **79:**1315–13165.

Nardelli-Haefliger, D., Roden, R. B. S., Benyacoub, J., Sahli, R., Kraehenhuhl, J. P., Schiller, J. T., Lachat, P., Potts, A., and De Grande, P. (1997). Human papillomavirus type 16 virus-like particles expressed in attenuated *Salmonella typhimurium* elicit mucosal and systemic neutralizing antibodies in mice. *Infect. Immun.* **65:**3328–3336.

Nguyen, M. L., Nguyen, M. M., Lee, D., Griep, A. E., and Lambert, P. F. (2003). The PDZ ligand domain of the human papillomavirus type 16 E6 protein is required for E6's induction of epithelial hyperplasia *in vivo*. *J. Virol.* **77:**6957–6964.

Noya, F., Chien, W.-M., Broker, T. R., and Chow, L. T. (2001). p21cip1 degradation in differentiated keratinocytes is abrogated by co-stabilization with cyclin E induced by HPV E7. *J. Virol.* **75:**6121–6134.

Oberg, D., Collier, B., Zhao, X., and Schwartz, S. (2003). Mutational inactivation of two distinct negative RNA elements in the human papillomavirus type 16 L2 coding region induces production of high levels of L2 in human cells. *J. Virol.* **77:**11674–11684.

Oda, D., Bigler, L., Mao, E. J., and Disteche, C. M. (1996). Chromosomal abnormalities in HPV-16-immortalized oral epithelial cells. *Carcinogenesis* **17:**2003–2008.

Oh, S. T., Kyo, S., and Laimins, L. A. (2001). Telomerase activation by human papillomavirus type 16 E6 protein: Induction of human telomerase reverse transcriptase expression through Myc and GC-rich Sp1 binding sites. *J. Virol.* **75:**5559–5566.

Ohlschlager, P., Osen, W., Dell, K., Faath, S., Garcea, R. L., Jochmus, I., Muller, M., Pawlita, M., Schafer, K., Schr, P., Staib, C., Sutter, G., *et al.* (2003). Human papillomavirus type 16 L1 capsomeres induce L1-specific cytotoxic T lymphocytes and tumor regression in C57BL/6 mice. *J. Virol.* **77:**4635–4645.

Ordonez, R. M., Espinosa, A. M., Sanchez-Gonzalez, D. J., Armendariz-Borunda, J., and Berumen, J. (2004). Enhanced oncogenicity of Asian-American human papillomavirus 16 is associated with impaired E2 repression of E6/E7 oncogene transcription. *J. Gen. Virol.* **85:**1433–1444.

Ozbun, M. A., and Meyers, C. (1998). Temporal usage of multiple promoters during the life cycle of human papillomavirus type 31b. *J. Virol.* **72:**2715–2722.

Palefsky, J. M., and Holly, E. A. (2003). Chapter 6: Immunosuppression and co-infection with HIV. *J. Natl. Cancer Inst. Monogr.* **31:**41–46.

Pan, H., and Griep, A. E. (1994). Altered cell cycle regulation in the lens of HPV-16 E6 or E7 transgenic mice: Implications for tumor suppressor gene function in development. *Genes Dev.* **8:**1285–1299.

Park, J. S., Kim, E. J., Kwon, H. J., Hwang, E. S., Namkoong, S. E., and Um, S. J. (2000). Inactivation of interferon regulatory factor-1 tumor suppressor protein by HPV E7 oncoprotein. Implication for the E7-mediated immune evasion mechanism in cervical carcinogenesis. *J. Biol. Chem.* **275:**6764–6769.

Park, P., Copeland, W., Yang, L., Wang, T., Botchan, M. R., and Mohr, I. J. (1994). The cellular DNA polymerase alpha-primase is required for papillomavirus DNA replication and associates with the viral E1 helicase. *Proc. Natl. Acad. Sci. USA* **91:**8700–8704.

Park, R. B., and Androphy, E. J. (2002). Genetic analysis of high-risk E6 in episomal maintenance of human papillomavirus genomes in primary human keratinocytes. *J. Virol.* **76:**11359–11364.

Parkin, D. V., Bray, F., Ferlay, J., and Pisani, P. (2001). Estimating the world cancer burden: Globocan 2000. *Int. J. Cancer* **94:**153–156.

Pecoraro, G., Lee, M., Morgan, D., and Defendi, V. (1991). Evolution of *in vitro* transformation and tumorigenesis of HPV16 and HPV18 immortalized primary cervical epithelial cells. *Am. J. Pathol.* **138:**1–8.

Peh, W. L., Brandsma, J. L., Christensen, N. D., Cladel, N. M., Wu, X., and Doorbar, J. (2004). The viral E4 protein is required for the completion of the cottontail rabbit papillomavirus productive cycle *in vivo*. *J. Virol.* **78:**2142–2151.

Perea, S. E., Massimi, P., and Banks, L. (2000). Human papillomavirus type 16 E7 impairs the activation of the interferon regulatory factor-1. *Int. J. Mol. Med.* **5:**661–666.

Petry, K. U., Scheffel, D., Bode, U., Gabrysiak, T., Kochel, H., Kupsch, E., Glaubitz, M., Niesert, S., Kuhnle, H., and Schedel, I. (1994). Cellular immunodeficiency enhances the progression of human papillomavirus-associated cervical lesions. *Int. J. Cancer* **57:**836–840.

Petti, L., Nilson, L. A., and DiMaio, D. (1991). Activation of the platelet-derived growth factor receptor by the bovine papillomavirus E5 transforming protein. *EMBO J.* **10:**845–855.

Piirsoo, M., Ustav, E., Mandel, T., Stenlund, A., and Ustav, M. (1996). Cis and trans requirements for stable episomal maintenance of the BPV-1 replicator. *EMBO J.* **15:**1–11.

Pirisi, L., Yasumoto, S., Feller, M., Doniger, J., and DiPaolo, J. A. (1987). Transformation of human fibroblasts and keratinocytes with human papillomavirus type 16 DNA. *J. Virol.* **61:**1061–1066.

Pirisi, L., Creek, K. E., Doniger, J., and DiPaolo, J. A. (1988). Continuous cell lines with altered growth and differentiation properties originate after transfection of human keratinocytes with human papillomavirus type 16 DNA. *Carcinogenesis* **9:**1573–1579.

Psyrri, A., DeFilippis, R. A., Edwards, A. P., Yates, K. E., Manuelidis, L., and DiMaio, D. (2004). Role of the retinoblastoma pathway in senescence triggered by repression of the human papillomavirus E7 protein in cervical carcinoma cells. *Cancer Res.* **64:**3079–3086.

Ressing, M. E., Offringa, R., Toes, R. E., Ossendorp, F., de Jong, J. H., Brandt, R. M., Kast, W. M., and Melief, C. J. (1996). Immunotherapy of cancer by peptide-based vaccines for the induction of tumor-specific T cell immunity. *Immunotechnology* **2:**241–251.

Rey, O., Lee, S., and Park, N. H. (1999). Impaired nucleotide excision repair in UV-irradiated human oral keratinocytes immortalized with type 16 human papillomavirus genome. *Oncogene* **18:**6997–7001.

Ronco, L. V., Karpova, A. Y., Vidal, M., and Howley, P. M. (1998). Human papillomavirus 16 E6 oncoprotein binds to interferon regulatory factor-3 and inhibits its transcriptional activity. *Genes Dev.* **12:**2061–2072.

Rose, B., Steger, G., Dong, X. P., Thompson, C., Cossart, Y., Tattersall, M., and Pfister, H. (1998). Point mutations in SP1 motifs in the upstream regulatory region of human papillomavirus type 18 isolates from cervical cancers increase promoter activity. *J. Gen. Virol.* **79:**1659–1663.

Rose, R. C., Bonnez, W., Reichman, R. C., and Garcea, R. L. (1993). Expression of human papillomavirus type 11 L1 protein in insect cells: *In vivo* and *in vitro* assembly of virus-like particles. *J. Virol.* **67:**1936–1944.

Rose, R. C., Reichman, R. C., and Bonnez, W. (1994). Human papillomavirus (HPV) type 11 recombinant virus-like particles induce the formation of neutralizing antibodies and detect HPV-specific antibodies in human sera. *J. Gen. Virol.* **75:**2075–2079.

Sanchez-Perez, A. M., Soriano, S., Clarke, A. R., and Gaston, K. (1997). Disruption of the human papillomavirus type 16 E2 gene protects cervical carcinoma cells from E2F-induced apoptosis. *J. Gen. Virol.* **78:**3009–3018.

Sanders, C. M., and Stenlund, A. (1998). Recruitment and loading of the E1 initiator protein: An ATP-dependent process catalysed by a transcription factor. *EMBO J.* **17:**7044–7055.

Schapiro, F., Sparkowski, J., Adduci, A., Suprynowicz, F., Schlegel, R., and Grinstein, S. (2000). Golgi alkalinization by the papillomavirus E5 oncoprotein. *J. Cell Biol.* **148:**305–315.

Scheffner, M., Werness, B. A., Huibregtse, J. M., Levine, A. J., and Howley, P. M. (1990). The E6 oncoprotein encoded by human papillomavirus type 16 and 18 promotes the degradation of p53. *Cell* **63:**1129–1136.

Scheffner, M., Huibregtse, J. M., Vierstra, R. D., and Howley, P. M. (1993). The HPV-16 E6 and E6-AP complex functions as a ubiquitin-protein ligase in the ubiquitination of p53. *Cell* **75:**495–505.

Schiffman, M., and Castle, P. E. (2005). The promise of global cervical-cancer prevention. *N. Engl. J. Med.* **353:**2101–2104.

Schiffman, M., Herrero, R., Desalle, R., Hildesheim, A., Wacholder, S., Rodriguez, A. C., Bratti, M. C., Sherman, M. E., Morales, J., Guillen, D., Alfaro, M., Hutchinson, M., *et al.* (2005a). The carcinogenicity of human papillomavirus types reflects viral evolution. *Virology* **337:**76–84.

Schiffman, M., Khan, M. J., Solomon, D., Herrero, R., Wacholder, S., Hildesheim, A., Rodriguez, A. C., Bratti, M. C., Wheeler, C. M., and Burk, R. D. (2005b). A study of the impact of adding HPV types to cervical cancer screening and triage tests. *J. Natl. Cancer Inst.* **97:**147–150.

Schlecht, N. F., Kulaga, S., Robitaille, J., Ferreira, S., Santos, M., Miyamura, R. A., Duarte-Franco, E., Rohan, T. E., Ferenczy, A., Villa, L. L., and Franco, E. L. (2001). Persistent human papillomavirus infection as a predictor of cervical intraepithelial neoplasia. *JAMA* **286:**3106–3114.

Schlegel, R., Phelps, W. C., Zhang, Y. L., and Barbosa, M. (1988). Quantitative keratinocyte assay detects two biological activities of human papillomavirus DNA and identifies viral types associated with cervical carcinoma. *EMBO J.* **7:**3181–3187.

Schneider-Maunoury, S., Croissant, O., and Orth, G. (1987). Integration of human papillomavirus type 16 DNA sequences: A possible early event in the progression of genital tumors. *J. Virol.* **61:**3295–3298.

Schwarz, E., Freese, U. K., Gissmann, L., Mayer, W., Roggenbuck, B., Stremlau, A., and zur Hausen, H. (1985). Structure and transcription of human papillomavirus sequences in cervical carcinoma cells. *Nature* **314:**111–114.

Scotto, J., and Bailar, J. C. III, (1969). Rigoni-Stern and medical statistics. A nineteenth-century approach to cancer research. *J. Hist. Med. Allied Sci.* **24:**65–75.

Sedman, J., and Stenlund, A. (1995). Co-operative interaction between the initiator E1 and the transcriptional activator E2 is required for replicator specific DNA replication of bovine papillomavirus *in vivo* and *in vitro*. *EMBO J.* **14:**6218–6228.

Sedman, J., and Stenlund, A. (1998). The papillomavirus E1 protein forms a DNA-dependent hexameric complex with ATPase and DNA helicase activities. *J. Virol.* **72:**6893–6897.

Seo, Y. S., Muller, F., Lusky, M., and Hurwitz, J. (1993). Bovine papilloma virus (BPV)-encoded E1 protein contains multiple activites required for BPV DNA replication. *Proc. Natl. Acad. Sci. USA* **90:**702–706.

Serraino, D., Carrieri, P., Pradier, C., Bidoli, E., Dorrucci, M., Ghetti, E., Schiesari, A., Zucconi, R., Pezzotti, P., Dellamonica, P., Franceschi, S., and Rezza, G. (1999). Risk of invasive cervical cancer among women with or at risk for HIV infection. *Int. J. Cancer* **82:**334–337.

Shafti-Keramat, S., Handisurya, A., Kriehuber, E., Meneguzzi, G., Slupetzky, K., and Kirnbauer, R. (2003). Different heparan sulfate proteoglycans serve as cellular receptors for human papillomaviruses. *J. Virol.* **77:**13125–13135.

Sherwood, J. B., Shivapurkar, N., Lin, W. M., Ashfaq, R., Miller, D. S., Gazdar, A. F., and Muller, C. Y. (2000). Chromosome 4 deletions are frequent in invasive cervical cancer and differ between histologic variants. *Gynecol. Oncol.* **79:**90–96.

Shin, K. H., Tannyhill, R. J., Liu, X., and Park, N. H. (1996). Oncogenic transformation of HPV-immortalized human oral keratinocytes is associated with the genetic instability of cells. *Oncogene* **12:**1089–1096.

Skiadopoulos, M. H., and McBride, A. A. (1998). Bovine papillomavirus type 1 genomes and the E2 transactivator protein are closely associated with mitotic chromatin. *J. Virol.* **72:**2079–2088.

Slebos, R. J., Kessis, T. D., Chen, A. W., Han, S. M., Hedrick, L., and Cho, K. R. (1995). Functional consequences of directed mutations in human papillomavirus E6 proteins: Abrogation of p53-mediated cell cycle arrest correlates with p53 binding and degradation *in vitro*. *Virology* **208:**111–120.

Slebos, R. J. C., Lee, M. H., Plunkett, B. S., Kessis, T. D., Williams, B. O., Jacks, T., Hedrick, L., Kastan, M. B., and Cho, K. R. (1994). p53-dependent G(1) arrest involves pRB-related proteins and is disrupted by the human papillomavirus 16 E7 oncoprotein. *Proc. Natl. Acad. Sci. USA* **91:**5320–5324.

Solinas-Toldo, S., Durst, M., and Lichter, P. (1997). Specific chromosomal imbalances in human papillomavirus-transfected cells during progression toward immortality. *Proc. Natl. Acad. Sci. USA* **94:**3854–3859.

Song, S., Gulliver, G. A., and Lambert, P. F. (1998). Human papillomavirus type 16 E6 and E7 oncogenes abrogate radiation-induced DNA damage responses *in vivo* through p53-dependent and p53-independent pathways. *Proc. Natl. Acad. Sci. USA* **95:**2290–2295.

Spalholz, B. A., Yang, Y. C., and Howley, P. M. (1985). Transactivation of a bovine papilloma virus transcriptional regulatory element by the E2 gene product. *Cell* **42:**183–191.

Spalholz, B. A., Lambert, P. F., Yee, C. L., and Howley, P. M. (1987). Bovine papillomavirus transcriptional regulation: Localization of the E2 responsive elements of the long control region. *J. Virol.* **61:**2128–2137.

Srivenugopal, K. S., and Ali-Osman, F. (2002). The DNA repair protein, O(6)-methylguanine-DNA methyltransferase is a proteolytic target for the E6 human papillomavirus oncoprotein. *Oncogene* **21:**5940–5945.

Stanley, M. A. (2002). Human papillomavirus vaccines. *Curr. Opin. Mol. Ther.* **4:**15–22.

Steele, C., Sacks, P. G., Adler-Storthz, K., and Shillitoe, E. J. (1992). Effect on cancer cells of plasmids that express antisense RNA of human papillomavirus type 18. *Cancer Res.* **52:**4706–4711.

Steele, J. C., Mann, C. H., Rookes, S., Rollason, T., Murphy, D., Freeth, M. G., Gallimore, P. H., and Roberts, S. (2005). T-cell responses to human papillomavirus type 16 among women with different grades of cervical neoplasia. *Br. J. Cancer* **93:**248–259.

Steenbergen, R. D., Hermsen, M. A., Walboomers, J. M., Meijer, G. A., Baak, J. P., Meijer, C. J., and Snijders, P. J. (1998). Non-random allelic losses at 3p, 11p and 13q during HPV-mediated immortalization and concomitant loss of terminal differentiation of human keratinocytes. *Int. J. Cancer* **76:**412–417.

Steger, G., and Corbach, S. (1997). Dose-dependent regulation of the early promoter of human papillomavirus type 18 by the viral E2 protein. *J. Virol.* **71:**50–58.

Sterlinko Grm, H., and Banks, L. (2004). HPV proteins as targets for therapeutic intervention. *Antivir. Ther.* **9:**665–678.

Stoppler, H., Stoppler, M. C., Johnson, E., Simbulan-Rosenthal, C. M., Smulson, M. E., Iyer, S., Rosenthal, D. S., and Schlegel, R. (1998). The E7 protein of human papillomavirus type 16 sensitizes primary human keratinocytes to apoptosis. *Oncogene* **17:**1207–1214.

Storey, A., Oates, D., Banks, L., Crawford, L., and Crook, T. (1991). Anti-sense phosphorothioate oligonucleotides have both specific and non-specific effects on cells containing human papillomavirus type 16. *Nucleic Acids Res.* **19:**4109–4114.

Storey, A., Thomas, M., Kalita, A., Harwood, C., Gardiol, D., Mantovani, F., Breuer, J., Leigh, I. M., Matlashewski, G., and Banks, L. (1998). Role of a p53 polymorphism in the development of human papillomavirus-associated cancer. *Nature* **393:**229–234.

Straight, S. W., Hinkle, P. M., Jewers, R. J., and McCance, D. J. (1993). The E5 oncoprotein of human papillomavirus type 16 transforms fibroblasts and effects the downregulation of the epidermal growth factor receptor in keratinocytes. *J. Virol.* **67:**4521–4532.

Straight, S. W., Herman, B., and McCance, D. J. (1995). The E5 oncoprotein of human papillomavirus type 16 inhibits the acidification of endosomes in human keratinocytes. *J. Virol.* **69:**3185–3192.

Suzich, J. A., Ghim, S., Palmer-Hill, F. J., White, W. I., Tamura, J. K., Bell, J., Newsome, J. A., Jenson, A. B., and Schlegel, R. (1995). Systemic immunization with papillomavirus L1 protein completely prevents the development of viral mucosal papillomas. *Proc. Natl. Acad. Sci. USA* **92:**11553–11557.

Terhune, S. S., Milcarek, C., and Laimins, L. A. (1999). Regulation of human papillomavirus type 31 polyadenylation during the differentiation-dependent life cycle. *J. Virol.* **73:**7185–7192.

Thierry, F., and Yaniv, M. (1987). The BPV1-E2 trans-acting protein can be either an activator or a repressor of the HPV18 regulatory region. *EMBO J.* **6:**3391–3397.

Thomas, J. T., and Laimins, L. A. (1998). Human papillomavirus oncoproteins E6 and E7 independently abrogate the mitotic spindle checkpoint. *J. Virol.* **72:**1131–1137.

Thomas, J. T., Hubert, W. G., Ruesch, M. N., and Laimins, L. A. (1999). Human papillomavirus type 31 oncoproteins E6 and E7 are required for the maintenance of episomes during the viral life cycle in normal human keratinocytes. *Proc. Natl. Acad. Sci. USA* **96:**8449–8454.

Tommasino, M., Adamczewski, J. P., Carlotti, F., Barth, C. F., Manetti, R., Contorni, M., Cavalieri, F., Hunt, T., and Crawford, L. (1993). HPV16 E7 protein associates with the protein kinase p33CDK2 and cyclin A. *Oncogene* **8:**195–202.

Ustav, M., and Stenlund, A. (1991). Transient replication of BPV-1 requires two viral polypeptides encoded by the E1 and E2 open reading frames. *EMBO J.* **10:**449–457.

Ustav, E., Ustav, M., Szymanski, P., and Stenlund, A. (1993). The bovine papillomavirus origin of replication requires a binding site for the E2 transcriptional activator. *Proc. Natl. Acad. Sci. USA* **90:**898–902.

van Driel, W. J., Ressing, M. E., Kenter, G. G., Brandt, R. M., Krul, E. J., van Rossum, A. B., Schuuring, E., Offringa, R., Bauknecht, T., Tann-Hermelink, A., van Dam,

P. A., Fleuren, G. J., *et al.* (1999). Vaccination with HPV16 peptide of patients with advanced cervical carcinoma: Clinical evaluation of a phase I-II trial. *Eur. J. Cancer* **35:**946–952.

Van Tine, B. A., Dao, L. D., Wu, S.-Y., Sonbuchner, T. M., Lin, B. Y., Zou, N., Chiang, C.-M., Broker, T. R., and Chow, L. T. (2004a). HPV origin binding protein associates with mitotic spindles to enable viral DNA partitioning. *Proc. Natl. Acad. Sci. USA* **101:**4030–4035.

Van Tine, B. A., Kappes, J. C., Banerjee, N. S., Knops, J., Lai, L., Steenberger, R. D. M., Meijer, C. L. J. M., Snijders, P. J. F., Chatis, P., Broker, T. R., Moen, J. P. T., and Chow, L. T. (2004b). Clonal selection for transcriptionally active viral oncogenes during progression to cancer by DNA methylation-mediated silencing. *J. Virol.* **78:**11172–11186.

Vaziri, H., and Benchimol, S. (1999). Alternative pathways for the extension of cellular life span: Inactivation of p53/pRb and expression of telomerase. *Oncogene* **18:**7676–7680.

Velders, M. P., McElhiney, S., Cassetti, M. C., Eiben, G. L., Higgins, T., Kovacs, G. R., Elmishad, A. G., Kast, W. M., and Smith, L. R. (2001). Eradication of established tumors by vaccination with Venezuelan equine encephalitis virus replicon particles delivering human papillomavirus 16 E7 RNA. *Cancer Res.* **61:**7861–7867.

Veldman, T., Horikawa, I., Barrett, J. C., and Schlegel, R. (2001). Transcriptional activation of the telomerase hTERT gene by human papillomavirus type 16 E6 oncoprotein. *J. Virol.* **75:**4467–4472.

Villa, L. L., Sichero, L., Rahal, P., Caballero, O., Ferenczy, A., Rohan, T. E., and Franco, E. L. (2000). Molecular variants of human papillomavirus types 16 and 18 preferentially associated with cervical neoplasia. *J. Gen. Virol.* **81:**2959–2968.

Villa, L. L., Costa, R. L., Petta, C. A., Andrade, R. P., Ault, K. A., Giuliano, A. R., Wheeler, C. M., Koutsky, L. A., Malm, C., Lehtinen, M., Skjeldestad, F. E., Olsson, S. E., *et al.* (2005). Prophylactic quadrivalent human papillomavirus (types 6, 11, 16, and 18) L1 virus-like particle vaccine in young women: A randomised double-blind placebo-controlled multicentre phase II efficacy trial. *Lancet Oncol.* **6:**271–278.

von Knebel Doeberitz, M., Oltersdorf, T., Schwarz, E., and Gissmann, L. (1988). Correlation of modified human papilloma virus early gene expression with altered growth properties in C4-1 cervical carcinoma cells. *Cancer Res.* **48:**3780–3786.

Vonka, V., Kanka, J., Hirsch, I., Zavadova, H., Kremar, M., Suchankova, A., Rezacova, D., Broucek, J., Press, M., and Domorazkova, E. (1984). Prospective study on the relationship between cervical neoplasia and herpes simplex type-2 virus. II. Herpes simplex type-2 antibody presence in sera taken at enrollment. *Int. J. Cancer* **33:**61–66.

Vonka, V., Kanka, J., and Roth, Z. (1987). Herpes simplex type 2 virus and cervical neoplasia. *Adv. Cancer Res.* **48:**149–191.

Walboomers, J. M., Jacobs, M. V., Manos, M. M., Bosch, F. X., Kummer, J. A., Shah, K. V., Snijders, P. J., Peto, J., Meijer, C. J., and Munoz, N. (1999). Human papillomavirus is a necessary cause of invasive cervical cancer worldwide. *Pathology* **189:**12–19.

Wallin, K.-L., Wiklund, F., Angstrom, T., Bergman, F., Stendahl, U., Wadell, G., Hallmans, G., and Dillner, J. (1999). Type-specific persistence of human papillomavirus DNA before the development of invasive cervical cancer. *N. Engl. J. Med.* **341:**1633–1638.

Webster, K., Parish, J., Pandya, M., Stern, P. L., Clarke, A. R., and Gaston, K. (2000). The human papillomavirus (HPV) 16 E2 protein induces apoptosis in the absence of other HPV proteins and via a p53-dependent pathway. *J. Biol. Chem.* **275:**87–94.

Wells, S. I., Francis, D. A., Karpova, A. Y., Dowhanick, J. J., Benson, J. D., and Howley, P. M. (2000). Papillomavirus E2 induces senescence in HPV-positive cells via pRB- and p21(CIP)-dependent pathways. *EMBO J.* **19:**5762–5771.

Werness, B. A., Levine, A. J., and Howley, P. M. (1990). Association of human papillomavirus types 16 and 18 E6 proteins with p53. *Science* **248:**76–79.

White, A. E., Livanos, E. M., and Tlsty, T. D. (1994). Differential disruption of genomic integrity and cell cycle regulation in normal human fibroblasts by the HPV oncoproteins. *Genes Dev.* **8:**666–677.

White, P. W., Titolo, S., Brault, K., Thauvette, L., Pelletier, A., Welchner, E., Bourgon, L., Dovon, L., Ogilvie, W. W., Yoakim, C., Cordingley, M. G., and Archambault, J. (2003). Inhibition of human papillomavirus DNA replication by small molecule antagonists of the E1-E2 protein interaction. *J. Biol. Chem.* **278:**26765–26772.

Wilson, R., Fehrmann, F., and Laimins, L. A. (2005). Role of the E1–E4 protein in the differentiation-dependent life cycle of human papillomavirus type 31. *J. Virol.* **79:**6732–6740.

Wilson, V. G., and Ludes-Meyers, J. (1991). A bovine papillomavirus E1-related protein binds specifically to bovine papillomavirus DNA. *J. Virol.* **65:**5314–5322.

Woodworth, C. D., Bowden, P. E., Doniger, J., Pirisi, L., Barnes, W., Lancaster, W. D., and DiPaolo, J. A. (1988). Characterization of normal human exocervical epithelial cells immortalized *in vitro* by papillomavirus types 16 and 18 DNA. *Cancer Res.* **48:**4620–4628.

Woodworth, C. D., Doniger, J., and DiPaolo, J. A. (1989). Immortalization of human foreskin keratinocytes by various human papillomavirus DNAs corresponds to their association with cervical carcinoma. *J. Virol.* **63:**159–164.

Wu, L., Goodwin, E. C., Naeger, L. K., Vigo, E., Galaktionov, K., Helin, K., and DiMaio, D. (2000). E2F-Rb complexes assemble and inhibit cdc25A transcription in cervical carcinoma cells following repression of human papillomavirus oncogene expression. *Mol. Cell. Biol.* **20:**7059–7067.

Wu, X., Xiao, W., and Brandsma, J. L. (1994). Papilloma formation by cottontail rabbit papillomavirus requires E1 and E2 regulatory genes in addition to E6 and E7 transforming genes. *J. Virol.* **68:**6097–6102.

Xi, L. F., Koutsky, L. A., Galloway, D. A., Kuypers, J., Hughes, J. P., Wheeler, C. M., Holmes, K. K., and Kiviat, N. B. (1997). Genomic variation of human papillomavirus type 16 and risk for high grade cervical intraepithelial neoplasia. *J. Natl. Cancer Inst.* **89:**796–802.

Yang, L., Li, R., Mohr, I. J., Clark, R., and Botchan, M. R. (1991). Activation of BPV-1 replication *in vitro* by the transcription factor E2. *Nature* **353:**628–632.

Yang, L., Mohr, I. J., Fouts, E., Lim, D. A., Nohaile, M., and Botchan, M. (1993). The E1 protein of bovine papilloma virus 1 is an ATP-dependent DNA helicase. *Proc. Natl. Acad. Sci. USA* **90:**5086–5090.

Yee, C. L., Krishnan-Hewlett, I., Baker, C. C., Schlegel, R., and Howley, P. M. (1985). Presence and expression of human papillomavirus sequences in human cervical carcinoma cell lines. *Am. J. Pathol.* **119:**361–366.

You, J., Croyle, J. L., Nishimura, A., Ozato, K., and Howley, P. M. (2004). Interaction of the bovine papillomavirus E2 protein with Brd4 tethers the viral DNA to host mitotic chromosomes. *Cell* **117:**349–360.

Yuan, H., Estes, P. A., Chen, Y., Newsome, J., Olcese, V. A., Garcea, R. L., and Schlegel, R. (2001). Immunization with a pentameric L1 fusion protein protects against papillomavirus infection. *J. Virol.* **75:**7848–7853.

Zerfass-Thome, K., Zwerschke, W., Mannhardt, B., Tindle, R., Botz, J. W., and Jansen-Durr, P. (1996). Inactivation of the cdk inhibitor p27KIP1 by the human papillomavirus type 16 E7 oncoprotein. *Oncogene* **13:**2323–2330.

Zhang, B., Spandau, D. F., and Roman, A. (2002). E5 protein of human papillomavirus type 16 protects human foreskin keratinocytes from UV B-irradiation-induced apoptosis. *J. Virol.* **76:**220–231.

Zhang, B., Li, P., Wang, E., Brahmi, Z., Dunn, K. W., Blum, J. S., and Roman, A. (2003). The E5 protein of human papillomavirus type 16 perturbs MHC class II antigen maturation in human foreskin keratinocytes treated with interferon-gamma. *Virology* **310:**100–108.

Zhang, B., Srirangam, A., Potter, D. A., and Roman, A. (2005). HPV16 E5 protein disrupts the c-Cbl-EGFR interaction and EGFR ubiquitination in human foreskin keratinocytes. *Oncogene* **24:**2585–2588.

Zhao, X., Rush, M., and Schwartz, S. (2004). Identification of an hnRNP A1-dependent splicing silencer in the human papillomavirus type 16 L1 coding region that prevents premature expression of the late L1 gene. *J. Virol.* **78:**10888–10905.

Zhou, J., Sun, X. Y., Stenzel, D. J., and Frazer, I. H. (1991). Expression of vaccinia recombinant HPV16 L1 and L2 ORF proteins in epithelial cells is sufficient for assembly of HPV virion-like particles. *Virology* **185:**251–257.

zur Hausen, H. (2000). Papillomaviruses causing cancer: Evasion from host-cell control in early events in carcinogenesis. *J. Natl. Cancer Inst.* **92:**690–698.

zur Hausen, H., de Villiers, E.-M., and Gissmann, L. (1981). Papillomavirus infections and human genital cancer. *Gynecol. Oncol.* **12:**S124–S128.

This page intentionally left blank

ADVANCES IN VIRUS RESEARCH, VOL 66

PLANT SIGNAL TRANSDUCTION AND DEFENSE AGAINST VIRAL PATHOGENS

Pradeep Kachroo,* A. C. Chandra-Shekara,* and Daniel F. Klessig†

*Department of Plant Pathology, University of Kentucky, Lexington, Kentucky 40546
†Boyce Thompson Institute for Plant Research, Ithaca, New York 14853

ABSTRACT

Viral infection of plants is a complex process whereby the virus parasitizes the host and utilizes its cellular machinery to multiply and spread. In turn, plants have evolved signaling mechanisms that ultimately limit the ingress and spread of viral pathogens, resulting in resistance. By dissecting the interaction between host and virus, knowledge of signaling pathways that are deployed for resistance against these pathogens has been gained. Advances in this area have shown that resistance signaling against viruses does not follow a prototypic pathway but rather different host factors may play a role in resistance to different viral pathogens. Some components of viral resistance signaling pathways also appear to be conserved with those

0065-3527/06 $35.00
DOI: 10.1016/S0065-3527(06)66004-1

functioning in signaling pathways operational against other nonviral pathogens, however, these pathways may or may not overlap. This review aims to document the advances that have improved our understanding of plant resistance to viruses.

I. Introduction

Plant viruses are a major threat to the cultivation of many agricultural crops, causing serious economic losses worldwide. For many years, these pathogens have been controlled by conventional plant protection methods such as crop rotation, destruction of infected sources, breeding for resistance, and chemical control of relevant insect vectors (Bos, 2000; Hull, 2002).

Most plant species are resistant to most plant viruses, which suggests that susceptibility to viral pathogens is the exception rather than the rule. Resistance may be due to a variety of factors. For example, the plant may lack a factor(s) that is required for viral replication and/or movement. Alternatively, the plant's basal defenses may be sufficient to prevent viral replication and spread. The above two forms of resistance are often grouped under a phenomenon known as nonhost resistance. Basal defenses may include silencing of the viral genetic material either by degradation of the viral RNA or via inhibition of its translation (Dunoyer and Voinnet, 2005). RNA silencing has been an active area of research over the past decade, and the results are covered in several excellent reviews (Baulcombe, 2004; Dunoyer and Voinnet, 2005; Qu and Morris, 2005). Hence, it is not the focus of this chapter and will be only briefly discussed near the end of the chapter for completeness.

In comparison to nonhost resistance, some plants prevent viral infection by activating defense responses following pathogen recognition. This process involves strain-specific recognition of a virus-encoded avirulence (Avr) factor through direct or indirect interaction with the corresponding host resistance (*R*) gene product. Since resistance is dependent on the presence of both the pathogen Avr factor and its corresponding host R protein, it is termed gene-for-gene-mediated resistance (Flor, 1971). Such an interaction (also known as an incompatible interaction) triggers one or more defense signaling cascades and is often associated with induction of a hypersensitive response (HR). The HR is a form of programmed cell death, which results in the formation of necrotic lesions due to death of plant cells at and around the site of pathogen entry. An HR is one of the first visible

manifestations of pathogen-induced host defense responses and it is thought to help prevent pathogen multiplication and spread by confining the pathogen to the dead cells. However, increasing evidence suggests that the HR is not a prerequisite for gene-for-gene-mediated disease resistance. For example, a visible HR does not develop either in potato during *Rx*-mediated resistance against *Potato virus X* (PVX) (Kohm *et al*., 1993) or in *Arabidopsis* plants overexpressing the *R* gene *HRT*, which confers an HR to *Turnip crinkle virus* (TCV). Nonetheless, these plants are resistant to their respective viral pathogens (Chandra-Shekara *et al*., 2004; Cooley *et al*., 2000). Moreover, HR and resistance can be uncoupled in the *Arabidopsis*–TCV pathosystem; susceptible plants show similar amounts of virus in their systemic tissue irrespective of the presence or absence of an HR on their inoculated leaves. This result suggests that the HR by itself is not sufficient to prevent viral spread to the uninoculated tissues. Thus, while an HR is frequently associated with resistance, it is not necessarily required or sufficient for resistance.

R gene-mediated pathogen recognition often involves the accumulation of various phytohormones, including salicylic acid (SA), jasmonic acid (JA), and/or ethylene, which in turn signal the activation of defense gene expression. These phytohormones trigger separate and/or overlapping pathways whose combined effects confer resistance and prevent spread of the pathogen to the uninoculated parts of the plant.

R genes cloned to date can be grouped into six classes, based on their structural characteristics and protein motifs (Martin *et al*., 2003). These include proteins with a serine/threonine kinase catalytic domain and an N-terminal myristylation motif (class I, for example, Pto in tomato), proteins with leucine-rich repeats (LRRs), a nucleotide binding site (NBS), and an N-terminal coiled coil (CC) sequence (class II, for example, HRT in *Arabidopsis*, and Xa1 in rice), proteins similar to those in class II except for the presence of a Toll-interleukin-1 receptor (TIR)-like domain instead of a CC domain at their N-terminus (class III, for example, N in tobacco, L in flax, and RPP5 in *Arabidopsis*), proteins that have a transmembrane (TM) domain, an extracellular LRR and a small putative cytoplasmic tail without any identifiable motifs (class IV, for example, Cf2 and Cf9 in tomato), and proteins that contain an extracellular LRR, a TM domain, and a cytoplasmic serine/threonine kinase domain (class V, for example, Xa21 in rice). Class VI is composed of R proteins that do not show characteristics similar to proteins belonging to any of the above classes (for example, RPW8 in *Arabidopsis* and Ve1 and Ve2 in tomato). The proteins belonging to classes I–III lack a TM domain and are therefore thought to be localized intracellularly.

Strikingly, most of the *R* genes cloned thus far belong either to class II or III, suggesting that NBS-LRR type R proteins predominate over the other classes. It is, therefore, no particular surprise that a majority of the cloned *R* genes specifying resistance to viral pathogens also belong to the NBS-LRR category (Table I). Analysis of downstream signaling reveals that a few viral *R* genes activate resistance via unique pathways not used by other *R* genes. By contrast, other viral *R* genes utilize pathways in which at least some of the downstream components are shared, in many cases these components are also common to pathways triggered by *R* genes specifying resistance to nonviral pathogens.

Host resistance to viral pathogens is genetically accessible and, therefore, has been used widely in crop breeding. This approach continues to be a cost effective and commercially feasible method for providing protection against viral pathogens (Lecoq *et al.*, 2004). Molecular cloning of *R* genes has not only aided in crop breeding but also has facilitated investigation of the mechanisms underlying resistance to viruses. However, our understanding of resistance signaling is far from clear and, certainly, more work is needed to elucidate the complex signaling cascades leading to resistance. This review covers various aspects of resistance signaling employed by plants to counter viral pathogens and details several *R* gene-specified pathways operational against different viral pathogens.

II. *R* Gene-Mediated Resistance to Viral Pathogens

A. N *Gene-Mediated Resistance to* Tobacco mosaic virus *in Tobacco*

The interaction between *Tobacco mosaic virus* (TMV) and tobacco plants containing the *N* gene is a classic example of gene-for-gene resistance (Holmes, 1938). The *N* gene encodes a TIR-NBS-LRR protein (Whitham *et al.*, 1994) that interacts directly or indirectly with the helicase domain of the TMV replicase (Erickson *et al.*, 1999; Padgett *et al.*, 1997). N-mediated recognition of TMV leads to HR development in the host, which helps restrict the virus to a region in and immediately surrounding the necrotic lesions. By contrast, tobacco plants lacking the *N* gene fail to develop an HR and allow systemic spread of TMV, resulting in mosaic disease symptoms characterized by intermingled areas of light and dark green leaf tissue. Upon TMV inoculation, *N*-gene expression is upregulated in both the inoculated and uninoculated tissues of resistant plants (Levy *et al.*, 2004). The approximately fourfold increase in *N* transcripts in uninoculated tissues suggests that

TABLE I

LIST OF DOMINANT *R* GENES AGAINST PLANT VIRUSES, THEIR PROTEIN STRUCTURE, AND CORRESPONDING AVIRULENCE FACTORS

R gene	Host*	Pathogen†	Avr factor‡	Predicted domains§	Reference
N	*N. tabacum*	TMV	Helicase	TIR-NBS-LRR	Whitham *et al*., 1994
HRT	*A. thaliana*	TCV	CP	CC-NBS-LRR	Cooley *et al*., 2000
RCY1	*A. thaliana*	CMV	CP	CC-NBS-LRR	Takahashi *et al*., 2002
RTM1	*A. thaliana*	TEV	–¶	Jacaline-like	Chisholm *et al*., 2000
RTM2	*A. thaliana*	TEV	–	Small HSP-like	Whitham *et al*., 2000
Rx1	*S. tuberosum*	PVX	CP	CC-NBS-LRR	Bendahmane *et al*., 1999
Rx2	*S. tuberosum*	PVX	CP	CC-NBS-LRR	Bendahmane *et al*., 2000
Nb	*S. tuberosum*	PVX	MP	–	Marano *et al*., 2002
Ny_{tbr}	*S. tuberosum*	PVY	–	–	Celebi-Toprak *et al*., 2002
Ry	*S. tuberosum*	PVY	NIaPro	–	Mestre *et al*., 2003
Sw-5	*L. esculentum*	TSWV	–	CC-NBS-LRR	Brommonschenkel *et al*., 2000
Tm-1	*L. esculentum*	ToMV	RdRp	–	Meshi *et al*., 1988
Tm-2	*L. esculentum*	ToMV	MP	CC-NBS-LRR	Lanfermeijer *et al*., 2005
$Tm\text{-}2^2$	*L. esculentum*	ToMV	MP	CC-NBS-LRR	Lanfermeijer *et al*., 2003
Rsv1	*G. max*	SMV	HC-Pro and P3	CC-NBS-LRR	Hayes *et al*., 2004
TuRBO1	*B. napus*	TuMV	CI	–	Jenner *et al*., 2000
TuRBO1b	*B. napus*	TuMV	CI	–	Jenner *et al*., 2000
TuRBO3	*B. napus*	TuMV	P3	–	Hughes *et al*., 2003
RuRBO4	*B. napus*	TuMV	P3	–	Jenner *et al*., 2002
RuRBO5	*B. napus*	TuMV	CI	–	Jenner *et al*., 2002
L^1, L^2, L^3, L^4	*C. annum*	TMV	CP	–	Berzal-Herranz *et al*., 1995

* *A. thaliana*, *Arabidopsis thaliana*; *N. tabacum*, *Nicotiana tabacum*; *S. tuberosum*, *Solanum tuberosum*; *L. esculentum*, *Lycopersicum esculentum*; *G. max*, *Glycine max*; *B. napus*, *Brassica napus*; *C. annum*, *Capsicum annum*.

† TCV, *Turnip crinkle virus*; CMV, *Cucumber mosaic virus*; TMV, *Tobacco mosaic virus*; PVX, *Potato virus X*; PVY, *Potato virus Y*; TSWV, *Tomato spotted wilt virus*; ToMV, *Tomato mosaic virus*; SMV, *Soybean mosaic virus*; TEV, *Tobacco etch virus*; TuMV, *Turnip mosaic virus*.

‡ CP, coat protein; MP, movement protein; RdRp, RNA dependent RNA polymerase; CI, cylindrical inclusion; P3, protein 3; NIaPro, protease domain of nuclear inclusion; HC-Pro, helper component protease.

§ TIR-NBS-LRR, Toll-interleukin-1 receptor-nucleotide binding site-leucine-rich repeat; CC-NBS-LRR, coiled coil-nucleotide binding site-leucine-rich repeat; HSP, heat shock protein.

¶ Not known.

a TMV-induced systemic signal is involved in induction of *N* gene expression and resistance to TMV (Levy *et al.*, 2004). Similar to a few other TIR-NBS-LRR *R* genes (Ayliffe *et al.*, 1999; Parker *et al.*, 1997), *N* transcripts undergo alternative splicing to generate two mRNAs, designated as N_S and N_L (Dinesh-Kumar and Baker, 2000). N_S and N_L are predicted to encode full-length and truncated N proteins, respectively (Dinesh-Kumar and Baker, 2000); the relative levels of these transcripts change after TMV infection. N_S transcript levels are higher through 3 h after TMV infection while the N_L transcript predominates 4–8 h after infection. Notably, both transcripts are required to attain resistance to TMV (Dinesh-Kumar and Baker, 2000). The molecular mechanism(s) regulating alternative splicing is not known, but it has been suggested that protein kinases involved in the N–TMV interaction or rapid cellular changes function as a trigger to induce alternative splicing (Dinesh-Kumar and Baker, 2000).

N-mediated resistance to TMV is dependent on SA, and increased SA levels are observed during the HR to TMV in both inoculated and systemic tissues. These increases correlate with the induction of pathogenesis-related (*PR*) genes in both tissues (Delaney *et al.*, 1994; Malamy *et al.*, 1992). Studies have suggested that nitric oxide (NO) also plays a role in signaling TMV resistance. NO synthase (NOS) activity is induced by TMV infection in an *N* gene-dependent manner (Durner *et al.*, 1998). Furthermore, exogenous application of NO or an NO donor induces SA accumulation and triggers *PR-1* and phenylalanine ammonia lyase gene expression. Conversely, exogenous application of NOS inhibitors abolishes TMV-induced *PR-1* expression in an *N* gene-dependent manner (Durner *et al.*, 1998). SA appears to be necessary for NO function, since exogenous application of NO donors failed to induce *PR-1* in SA-deficient nahG transgenic tobacco (Durner *et al.*, 1998). SA also has been shown to induce the expression of a tobacco RNA-dependent RNA polymerase (*RdRP*) gene; RdRPs have been implicated in RNA silencing and in limiting the accumulation and spread of RNA viruses (Xie *et al.*, 2001). In addition, increased SA levels can contribute to N-mediated resistance by inhibiting the respiratory electron transport chain, leading to an increase in mitochondrial reactive oxygen species (Chivasa and Carr, 1998; Gilliland *et al.*, 2003; Singh *et al.*, 2004).

The signaling pathway leading to N-mediated resistance also has been shown to involve polyamine metabolism. The HR to TMV is associated with an ~20-fold increase in spermine levels in the inoculated leaves (Yamakawa *et al.*, 1998). Moreover, exogenous treatment with spermine induces expression of acidic *PR* genes and reduces the

size of TMV-induced lesions. However, spermine treatment does not induce SA accumulation and, conversely, exogenous application of SA does not enhance spermine accumulation (Yamakawa *et al*., 1998). Spermine-derived signaling involves a Cys2/His2-type zinc finger protein (ZFT1) that is upregulated during TMV infection in an N-dependent manner. TMV-induced expression of *ZFT1* remains unimpaired in *nahG* transgenic tobacco plants, indicating that spermine signaling involves an SA-independent pathway. It has been suggested that ZFT1 functions as a transcriptional repressor for spermine signaling and it may restrict the virus by accelerating necrotic lesion formation (Uehara *et al*., 2005). Consistent with this possibility, overexpression of *ZFT1* resulted in enhanced tolerance to TMV (Uehara *et al*., 2005).

Characterization of N-mediated signaling has led to the identification of several proteins that play important roles in resistance responses to TMV (Fig. 1). Remarkably, several of these downstream components were first identified in *Arabidopsis* as signal transducers for pathways leading to resistance against nonviral pathogens. This finding suggests that resistance signaling components are conserved not only across plant species but also for different types of pathogens. In tobacco, N-mediated resistance is dependent on RAR1, SGT1, and NPR1-like proteins (Liu *et al*., 2002a). RAR1 and SGT1 can participate in resistance pathways triggered by either TIR- or CC-NBS-LRR-type R proteins (Aarts *et al*., 1998; Austin *et al*., 2002; Azevedo *et al*., 2002; Liu *et al*., 2002a; Muskett *et al*., 2002; Tör *et al*., 2002). Both RAR1 and SGT1 physically interact with each other, as well as with other proteins (Azevedo *et al*., 2002; Liu *et al*., 2002a). SGT1 is a component of the SCF-type E3 ubiquitin ligase complex (Kitagawa *et al*., 1999; Lyapina *et al*., 2001; Matsuzawa and Reed, 2001), which facilitates the attachment of ubiquitin to specific protein substrates for subsequent degradation by the 26S proteasome (Deshaies, 1999). In addition to RAR1, SGT1 also interacts with SKP1, which is another component of the SCF-type E3 ubiquitin ligase complex (Liu *et al*., 2002b). Silencing of *SKP1* results in loss of resistance to TMV, and the effect is similar to that seen upon silencing *N* (Liu *et al*., 2002b). Both RAR1 and SGT1 are also known to interact with the COP9 signalosome, which is an evolutionarily conserved multiprotein complex involved in protein degradation and light signaling (Wei and Deng, 1999; Wei *et al*., 1998). The COP9 multiprotein complex can, in turn, interact with the components of the SCF-type 3 ubiquitin ligase complex (Lyapina *et al*., 2001), and silencing of the CSN3 and CSN8 subunits of the COP9 complex abolishes N-mediated resistance to

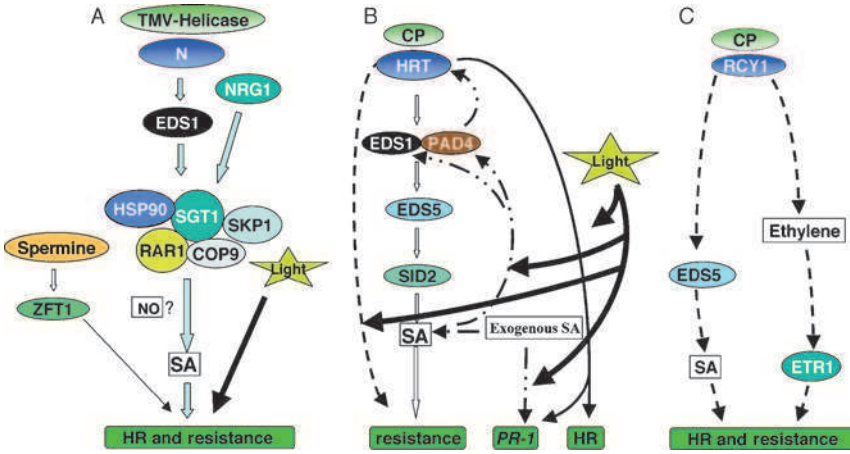

FIG 1. A sketch of components involved in the N- (A), HRT- (B), and RCY1- (C) mediated resistance-signaling pathways, which confer resistance to TMV in tobacco and to TCV and CMV in *Arabidopsis*, respectively. Defense signaling in each of these R protein-triggered pathways is initiated upon indirect interaction between the R protein and its corresponding Avr factor encoded by the virus. Thick lines in (A) and (B) indicate light-mediated regulation of defense pathways. NO-mediated signaling plays a positive role in N-mediated resistance to TMV, but it is not yet clear if NO acts upstream or downstream of EDS1 or the SGT1-RAR1 complex. Dash-dotted lines in (B) indicate SA-mediated feedback regulation of EDS1 and PAD4. A positive feedback mechanism also regulates SA-mediated induction of HRT. The dashed line in (B) indicates resistance triggered by overexpression of HRT, which appears to act independently of SA. Dashed lines in (C) indicate partial dependence of RCY1-mediated signaling on the SA and ethylene pathways.

TMV (Liu *et al.*, 2002b). It is possible that the COP9 signalosome modulates resistance by affecting the functions of its interacting partners or via its role in light signaling. The latter possibility is supported by the observation that HR formation and TMV resistance are compromised in the dark (Chandra-Shekara *et al.*, 2006).

Signal transduction via the N protein also involves heat shock protein 90 (HSP90). HSP90 interacts with N, and silencing of *HSP90* results in loss of resistance to TMV (Liu *et al.*, 2004a). Heat shock proteins are known to play roles in the folding, activation, and assembly of proteins involved in signal transduction, cell cycle control, or transcriptional regulation; they may serve a similar function in N-mediated signaling (Picard, 2002; Richter and Buchner, 2001). Since HSP90 interacts with SGT1 and RAR1, these proteins, together with N, may exist as a complex (Liu *et al.*, 2004a). Like RAR1 and SGT1, HSP90

functions in other *R* gene-signaling pathways. For example, all three proteins are required for the function of *RPS2*, which mediates resistance to *Pseudomonas syringae* pv. *tomato* DC3000 in *Arabidopsis* (Takahashi *et al*., 2003).

A CC-NBS-LRR class resistance protein, N requirement gene 1 (NRG1), was shown to play a critical role in N-mediated resistance (Peart *et al*., 2005). In tobacco containing the *N* gene, silencing of *NRG1* resulted in loss of HR and resistance to TMV. This suggests that resistance to TMV requires both TIR-NBS-LRR and CC-NBS-LRR classes of resistance proteins (Peart *et al*., 2005), and that NRG1 may be acting downstream of or in parallel to the N signaling pathway. N-mediated signaling, but not NRG1-mediated signaling, is dependent on EDS1, whereas both N- and NRG1-mediated pathways are dependent on SGT1 (Peart *et al*., 2005). Results obtained from other systems also provide compelling evidence that multiple NBS-LRR proteins are a common feature of resistance signaling pathways. For example, RPP2-mediated resistance against *Peronospora parasitica* requires two NBS-LRR proteins encoded by the adjacent genes *RPP2a* and *RPP2b* (Sinapidou *et al*., 2004).

N-mediated resistance to TMV is also associated with the activation of several mitogen-activated protein kinases (MAPKs), including the SA-induced protein kinase (SIPK), the wound-induced protein kinase (WIPK), and an MAPKK, NtMEK2, which acts as an upstream kinase of SIPK and WIPK. These kinases also are activated by various elicitors, suggesting that they function as convergence points after the perception of different pathogens, pathogen-derived elicitors, and nonbiotic stresses (Cardinale *et al*., 2000; Desikan *et al*., 2001; Jin *et al*., 2003; Lee *et al*., 2001a; Mikolajczyk *et al*., 2000; Nühse *et al*., 2000; Romeis *et al*., 1999; Zhang and Klessig, 1998a,b; Zhang *et al*., 1998, 2000). Since TMV resistance is compromised in tobacco silenced for expression of NtMEK2, SIPK, or WIPK, these kinases appear to play important roles in N-mediated signaling (Jin *et al*., 2003; Liu *et al*., 2004b).

B. HRT-Mediated Resistance to Turnip crinkle virus *in* Arabidopsis

The carmovirus TCV has a wide host range that includes several members of the cruciferous family such as *Arabidopsis*. Most *Arabidopsis* ecotypes are susceptible to TCV; however, a resistant line, designated Di-17 was isolated from the Dijon (Di) ecotype (Dempsey *et al*., 1993). Following TCV infection, Di-17 plants develop an HR, express several defense genes, including *PR-1*, *PR-2*, *PR-5*, and *GST1*,

and accumulate SA and the phytoalexin, camelexin (Dempsey *et al.*, 1997; Kachroo *et al.*, 2000). By contrast, plants lacking *HRT* fail to develop an HR after TCV infection, they also exhibit basal-level expression of the *PR* and *GST1* genes and accumulate low levels of SA and camelexin. These plants allow systemic spread of the virus, which is associated with appearance of crinkled leaves and drooping bolts followed by death of the plant (Dempsey *et al.*, 1997; Kachroo *et al.*, 2000). The HR to TCV is conferred by a CC-NBS-LRR type R protein, designated HRT (hypersensitive response to TCV) (Cooley *et al.*, 2000). In addition to its role in HR development, HRT is required for resistance to TCV. However, HRT alone is not sufficient to confer resistance to TCV, as F1 plants and ~75% of HR-developing F2 plants derived from a cross between resistant (Di-17) and susceptible (Columbia-0 [Col-0]) ecotypes succumb to disease. Furthermore, ~90% of transgenic Col-0 plants expressing an *HRT* transgene develop an HR but are still susceptible, confirming that HRT alone is insufficient and that other loci also may regulate resistance to TCV (Cooley *et al.*, 2000). Subsequent studies revealed that a recessive allele at a second locus, designated *RRT* (regulates resistance to TCV), is required together with *HRT* to confer resistance (Chandra-Shekara *et al.*, 2004; Kachroo *et al.*, 2000). Analysis of *HRT RRT* homozygous plants suggests that *RRT* does not have a role in HR development or *PR* gene induction (Chandra-Shekara *et al.*, 2004).

Analysis of the downstream signaling pathway indicates that HRT-mediated resistance is independent of JA and ethylene but dependent on SA (Fig. 1; Chandra-Shekara *et al.*, 2004; Kachroo *et al.*, 2000). TCV induces approximately a 10-fold increase in SA levels in Di-17 but not in Col-0. This increase appears to be critical for signaling resistance since SA-deficient plants expressing the *nahG* transgene, which encodes the SA-degrading enzyme salicylate hydroxylase, are compromised for HRT-mediated resistance. Similarly, mutations in the *EDS1*, *EDS5*, *PAD4*, or *SID2* genes, which suppress SA accumulation following TCV infection, compromise HRT-mediated resistance (Chandra-Shekara *et al.*, 2004). It has previously been demonstrated that mutations in *EDS1*, *EDS5*, *PAD4*, or *SID2* enhance susceptibility to various bacterial and oomycete pathogens by affecting SA perception or accumulation (Falk *et al.*, 1999; Jirage *et al.*, 1999; Nawrath *et al.*, 2002; Wildermuth *et al.*, 2001). The SA level is affected not only by the gene products directly involved in SA synthesis [such as *SID2*, which encodes isochorismate synthase (Wildermuth *et al.*, 2001)] but also by factors that participate in resistance signaling, and directly or indirectly affect SA synthesis and/or accumulation (such as *EDS1*, *PAD4*, *EDS5*). For example, mutations in *EDS1* and *PAD4* compromise

SA synthesis and cause increased susceptibility to bacterial and oomycete pathogens (Falk *et al*., 1999; Jirage *et al*., 1999). The *eds1* and *pad4* mutations also block the pathogen-activated expression of *EDS5*, which encodes another component of the SA-signaling pathway.

HRT-mediated signaling, unlike most CC-NBS-LRR R proteins, is dependent on EDS1 but independent of NDR1. This finding is unexpected since R proteins with a CC-NBS-LRR structure, such as HRT, usually require NDR1 to signal resistance responses, while R proteins with a TIR-NBS-LRR structure utilize EDS1 (Aarts *et al*., 1998; Dangl and Jones, 2001). Besides HRT, the only other CC domain-containing R protein that utilizes an EDS1-dependent pathway is RPW8, which confers broad-spectrum resistance to powdery mildew (Xiao *et al*., 2005). However, RPW8 is not an NBS-LRR type R protein; it contains an N-terminal TM domain in addition to the CC domain. The *HRT* paralog *RPP8* found in the Landsberg ecotype requires neither NDR1 nor EDS1 for its downstream signaling (McDowell *et al*., 2000). It is possible that EDS1 plays a signaling role in HRT-mediated resistance and/or has an effect on resistance to TCV via its effect on SA levels, which appear to be critical for resistance (Chandra-Shekara *et al*., 2004). In contrast, HRT-mediated resistance is independent of two other downstream factors RAR1 and SGT1b.

HRT-mediated resistance is dependent on PAD4, which like EDS1 and EDS5, is involved in regulating SA levels. PAD4 also regulates SA-induced expression of *HRT*, which suggests that besides governing SA levels, PAD4 has other regulatory functions in the HRT-triggered pathway. Both PAD4 and EDS1 show homology to triacylglycerol lipases/esterases. This raises the possibility that lipid/fatty acid signaling is involved in resistance to viral pathogens. A role for lipids/fatty acids in resistance to viral pathogens also is suggested by the finding that a mutation in the yeast delta-9 desaturase impairs replication of *Brome mosaic virus* (BMV) (Lee *et al*., 2001). Since delta-9 desaturase catalyzes the formation of oleic acid, the level of oleic acid may influence BMV replication. Replication of BMV is much more sensitive than yeast growth to reduced levels of this unsaturated fatty acid (Lee *et al*., 2001b). In plants, an equivalent of the yeast delta-9 desaturase is stearoyl-acyl carrier protein desaturase; similar to the yeast enzyme, a mutation in the plant desaturase lowers oleic acid levels (Kachroo *et al*., 2001). Analysis of a stearoyl-acyl carrier protein desaturase-defective mutant, designated *ssi2*, showed that it is partially resistant to *Cucumber mosaic virus* (CMV) (Takahashi *et al*., 2004). Second-site mutations, which restore oleic acid levels in *ssi2* plants, were sufficient to restore CMV susceptibility. Thus, *ssi2*-mediated resistance to CMV is likely due to reduced levels of oleic acid. Oleic acid also has been

implicated in regulating other defense responses (Kachroo *et al.*, 2001, 2003a,b, 2004, 2005). However, oleic acid levels do not appear to be critical for TCV resistance since *ssi2* plants are susceptible to this pathogen (Chandra-Shekara *et al.*, 2004).

Analysis of the HRT signaling pathway has revealed that light conditions also influence TCV resistance. We previously demonstrated that high SA levels, due to exogenously supplied SA or the presence of a mutation stimulating endogenous SA accumulation, enhance TCV resistance in an HRT-dependent, rrt-independent manner by upregulating *HRT* expression (Chandra-Shekara *et al.*, 2004, 2006). Light plays an important role in the SA-mediated upregulation of *HRT* expression and TCV resistance. When *HRT*-overexpressing transgenic Col-0 plants were subjected to a dark period immediately following TCV inoculation, TCV resistance was abolished (Chandra-Shekara *et al.*, 2006). Strikingly, dark treatment impaired resistance without affecting the levels of *HRT* transcript or free SA. However, increased expression of *HRT*, coupled with high endogenous SA levels, partially overcame the light requirement (Chandra-Shekara *et al.*, 2006).

Light also is required for the HR to TCV, since a dark period immediately following inoculation abolishes both the HR and *PR-1* gene expression (Chandra-Shekara *et al.*, 2006). Unlike resistance, the HR to TCV is independent of EDS1, PAD4, EDS5, and SID2. This suggests that, upon recognition of the pathogen, HRT induces at least two distinct pathways that differ in their requirement for downstream factors (Fig. 1). Since SA levels in *HRT sid2* plants do not rise after TCV inoculation, both HR formation and *PR-1* expression appear to be SA independent. In this regard, the HRT-triggered signaling pathway may overlap with that of its RPP8 paralog, which confers resistance to *P. parasitica* in an SA-independent manner (McDowell *et al.*, 1998). TCV-induced HR and *PR-1* gene expression also are independent of NDR1, RAR1, and SGT1. A mutation in NPR1, a positive regulator of SA signaling and systemic acquired resistance, partially compromises TCV-induced *PR-1* gene expression but does not affect the HR or resistance (Kachroo, 2005; Kachroo *et al.*, 2000).

C. RCY1-Mediated Resistance to Cucumber mosaic virus *in* Arabidopsis

The interaction between *Arabidopsis* ecotype C24 and CMV, a cucumovirus, represents the only other *Arabidopsis*–virus pathosystem, besides the *Arabidopsis*–TCV system, in which viral resistance is the result of pathogen-induced defense responses. Inoculation of CMV on

plants from the resistant ecotype C24 elicits an HR on the inoculated leaves, which is accompanied by increased expression of the SA-responsive genes, *PR-1* and *PR-5* (Takahashi *et al*., 1994, 2004). Unlike the *Arabidopsis*–TCV system, the HR to CMV is associated not only with the induction of SA-responsive genes, but also with upregulation of the JA/ethylene-responsive gene *PDF1.2* (encoding a plant defensin protein). This finding suggests that both SA- and JA/ethylene-regulated pathways are triggered during the resistance response to CMV. Consistent with this possibility, CMV-induced expression of the *PR* and *PDF1.2* genes was abolished by mutations in *EDS5* and *COI1*, respectively. Both the HR and resistance to CMV are conferred by a CC-NBS-LRR type R protein designated RCY1 (resistance to CMV strain Y1) (Takahashi *et al*., 2002). However, unlike the HRT-TCV system, RCY1-mediated resistance is only partially dependent on SA and *EDS5* (Fig. 1). Furthermore, the *coi1* mutation, which results in JA insensitivity, abolishes RCY1-induced expression of PDF1.2 but restores CMV resistance in *RCY1 eds5* plants (Takahashi *et al*., 2004). This result suggests that *PDF1.2* expression does not contribute to CMV resistance and that cross talk between SA and JA pathways modulates this resistance. Since *PR-1* expression is abolished in *RCY1 eds5* plants (Takahashi *et al*., 2004), it is likely that the partial dependence on *EDS5* is because the *eds5* mutation affects SA accumulation. Consistent with the involvement of SA in resistance, Mayers *et al.* (2005) found that exogenous application of SA delays the onset of systemic movement of CMV in susceptible ecotypes of *Arabidopsis*. *RCY1*-mediated resistance is partially dependent on ethylene but independent of *NPR1* (Takahashi *et al*., 2002).

Although the predicted proteins encoded by *RCY1* and its paralogs *HRT* and *RPP8* show ~90% similarity at the amino acid level, they confer resistance to very different pathogens. It has been hypothesized that intragenic recombination and positive selection are responsible for evolution of the *HRT*/*RPP8*/*RCY1* genes (Cooley *et al*., 2000; McDowell *et al*., 1998). Even though RCY1, HRT, and RPP8 share a high level of similarity, they appear to regulate distinct resistance pathways that are unique to each pathosystem. Moreover, comparison of the TCV and CMV coat proteins (CP), which are the Avr factors for these viruses (Oh *et al*., 1995; Takahashi *et al*., 2001; Zhao *et al*., 2000), fails to reveal any similarity at the amino acid or DNA levels. Thus, HRT and RCY1 may have evolved to recognize completely different ligands; alternatively, the interaction between these R proteins and their Avr factors may involve other common accessory factors. Given that HRT and TCV CP interact at the genetic level, but there

is no biochemical evidence for their direct physical interaction, the latter possibility is likely to be the case (Cooley *et al.*, 2000; Ren *et al.*, 2000; Wu and Klessig, unpublished data). Moreover, HRT-mediated resistance requires a physical interaction between the TCV CP and a protein belonging to the NAC family of transcription activators, designated TIP (TCV interacting protein) (Ren *et al.*, 2000). These and other studies with various R and Avr proteins suggest that interactions between most R proteins and their corresponding Avr factors do not occur directly, but instead require other accessory proteins/factors (Luderer and Joosten, 2001).

While expression of an *HRT* transgene in susceptible Col-0 plants confers HR formation after TCV infection, expression of an *RCY1* transgene in a susceptible ecotype did not confer a CMV-induced HR; however, resistance was observed in 50% of these plants (Takahashi *et al.*, 2002). This observation suggests that HR development and CMV resistance either are influenced by the level of *RCY1* transgene expression, or that another locus (loci) is required for HR formation and/or resistance. Supporting the latter possibility, F2 progeny from a cross between C24 and the susceptible Landsberg ecotype showed digenic segregation for HR formation, which suggests that a recessive gene influences HR development (Takahashi *et al.*, 1994).

D. RTM1-Mediated Resistance to Tobacco etch virus *in* Arabidopsis

Resistance to *Tobacco etch virus* (TEV) in *Arabidopsis* is governed by the dominant gene, *RTM1*, which functions by blocking long distance movement of the virus. *RTM1*-mediated resistance to TEV differs from that of a typical *R* gene because it does not involve HR formation or induction of defense genes associated with systemic acquired resistance (SAR). RTM1-mediated resistance also is unaffected by expression of a *nahG* transgene and is independent of NPR1, EDS1, PAD4, and NDR1 (Mahajan *et al.*, 1998). These observations suggest that RTM1-mediated signaling either acts downstream of the various *R* gene-associated functions or is independent of them. In addition to *RTM1*, another dominant locus, *RTM2* is involved in restricting TEV long distance movement. Both RTM1 and RTM2 are specific to TEV, since they do not appear to function as general defense controls against long distance viral movement. The *RTM1* gene encodes a lectin-like protein, which has led to the suggestion that it restricts TEV long distance movement either by physically blocking viral entry into the vascular tissue or by inhibiting a factor required for long distance movement. *RTM2* encodes a multidomain protein con-

taining an N-terminal region with high similarity to that of plant small HSPs (Whitham *et al*., 2000). Although RTM2's small HSP-like domain is evolutionarily distinct from plant small HSPs, the discovery that HSPs can act as molecular chaperones in *R* gene-triggered signaling pathways (Hubert *et al*., 2003; Liu *et al*., 2004a; Takahashi *et al*., 2003) has prompted speculation that *RTM*-mediated signaling is somehow linked with active resistance conferred by typical *R* genes.

E. Rx- and Rx2-Mediated Resistance to Potato virus X *(PVX) in Potato*

Resistance to PVX is conferred by either of two genes, designated *Rx* and *Rx2*, which encode CC-NBS-LRR type proteins. Both R proteins display the same specificity for the PVX CP, which acts as the Avr factor. The resistance response to PVX, commonly referred to as extreme resistance, involves rapid arrest of PVX replication in the initially infected cell; this prevents viral accumulation and minimizes the HR to a single cell (Goulden *et al*., 1993; Kohm *et al*., 1993). However, an HR to PVX is observed when Rx is transiently coexpressed with the PVX CP in *N. benthamiana* (Moffett *et al*., 2002). Resistance signaling mediated by *Rx* is dependent on SGT1, HSP90, and a MAPKKK (Lu *et al*., 2003; Peart *et al*., 2002a) but is independent of EDS1 and RAR1 (Bieri *et al*., 2004; Peart *et al*., 2002b).

F. Nb-Mediated Resistance to PVX in Potato

Nb is a single dominant *R* locus that maps to chromosome V in potato and confers resistance to PVX isolates from strain groups 1 and 2. Unlike *Rx*-mediated signaling, *Nb* gene-dependent resistance is characterized by development of an HR, which is elicited by a 25-kDa protein from the pathogen (Marano *et al*., 2002). The *Rx* gene is epistatic to *Nb* (Marano *et al*., 2002), since it masks the *Nb*-associated resistance phenotype (Cockerham, 1970).

G. Ry- and Ny_{tbr}*-Mediated Resistance to* Potato virus Y *in Potato*

Resistance to *Potato virus Y* (PVY) in potato is conferred by two different *R* genes, *Ry* and Ny_{tbr}. *Ry* is a single dominant gene conferring extreme resistance to PVY, while Ny_{tbr} confers HR-associated resistance. *Ry* and Ny_{tbr} map on chromosomes XI and IV of potato, respectively (Hamalainen *et al*., 1997; Leister *et al*., 1996). Plants carrying Ny_{tbr} exhibit both local and systemic HR to PVY. This systemic HR has been attributed to a low affinity interaction between the elicitor (Avr

factor) and the receptor (R protein) and/or when elicitor is produced at a late stage in the infection cycle (Celebi-Toprak *et al.*, 2002). The *Ry* gene has been mapped in two different species of potato, and the identified genes were designated Ry_{adg} and Ry_{sto} and mapped to chromosomes XI and XII, respectively (Brigneti *et al.*, 1997; Song *et al.*, 2005). A coding region designated Y-1, which was found to co-segregate with Ry_{adg}, has been cloned and is predicted to encode a TIR-NBS-LRR class of resistance protein. Expression of the *Y-1* transgene in a susceptible cultivar results in development of an HR to PVY, but the transgenic plants failed to prevent systemic viral spread (Vidal *et al.*, 2002). The Avr factor for PVY appears to be the protease domain of the nuclear inclusion protein, NIaPro, since this protein is able to elicit Ry-mediated resistance responses. However, evidence suggests that a host factor(s) also plays a role in eliciting resistance responses (Mestre *et al.*, 2003).

H. Sw-5-Mediated Resistance to Tomato spotted wilt virus *in Tomato*

Resistance to *Tomato spotted wilt virus* (TSWV) is conferred by *Sw-5*, which encodes a CC-NBS-LRR class of resistance protein. Resistance to TSWV is associated with development of an HR, which helps prevent the systemic spread of the virus (Jansen and Lenoire, 1998). *Sw-5* shares a high level of similarity with another tomato *R* gene, *Mi*, which confers resistance to nematodes (Brommonschenkel *et al.*, 2000).

Sw-5 gene confers broad spectrum resistance to TSWV isolates collected from different geographical regions as well as to two other tospoviruses, *Tomato chlorotic spot virus* and *Groundnut ring spot virus*, which infect tomato (Boiteux and Giordano, 1993; Stevens *et al.*, 1992). In addition to *Sw-5*, tomato contains five different genes (two dominant, three recessive; *Sw-a1*, *Sw-b1*, *Sw-2*, *Sw-3*, and *Sw-4*) that confer resistance to various isolates of TSWV. All five genes confer isolate-specific resistance, which can be easily overcome by different TSWV isolates and other tospoviruses (Boiteux and Giordano, 1993; Stevens *et al.*, 1992).

I. Tm-2^2-Mediated Resistance to Tomato mosaic virus *in Tomato*

Resistance to the tobamovirus, *Tomato mosaic virus* (ToMV), is conferred by three dominant *R* genes (*Tm-1*, *Tm-2*, and *Tm-2^2*) that are present in different tomato accessions and are widely used in tomato breeding to protect against ToMV. *Tm-1* was introgressed into the cultivated species (*Lycopersicum esculentum*) from its distant relative,

L. hirsutum, while *Tm-2* and *Tm-2*^{2} were introgressed from *L. peruvianum* (Hall, 1980; Pelham, 1966). The *Tm-2* and *Tm-2*^{2} genes encode CC-NBS-LRR-type R proteins and are considered to be allelic to each other (Lanfermeijer *et al*., 2005; Tanksley *et al*., 1992). *Tm-2*^{2}-conferred resistance is more durable than that conferred by *Tm-2* (Fraser *et al*., 1989); this difference in durability has been attributed to four amino acid differences between these proteins (Lanfermeijer *et al*., 2005). Both *Tm-2* and *Tm-2*^{2} recognize the movement protein of ToMV as the Avr factor (Calder and Palukaitis, 1992; Meshi *et al*., 1989; Weber and Pfitzner, 1998).

J. Rsv1-Mediated Resistance to Soybean mosaic virus *in Soybean*

Soybean *Rsv*1 is a single-locus, multi-allelic gene conferring resistance to *Soybean mosaic virus* (SMV). Different *Rsv*1 alleles condition diverse responses to the seven strains of SMV (G1–G7), ranging from extreme resistance and necrosis to mosaic symptoms. These genes encode a CC-NBS-LRR class of R protein. The *3gG2* gene within the *Rsv1* locus is a strong candidate for the major *Rsv1* gene mediating resistance to SMV (Hayes *et al*., 2004).

K. L Locus-Mediated Resistance to Tobamoviruses in Pepper

Resistance to tobamoviruses is governed by four dominant genes, L^1–L^4 in *Capsicum annum*. These genes are allelic and can be differentiated based on the induction of an HR by specific strains of tobamoviruses (Boukema, 1982; Boukema *et al*., 1980). L^3 gene-mediated resistance is most effective against all but the *Pepper mild mottle tobamovirus* strain (Garcia-Luque *et al*., 1993). Unlike most *R* gene-mediated responses, L^3-mediated resistance shows a strong dosage-dependent response. When L^3 is homozygous, it confers extreme resistance. By contrast, plants heterozygous for L^3 do not exhibit an HR and are mildly susceptible (Boukema *et al*., 1980).

III. Other Signaling Mechanisms Contributing to Viral Resistance

A. Pathogen-Derived Resistance: Recruiting Part of the Enemy for Defense

Resistance to viral pathogens also can be achieved by expressing a portion of viral genetic material in the plant. This form of resistance, popularly known as "pathogen-derived resistance," is a commonly used approach to engineer viral resistance. For example, expression of the

TMV *CP* gene in tobacco blocks the disassembly of infecting virion thereby preventing replication and movement of TMV (Powell-Abel *et al.*, 1986; Register and Beachy, 1988). This CP-mediated resistance (CPMR) is effective against virions but ineffective against unencapsidated virus or high inoculation titer. CPMR has been shown to work against a number of RNA viruses including PVX, *Alfalfa mosaic virus* (AlMV), CMV, TEV, *Potato mop-top virus*, *Papaya ringspot virus*, and *Tobacco ringspot virus* (Chapman *et al.*, 1992; reviewed in Barker *et al.*, 1998; Baulcombe, 1996; Beachy, 1994; Ferreira *et al.*, 2002; Wilson, 1993; Zadeh and Foster, 2004). Pathogen-derived resistance also can be achieved by expression of defective movement proteins, defective replicase subunits, or symptom-suppressing viral satellite RNAs (sat-RNAs) (Anderson *et al.*, 1992; Audy *et al.*, 1994; Baulcombe, 1994; Brederode *et al.*, 1995; Carr *et al.*, 1994; Lapidot *et al.*, 1993; Lomonossoff, 1995; Palukaitis and Zaitlin, 1997). Movement protein-mediated resistance has an advantage over CPMR since it provides resistance to several viruses. For example, expression of a defective movement protein of TMV confers resistance to tobamo-, cucumo-, potex-, and tobra-viral groups (Cooper *et al.*, 1995). A peptide-mediated resistance strategy has been developed that involves expressing a 29-amino acid peptide in plants (Rudolph *et al.*, 2003). This peptide, which was derived from the TSWV nucleocapsid protein, interacts with nucleoproteins from several members of the tospovirus group. Transgenic plants expressing this peptide exhibit enhanced resistance to TSWV, *Tomato chlorotic spot virus, Groundnut ring spot virus*, and *Chrysanthemum stem necrosis virus* (Rudolph *et al.*, 2003).

B. Viral Gene Silencing: A Tug-of-War Between Host and Pathogen

Another way to achieve resistance to viral pathogens containing an RNA genome is to selectively target the viral RNA for degradation. When an RNA virus infects a host cell, it can activate a host defense mechanism known as RNA silencing (Ratcliff *et al.*, 1999). RNA silencing is an epigenetic phenomenon manifested as posttranscriptional gene silencing (PTGS) in plants; it provides a highly specific, efficient surveillance system against parasitic RNA. Mechanistically, RNA silencing is triggered by formation of double-stranded RNA (dsRNA) (Fire *et al.*, 1998; Klahre *et al.*, 2002; Metzlaff *et al.*, 1997; Waterhouse *et al.*, 1998), which is subsequently cleaved by a dsRNA-specific RNase (commonly known as dicer) to produce small guide molecules 21–24 nucleotides long, termed short interfering RNAs (siRNAs) (Hamilton and Balcombe, 1999; Martinez *et al.*, 2002). The antisense strand of the

siRNA associates with an RNAi silencing complex to target homologous RNA for degradation (reviewed in Bartel, 2004; Baulcombe, 1999; Chicas and Macino, 2001; Matzke *et al*., 2001; Vance and Vaucheret, 2001; Waterhouse *et al*., 2001). The RNA silencing signal is also transported to other cells in the form of siRNAs, through plasmodesmata and phloem, to trigger silencing throughout the plant (Mlotshwa *et al*., 2002; Yoo *et al*., 2004). The mechanism of RNA silencing is highly conserved in plants and animals and is implicated in viral resistance (Covey *et al*., 1997; Ratcliff *et al*., 1997), genome maintenance (Assaad *et al*., 1993), and developmental control (Boerjan *et al*., 1994).

Silencing and degradation of viral RNA can be engineered by expressing a portion of viral RNA in the host genome. For example, expression of a nontranslatable version of the TEV CP in tobacco confers resistance to subsequent TEV infection. Resistance to TEV, due to silencing of the CP, is specific to TEV and does not provide resistance to other viruses such as CMV, AlMV, or PVY (Lindbo and Dougherty, 1992; Lindbo *et al*., 1993). Another method for engineering viral resistance exploits the effect of sat-RNAs, which are subgenomic viral RNAs that depend on the viral genomic RNA (helper virus) for replication, encapsidation, and movement. Some sat-RNAs are known to either attenuate or exacerbate disease symptoms caused by their helper viruses (Kong *et al*., 1997; Roossinck *et al*., 1992). Thus, expression of sat-RNAs in transgenic tobacco has been used to confer resistance against *Groundnut rosette virus* (Taliansky *et al*., 1998). Similarly, resistance to sat-RNA-free strains of CMV was obtained when a benign variant of a CMV sat-RNA was expressed in tomato (Cillo *et al*., 2004).

In addition to using portions of the viral genome or sat-RNAs, resistance has been engineered using constructs encoding an intron-spliced RNA with a hairpin loop structure. The PTGS mediated by hairpin RNA (hpRNA) was stable and more efficient than PTGS mediated by expressing sense or antisense constructs (Smith *et al*., 2000). Transient expression of hpRNAs containing sequences derived from viral pathogens has been shown to effectively confer resistance. For example, tobacco infiltrated with *Agrobacterium* carrying hpRNA derived from *Pepper mild mottle virus* were resistant to subsequent infection by this virus (Tenllado *et al*., 2004). In a novel study, expression of self-complementary hpRNA in tobacco was placed under control of the *rolC* promoter of *Agrobacterium rhizogenes*. The *rolC* promoter is tissue specific as it is expressed only in vascular tissues (Schmülling *et al*., 1989; Sugaya and Uchimiya, 1992); the resultant plants displayed systemic resistance to *Plum pox virus* (Pandolfini *et al*., 2003).

Plant viruses have evolved counter defenses to overcome RNA silencing in their host. One strategy is to encode proteins that suppress host-mediated RNA silencing thereby facilitating replication and systemic movement of the virus (Anandalakshmi *et al.*, 1998; Brigneti *et al.*, 1998; Kasschau and Carrington, 1998; Mallory *et al.*, 2001; Soosaar *et al.*, 2005; Voinnet, 2001, 2005). An interesting feature of these viral suppressors of host-mediated RNA silencing is that they do not share obvious sequence or structural similarity to one another. Furthermore, suppressor activity has been identified in a variety of viral proteins that serve different functions, including structural proteins (such as CP) and nonstructural proteins (such as replicases). This suggests that several different mechanisms are involved in suppressing RNA silencing. Suppressors of RNA silencing appear to function in both animal and plant cells, regardless of the host origin of the virus (Dunoyer *et al.*, 2004; Lakatos *et al.*, 2004). Thus, the silencing machinery and/or host signaling leading to RNA silencing appear to be conserved between plants and animals.

IV. Conclusions

The past decade has witnessed a substantial growth in our understanding of *R* gene signaling and RNA silencing pathways. While it is probable that these pathways communicate with each during the development of an effective resistance response to viral attack, the evidence to support such a link is rather scarce. A possible connection between resistance mediated by *R* genes and RNA silencing is indicated by the observation that in certain host–virus interactions (e.g., Di-17 and TCV) the same viral protein can function as both an Avr factor and a suppressor of RNA silencing. In addition, the ability of SA to induce host *RdRps*, which are components of the RNA silencing pathway, further suggests an overlap between these pathways. Improved understanding of *R* gene-mediated resistance and the RNA silencing pathways should facilitate better control of viral diseases by making it possible to further manipulate and enhance resistance in plants.

Acknowledgments

We are grateful to D'Maris Dempsey and David Smith for critical comments on the manuscript and to Ludmila Lapchyk for help with editing. Our work described in this review was supported by grants from the USDA-NRI (99–35303–8087 and

2003–35319–13312), NSF (MCB-0110404, MCB-0421914, and IBN-0525330), and the Kentucky Science and Engineering Foundation (KSEF-555-RDE-005).

References

Aarts, N., Metz, M., Holub, E., Staskawicz, B. J., Daniels, M. J., and Parker, J. E. (1998). Different requirements for EDS1 and NDR1 by disease resistance genes define at least two *R* gene-mediated signaling pathways in Arabidopsis. *Proc. Natl. Acad. Sci. USA* **95:**10306–10311.

Anandalakshmi, R., Pruss, G. J., Ge, X., Marathe, R., Mallory, A. C., Smith, T. H., and Vance, V. B. (1998). A viral suppressor of gene silencing in plants. *Proc. Natl. Acad. Sci. USA* **95:**13079–13084.

Anderson, J. M., Palukaitis, P., and Zaitilin, M. (1992). A defective replicase gene induces resistance to cucumber mosaic virus in transgenic tobacco plants. *Proc. Natl. Acad. Sci. USA* **89:**8759–8763.

Assaad, F. F., Tucker, K. L., and Signer, E. R. (1993). Epigenetic repeat-induced gene silencing (RIGS) in Arabidopsis. *Plant Mol. Biol.* **22:**1067–1085.

Audy, P., Palukaitis, P., Slack, S. A., and Zaitlin, M. (1994). Replicase-mediated resistance to potato virus Y in transgenic plants. *Mol. Plant Microbe Interact.* **7:**15–22.

Austin, M. J., Muskett, P., Kahn, K., Feys, B. J., Jones, J. D., and Parker, J. E. (2002). Regulatory role of SGT1 in early *R* gene-mediated plant defenses. *Science* **295:**2077–2080.

Ayliffe, M. A., Frost, D. V., Finnegan, E. J., Lawrence, G. J., Anderson, P. A., and Ellis, J. G. (1999). Analysis of alternative transcripts of the flax *L6* rust resistance gene. *Plant J.* **17:**287–292.

Azevedo, C., Sadanandom, A., Kitagawa, K., Freialdenhoven, A., Shirasu, K., and Schulze-Lefert, P. (2002). The RAR1 interactor SGT1, an essential component of R gene-triggered disease resistance. *Science* **295:**2073–2076.

Barker, I., Henry, C. M., Thomas, M. R., and Stratford, R. (1998). Potential benefits of the transgenic control of plant viruses in the United Kingdom. *Methods Mol. Biol.* **81:**557–566.

Bartel, D. P. (2004). MicroRNAs: Genomics, biogenesis, mechanism, and function. *Cell* **116:**281–297.

Baulcombe, D. C. (1994). Replicase-mediated resistance: A novel type of virus resistance in transgenic plants? *Trends Microbiol.* **2:**60–63.

Baulcombe, D. C. (1996). Mechanisms of pathogen-derived resistance to viruses in transgenic plants. *Plant Cell* **8:**1833–1844.

Baulcombe, D. C. (1999). Gene silencing: RNA makes no protein. *Curr. Biol.* **9:** R599–R601.

Baulcombe, D. C. (2004). RNA silencing in plants. *Nature* **431:**356–363.

Beachy, R. N. (1994). Introduction: Transgenic resistance to plant viruses. *Semin. Virol.* **4:**327–328.

Bendahmane, A., Kanyuka, K., and Baulcombe, D. C. (1999). The *Rx* gene from potato controls separate virus resistance and cell death responses. *Plant Cell* **11:**781–92.

Bendahmane, A., Querci, M., Kanyuka, K., and Baulcombe, D. C. (2000). Agrobacterium transient expression system as a tool for the isolation of disease resistance genes: Application to the *Rx2* locus in potato. *Plant J.* **21:**73–81.

Berzal-Herranz, A., de la Cruz, A., Tenllado, F., Diaz-Ruiz, J. R., Lopez, L., Sanz, A. I., Vaquero, C., Serra, M. T., and Garcia-Luque, I. (1995). The Capsicum *L3* gene-mediated resistance against the tobamoviruses is elicited by the coat protein. *Virology* **209:**498–505.

Bieri, S., Mauch, S., Shen, Q. H., Peart, J., Devoto, A., Casais, C., Ceron, F., Schulze, S., Steinbiss, H. H., Shirasu, K., and Schulze-Lefert, P. (2004). RAR1 positively controls steady state levels of barley MLA resistance proteins and enables sufficient MLA6 accumulation for effective resistance. *Plant Cell* **16:**3480–3495.

Boerjan, W., Bauw, G., Van Montagu, M., and Inze, D. (1994). Distinct phenotypes generated by overexpression and suppression of S-adenosyl-L-methionine synthetase reveal developmental patterns of gene silencing in tobacco. *Plant Cell* **6:**1401–1414.

Boiteux, L. S., and Giordano, L.deB. (1993). Genetic basis of resistance against two Tospovirus species in tomato (*Lycopersicon esculentum*). *Euphytica* **71:**151–154.

Bos, L. (2000). *In* "Plant Viruses, Unique and Intriguing Pathogens," p. 358. Backhuys Publishers, Leiden.

Boukema, I. W. (1982). Resistance to TMV in *Capsicum chacoense* Hunz is governed by an allele of the L-locus. *Capsicum Newslett.* **3:**47–48.

Boukema, I. W., Jansen, K., and Hofman, K. (1980). Strains of TMV and genes for resistance in Capsicum. *In* "Proc 4th Capsicum Eucarpia Meeting," pp. 44–48. Wageningen, The Netherlands.

Brederode, F. T., Taschner, P. E. Y., Posthumus, E., and Boi, J. F. (1995). Replicase-mediated resistance to alfalfa mosaic virus. *Virology* **207:**467–474.

Brigneti, G., Garcia-Mas, J., and Baulcombe, D. C. (1997). Molecular mapping of the Potato Virus Y resistance gene Ry_{sto} in potato. *Theor. Appl. Genet.* **94:**198–203.

Brommonschenkel, S. H., Frary, A., Frary, A., and Tanksley, S. D. (2000). The broad-spectrum tospovirus resistance gene Sw-5 of tomato is a homolog of the root-knot nematode resistance gene Mi. *Mol. Plant-Microbe Interact.* **13:**1130–1138.

Calder, V. L., and Palukaitis, P. (1992). Nucleotide sequence analysis of the movement genes of resistance breaking strains of tomato mosaic virus. *J. Gen. Virol.* **73:**165–168.

Cardinale, F., Jonak, C., Ligterink, W., Niehaus, K., Boller, T., and Hirt, H. (2000). Differential activation of four specific MAPK pathways by distinct elicitors. *J. Biol. Chem.* **275:**36734–36740.

Carr, J. P., Gal-On, A., Palukaltis, P., and Zaltiin, M. (1994). Replicase-mediated resistance to cucumber mosaic virus in transgenic plants involves suppression of both virus replication in the inoculated leaves and long distance movement. *Virology* **199:**439–447.

Celebi-Toprak, F., Slack, S. A., and Jahn, M. M. (2002). A new gene, Ny_{tbr}, for hypersensitivity to potato virus Y from *Solanum tuberosum* maps to chromosome IV. *Theor. Appl. Genet.* **104:**669–674.

Chandra-Shekara, A. C., Navarre, D., Kachroo, A., Kang, H-G., Klessig, D., and Kachroo, P. (2004). Signaling requirements and role of salicylic acid in *HRT*- and *rrt*-mediated resistance to turnip crinkle virus in Arabidopsis. *Plant J.* **5:**647–659.

Chandra-Shekara, A. C., Gupte, M., Navarre, D., Raina, S., Raina, R., Klessig, D., and Kachroo, P. (2006). Light-dependent hypersensitive response and resistance signaling against *Turnip crinkle virus* in *Arabidopsis*. *Plant J.* **45:**320–334.

Chapman, S. N., Kavanagh, T. A., and Baulcombe, D. C. (1992). Potato virus X as a vector for gene expression in plants. *Plant J.* **2:**549–557.

Chicas, A., and Macino, G. (2001). Characteristics of post-transcriptional gene silencing. *EMBO Rep.* **2:**992–996.

Chisholm, S. T., Mahajan, S. K., Whitham, S. A., Yamamoto, M. L., and Carrington, J. C. (2000). Cloning of the Arabidopsis *RTM1* gene, which controls restriction of long-distance movement of tobacco etch virus. *Proc. Natl. Acad. Sci. USA* **97:**489–494.

Chivasa, S., and Carr, J. P. (1998). Cyanide restores *N* gene-mediated resistance to tobacco mosaic virus in transgenic tobacco expressing salicylic acid hydroxylase. *Plant Cell* **10:**1489–1498.

Cillo, F., Finetti-Sialer, M. M., Papanice, M. A., and Gallitelli, D. (2004). Analysis of mechanisms involved in the cucumber mosaic virus satellite RNA-mediated transgenic resistance in tomato plants. *Mol. Plant-Microbe Interact.* **17:**98–108.

Cockerham, G. (1970). Genetical studies on resistance to potato viruses X and Y. *Heredity* **25:**309–348.

Cooley, M. B., Pathirana, S., Wu, H. J., Kachroo, P., and Klessig, D. F. (2000). Members of the Arabidopsis *HRT/RPP8* family of resistance genes confer resistance to both viral and oomycete pathogens. *Plant Cell* **12:**663–676.

Cooper, B., Lapidot, M., Heick, J. A., Dodds, J. A., and Beachy, R. N. (1995). A defective movement protein of TMV in transgenic plants confers resistance to multiple viruses whereas the functional analog increases susceptibility. *Virology* **206:**307–313.

Covey, S. N., Al-Kaff, N. S., Langara, A., and Turner, D. S. (1997). Plants combat infections by gene silencing. *Nature* **385:**781–782.

Dangl, J. L., and Jones, J. D. (2001). Defense responses to infection. *Nature* **411:**826–833.

Delaney, T. P., Uknes, S., Vernooij, B., Friedrich, L., Weymann, K., Negrotto, D., Gaffney, T., Gut-Rella, M., Kessmann, H., Ward, E., and Ryals, J. A. (1994). A central role of salicylic acid in plant disease resistance. *Science* **266:**1247–1250.

Dempsey, D. A., Wobbe, K. K., and Klessig, D. F. (1993). Resistance and susceptible responses of *Arabidopsis thaliana* to turnip crinkle virus. *Phytopathology* **83:**1021–1029.

Dempsey, D. A., Pathirana, M. S., Wobbe, K. K., and Klessig, D. F. (1997). Identification of an Arabidopsis locus required for resistance to turnip crinkle virus. *Plant J.* **2:**301–311.

Deshaies, R. J. (1999). SCF and Cullin/Ring H2-based ubiquitin ligases. *Annu. Rev. Cell Dev. Biol.* **15:**435–467.

Desikan, R., Hancock, J. T., Ichimura, K., Shinozaki, K., and Neill, S. J. (2001). Harpin-induced activation of the Arabidopsis mitogen-activated protein kinases AtMPK4 and AtMPK6. *Plant Physiol.* **126:**1579–1587.

Dinesh-Kumar, S. P., and Baker, B. J. (2000). Alternatively spliced *N* resistance gene transcripts: Their possible role in tobacco mosaic virus resistance. *Proc. Natl. Acad. Sci. USA* **97:**1908–1913.

Dunoyer, P., and Voinnet, O. (2005). The complex interplay between plant viruses and host RNA-silencing pathways. *Curr. Opin. Plant Biol.* **4:**415–423.

Dunoyer, P., Lecellier, C. H., Parizotto, E. A., Himber, C., and Voinnet, O. (2004). Probing the microRNA and small interfering RNA pathways with virus-encoded suppressors of RNA silencing. *Plant Cell* **16:**1235–1250.

Durner, J., Wendehenne, D., and Klessig, D. F. (1998). Defense gene induction in tobacco by nitric oxide, cyclic GMP, and cyclic ADP-ribose. *Proc. Natl. Acad. Sci. USA* **95:**10328–10333.

Erickson, F. L., Holzberg, S., Calderon-Urrea, A., Handley, V., Axtell, M., Corr, C., and Baker, B. (1999). The helicase domain of the TMV replicase proteins induces the N-mediated defense response in tobacco. *Plant J.* **18:**67–75.

Falk, A., Feys, B. J., Frost, L. N., Jones, J. D., Daniels, M. J., and Parker, J. E. (1999). EDS1, an essential component of *R* gene-mediated disease resistance in Arabidopsis has homology to eukaryotic lipases. *Proc. Natl. Acad. Sci. USA* **96:**3292–3297.

Ferreira, S. A., Pitz, K. Y., Manshardt, R., Zee, F., Fitch, M., and Gonsalves, D. (2002). Virus coat protein transgenic papaya provides practical control of papaya ringspot virus in Hawaii. *Plant Dis.* **86:**101–105.

Fire, A., Xu, S., Montgomery, M. K., Kostas, S. A., Driver, S. E., and Mello, C. C. (1998). Potent and specific genetic interference by double-stranded RNA in *Caenorhabditis elegans*. *Nature* **391:**806–811.

Flor, H. (1971). Current status of gene-for-gene concept. *Annu. Rev. Phytopathol.* **9:**275–296.

Fraser, R. S. S., Gerwitz, A., and Betti, L. (1989). Deployment of resistance genes: Implications from studies on resistance-breaking isolates of tobacco mosaic virus. *In* "Proc. of the IV Intl. Plant Virus Epidemiology Workshop," pp. 154–155. Montpellier, France.

Garcia-Luque, I., Ferrero, M. L., Rodriguez, J. M., Alonso, E., de la Cruz, A., Sanz, A. I., Vaquero, C., Serra, M. T., and Diaz-Ruiz, J. R. (1993). The nucleotide sequence of the coat protein genes and 3′ non-coding regions of two resistance-breaking tobamoviruses in pepper shows that they are different viruses. *Arch. Virol.* **131:**75–88.

Gilliland, A., Singh, D. P., Hayward, J. M., Moore, C. A., Murphy, A. M., York, C. J., Slator, J., and Carr, J. P. (2003). Genetic modification of alternative respiration has differential effects on antimycin A-induced versus salicylic acid-induced resistance to tobacco mosaic virus. *Plant Physiol.* **132:**1518–1528.

Goulden, M. G., Kohm, B. A., Santa Cruz, S., Kavanagh, T. A., and Baulcombe, D. C. (1993). A feature of the coat protein of potato virus X affects both induced virus resistance in potato and viral fitness. *Virology* **197:**293–302.

Hall, T. J. (1980). Resistance at the Tm-2 locus in the tomato to tomato mosaic virus. *Euphytica* **29:**189–197.

Hamalainen, J. H., Watanabe, K. N., Valkonen, J. P. T., Arihara, A., and Plaisted, R. L. (1997). Mapping and marker-assisted selection for a gene for extreme resistance to potato virus Y. *Theor. Appl. Genet.* **94:**192–197.

Hamilton, A. J., and Baulcombe, D. C. (1999). A species of small antisense RNA in post-transcriptional gene silencing in plants. *Science* **286:**950–952.

Hayes, A. J., Jeong, S. C., Gore, M. A., Yu, Y. G., Buss, G. R., Tolin, S. A., and Maroof, M. A. (2004). Recombination within a nucleotide-binding-site/leucine-rich-repeat gene cluster produces new variants conditioning resistance to soybean mosaic virus in soybeans. *Genetics* **166:**493–503.

Holmes, F. O. (1938). Inheritance of resistance to tobacco-mosaic disease in tobacco. *Phytopathology* **28:**553–561.

Hubert, D. A., Tornero, P., Belkhadir, Y., Krishna, P., Takahashi, A., Shirasu, K., and Dangl, J. L. (2003). Cytosolic HSP90 associates with and modulates the Arabidopsis RPM1 disease resistance protein. *EMBO J.* **22:**5679–5689.

Hughes, S. L., Hunter, P. J., Sharpe, A. G., Kearsey, M. J., Lydiate, D. J., and Walsh, J. A. (2003). Genetic mapping of the novel turnip mosaic virus resistance gene *TuRB03* in *Brassica napus*. *Theor. Appl. Genet.* **107:**1169–1173.

Hull, R. (2002). *In* "Matthews' Plant Virology," p. 1001. Academic Press, London.

Jansen, F., and Lenoire, R. (1998). *Molecular and biological aspects of tospoviruses.* http://www.spg.wau.nl/viro/research/tospo.html.

Jenner, C. E., Sanchez, F., Nettleship, S. B., Foster, G. D., Ponz, F., and Walsh, J. A. (2000). The cylindrical inclusion gene of turnip mosaic virus encodes a pathogenic determinant to the Brassica resistance gene *TuRB01*. *Mol. Plant-Microbe Interact.* **13:**1102–1108.

Jenner, C. E., Tomimura, K., Ohshima, K., Hughes, S. L., and Walsh, J. A. (2002). Mutations in turnip mosaic virus P3 and cylindrical inclusion proteins are separately required to overcome two *Brassica napus* resistance genes. *Virology* **300:**50–59.

Jin, H., Liu, Y., Yang, K. Y., Kim, C. Y., Baker, B., and Zhang, S. (2003). Function of a mitogen-activated protein kinase pathway in *N* gene-mediated resistance in tobacco. *Plant J.* **33:**719–731.

Jirage, D., Tootle, T. L., Reuber, T. L., Frost, L. N., Feys, B. J., Parker, J. E., Ausubel, F. M., and Glazebrook, J. (1999). *Arabidopsis thaliana PAD4* encodes a lipase-like gene that is important for salicylic acid signaling. *Proc. Natl. Acad. Sci. USA* **96:**13583–13588.

Kachroo, P. (2006). Host gene-mediated virus resistance mechanisms and signaling in Arabidopsis. *In* "Natural Resistance Mechanisms of Plants to Viruses" (G. Loebenstein and J. P. Carr, eds.). Kluwer Academic Publishers, The Netherlands.

Kachroo, P., Yoshioka, K., Shah, J., Dooner, H. K., and Klessig, D. F. (2000). Resistance to turnip crinkle virus in Arabidopsis is regulated by two host genes, is salicylic acid dependent but *NPR1*, ethylene and jasmonate independent. *Plant Cell* **12:**677–690.

Kachroo, P., Shanklin, J., Shah, J., Whittle, E. J., and Klessig, D. F. (2001). A fatty acid desaturase modulates the activation of defense signaling pathways in plants. *Proc. Natl. Acad. Sci. USA* **98:**9448–9453.

Kachroo, P., Kachroo, A., Lapchyk, L., Hildebrand, D., and Klessig, D. (2003a). Restoration of defective cross talk in *ssi2* mutants; Role of salicylic acid, jasmonic acid and fatty acids in SSI2-mediated signaling. *Mol. Plant-Microbe Interact.* **11:**1022–1029.

Kachroo, A., Lapchyk, L., Fukushigae, H., Hildebrand, D., Klessig, D., and Kachroo, P. (2003b). Plastidial fatty acid signaling modulates salicylic acid- and jasmonic acid-mediated defense pathways in the Arabidopsis *ssi2* mutant. *Plant Cell* **15:**2952–2965.

Kachroo, A., Srivathsa, C. V., Lapchyk, L., Falcone, D., Hildebrand, D., and Kachroo, P. (2004). Oleic acid levels regulated by glycerolipid metabolism modulate defense gene expression in Arabidopsis. *Proc. Natl. Acad. Sci. USA* **101:**5152–5157.

Kachroo, P., Venugopal, S. C., Navarre, D. A., Lapchyk, L., and Kachroo, A. (2005). Role of salicylic acid and fatty acid desaturation pathways in *ssi2*-mediated signaling. *Plant Physiol.* **139:**1–19.

Kasschau, K. D., and Carrington, J. C. (1998). A counter defensive strategy of plant viruses: Suppression of posttranscriptional gene silencing. *Cell* **95:**461–470.

Kitagawa, K., Skowyra, D., Elledge, S. J., Harper, J. W., and Hieter, P. (1999). SGT1 encodes an essential component of the yeast kinetochore assembly pathway and a novel subunit of the SCF ubiquitin ligase complex. *Mol. Cell* **4:**21–33.

Klahre, U., Crete, P., Leuenberger, S. A., Iglesias, V. A., and Meins, F., Jr. (2002). High molecular weight RNAs and small interfering RNAs induce systemic posttranscriptional gene silencing in plants. *Proc. Natl. Acad. Sci. USA* **99:**11981–11986.

Kohm, B. A., Goulden, M. G., Gilbert, J. E., Kavanagh, T. A., and Baulcombe, D. C. (1993). A Potato Virus X resistance gene mediates an induced, nonspecific resistance in protoplasts. *Plant Cell* **8:**913–920.

Kong, Q., Wang, J., and Simon, A. E. (1997). Satellite RNA-mediated resistance to turnip crinkle virus in Arabidopsis involves a reduction in virus movement. *Plant Cell* **9:**2051–2063.

Lakatos, L., Szittya, G., Silhavy, D., and Burgyan, J. (2004). Molecular mechanism of RNA silencing suppression mediated by p19 protein of tombusviruses. *EMBO J.* **23:**876–884.

Lanfermeijer, F. C., Dijkhuis, J., Sturre, M. J., de Haan, P., and Hille, J. (2003). Cloning and characterization of the durable tomato mosaic virus resistance gene *Tm-2(2)* from *Lycopersicum esculentum. Plant Mol. Biol.* **52:**1037–1049.

Lanfermeijer, F. C., Warmink, J., and Hille, J. (2005). The products of the broken *Tm-2* and the durable *Tm-2*^{2} resistance genes from tomato differ in four amino acids. *J. Exp. Bot.* **56:**2925–2933.

Lapidot, M., Gafny, R., Ding, E., Wolf, S., Lucas, W. J., and Beachy, R. N. (1993). A dysfunctional movement protein of tobacco mosaic virus that partially modifies the plasmodesmata and limits virus spread in transgenic plants. *Plant J.* **4:**959–970.

Lecoq, H., Moury, B., Desbiez, C., Palloix, A., and Pitrat, M. (2004). Durable virus resistance in plants through conventional approaches: A challenge. *Virus Res.* **100:**31–39.

Lee, J., Klessig, D. F., and Nürnberger, T. (2001a). A harpin binding site in tobacco plasma membranes mediates activation of the pathogenesis-related gene HIN1 independent of extracellular calcium but dependent on mitogen-activated protein kinase activity. *Plant Cell* **13:**1079–1093.

Lee, W.-M., Ishikawa, M., and Ahlquist, P. (2001b). Mutations of host Δ9 fatty acid desaturase inhibits brome mosaic virus RNA replication between template recognition and RNA synthesis. *J. Virol.* **75:**2097–2106.

Leister, D., Ballvora, A., Salamani, F., and Gebhardt, C. (1996). A PCR-based approach for isolating pathogen resistance genes from potato with potential for wide application in plants. *Nat. Genet.* **14:**421–429.

Levy, M., Edelbaum, O., and Sela, I. (2004). Tobacco mosaic virus regulates the expression of its own resistance gene *N*. *Plant Physiol.* **135:**2392–2397.

Lindbo, J. A., and Dougherty, W. G. (1992). Untranslatable transcripts of the tobacco etch virus coat protein gene sequence can interfere with tobacco etch virus replication in transgenic plants and protoplasts. *Virology* **189:**725–733.

Lindbo, J. A., Silva-Rosales, L., Proebsting, W. M., and Dougherty, W. G. (1993). Induction of a highly specific antiviral state in transgenic plants: Implications for regulation of gene expression and virus resistance. *Plant Cell* **5:**1749–1759.

Liu, Y., Schiff, M., Marathe, R., and Dinesh-Kumar, S. P. (2002a). Tobacco RAR1, EDS1 and NPR1/NIM1 like genes are required for *N*-mediated resistance to tobacco mosaic virus. *Plant J.* **30:**415–429.

Liu, Y., Schiff, M., Serino, G., Deng, X. W., and Dinesh-Kumar, S. P. (2002b). Role of SCF ubiquitin-ligase and the COP9 signalosome in the *N* gene-mediated resistance response to tobacco mosaic virus. *Plant Cell* **14:**1483–1496.

Liu, Y., Burch-Smith, T., Schiff, M., Feng, S., and Dinesh-Kumar, S. P. (2004a). Molecular chaperone Hsp90 associates with resistance protein N and its signaling proteins SGT1 and RAR1 to modulate an innate immune response in plants. *J. Biol. Chem.* **279:**2101–2108.

Liu, Y., Schiff, M., and Dinesh-Kumar, S. P. (2004b). Involvement of MEK1, MAPKK, NTF6 MAPK, WRKY/MYB transcription factors, COI1 and CTR1 in N-mediated resistance to tobacco mosaic virus. *Plant J.* **38:**800–809.

Lomonossoff, G. P. (1995). Pathogen-derived resistance to plant viruses. *Annu. Rev. Phytopathol.* **33:**323–343.

Lu, R., Malcuit, I., Moffett, P., Ruiz, M. T., Peart, J., Wu, A. J., Rathjen, J. P., Bendahmane, A., Day, L., and Baulcombe, D. C. (2003). High throughput virus-induced gene silencing implicates heat shock protein 90 in plant disease resistance. *EMBO J.* **22:**5690–5699.

Luderer, R., and Joosten, M. H. A. J. (2001). Avirulence proteins of plant pathogens: Determinants of victory and defeat. *Mol. Plant Pathol.* **2:**355–364.

Lyapina, S., Cope, G., Shevchenko, A., Serino, G., Tsuge, T., Zhou, C., Wolf, D. A., Wei, N., Shevchenko, A., and Deshaies, R. J. (2001). Promotion of NEDD-CUL1 conjugate cleavage by COP9 signalosome. *Science* **292:**1382–1385.

Mahajan, S. K., Chisholm, S. T., Whitham, S. A., and Carrington, J. C. (1998). Identification and characterization of a locus (*RTM1*) that restricts long-distance movement of tobacco etch virus in *Arabidopsis thaliana*. *Plant J.* **14:**177–186.

Malamy, J., Hennig, J., and Klessig, D. F. (1992). Temperature-dependent induction of salicylic acid and its conjugates during the resistance response to tobacco mosaic virus infection. *Plant Cell* **4:**359–366.

Mallory, A. C., Ely, L., Smith, T. H., Marathe, R., Anandalakshmi, R., Fagard, M., Vaucheret, H., Pruss, G., Bowman, L., and Vance, V. B. (2001). HC-Pro suppression of transgene silencing eliminates the small RNAs but not transgene methylation or the mobile signal. *Plant Cell* **13:**571–583.

Marano, R., Malcuit, I., De Jong, W., and Baulcombe, D. C. (2002). High-resolution genetic map of *Nb*, a gene that confers hypersensitive resistance to potato virus X in *Solanum tuberosum*. *Theor. Appl. Genet.* **105:**192–200.

Martin, G. B., Bogdanove, A. J., and Sessa, G. (2003). Understanding the functions of plant disease resistance proteins. *Annu. Rev. Plant Biol.* **54:**23–61.

Martinez, J., Patkaniowska, A., Urlaub, H., Luhrmann, R., and Tuschl, T. (2002). Single-stranded antisense siRNAs guide target RNA cleavage in RNAi. *Cell* **110:**563–574.

Matsuzawa, S. I., and Reed, J. C. (2001). Siah-1, SIP, and Ebi collaborate in a novel pathway for beta-catenin degradation linked to p53 responses. *Mol. Cell* **7:**915–926.

Matzke, M. A., Matzke, A. J., Pruss, G. J., and Vance, V. B. (2001). RNA-based silencing strategies in plants. *Curr. Opin. Genet. Dev.* **11:**221–227.

Mayers, C. N., Lee, K. C., Moore, C. A., Wong, S. M., and Carr, J. P. (2005). Salicylic acid-induced resistance to cucumber mosaic virus in squash and *Arabidopsis thaliana*: Contrasting mechanisms of induction and antiviral action. *Mol. Plant-Microbe Interact.* **18:**428–434.

McDowell, J. M., Dhandaydham, M., Long, T. A., Aarts, M. G., Goff, S., Holub, E. B., and Dangl, J. L. (1998). Intragenic recombination and diversifying selection contribute to the evolution of downy mildew resistance at the *RPP8* locus of Arabidopsis. *Plant Cell* **10:**1861–1874.

McDowell, J. M., Cuzick, A., Can, C., Beynon, J., Dangl, J. L., and Holub, E. B. (2000). Downy mildew (*Peronospora parasitica*) resistance genes in Arabidopsis vary in functional requirements for *NDR1*, *EDS1*, *NPR1* and salicylic acid accumulation. *Plant J.* **22:**523–529.

Meshi, T., Motoyoshi, F., Adachi, A., Watanabe, Y., Takamatsu, N., and Okada, Y. (1988). Two concomitant base substitutions in the putative replicase genes of tobacco mosaic virus confer the ability to overcome the effects of a tomato resistance gene, Tm-1. *EMBO J.* **7:**1575–1581.

Meshi, T., Motoyoshi, F., Maeda, T., Yoshiwoka, S., Watanabe, H., and Okada, Y. (1989). Mutations in the tobacco mosaic virus 30-kD protein gene overcome Tm-2 resistance in tomato. *Plant Cell* **1:**515–522.

Mestre, P., Brigneti, G., Durrant, M. C., and Baulcombe, D. C. (2003). Potato virus Y NIa protease activity is not sufficient for elicitation of Ry-mediated disease resistance in potato. *Plant J.* **36:**755–761.

Metzlaff, M., O'Dell, M., Cluster, P. D., and Flavell, R. B. (1997). RNA-mediated RNA degradation and chalcone synthase A silencing in petunia. *Cell* **88:**845–854.

Mikolajczyk, M., Awotunde, O. S., Muszynska, G., Klessig, D. F., and Dobrowolska, G. (2000). Osmotic stress induces rapid activation of a salicylic acid-induced protein kinase and a homolog of protein kinase ASK1 in tobacco cells. *Plant Cell* **12:**165–178.

Mlotshwa, S., Voinnet, O., Mette, M. F., Matzke, M., Vaucheret, H., Ding, S. W., Pruss, G., and Vance, V. B. (2002). RNA silencing and the mobile silencing signal. *Plant Cell* **14:**S289–S301.

Moffett, P., Farnham, G., Peart, J., and Baulcombe, D. C. (2002). Interaction between domains of a plant NBS-LRR protein in disease resistance-related cell death. *EMBO J.* **21:**4511–4519.

Muskett, P. R., Kahn, K., Austin, M. J., Moisan, L. J., Sadanandom, A., Shirasu, K., Jones, J. D., and Parker, J. E. (2002). Arabidopsis RAR1 exerts rate-limiting control of *R* gene-mediated defenses against multiple pathogens. *Plant Cell* **14:**979–992.

Nawrath, C., Heck, S., Parinthawong, N., and Metraux, J. P. (2002). EDS5, an essential component of salicylic acid-dependent signaling for disease resistance in Arabidopsis, is a member of the MATE transporter family. *Plant Cell* **14:**275–286.

Nühse, T., Peck, S. C., Hirt, H., and Boller, T. (2000). Microbial elicitors induce activation and dual phosphorylation of the *Arabidopsis thaliana* MAPK6. *J. Biol. Chem.* **275:**7521–7526.

Oh, J.-W., Kong, W., Song, C., Carpenter, C. D., and Simon, A. E. (1995). Open reading frames of turnip crinkle virus involved in satellite symptom expression and incompatibility with *Arabidopsis thaliana* ecotype Dijon. *Mol. Plant-Microbe Interact.* **8:**979–987.

Padgett, H. S., Watanabe, Y., and Beachy, R. N. (1997). Identification of the TMV replicase sequence that activates the *N* gene-mediated hypersensitive response. *Mol. Plant-Microbe Interact.* **10:**709–715.

Palukaitis, P., and Zaitlin, M. (1997). Replicase-mediated resistance to plant virus disease. *Adv. Virus Res.* **48:**349–377.

Pandolfini, T., Molesini, B., Avesani, L., Spena, A., and Polverari, A. (2003). Expression of self-complementary hairpin RNA under the control of the *rolC* promoter confers systemic disease resistance to plum pox virus without preventing local infection. *BMC Biotechnol.* **3:**7.

Parker, J. E., Coleman, M. J., Szabo, V., Frost, L. N., Schmidt, R., van der Biezen, E. A., Moores, T., Dean, C., Daniels, M. J., and Jones, J. D. (1997). The Arabidopsis downy mildew resistance gene *RPP5* shares similarity to the toll and interleukin-1 receptors with N and L6. *Plant Cell* **9:**879–894.

Peart, J. R., Lu, R., Sadanandom, A., Malcuit, I., Moffett, P., Brice, D. C., Schauser, L., Jaggard, D. A., Xiao, S., Coleman, M. J., Dow, M., Jones, M. *et al.* (2002a). Ubiquitin ligase-associated protein SGT1 is required for host and nonhost disease resistance in plants. *Proc. Natl. Acad. Sci. USA* **99:**10865–10869.

Peart, J. R., Cook, G., Feys, B. J., Parker, J. E., and Baulcombe, D. C. (2002b). An EDS1 orthologue is required for N-mediated resistance against tobacco mosaic virus. *Plant J.* **29:**569–579.

Peart, J. R., Mestre, P., Lu, R., Malcuit, I., and Baulcombe, D. C. (2005). NRG1, a CC-NB-LRR protein, together with N, a TIR-NB-LRR protein, mediates resistance against tobacco mosaic virus. *Curr. Biol.* **15:**968–973.

Pelham, J. (1966). Resistance in tomato to tobacco mosaic virus. *Euphytica* **15:**258–267.

Picard, D. (2002). Heat-shock protein 90, a chaperone for folding and regulation. *Cell. Mol. Life Sci.* **59:**1640–1648.

Powell-Abel, P., Nelson, R. S., De, B., Hoffmann, N., Rogen, S. G., Fraley, R. T., and Beachy, R. N. (1986). Delay of disease development in transgenic plants that express the tobacco mosaic virus coat protein gene. *Science* **232:**738–743.

Qu, F., and Morris, T. J. (2005). Suppressors of RNA silencing encoded by plant viruses and their role in viral infections. *FEBS Lett.* **579:**5958–5964.

Ratcliff, F., Harrison, B. D., and Baulcombe, D. C. (1997). A similarity between viral defense and gene silencing in plants. *Science* **276:**1558–1560.

Ratcliff, F. G., MacFarlane, S. A., and Baulcombe, D. C. (1999). Gene silencing without DNA. RNA-mediated cross-protection between viruses. *Plant Cell* **11:**1207–1216.

Register, J. C., and Beachy, R. N. (1988). Resistance to TMV in transgenic plants results from interference with an early event in infection. *Virology* **166:**524–532.

Ren, T., Qu, F., and Morris, T. J. (2000). HRT gene function requires interaction between a NAC protein and viral capsid protein to confer resistance to turnip crinkle virus. *Plant Cell* **12:**1917–1926.

Richter, K., and Buchner, J. (2001). Hsp90: Chaperoning signal transduction. *J. Cell Physiol.* **188:**281–290.

Romeis, T., Piedras, P., Zhang, S., Klessig, D. F., Hirt, H., and Jones, J. (1999). Rapid Avr9- and Cf-9-dependent activation of MAP kinases in tobacco cell cultures and leaves: Convergence of resistance gene, elicitor, wound and salicylate responses. *Plant Cell* **11:**273–287.

Roossinck, M. J., Sleat, D., and Palukaitis, P. (1992). Satellite RNAs of plant viruses: Structures and biological effects. *Microbiol. Rev.* **56:**265–279.

Rudolph, C., Schreier, P. H., and Uhrig, J. F. (2003). Peptide-mediated broad-spectrum plant resistance to tospoviruses. *Proc. Natl. Acad. Sci. USA* **100:**4429–4434.

Schmülling, T., Schell, J., and Spena, A. (1989). Promoters of the *rol A*, *B*, and *C* genes of *Agrobacterium rhizogenes* are differentially regulated in transgenic plants. *Plant Cell* **1:**665–670.

Sinapidou, E., Williams, K., Nott, L., Bahkt, S., Tor, M., Crute, I., Bittner-Eddy, P., and Beynon, J. (2004). Two TIR:NB:LRR genes are required to specify resistance to *Peronospora parasitica* isolate Cala2 in Arabidopsis. *Plant J.* **38:**898–909.

Singh, D. P., Moore, C. A., Gilliland, A., and Carr, J. P. (2004). Activation of multiple antiviral defence mechanisms by salicylic acid. *Mol. Plant. Pathol.* **5:**57–63.

Smith, N. A., Singh, S. P., Wang, M. B., Stoutjesdijk, P. A., Green, A. G., and Waterhouse, P. M. (2000). Total silencing by intron-spliced hairpin RNAs. *Nature* **407:**319–320.

Song, Y. S., Hepting, L., Schweizer, G., Hartl, L., Wenzel, G., and Schwarzfischer, A. (2005). Mapping of extreme resistance to PVY (Ry_{sto}) on chromosome XII using anther-culture-derived primary dihaploid potato lines. *Theor. Appl. Genet.* **111:**879–887.

Soosaar, J. L., Burch-Smith, T. M., and Dinesh-Kumar, S. P. (2005). Mechanisms of plant resistance to viruses. *Nat. Rev. Microbiol.* **3:**789–798.

Stevens, M. R., Scott, J. W., and Gergerich, R. C. (1992). Inheritance of a gene for resistance to tomato spotted wilt virus (TSWV) from *Lycopersicum peruvianum* Mill. *Euphytica* **59:**9–17.

Sugaya, H., and Uchimiya, S. (1992). Deletion analysis of the 5′-upstream region of the *Agrobacterium rhizogenes* Ri plasmid *rolC* gene required for tissue-specific expression. *Plant Physiol.* **99:**464–467.

Takahashi, A., Casais, C., Ichimura, K., and Shirasu, K. (2003). HSP90 interacts with RAR1 and SGT1 and is essential for RPS2-mediated disease resistance in Arabidopsis. *Proc. Natl. Acad. Sci. USA* **100:**11777–11782.

Takahashi, H., Goto, N., and Ehara, Y. (1994). Hypersensitive response in cucumber mosaic virus-inoculated *Arabidopsis thaliana*. *Plant J.* **6:**369–377.

Takahashi, H., Suzuki, M., Natsuaki, K., Shigyo, T., Hino, K., Teaoka, T., Hosokawa, D., and Ehara, Y. (2001). Mapping the virus and host genes involved in resistance response in cucumber mosaic virus-infected *Arabidopsis thaliana*. *Plant Cell Physiol.* **42:**340–347.

Takahashi, H., Miller, J., Nozaki, Y., Takeda, M., Shah, J., Hase, S., Ikegami, M., Ehara, Y., and Dinesh-Kumar, S. P. (2002). RCY1, an *Arabidopsis thaliana RPP8/HRT* family resistance gene, conferring resistance to cucumber mosaic virus requires salicylic acid, ethylene and a novel signal transduction mechanism. *Plant J.* **32:**655–667.

Takahashi, H., Kanayama, Y., Zheng, M. S., Kusano, T., Hase, S., Ikegami, M., and Shah, J. (2004). Antagonistic interactions between the SA and JA signaling pathways in Arabidopsis modulate expression of defense genes and gene-for-gene resistance to cucumber mosaic virus. *Plant Cell Physiol.* **45:**803–809.

Taliansky, M. E., Ryabov, E. V., and Robinson, D. J. (1998). Two distinct mechanisms of transgenic resistance mediated by groundnut rosette virus satellite RNA sequences. *Mol. Plant-Microbe Interact.* **11:**367–374.

Tanksley, S. D., Ganal, M. W., Prince, J. P., de Vicente, M. C., Bonierbale, M. W., Broun, P., Fulton, T. M., Giovannoni, J. J., Grandillo, S., and Martin, G. B. (1992). High density molecular linkage maps of the tomato and potato genomes. *Genetics* **132:**1141–1160.

Tenllado, F., Llave, C., and Diaz-Ruiz, J. R. (2004). RNA interference as a new biotechnological tool for the control of virus diseases in plants. *Virus Res.* **102:**85–96.

Tör, M., Gordon, P., Cuzick, A., Eulgem, T., Sinapidou, E., Mert-Turk, F., Can, C., Dangl, J. L., and Holub, E. B. (2002). Arabidopsis SGT1b is required for defense signaling conferred by several downy mildew resistance genes. *Plant Cell* **14:**993–1003.

Uehara, Y., Takahashi, Y., Berberich, T., Miyazaki, A., Takahashi, H., Matsui, K., Ohme-Takagi, M., Saitoh, H., Terauchi, R., and Kusano, T. (2005). Tobacco ZFT1, a transcriptional repressor with a Cys(2)/His(2) type zinc finger motif that functions in spermine-signaling pathway. *Plant Mol. Biol.* **59:**435–448.

Vance, V., and Vaucheret, H. (2001). RNA silencing in plants defense and counter defense. *Science* **292:**2277–2280.

Vidal, S., Cabrera, H., Andersson, R. A., Fredriksoon, A., and Valkonen, J. P. (2002). Potato gene *Y-1* is an *N* gene homolog that confers cell death upon infection with Potato Virus Y. *Mol. Plant-Microbe Interact.* **15:**717–727.

Voinnet, O. (2001). RNA silencing as a plant immune system against viruses. *Trends Genet.* **17:**449–459.

Voinnet, O. (2005). Induction and suppression of RNA silencing: Insights from viral infections. *Nat. Rev. Genet.* **6:**206–220.

Waterhouse, P. M., Graham, M. W., and Wang, M. B. (1998). Virus resistance and gene silencing in plants can be induced by simultaneous expression of sense and antisense RNA. *Proc. Natl. Acad. Sci. USA* **95:**13959–13964.

Waterhouse, P. M., Wang, M. B., and Finnegan, E. J. (2001). Role of short RNAs in gene silencing. *Trends Plant Sci.* **6:**297–301.

Weber, H., and Pfitzner, A. J. (1998). *Tm-2*^{2} resistance in tomato requires recognition of the carboxy terminus of the movement protein of tomato mosaic virus. *Mol. Plant-Microbe Interact.* **11:**498–503.

Wei, N., and Deng, X. W. (1999). Making sense of the COP9 signalosome. A regulatory protein complex conserved from Arabidopsis to human. *Trends Genet.* **15:**98–103.

Wei, N., Tsuge, T., Serino, G., Dohmae, N., Takio, K., Matsui, M., and Deng, X. W. (1998). The COP9 complex is conserved between plants and mammals and is related to the 26S proteasome regulatory complex. *Curr. Biol.* **8:**919–922.

Whitham, S., Dinesh-Kumar, S. P., Choi, D., Hehl, R., Corr, C., and Baker, B. (1994). The product of the tobacco mosaic virus resistance gene N: Similarity to toll and the interleukin-1 receptor. *Cell* **78:**1101–1115.

Whitham, S. A., Anderberg, R. J., Chisholm, S. T., and Carrington, J. C. (2000). Arabidopsis *RTM2* gene is necessary for specific restriction of tobacco etch virus and encodes an unusual small heat shock-like protein. *Plant Cell* **12:**569–582.

Wildermuth, M. C., Dewdney, J., Wu, G., and Ausubel, F. M. (2001). Isochorismate synthase is required to synthesize salicylic acid for plant defense. *Nature* **414:**562–565.

Wilson, T. M. (1993). Strategies to protect crop plants against viruses: Pathogen-derived resistance blossoms. *Proc. Natl. Acad. Sci. USA* **90:**3134–3141.

Xiao, S., Calis, O., Patrick, E., Zhang, G., Charoenwattana, P., Muskett, P., Parker, J. E., and Turner, J. G. (2005). The atypical resistance gene, *RPW8*, recruits components of basal defence for powdery mildew resistance in Arabidopsis. *Plant J.* **42:**95–110.

Xie, Z., Fan, B., Chen, C., and Chen, Z. (2001). An important role of an inducible RNA-dependent RNA polymerase in plant antiviral defense. *Proc. Natl. Acad. Sci. USA* **98:**6516–6521.

Yamakawa, H., Kamada, H., Satoh, M., and Ohashi, Y. (1998). Spermine is a salicylate-independent endogenous inducer for both tobacco acidic pathogenesis-related proteins and resistance against tobacco mosaic virus infection. *Plant Physiol.* **118:**1213–1222.

Yoo, B. C., Kragler, F., Varkonyi-Gasic, E., Haywood, V., Archer-Evans, S., Lee, Y. M., Lough, T. J., and Lucas, W. J. (2004). A systemic small RNA signaling system in plants. *Plant Cell* **16:**1979–2000.

Zadeh, A. H., and Foster, G. D. (2004). Transgenic resistance to tobacco ringspot virus. *Acta Virol.* **48:**145–152.

Zhang, S., and Klessig, D. F. (1998a). *N* resistance gene-mediated *de novo* synthesis and activation of a tobacco MAP kinase by TMV infection. *Proc. Natl. Acad. Sci. USA* **95:**7433–7438.

Zhang, S., and Klessig, D. F. (1998b). The tobacco wounding-activated mitogen-activated protein kinase is encoded by SIPK. *Proc. Natl. Acad. Sci. USA* **95:**7225–7230.

Zhang, S., Du, H., and Klessig, D. F. (1998). Activation of tobacco SIP kinase by both a cell wall-derived carbohydrate elicitor and purified proteinaceous elicitins from *Phytophthora* spp. *Plant Cell* **10:**435–449.

Zhang, S., Liu, Y., and Klessig, D. F. (2000). Multiple levels of tobacco WIPK activation during the induction of cell death by fungal elicitins. *Plant J.* **23:**339–347.

Zhao, Y., DelGrosso, L., Yigit, E., Dempsey, D. A., Klessig, D. F., and Wobbe, K. K. (2000). The amino terminus of the coat protein of turnip crinkle virus is the AVR factor recognized by resistant Arabidopsis. *Mol. Plant-Microbe Interact.* **13:**1015–1018.

This page intentionally left blank

ADVANCES IN VIRUS RESEARCH, VOL 66

THE MOLECULAR BIOLOGY OF CORONAVIRUSES

Paul S. Masters

Wadsworth Center, New York State Department of Health
Albany, New York 12201

Abstract

Coronaviruses are large, enveloped RNA viruses of both medical and veterinary importance. Interest in this viral family has intensified in the past few years as a result of the identification of a newly emerged coronavirus as the causative agent of severe acute respiratory syndrome (SARS). At the molecular level, coronaviruses employ a variety of unusual strategies to accomplish a complex program of gene expression. Coronavirus replication entails ribosome frameshifting during genome translation, the synthesis of both genomic and multiple subgenomic RNA species, and the assembly of progeny virions by a pathway that is unique among enveloped RNA viruses. Progress in the investigation of these processes has been enhanced by the development of reverse genetic systems, an advance that was heretofore obstructed

0065-3527/06 $35.00
DOI: 10.1016/S0065-3527(06)66005-3

by the enormous size of the coronavirus genome. This review summarizes both classical and contemporary discoveries in the study of the molecular biology of these infectious agents, with particular emphasis on the nature and recognition of viral receptors, viral RNA synthesis, and the molecular interactions governing virion assembly.

I. Introduction

Coronaviruses are a family of enveloped RNA viruses that are distributed widely among mammals and birds, causing principally respiratory or enteric diseases but in some cases neurologic illness or hepatitis (Lai and Holmes, 2001). Individual coronaviruses usually infect their hosts in a species-specific manner, and infections can be acute or persistent. Infections are transmitted mainly via respiratory and fecal-oral routes. The most distinctive feature of this viral family is genome size: coronaviruses have the largest genomes among all RNA viruses, including those RNA viruses with segmented genomes. This expansive coding capacity seems to both provide and necessitate a wealth of gene-expression strategies, most of which are incompletely understood.

Two prior reviews with the same title as this one have appeared in the *Advances in Virus Research* series (Lai and Cavanagh, 1997; Sturman and Holmes, 1983). The earlier of the two noted that the recognition of coronaviruses as a separate virus family occurred in the 1960s, in the wake of the discovery of several new human respiratory pathogens, certain of which, it was realized, appeared highly similar to the previously described avian infectious bronchitis virus (IBV) and mouse hepatitis virus (MHV) (Almeida and Tyrrell, 1967). These latter viruses had a characteristic morphology in negative-stained electron microscopy, marked by a "fringe" of surface structures described as "spikes" (Berry *et al.*, 1964) or "club-like" projections (Becker *et al.*, 1967). Such structures were less densely distributed and differently shaped than those of the myxoviruses. To some, the fringe resembled the solar corona, giving rise to the name that was ultimately assigned to the group (Almeida *et al.*, 1968). Almost four decades later, recognition of the same characteristic virion morphology alerted the world to the emergence of another new human respiratory pathogen: the coronavirus responsible for the devastating outbreak of severe acute respiratory syndrome (SARS) in 2002–2003 (Ksiazek *et al.*, 2003; Peiris *et al.*, 2003). The sudden appearance of SARS has stimulated a burst of new research to understand the basic replication mechanisms of members of

this family of viral agents, as a means toward their control and prophylaxis. Thus, the time is right to again assess the state of our collective knowledge about the molecular biology of coronaviruses.

Owing to limitations imposed by both space and the expertise of the author, "molecular biology" will be considered here in the more narrow sense, that is, the molecular details of the cellular replication of coronaviruses. No attempt will be made to address matters of pathogenesis, viral immunology, or epidemiology. For greater depth and differences of emphasis in particular areas, as well as for historical perspectives, the reader is referred to the two excellent predecessors of this review (Lai and Cavanagh, 1997; Sturman and Holmes, 1983) and also to volumes edited by Siddell (1995) and Enjuanes (2005).

II. Taxonomy

Coronaviruses are currently classified as one of the two genera in the family *Coronaviridae* (Enjuanes *et al.*, 2000b). However, it is likely that the coronaviruses, as well as the other genus within the *Coronaviridae*, the toroviruses (Snijder and Horzinek, 1993), will each be accorded the taxonomic status of family in the near future (González *et al.*, 2003). Therefore, throughout this review, the coronaviruses are referred to as a family. Both the coronaviruses and the toroviruses, in addition to two other families, the *Arteriviridae* (Snijder and Meulenberg, 1998) and the *Roniviridae* (Cowley *et al.*, 2000; Dhar *et al.*, 2004), have been grouped together in the order *Nidovirales*. This higher level of organization recognizes a relatedness among these families that sets them apart from other nonsegmented positive-strand RNA viruses. The most salient features that all nidoviruses have in common are: gene expression through transcription of a set of multiple 3′-nested subgenomic RNAs; expression of the replicase polyprotein via ribosomal frameshifting; unique enzymatic activities among the replicase protein products; a virion membrane envelope; and a multispanning integral membrane protein in the virion. The first of these qualities provides the name for the order, which derives from the Latin *nido* for nest (Enjuanes *et al.*, 2000a). In contrast to their commonalities, however, nidovirus families differ from one another in distinct ways, most conspicuously in the numbers, types, and sizes of the structural proteins in their virions and in the morphologies of their nucleocapsids. A more detailed comparison of characteristics of these virus families has been given by Enjuanes *et al.* (2000b) and Lai and Cavanagh (1997).

Members of the coronavirus family have been sorted into three groups (Table I), which, it has been proposed, are sufficiently divergent to merit the taxonomic status of genera (González *et al.*, 2003). Classification into groups was originally based on antigenic relationships. However, such a criterion reflects the properties of a limited subset of viral proteins, and cases have arisen where clearly related viruses in group 1 were found not to be serologically cross-reactive (Sanchez *et al.*, 1990). Consequently, sequence comparisons of entire viral genomes (or of as much genomic sequence as is available) have come to be the basis for group classification (Gorbalenya *et al.*, 2004). Almost all group 1 and group 2 viruses have mammalian hosts, with human coronaviruses falling into each of these groups. Viruses of group 3, by contrast, have been isolated solely from avian hosts. Most of the coronaviruses in Table I have been studied for decades, and, by the turn of the century, the scope of the family seemed to be fairly well-defined. Accordingly, it came as quite a shock, in 2003, when the causative agent of SARS was found to be a coronavirus (SARS-CoV). Equally astonishing have been the outcomes of renewed efforts, following the SARS epidemic, to detect previously unknown viruses; these investigations have led to the discovery of two more human respiratory coronaviruses, HCoV-NL63 (van der Hoek *et al.*, 2004) and HCoV-HKU1 (Woo *et al.*, 2005). Three distinct bat coronaviruses have also been isolated: two are members of group 1, and the third, in group 2, is a likely precursor of the human SARS-CoV (Lau *et al.*, 2005; Li *et al.*, 2005c; Poon *et al.*, 2005). In addition, new IBV-like viruses have been found that infect geese, pigeons, and ducks (Jonassen *et al.*, 2005).

In almost all cases, the assignment of a coronavirus species to a given group has been unequivocal. Exceptionally, the classification of SARS-CoV has provoked considerable controversy. The original, unrooted, phylogenetic characterizations of the SARS-CoV genome sequence posited this virus to be roughly equidistant from each of the three previously established groups. It was thus proposed to be the first recognized member of a fourth group of coronaviruses (Marra *et al.*, 2003; Rota *et al.*, 2003). However, a subsequently constructed phylogeny based on gene *1b*, which contains the viral RNA-dependent RNA polymerase and which was rooted in the toroviruses as an outgroup, concluded that SARS-CoV is most closely related to the group 2 coronaviruses (Snijder *et al.*, 2003). In the same vein, it was noted that regions of gene *1a* of SARS-CoV contain domains that are unique to the group 2 coronaviruses (Gorbalenya *et al.*, 2004). Other analyses of a subset of structural gene sequences (Eickmann *et al.*, 2003) and of RNA secondary structures in the 3′ untranslated region (3′ UTR) of the genome (Goebel

TABLE I
CORONAVIRUS SPECIES AND GROUPS

Group	Designation	Species	Host	GenBank accession number*	
1	TGEV	Transmissible gastroenteritis virus	Pig	AJ271965	[g]
	PRCoV	Porcine respiratory coronavirus	Pig	Z24675	[p]
	FIPV	Feline infectious peritonitis virus	Cat	AY994055	[g]
	FCoV	Feline enteric coronavirus	Cat	Y13921	[p]
	CCoV	Canine coronavirus	Dog	D13096	[p]
	HCoV-229E	Human coronavirus strain 229E	Human	AF304460	[g]
	PEDV	Porcine epidemic diarrhea virus	Pig	AF353511	[g]
	HCoV-NL63	Human coronavirus strain NL63	Human	AY567487	[g]
	Bat-CoV-61	Bat coronavirus strain 61	Bat	AY864196	[p]
	Bat-CoV-HKU2	Bat coronavirus strain HKU2	Bat	AY594268	[p]
2	MHV	Mouse hepatitis virus	Mouse	AY700211	[g]
	BCoV	Bovine coronavirus	Cow	U00735	[g]
	RCoV	Rat coronavirus	Rat	AF088984	[p]
	SDAV	Sialodacryoadenitis virus	Rat	AF207551	[p]
	HCoV-OC43	Human coronavirus strain OC43	Human	AY903460	[g]
	HEV	Hemagglutinating encephalomyelitis virus	Pig	AF481863	[p]
	PCoV[†]	Puffinosis coronavirus	Puffin	AJ544718	[p]
	ECoV	Equine coronavirus	Horse	AY316300	[p]
	CRCoV	Canine respiratory coronavirus	Dog	CQ772298	[p]
	SARS-CoV	SARS coronavirus	Human	AY278741	[g]
	HCoV-HKU1	Human coronavirus strain HKU1	Human	AY597011	[g]
	Bat-SARS-CoV	Bat SARS coronavirus	Bat	DQ022305	[g]

(*continues*)

TABLE I (*continued*)

Group	Designation	Species	Host	GenBank accession number*	
3	IBV	Infectious bronchitis virus	Chicken	AJ311317	[g]
	TCoV	Turkey coronavirus	Turkey	AY342357	[p]
	PhCoV	Pheasant coronavirus	Pheasant	AJ618988	[p]
	GCoV	Goose coronavirus	Goose	AJ871017	[p]
	PCoV†	Pigeon coronavirus	Pigeon	AJ871022	[p]
	DCoV	Duck coronavirus	Mallard	AJ871024	[p]

* One representative GenBank accession number is given for each species. When available, a complete genomic sequence (denoted [g]) is provided; otherwise, the largest available partial sequence (denoted [p]) is given.

† Unique designations have not yet been formulated for these two viruses.

et al., 2004b) also supported a group 2 assignment. By contrast, some authors have argued, based on bioinformatics methods, that the ancestor of SARS-CoV was derived from multiple recombination events among progenitors from all three groups (Rest and Mindell, 2003; Stanhope *et al.*, 2004; Stavrinides and Guttman, 2004). While these latter studies assume that historically there has been limitless opportunity for intergroup recombination, there is no well-documented example of recombination between extant coronaviruses of different groups. Moreover, it is not clear that intergroup recombination is even possible, owing to replicative incompatibilities among the three coronavirus groups (Goebel *et al.*, 2004b). Therefore, although SARS-CoV does indeed have unique features, the currently available evidence best supports the conclusion that it is more closely allied with the group 2 coronaviruses and that it has not sufficiently diverged to constitute a fourth group (Gorbalenya *et al.*, 2004).

III. Virion Morphology, Structural Proteins, and Accessory Proteins

A. Virus and Nucleocapsid

Coronaviruses are roughly spherical and moderately pleiomorphic (Fig. 1). Virions have typically been reported to have average diameters of 80–120 nm, but extreme sizes as small as 50 nm and as large

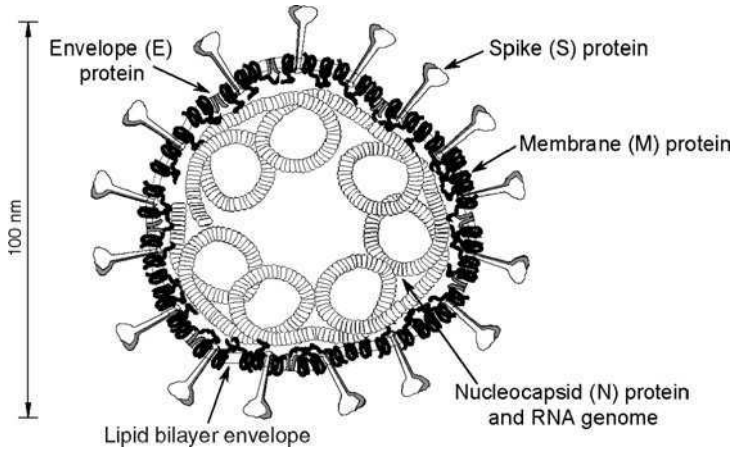

FIG 1. Schematic of the coronavirus virion, with the minimal set of structural proteins.

as 200 nm are occasionally given in the older literature (Oshiro, 1973; McIntosh, 1974). The surface spikes or peplomers of these viruses, variously described as club-like, pear-shaped, or petal-shaped, project some 17–20 nm from the virion surface (McIntosh, 1974), having a thin base that swells to a width of about 10 nm at the distal extremity (Sugiyama and Amano, 1981). For some coronaviruses a second set of projections, 5–10-nm long, forms an undergrowth beneath the major spikes (Guy *et al.*, 2000; Patel *et al.*, 1982; Sugiyama and Amano, 1981). These shorter structures are now known to be the hemagglutinin-esterase (HE) protein that is found in a subset of group 2 coronaviruses (Section III.G).

At least some of the heterogeneity in coronavirus particle morphology can be attributed to the distorting effects of negative-staining procedures. Freeze-dried (Roseto *et al.*, 1982) and cryo-electron microscopic (Risco *et al.*, 1996) preparations of BCoV and TGEV, respectively, showed much more homogeneous populations of virions, with diameters 10–30 nm greater than virions in comparable samples prepared by negative staining. Extraordinary three-dimensional images have been obtained for SARS-CoV virions emerging from infected Vero cells (Ng *et al.*, 2004). These scanning electron micrographs and atomic force micrographs reveal knobby, rosette-like viral particles resembling tiny cauliflowers. It will be exciting to see future applications of advanced imaging techniques to the study of coronavirus structure.

The internal component of the coronavirus virion is obscure in electron micrographs of whole virions. In negative-stained images the

core appears as an indistinct mass with a densely staining center, giving the virion a "punched-in" spherical appearance. Imaging of virions that have burst spontaneously, expelling their contents, or that have been treated with nonionic detergents has allowed visualization of the coronavirus core. Such analyses led to the attribution of another distinguishing characteristic to the coronavirus family: that its members possess helically symmetric nucleocapsids. Such nucleocapsid symmetry is the rule for negative-strand RNA viruses, but almost all positive-strand RNA animal viruses have icosahedral ribonucleoprotein capsids. However, although it is fairly well accepted that coronaviruses have helical nucleocapsids, there are surprisingly few published data that bear on this issue. Additionally, the reported results vary considerably with both the viral species and the method of preparation. The earliest study of nucleocapsids from spontaneously disrupted HCoV-229E virions found tangled, threadlike structures 8–9 nm in diameter; these were unraveled or clustered to various degrees and, in rare cases, retained some of the shape of the parent virion (Kennedy and Johnson-Lussenburg, 1975/76). A subsequent analysis of spontaneously disrupted virions of HCoV-229E and MHV observed more clearly helical nucleocapsids, with diameters of 14–16 nm and hollow cores of 3–4 nm (Macnaughton *et al.*, 1978). The most highly resolved images of any coronavirus nucleocapsid were obtained with NP-40-disrupted HCoV-229E virions (Caul *et al.*, 1979). These preparations showed filamentous structures 9–11 or 11–13 nm in diameter, depending on the method of staining, with a 3–4-nm central canal. The coronavirus nucleocapsid was noted to be thinner in cross-section than those of paramyxoviruses and also to lack the sharply segmented "herringbone" appearance characteristic of paramyxovirus nucleocapsids. By contrast, in early studies, IBV and TGEV nucleocapsids were refractory to the techniques that had been successful with other viruses. Visualization of IBV nucleocapsids, which seemed to be very sensitive to degradation (Macnaughton *et al.*, 1978), was finally achieved by electron microscopy of viral samples prepared by carbon-platinum shadowing (Davies *et al.*, 1981). This revealed linear strands, some as long as 6–7 μm, which were only 1.5-nm thick, suggesting that they represented unwound helices. TGEV, on the other hand, was found to be more resistant to nonionic detergents. Treatment of virions of this species with NP-40 resulted in spherical subviral particles with no threadlike substructure visible (Garwes *et al.*, 1976). The TGEV core was later seen as a spherically symmetric, possibly icosahedral, superstructure that only dissociated further into a helical nucleocapsid following Triton X-100 treatment of virions (Risco *et al.*, 1996). Such a collection of incomplete and often discrepant results makes it clear that

much further examination of the internal structure of coronavirus virions is warranted. It would substantially aid our understanding of coronavirus structure and assembly if we had available a detailed description of nucleocapsid shape, length, diameter, helical repeat distance, and protein:RNA stoichiometry.

B. Spike Protein (S)

There are three protein components of the viral envelope (Fig. 1). The most prominent of these is the S glycoprotein (formerly called E2) (Cavanagh, 1995), which mediates receptor attachment and viral and host cell membrane fusion (Collins *et al.*, 1982). The S protein is a very large, N-exo, C-endo transmembrane protein that assembles into trimers (Delmas and Laude, 1990; Song *et al.*, 2004) to form the distinctive surface spikes of coronaviruses (Fig. 2). S protein is inserted into the endoplasmic reticulum (ER) via a cleaved, amino-terminal signal peptide (Cavanagh *et al.*, 1986b). The ectodomain makes up most of the molecule, with only a small carboxy-terminal segment (of 71 or fewer of the total 1162–1452 residues) constituting the transmembrane domain and endodomain. Monomers of S protein, prior to glycosylation, are 128–160 kDa, but molecular masses of the glycosylated forms of

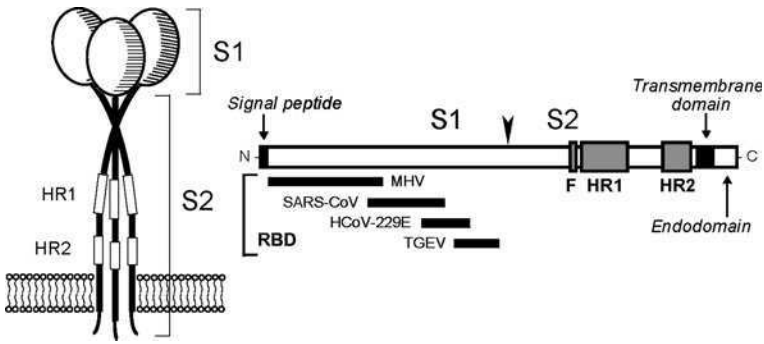

FIG 2. The spike (S) protein. At the right is a linear map of the protein, denoting the amino-terminal S1 and the carboxy-terminal S2 portions of the molecule. The arrowhead marks the site of cleavage for those S proteins that become cleaved by cellular protease(s). The signal peptide and regions of mapped receptor-binding domains (RBDs) are shown in S1. The heptad repeat regions (HR1 and HR2), putative fusion peptide (F), transmembrane domain, and endodomain are indicated in S2. At the left is a model for the S protein trimer.

full-length monomers fall in the range of 150–200 kDa. The S molecule is thus highly glycosylated, and this modification is exclusively N-linked (Holmes *et al.*, 1981; Rottier *et al.*, 1981). S protein ectodomains have from 19 to 39 potential consensus glycosylation sites, but a comprehensive mapping of actual glycosylation has not yet been reported for any coronavirus. A mass spectrometric analysis of the SARS-CoV S protein has shown that at least 12 of the 23 candidate sites are glycosylated in this molecule (Krokhin *et al.*, 2003). For the TGEV S protein, it has been demonstrated that the early steps of glycosylation occur cotranslationally, but that terminal glycosylation is preceded by trimerization, which can be rate-limiting in S protein maturation (Delmas and Laude, 1990). In addition, glycosylation of TGEV S may assist monomer folding, given that tunicamycin inhibition of high-mannose transfer was found to also block trimerization.

The S protein ectodomain has between 30 and 50 cysteine residues, and within each coronavirus group the positions of cysteines are well conserved (Abraham *et al.*, 1990; Eickmann *et al.*, 2003). However, as with glycosylation, a comprehensive mapping of disulfide linkages has not yet been achieved for any coronavirus S protein.

In most group 2 and all group 3 coronaviruses, the S protein is cleaved by a trypsin-like host protease into two polypeptides, S1 and S2, of roughly equal sizes. Even for uncleaved S proteins, that is, those of the group 1 coronaviruses and SARS-CoV, the designations S1 and S2 are used for the amino-terminal and carboxy-terminal halves of the S protein, respectively. Peptide sequencing has shown that cleavage occurs following the last residue in a highly basic motif: RRFRR in IBV S protein (Cavanagh *et al.*, 1986b), RRAHR in MHV strain A59 S protein (Luytjes *et al.*, 1987), and KRRSRR in BCoV S protein (Abraham *et al.*, 1990). Similar cleavage sites are predicted from the sequences of other group 2 S proteins, except that of SARS-CoV. It has been noted that the S protein of MHV strain JHM has a cleavage motif (RRARR) more basic than that found in MHV strain A59 (RRAHR). An expression study has shown that this difference accounts for the almost total extent of cleavage of the JHM S protein that is seen in cell lines in which the A59 S protein undergoes only partial cleavage (Bos *et al.*, 1995).

The S1 domain is the most divergent region of the molecule, both across and within the three coronavirus groups. Even among strains and isolates of a single coronavirus species, the sequence of S1 can vary extensively (Gallagher *et al.*, 1990; Parker *et al.*, 1989; Wang *et al.*, 1994). By contrast, the most conserved part of the molecule across the three coronavirus groups is a region that encompasses the

S2 portion of the ectodomain, plus the start of the transmembrane domain (de Groot *et al.*, 1987). An early model for the coronavirus spike, which has held up well in light of subsequent work, proposed that the S1 domains of the S protein oligomer constitute the bulb portion of the spike. The stalk portion of the spike, on the other hand, was envisioned to be a coiled-coil structure, analogous to that in influenza HA protein, formed by association of heptad repeat regions of the S2 domains of monomers (de Groot *et al.*, 1987). The roles of these two regions of the S protein in the initiation of infection will be discussed (Section IV.A).

C. Membrane Protein (M)

The M glycoprotein (formerly called E1) is the most abundant constituent of coronaviruses (Sturman, 1977; Sturman *et al.*, 1980) and gives the virion envelope its shape. The preglycosylated M polypeptide ranges in size from 25 to 30 kDa (221–262 amino acids), but multiple higher-molecular-mass glycosylated forms are often observed by SDS-PAGE (Krijnse Locker *et al.*, 1992a). The M protein of MHV has also been noted to multimerize under standard conditions of SDS-PAGE (Sturman, 1977).

M is a multispanning membrane protein with a small, amino-terminal domain located on the exterior of the virion, or, intracellularly, in the lumen of the ER (Fig. 3). The ectodomain is followed by three

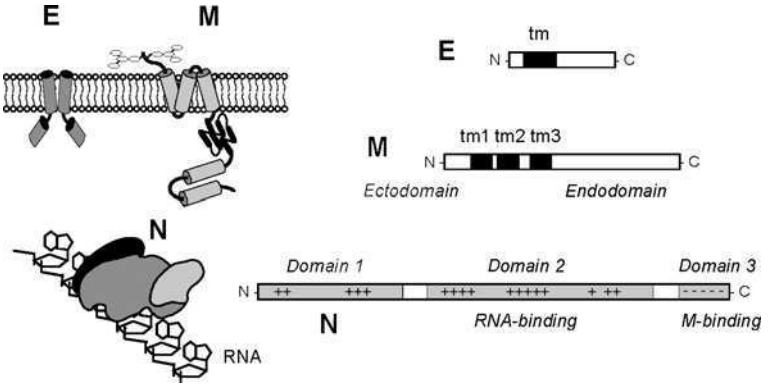

FIG 3. The membrane (M), envelope (E), and nucleocapsid (N) proteins. At the right are linear maps of the proteins, denoting known regions of importance, including transmembrane (tm) domains. At the left are models for the three proteins.

transmembrane segments and then a large carboxy terminus comprising the major part of the molecule. This latter domain is situated in the interior of the virion or on the cytoplasmic face of intracellular membranes (Rottier, 1995). M proteins within each coronavirus group are moderately well conserved, but they are quite divergent across the three groups. The region of M protein showing the most conservation among all coronaviruses is a segment of some 25 residues encompassing the end of the third transmembrane domain and the start of the endodomain; a portion of this segment even retains homology to its torovirus counterpart (den Boon *et al.*, 1991). The ectodomain, which is the least conserved part of the M molecule, is glycosylated. For most group 2 coronaviruses, glycosylation is O-linked, although two exceptions to this pattern are MHV strain 2 (Yamada *et al.*, 2000) and SARS-CoV (Nal *et al.*, 2005), both of which have M proteins with N-linked carbohydrate. Group 1 and group 3 coronavirus M proteins, by contrast, exhibit N-linked glycosylation exclusively (Cavanagh and Davis, 1988; Garwes *et al.*, 1984; Jacobs *et al.*, 1986; Stern and Sefton, 1982). At the time of its discovery in the MHV M protein, O-linked glycosylation had not previously been seen to occur in a viral protein (Holmes *et al.*, 1981), and MHV M has since been used as a model to study the sites and mechanism of this type of posttranslational modification (de Haan *et al.*, 1998b; Krijnse Locker *et al.*, 1992a; Niemann *et al.*, 1982). Although the roles of M protein glycosylation are not fully understood, the glycosylation status of M can influence both organ tropism *in vivo* and the capacity of some coronaviruses to induce alpha interferon *in vitro* (Charley and Laude, 1988; de Haan *et al.*, 2003a; Laude *et al.*, 1992).

The coronavirus M protein was the first polytopic viral membrane protein to be described (Armstrong *et al.*, 1984; Rottier *et al.*, 1984), and the atypical topology of the MHV and IBV M proteins was examined in considerable depth in cell-free translation and cellular expression studies. For both of these M proteins, the entire ectodomain was found to be protease sensitive. However, at the other end of the molecule, no more than 20–25 amino acids could be removed from the carboxy terminus by protease treatment (Cavanagh *et al.*, 1986a; Mayer *et al.*, 1988; Rottier *et al.*, 1984, 1986). This pattern suggested that almost all of the endodomain of M is tightly associated with the surface of the membrane or that it has an unusually compact structure that is refractory to proteolysis (Rottier, 1995). Most M proteins do not possess a cleaved amino-terminal signal peptide (Cavanagh *et al.*, 1986b; Rottier *et al.*, 1984), and for both IBV and MHV it was demonstrated that either the first or the third transmembrane domain alone is sufficient to function as the signal for insertion and anchoring of the

protein in its native orientation in the membrane (Krijnse Locker *et al.*, 1992b; Machamer and Rose, 1987; Mayer *et al.*, 1988). The M proteins of a subset of group 1 coronaviruses (TGEV, FIPV, and CCoV) each contain a cleavable amino-terminal signal sequence (Laude *et al.*, 1987), although this element may not be required for membrane insertion (Kapke *et al.*, 1988; Vennema *et al.*, 1991). Another anomalous feature of at least one group 1 coronavirus, TGEV, is that roughly one-third of its M protein assumes a topology in which part of the endodomain constitutes a fourth transmembrane segment, thereby positioning the carboxy terminus of the molecule on the exterior of the virion (Risco *et al.*, 1995). This alternative configuration of M has yet to be demonstrated for other coronavirus family members.

D. Envelope Protein (E)

The E protein (formerly called sM) is a small polypeptide, ranging from 8.4 to 12 kDa (76–109 amino acids), that is only a minor constituent of virions (Fig. 3). Owing to its tiny size and limited quantity, E was recognized as a virion component much later than were the other structural proteins, first in IBV (Liu and Inglis, 1991) and then in TGEV (Godet *et al.*, 1992) and MHV (Yu *et al.*, 1994). Its significance was also obscured by the fact that in some coronaviruses, the coding region for E protein occurs as the furthest-downstream open reading frame (ORF) in a bi- or tricistronic mRNA and must therefore be expressed by a nonstandard translational mechanism (Boursnell *et al.*, 1985; Budzilowicz and Weiss, 1987; Leibowitz *et al.*, 1988; Liu *et al.*, 1991; Skinner *et al.*, 1985; Thiel and Siddell, 1994). E protein sequences are extremely divergent across the three coronavirus groups and in some cases, among members of a single group. Nevertheless, the same general architecture can be discerned in all E proteins: a short hydrophilic amino terminus (8–12 residues), followed by a large hydrophobic region (21–29 residues) containing two to four cysteines, and a then hydrophilic carboxy-terminal tail (39–76 residues), the latter constituting most of the molecule.

E is an integral membrane protein, as has been shown for both the MHV and IBV E proteins by the criterion of resistance to alkaline extraction (Corse and Machamer, 2000; Vennema *et al.*, 1996), and membrane insertion occurs without cleavage of a signal sequence (Raamsman *et al.*, 2000). The E protein of IBV has been shown to be palmitoylated on one or both of its two cysteine residues (Corse and Machamer, 2002), but it is not currently clear whether this modification is a general characteristic. One study of MHV E showed

a gel mobility shift of E caused by hydroxylamine treatment, which cleaves thioester linkages (Yu *et al.*, 1994), but attempts to incorporate labeled palmitic acid into either the TGEV or MHV E protein have been unsuccessful (Godet *et al.*, 1992; Raamsman *et al.*, 2000). The topology of E in the membrane is at least partially resolved. Although one early report suggested a C-exo, N-endo membrane orientation for the TGEV E protein (Godet *et al.*, 1992), more extensive investigations of the MHV and IBV E proteins both concluded that the carboxy-terminal tail of the molecule is cytoplasmic (or, correspondingly, is situated in the interior of the virion) (Corse and Machamer, 2000; Raamsman *et al.*, 2000). Moreover, for IBV E, it was shown that the carboxy-terminal tail, in the absence of the membrane-bound domain, specifies targeting to the budding compartment (Corse and Machamer, 2002). The status of the amino terminus is less clear, however. The IBV E protein amino terminus was inaccessible to antibodies at the cytoplasmic face of the Golgi membrane, suggesting that this end of the molecule is situated in the lumen (corresponding to the exterior of the virion) (Corse and Machamer, 2000). Such a single transit, placing the termini of the protein on opposite faces of the membrane, would be consistent with prediction, by molecular dynamics simulations, that a broad set of E proteins occur as transmembrane oligomers (Torres *et al.*, 2005). Conflicting results were obtained with MHV E, though. Based on the cytoplasmic reactivity of an engineered amino-terminal epitope tag, it was proposed that the MHV E protein amino terminus is buried within the membrane near the cytoplasmic face (Maeda *et al.*, 2001). This result also accords with the finding that no part of the MHV E protein in purified virions is accessible to protease treatment (Raamsman *et al.*, 2000). Such an orientation would mean that the hydrophobic domain of E protein forms a hairpin, looping back through the membrane. This topology agrees with the outcome of a biophysical analysis of the SARS-CoV E protein transmembrane domain (Arbely *et al.*, 2004). However, in the latter study it was asserted that the palindromic hairpin configuration of the transmembrane segment is unique to the SARS-CoV E protein, which begs the question of how the other coronavirus E proteins are situated in the membrane and why the E protein of SARS-CoV should differ.

E. Nucleocapsid Protein (N)

The N protein, which ranges from 43 to 50 kDa, is the protein component of the helical nucleocapsid and is thought to bind the genomic RNA in a beads-on-a-string fashion (Laude and Masters, 1995) (Fig. 3). Based on a comparison of sequences of multiple strains, it has been

proposed that the MHV N protein is divided into three conserved domains, which are separated by two highly variable spacer regions (Parker and Masters, 1990). Domains 1 and 2, which constitute most of the molecule, are rich in arginines and lysines, as is typical of many viral RNA-binding proteins. In contrast, the short, carboxy-terminal domain 3 has a net negative charge resulting from an excess of acidic over basic residues. While there is now considerable evidence to support the notion that domain 3 truly constitutes a separate domain (Hurst *et al.*, 2005; Koetzner *et al.*, 1992), little is known about the structure of the other two putative domains. The overall features of the three-domain model appear to extend to N proteins of coronaviruses in groups 1 and 3, although the boundaries between domains appear to be less clearly defined for these latter N proteins. There is not a high degree of intergroup sequence homology among N proteins, with the exception of a strongly conserved stretch of 30 amino acids, near the junction of domains 1 and 2, which contains many aromatic hydrophobic residues (Laude and Masters, 1995).

The main activity of N protein is to bind to the viral RNA. Unlike the helical nucleocapsids of nonsegmented negative-strand RNA viruses, coronavirus ribonucleoprotein complexes are quite sensitive to the action of ribonucleases (Macnaughton *et al.*, 1978). A significant portion of the stability of the nucleocapsid may derive from N–N monomer interactions (Narayanan *et al.*, 2003b). Both sequence-specific and nonspecific modes of RNA binding by N have been assayed *in vitro* (Chen *et al.*, 2005; Cologna *et al.*, 2000; Masters, 1992; Molenkamp and Spaan, 1997; Nelson and Stohlman, 1993; Nelson *et al.*, 2000; Robbins *et al.*, 1986; Stohlman *et al.*, 1988; Zhou *et al.*, 1996). Specific RNA substrates that have been identified for N protein include the positive-sense transcription regulating sequence (Chen *et al.*, 2005; Nelson *et al.*, 2000; Stohlman *et al.*, 1988), regions of the 3′ UTR (Zhou *et al.*, 1996) and the *N* gene (Cologna *et al.*, 2000), and the genomic RNA packaging signal (Cologna *et al.*, 2000; Molenkamp and Spaan, 1997) (Section IV.C). The RNA-binding capability of the MHV N protein has been mapped to domain 2 of this molecule (Masters, 1992; Nelson and Stohlman, 1993). However, for IBV, two separate RNA-binding sites have been found to map, respectively, to amino- and carboxy-terminal fragments of N protein (Zhou and Collisson, 2000), and RNA-binding activity has been reported for a fragment of the SARS-CoV N protein containing parts of domains 1 and 2 (Huang *et al.*, 2004b).

N is a phosphoprotein, as has been shown for MHV, IBV, BCoV, TGEV, and SARS-CoV (Calvo *et al.*, 2005; King and Brian, 1982; Lomniczi and Morser, 1981; Stohlman and Lai, 1979; Zakhartchouk *et al.*, 2005). For MHV N, phosphorylation occurs exclusively on serine resi-

dues (Siddell *et al.*, 1981; Stohlman and Lai, 1979), but in IBV N a phosphothreonine residue was also found (Chen *et al.*, 2005). Kinetic analysis has shown that MHV N protein acquires phosphates rapidly following its synthesis (Siddell *et al.*, 1981; Stohlman *et al.*, 1983), and phosphorylation may lead to the association of N with intracellular membranes (Calvo *et al.*, 2005; Stohlman *et al.*, 1983). Although some 15% of the amino acids of coronavirus N proteins are candidate phosphoacceptor serines and threonines, phosphorylation appears to be targeted to a small subset of residues. For MHV, this was concluded both from the degree of charge heterogeneity of N protein observed in two-dimensional gel electrophoresis and from the limited number of tryptic phosphopeptides of N that could be separated by HPLC (Bond *et al.*, 1979; Wilbur *et al.*, 1986). Mass spectrometry has been employed to map the sites of phosphorylation of the IBV and TGEV N proteins. For IBV N, this was accomplished by comparison of unphosphorylated N protein expressed in bacteria with phosphorylated N protein expressed in insect cells (Chen *et al.*, 2005). Four sites of phosphorylation were found, two each in domains 2 and 3: Ser190, Ser192, Thr378, and Ser379. For TGEV N, purified virions and multiple fractions from infected cells were analyzed (Calvo *et al.*, 2005). Here also, four sites of phosphorylation were found, one in domain 1 and three in domain 2: Ser9, Ser156, Ser254, and Ser256. In both of these analyses, the degree of sequence coverage achieved did not entirely rule out the possibility of additional, undetected phosphorylated residues in each of these N proteins.

The role of N protein phosphorylation is currently unresolved, but this modification has long been speculated to have regulatory significance. *In vitro* binding evidence has been presented that phosphorylated IBV N is better able to distinguish between viral and nonviral RNA substrates than is nonphosphorylated N (Chen *et al.*, 2005). Possibly related to this result is the early conclusion, inferred from the differential accessibilities of some monoclonal antibodies, that phosphorylation induces a conformational change in the MHV N protein (Stohlman *et al.*, 1983). It has also been found that only a subset of the intracellular phosphorylated forms of BCoV N protein are incorporated into virions, suggesting that phosphorylation is linked to virion assembly and maturation (Hogue, 1995). The recent mapping of at least some of the N phosphorylation sites in some coronaviruses has now laid the groundwork for testing of the hypothetical functions of phosphorylation by reverse genetic methods.

A number of potential activities, other than its structural role in the virion, have been put forward for N protein. Based on the specific

binding of N protein to the transcription-regulating sequence within the leader RNA, it has been proposed that N participates in viral transcription (Baric *et al.*, 1988; Choi *et al.*, 2002; Stohlman *et al.*, 1988). However, an engineered HCoV-229E replicon RNA that was devoid of the *N* gene and all other structural protein genes retained the capability to synthesize subgenomic RNA (Thiel *et al.*, 2001b). Thus, if N protein does function in transcription, it must be in a modulatory, but not essential, capacity. Likewise, the binding of N protein to leader RNA has been implicated as a means for preferential translation of viral mRNAs (Tahara *et al.*, 1994, 1998), although data supporting this attractive hypothesis are, as yet, incomplete. N protein has also been found to enhance the efficiency of replication of replicon or genomic RNA in reverse genetic systems in which infections are initiated from engineered viral RNA (Almazan *et al.*, 2004; Schelle *et al.*, 2005; Thiel *et al.*, 2001a; Yount *et al.*, 2002). This may be indicative of a direct role of N in RNA replication, but it remains possible that the enhancement actually results from the sustained translation of a limiting replicase component.

Finally, it was shown that, in addition to its presence in the cytoplasm, IBV N protein localized to the nucleoli of about 10% of cells that were infected with IBV or were independently expressing N protein (Hiscox *et al.*, 2001). This observation was extended to the N proteins of MHV and TGEV, suggesting that nucleolar localization is a general feature of all three coronavirus groups. Such localization was proposed to correlate with the arrest of cell division (Wurm *et al.*, 2001). Additionally, both MHV and IBV N proteins were found to bind to two nucleolar proteins, fibrillarin and nucleolin (Chen *et al.*, 2002). It must be noted, however, that nucleolar localization of N was not observed in TGEV-infected or SARS-CoV-infected cells by other groups of investigators (Calvo *et al.*, 2005; Rowland *et al.*, 2005). All steps of coronavirus replication are thought to occur outside of the nucleus. For MHV, it was shown some time ago that viral replication could occur in enucleated cells or in cells treated with actinomycin D or α-amanitin, host RNA polymerase inhibitors (Brayton *et al.*, 1981; Wilhelmsen *et al.*, 1981). By contrast, other studies reported that similar conditions reduced the growth yield of IBV, HCoV-229E, or FCoV (Evans and Simpson, 1980; Kennedy and Johnson-Lussenburg, 1979; Lewis *et al.*, 1992). Even if coronavirus replication does not have an absolute dependence on the nucleus, the possibility remains that some viruses can alter host nuclear functions so as to create an environment more

favorable for viral infection. Such a modification might be brought about through the nuclear trafficking of one or more viral components.

F. Genome

The genomes of coronaviruses are nonsegmented, single-stranded RNA molecules of positive sense, that is, the same sense as mRNA (Fig. 4) (Lai and Stohlman, 1978; Lomniczi and Kennedy, 1977; Schochetman *et al.*, 1977; Wege *et al.*, 1978). Structurally they resemble most eukaryotic mRNAs, in having both 5′ caps (Lai and Stohlman, 1981) and 3′ poly(A) tails (Lai and Stohlman, 1978; Lomniczi, 1977; Schochetman *et al.*, 1977; Wege *et al.*, 1978). Unlike most eukaryotic mRNAs, coronavirus genomes are extremely large—nearly three times the size of alphavirus and flavivirus genomes and four times the size of picornavirus genomes. Indeed, at lengths ranging from 27.3 (HCoV-229E) to 31.3 kb (MHV), coronavirus genomes are among the largest mature RNA molecules known to biology. Again, unlike most eukaryotic mRNAs, coronavirus genomes contain multiple ORFs. The genes for the four canonical structural proteins discussed previously account for less than one-third of the coding capacity of the genome and are clustered at the 3′ end. A single gene, which encodes the viral replicase, occupies the 5′-most two-thirds of the genome. The invariant gene order in all members of the coronavirus family is 5′-replicase-S-E-M-N-3′. However, engineered rearrangement of the gene order of MHV was found to be completely tolerated by the virus (de Haan *et al.*, 2002b). This implies that the native order, although it became fixed

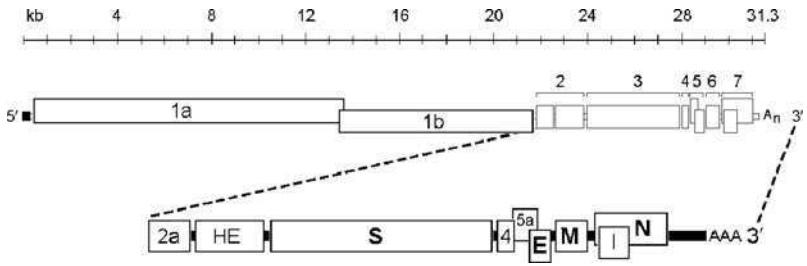

FIG 4. Coronavirus genomic organization. The layout of the MHV genome is shown as an example. All coronavirus genomes have a 5′ cap and 3′ poly(A) tail. The invariant order of the canonical genes is replicase-S-E-M-N. The replicase contains two ORFs, 1a and 1b, complete expression of which is accomplished via ribosomal frameshifting. Accessory proteins (2a, HE, 4, 5a, and I, in the case of MHV) occur at various positions among the canonical genes.

early in the evolution of the family, is not functionally essential. At the termini of the genome are a 5′ UTR, ranging from 210 to 530 nucleotides, and a 3′ UTR, ranging from 270 to 500 nucleotides. The noncoding regions between the ORFs are generally quite small; in some cases, there is a small overlap between adjacent ORFs. Additionally, one or a number of accessory genes are intercalated among the structural protein genes.

In common with almost all other positive-sense RNA viruses, the genomic RNA of coronaviruses is infectious when transfected into permissive host cells, as was originally shown for TGEV (Norman *et al.*, 1968), IBV (Lomniczi, 1977; Schochetman *et al.*, 1977), and MHV (Wege *et al.*, 1978). The genome has multiple functions during infection. It acts initially as an mRNA that is translated into the huge replicase polyprotein, the complete synthesis of which requires a ribosomal frameshifting event (Section V.C.1). The replicase is the only translation product derived from the genome; all downstream ORFs are expressed from subgenomic RNAs. The genome next serves as the template for replication and transcription (Section V). Finally, the genome plays a role in assembly, as progeny genomes are incorporated into progeny virions (Section IV.C).

G. Accessory Proteins

Interspersed among the set of canonical genes, replicase, S, E, M, and N, all coronavirus genomes contain additional ORFs, in a wide range of configurations. As shown in Table II, these "extra" genes can fall in any of the genomic intervals among the canonical genes and can vary from as few as one (PEDV and HCoV-NL63) to as many as eight genes (SARS-CoV). In some cases, accessory genes can be entirely embedded in another ORF, as the internal (I) gene found within the *N* gene of many group 2 coronviruses (Fischer *et al.*, 1997a; Lapps *et al.*, 1987; Senanayake *et al.*, 1992), or they can be extensively overlapped with another gene, as the *3b* gene of SARS-CoV. In addition, many accessory genes do not constitute the 5′-most ORF in the largest subgenomic RNA in which they appear, and they therefore must require nonstandard translation mechanisms for their expression (Liu *et al.*, 1991). Intracellular expression has been demonstrated for a number of accessory proteins, but for many others it is at present merely speculative.

The coronavirus accessory genes were originally labeled nonstructural, but this is not entirely apt, since the products of some of them, the group 2 HE protein, the I protein (Fischer *et al.*, 1997a), and the

TABLE II
CORONAVIRUS ACCESSORY PROTEINS

Group	Virus species	Accessory genes (Proteins)*
1	TGEV	[rep] - [*S*] - 3a, 3b - [*E*] - [*M*] - [*N*] - 7
	FIPV	[rep] - [*S*] - 3a, 3b, 3c - [*E*] - [*M*] - [*N*] - 7a, 7b
	HCoV-229E	[rep] - [*S*] - 4a, 4b - [*E*] - [*M*] - [*N*]
	PEDV	[rep] - [*S*] - 3 - [*E*] - [*M*] - [*N*]
	HCoV-NL63	[rep] - [*S*] - 3 - [*E*] - [*M*] - [*N*]
2	MHV	[rep] - 2a, 2b(HE) - [*S*] - 4 - 5a, [*E*] - [*M*] - [*N*], 7b(I)
	BCoV	[rep] - 2a - 2b(HE) - [*S*] - 4a(4.9k), 4b(4.8k) - 5(12.7k) [*E*] - [*M*] - [*N*], 7b(I)
	HCoV-OC43	[rep] - 2a - 2b(HE) - [*S*] - 5(12.9k) - [*E*] - [*M*] - [*N*], 7b(I)
	SARS-CoV	[rep] - [*S*] - 3a, 3b - [*E*] - [*M*] - 6 - 7a, 7b - 8a, 8b - [*N*], 9b(I)
	HCoV-HKU1	[rep] - 2(HE) - [*S*] - 4 - [*E*] - [*M*] - [*N*], 7b(I)
	Bat-SARS-CoV	[rep] - [*S*] - 3 - [*E*] - [*M*] - 6 - 7a, 7b - 8 - [*N*], 9b(I)
3	IBV	[rep] - [*S*] - 3a, 3b, 3c - [*E*] - [*M*] - 5a, 5b - [*N*]

* Accessory genes and proteins are listed only for coronaviruses for which a complete genomic sequence is available. The protein product is indicated in parentheses in cases where it has a different designation than the gene. Products of separate transcripts are separated by hyphens; the transcription of accessory genes may vary among different strains of the same virus species (O'Connor and Brian, 1999). The canonical coronavirus genes are indicated in brackets; rep denotes replicase.

SARS-CoV 3a protein, have been shown to be components of virions. Accessory genes were also previously called group-specific genes, but this appellation has become a misnomer in light of the diversity revealed by recently discovered coronaviruses. In general, accessory genes are numbered according to the subgenomic RNA in whose unique region they appear, but this nomenclature system is sometimes overridden by historical precedent. As a result, identically numbered genes in two different viruses, for example, the *5a* genes of MHV and IBV, do not necessarily occupy the same genomic position. Likewise, two identically numbered genes, for example, the *3a* genes of SARS-CoV and TGEV, do not necessarily have any sequence homology.

It is often speculated that the coronavirus accessory genes were horizontally acquired from cellular or heterologous viral sources, but only in two cases, the group 2 HE and *2a* genes, is there good evidence for this proposal. HE, the most clear-cut example, is discussed later. A possible function for the 2a protein has been inferred from a bioinformatics analysis, which places it in a very large family of cellu-

lar and viral 2′,3′-cyclic phosphodiesterases (Mazumder *et al.*, 2002). Besides its presence in some group 2 coronaviruses, this gene also appears in another family within the *Nidovirales* order, the toroviruses (Snijder *et al.*, 1990). Curiously, in the toroviruses, the 2a homolog is situated as a module within the replicase polyprotein, suggesting either that it was acquired independently or that there was nonhomologous recombination between ancestors of viruses within the two families (Snijder *et al.*, 1991). However, most accessory gene ORFs have no obvious homology to any other viral or cellular sequence in public databases. It is conceivable that many of them evolved in individual coronaviruses by the scavenging of ORFs from the virus's own genome, through duplication and subsequent mutation, as has been proposed for several of the accessory proteins of SARS-CoV (Inberg and Linial, 2004). It is tempting to regard this as a possible origin for the SARS-CoV 3a protein, which has a topology and size remarkably similar to that of the M protein, although there is no sequence similarity between the two. Such a relationship would parallel that in the arteriviruses, another *Nidovirales* family, in which the major envelope glycoprotein is also a triple-spanning membrane protein and forms heterodimers with its M protein (Snijder and Meulenberg, 1998).

It also needs to be considered that, although there is evidence that some accessory genes encode "luxury" functions for their respective viruses, other accessory genes may be genetic junk. Many isolates of IBV contain an extremely diverged segment of some 200 nucleotides between the *N* gene and the 3′ UTR (Sapats *et al.*, 1996). This was long considered to be a hypervariable region of the 3′ UTR, although it was shown to be dispensable for RNA synthesis (Dalton *et al.*, 2001). Intriguingly, coronavirus sequences closely related to IBV have been characterized in pigeons and geese. These sequences have one and two additional ORFs, respectively, between the *N* gene and the 3′ UTR (Jonassen *et al.*, 2005). This finding suggests that the IBV hypervariable region and the PCoV ORF are degenerate remnants of a precursor retained in the GCoV sequence. The two GCoV ORFs, in turn, may be vestiges of one or more functional ancestral genes, or they may be derived from horizontally acquired sequences that there has been no selective pressure to eliminate. A similar situation probably pertains for the SARS-CoV *8a* and *8b* genes. Isolates of SARS-CoV from marketplace animals near the source of the epidemic were found to contain an additional 29 nucleotides absent from all but one previously reported human isolate, and this apparent insertion resulted in the fusion of ORFs 8a and 8b into a single ORF 8 (Guan *et al.*, 2003).

One scenario consistent with this observation is that loss of the 29-nt sequence was concomitant with the jump of the virus from animals to humans, although the functional significance of this loss, if any, is not yet clear.

In all cases examined, through natural or engineered mutants, accessory protein genes have been found to be nonessential for viral replication in tissue culture. This dispensability has been determined for the *2a* and *HE* genes of MHV (de Haan *et al.*, 2002a; Schwarz *et al.*, 1990), genes *4* and *5a* of MHV (de Haan *et al.*, 2002a; Weiss *et al.*, 1993; Yokomori and Lai, 1991), the *I* gene of MHV (Fischer *et al.*, 1997a), gene *7* of TGEV (Ortego *et al.*, 2003), genes *7a* and *7b* of FIPV (Haijema *et al.*, 2003, 2004), and genes *5a* and *5b* of IBV (Casais *et al.*, 2005; Youn *et al.*, 2005). Similarly, some accessory protein genes do not seem to play any role in infection of the natural host. For gene *4* (Ontiveros *et al.*, 2001) and the *I* gene (Fischer *et al.*, 1997a) of MHV, and for gene *7b* of FIPV (Haijema *et al.*, 2003), selective knockout produced no detectable effect on pathogenesis in mice or cats, respectively. By contrast, disruption of gene *7* of TGEV greatly reduced viral replication in the lung and gut of infected piglets (Ortego *et al.*, 2003). In the same manner, viruses with knockouts of either the *3abc* gene cluster or genes *7a* and *7b* in FIPV produced no clinical symptoms in cats at doses that were fatal with wild-type virus (Haijema *et al.*, 2004). The deletion of genes *2a* and HE, or of genes *4* and *5a*, in MHV completely abrogated the lethality of intracranial infection in mice (de Haan *et al.*, 2002a). Even a single point mutation in MHV ORF 2a, which had no effect in tissue culture, was found to greatly attenuate virulence *in vivo* (Sperry *et al.*, 2005). In a study that took the opposite approach to assessing accessory protein function, it was discovered that engineered insertion of gene *6* of SARS-CoV greatly enhanced the virulence of an attenuated variant of MHV (Pewe *et al.*, 2005).

The most extensively characterized accessory protein is HE (formerly called E3), which is a fourth constituent of the membrane envelope in many group 2 coronaviruses (Brian *et al.*, 1995). HE forms a second set of small spikes that appear as an understory among the tall S protein spikes. It was first identified as a hemagglutinin in HEV (Callebaut and Pensaert, 1980) and BCoV (King and Brian, 1982; King *et al.*, 1985). The HE monomer has an N-exo, C-endo transmembrane topology, with an amino-terminal signal peptide, a large ectodomain, a transmembrane anchor, and a very short, carboxy-terminal endodomain. Monomers of HE, prior to glycosylation are 48 kDa; this size increases to 65 kDa after addition and processing of oligosaccharide, which is exclusively N-linked (Hogue *et al.*, 1989; Kienzle *et al.*, 1990; Yokomori *et al.*,

1989). The mature protein is a homodimer that is stabilized by both intrachain and interchain disulfide bonds (Hogue *et al.*, 1989). The hemagglutinating property of HE raised the possibility that, in the viruses in which it appears, this protein may duplicate or replace the role that is assigned to the coronavirus S protein. However, it has been shown, through the construction of MHV-BCoV chimeric viruses, that the BCoV HE protein, in the absence of BCoV S protein, is not sufficient for initiation of infection in tissue culture (Popova and Zhang, 2002).

The HE protein also contains an acetylesterase activity. This was originally discovered in BCoV and HCoV-OC43, where it was shown to be similar to the receptor-binding and receptor-destroying activity found in influenza C virus (Vlasak *et al.*, 1988a, b). The nature of the esterase enzyme has subsequently been comprehensively studied and compared among a number of group 2 coronaviruses (Klausegger *et al.*, 1999; Regl *et al.*, 1999; Smits *et al.*, 2005). HE proteins of BCoV, HCoV-OC43, ECoV, and MHV strain DVIM were found to be sialate-9-*O*-acetylesterases. By contrast, HE proteins of RCoV, and MHV strains S and JHM were found to be sialate-4-*O*-acetylesterases. Surprisingly, the coronavirus *HE* gene is clearly related to the influenza C virus *HA1* gene (Luytjes *et al.*, 1988). Equally remarkably, toroviruses also possess a homolog of the *HE* gene but at a different genomic locus than where it appears in the group 2 coronaviruses (Cornelissen *et al.*, 1997). This may be evidence of genetic trafficking among pairs of ancestors of these three viruses, as was originally proposed (Luytjes *et al.*, 1988; Snijder *et al.*, 1991). Alternatively, it may indicate that members of different virus families independently acquired the *HE* gene by horizontal transfer from cellular sources (Cornelissen *et al.*, 1997).

There are two ways in which HE could act in coronavirus replication. It could serve as a cofactor for S, assisting attachment of virus to host cells. Additionally, it could prevent aggregation of progeny virions and travel of virus through the extracellular mucosa (Cornelissen *et al.*, 1997). The role of HE protein in coronavirus infection has been systematically documented in a recent pair of elegant studies (Kazi *et al.*, 2005; Lissenberg *et al.*, 2005). To evaluate the cost and benefit of the *HE* gene, three isogenic MHV mutants were engineered: HE^{+}, with an expressed and functional *HE* gene; HE^{0}, with an expressed *HE* gene that was inactive, owing to active site point mutations; and HE^{-}, which lacked HE expression because of an introduced frameshift. It was demonstrated that, following multiple passages, there was rapid loss of HE expression in the HE^{+} virus. Moreover, competition experiments showed a growth advantage for the HE^{-} virus, but not the HE^{0}

virus. Consistent with this, examination of esterase-negative mutants arising from the HE^+ virus showed that it was not loss of activity, but, rather, loss of the ability of HE to be incorporated into virions that correlated with the growth advantage of HE^- viruses (Lissenberg *et al.*, 2005). By contrast, in infections of mice, it was found that the presence of HE (whether or not it was enzymatically active) dramatically enhanced neurovirulence, as measured by viral spread and lethality (Kazi *et al.*, 2005). These results imply that sialic acid–bearing coreceptors can function to influence the course of MHV infection. Thus, the HE protein is a burden *in vitro* but provides an advantage to the virus *in vivo*. The selection against HE *in vitro* provides a cautionary example that tissue culture adaptation of a virus can rapidly lead to selection of a variant that differs from the natural isolate.

IV. Viral Replication Cycle and Virion Assembly

Coronavirus infections are initiated by the binding of virions to cellular receptors (Fig. 5). This sets off a series of events culminating in the deposition of the nucleocapsid into the cytoplasm, where the viral genome becomes available for translation. The positive-sense genome, which also serves as the first mRNA of infection, is translated into the enormous replicase polyprotein. The replicase then uses the genome as the template for the synthesis, via negative-strand intermediates, of both progeny genomes and a set of subgenomic mRNAs. The latter are translated into structural proteins and accessory proteins. The membrane-bound structural proteins, M, S, and E, are inserted into the ER, from where they transit to the endoplasmic reticulum-Golgi intermediate compartment (ERGIC). Nucleocapsids are formed from the encapsidation of progeny genomes by N protein, and these coalesce with the membrane-bound components, forming virions by budding into the ERGIC. Finally, progeny virions are exported from infected cells by transport to the plasma membrane in smooth-walled vesicles, or Golgi sacs, that remain to be more clearly defined. During infection by some coronaviruses, but not others, a fraction of S protein that has not been assembled into virions ultimately reaches the plasma membrane. At the cell surface S protein can cause the fusion of an infected cell with adjacent, uninfected cells, leading to the formation of large, multinucleate syncytia. This enables the spread of infection independent of the action of extracellular virus, thereby providing some measure of escape from immune surveillance. Key aspects of

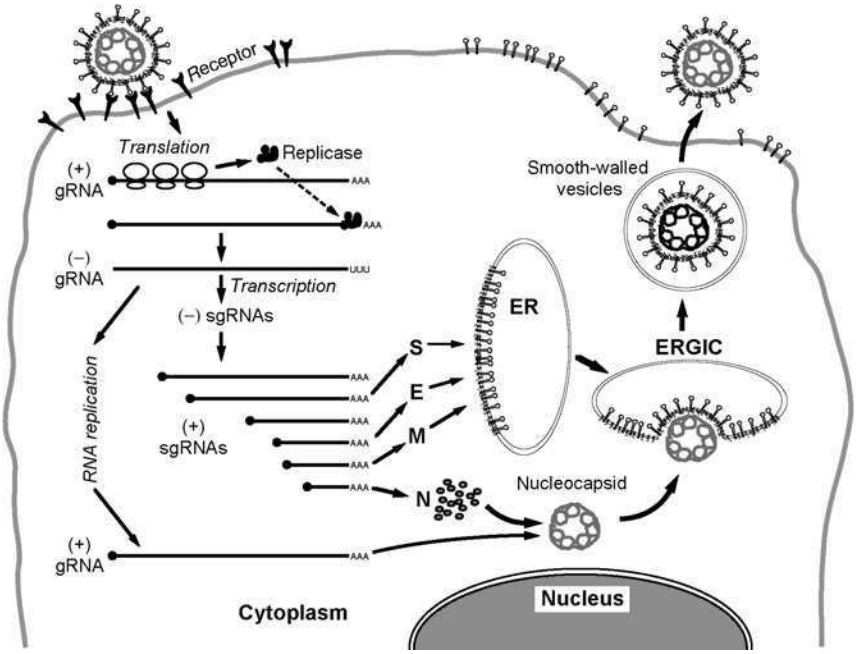

FIG 5. The coronavirus life cycle.

the coronavirus replication cycle are discussed in more detail in the remainder of this section and in the next section (Section V).

A. Receptors and Entry

1. Receptors

The pairings of coronaviruses and their corresponding receptors are generally highly species specific, but the adaptation of SARS-CoV to the human population has reminded us that this allegiance is mutable. Well prior to the emergence of SARS, it was clearly documented that another coronavirus, BCoV, was capable of sporadic cross-species transmission (Saif, 2004). Viruses very closely related to BCoV had been isolated from wild ruminants (Tsunemitsu *et al.*, 1995), domestic dogs (Erles *et al.*, 2003), and, in one case, a human child (Zhang *et al.*, 1994). Nevertheless, the interaction between S protein and receptor remains the principal, if not sole, determinant of coronavirus host

species range and tissue tropism. At the cellular level, this has been demonstrated by manipulation of each of the interacting partners. First, expression of an identified receptor in nonpermissive cells, often of a heterologous species, invariably has rendered those cells permissive for the corresponding coronavirus (Delmas *et al.*, 1992; Dveksler *et al.*, 1991; Li *et al.*, 2003, 2004; Mossel *et al.*, 2005; Tresnan *et al.*, 1996; Yeager *et al.*, 1992). Second, the engineered swapping of S protein ectodomains has been shown to change the *in vitro* host cell species specificity of MHV to that of FIPV (Kuo *et al.*, 2000) or, conversely, of FIPV to that of MHV (Haijema *et al.*, 2003). Similarly, exchange of the relevant regions of S protein ectodomains was shown to transform a strictly respiratory isolate of TGEV into a more virulent, enterotropic strain (Sanchez *et al.*, 1999). Replacement of the S protein ectodomain of MHV strain A59 caused the virus to acquire the highly virulent neurotropism of MHV strain 4 (Phillips *et al.*, 1999) or the highly virulent hepatotropism of MHV strain 2 (Navas *et al.*, 2001).

Table III lists the known cellular receptors for coronaviruses of groups 1 and 2; to date no receptors have been identified for coronaviruses of group 3. Group 2 coronavirus receptors include the earliest and the most recent of the items in Table III. The MHV receptor (formerly MHVR1, now called mCEACAM1) is a member of the carcinoembryonic antigen (CEA) family, a group of proteins within the immunoglobulin (Ig) superfamily. CEACAM1 was the first receptor discovered for a coronavirus, and, indeed, it was one of the first receptors found for any virus (Williams *et al.*, 1990, 1991). Cloning of cDNA to the largest mRNA for this protein revealed that full-length CEACAM1 has four Ig-like domains (Dveksler *et al.*, 1991), but a number of two- and four-domain versions of the molecule were later found to be expressed in mouse cells. This diversity of MHV receptor isoforms was found to be generated by multiple alleles of the *Ceacam1* gene as well as by the existence of multiple alternative splicing variants of its mRNA (Compton, 1994; Dveksler *et al.*, 1993a,b; Ohtsuka and Taguchi, 1997; Ohtsuka *et al.*, 1996; Yokomori and Lai, 1992). The wide range of pathogenicity of MHV in mice is therefore thought to result from the interactions of S proteins of different virus strains with the tissue-specific spectra of receptor variants displayed in mice having different genetic backgrounds. A number of lines of evidence argue that CEACAM1 is the only biologically relevant receptor for MHV. This was initially suggested by an early experiment showing that *in vivo* administration of a monoclonal antibody to CEACAM1 greatly enhanced the frequency of survival of mice subsequently given a lethal challenge of MHV (Smith *et al.*, 1991). More definitively, it was demon-

TABLE III
CORONAVIRUS RECEPTORS

Group	Virus species	Receptor	Reference
1	TGEV	Porcine aminopeptidase N (pAPN)	Delmas *et al.*, 1992
	PRCoV	Porcine aminopeptidase N (pAPN)	Delmas *et al.*, 1994b
	FIPV	Feline aminopeptidase N (fAPN)	Tresnan *et al.*, 1996
	FCoV	Feline aminopeptidase N (fAPN)	Tresnan *et al.*, 1996
	CCoV	Canine aminopeptidase N (cAPN)	Benbacer *et al.*, 1997
	HCoV-229E	Human aminopeptidase N (hAPN)	Yeager *et al.*, 1992
	HCoV-NL63	Angiotensin-converting enzyme 2 (ACE2)	Hofmann *et al.*, 2005
2	MHV	Murine carcinoembryonic antigen-related adhesion molecules 1 and 2* (mCEACAM1, mCEACAM2*)	Nedellec *et al.*, 1994*; Williams *et al.*, 1991
	BCoV	9-*O*-acetyl sialic acid	Schultze *et al.*, 1991
	SARS-CoV	Angiotensin-converting enzyme 2 (ACE2)	Li *et al.*, 2003
		CD209L (L-SIGN)	Jeffers *et al.*, 2004

* The mCEACAM2 molecule functions as a weak MHV receptor in tissue culture but does not serve as an alternate receptor *in vivo* (Hemmila *et al.*, 2004).

strated that homozygous *Ceacam1* knockout mice were totally resistant to infection by high doses of MHV (Hemmila *et al.*, 2004). Thus, even though CEACAM2, the product of the other murine *Ceacam* gene family member, can function as a weak MHV receptor in tissue culture (Nedellec *et al.*, 1994), it cannot be used as an alternative receptor *in vivo*.

Initial studies of the structural requirements for CEACAM1 function showed that the molecule must be glycosylated in order to be functional as an MHV receptor (Pensiero *et al.*, 1992). Moreover, the amino-terminal Ig-like domain was found to be the part of the molecule that is bound both by MHV S protein and by the monoclonal antibody originally used to identify the receptor (Dveksler *et al.*, 1993b). The essential difference between high-affinity and low-affinity S binding receptor alleles has been mapped to a determinant as small as six amino acid residues on the amino-terminal domain (Rao *et al.*, 1997; Wessner *et al.*, 1998). These critical residues, it turns out, fall within a prominent, uniquely convoluted loop in the recently solved x-ray crystallographic structure for a two-Ig-domain isoform

of CEACAM1 (Tan *et al.*, 2002). Notably, this loop was found to be topologically similar to protruding loops of the virus-binding domains of the receptors for rhinoviruses, HIV, and measles, all of which, like CEACAM1, are cell adhesion molecules. The CEACAM1 structure now provides the basis for beginning to understand the relative affinities of receptor variants for different S protein ligands.

Other group 2 coronaviruses use different receptors. The rat coronaviruses RCoV and SDAV, although closely related to MHV and able to grow in some of the same cell lines as does MHV, do not gain entry to cells via mCEACAM1. Anti-CEACAM1 monoclonal antibody, which totally blocks MHV infection, was shown to have no effect on infection by rat coronaviruses; moreover, expression of mCEACAM1 in nonpermissive BHK cells rendered them susceptible to MHV but not to rat coronaviruses (Gagneten *et al.*, 1996). BCoV is phylogenetically close to MHV, but the two viruses neither share common hosts nor are they supported by any of the same cell lines in tissue culture. To date, the only identified cell attachment factor for BCoV is 9-*O*-acetyl sialic acid (Schultze *et al.*, 1991), but it is not yet clear whether this moiety must be linked to specific proteins or glycolipids or whether there is also a specific cellular protein receptor for BCoV.

Not surprisingly, SARS-CoV, which is phylogenetically most distant from all other group 2 coronaviruses, uses a receptor wholly unrelated to CEACAMs. The SARS-CoV receptor, which was found in remarkably short order after the discovery of the virus, is angiotensin-converting enzyme 2 (ACE2). This was identified through the use of a SARS-CoV S1-IgG fusion protein to immunoprecipitate membrane proteins from Vero E6 cells, an African green monkey kidney cell line that is the best *in vitro* host for SARS-CoV (Li *et al.*, 2003). Binding of S1-IgG to Vero E6 cells was inhibited by soluble ACE2 protein but not by a related protein, ACE1. Expression of cloned cDNA for ACE2 was then shown to render nonpermissive cells susceptible to infection by SARS-CoV (Li *et al.*, 2003). ACE2 was also identified by expression cloning of an S1-binding activity, and it was shown to render cells infectable by a retroviral pseudotype carrying the SARS-CoV S protein (Wang *et al.*, 2004).

ACE2 is a zinc-binding carboxypeptidase that is involved in regulation of heart function. It is an N-exo, C-endo transmembrane glycoprotein with a broad tissue distribution. Active-site mutants of ACE2 showed no detectable defects in binding to SARS-CoV S protein (Moore *et al.*, 2004) or in promoting S protein-mediated syncytia formation (Li *et al.*, 2003), suggesting that ACE2 catalytic activity is not required for receptor function. This conclusion needs to be verified by

direct SARS-CoV infection, however. Recently solved x-ray structures for ACE2 have revealed that a large conformational change is induced by the binding of an inhibitor in the active site of the enzyme (Towler *et al.*, 2004). Although this finding raised the possibility of a means to interfere with the initiation of infection, the inhibitor does not affect S protein binding or receptor function of ACE2 (Li *et al.*, 2005a).

Numerous cell lines from a range of species have been classified with respect to their permissivity or nonpermissivity to SARS-CoV (Gillim-Ross *et al.*, 2004; Giroglou *et al.*, 2004; Mossel *et al.*, 2005), thereby allowing inferences as to which species homologs of ACE2 could have some degree of SARS-CoV receptor activity. In direct tests of S1 binding, human ACE2 was shown to be a much better receptor than was mouse ACE2; the receptor activity of rat ACE2, however, was barely detectable above background (Li *et al.*, 2004). In all cases tested, nonpermissive cells were shown to be made permissive by expression of human ACE2 (Mossel *et al.*, 2005). The full picture of factors influencing SARS-CoV host and tissue tropism is still developing. Human CD209L (also called L-SIGN or DC-SIGNR), a lectin family member, has been found to act as a second receptor for SARS-CoV, but it has much lower efficiency than does ACE2 (Jeffers *et al.*, 2004). A related lectin, DC-SIGN, was identified as a coreceptor, since it was able to transfer the virus from dendritic cells to susceptible cells; DC-SIGN could not act as receptor on its own, however (Marzi *et al.*, 2004; Yang *et al.*, 2004).

Many group 1 coronaviruses use the aminopeptidase N (APN) of their cognate species as a receptor (Table III) (Delmas *et al.*, 1992; Tresnan *et al.*, 1996; Yeager *et al.*, 1992). APN (also called CD13) is a cell-surface, zinc-binding protease that contributes to the digestion of small peptides in respiratory and enteric epithelia; it is also found in human neural tissue that is susceptible to HCoV-229E (Lachance *et al.*, 1998). The APN molecule is a homodimer; each monomer has a C-exo, N-endo membrane orientation and is heavily glycosylated. Competition experiments with monoclonal antibodies suggested that there is some overlap between the catalytic domain of hAPN and the binding site for HCoV-229E (Yeager *et al.*, 1992). However, neither the use of specific APN inhibitors, nor the mutational disruption of the catalytic site of pAPN, affected its TGEV receptor activity, indicating that the enzymatic activity of APN, per se, is not required for initiation of infection (Delmas *et al.*, 1994a). In general, the receptor activities of APN homologs are not interchangeable: hAPN cannot act as a receptor for TGEV (Delmas *et al.*, 1994a), and pAPN cannot act as a receptor for HCoV229E (Kolb *et al.*, 1996). Curiously, fAPN can serve as a receptor not

only for FIPV but also for CCoV, TGEV, and HCoV-229E (Tresnan *et al.*, 1996). These contrasting properties have been used as the framework for dissecting the basis of species-specific or -nonspecific function, through the construction and analysis of chimeric receptors (Benbacer *et al.*, 1997; Delmas *et al.*, 1994a; Hegyi and Kolb, 1998; Kolb *et al.*, 1996, 1997). However, chimera construction has not revealed a single linear determinant for virus binding. Rather, two different regions of the molecule have been found to influence receptor activity with respect to a given coronavirus. A detailed study of one of these regions showed that the critical characteristic in chimeras that exclude HCoV-229E is a particular glycosylation site. HCoV-229E likely does not directly bind to this region of APN, but it is hindered from doing so in homologs that are glycosylated at this locus (Wentworth and Holmes, 2001).

Not all group 1 coronaviruses use APN as a receptor, however. It has been proposed that one subset of FIPV strains uses a different receptor, since an antibody to fAPN blocked replication of type II strains of FIPV but not replication of type I strains of FIPV (Hohdatsu *et al.*, 1998). This conclusion is consistent with the observation that there is greater sequence divergence between type I FIPV S proteins and type II FIPV S proteins than there is between type II FIPV S proteins and the S proteins of CCoV or TGEV (Herrewegh *et al.*, 1998; Motokawa *et al.*, 1996). Likewise, although it has been suggested that pAPN can facilitate cellular entry of PEDV (Oh *et al.*, 2003), the major receptor for PEDV probably differs from that for TGEV, since the two viruses are able to grow in mutually exclusive sets of cells lines derived from different species (Hofmann and Wyler, 1988). The most outstanding exception to the generality of APN as a receptor for group 1 coronaviruses is the discovery that HCoV-NL63 cannot use hAPN to initiate infection; instead it is able to employ the same receptor as SARS-CoV, namely ACE2 (Hofmann *et al.*, 2005). This finding raises very interesting questions, one of which is why HCoV-NL63 causes a much milder respiratory disease than does SARS-CoV. Another is why two very different, zinc-binding, cell-surface peptidases, APN and ACE2, should serve as receptors for such a substantial number of coronaviruses. This situation can currently be ascribed to an amazing coincidence, but it may later be found to have deeper significance.

2. Receptor Recognition

The more variable of the two portions of the spike molecule, S1, is the part that binds to the receptor. Binding leads to a conformational change that results in the more highly conserved portion of the spike molecule, S2, mediating fusion between virion and cell membranes.

Just as different coronaviruses can bind to different receptors, coronaviruses also appear to use different regions of S1 with which to do so. Receptor-binding domains (RBDs) have so far been mapped in four S proteins (Fig. 2). In the group 1 coronavirus TGEV, the RBD was localized to amino acids 579–655, a region highly conserved among the S proteins of TGEV, PRCoV, FIPV, FCoV, and CCoV (Godet *et al.*, 1994). For the more distantly related group 1 coronavirus HCoV-229E, the RBD was found to fall in an adjacent, nonoverlapping segment of S1, amino acids 417–547 (Bonavia *et al.*, 2003). By contrast, the RBD of MHV was localized to the amino terminus of the S molecule, amino acids 1–330 (Kubo *et al.*, 1994; Suzuki and Taguchi, 1996; Taguchi, 1995). Finally, the RBD of SARS-CoV was mapped to amino acids 270–510 or 303–537 by binding of S protein fragments to Vero cells (Babcock *et al.*, 2004; Xiao *et al.*, 2003). These loci were contained within a domain shown to harbor the epitope for a neutralizing single-chain antibody fragment that blocked S1 association with the ACE2 receptor (Sui *et al.*, 2004). The SARS-CoV RBD was more finely delimited, to amino acids 318–510, by analysis of the binding to ACE2 of a large set of S1 constructs (Wong *et al.*, 2004). Thus, on a linear map of S proteins aligned principally by their S2 domains, the MHV RBD falls near the amino end of S1, the SARS-CoV RBD is in the middle of S1, and the TGEV and HCoV-229E RBDs fall near the carboxyl end of S1. The complementarity of the MHV and TGEV RBD loci is further emphasized by the fact that substantial deletions are tolerated in TGEV S1 in the region that corresponds to the MHV RBD (Laude *et al.*, 1995). Conversely, substantial deletions are tolerated in MHV S1 in the region that corresponds to the TGEV RBD (Parker *et al.*, 1989; Rowe *et al.*, 1997).

For MHV, persistent infection in tissue culture was shown to lead to the selection of variant viruses with an extended host range (Baric *et al.*, 1997, 1999; Schickli *et al.*, 1997). These viruses gained the ability to grow in cell lines from numerous species not permissive to wild-type MHV through an acquired recognition of receptors other than CEACAM1. Analysis and engineered reconstruction of one of these selected variants showed that a relatively small number of amino acid changes in the S protein RBD accounted for its extended host range (Schickli *et al.*, 2004; Thackray and Holmes, 2004). Comparison of the RBDs of various strains of MHV, of the extended host range mutant of MHV, and of other group 2 coronaviruses allowed the identification of five residues in the RBD that were uniquely conserved among MHV strains (Thackray *et al.*, 2005). Mutations in some of these residues were lethal or resulted in viruses that formed very small plaques; in

particular, a tyrosine at position 162 of the RBD was proposed as a candidate element in a key interaction with the receptor.

A set of elegant studies with the SARS-CoV S protein and ACE2 has provided the most detailed image of RBD-receptor interactions yet available for any coronavirus. Aided by the x-ray structure of ACE2, Li *et al.* (2005a) used the rat ACE2 molecule, which has negligible receptor activity, as a scaffold to identify critical residues in human ACE2. Transfer of as few as four human ACE 2 residues to rat ACE2 enabled the latter to bind S protein almost as well as human ACE2 did. A similar approach was used to determine key S1 residue changes that allowed the interspecies jump of SARS-CoV. The S1 domains of two SARS-CoV isolates were compared in this analysis: one (TOR2) from the main 2002–2003 SARS outbreak, and one (GD) from the subsequent 2003–2004 outbreak; the latter outbreak was much less severe and did not include any human-to-human transmission. Both the TOR2 and GD viruses are thought to have been transmitted to humans from palm civets, the final intermediary host in the jump of SARS-CoV from an unknown natural reservoir. However, only the TOR2 virus efficiently adapted to humans. Correspondingly, it was found that the S1 domains of both the TOR2 and GD viruses bound to palm civet ACE2, but only TOR2 S1 bound to human ACE2 (Li *et al.*, 2005a). Binding experiments with numerous chimeric variants were used to chart precisely which of the multiple coordinated changes in both the S1 RBD and in the human and palm-civet ACE2 could account for differences in the mutual affinities of the two molecules. The basis for the results that were obtained was then deduced from the x-ray structure of human ACE2 in a complex with the SARS-CoV S protein RBD (Li *et al.*, 2005b). The RBD was found to bind to the amino-terminal, catalytic domain of ACE2, contacting the latter with a concave, 71-residue loop. Inspection of the interface of this contact revealed that an astonishingly small number of RBD amino acid changes were critical to the adaptation of the virus from one species homolog of ACE2 to another. A change as subtle as the gain of a methyl group (serine to threonine at residue 487 of the RBD) that fits into a hydrophobic pocket on the receptor could account for a 20-fold increase in affinity of S1 for human ACE2.

3. S Protein Conformational Change and Fusion

The binding of spike to its cellular receptor triggers a major conformational change in the S molecule. In some cases, induction of this conformational change may also require a shift to an acidic pH. Thus, some coronaviruses, such as MHV, fuse with the plasma membrane at

the cell surface (Sturman *et al.*, 1990; Weismiller *et al.*, 1990), while others, such as TGEV (Hansen *et al.*, 1998), HCoV-229E (Nomura *et al.*, 2004), and SARS-CoV (Hofmann *et al.*, 2004; Simmons *et al.*, 2004; Yang *et al.*, 2004), appear to enter the cell via receptor-mediated endocytosis and then fuse with the membranes of acidified endosomes. There may be a very fine balance between these two states. For MHV, it was found that as few as three amino acid changes in a heptad repeat region in S2 could govern the switch from plasma membrane fusion to strictly acid pH-dependent fusion (Gallagher *et al.*, 1991; Nash and Buchmeier, 1997). For SARS-CoV, protease treatment of cells at the earliest steps of infection was found to allow the virus to enter cells from the surface, rather than through an endocytic pathway (Matsuyama *et al.*, 2005). Such treatment enhanced the infectivity of the virus by orders of magnitude, and this enhancement was receptor dependent. Although SARS-CoV S protein is not detectably cleaved in virions or pseudovirions produced in tissue culture (Simmons *et al.*, 2004; Song *et al.*, 2004), protease treatment may mimic the environment resulting from an inflammatory response in infected lungs.

Much of the characterization of the receptor-induced conformational change in S was initially carried out with the MHV S protein, for which it was found that the effects of receptor binding could also be elicited by treatment of virions at mild alkaline pH (Sturman *et al.*, 1990). Such treatment caused the dissociation and release of the cleaved S1 subunit and the aggregation of S2 subunits; the accompanying conformational changes in S1 were monitored by differential access of a panel of monoclonal antibodies at neutral and alkaline pH (Weismiller *et al.*, 1990). Disulfide bond formation plays an important role in S protein folding, and disulfides in S1 may become rearranged during the conformational transitions of S1 following receptor binding (Lewicki and Gallagher, 2002; Opstelten *et al.*, 1993; Sturman *et al.*, 1990). The S protein of the highly virulent MHV strain 4 (JHM) has been shown to exist in a particularly metastable configuration. This results in a hair-trigger spike so highly fusogenic that it can mediate fusion between infected cells and cells lacking receptors, thereby leading to more extensive neuropathogenesis than occurs with other MHV strains (Gallagher and Buchmeier, 2001; Gallagher *et al.*, 1992; Krueger *et al.*, 2001; Nash and Buchmeier, 1996).

In the normal spike-receptor interaction, both the S1-binding and the S1-activation functions were found to reside in the amino-terminal Ig domain of CEACAM1 (Miura *et al.*, 2004). The role of the additional Ig domain(s) in the various CEACAM isoforms is apparently to give the

virus access to the amino-terminal Ig domain. Similarly, although the RBD of the MHV S protein lies near the amino terminus of S1, portions of the molecule distal to this site can significantly influence the stability of the S1-receptor interaction (Gallagher, 1997). The conformational change that separates S1 from the rest of the molecule, in turn, transmits a major change to S2. This secondary change has been monitored by the differential susceptibility of S2 to protease treatment before and after the binding of S1 to soluble receptor (Matsuyama and Taguchi, 2002). Additionally, the same changes were shown to be caused, in the absence of receptor, by mild alkaline pH, which induced a fusogenic state in S2 that could be measured by a liposome flotation assay (Zelus *et al.*, 2003).

It has been realized that the coronavirus S protein is a type I viral fusion protein with functional similarities to the fusion proteins of phylogenetically distant RNA viruses such as influenza virus, HIV, and Ebola virus (Bosch *et al.*, 2003). Similar to its counterparts in other viruses, the coronavirus S2 domain contains two separated heptad repeats, HR1 and HR2, with a fusion peptide upstream of HR1 and the transmembrane domain immediately downstream of HR2 (Fig. 2). Mutations in the MHV S protein HR1 and HR2 regions were shown to inhibit or abolish fusion (Luo and Weiss, 1998; Luo *et al.*, 1999). Unlike its counterparts, however, the coronavirus S protein does not require cleavage to be fusogenic, and it contains an internal fusion peptide, although the exact assignment of this domain is not agreed upon (Guillen *et al.*, 2005; Sainz *et al.*, 2005). Even for MHV S and other cleaved S proteins, the fusion peptide is not the amino terminus of S2 created by cleavage (Luo and Weiss, 1998), as is the case in other type I fusion proteins.

The receptor-mediated conformational change in S1 and the dissociation of S1 from S2 are thought to initiate a major rearrangement in the remaining S2 trimer. This rearrangement exposes a fusion peptide that interacts with the host cellular membrane, and it brings together the two heptad repeats in each monomer so as to form an antiparallel, six-helix "trimer-of-dimers" bundle. The result is the juxtaposition of the viral and cellular membranes in sufficient proximity to allow the mixing of their lipid bilayers and the delivery of the contents of the virion into the cytoplasm. The trimer of dimers is extremely stable, forming a rod-like, protease-resistant complex, the biophysical properties of which have been studied in depth for the S proteins of MHV (Bosch *et al.*, 2003) and SARS-CoV (Bosch *et al.*, 2003, 2004; Ingallinella *et al.*, 2004; Liu *et al.*, 2004; Tripet *et al.*, 2004) by the use of model peptides. X-ray crystallographic structures have been solved

for peptide complexes for both the MHV S protein (Xu *et al.*, 2004a) and the SARS-CoV S protein (Duquerroy *et al.*, 2005; Supekar *et al.*, 2004; Xu *et al.*, 2004b). In the six-helix bundle, the three HR1 helices were found to form a central, coiled-coil core, and the three HR2 helices, in an antiparallel orientation, pack into the grooves between the HR1 monomers. There is no contact between the HR2 monomers, each of which associates with the HR1 grooves through hydrophobic interactions. The overall structures obtained for MHV S and SARS-CoV S are highly similar to each other and strongly resemble the structures of the fusion cores of influenza virus HA and HIV gp41. Noteworthy differences are that the coronavirus HR1 coiled-coil is two to three times larger than its counterparts in other viruses and that the much shorter coronavirus HR2 helices assume a unique conformation within the bundle. A major goal of these studies is the design of peptides that are able to inhibit formation of this complex in SARS-CoV infections.

In addition to the mechanisms of the conformational rearrangements of S1 and S2, other factors influence coronavirus fusion and entry, in ways that are not yet well understood. For two coronaviruses, the role of cholesterol in virus entry has been investigated. Cholesterol supplementation was found to augment MHV replication, while cholesterol depletion was inhibitory; these effects were shown to occur at the earliest stages of infection (Thorp and Gallagher, 2004). Contrary to expectations, the basis for the action of cholesterol was not through clustering of CEACAM receptors into lipid rafts, either before or after the binding of virus to receptor (Choi *et al.*, 2005; Thorp and Gallagher, 2004). However, cell-bound virions did cluster into lipid rafts, suggesting that MHV S protein associates with some host factor other than CEACAM prior to entry (Choi *et al.*, 2005). For HCoV-229E, on the other hand, both virus and hAPN receptor were found to redistribute on the cell surface from an initially disperse pattern to clusters within caveolin-1-rich lipid rafts (Nomura *et al.*, 2004). Thus, the mechanism by which cholesterol assists infection may differ between coronaviruses that enter the cell via receptor-mediated endocytosis and those that fuse with the plasma membrane.

For those coronaviruses that bring about syncytia formation, cell–cell fusion appears to have different requirements than virus–cell fusion. Studies with MHV have long noted a correlation between the degree of S protein cleavage and the amount of cell–cell fusion, both of which could be enhanced by trypsin treatment (Sturman *et al.*, 1985). The extent and kinetics of S protein cleavage were shown to vary among different cell lines, implicating the involvement of a cellular, rather than viral, protease (Frana *et al.*, 1985). Consistent with this,

an MHV strain A59 mutant isolated from persistently infected glial cells was found to have an altered cleavage site, RRADR instead of the wild-type RRAHR (Gombold *et al.*, 1993); this change caused an extreme delay, but not abrogation, of fusion of infected cells. Studies of expressed MHV S proteins with wild-type or mutated cleavage sites gave essentially the same results, showing that the fusion delay was strictly a property of mutant S protein (Bos *et al.*, 1995; Stauber *et al.*, 1993; Taguchi, 1993). However, S protein was found not to be cleaved at all in MHV-infected primary glial cells or hepatocytes, indicating that cleavage was not a requirement for virus–cell fusion (Hingley *et al.*, 1998). It was demonstrated that furin or a furin-like protease is responsible for MHV S cleavage in tissue culture (de Haan *et al.*, 2004). Treatment of cells with a specific furin inhibitor blocked both cleavage and cell–cell fusion, but it had no effect on virus–cell fusion.

Another component of the MHV S protein that operates in cell–cell fusion is the cysteine-rich region of the endodomain, mutation of which delays or abrogates syncytia formation (Bos *et al.*, 1995; Chang *et al.*, 2000). It is currently not known how this segment of the S molecule, which is on the opposite side of the membrane from the six-helix bundle, participates in the fusion process. The cysteine-rich region of the endodomain is a possible target for palmitoylation (Bos *et al.*, 1995), which is a known modification of MHV S (Niemann and Klenk, 1981), but, as yet, a role for palmitoylation has not been established.

B. Virion Assembly Interactions

Once the full program of viral gene expression is underway, through transcription, translation, and genome replication, progeny viruses can begin to assemble. Coronavirus virion assembly occurs through a series of cooperative interactions that occur in the ER and the ERGIC among the canonical set of structural proteins, S, M, E, and N. The M protein is a party to most, if not all, of these interactions and has come to be recognized as the central organizer of the assembly process. Despite its dominant role, however, M protein alone is not sufficient for virion formation. Independent expression of M protein does not result in its assembly into virion-like structures. Under these circumstances, M was shown to traverse the secretory pathway as far as the *trans*-Golgi (Klumperman *et al.*, 1994; Machamer and Rose, 1987; Machamer *et al.*, 1990; Rottier and Rose, 1987; Swift and Machamer, 1991), where it forms large, detergent-insoluble complexes (Krijnse Locker *et al.*, 1995; Weisz *et al.*, 1993). By contrast, MHV, IBV, TGEV, and FIPV, representative species from each of the three coronavirus

groups, were found to bud into a proximal compartment, the ERGIC (Klumperman *et al.*, 1994; Krijnse Locker *et al.*, 1994; Tooze *et al.*, 1984, 1988). These observations suggested that some factor, in addition to M, must determine the site of virion assembly and budding.

The identification of the unknown factor came from the development of virus-like particle (VLP) systems for coronaviruses. Such studies showed that, for MHV, coexpression of both M protein and the minor virion component, E protein, was necessary and sufficient for the formation of particles (Bos *et al.*, 1996; Vennema *et al.*, 1996). The resulting VLPs were morphologically identical to virions (minus spikes) and were released from cells by a pathway similar to that used by virions. Notably, neither the S protein nor the nucleocapsid was found to be required for VLP formation. These results were subsequently generalized for coronaviruses from all three groups: BCoV and TGEV (Baudoux *et al.*, 1998), IBV (Corse and Machamer, 2000, 2003), and SARS-CoV (Mortola and Roy, 2004). Currently, there is one known exception to this trend: in a separate study of SARS-CoV, M and N proteins were reported to be necessary and sufficient for VLP formation, whereas E protein was dispensable (Huang *et al.*, 2004a). This latter contradiction remains to be resolved. It may reflect a unique aspect of SARS-CoV virion assembly, or, alternatively, it may indicate that VLP requirements can vary with different expression systems.

1. M Protein–M Protein Interactions

Since VLPs contain very little E protein, it is assumed that lateral interactions between M protein monomers are the driving force for virion envelope formation. These interactions have been explored through examination of the ability of constructed M protein mutants to support or to interfere with VLP formation. A study that tested the structural requirements of the M protein found that mutations either in the ectodomain, or in any of the three transmembrane domains, or in the carboxy-terminal endodomain, could inhibit or abolish VLP formation (de Haan *et al.*, 1998a). In particular, the carboxy terminus of M was extremely sensitive to small deletions or even to point mutations of the final residue of the molecule. Construction of many of these latter mutations in the viral genome revealed a consistent set of effects on viral viability. Yet, virions were better able than VLPs to tolerate carboxy-terminal alterations in M protein, presumably because virions were stabilized by additional intermolecular interactions not present in VLPs. In experiments in which both wild-type and mutant M proteins were coexpressed with E protein, wild-type M protein was able to rescue low concentrations of assembly-defective mutant M proteins

into VLPs (de Haan *et al.*, 1998a). This finding, coupled with results from coimmunoprecipitation analyses, provided the basis for further work, which concluded that monomers of M interact via multiple contacts throughout the molecule and particularly in the transmembrane domains (de Haan *et al.*, 2000).

2. S Protein–M Protein Interactions

That VLPs could be formed in the absence of S protein (Bos *et al.*, 1996; Vennema *et al.*, 1996) confirmed the much earlier discovery that treatment of MHV-infected cells with the glycosylation inhibitor tunicamycin led to the assembly and release of spikeless (and consequently, noninfectious) virions (Holmes *et al.*, 1981; Rottier *et al.*, 1981). These findings were also consistent with the properties of certain classical temperature-sensitive mutants of MHV and IBV, which, owing to *S* gene lesions, failed to incorporate spikes into virions at the nonpermissive temperature (Luytjes *et al.*, 1997; Ricard *et al.*, 1995; Shen *et al.*, 2004). Independently expressed MHV, FIPV, or IBV S proteins enter the default secretory pathway and ultimately reach the plasma membrane (Vennema *et al.*, 1990). In the presence of M protein, however, a major fraction of S is retained in intracellular membranes, as was shown by coimmunoprecipitation of S and M proteins from MHV-infected cells (Opstelten *et al.*, 1995). Moreover, the interaction of M with S was demonstrated to be specific; complexes of M did not impede the progress of a heterologous glycoprotein (the VSV G protein) to the plasma membrane. Additionally, kinetic experiments revealed that the folding and oligomerization of S protein in the ER is rate limiting in the M–S interaction, in which nascent M protein immediately participates (Opstelten *et al.*, 1995). Complexes of the M and S proteins were similarly observed in BCoV-infected cells, for which it was found that M also determines the selection of HE protein for incorporation into virions (Nguyen and Hogue, 1997). The simplest picture to be drawn from all this evidence, then, is that S protein is entirely passive in assembly but becomes trapped by M protein upon passage through the ER. Nevertheless, there are indications that, in some cases, S cooperates in its own capture. By the criterion of acquisition of endo H resistance, independently expressed S protein was found to be transported to the cell surface with much slower kinetics than S protein that was incorporated into virions. This led to the proposal that free S protein harbors intracellular retention signals that become hidden during virion assembly (Vennema *et al.*, 1990). Such signals have been found in the (group 3) IBV S protein cytoplasmic endodomain, which

contains both a dilysine motif that was shown to specify retention in the ERGIC and a tyrosine-based motif that causes retrieval by endocytosis from the plasma membrane (Lontok *et al.*, 2004). Additionally, a novel dibasic ERGIC retention signal was identified in the S protein endodomains of group 1 coronaviruses (TGEV, FIPV, and HCoV-229E) and SARS-CoV, but not other group 2 coronaviruses, such as MHV and BCoV.

Although the S protein is not required for VLP formation, it does become incorporated into VLPs if it is coexpressed with the M and E proteins (Bos *et al.*, 1996; Vennema *et al.*, 1996). VLP manipulations thus made it possible to begin to dissect the molecular basis for the specific selection of S protein by M protein. As for M–M homotypic interactions, the sites within M protein that bind to S protein have not yet been pinpointed. On a broader scale, deletion mapping has indicated that the ectodomain of M protein and the carboxy-terminal 25 residues of the endodomain do not participate in interactions with S, even though both of these regions are critical for VLP formation (de Haan *et al.*, 1999). The residues of S protein that interact with M protein, on the other hand, have been much more precisely localized. This mapping began with the swapping of ectodomains between the very divergent S proteins of MHV and FIPV (Godeke *et al.*, 2000). This type of exchange showed that the incorporation of S protein into VLPs of a given species was determined by the presence of merely the transmembrane domain and endodomain of S protein from the same species. The source of the S ectodomain did not matter. The assembly competence of the 1324-residue MHV S protein or the 1452-residue FIPV S protein was therefore restricted to just the 61-amino-acid, carboxy-terminal region of each of these molecules. That the domain-switched S molecules were completely functional was demonstrated by the construction of an MHV mutant, designated fMHV, in which the ectodomain of the MHV S protein was replaced by that of the FIPV S protein (Kuo *et al.*, 2000). As predicted, this mutant gained the ability to grow in feline cells, while losing the ability to grow in mouse cells. The fMHV chimera provided the basis for powerful selections, based on host cell species restriction, that have been used with the reverse genetic system of targeted RNA recombination (Section VI) (Kuo and Masters, 2002; Masters, 1999; Masters and Rottier, 2005). The converse construct, an FIPV mutant designated mFIPV, in which the ectodomain of the FIPV S protein was replaced by that of the MHV S protein, had properties exactly complementary to those of fMHV (Haijema *et al.*, 2003).

More detailed dissection of the transmembrane domain and endodomain of the MHV S protein has been carried out to further localize the determinants of S incorporation into virions (Bosch *et al.*, 2005; Ye *et al.*, 2004). In one study, the S protein transmembrane domain, or the endodomain, or both, were swapped with the corresponding region(s) of a heterologous transmembrane protein, which was expressed as an extra viral gene product (Ye *et al.*, 2004). Mutations were constructed in this surrogate virion structural protein, or, alternatively, directly in the S protein. From this work, the virion assembly property of S was found to map solely to the 38-residue endodomain, with a major role assigned to the charge-rich, carboxy-terminal region of the endodomain. Additionally, it was observed that the adjacent, membrane-proximal, cysteine-rich region of the endodomain was critical for cell–cell fusion during infection, consistent with results previously reported from investigations using S protein expression systems (Bos *et al.*, 1995; Chang *et al.*, 2000). A second study, based on analysis of a progressive series of carboxy-terminal truncations of the S protein in VLPs and in viral mutants, also mapped the virion assembly competence of S to the endodomain (Bosch *et al.*, 2005). In this work, however, the major role in assembly was attributed to the cysteine-rich region of the endodomain, and the overall size, rather than the sequence of the endodomain, was seen to be critical. Thus, the precise nature of the interaction between the S protein endodomain and the M protein remains to be resolved.

3. N Protein–M Protein Interactions

The interaction of the viral nucleocapsid with M protein was originally examined by the fractionation of purified MHV virions (Sturman *et al.*, 1980). At 4°C, M protein was separated from other components on density gradient centrifugation of NP-40-solubilized virion preparations, but M reassociated with the nucleocapsid when the temperature was elevated to 37°C. Further analysis suggested that, contrary to expectations, this temperature-dependent association was mediated by M binding to viral RNA, rather than to N protein. The notion of M protein as an RNA-binding protein has been revived in light of recent results on the mechanism of genome packaging (Section IV.C) (Narayanan *et al.*, 2003a).

For TGEV virions, the use of particular low-ionic-strength conditions of NP-40 treatment similarly resulted in the finding that a fraction of M protein was persistently integrated with subviral cores (Risco *et al.*, 1996). For assay of this association, *in vitro*-translated M protein was bound to immobilized nucleocapsid purified from virions (Escors

et al., 2001). Through the combined approaches of deletion mapping, inhibition by antibodies of defined specificity, and peptide competition, the M-nucleocapsid interaction was localized to a segment of 16 residues adjacent to the carboxy terminus of the 262-residue TGEV M protein.

Studies of MHV have taken genetic avenues to explore the N protein–M protein interaction. In one report, a viral mutant was constructed in which the carboxy-terminal two amino acids of the 228-residue MHV M protein were deleted (Kuo and Masters, 2002), a lesion previously known to abolish VLP formation (de Haan *et al.*, 1998a). The resulting highly impaired virus, designated MΔ2, formed tiny plaques and grew to maximal titers many orders of magnitude lower than those of the wild type. Multiple independent second-site revertants of the *MΔ2* mutant were isolated and mapped to either the carboxy terminus of M or that of N. Reconstruction of some of these compensating mutations, in the presence of the original MΔ2 mutation, provided evidence for a structural interaction between the carboxy termini of the M and the N proteins. In a complementary analysis, a set of viral mutants were created containing all possible clustered charged-to-alanine mutations in the carboxy-terminal domain 3 of the N protein (Hurst *et al.*, 2005). One of the members of this set, designated N-CCA4, was extremely defective, having a phenotype similar to that of the *MΔ2* mutant. Multiple independent second-site suppressors of N-CCA4 were found to map in the carboxy-terminal region of either the N or the M protein, thereby reciprocating the genetic cross-talk uncovered with the *MΔ2* mutant. Additionally, it was shown that the transfer of N protein domain 3 to a heterologous protein allowed incorporation of that protein into MHV virions.

4. Role of E Protein

In contrast to the more overt structural roles of the M, S, and N proteins, the part played by E protein in assembly is enigmatic. On discovery of the essential nature of E in VLP formation, it was speculated that the low amount of E protein in virions and VLPs indicated a catalytic, rather than structural, function for this factor. E protein might serve to induce membrane curvature in the ERGIC, or it might act to pinch off the neck of the viral particle in the final stage of the budding process (Vennema *et al.*, 1996). In a search for evidence correlating the VLP findings to the situation in whole virions, a set of clustered charged-to-alanine mutations were constructed in the *E* gene of MHV. One of the resulting mutants was markedly thermolabile, and

its assembled virions had striking morphologic defects, exhibiting pinched and elongated shapes that were rarely seen among wild-type virions (Fischer *et al.*, 1998). This phenotype clearly supported a critical role for E protein in virion assembly. Surprisingly, however, it was later found to be possible to entirely delete the *E* gene from the MHV genome, although the resulting Δ*E* mutant virus was only minimally viable compared to the wild type (Kuo and Masters, 2003). This indicated that, for MHV, the E protein is important, but not absolutely essential, to virion assembly. By contrast, for TGEV, two independent reverse genetic studies showed that knockout of the *E* gene was lethal. Viable virus could be recovered only if E protein was provided *in trans* (Curtis *et al.*, 2002; Ortego *et al.*, 2002). This discordance may point to basic morphogenic differences between group 2 coronaviruses (such as MHV) and group 1 coronaviruses (such as TGEV). Alternatively, it is possible that E protein has multiple activities, one of which is essential for group 1 coronaviruses but is largely dispensable for group 2 coronaviruses.

The information available about E protein at this time is not sufficiently complete to allow us to understand the function of this tiny molecule. One of the most intriguing questions is whether it is necessary for E protein to directly physically interact with M protein, or whether E acts at a distance. If E protein has multiple roles, then perhaps both of these possibilities are applicable. Direct interaction between the E and M proteins is implied by the observation that, at least in some cases, coexpression of E and M proteins from different species does not support VLP formation (Baudoux *et al.*, 1998). The demonstration that IBV E and M can be cross-linked to one another also has established that the two proteins are in close physical proximity in infected or transfected cells (Corse and Machamer, 2003). Contrary to this, some data appear to argue that E acts independently of M. The individual expression of MHV or IBV E protein results in membrane vesicles that are exported from cells (Corse and Machamer, 2000; Maeda *et al.*, 1999). Additionally, it has been shown that the expression of MHV E protein alone leads to the formation of clusters of convoluted membranous structures highly similar to those seen in coronavirus-infected cells (Raamsman *et al.*, 2000). This suggests that the E protein, without other viral proteins, acts to induce membrane curvature in the ERGIC. Some indirect evidence may also be taken to indicate that E does not directly contact other viral proteins. Multiple revertant searches with *E* gene mutants failed to identify any suppressor mutations that map in *M* or in any gene other than *E* (Fischer *et al.*, 1998). Similarly, none of the intergenic suppressors of the *MΔ2*

mutant mapped to the *E* gene (Kuo and Masters, 2002). It has been found that the SARS-CoV E protein forms cation-selective ion channels in a model membrane system (Wilson *et al.*, 2004). Moreover, this channel-forming property was contained in the amino-terminal 40 residues of the 76-residue SARS-CoV E molecule. Such an activity made be the basis for an independent mode of action of E protein.

C. Genome Packaging

Although a variety of positive- and negative-strand viral RNA species are synthesized during the course of infection (Section V), coronaviruses selectively incorporate genomic (positive-strand) RNA into assembled virions. This may be accomplished with varying degrees of stringency by different members of the family. Sucrose gradient-purified virions of MHV have been found to exclusively contain genomic RNA (Makino *et al.*, 1990). By contrast, similarly purified virions of BCoV (Hofmann *et al.*, 1990), TGEV (Sethna *et al.*, 1989, 1991), and IBV (Zhao *et al.*, 1993) have been reported to contain significant quantities of subgenomic mRNA, in some cases in molar amounts exceeding those of the genomic RNA. However, in a study of TGEV, in which virions were extensively purified by an ELISA-based immunopurification procedure, a very high degree of selectivity for genomic RNA packaging was observed (Escors *et al.*, 2003).

In those viruses in which it has been mapped, the RNA element that specifies selective packaging falls, as would be expected, in a region of the genome that is not found in any of the subgenomic mRNAs. In MHV, the genomic packaging signal was localized through analysis of defective interfering (DI) RNAs. DI RNAs are extensively deleted variants of the genome that propagate as molecular parasites, using the replicative machinery of a helper virus. Some DI RNAs are packaged efficiently, while others have lost such a capability. Dissection of particular members of the former class revealed that a relatively small span of internal sequence could account for packaging competence (Makino *et al.*, 1990; van der Most *et al.*, 1991). The exact boundaries of the MHV packaging signal are not precisely defined, but reports from different groups have converged on RNA segments of 180–190 nt, within a 220-nt region that is centered some 20.3 kb from the 5′ end of the genome (Fosmire *et al.*, 1992; Molenkamp and Spaan, 1997). The MHV packaging element is thus embedded in the coding sequence of nsp15, at the distal end of the replicase gene. A core 69-nt RNA secondary structural element can act as a minimal signal for packaging (Fosmire *et al.*, 1992; Woo *et al.*, 1997), but larger versions of the

element, consisting of the core plus flanking sequences, function more efficiently (Cologna and Hogue, 2000; Narayanan and Makino, 2001). Even the larger versions of the element may not be entirely sufficient, however: some data suggest that other *cis*-acting sequences found in genomic, but not subgenomic, DI RNA contribute to the overall efficiency of packaging (Bos *et al.*, 1997).

For the closely related group 2 coronavirus BCoV, the 190-nt genomic region homologous to the MHV packaging signal has been shown to have the same function as its MHV counterpart. Moreover, the MHV and BCoV packaging signals are able to act in a reciprocal fashion: a nonviral RNA containing the MHV packaging signal can be packaged by BCoV helper virus, and a nonviral RNA containing the BCoV packaging signal can be packaged by MHV helper virus (Cologna and Hogue, 2000). This functional homology does not appear to extend across group boundaries, though. For the group 1 coronavirus TGEV, the packaging signal was also shown to be retained in particular DI RNAs, which were found to be incorporated into defective virions that could be separated from helper virus by density gradient centrifugation (Mendez *et al.*, 1996). Surprisingly, dissection of the smallest packaged DI RNA revealed that the packaging signal for TGEV maps to the upstream end of the replicase gene, localizing in the region of 100–649 nt from the 5′ end of the genome (Escors *et al.*, 2003). For the group 3 coronavirus IBV, a packaged DI RNA has been isolated and characterized (Penzes *et al.*, 1994), but mapping of the packaging element in this RNA has thus far been inconclusive, owing to the need to decouple requirements for replication from those for packaging (Dalton *et al.*, 2001). Nevertheless, it is clear that the IBV DI RNA does not harbor a region of the IBV genome homologous to the region that contains the packaging signal in MHV. Similarly, the IBV DI RNA may also lack the counterpart of the TGEV packaging signal. It will be interesting to see whether the packaging signals of viruses in the three coronavirus groups, once they are completely characterized, are found to retain structural similarities despite differences in sequence and location.

The mechanism by which packaging signals operate is not yet clear, and results with MHV have in fact taken an unanticipated turn. In this context, it is important to note the distinction between encapsidation and packaging, two terms that are often used interchangeably in the coronavirus literature. Encapsidation is the process of formation of the nucleocapsid, that is, the cooperative binding of N protein to viral RNA. Packaging is the incorporation of the nucleocapsid into virions. For enveloped viruses, the two processes are not necessarily

the same. For example, for nonsegmented negative-strand viruses, both genomic and antigenomic RNA are encapsidated, but only genomic RNA is packaged. For coronaviruses, it was logical to assume that encapsidation is initiated by the N protein. Indeed, specific binding of MHV N protein to the packaging signal RNA has been demonstrated *in vitro* (Molenkamp and Spaan, 1997). However, *in vitro* RNA binding experiments have also shown a specific interaction between the MHV N protein and the leader RNA, which is located at the 5′ end of subgenomic and genomic RNA (Nelson *et al.*, 2000; Stohlman *et al.*, 1988). It remains to be seen whether either of these sequence-specific modes of RNA binding represents a nucleation step ultimately leading to encapsidation by multiple monomers of N. The binding of N to leader RNA appears incongruent with the specificity of packaging, but it is consistent with the observation that anti-N antibodies coimmunoprecipitate both subgenomic and genomic RNA from cells infected with MHV or BCoV (Baric *et al.*, 1988; Cologna *et al.*, 2000; Narayanan *et al.*, 2000). A possible resolution of this paradox has come from findings that reveal a role for M protein in the selectivity of packaging. Antibodies to MHV M protein were shown to coimmunoprecipitate the fraction of N protein that is bound to genomic RNA, but not N protein that is bound to subgenomic RNA (Narayanan *et al.*, 2000). Furthermore, this specific M–N interaction is dependent on the presence of the MHV packaging signal (Narayanan and Makino, 2001). Remarkably, recent work with coexpressed MHV proteins has attributed the direct selection of packaging signal RNA to the M protein. Thus, VLPs formed by M and E proteins, but devoid of N protein, were found to incorporate a heterologous RNA molecule only if it contained the MHV packaging signal (Narayanan *et al.*, 2003a). If this discovery turns out to generalize to all coronaviruses, then it will mean that M protein orchestrates every single interaction necessary for virion assembly.

V. RNA Synthesis

A. Replication and Transcription

Coronavirus RNA synthesis proceeds by a complex and incompletely understood mechanism, portions of which involve interactions between distant segments of the genome (Lai and Cavanagh, 1997; Lai and Holmes, 2001; van der Most and Spaan, 1995). Following its translation into the replicase polyproteins, the genomic RNA (gRNA) next acts as the template for synthesis of negative-sense RNA species.

Further events produce a series of smaller, subgenomic RNAs (sgRNAs) of both polarities (Fig. 6) (Baric and Yount, 2000; Sethna *et al.*, 1989, 1991). The positive-sense sgRNAs, each of which serves as the message for one of the ORFs downstream of the replicase ORF, have compositions equivalent to large genomic deletions. Positive-sense sgRNAs contain a 70–100-nt leader RNA, which is identical to the 5′ end of the genome, joined at a downstream site to a stretch of sequence (the body of the sgRNA), which is identical to the 3′ end of the genome. Collectively, the sgRNAs are said to form a 3′-nested set. The 3′-nested set of sgRNAs, with or without a leader sequence, is a defining feature of the order *Nidovirales* (Enjuanes *et al.*, 2000a; van Vliet *et al.*, 2002). The negative-sense sgRNAs, roughly a tenth to a hundredth as abundant as their positive-sense counterparts, each possess the complement of this arrangement, including a 5′ oligo(U) tract of 9–26 residues (Hofmann and Brian, 1991) and a 3′ antileader (Sethna *et al.*, 1991).

Many advances in understanding the mechanism of coronavirus RNA synthesis were facilitated by the discovery and cloning of DI RNAs of MHV (Makino *et al.*, 1985, 1988; van der Most *et al.*, 1991)

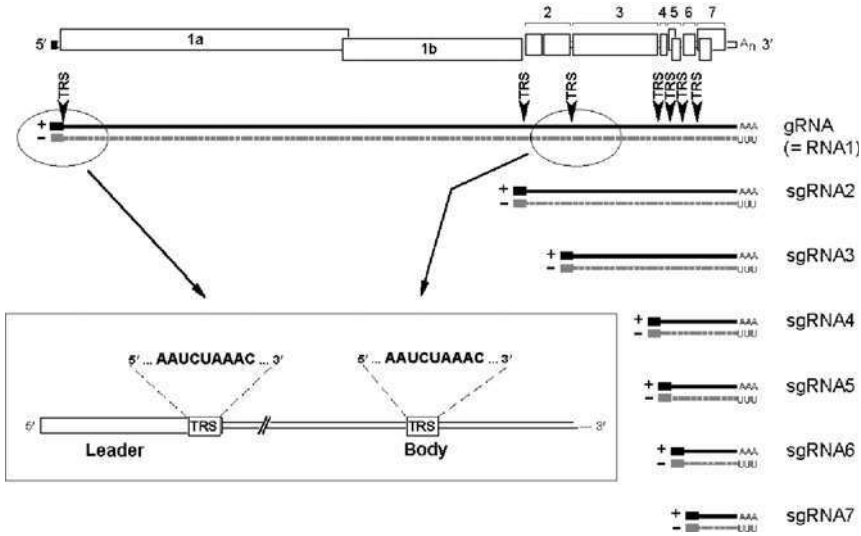

FIG 6. Coronavirus RNA synthesis. The nested set of positive- and negative-strand RNAs produced during replication and transcription are shown, using MHV as an example. The inset shows details of the arrangement of leader and body copies of the transcription-regulating sequence (TRS).

and, subsequently, of other coronaviruses (Chang *et al.*, 1994; Mendez *et al.*, 1996; Penzes *et al.*, 1994). Because they are extensively deleted genomic variants that propagate by competing for the viral RNA synthesis machinery, DI RNAs have evolved to retain *cis*-acting sequence elements necessary for replication. Manipulations of naturally occurring and artificially constructed DI RNAs, which are studied by transfection into infected cells, enabled the mapping of elements from the genome that participate in replication and transcription (Brian and Baric, 2005).

In studies of replication, deletion analyses of various cloned MHV DI RNAs have demonstrated that either 466, 474, or 859 nucleotides at the 5′ end of the MHV genome are required to support replication (Kim *et al.*, 1993; Lin and Lai, 1993; Luytjes *et al.*, 1996). The exact magnitude of this value appears to have been dependent on which MHV genomic regions were present in the individual DI RNA with which a particular analysis was begun. In the very closely related BCoV, 498 nucleotides at the 5′ end of a naturally occurring DI RNA have been shown to suffice for replication (Chang *et al.*, 1994). For TGEV and IBV, the minimal 5′ *cis*-acting replication signals have thus far been limited to 1348 and 544 nucleotides, respectively (Dalton *et al.*, 2001; Izeta *et al.*, 1999). In all cases, this region extends well beyond the leader RNA and includes a portion of the 5′ end of the replicase ORF. This means that coronavirus sgRNAs do not have a sufficient extent of 5′ sequence to function as replicons, as was once proposed (Sethna *et al.*, 1989). Only in BCoV has the 5′ *cis*-acting replication signal been further defined. Detailed dissections of this element, through structural probing and functional mutational analyses, have identified four stem-loop structures essential for RNA replication (Chang *et al.*, 1994, 1996; Raman and Brian, 2005; Raman *et al.*, 2003). For stems III and IV, secondary structure, rather than primary sequence, has been shown to be of functional importance; these structures were found to be conserved in the more closely related group 2 coronaviruses but not in SARS-CoV.

At the other end of the genome, deletion analyses found that the minimal stretch of the 3′ terminus able to sustain MHV DI RNA replication falls between 436 and 462 nucleotides (Kim *et al.*, 1993; Lin and Lai, 1993; van der Most *et al.*, 1995). Notably, this range of sequence would include a portion of the adjacent *N* gene as well as the entire 301-nucleotide 3′ UTR. By contrast, the minimal 3′ *cis*-acting replication signals for TGEV and IBV were 492 and 338 nucleotides, respectively. DI RNAs containing such minimal elements were devoid of any part of the *N* gene (Dalton *et al.*, 2001; Izeta *et al.*, 1999).

Consistent with this latter finding, it was shown for engineered mutants of MHV that translocation of the *N* gene to an upstream genomic position had no effect on replication (Goebel *et al.*, 2004a). This argues strongly that no essential 3′ *cis*-acting region is present in the *N* gene within the intact MHV genome. If any such region does exist, it must be able to act at a distance of nearly 1.5 kb. Given the requirement in MHV for the entire 3′ UTR, it was somewhat paradoxical when further study showed that a minimum of 45–55 nucleotides at the 3′ end of the genome, plus an indeterminate amount of poly(A) tail, sufficed to support negative-strand RNA synthesis (Lin *et al.*, 1994). From this result it was concluded that the promoter for negative-strand initiation lies completely within the last 55 nucleotides of the genome and that the remainder of the 3′ *cis*-acting element must be required for positive-strand RNA synthesis. Alternatively, the 3′-most 45–55 nucleotides of the genome may constitute the minimal region able to associate *in trans* with helper virus genome so as to allow initiation of negative-strand synthesis. A finer examination of the 3′ poly(A) tail requirement found that, for both MHV and BCoV DI RNAs, no fewer than 5–10 A residues are necessary for replication, and there is a correlation between DI RNA replication competence and the ability to bind poly(A)-binding protein (Spagnolo and Hogue, 2000).

Further investigation of the 3′ UTR in MHV and BCoV has produced a fairly complete picture of the RNA landscape of this region. At the upstream end of the 3′ UTR, two functionally essential structures have been demonstrated by chemical and enzymatic probing and by genetic studies with both DI RNAs and constructed viral mutants. The first structure is a bulged stem-loop (Hsue and Masters, 1997; Hsue *et al.*, 2000; Goebel *et al.*, 2004a); the second is an adjacent RNA pseudoknot (Goebel *et al.*, 2004a; Williams *et al.*, 1999). An intriguing property of these upstream RNA elements is that they partially overlap, that is, the bulged stem-loop and the pseudoknot would not be able to fold up simultaneously. It has thus been proposed that they constitute components of a molecular switch that is operative at some stage of RNA synthesis, although a target of their putative regulation has not yet been identified (Goebel *et al.*, 2004a). Further downstream in the MHV genome is a complex RNA secondary structural element that takes up most of the remainder of the 3′ UTR (Johnson *et al.*, 2005; Liu *et al.*, 2001). Although this structure is only poorly conserved with the structure predicted for the corresponding region of the BCoV 3′ UTR, mutations made in one stem that is highly conserved between the two viruses were found to be deleterious to DI RNA replication. Surprisingly, in the heart of this most divergent region of the 3′ UTR is found

an octanucleotide motif, 5′-GGAAGAGC-3′, that is absolutely conserved in the 3′ UTRs of all coronaviruses in all three groups.

The presence of the 3′ UTR stem-loop and pseudoknot appears to be a distinguishing feature of the group 2 coronaviruses. The group 1 coronaviruses all contain a highly conserved pseudoknot (Williams *et al.*, 1999), but no detectable counterpart of the bulged stem-loop in either upstream or downstream proximity to it. On the other hand, the group 3 coronaviruses have a highly conserved and functionally essential stem-loop (Dalton *et al.*, 2001), but merely a poor candidate for the pseudoknot structure can be found nearby (Williams *et al.*, 1999). Only the group 2 coronaviruses have both elements, and, in all cases, the elements overlap in the same fashion. Despite sequence divergence among the 3′ UTRs of group 2 coronaviruses, these genomic segments are functionally equivalent. The BCoV 3′ UTR was found to be able to entirely replace the MHV 3′ UTR (Hsue and Masters, 1997). Moreover, it was demonstrated that replication of a BCoV DI RNA could be supported by any of a number of closely related group 2 helper viruses, including MHV (Wu *et al.*, 2003). More strikingly yet, the SARS-CoV 3′ UTR was found to be able to entirely replace the MHV 3′ UTR (Goebel *et al.*, 2004b). Thus, the replicase machinery of a group 2 coronavirus, MHV, is able to recognize and use the 3′ *cis*-acting structures and sequences of other group 2 coronaviruses, BCoV and SARS-CoV. By contrast, the MHV 3′ UTR cannot be replaced with either the group 1 TGEV 3′ UTR or the group 3 IBV 3′ UTR.

Numerous investigations have focused on the intriguing nature of coronavirus sgRNA transcription. The sites of leader-to-body fusion in the sgRNAs occur at loci in the genome that contain a short run of sequence that is identical, or nearly identical, to the 3′ end of the leader RNA (Fig. 6). These sites are called transcription-regulating sequences (TRSs); they have also been designated transcription-associated sequences (TASs) or intergenic sequences (IGs or IGSs). TRSs are fairly well conserved within each coronavirus group. The core consensus TRS is 5′-AACUAAAC-3′ for group 1; 5′-AAUCUAAAC-3′ for group 2 (except for SARS-CoV, for which it is 5′-AAACGAAC-3′); and 5′-CUUAACAA-3′ for group 3 (Thiel *et al.*, 2003a; van der Most and Spaan, 1995). Not every TRS in a given virus conforms exactly to the consensus sequence; a number of allowable variant bases are found in individual TRSs.

It was clear from very early studies that the sgRNAs are formed by a discontinuous, cotranscriptional process and that they are not produced by splicing of a full-length genomic precursor (Jacobs *et al.*, 1981; Stern and Sefton, 1982). As for RNA replication, the first

systematic means of addressing the mechanism of transcription came from the manipulation of engineered DI RNAs. The efficiency of fusion at a given TRS was at first thought to be mediated solely by base-pairing between the 3′ end of the leader and the complement of the TRS. However, studies with DI RNAs containing authentic and mutated TRSs led many investigators to conclude that, beyond a minimum threshold of potential base pairing, other factors must predominate (Hiscox *et al.*, 1995; Makino *et al.*, 1991; van der Most *et al.*, 1994). DI RNA studies thus provided the first indication of the importance of the local sequence context of the TRS and the position of the TRS relative to the 3′ end of the genome (Joo and Makino, 1995; Krishnan *et al.*, 1996; Ozdarendeli *et al.*, 2001; van Marle *et al.*, 1995).

The original conceptual framework for many studies was that of leader-primed transcription. In this model, sgRNAs were envisioned to be generated during positive-strand RNA synthesis. It was proposed that the polymerase pauses near the end of the leader sequence and detaches with the nascent free leader RNA. This step is followed by reattachment of the leader RNA to the complement of a TRS at an internal portion of the negative-strand template, from where the nascent RNA is then elongated (Lai, 1986). A refinement of this idea was that leader-to-body fusion results from quasi-continuous synthesis across two distant portions of a looped-out template, which are brought together via protein-RNA and protein–protein interactions (Lai *et al.*, 1994; Zhang *et al.*, 1994).

More recently, accumulated experimental results, while retaining the notion of a looped-out template, have been taken to support a mechanism in which the discontinuous step in sgRNA synthesis occurs during negative-strand RNA synthesis (Fig. 7) (Sawicki and Sawicki, 1998, 2005). In this model, the viral polymerase, starting from the 3′ end of a genomic template, switches templates at an internal TRS and resumes synthesis at the homologous TRS sequence at the 3′ end of the genomic leader RNA. The resulting negative-strand sgRNA, in association with positive-strand gRNA, then serves as the template for synthesis of multiple copies of the corresponding positive-strand sgRNA. This new view originated with the discovery of negative-strand sgRNAs (Sethna *et al.*, 1989) and with the demonstration that free leader RNA could not be detected in infected cells (Chang *et al.*, 1994). Most (Baric and Yount, 2000; Sawicki and Sawicki, 1990; Sawicki *et al.*, 2001; Schaad and Baric, 1994), although not all (An and Makino, 1998; An *et al.*, 1998; Mizutani *et al.*, 2000), subsequent biochemical work supported the contention that the negative-strand sgRNA species are kinetically competent to serve as templates for

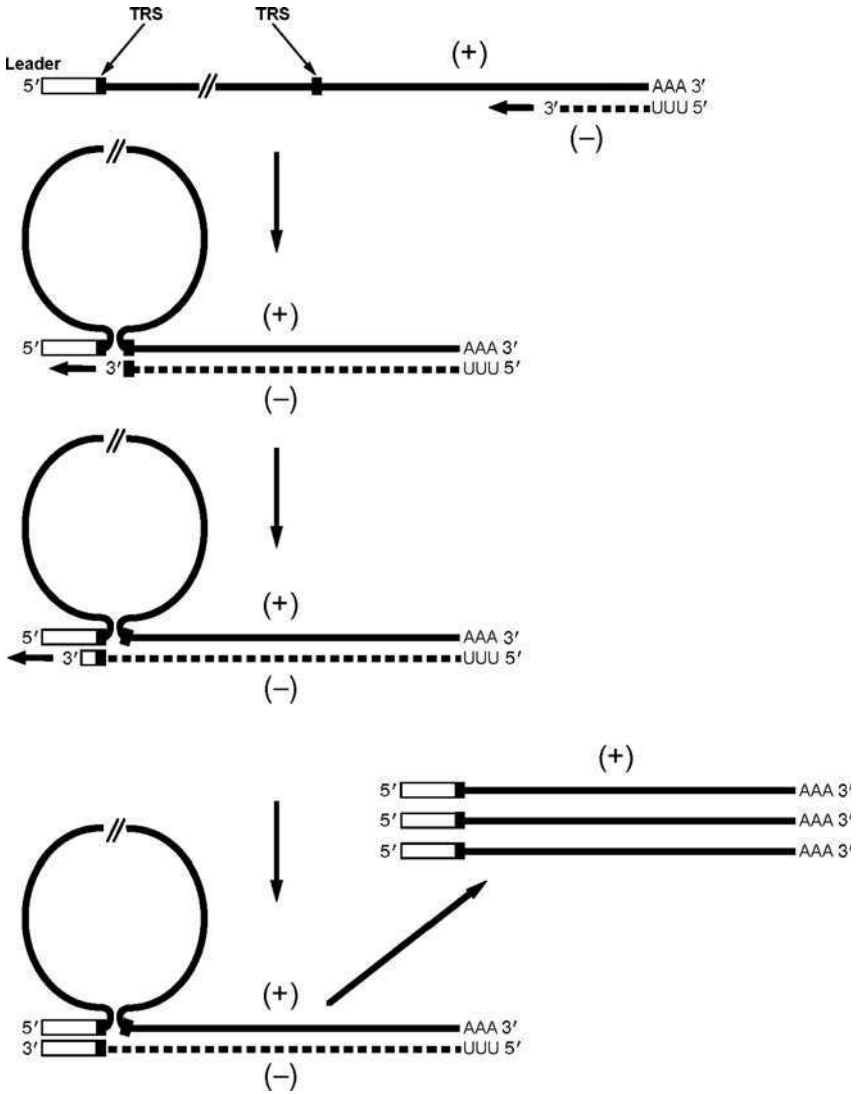

FIG 7. Model for discontinuous negative-strand transcription. Negative-strand sgRNAs are initiated at the 3′ end of the gRNA template. Elongation proceeds as far as a body copy of a transcription-regulating sequence (TRS). A strand-switching event then occurs, pairing the newly transcribed negative-sense body TRS with the leader copy of the TRS, from which point transcription resumes. A complex of the (+)gRNA and the (−)sgRNA then serves as the template for synthesis of multiple (+)sgRNAs.

positive-strand sgRNAs. In addition, some of the strongest evidence for negative-strand discontinuous sgRNA synthesis came from landmark studies using a full-length infectious cDNA of equine arterivirus, the prototype member of the closely related arterivirus family. This work made use of a robust system in which both the leader copy and one or multiple body copies of the TRS were singly or simultaneously mutated in the genome; RNA synthesis in this system was able to be assayed in the initial passage of infectious RNA (Pasternak *et al.*, 2001, 2003, 2004; van Marle *et al.*, 1999). The arterivirus results have been corroborated, in part, by experiments enabled by the development of reverse genetic approaches for TGEV and MHV (Alonso *et al.*, 2002; Curtis *et al.*, 2004; de Haan *et al.*, 2002a,b; Sola *et al.*, 2005; Zuniga *et al.*, 2004). At this time, there is a broad, but not universal, consensus that for coronaviruses, as well as for other nidoviruses, both replication and transcription initiate with negative-strand RNA synthesis. However, much further work needs to be done to elucidate the details of the template-switching step of discontinuous transcription. It will also be necessary to extend to the coronaviruses principles that have been more clearly established for the arteriviruses.

B. RNA Recombination

An important feature of coronavirus RNA synthesis is the high rate of homologous and nonhomologous RNA–RNA recombination that has been demonstrated to occur among selected and unselected markers during the course of infection. Although most experimental work in this area has been performed with MHV (Keck *et al.*, 1987, 1988a,b; Makino *et al.*, 1986, 1987), a high frequency of homologous recombination is clearly an attribute of the entire coronavirus family, given that it has been observed in other viruses in all three groups: TGEV (Sanchez *et al.*, 1999), FIPV (Haijema *et al.*, 2003; Herrewegh *et al.*, 1998), BCV (Chang *et al.*, 1996), and IBV (Cavanagh *et al.*, 1992; Kottier *et al.*, 1995; Kusters *et al.*, 1990; Wang *et al.*, 1993). In addition, nonhomologous recombination was likely, in all three groups, to be the mechanism of acquisition of the various accessory protein genes.

RNA recombination is thought to result from a copy-choice mechanism, as originally described for poliovirus (Kirkegaard and Baltimore, 1986). In this scheme, the viral polymerase, with its nascent RNA strand intact, detaches from one template and resumes elongation at the identical position, or a similar position, on another template. In MHV, recombination has been shown to take place along the entire length of the genome at an estimated frequency of 1% per 1.3 kb

(almost 25% over the entire genome), the highest rate observed for any RNA virus (Baric *et al.*, 1990). On a fine scale, the sites of recombination were seen to be random (Banner and Lai, 1991), although strong selective pressures were able to create the appearance of local clustering of recombinational hot spots in one study (Banner *et al.*, 1990). Some results suggest that the rate of recombination increases across the entire MHV genome, from 5′ to 3′ end (Fu and Baric, 1992, 1994). This gradient may result from homologous recombination between genomic and subgenomic RNAs, since the latter would provide a source of donor and acceptor templates that would become more numerous as a function of proximity to the 3′ end of the genome.

Most evidence supports a model for viral RNA recombination having three mechanistic requirements (Lai, 1992). First, the RNA polymerase must pause during synthesis. This may be an intrinsic property of the enzyme, or it may result from the enzyme encountering a template secondary structure that exceeds a certain stability threshold. Second, a new template must be in physical proximity. Third, some property of the new template must allow the transfer of the nascent RNA strand and the resumption of RNA synthesis. Alternatively, strand transfer could result from a processive mechanism that does not require polymerase dissociation (Jarvis and Kirkegaard, 1991). For poliovirus, classical experiments showed that RNA recombination occurs during negative-strand RNA synthesis (Kirkegaard and Baltimore, 1986), most likely because positive-strand acceptor templates far outnumber negative strands (Jarvis and Kirkegaard, 1992). The same is likely to be true for coronaviruses, since they, too, have a high ratio of positive-strand to negative-strand RNA (Sawicki and Sawicki, 1986, 1990; Sethna *et al*., 1989). Moreover, for MHV, most or all negative-strand RNA is found duplexed with positive-strand RNA (Lin *et al.*, 1994; Sawicki and Sawicki, 1986). Thus, there may be a bias toward negative-strand recombination simply because positive-strand RNA is the most available (single-stranded) acceptor template. However, instances of coronavirus homologous recombination that occurred during positive-strand RNA synthesis have been documented (Liao and Lai, 1992). Also, work with extremely defective MHV mutants has shown that sufficiently strong selective pressures can reveal unusual nonhomologous rearrangements, including recombination between negative- and positive-strand RNA, which are likely to be constantly occurring at a low frequency during viral RNA synthesis.

One form of nonhomologous recombination that occurs between genomic and subgenomic RNA has been hypothesized to result from the collapse of the transcription complex during negative-strand

discontinuous transcription (Kuo and Masters, 2002). Such a disruption, followed by resumption of replicative antigenome synthesis, would leave a partial copy of the leader sequence embedded at an internal point in the genome, near the junction between two genes. This type of recombinant was selected repeatedly in revertants of a severely impaired MHV M protein mutant. However, similar transcriptional collapse events may have been a significant factor in coronavirus evolution. Remnants of leader RNAs were found in the genomes of wild-type HCoV-OC43 (Mounir and Talbot, 1993) and in a mutant of MHV strain S (Taguchi *et al.*, 1994). Most strikingly, the recently described HCoV-HKU1 genome contains two very significant segments of embedded leader sequence (Woo *et al.*, 2005). Each of these leader remnants occurs at a site where there is an apparent deletion of an entire accessory gene, with respect to the genomic layouts of the closest relatives of this virus, MHV and BCoV.

C. Replicase Complex

1. Ribosomal Frameshifting

The replicase complex that carries out the intricacies of viral RNA replication and transcription is encoded by the first gene of the coronavirus genome. This huge gene occupies roughly two-thirds of the genome and contains two ORFs, the complete expression of which is dependent on a programmed ribosomal frameshift. The discovery of coronavirus ribosomal frameshifting resulted from the completion of the sequence of IBV, the first member of the family for which an entire genomic sequence was obtained (Brierley *et al.*, 1987). This revealed a small (43 nt) overlap between ORF 1a (11.9 kb) and ORF 1b (8.1 kb), the latter in the −1 frame relative to the former; moreover, there was no sgRNA that could serve as the mRNA for ORF 1b. This arrangement was subsequently found to exist for all coronaviruses. Thus, ribosomal frameshifting, which had previously been seen only in retroviruses (Jacks *et al.*, 1988), was proposed as a mechanism for expression of ORF 1b. Programmed frameshifting was demonstrated for the IBV gene *1a/1b* overlap region in reporter gene constructs in experiments using *in vitro* translation systems and, in some cases, cellular expression systems (Brierley *et al.*, 1989). In such systems, a frameshifting incidence of 25–30% was measured, representing an efficiency far greater than the 5% seen at the retroviral *gag-pol* junction. It should be noted, however, that the efficiency of *in vivo* frameshifting occurring in cells infected with IBV, or any other coronavirus,

has not yet been quantitated; nor is it known whether that value remains constant over the course of infection.

IBV ribosomal frameshifting was found to depend on two genomic RNA elements (Fig. 8): a heptanucleotide "slippery sequence" (UUUAAAC) and a downstream, hairpin-type pseudoknot (Brierley *et al.*, 1989). In addition, the spacing between these elements is critical. It is thought that the pseudoknot impedes the progress of the elongating ribosome. With some fixed probability, the delay required for the ribosome to melt out this secondary structural element allows the simultaneous slippage of the P and A site tRNAs by one base in the −1 direction. Normal translational elongation then resumes. Studies of the kinetics of translation, using a model mRNA based on the IBV frameshifting region, support the idea of ribosomal pausing at the pseudoknot (Somogyi *et al.*, 1993). Moreover, mutational studies of IBV frameshifting (Brierley *et al.*, 1989) and direct mass spectrometric analysis of the SARS-CoV frameshifted polypeptide product (Baranov *et al.*, 2005) have confirmed both the locus of the slippage site and the occurrence of simultaneous slippage. The reason why coronaviruses employ ribosomal frameshifting as a gene expression strategy is less well established at this time. The explanation most commonly given is that, as for retroviruses, the frameshifting mechanism provides a fixed ratio of translation products, in the necessary proximity of one another, for assembly into a macromolecular complex. It could also be speculated that frameshifting forestalls expression of the enzymatic

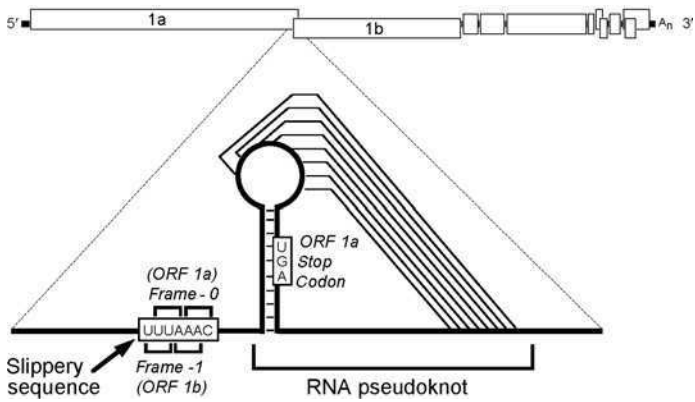

FIG 8. RNA elements required for ribosomal frameshifting. The expanded region shows RNA sequences and secondary structures that program the frameshift, using IBV as an example.

products of ORF 1b until a platform and a cellular environment for them have been prepared by the products of ORF 1a.

The two genomic components required for ribosomal frameshifting have been investigated in considerable detail. Exhaustive mutagenesis of the slippery sequence showed that frameshifting could be facilitated by a number of heptameric sequences of the form XXXYYYN, where XXX and YYY are the postslippage P and A site codons, respectively (Brierley *et al.*, 1992). Hierarchies of preferred combinations of X, Y, and N were defined, and these indicated a major role for the strength of the A-site tRNA interaction. However, although some heptanucleotides showed a frameshifting efficiency nearly as high as that of the wild type, it must be noted that, to date, all known coronaviruses have been found to contain a slippery sequence of UUUAAAC (Brian and Baric, 2005; Plant *et al.*, 2005).

The second component, the pseudoknot, has similarly been examined through exhaustive mutagenesis (Brierley *et al.*, 1991). Although the involvement of a downstream RNA secondary structural element in ribosomal frameshifting was first recognized with retroviruses (Jacks *et al.*, 1988), the earliest demonstration that the requisite structure is a pseudoknot came from the study of IBV (Brierley *et al.*, 1989). This demonstration was initially by classic stem replacement mutagenesis, and, subsequently, by intensive modification of pseudoknot elements; all of the results of both types of studies supported the proposed structure. It was also revealed that the length of stem 1 is very important for frameshifting efficiency (Napthine *et al.*, 1999) and that it is the structure, not the primary sequence, that is significant for both stems 1 and 2. Higher-order structure was also found to be critical: the pseudoknot could not be replaced by a single stem-loop of the same stability, containing the identical base pairs as the sum of the two pseudoknot stems (Brierley *et al.*, 1991).

The frameshifting signals of other coronaviruses have been found to generally conform to the rules defined for IBV, although additional complexities have emerged. With the completion of the genomic sequences of the group 1 coronaviruses HCoV-229E (Herold and Siddell, 1993) and TGEV (Eleouet *et al.*, 1995), an "elaborated" pseudoknot was proposed for members of this group, containing a third stem falling within an unusually large loop 2. It is currently unresolved whether the group 1 elaborated pseudoknot is the operative structure in frameshifting, as suggested by some mutational evidence (Herold and Siddell, 1993). By contrast, loop 2 can be assigned as for the other coronaviruses, with the extra group 1-specific element providing an alternative, long-range kissing loop interaction between the upstream

arm of pseudoknot stem 2 and the loop of a downstream stem-loop (Plant *et al.*, 2005). Analysis of the sequence of the frameshifting region of the SARS-CoV genome led to the prediction of a third stem-loop within loop 2 of the pseudoknot (Ramos *et al.*, 2004). This third element is situated differently from the additional stem of the group 1 elaborated pseudoknot, but it is similar to the potential bulged stem-loop that was earlier proposed to reside in loop 2 of the pseudoknot of the torovirus Berne virus (Snijder *et al.*, 1990). Further computational analysis has similarly found a possible third stem within loop 2 of the frameshifting pseudoknots of all coronaviruses, and the SARS-CoV stem 3 structure has been shown to be consistent with NMR data and nuclease mapping (Plant *et al.*, 2005). The role of stem 3 in ribosomal frameshifting is, as yet, unclear. Contrary to the previous results in the IBV system, mutagenesis studies suggest that both the primary sequence and the structures of the SARS-CoV stems 2 and 3 affect the efficiency of frameshifting (Baranov *et al.*, 2005; Plant *et al.*, 2005). On the other hand, the complete deletion of stem 3 is not detrimental to frameshifting. This seeming discrepancy has led to the suggestion that stem 3 plays an as yet undiscovered regulatory role, perhaps in the switch from genome translation to replication (Plant *et al.*, 2005).

2. Replicase Proteins

The end result of the ribosomal frameshifting-mediated translation of the replicase gene is the synthesis of two very large polyproteins, pp1a and pp1ab. These range from 440 to 500 kDa and from 740 to 810 kDa, respectively, and they are cotranslationally processed by two or three internally contained proteinase activities. The Herculean task of mapping all of the polyprotein processing events began at a time before investigators were even aware of the full sizes of coronavirus genomes (Denison and Perlman, 1986, 1987; Soe *et al.*, 1987). Only relatively recently have replicase cleavage maps been completed for at least one representative from each coronavirus group (Bonilla *et al.*, 1997; Kanjanahaluethai *et al.*, 2003; Lim and Liu, 1998; Liu *et al.*, 1998; Lu and Denison, 1997; Pinon *et al.*, 1997; Schiller *et al.*, 1998; Xu *et al.*, 2001; Ziebuhr and Siddell, 1999; Ziebuhr *et al.*, 2001). Knowledge gained from these efforts allowed the informed prediction (Snijder *et al.*, 2003; Thiel *et al.*, 2003a) and rapid experimental verification (Harcourt *et al.*, 2004; Prentice *et al.*, 2004b) of the processing pathway for the SARS-CoV replicase.

The final products of the autoproteolytic cleavage of pp1a and pp1ab are 16 nonstructural proteins, designated nsp1–nsp16 (Fig. 9).

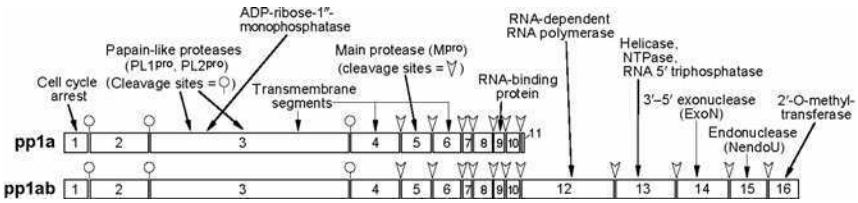

FIG 9. Protein products of the replicase gene. Cleavage sites and processed products of pp1a (nsp1–nsp11) and of pp1ab (nsp1–nsp10, nsp12–nsp16) are shown. Predicted and/or experimentally demonstrated activities are indicated.

Nsp1–nsp11 are derived from pp1a, whereas nsp1–nsp10 and nsp12–nsp16 are derived from pp1ab. Thus, all products processed from pp1a are common to those processed from pp1ab, except for nsp11, which is an oligopeptide generated when ribosomal frameshifting does not occur. For IBV, which lacks a counterpart of nsp1, there are 15 final products of polyprotein cleavage. These are numbered beginning with nsp2, in order to maintain correspondence with their homologs in the other coronaviruses. Comparative layouts and processing schemes for the replicase genes of all three coronavirus groups can be found in the review by Ziebuhr (2005) and references therein. Detailed lists and schematics of cleavage sites, the proteinases responsible, and the resulting nsp products for HCoV-229E, MHV, and IBV can be found in Table 2 and Figure 2 of the review by Ziebuhr *et al.* (2000). It should be noted that partial proteolytic products may also be significant in the processing scheme. The efficiency of cleavage at particular polyprotein sites may be regulated by both the exact primary sequence at the site and the site's accessibility to the proteinase (Ziebuhr, 2005; Ziebuhr *et al.*, 2000).

Elucidation of the precise roles of nsp1–nsp16 will be the next major undertaking. Functions for many domains of the coronavirus replicase were predicted by pioneering bioinformatics methods well before the term "bioinformatics" was invented (Gorbalenya *et al.*, 1989; Lee *et al.*, 1991). While knowledge about many of the replicase proteins is still at a very early stage, substantial progress has been made for others. Research in this field is proceeding at an unprecedented pace for reasons of both opportunity and necessity. First, tools that were not previously available, most notably reverse genetics systems for the replicase gene, are now at the disposal of coronavirus researchers. Second, the replicase products present a wide array of promising targets for anti-SARS therapeutics. The information that is currently at hand points to a correspondence between the genomic order of the

encoded activities of the replicase gene and the temporal program of infection. The products of pp1a appear to function to prepare the cell for infection and to assemble the machinery for RNA synthesis. Then, the products that are unique to pp1ab carry out the actual catalysis of RNA replication and transcription.

The very first mature translation product for MHV pp1a, nsp1, has been shown to play a role in cell cycle arrest. It may thus prepare a favorable cellular environment for viral replication (Chen and Makino, 2004; Chen *et al.*, 2004). The next cleavage product, nsp2, diverges considerably among different coronaviruses, and no function for it has yet been predicted or demonstrated. Surprisingly, deletion of the complete nsp2 region from the genome of MHV or SARS-CoV was not lethal. However, nsp2 deletion mutants showed delayed viral growth kinetics (Graham *et al.*, 2005). Other early replicase products are the enzymes that carry out the processing of the polyproteins: papain-like proteinases, which are in nsp3 (Baker *et al.*, 1993), and the main proteinase, which is in nsp5 (Lu *et al.*, 1995). Most coronaviruses have two papain-like proteinases, designated $PL1^{pro}$ and $PL2^{pro}$. By contrast, IBV and SARS-CoV have a single PL^{pro}. $PL1^{pro}$ and $PL2^{pro}$ may have arisen by duplication, and *in vitro*, they appear to have some redundancy in their activities. However, for HCoV-229E, a genetic analysis showed that $PL2^{pro}$ is essential, and the presence of both $PL1^{pro}$ and $PL2^{pro}$ was found to confer a clear advantage in viral fitness (Thiel and Siddell, 2005). In addition to the papain-like proteinases, nsp3 in many coronaviruses contains a domain that harbors ADP-ribose-1″-monophosphatase activity (Putics *et al*., 2005). The construction of active-site mutants has shown that this activity is dispensable for replication of HCoV-229E in tissue culture. Although the cellular homolog of this enzyme plays a role in tRNA processing, the biological significance of the virally encoded activity is unknown. Nsp3 can also contain some variable domains. In HCoV-HKU1, as many as 14 tandem repeats of an acidic decapeptide are present in an amino-terminal segment of nsp3 (Woo *et al.*, 2005 [note: nsp3 is misidentified as nsp1 in this reference]). In SARS-CoV, nsp3 contains a "SARS-unique" domain that is not found in any other coronavirus (Snijder *et al.*, 2003).

The coronavirus main proteinase, designated M^{pro}, constitutes all of nsp5. This enzyme has also been called the 3C-like proteinase ($3CL^{pro}$), because of its resemblance to the 3C proteinases of picornaviruses. Crystal structures have been solved for M^{pro} for HCoV-229E (Anand *et al.*, 2002), TGEV (Anand *et al.*, 2003), and SARS-CoV (Yang *et al.*, 2003). These reveal that M^{pro} is a dimer, each monomer of which has a three-domain structure, with an active site located in a cleft between

the first and second domains in each monomer. At the carboxy terminus is an extra domain not found in the $3CL^{pro}$ of other viral families. Multiple structures determined for the SARS-CoV M^{pro} showed that the entire molecule undergoes major pH-dependent conformational changes, which have been proposed to regulate activity.

At the carboxy-terminal end of pp1a is a cluster of small proteins, nsp7–nsp10. The crystal structure of SARS-CoV nsp9 was solved independently by two groups (Egloff *et al*., 2004; Sutton *et al*., 2004). In addition, prompted by features of the structure, investigators found that nsp9 has nonspecific RNA-binding activity. Biophysical evidence has also been presented for an interaction between nsp9 and nsp8 (Sutton *et al*., 2004). Therefore, although nsp9 was found to occur as a dimer in the crystals, its natural binding partner may be nsp8. A solution structure for SARS-CoV nsp7 was determined by NMR; this structure showed potential protein–protein interaction surfaces for this small polypeptide (Peti *et al*., 2005). Moreover, a cocrystal structure of SARS-CoV nsp7 with nsp8 revealed a complex of eight monomers of each protein forming a hollow cylindrical structure. This hexadecameric assembly was proposed to be able to encircle an RNA template, possibly acting as a processivity factor for the RNA polymerase (Zhai *et al*., 2005). Thus, a picture of a putative complex of all four of the nsp7–nsp10 polypeptides is being gradually pieced together, but, as yet, there is a paucity of functional data to complement this wealth of structural information.

Transmembrane domains in nsp3, nsp4, and nsp6 anchor the replicase complex to intracellular membranes, and these proteins may be involved in the remodeling of the latter, to form double-membrane compartments that are dedicated to viral RNA synthesis (Bi *et al.*, 1999; Gosert *et al.*, 2002; Prentice *et al.*, 2004a; Shi *et al.*, 1999; van der Meer *et al.*, 1999). These double-membrane vesicles, which colocalize with nascent viral RNA, are distinct from the sites of virion assembly and budding. Coronavirus RNA synthesis may thus take place in structures that are similar to the autophagosomal RNA synthesis compartments that have been characterized in picornavirus-infected cells (Jackson *et al.*, 2005). The nsp7–nsp10 products localize in discrete perinuclear and cytoplasmic foci in infected cells (Bost *et al.*, 2000), in a membrane-associated complex that also includes nsp2. This complex colocalizes with N protein and the viral helicase (nsp13) early in infection. However, late in infection, N protein and the helicase segregate into biochemically distinct membranes in the ERGIC that also contain M protein, suggesting a role for the helicase in genome encapsidation or packaging (Bost *et al.*, 2001; Sims *et al.*, 2000).

The postribosomal frameshift products of the replicase, nsp12–nsp16, contain the actual enzymes of RNA replication and transcription. The coronavirus RNA-dependent RNA polymerase (RdRp) is contained within nsp12, the first part of pp1ab synthesized after frameshifting. This protein has the fingers, palm, and thumb domains common to a number of viral RdRps and reverse transcriptases. In addition, the RdRp contains a very large, amino-terminal domain that is unique to the coronaviruses. For MHV, the ability of the RdRp to associate with intracellular membranes was mapped to a 38-amino acid segment of the unique domain (Brockway *et al.*, 2003). Membrane association of expressed RdRp also depended on MHV infection, indicating that other viral components are required for this targeting. In addition, the RdRp was shown to form intermolecular associations with M^{pro}, nsp8, and nsp9. For the SARS-CoV RdRp, preliminary biochemical characterization of the bacterially expressed enzyme suggests that the coronavirus-unique domain is essential for activity (Cheng *et al.*, 2005).

Nsp13 contains multiple activities that have been extensively characterized for HCoV-229E and SARS-CoV (Ivanov and Ziebuhr, 2004; Ivanov *et al.*, 2004a; Seybert *et al.*, 2000). This protein is a helicase with a highly processive duplex unwinding activity for both DNA and RNA substrates. The nsp13 helicase unwinds with 5′–3′ polarity, suggesting that it has a role in preparing the template for the RdRp. Nsp13 also has RNA-dependent NTPase and dNTPase activities, which probably provide the energy for its translocation along RNA templates. In addition, nsp13 is a RNA 5′-triphosphatase, making it a candidate to carry out the initial step of RNA capping.

Nsp14 and nsp15 have each been assigned ribonucleolytic functions. Such activities would, at first glance, seem to be out of place in an RNA virus. Nsp14 has been predicted to be an exonuclease (designated ExoN), which, it is speculated, could be involved in an RNA processing step integral to coronavirus transcription (Snijder *et al.*, 2003). This activity has not yet been demonstrated, but a point mutation in nsp14 of MHV was shown to be markedly attenuating in the mouse host (Sperry *et al.*, 2005). Nsp15 is an endoribonuclease, designated NendoU, that is found only in the nidoviruses (Snijder *et al.*, 2003). This enzyme, from HCoV-229E and SARS-CoV, has been shown to hydrolyze both single- and double-stranded RNA, with a specificity for cleavage immediately upstream and downstream of uridylate residues (Bhardwaj *et al.*, 2004; Ivanov *et al.*, 2004b). NendoU exhibited optimal activity with manganese ion, rather than magnesium ion, and it was essentially inactive with 2′-*O*-ribose-methylated RNA

substrates (Ivanov *et al*., 2004b). Mutation of the active site of nsp15 of HCoV-229E was found to be lethal.

Finally, nsp16, the carboxy-terminal product of pp1ab, has been predicted to contain 2′-*O*-methyltransferase activity (Snijder *et al*., 2003; von Grotthuss *et al.*, 2003 [note: nsp16 is misidentified as nsp13 in this reference]). Such an activity, which has not yet been demonstrated, would have a most obvious role in RNA capping. However, the possibility has been raised that 2′-*O*-methylation serves to protect a segment of duplex RNA from the NendoU activity of nsp15 in one stage of discontinuous negative-strand RNA synthesis (Ivanov *et al*., 2004b). Relevant to RNA capping, it must be noted that if coronaviruses possess their own guanylyltransferase or cap 7-methyltranferase activities, these have not yet been identified among the many replicase proteins.

3. Host Factors

RNA viruses often expropriate and redirect host cell components, to assist in mechanisms of their own gene expression (Ahlquist *et al*., 2003). A number of host factors have been proposed to participate in coronavirus RNA synthesis. To date, all of these have been discovered with either MHV or BCoV, and all were originally identified on the basis of their ability to bind *in vitro* to RNA segments of functional importance. The most completely characterized coronavirus host factor is heterogeneous nuclear ribonucleoprotein A1 (hnRNP A1), which was initially found as a member of a set of proteins that bound to the negative strand of the MHV TRS (Furuya and Lai, 1993; Li *et al.*, 1997; Zhang and Lai, 1995). Its RNA-binding property, its affinity for MHV N protein, and its propensity to dimerize, all made hnRNP A1 attractive as a potential mediator of the antigenome looping-out event envisaged by the leader-primed transcription model (Wang and Zhang, 1999; Zhang and Lai, 1995; Zhang *et al*., 1999). Overexpression of hnRNP A1 was shown to result in a marked increase in the kinetics of MHV RNA synthesis, suggesting that this factor affects genome replication as well as transcription. Additionally, expression of a truncated form of hnRNP A1 had a dominant-negative effect on MHV replication (Shi *et al*., 2000). The role of hnRNP A1 was questioned on the basis of the finding that MHV replication and RNA synthesis were completely unimpaired in CB3 cells, a mutant murine cell line that does not express hnRNP A1 (Ben-David *et al.*, 1992; Shen and Masters, 2001). In addition, high-affinity hnRNP A1 binding sites (Burd and Dreyfuss, 1994), when placed in the MHV genome, did not act in lieu of a TRS and did not displace the site of leader-body fusion away from a

TRS (Shen and Masters, 2001). However, it was subsequently shown that other hnRNP A/B family members, which are present in CB3 cells, could replace hnRNP A1; further, overexpression of hnRNP A/B was shown to enhance MHV RNA synthesis (Shi *et al*., 2003).

Other members of the hnRNP family have also been implicated in MHV RNA synthesis. Pyrimidine tract-binding protein (PTB, also known as hnRNP I) was shown to bind to pentanucleotide repeats upstream of the positive-strand leader copy of the TRS (Li *et al.*, 1999). In addition, PTB bound the negative strand of the 3′ UTR, specifically at the complement of the invariant octanucleotide motif (Huang and Lai, 1999). The positive strand of the same region of the 3′ UTR was also bound by hnRNP A1, and deletions in this region inhibited DI RNA synthesis (Huang and Lai, 2001). Another hnRNP, synaptotagmin-binding cytoplasmic RNA-interacting protein (SYNCRIP), was found to bind to both positive- and negative-strand MHV RNA near the region of the leader pentanucleotide repeats (Choi *et al.*, 2004). Moreover, RNAi-mediated downregulation of SYNCRIP delayed the kinetics of MHV RNA synthesis. In the BCoV 5′ UTR, multiple complexes of six proteins have been found to bind specifically to the stem-loop IV that is required for DI RNA replication (Raman and Brian, 2005). It is not yet clear whether some of these proteins are previously identified hnRNPs or whether they represent new cellular factors.

In the 3′ UTR of MHV, a complex of proteins was found to bind to two similar 11-base motifs in positive-strand RNA, at distances of 26–36 and 129–139 nucleotides from the poly(A) tail (Liu *et al.*, 1997; Yu and Leibowitz, 1995a,b). DI RNAs with mutations in either of these elements were defective in replication. The largest member of the protein complex was identified as mitochondrial aconitase, a protein not previously known to have RNA-binding activity (Nanda and Leibowitz, 2001). Other components of the complex were then found to be the chaperones HSP60, HSP40, and mitochondrial HSP70 (Nanda *et al*., 2004). Although MHV replication does not have any known involvement with mitochondria, both mitochondrial aconitase and mitochondrial HSP70 have substantial cytoplasmic fractions. Finally, at the furthest downstream ends of the genomes of MHV and BCoV, poly(A) binding protein binds to the poly(A) tail and appears to play a role in RNA synthesis beyond its function in translation (Spagnolo and Hogue, 2000).

Among the array of candidate host factors in coronavirus RNA synthesis, it remains to be established which are essential and which play enhancing roles, either as RNA chaperones or in some other capacity.

Such assessments can be difficult, because many of these factors are critical or essential to normal cellular functions. Thus, the validation of host factors will likely require the establishment of an efficient *in vitro* RNA replication and transcription system, in which reconstitution of coronavirus RNA synthesis can be achieved from isolated components and precursors.

VI. Genetics and Reverse Genetics

Numerous classical coronavirus mutants have been isolated over the past 25 years, mainly with MHV (Lai and Cavanagh, 1997). Mutants were either identified as naturally occurring viral variants (often on the basis of causing atypical pathogenesis), or else they were obtained through selection criteria such as escape from neutralization by monoclonal antibodies. A number of sets of MHV mutants were generated by chemical mutagenesis, followed by screening for temperature-sensitive phenotypes (Koolen *et al.*, 1983; Martin *et al.*, 1988; Robb *et al.*, 1979; Schaad *et al.*, 1990) or, in one case, for aberrant cytopathic effects or plaque morphologies (Sturman *et al.*, 1987). Although the latter search yielded an unusually high proportion of structural protein mutants, viruses with conditionally lethal, RNA-negative phenotypes were the predominant isolates in all searches. The arrangement of the coronavirus genome dictates that the vast majority of randomly generated mutations will fall in the replicase gene, owing to its large target size. Despite assiduous efforts that applied classical genetic methods to the study of the replicase (Baric *et al.*, 1990; Fu and Baric, 1992, 1994; Schaad *et al.*, 1990), progress was limited by the technology available at the time, and exploitation of the full value of these mutants would await the development of reverse genetic techniques.

The basic blueprint for positive-strand RNA virus reverse genetics—the transcription of infectious RNA from a full-length cDNA copy of the viral genome—was established more than two decades ago with poliovirus (Racaniello and Baltimore, 1981). It became possible only recently to apply this scheme to coronaviruses, however, owing to the need to surmount a number of formidable hurdles. Most notable were the obstacles posed by the huge sizes of coronavirus genomes and the high instabilities of various regions of the replicase gene when they were propagated as cloned cDNA in *E. coli*. The first reverse genetic system for coronaviruses, targeted RNA recombination, was developed to circumvent these barriers, at a time when it was far from clear whether the construction of full-length infectious cDNA clones would ever be

technically feasible (Masters, 1999; Masters and Rottier, 2005). This method, originally developed in MHV, takes advantage of the high rate of homologous RNA recombination in coronaviruses. A synthetic donor RNA bearing the mutation of interest is introduced into cells that have been infected with a recipient parent virus possessing some characteristic that can be selected against. Mutant recombinants that arise among progeny viruses are then identified by counterselection of the recipient parent virus.

The earliest form of targeted RNA recombination employed, as the recipient parent virus, a classical MHV mutant that was thermolabile owing to an internal deletion in the *N* gene (Koetzner *et al.*, 1992; Peng *et al.*, 1995a), which is the 3′-most gene in the genome. Mutations were introduced into the *N* gene or the 3′ UTR by means of *in vitro*-synthesized donor RNAs corresponding to the smallest MHV sgRNA. Recombinants, which were identified as survivors of a heat-killing selection, had restored the region deleted in the parent virus and, concomitantly, had acquired marker mutations planted in the donor RNA. The efficiency of this system was subsequently increased by the incorporation of 5′-*cis*-acting elements that converted the donor RNA into a replicating DI RNA (Masters *et al.*, 1994; van der Most *et al.*, 1992). The scope of this technique was then extended through the addition of 3′-contiguous genomic sequence to donor RNAs, ultimately allowing reverse-genetic access to all of the structural genes of MHV (Fischer *et al.*, 1997a,b, 1998; Peng *et al.*, 1995b). The strength and versatility of targeted RNA recombination were substantially enhanced as a result of the construction of the interspecies coronavirus mutant fMHV, a chimera in which the S protein ectodomain of MHV was replaced by the S protein ectodomain from FIPV (Kuo *et al.*, 2000). This replacement resulted in a virus that had acquired the ability to grow in feline cells and had simultaneously lost the ability to grow in murine cells. Although the immediate rationale for the creation of fMHV was to dissect domain requirements for virion assembly (Section IV.B.2), it was readily apparent that this chimera offered a tremendous selective advantage in targeted RNA recombination. The use of fMHV as the recipient parent virus allowed the selection of recombinants harboring virtually any nonlethal MHV mutation in the 3′-most 10 kb of the genome, on the basis of their having regained the ability to grow in murine cells. Numerous mutants, many with extremely fragile phenotypes, have since been obtained by this method (de Haan *et al.*, 2002a,b; Goebel *et al.*, 2004a,b; Hurst *et al.*, 2005; Kuo *et al.*, 2002, 2003). The generality of this host-range-based selection system has been established by the extension of the method to another strain of

MHV (Ontiveros *et al.*, 2001) and by use of an analogous chimera, mFIPV, for the construction of FIPV mutants (Haijema *et al.*, 2003, 2004).

Despite its value, however, targeted RNA recombination can be used to engineer only the downstream one-third of the genome. The complete extent of reverse genetics did not become available to coronavirus research until relatively recently. Through the exceptional perseverance and inventiveness of three independent laboratories, systems based on full-length cDNA clones have been developed, each using a different strategy to overcome the stability problems inherent to coronavirus cDNA. These systems all provide a capability of great importance that is effectively beyond the scope of targeted RNA recombination: access to the replicase gene. In the first such method (Enjuanes *et al.*, 2005), a full-length cDNA copy of the TGEV genome was assembled in a low copy-number bacterial artificial chromosome (BAC) vector. Infectious coronavirus RNA was produced in this system by a "DNA-launch," *in vivo* nuclear transcription by host RNA polymerase II from an engineered CMV promoter (Almazan *et al.*, 2000). The DNA launch ensured complete capping of the viral RNA, and it bypassed potential limitations of the system arising from the efficiency of *in vitro* transcription of genomic RNA. Heterologous sequence was removed from the 3′ end of the transcribed RNA through the action of an incorporated hepatitis delta virus ribozyme. Further stabilization of the full-length BAC clone in bacteria was achieved through the insertion of a eukaryotic intron into either of two positions in the mapped toxic region of the TGEV cDNA (González *et al.*, 2002). This allowed stable propagation of the BAC for over 200 bacterial generations.

In the second method, full-length genomic cDNAs were assembled by *in vitro* ligation of smaller, more stable subcloned cDNAs (Baric and Sims, 2005). Infectious RNA was then transcribed *in vitro* from the ligated product. The boundaries of the subcloned genomic cDNA fragments were chosen so as to allow ease of manipulation for site-directed mutagenesis applications. Most importantly, some fragment boundaries were arranged in such a way as to interrupt regions of cloned cDNA instability. This is essentially the same scheme that had been earlier used to produce infectious RNA for yellow fever virus, a flavivirus (Rice *et al*., 1989). However, for coronaviruses, the scheme had to be executed on a much grander scale, with five to seven fragments instead of two. To facilitate this approach, the innovation was introduced of directing the unique assembly of fragments by means of nonsymmetric overhangs generated by restriction enzymes that cut

at a distance from their recognition sequences. This ensured that the fragments became connected in a predetermined order by ligation, without the generation of rearranged byproducts. Originally demonstrated with TGEV (Yount *et al.*, 2000), this *in vitro* assembly technique has subsequently been successfully used to engineer the genomes of MHV (Yount *et al.*, 2002), SARS-CoV (Yount *et al.*, 2003), and IBV (Youn *et al.*, 2005).

In the third method, entire coronavirus cDNAs, generated by long-range RT-PCR (Thiel *et al.*, 1997), were inserted into a unique restriction site in the genome of vaccinia virus (Thiel and Siddell, 2005). In this scheme, vaccinia virus served as a huge cloning vehicle, in which the coronavirus genome cDNAs did not exhibit the instabilities encountered in *E. coli* plasmids. Infectious RNA was produced by *in vitro* transcription from purified vaccinia virus DNA (Thiel *et al.*, 2001a). Alternatively, a DNA launch was carried out *in vivo* with transfected cDNA and fowlpox-encoded T7 RNA polymerase (Casais *et al.*, 2001). The use of vaccinia as a vector has allowed manipulation of the resulting cloned cDNA by any among the suite of methods that have been developed for poxvirus reverse genetics. In particular, transient dominant selection has been used to carry out site-directed mutagenesis (Britton *et al.*, 2005). Engineered mutations have also been directly recombined from PCR products into vaccinia clones, through exploitation of both negative and positive selection of a *gpt* cassette (Coley *et al.*, 2005). A further innovation came from the rescue of recombinant coronaviruses from cell lines expressing N protein, given that N protein has been shown to greatly enhance recovery of virus in all three full-length cDNA systems (Almazan *et al.*, 2004; Schelle *et al.*, 2005; Thiel *et al.*, 2001a; Yount *et al.*, 2002). This poxvirus-vectored technique was originally applied to HCoV-229E (Thiel *et al.*, 2001a), and it has since been used to engineer the genomes of IBV (Casais *et al.*, 2001) and MHV (Coley *et al.*, 2005).

The two main options for reverse genetic systems both have their own relative advantages. For reverse genetic studies involving coronavirus structural genes or the 3′ UTR, targeted RNA recombination is currently the easier system to manipulate, and it has the power to recover extremely defective mutants. Another asset of targeted RNA recombination is that it lends itself well to studies involving domain exchange between different proteins (Peng *et al.*, 1995b) or the exchange of genomic elements (Hsue and Masters, 1997). In these cases, the system, through its own selection of allowable crossover sites, can reveal which substitutions retain functionality and which are lethal. On the other hand, full-length cDNA reverse-genetic strategies provide

the capacity to site-specifically mutagenize the exceedingly large viral RNA replicase gene. This advantage is just beginning to be exploited, and it can be expected to play a major role in the future in the acquisition of an understanding of the workings of the complex RNA synthesis machinery. In addition to molecular biological studies, coronavirus reverse-genetic investigations have opened the door to the development of these viruses, and their derivative replicons, for vaccines (Alonso *et al.*, 2002; Haijema *et al.*, 2004), expression systems (de Haan *et al.*, 2003b, 2005), and gene delivery vectors (Thiel *et al.*, 2001b, 2003b).

Acknowledgments

I am indebted to Lawrence Sturman for first telling me what coronaviruses are and why I should care. I am grateful to Adriana Verschoor, Wadsworth Center Publications Editor, for improving the style and accuracy of the manuscript. This work was supported in part by Public Health Service grants AI 45695, AI 60755, and AI 64603 from the National Institutes of Health.

References

Abraham, S., Kienzle, T. E., Lapps, W., and Brian, D. A. (1990). Deduced sequence of the bovine coronavirus spike protein and identification of the internal proteolytic cleavage site. *Virology* **176:**296–301.

Ahlquist, P., Noueiry, A. O., Lee, W. M., Kushner, D. B., and Dye, B. T. (2003). Host factors in positive-strand RNA virus genome replication. *J. Virol.* **77:**8181–8186.

Almazan, F., Gonzalez, J. M., Penzes, Z., Izeta, A., Calvo, E., Plana-Duran, J., and Enjuanes, L. (2000). Engineering the largest RNA virus genome as an infectious bacterial artificial chromosome. *Proc. Natl. Acad. Sci. USA* **97:**5516–5521.

Almazan, F., Galan, C., and Enjuanes, L. (2004). The nucleoprotein is required for efficient coronavirus genome replication. *J. Virol.* **78:**12683–12688.

Almeida, J. D., and Tyrrell, D. A. (1967). The morphology of three previously uncharacterized human respiratory viruses that grow in organ culture. *J. Gen. Virol.* **1:**175–178.

Almeida, J. D., Berry, D. M., Cunningham, C. H., Hamre, D., Hofstad, M. S., Mallucci, L., McIntosh, K., and Tyrrell, D. A. J. (1968). Coronaviruses. *Nature* **220:**650.

Alonso, S., Sola, I., Teifke, J. P., Reimann, I., Izeta, A., Balasch, M., Plana-Duran, J., Moormann, R. J., and Enjuanes, L. (2002). *In vitro* and *in vivo* expression of foreign genes by transmissible gastroenteritis coronavirus-derived minigenomes. *J. Gen. Virol.* **83:**567–579.

An, S., and Makino, S. (1998). Characterizations of coronavirus *cis*-acting RNA elements and the transcription step affecting its transcription efficiency. *Virology* **243:**198–207.

An, S., Maeda, A., and Makino, S. (1998). Coronavirus transcription early in infection. *J. Virol.* **72:**8517–8524.

Anand, K., Palm, G. J., Mesters, J. R., Siddell, S. G., Ziebuhr, J., and Hilgenfeld, R. (2002). Structure of coronavirus main proteinase reveals combination of a chymotrypsin fold with an extra alpha-helical domain. *EMBO J.* **21:**3213–3224.

Anand, K., Ziebuhr, J., Wadhwani, P., Mesters, J. R., and Hilgenfeld, R. (2003). Coronavirus main proteinase (3CLpro) structure: Basis for design of anti-SARS drugs. *Science* **300:**1763–1767.

Arbely, E., Khattari, Z., Brotons, G., Akkawi, M., Salditt, T., and Arkin, I. T. (2004). A highly unusual palindromic transmembrane helical hairpin formed by SARS coronavirus E protein. *J. Mol. Biol.* **341:**769–779.

Armstrong, J., Niemann, H., Smeekens, S., Rottier, P., and Warren, G. (1984). Sequence and topology of a model intracellular membrane protein, E1 glycoprotein, from a coronavirus. *Nature* **308:**751–752.

Babcock, G. J., Esshaki, D. J., Thomas, W. D., Jr., and Ambrosino, D. M. (2004). Amino acids 270 to 510 of the severe acute respiratory syndrome coronavirus spike protein are required for interaction with receptor. *J. Virol.* **78:**4552–4560.

Baker, S. C., Yokomori, K., Dong, S., Carlisle, R., Gorbalenya, A. E., Koonin, E. V., and Lai, M. M. C. (1993). Identification of the catalytic sites of a papain-like cysteine proteinase of murine coronavirus. *J. Virol.* **67:**6056–6063.

Banner, L. R., and Lai, M. M. C. (1991). Random nature of coronavirus RNA recombination in the absence of selective pressure. *Virology* **185:**441–445.

Banner, L. R., Keck, J. G., and Lai, M. M. C. (1990). A clustering of RNA recombination sites adjacent to a hypervariable region of the peplomer gene of murine coronavirus. *Virology* **175:**548–555.

Baranov, P. V., Henderson, C. M., Anderson, C. B., Gesteland, R. F., Atkins, J. F., and Howard, M. T. (2005). Programmed ribosomal frameshifting in decoding the SARS-CoV genome. *Virology* **332:**498–510.

Baric, R. S., and Sims, A. C. (2005). Development of mouse hepatitis virus and SARS-CoV infectious cDNA constructs. *Curr. Top. Microbiol. Immunol.* **287:**229–252.

Baric, R. S., and Yount, B. (2000). Subgenomic negative-strand RNA function during mouse hepatitis virus infection. *J. Virol.* **74:**4039–4046.

Baric, R. S., Nelson, G. W., Fleming, J. O., Deans, R. J., Keck, J. G., Casteel, N., and Stohlman, S. A. (1988). Interactions between coronavirus nucleocapsid protein and viral RNAs: Implications for viral transcription. *J. Virol.* **62:**4280–4287.

Baric, R. S., Fu, K., Schaad, M. C., and Stohlman, S. A. (1990). Establishing a genetic recombination map for murine coronavirus strain A59 complementation groups. *Virology* **177:**646–656.

Baric, R. S., Yount, B., Hensley, L., Peel, S. A., and Chen, W. (1997). Episodic evolution mediates interspecies transfer of a murine coronavirus. *J. Virol.* **71:**1946–1955.

Baric, R. S., Sullivan, E., Hensley, L., Yount, B., and Chen, W. (1999). Persistent infection promotes cross-species transmissibility of mouse hepatitis virus. *J. Virol.* **73:**638–649.

Baudoux, P., Carrat, C., Besnardeau, L., Charley, B., and Laude, H. (1998). Coronavirus pseudoparticles formed with recombinant M and E proteins induce alpha interferon synthesis by leukocytes. *J. Virol.* **72:**8636–8643.

Becker, W.B, McIntosh, K., Dees, J. H., and Chanock, R. M. (1967). Morphogenesis of avian infectious bronchitis virus and a related human virus (strain 229E). *J. Virol.* **1:**1019–1027.

Benbacer, L., Kut, E., Besnardeau, L., Laude, H., and Delmas, B. (1997). Interspecies aminopeptidase-N chimeras reveal species-specific receptor recognition by canine coronavirus, feline infectious peritonitis virus, and transmissible gastroenteritis virus. *J. Virol.* **71:**734–737.

Ben-David, Y., Bani, M.-R., Chabot, B., De Koven, A., and Bernstein, A. (1992). Retroviral insertions downstream of the heterogeneous nuclear ribonucleoprotein A1 gene in erythroleukemia cells: Evidence that A1 is not essential for cell growth. *Mol. Cell. Biol.* **12:**4449–4455.

Berry, D. M., Cruickshank, J. G., Chu, H. P., and Wells, R. J. (1964). The structure of infectious bronchitis virus. *Virology* **23:**403–407.

Bhardwaj, K., Guarino, L., and Kao, C. C. (2004). The severe acute respiratory syndrome coronavirus Nsp15 protein is an endoribonuclease that prefers manganese as a cofactor. *J. Virol.* **78:**12218–12224.

Bi, W., Pinon, J. D., Hughes, S., Bonilla, P. J., Holmes, K. V., Weiss, S. R., and Leibowitz, J. L. (1999). Localization of mouse hepatitis virus open reading frame 1A derived proteins. *J. Neurovirol.* **4:**594–605.

Bonavia, A., Zelus, B. D., Wentworth, D. E., Talbot, P. J., and Holmes, K. V. (2003). Identification of a receptor-binding domain of the spike glycoprotein of human coronavirus HCoV-229E. *J. Virol.* **77:**2530–2538.

Bond, C. W., Leibowitz, J. L., and Robb, J. A. (1979). Pathogenic murine coronaviruses: II. characterization of virus-specific proteins of murine coronaviruses JHMV and A59V. *Virology* **94:**371–384.

Bonilla, P. J., Hughes, S. A., and Weiss, S. R. (1997). Characterization of a second cleavage site and demonstration of activity in *trans* by the papain-like proteinase of the murine coronavirus mouse hepatitis virus strain A59. *J. Virol.* **71:**900–909.

Bos, E. C. W., Heijnen, L., Luytjes, W., and Spaan, W. J. M. (1995). Mutational analysis of the murine coronavirus spike protein: Effect on cell-to-cell fusion. *Virology* **214:**453–463.

Bos, E. C. W., Luytjes, W., van der Meulen, H., Koerten, H. K., and Spaan, W. J. M. (1996). The production of recombinant infectious DI-particles of a murine coronavirus in the absence of helper virus. *Virology* **218:**52–60.

Bos, E. C. W., Dobbe, J. C., Luytjes, W., and Spaan, W. J. M. (1997). A subgenomic mRNA transcript of the coronavirus mouse hepatitis virus strain A59 defective interfering (DI) RNA is packaged when it contains the DI packaging signal. *J. Virol.* **71:**5684–5687.

Bosch, B. J., van der Zee, R., de Haan, C. A. M., and Rottier, P. J. M. (2003). The coronavirus spike protein is a class I virus fusion protein: Structural and functional characterization of the fusion core complex. *J. Virol.* **77:**8801–8811.

Bosch, B. J., Martina, B. E., Van Der Zee, R., Lepault, J., Haijema, B. J., Versluis, C., Heck, A. J., De Groot, R., Osterhaus, A. D., and Rottier, P. J. M. (2004). Severe acute respiratory syndrome coronavirus (SARS-CoV) infection inhibition using spike protein heptad repeat-derived peptides. *Proc. Natl. Acad. Sci. USA* **101:**8455–8460.

Bosch, B. J., de Haan, C. A. M., Smits, S. L., and Rottier, P. J. M. (2005). Spike protein assembly into the coronavirion: Exploring the limits of its sequence requirements. *Virology* **334:**306–318.

Bost, A. G., Carnahan, R. H., Lu, X. T., and Denison, M. R. (2000). Four proteins processed from the replicase gene polyprotein of mouse hepatitis virus colocalize in the cell periphery and adjacent to sites of virion assembly. *J. Virol.* **74:**3379–3387.

Bost, A. G., Prentice, E., and Denison, M. R. (2001). Mouse hepatitis virus replicase protein complexes are translocated to sites of M protein accumulation in the ERGIC at late times of infection. *Virology* **285:**21–29.

Boursnell, M. E. G., Binns, M. M., and Brown, T. D. K. (1985). Sequencing of coronavirus IBV genomic RNA: Three open reading frames in the 5′ 'unique' region of mRNA D. *J. Gen. Virol.* **66:**2253–2258.

Brayton, P. R., Ganges, R. G., and Stohlman, S. A. (1981). Host cell nuclear function and murine hepatitis virus replication. *J. Gen. Virol.* **56:**457–460.

Brian, D. A., and Baric, R. S. (2005). Coronavirus genome structure and replication. *Curr. Top. Microbiol. Immunol.* **287:**1–30.

Brian, D. A., Hogue, B. G., and Kienzle, T. E. (1995). *In* "The Coronaviridae" (S. G. Siddell, ed.), pp. 165–179. Plenum, New York.

Brierley, I., Boursnell, M. E., Binns, M. M., Bilimoria, B., Blok, V. C., Brown, T. D., and Inglis, S. C. (1987). An efficient ribosomal frame-shifting signal in the polymerase-encoding region of the coronavirus IBV. *EMBO J.* **6:**3779–3785.

Brierley, I., Digard, P., and Inglis, S. C. (1989). Characterization of an efficient coronavirus ribosomal frameshifting signal: Requirement for an RNA pseudoknot. *Cell* **57:**537–547.

Brierley, I., Rolley, N. J., Jenner, A. J., and Inglis, S. C. (1991). Mutational analysis of the RNA pseudoknot component of a coronavirus ribosomal frameshifting signal. *J. Mol. Biol.* **220:**889–902.

Brierley, I., Jenner, A. J., and Inglis, S. C. (1992). Mutational analysis of the "slippery-sequence" component of a coronavirus ribosomal frameshifting signal *J. Mol. Biol.* **227:**463–479.

Britton, P., Evans, S., Dove, B., Davies, M., Casais, R., and Cavanagh, D. (2005). Generation of a recombinant avian coronavirus infectious bronchitis virus using transient dominant selection. *J. Virol. Methods* **123:**203–211.

Brockway, S. M., Clay, C. T., Lu, X. T., and Denison, M. R. (2003). Characterization of the expression, intracellular localization, and replication complex association of the putative mouse hepatitis virus RNA-dependent RNA polymerase. *J. Virol.* **77:**10515–10527.

Budzilowicz, C. J., and Weiss, S. R. (1987). *In vitro* synthesis of two polypeptides from a nonstructural gene of coronavirus mouse hepatitis virus strain A59. *Virology* **157:**509–515.

Burd, C. G., and Dreyfuss, G. (1994). RNA binding specificity of hnRNP A1: Significance of hnRNP A1 high-affinity binding sites in pre-mRNA splicing. *EMBO J.* **13:**1197–1204.

Callebaut, P. E., and Pensaert, M. B. (1980). Characterization and isolation of structural polypeptides in haemagglutinating encephalomyelitis virus. *J. Gen. Virol.* **48:**193–204.

Calvo, E., Escors, D., Lopez, J. A., Gonzalez, J. M., Alvarez, A., Arza, E., and Enjuanes, L. (2005). Phosphorylation and subcellular localization of transmissible gastroenteritis virus nucleocapsid protein in infected cells. *J. Gen. Virol.* **86:**2255–2267.

Casais, R., Thiel, V., Siddell, S. G., Cavanagh, D., and Britton, P. (2001). Reverse genetics system for the avian coronavirus infectious bronchitis virus. *J. Virol.* **75:**12359–12369.

Casais, R., Davies, M., Cavanagh, D., and Britton, P. (2005). Gene 5 of the avian coronavirus infectious bronchitis virus is not essential for replication. *J. Virol.* **79:**8065–8078.

Caul, E. O., Ashley, C. R., Ferguson, M., and Egglestone, S. I. (1979). Preliminary studies on the isolation of coronaviruse 229E nucleocapsids. *FEMS Microbiol. Lett.* **5:**101–105.

Cavanagh, D. (1995). *In* "The Coronaviridae" (S. G. Siddell, ed.), pp. 73–113. Plenum, New York.

Cavanagh, D., and Davis, P. J. (1988). Evolution of avian coronavirus IBV: Sequence of the matrix glycoprotein gene and intergenic region of several serotypes. *J. Gen. Virol.* **69:**621–629.

Cavanagh, D., Davis, P. J., and Pappin, D. J. C. (1986a). Coronavirus IBV glycopolypeptides: Locational studies using proteases and saponin, a membrane permeabilizer. *Virus Res.* **4:**145–156.

Cavanagh, D., Davis, P. J., Pappin, D. J., Binns, M. M., Boursnell, M. E., and Brown, T. D. (1986b). Coronavirus IBV: Partial amino terminal sequencing of spike polypeptide S2 identifies the sequence Arg-Arg-Phe-Arg-Arg at the cleavage site of the spike precursor propolypeptide of IBV strains Beaudette and M41. *Virus Res.* **4:**133–143.

Cavanagh, D., Davis, P. J., and Cook, J. K. A. (1992). Infectious bronchitis virus: Evidence for recombination within the Massachusetts serotype. *Avian Pathol.* **21:**401–408.

Chang, K. W., Sheng, Y. W., and Gombold, J. L. (2000). Coronavirus-induced membrane fusion requires the cysteine-rich domain in the spike protein. *Virology* **269:**212–224.

Chang, R.-Y., Hofmann, M. A., Sethna, P. B., and Brian, D. A. (1994). A *cis*-acting function for the coronavirus leader in defective interfering RNA replication. *J. Virol.* **68:**8223–8231.

Chang, R.-Y., Krishnan, R., and Brian, D. A. (1996). The UCUAAAC promoter motif is not required for high-frequency leader recombination in bovine coronavirus defective interfering RNA. *J. Virol.* **70:**2720–2729.

Charley, B., and Laude, H. (1988). Induction of alpha interferon by transmissible gastroenteritis coronavirus: Role of transmembrane glycoprotein E1. *J. Virol.* **62:**8–11.

Chen, C.-J., and Makino, S. (2004). Murine coronavirus replication induces cell cycle arrest in G0/G1 phase. *J. Virol.* **78:**5658–5669.

Chen, C.-J., Sugiyama, K., Kubo, H., Huang, C., and Makino, S. (2004). Murine coronavirus nonstructural protein p28 arrests cell cycle in G0/G1 phase. *J. Virol.* **78:**10410–10419.

Chen, H., Wurm, T., Britton, P., Brooks, G., and Hiscox, J. A. (2002). Interaction of the coronavirus nucleoprotein with nucleolar antigens and the host cell. *J. Virol.* **76:**5233–5250.

Chen, H., Gill, A., Dove, B. K., Emmett, S. R., Kemp, C. F., Ritchie, M. A., Dee, M., and Hiscox, J. A. (2005). Mass spectroscopic characterization of the coronavirus infectious bronchitis virus nucleoprotein and elucidation of the role of phosphorylation in RNA binding by using surface plasmon resonance. *J. Virol.* **79:**1164–1179.

Cheng, A., Zhang, W., Xie, Y., Jiang, W., Arnold, E., Sarafianos, S. G., and Ding, J. (2005). Expression, purification, and characterization of SARS coronavirus RNA polymerase. *Virology* **335:**165–176.

Choi, K. S., Huang, P., and Lai, M. M. C. (2002). Polypyrimidine-tract-binding protein affects transcription but not translation of mouse hepatitis virus RNA. *Virology* **303:**58–68.

Choi, K. S., Mizutani, A., and Lai, M. M. C. (2004). SYNCRIP, a member of the heterogeneous nuclear ribonucleoprotein family, is involved in mouse hepatitis virus RNA synthesis. *J. Virol.* **78:**13153–13162.

Choi, K. S., Aizaki, H., and Lai, M. M. C. (2005). Murine coronavirus requires lipid rafts for virus entry and cell–cell fusion but not for virus release. *J. Virol.* **79:**9862–9871.

Coley, S. E., Lavi, E., Sawicki, S. G., Fu, L., Schelle, B., Karl, N., Siddell, S. G., and Thiel, V. (2005). Recombinant mouse hepatitis virus strain A59 from cloned, full-length cDNA replicates to high titers *in vitro* and is fully pathogenic *in vivo*. *J. Virol.* **79:**3097–3106.

Collins, A. R., Knobler, R. L., Powell, H., and Buchmeier, M. J. (1982). Monoclonal antibodies to murine hepatitis virus-4 (strain JHM) define the viral glycoprotein responsible for attachment and cell–cell fusion. *Virology* **119:**358–371.

Cologna, R., and Hogue, B. G. (2000). Identification of a bovine coronavirus packaging signal. *J. Virol.* **74:**580–583.

Cologna, R., Spagnolo, J. F., and Hogue, B. G. (2000). Identification of nucleocapsid binding sites within coronavirus-defective genomes. *Virology* **277:**235–249.

Compton, S. R. (1994). Enterotropic strains of mouse coronavirus differ in their use of murine carcinoembryonic antigen-related glycoprotein receptors. *Virology* **203:**197–201.

Cornelissen, L. A., Wierda, C. M., van der Meer, F. J., Herrewegh, A. A., Horzinek, M. C., Egberink, H. F., and de Groot, R. J. (1997). Hemagglutinin-esterase, a novel structural protein of torovirus. *J. Virol.* **71:**5277–5286.

Corse, E., and Machamer, C. E. (2000). Infectious bronchitis virus E protein is targeted to the Golgi complex and directs release of virus-like particles. *J. Virol.* **74:**4319–4326.

Corse, E., and Machamer, C. E. (2002). The cytoplasmic tail of infectious bronchitis virus E protein directs Golgi targeting. *J. Virol.* **76:**1273–1284.

Corse, E., and Machamer, C. E. (2003). The cytoplasmic tails of infectious bronchitis virus E and M proteins mediate their interaction. *Virology* **312:**25–34.

Cowley, J. A., Dimmock, C. M., Spann, K. M., and Walker, P. J. (2000). Gill-associated virus of Penaeus monodon prawns: An invertebrate virus with ORF1a and ORF1b genes related to arteri- and coronaviruses. *J. Gen. Virol.* **81:**1473–1484.

Curtis, K. M., Yount, B., and Baric, R. S. (2002). Heterologous gene expression from transmissible gastroenteritis virus replicon particles. *J. Virol.* **76:**1422–1434.

Curtis, K. M., Yount, B., Sims, A. C., and Baric, R. S. (2004). Reverse genetic analysis of the transcription regulatory sequence of the coronavirus transmissible gastroenteritis virus. *J. Virol.* **78:**6061–6066.

Dalton, K., Casais, R., Shaw, K., Stirrups, K., Evans, S., Britton, P., Brown, T. D. K., and Cavanagh, D. (2001). *cis*-acting sequences required for coronavirus infectious bronchitis virus defective-RNA replication and packaging. *J. Virol.* **75:**125–133.

Davies, H. A., Dourmashkin, R. R., and Macnaughton, M. R. (1981). Ribonucleoprotein of avian infectious bronchitis virus. *J. Gen. Virol.* **53:**67–74.

de Groot, R. J., Luytjes, W., Horzinek, M. C., van der Zeijst, B. A., Spaan, W. J. M., and Lenstra, J. A. (1987). Evidence for a coiled-coil structure in the spike proteins of coronaviruses. *J. Mol. Biol.* **196:**963–966.

de Haan, C. A. M., Kuo, L., Masters, P. S., Vennema, H., and Rottier, P. J. M. (1998a). Coronavirus particle assembly: Primary structure requirements of the membrane protein. *J. Virol.* **72:**6838–6850.

de Haan, C. A. M., Roestenberg, P., de Wit, M., de Vries, A. A. F., Nilsson, T., Vennema, H., and Rottier, P. J. M. (1998b). Structural requirements for O-glycosylation of the mouse hepatitis virus membrane protein. *J. Biol. Chem.* **273:**29905–29914.

de Haan, C. A. M., Smeets, M., Vernooij, F., Vennema, H., and Rottier, P. J. M. (1999). Mapping of the coronavirus membrane protein domains involved in interaction with the spike protein. *J. Virol.* **73:**7441–7452.

de Haan, C. A. M., Vennema, H., and Rottier, P. J. M. (2000). Assembly of the coronavirus envelope: Homotypic interactions between the M proteins. *J. Virol.* **74:**4967–4978.

de Haan, C. A. M., Masters, P. S., Shen, X., Weiss, S., and Rottier, P. J. M. (2002a). The group-specific murine coronavirus genes are not essential, but their deletion, by reverse genetics, is attenuating in the natural host. *Virology* **296:**177–189.

de Haan, C. A. M., Volders, H., Koetzner, C. A., Masters, P. S., and Rottier, P. J. M. (2002b). Coronaviruses maintain viability despite dramatic rearrangements of the strictly conserved genome organization. *J. Virol.* **76:**12491–12493.

de Haan, C. A. M., de Wit, M., Kuo, L., Montalto-Morrison, C., Haagmans, B. L., Weiss, S. R., Masters, P. S., and Rottier, P. J. M. (2003a). The glycosylation status of the murine hepatitis coronavirus M protein affects the interferogenic capacity of the virus *in vitro* and its ability to replicate in the liver but not the brain. *Virology* **312:**395–406.

de Haan, C. A. M., van Genne, L., Stoop, J. N., Volders, H., and Rottier, P. J. M. (2003b). Coronaviruses as vectors: Position dependence of foreign gene expression. *J. Virol.* **77:**11312–11323.

de Haan, C. A. M., Stadler, K., Godeke, G. J., Bosch, B. J., and Rottier, P. J. M. (2004). Cleavage inhibition of the murine coronavirus spike protein by a furin-like enzyme affects cell–cell but not virus-cell fusion. *J. Virol.* **78:**6048–6054.

de Haan, C. A. M., Haijema, B. J., Boss, D., Heuts, F. W., and Rottier, P. J. M. (2005). Coronaviruses as vectors: Stability of foreign gene expression. *J. Virol.* **79:**12742–12751.

Delmas, B., and Laude, H. (1990). Assembly of coronavirus spike protein into trimers and its role in epitope expression. *J. Virol.* **64:**5367–5375.

Delmas, B., Gelfi, J., L'Haridon, R., Vogel, L. K., Sjostrom, H., Noren, O., and Laude, H. (1992). Aminopeptidase N is a major receptor for the entero-pathogenic coronavirus TGEV. *Nature* **357:**417–420.

Delmas, B., Gelfi, J., Kut, E., Sjostrom, H., Noren, O., and Laude, H. (1994a). Determinants essential for the transmissible gastroenteritis virus-receptor interaction reside within a domain of aminopeptidase-N that is distinct from the enzymatic site. *J. Virol.* **68:**5216–5224.

Delmas, B., Gelfi, J., Sjostrom, H., Noren, O., and Laude, H. (1994b). Further characterization of aminopeptidase-N as a receptor for coronaviruses. *Adv. Exp. Med. Biol.* **342:**293–298.

den Boon, J. A., Snijder, E. J., Locker, J. K., Horzinek, M. C., and Rottier, P. J. M. (1991). Another triple-spanning envelope protein among intracellularly budding RNA viruses: The torovirus E protein. *Virology* **182:**655–663.

Denison, M., and Perlman, S. (1987). Identification of putative polymerase gene product in cells infected with murine coronavirus A59. *Virology* **157:**565–568.

Denison, M. R., and Perlman, S. (1986). Translation and processing of mouse hepatitis virus virion RNA in a cell-free system. *J. Virol.* **60:**12–18.

Dhar, A. K., Cowley, J. A., Hasson, K. W., and Walker, P. J. (2004). Genomic organization, biology, and diagnosis of Taura syndrome virus and yellowhead virus of penaeid shrimp. *Adv. Virus Res.* **63:**353–421.

Duquerroy, S., Vigouroux, A., Rottier, P. J. M., Rey, F. A., and Bosch, B. J. (2005). Central ions and lateral asparagine/glutamine zippers stabilize the post-fusion hairpin conformation of the SARS coronavirus spike glycoprotein. *Virology* **335:**276–285.

Dveksler, G. S., Pensiero, M. N., Cardellichio, C. B., Williams, R. K., Jiang, G. S., Holmes, K. V., and Dieffenbach, C. W. (1991). Cloning of the mouse hepatitis virus (MHV) receptor: Expression in human and hamster cell lines confers susceptibility to MHV. *J. Virol.* **65:**6881–6891.

Dveksler, G. S., Dieffenbach, C. W., Cardellichio, C. B., McCuaig, K., Pensiero, M. N., Jiang, G. S., Beauchemin, N., and Holmes, K. V. (1993a). Several members of the mouse carcinoembryonic antigen-related glycoprotein family are functional receptors for the coronavirus mouse hepatitis virus-A59. *J. Virol.* **67:**1–8.

Dveksler, G. S., Pensiero, M. N., Dieffenbach, C. W., Cardellichio, C. B., Basile, A. A., Elia, P. E., and Holmes, K. V. (1993b). Mouse hepatitis virus strain A59 and blocking antireceptor monoclonal antibody bind to the N-terminal domain of cellular receptor. *Proc. Natl. Acad. Sci. USA* **90:**1716–1720.

Egloff, M. P., Ferron, F., Campanacci, V., Longhi, S., Rancurel, C., Dutartre, H., Snijder, E. J., Gorbalenya, A. E., Cambillau, C., and Canard, B. (2004). The severe acute respiratory syndrome-coronavirus replicative protein nsp9 is a single-stranded RNA-binding subunit unique in the RNA virus world. *Proc. Natl. Acad. Sci. USA* **101:**3792–3796.

Eickmann, M., Becker, S., Klenk, H. D., Doerr, H. W., Stadler, K., Censini, S., Guidotti, S., Masignani, V., Scarselli, M., Mora, M., Donati, C., Han, J. H. *et al.* (2003). Phylogeny of the SARS coronavirus. *Science* **302:**1504–1505.

Eleouet, J. F., Rasschaert, D., Lambert, P., Levy, L., Vende, P., and Laude, H. (1995). Complete sequence (20 kilobases) of the polyprotein-encoding gene 1 of transmissible gastroenteritis virus. *Virology* **206:**817–822.

Enjuanes, L., (ed.) (2005). Coronavirus replication and reverse genetics. In "Curr. Top. Microbiol. Immunol." vol. 287. Springer, New York.

Enjuanes, L., Spaan, W., Snijder, E., and Cavanagh, D. (2000a). Nidovirales. *In* "Virus Taxonomy. Seventh Report of the International Committee on Taxonomy of Viruses" (F. A. Murphy, C. M. Fauquet, D. H. L. Bishop, S. A. Ghabrial, A. W. Jarvis, G. P. Martelli, M. A. Mayo, and M. D. Summers, eds.), pp. 827–834. Academic Press, New York.

Enjuanes, L., Brian, D., Cavanagh, D., Holmes, K., Lai, M. M. C., Laude, H., Masters, P., Rottier, P. J. M., Siddell, S. G., Spaan, W. J. M., Taguchi, F., and Talbot, P. (2000b). Coronaviridae. *In* "Virus Taxonomy. Seventh Report of the International Committee on Taxonomy of Viruses" (F. A. Murphy, C. M. Fauquet, D. H. L. Bishop, S. A. Ghabrial, A. W. Jarvis, G. P. Martelli, M. A. Mayo, and M. D. Summers, eds.), pp. 835–849. Academic Press, New York.

Enjuanes, L., Sola, I., Alonso, S., Escors, D., and Zuniga, S. (2005). Coronavirus reverse genetics and development of vectors for gene expression. *Curr. Top. Microbiol. Immunol.* **287:**161–197.

Erles, K., Toomey, C., Brooks, H. W., and Brownlie, J. (2003). Detection of a group 2 coronavirus in dogs with canine infectious respiratory disease. *Virology* **310:**216–223.

Escors, D., Ortego, J., Laude, H., and Enjuanes, L. (2001). The membrane M protein carboxy terminus binds to transmissible gastroenteritis coronavirus core and contributes to core stability. *J. Virol.* **75:**1312–1324.

Escors, D., Izeta, A., Capiscol, C., and Enjuanes, L. (2003). Transmissible gastroenteritis coronavirus packaging signal is located at the 5′ end of the virus genome. *J. Virol.* **77:**7890–7902.

Evans, M. R., and Simpson, R. W. (1980). The coronavirus avian infectious bronchitis virus requires the cell nucleus and host transcriptional factors. *Virology* **105:**582–591.

Fischer, F., Peng, D., Hingley, S. T., Weiss, S. R., and Masters, P. S. (1997a). The internal open reading frame within the nucleocapsid gene of mouse hepatitis virus encodes a structural protein that is not essential for viral replication. *J. Virol.* **71:**996–1003.

Fischer, F., Stegen, C. F., Koetzner, C. A., and Masters, P. S. (1997b). Analysis of a recombinant mouse hepatitis virus expressing a foreign gene reveals a novel aspect of coronavirus transcription. *J. Virol.* **71:**5148–5160.

Fischer, F., Stegen, C. F., Masters, P. S., and Samsonoff, W. A. (1998). Analysis of constructed E gene mutants of mouse hepatitis virus confirms a pivotal role for E protein in coronavirus assembly. *J. Virol.* **72:**7885–7894.

Fosmire, J. A., Hwang, K., and Makino, S. (1992). Identification and characterization of a coronavirus packaging signal. *J. Virol.* **66:**3522–3530.

Frana, M. F., Behnke, J. N., Sturman, L. S., and Holmes, K. V. (1985). Proteolytic cleavage of the E2 glycoprotein of murine coronavirus: Host-dependent differences in proteolytic cleavage and cell fusion. *J. Virol.* **56:**912–920.

Fu, K., and Baric, R. S. (1992). Evidence for variable rates of recombination in the MHV genome. *Virology* **189:**88–102.

Fu, K., and Baric, R. S. (1994). Map locations of mouse hepatitis virus temperature-sensitive mutants: Confirmation of variable rates of recombination. *J. Virol.* **68:**7458–7466.

Furuya, T., and Lai, M. M. C. (1993). Three different cellular proteins bind to complementary sites on the 5′-end-positive and 3′-end-negative strands of mouse hepatitis virus RNA. *J. Virol.* **67:**7215–7222.

Gagneten, S., Scanga, C. A., Dveksler, G. S., Beauchemin, N., Percy, D., and Holmes, K. V. (1996). Attachment glycoproteins and receptor specificity of rat coronaviruses. *Lab. Anim. Sci.* **46:**159–166.

Gallagher, T. M. (1997). A role for naturally occurring variation of the murine coronavirus spike protein in stabilizing association with the cellular receptor. *J. Virol.* **71:**3129–3137.

Gallagher, T. M., and Buchmeier, M. J. (2001). Coronavirus spike proteins in viral entry and pathogenesis. *Virology* **279:**371–374.

Gallagher, T. M., Parker, S. E., and Buchmeier, M. J. (1990). Neutralization-resistant variants of a neurotropic coronavirus are generated by deletions within the amino-terminal half of the spike glycoprotein. *J. Virol.* **64:**731–741.

Gallagher, T. M., Escarmis, C., and Buchmeier, M. J. (1991). Alteration of the pH dependence of coronavirus-induced cell fusion: Effect of mutations in the spike glycoprotein. *J. Virol.* **65:**1916–1928.

Gallagher, T. M., Buchmeier, M. J., and Perlman, S. (1992). Cell receptor-independent infection by a neurotropic murine coronavirus. *Virology* **191:**517–522.

Garwes, D. J., Pocock, D. H., and Pike, B. V. (1976). Isolation of subviral components from transmissible gastroenteritis virus. *J. Gen. Virol.* **32:**283–294.

Garwes, D. J., Bountiff, L., Millson, G. C., and Elleman, C. J. (1984). Defective replication of porcine transmissible gastroenteritis virus in a continuous cell line. *Adv. Exp. Med. Biol.* **173:**79–93.

Gillim-Ross, L., Taylor, J., Scholl, D. R., Ridenour, J., Masters, P. S., and Wentworth, D. E. (2004). Discovery of novel human and animal cells infected by the severe acute respiratory syndrome coronavirus by replication-specific multiplex reverse transcription-PCR. *J. Clin. Microbiol.* **42:**3196–3206.

Giroglou, T., Cinatl, J., Jr., Rabenau, H., Drosten, C., Schwalbe, H., Doerr, H. W., and von Laer, D. (2004). Retroviral vectors pseudotyped with severe acute respiratory syndrome coronavirus S protein. *J. Virol.* **78:**9007–9015.

Godeke, G.-J., de Haan, C. A. M., Rossen, J. W., Vennema, H., and Rottier, P. J. M. (2000). Assembly of spikes into coronavirus particles is mediated by the carboxy-terminal domain of the spike protein. *J. Virol.* **74:**1566–1571.

Godet, M., L'haridon, R., Vautherot, J.-F., and Laude, H. (1992). TGEV corona virus ORF4 encodes a membrane protein that is incorporated into virions. *Virology* **188:**666–675.

Godet, M., Grosclaude, J., Delmas, B., and Laude, H. (1994). Major receptor-binding and neutralization determinants are located within the same domain of the transmissible gastroenteritis virus (coronavirus) spike protein. *J. Virol.* **68:**8008–8016.

Goebel, S. J., Hsue, B., Dombrowski, T. F., and Masters, P. S. (2004a). Characterization of the RNA components of a putative molecular switch in the 3′ untranslated region of the murine coronavirus genome. *J. Virol.* **78:**669–682.

Goebel, S. J., Taylor, J., and Masters, P. S. (2004b). The 3′ *cis*-acting genomic replication element of the severe acute respiratory syndrome coronavirus can function in the murine coronavirus genome. *J. Virol.* **78:**7846–7851.

Gombold, J. L., Hingley, S. T., and Weiss, S. R. (1993). Fusion-defective mutants of mouse hepatitis virus A59 contain a mutation in the spike protein cleavage signal. *J. Virol.* **67:**4504–4512.

González, J. M., Penzes, Z., Almazan, F., Calvo, E., and Enjuanes, L. (2002). Stabilization of a full-length infectious cDNA clone of transmissible gastroenteritis coronavirus by insertion of an intron. *J. Virol.* **76:**4655–4661.

González, J. M., Gomez-Puertas, P., Cavanagh, D., Gorbalenya, A. E., and Enjuanes, L. (2003). A comparative sequence analysis to revise the current taxonomy of the family *Coronaviridae*. *Arch. Virol.* **148:**2207–2235.

Gorbalenya, A. E., Koonin, E. V., Donchenko, A. P., and Blinov, V. M. (1989). Coronavirus genome: Prediction of putative functional domains in the non-structural polyprotein by comparative amino acid sequence analysis. *Nucleic Acids Res.* **17:**4847–4861.

Gorbalenya, A. E., Snijder, E. J., and Spaan, W. J. M. (2004). Severe acute respiratory syndrome coronavirus phylogeny: Toward consensus. *J. Virol.* **78:**7863–7866.

Gosert, R., Kanjanahaluethai, A., Egger, D., Bienz, K., and Baker, S. C. (2002). RNA replication of mouse hepatitis virus takes place at double-membrane vesicles. *J. Virol.* **76:**3697–3708.

Graham, R. L., Sims, A. C., Brockway, S. M., Baric, R. S., and Denison, M. R. (2005). The nsp2 replicase proteins of murine hepatitis virus and severe acute respiratory syndrome coronavirus are dispensable for viral replication. *J. Virol.* **79:**13399–13411.

Guan, Y., Zheng, B. J., He, Y. Q., Liu, X. L., Zhuang, Z. X., Cheung, C. L., Luo, S. W., Li, P. H., Zhang, L. J., Guan, Y. J., Butt, K. M., Wong, K. L. *et al.* (2003). Isolation and characterization of viruses related to the SARS coronavirus from animals in Southern China. *Science* **302:**276–278.

Guillen, J., Perez-Berna, A. J., Moreno, M. R., and Villalain, J. (2005). Identification of the membrane-active regions of the severe acute respiratory syndrome coronavirus spike membrane glycoprotein using a 16/18–mer peptide scan: Implications for the viral fusion mechanism. *J. Virol.* **79:**1743–1752.

Guy, J. S., Breslin, J. J., Breuhaus, B., Vivrette, S., and Smith, L. G. (2000). Characterization of a coronavirus isolated from a diarrheic foal. *J. Clin. Microbiol.* **38:**4523–4526.

Haijema, B. J., Volders, H., and Rottier, P. J. M. (2003). Switching species tropism: An effective way to manipulate the feline coronavirus genome. *J. Virol.* **77:**4528–4538.

Haijema, B. J., Volders, H., and Rottier, P. J. M. (2004). Live, attenuated coronavirus vaccines through the directed deletion of group-specific genes provide protection against feline infectious peritonitis. *J. Virol.* **78:**3863–3871.

Hansen, G. H., Delmas, B., Besnardeau, L., Vogel, L. K., Laude, H., Sjostrom, H., and Noren, O. (1998). The coronavirus transmissible gastroenteritis virus causes infection after receptor-mediated endocytosis and acid-dependent fusion with an intracellular compartment. *J. Virol.* **72:**527–534.

Harcourt, B. H., Jukneliene, D., Kanjanahaluethai, A., Bechill, J., Severson, K. M., Smith, C. M., Rota, P. A., and Baker, S. C. (2004). Identification of severe acute respiratory syndrome coronavirus replicase products and characterization of papain-like protease activity. *J. Virol.* **78:**13600–13612.

Hegyi, A., and Kolb, A. F. (1998). Characterization of determinants involved in the feline infectious peritonitis virus receptor function of feline aminopeptidase N. *J. Gen. Virol.* **79:**1387–1391.

Hemmila, E., Turbide, C., Olson, M., Jothy, S., Holmes, K. V., and Beauchemin, N. (2004). Ceacam1a−/− mice are completely resistant to infection by murine coronavirus mouse hepatitis virus A59. *J. Virol.* **78:**10156–10165.

Herold, J., and Siddell, S. G. (1993). An 'elaborated' pseudoknot is required for high frequency frameshifting during translation of HCV 229E polymerase mRNA. *Nucleic Acids Res.* **21:**5838–5842.

Herrewegh, A. A., Smeenk, I., Horzinek, M. C., Rottier, P. J. M., and de Groot, R. J. (1998). Feline coronavirus type II strains 79–1683 and 79–1146 originate from a double recombination between feline coronavirus type I and canine coronavirus. *J. Virol.* **72:**4508–4514.

Hingley, S. T., Leparc-Goffart, I., and Weiss, S. R. (1998). The spike protein of murine coronavirus mouse hepatitis virus strain A59 is not cleaved in primary glial cells and primary hepatocytes. *J. Virol.* **72:**1606–1609.

Hiscox, J. A., Mawditt, K. L., Cavanagh, D., and Britton, P. (1995). Investigation of the control of coronavirus subgenomic mRNA transcription by using T7-generated negative-sense RNA transcripts. *J. Virol.* **69:**6219–6227.

Hiscox, J. A., Wurm, T., Wilson, L., Britton, P., Cavanagh, D., and Brooks, G. (2001). The coronavirus infectious bronchitis virus nucleoprotein localizes to the nucleolus. *J. Virol.* **75:**506–512.

Hofmann, H., Hattermann, K., Marzi, A., Gramberg, T., Geier, M., Krumbiegel, M., Kuate, S., Uberla, K., Niedrig, M., and Pohlmann, S. (2004). S protein of severe acute respiratory syndrome-associated coronavirus mediates entry into hepatoma cell lines and is targeted by neutralizing antibodies in infected patients. *J. Virol.* **78:**6134–6142.

Hofmann, H., Pyrc, K., van der Hoek, L., Geier, M., Berkhout, B., and Pohlmann, S. (2005). Human coronavirus NL63 employs the severe acute respiratory syndrome coronavirus receptor for cellular entry. *Proc. Natl. Acad. Sci. USA* **102:**7988–7993.

Hofmann, M., and Wyler, R. (1988). Propagation of the virus of porcine epidemic diarrhea in cell culture. *J. Clin. Microbiol.* **26:**2235–2239.

Hofmann, M. A., and Brian, D. A. (1991). The 5′ end of coronavirus minus-strand RNAs contain a short poly(U) tract. *J. Virol.* **65:**6331–6333.

Hofmann, M. A., Sethna, P. B., and Brian, D. A. (1990). Bovine coronavirus mRNA replication continues throughout persistent infection in cell culture. *J. Virol.* **64:**4108–4114.

Hogue, B. G. (1995). Bovine coronavirus nucleocapsid protein processing and assembly. *Adv. Exp. Med. Biol.* **380:**259–263.

Hogue, B. G., Kienzle, T. E., and Brian, D. A. (1989). Synthesis and processing of the bovine enteric coronavirus haemagglutinin protein. *J. Gen. Virol.* **70:**345–352.

Hohdatsu, T., Izumiya, Y., Yokoyama, Y., Kida, K., and Koyama, H. (1998). Differences in virus receptor for type I and type II feline infectious peritonitis virus. *Arch. Virol.* **143:**839–850.

Holmes, K. V., Dollar, E. W., and Sturman, L. S. (1981). Tunicamycin resistant glycosylation of a coronavirus glycoprotein: Demonstration of a novel type of viral glycoprotein. *Virology* **115:**334–344.

Hsue, B., and Masters, P. S. (1997). A bulged stem-loop structure in the 3′ untranslated region of the genome of the coronavirus mouse hepatitis virus is essential for replication. *J. Virol.* **71:**7567–7578.

Hsue, B., Hartshorne, T., and Masters, P. S. (2000). Characterization of an essential RNA secondary structure in the 3′ untranslated region of the murine coronavirus genome. *J. Virol.* **74:**6911–6921.

Huang, P., and Lai, M. M. C. (1999). Polypyrimidine tract-binding protein binds to the complementary strand of the mouse hepatitis virus 3′ untranslated region, thereby altering RNA conformation. *J. Virol.* **73:**9110–9116.

Huang, P., and Lai, M. M. C. (2001). Heterogeneous nuclear ribonucleoprotein a1 binds to the 3′-untranslated region and mediates potential 5′-3′-end cross talks of mouse hepatitis virus RNA. *J. Virol.* **75:**5009–5017.

Huang, Q., Yu, L., Petros, A. M., Gunasekera, A., Liu, Z., Xu, N., Hajduk, P., Mack, J., Fesik, S. W., and Olejniczak, E. T. (2004b). Structure of the N-terminal RNA-binding domain of the SARS CoV nucleocapsid protein. *Biochemistry* **43:**6059–6063.

Huang, Y., Yang, Z. Y., Kong, W. P., and Nabel, G. J. (2004a). Generation of synthetic severe acute respiratory syndrome coronavirus pseudoparticles: Implications for assembly and vaccine production. *J. Virol.* **78:**12557–12565.

Hurst, K. R., Kuo, L., Koetzner, C. A., Ye, R., Hsue, B., and Masters, P. S. (2005). A major determinant for membrane protein interaction localizes to the carboxy-terminal domain of the mouse coronavirus nucleocapsid protein. *J. Virol.* **79:**13285–13297.

Inberg, A., and Linial, M. (2004). Evolutional insights on uncharacterized SARS coronavirus genes. *FEBS Lett.* **577:**159–164.

Ingallinella, P., Bianchi, E., Finotto, M., Cantoni, G., Eckert, D. M., Supekar, V. M., Bruckmann, C., Carfi, A., and Pessi, A. (2004). Structural characterization of the fusion-active complex of severe acute respiratory syndrome (SARS) coronavirus. *Proc. Natl. Acad. Sci. USA* **101:**8709–8714.

Ivanov, K. A., and Ziebuhr, J. (2004). Human coronavirus 229E nonstructural protein 13: Characterization of duplex-unwinding, nucleoside triphosphatase, and RNA 5′-triphosphatase activities. *J. Virol.* **78:**7833–7838.

Ivanov, K. A., Thiel, V., Dobbe, J. C., van der Meer, Y., Snijder, E. J., and Ziebuhr, J. (2004a). Multiple enzymatic activities associated with severe acute respiratory syndrome coronavirus helicase. *J. Virol.* **78:**5619–5632.

Ivanov, K. A., Hertzig, T., Rozanov, M., Bayer, S., Thiel, V., Gorbalenya, A. E., and Ziebuhr, J. (2004b). Major genetic marker of nidoviruses encodes a replicative endoribonuclease. *Proc. Natl. Acad. Sci. USA* **101:**12694–12699.

Izeta, A., Smerdou, C., Alonso, S., Penzes, Z., Mendez, A., Plana-Duran, J., and Enjuanes, L. (1999). Replication and packaging of transmissible gastroenteritis coronavirus-derived synthetic minigenomes. *J. Virol.* **73:**1535–1545.

Jacks, T., Madhani, H. D., Masiarz, F. R., and Varmus, H. E. (1988). Signals for ribosomal frameshifting in the Rous sarcoma virus gag-pol region. *Cell* **55:**447–458.

Jackson, W. T., Giddings, T. H., Jr., Taylor, M. P., Mulinyawe, S., Rabinovitch, M., Kopito, R. R., and Kirkegaard, K. (2005). Subversion of cellular autophagosomal machinery by RNA viruses. *PLoS Biol.* **3:**861–871.

Jacobs, L., Spaan, W. J. M., Horzinek, M. C., and van der Zeijst, B. A. M. (1981). Synthesis of subgenomic mRNAs of mouse hepatitis virus is initiated independently: Evidence from UV transcription mapping. *J. Virol.* **39:**401–406.

Jacobs, L., van der Zeijst, B. A., and Horzinek, M. C. (1986). Characterization and translation of transmissible gastroenteritis virus mRNAs. *J. Virol.* **57:**1010–1015.

Jarvis, T. C., and Kirkegaard, K. (1991). The polymerase in its labyrinth: Mechanisms and implications of RNA recombination. *Trends Genet.* **7:**186–191.

Jarvis, T. C., and Kirkegaard, K. (1992). Poliovirus RNA recombination: Mechanistic studies in the absence of selection. *EMBO J.* **11:**3135–3145.

Jeffers, S. A., Tusell, S. M., Gillim-Ross, L., Hemmila, E. M., Achenbach, J. E., Babcock, G. J., Thomas, W. D., Jr., Thackray, L. B., Young, M. D., Mason, R. J., Ambrosino, D. M., Wentworth, D. E. *et al.* (2004). CD209L (L-SIGN) is a receptor for severe acute respiratory syndrome coronavirus. *Proc. Natl. Acad. Sci. USA* **101:**15748–15753.

Johnson, R. F., Feng, M., Liu, P., Millership, J. J., Yount, B., Baric, R. S., and Leibowitz, J. L. (2005). Effect of mutations in the mouse hepatitis virus 3′(+)42 protein binding element on RNA replication. *J. Virol.* **79:**14570–14585.

Joo, M., and Makino, S. (1995). The effect of two closely inserted transcription consensus sequences on coronavirus transcription. *J. Virol.* **69:**272–280.

Jonassen, C. M., Kofstad, T., Larsen, I.-L., Lovland, A., Handeland, K., Follestad, A., and Lillehaug, A. (2005). Molecular identification and characterization of novel coronaviruses infecting graylag geese (Anser anser), feral pigeons (Columbia livia) and mallards (Anas platyrhynchos). *J. Gen. Virol.* **86:**1597–1607.

Kanjanahaluethai, A., Jukneliene, D., and Baker, S. C. (2003). Identification of the murine coronavirus MP1 cleavage site recognized by papain-like proteinase 2. *J. Virol.* **77:**7376–7382.

Kapke, P. A., Tung, F. Y., Hogue, B. G., Brian, D. A., Woods, R. D., and Wesley, R. (1988). The amino-terminal signal peptide on the porcine transmissible gastroenteritis coronavirus matrix protein is not an absolute requirement for membrane translocation and glycosylation. *Virology* **165:**367–376.

Kazi, L., Lissenberg, A., Watson, R., de Groot, R. J., and Weiss, S. R. (2005). Expression of hemagglutinin-esterase protein from recombinant mouse hepatitis virus enhances neurovirulence. *J. Virol.* **79:**15064–15073.

Keck, J. G., Stohlman, S. A., Soe, L. H., Makino, S., and Lai, M. M. C. (1987). Multiple recombination sites at the 5′-end of murine coronavirus RNA. *Virology* **156:**331–341.

Keck, J. G., Matsushima, G. K., Makino, S., Fleming, J. O., Vannier, D. M., Stohlman, S. A., and Lai, M. M. C. (1988a). *In vivo* RNA-RNA recombination of coronavirus in mouse brain. *J. Virol.* **62:**1810–1813.

Keck, J. G., Soe, L. H., Makino, S., Stohlman, S. A., and Lai, M. M. C. (1988). RNA recombination of murine coronaviruses: Recombination between fusion-positive mouse hepatitis virus A59 and fusion-negative mouse hepatitis virus 2. *J. Virol.* **62:**1989–1998.

Kennedy, D. A., and Johnson-Lussenburg, C. M. (1975/76). Isolation and morphology of the internal component of human coronavirus, strain 229E. *Intervirology* **6:**197–206.

Kennedy, D. A., and Johnson-Lussenburg, C. M. (1979). Inhibition of coronavirus 229E replication by actinomycin D. *J. Virol.* **29:**401–404.

Kienzle, T. E., Abraham, S., Hogue, B. G., and Brian, D. A. (1990). Structure and orientation of expressed bovine coronavirus hemagglutinin-esterase protein. *J. Virol.* **64:**1834–1838.

Kim, Y.-N., Jeong, Y. S., and Makino, S. (1993). Analysis of *cis*-acting sequences essential for coronavirus defective interfering RNA replication. *Virology* **197:**53–63.

King, B., and Brian, D. A. (1982). Bovine coronavirus structural proteins. *J. Virol.* **42:**700–707.

King, B., Potts, B. J., and Brian, D. A. (1985). Bovine coronavirus hemagglutinin protein. *Virus Res.* **2:**53–59.

Kirkegaard, K., and Baltimore, D. (1986). The mechanism of RNA recombination in poliovirus. *Cell* **47:**433–443.

Klausegger, A., Strobl, B., Regl, G., Kaser, A., Luytjes, W., and Vlasak, R. (1999). Identification of a coronavirus hemagglutinin-esterase with a substrate specificity different from those of influenza C virus and bovine coronavirus. *J. Virol.* **73:**3737–3743.

Klumperman, J., Krijnse Locker, J., Meijer, A., Horzinek, M. C., Geuze, H. J., and Rottier, P. J. M. (1994). Coronavirus M proteins accumulate in the Golgi complex beyond the site of virion budding. *J. Virol.* **68:**6523–6534.

Koetzner, C. A., Parker, M. M., Ricard, C. S., Sturman, L. S., and Masters, P. S. (1992). Repair and mutagenesis of the genome of a deletion mutant of the coronavirus mouse hepatitis virus by targeted RNA recombination. *J. Virol.* **66:**1841–1848.

Kolb, A. F., Maile, J., Heister, A., and Siddell, S. G. (1996). Characterization of functional domains in the human coronavirus HCV 229E receptor. *J. Gen. Virol.* **77:**2515–2521.

Kolb, A. F., Hegyi, A., and Siddell, S. G. (1997). Identification of residues critical for the human coronavirus 229E receptor function of human aminopeptidase N. *J. Gen. Virol.* **78:**2795–2802.

Koolen, M. J., Osterhaus, A. D., van Steenis, G., Horzinek, M. C., and van der Zeijst, B. A. M. (1983). Temperature-sensitive mutants of mouse hepatitis virus strain A59: Isolation, characterization and neuropathogenic properties. *Virology* **125:**393–402.

Kottier, S. A., Cavanagh, D., and Britton, P. (1995). Experimental evidence of recombination in coronavirus infectious bronchitis virus. *Virology* **213:**569–580.

Krijnse Locker, J., Griffiths, G., Horzinek, M. C., and Rottier, P. J. M. (1992a). O-glycosylation of the coronavirus M protein. Differential localization of sialyltransferases in N- and O-linked glycosylation. *J. Biol. Chem.* **267:**14094–14101.

Krijnse Locker, J., Rose, J. K., Horzinek, M. C., and Rottier, P. J. M. (1992b). Membrane assembly of the triple-spanning coronavirus M protein. Individual transmembrane domains show preferred orientation. *J. Biol. Chem.* **267:**21911–21918.

Krijnse Locker, J., Ericsson, M., Rottier, P. J. M., and Griffiths, G. (1994). Characterization of the budding compartment of mouse hepatitis virus: Evidence that transport from the RER to the Golgi complex requires only one vesicular transport step. *J. Cell. Biol.* **124:**55–70.

Krijnse Locker, J., Opstelten, D.-J. E., Ericsson, M., Horzinek, M. C., and Rottier, P. J. M. (1995). Oligomerization of a trans-Golgi/trans-Golgi network retained protein occurs in the Golgi complex and may be part of its recognition. *J. Biol. Chem.* **270:**8815–8821.

Krishnan, R., Chang, R.-Y., and Brian, D. A. (1996). Tandem placement of a coronavirus promoter results in enhanced mRNA synthesis from the downstream-most initiation site. *Virology* **218:**400–405.

Krueger, D. K., Kelly, S. M., Lewicki, D. N., Ruffolo, R., and Gallagher, T. M. (2001). Variations in disparate regions of the murine coronavirus spike protein impact the initiation of membrane fusion. *J. Virol.* **75:**2792–2802.

Krokhin, O., Li, Y., Andonov, A., Feldmann, H., Flick, R., Jones, S., Stroeher, U., Bastien, N., Dasuri, K. V., Cheng, K., Simonsen, J. N., Perreault, H. *et al.* (2003). Mass spectrometric characterization of proteins from the SARS virus: A preliminary report. *Mol. Cell Proteomics* **2:**346–356.

Ksiazek, T. G., Erdman, D., Goldsmith, C. S., Zaki, S. R., Peret, T., Emery, S., Tong, S., Urbani, C., Comer, J. A., Lim, W., Rollin, P. E., Dowell, S. *et al.* (2003). A novel coronavirus associated with severe acute respiratory syndrome. *N. Engl. J. Med.* **348:**1953–1966.

Kubo, H., Yamada, Y. K., and Taguchi, F. (1994). Localization of neutralizing epitopes and the receptor-binding site within the amino-terminal 330 amino acids of the murine coronavirus spike protein. *J. Virol.* **68:**5403–5410.

Kuo, L., and Masters, P. S. (2002). Genetic evidence for a structural interaction between the carboxy termini of the membrane and nucleocapsid proteins of mouse hepatitis virus. *J. Virol.* **76:**4987–4999.

Kuo, L., and Masters, P. S. (2003). The small envelope protein E is not essential for murine coronavirus replication. *J. Virol.* **77:**4597–4608.

Kuo, L., Godeke, G.-J., Raamsman, M. J. B., Masters, P. S., and Rottier, P. J. M. (2000). Retargeting of coronavirus by substitution of the spike glycoprotein ectodomain: Crossing the host cell species barrier. *J. Virol.* **74:**1393–1406.

Kusters, J. G., Jager, E. J., Niesters, H. G., and van der Zeijst, B. A. M. (1990). Sequence evidence for RNA recombination in field isolates of avian coronavirus infectious bronchitis virus. *Vaccine* **8:**605–608.

Lachance, C., Arbour, N., Cashman, N. R., and Talbot, P. J. (1998). Involvement of aminopeptidase N (CD13) in infection of human neural cells by human coronavirus 229E. *J. Virol.* **72:**6511–6519.

Lai, M. M. C. (1986). Coronavirus leader-RNA-primed transcription: An alternative mechanism to RNA splicing. *BioEssays* **5:**257–260.

Lai, M. M. C. (1992). RNA recombination in animal and plant viruses. *Microbiol. Rev.* **56:**61–79.

Lai, M. M. C., and Cavanagh, D. (1997). The molecular biology of coronaviruses. *Adv. Virus Res.* **48:**1–100.

Lai, M. M. C., and Holmes, K. V. (2001). *Coronaviridae:* The viruses and their replication. *In* "Fields Virology" (D. M. Knipe and P. M. Howley, eds.), 4th edn. pp. 1163–1185. Lippincott, Williams & Wilkins, Philadelphia.

Lai, M. M. C., and Stohlman, S. A. (1978). RNA of mouse hepatitis virus. *J. Virol.* **26:**236–242.

Lai, M. M. C., and Stohlman, S. A. (1981). Comparative analysis of RNA genomes of mouse hepatitis viruses. *J. Virol.* **38:**661–670.

Lai, M. M. C., Liao, C.-L., Lin, Y.-J., and Zhang, X. (1994). Coronavirus: How a large RNA viral genome is replicated and transcribed. *Infect. Agents Dis.* **3:**98–105.

Lapps, W., Hogue, B. G., and Brian, D. A. (1987). Sequence analysis of the bovine coronavirus nucleocapsid and matrix protein genes. *Virology* **157:**47–57.

Lau, S. K. P., Woo, P. C. Y., Li, K. S. M., Huang, Y., Tsoi, H.-W., Wong, B. H. L., Wong, S. S. Y., Leung, S.-Y., Chan, K.-H., and Yuen, K.-Y. (2005). Severe acute respiratory syndrome coronavirus-like virus in Chinese horseshoe bats. *Proc. Natl. Acad. Sci. USA* **102:**14040–14045.

Laude, H., and Masters, P. S. (1995). *In* "The Coronaviridae" (S. G. Siddell, ed.), pp. 141–163. Plenum, New York.

Laude, H., Rasschaert, D., and Huet, J. C. (1987). Sequence and N-terminal processing of the transmembrane protein E1 of the coronavirus transmissible gastroenteritis virus. *J. Gen. Virol.* **68:**1687–1693.

Laude, H., Gelfi, J., Lavenant, L., and Charley, B. (1992). Single amino acid changes in the viral glycoprotein M affect induction of alpha interferon by the coronavirus transmissible gastroenteritis virus. *J. Virol.* **66:**743–749.

Laude, H., Godet, M., Bernard, S., Gelfi, J., Duarte, M., and Delmas, B. (1995). Functional domains in the spike protein of transmissible gastroenteritis virus. *Adv. Exp. Med. Biol.* **380:**299–304.

Lee, H. J., Shieh, C. K., Gorbalenya, A. E., Koonin, E. V., La Monica, N., Tuler, J., Bagdzhadzhyan, A., and Lai, M. M. (1991). The complete sequence (22 kilobases) of murine coronavirus gene 1 encoding the putative proteases and RNA polymerase. *Virology* **180:**567–582.

Leibowitz, J. L., Perlman, S., Weinstock, G., DeVries, J. R., Budzilowicz, C., Weissemann, J. M., and Weiss, S. R. (1988). Detection of a murine coronavirus nonstructural protein encoded in a downstream open reading frame. *Virology* **164:**156–164.

Lewicki, D. N., and Gallagher, T. M. (2002). Quaternary structure of coronavirus spikes in complex with carcinoembryonic antigen-related cell adhesion molecule cellular receptors. *J. Biol. Chem.* **277:**19727–19734.

Lewis, E. L., Harbour, D. A., Beringer, J. E., and Grinsted, J. (1992). Differential *in vitro* inhibition of feline enteric coronavirus and feline infectious peritonitis virus by actinomycin D. *J. Gen. Virol.* **73:**3285–3288.

Li, F., Li, W., Farzan, M., and Harrison, S. C. (2005b). Structure of SARS coronavirus spike receptor-binding domain complexed with receptor. *Science* **309:**1864–1868.

Li, H.-P., Zhang, X., Duncan, R., Comai, L., and Lai, M. M. C. (1997). Heterogeneous nuclear ribonucleoprotein A1 binds to the transcription-regulatory region of mouse hepatitis virus RNA. *Proc. Natl. Acad. Sci. USA* **94:**9544–9549.

Li, H.-P., Huang, P., Park, S., and Lai, M. M. C. (1999). Polypyrimidine tract-binding protein binds to the leader RNA of mouse hepatitis virus and serves as a regulator of viral transcription. *J. Virol.* **73:**772–777.

Li, W., Moore, M. J., Vasilieva, N., Sui, J., Wong, S. K., Berne, M. A., Somasundaran, M., Sullivan, J. L., Luzuriaga, K., Greenough, T. C., Choe, H., and Farzan, M. (2003). Angiotensin-converting enzyme 2 is a functional receptor for the SARS coronavirus. *Nature* **426:**450–454.

Li, W., Greenough, T. C., Moore, M. J., Vasilieva, N., Somasundaran, M., Sullivan, J. L., Farzan, M., and Choe, H. (2004). Efficient replication of severe acute respiratory syndrome coronavirus in mouse cells is limited by murine angiotensin-converting enzyme 2. *J. Virol.* **78:**11429–11433.

Li, W., Zhang, C., Sui, J., Kuhn, J. H., Moore, M. J., Luo, S., Wong, S. K., Huang, I. C., Xu, K., Vasilieva, N., Murakami, A., He, Y. *et al.* (2005a). Receptor and viral determinants of SARS-coronavirus adaptation to human ACE2. *EMBO J.* **24:**1634–1643.

Li, W., Shi, Z., Yu, M., Ren, W., Smith, C., Epstein, J. H., Wang, H., Crameri, G., Hu, Z., Zhang, H., Zhang, J., McEachern, J. *et al.* (2005c). Bats are natural reservoirs of SARS-like coronaviruses. *Science* **310:**676–679.

Liao, C. L., and Lai, M. M. C. (1992). RNA recombination in a coronavirus: Recombination between viral genomic RNA and transfected RNA fragments. *J. Virol.* **66:**6117–6124.

Lim, K. P., and Liu, D. X. (1998). Characterization of the two overlapping papain-like proteinase domains encoded in gene 1 of the coronavirus infectious bronchitis virus and determination of the C-terminal cleavage site of an 87-kDa protein. *Virology* **245:**303–312.

Lin, Y.-J., and Lai, M. M. C. (1993). Deletion mapping of a mouse hepatitis virus defective interfering RNA reveals the requirement of an internal and discontiguous sequence for replication. *J. Virol.* **67:**6110–6118.

Lin, Y.-J., Liao, C.-L., and Lai, M. M. C. (1994). Identification of the *cis*-acting signal for minu-strand RNA synthesis of a murine coronavirus: Implications for the role of minus-strand RNA in RNA replication and transcription. *J. Virol.* **68:**8131–8140.

Lissenberg, A., Vrolijk, M. M., van Vliet, A. L. W., Langereis, M. A., de Groot-Mijnes, J. D. F., Rottier, P. J. M., and de Groot, R. J. (2005). Luxury at a cost? Recombinant mouse hepatitis viruses expressing the accessory hemagglutinin-esterase protein display reduced fitness *in vitro*. *J. Virol.* **79:**15054–15063.

Liu, D. X., and Inglis, S. C. (1991). Association of the infectious bronchitis virus 3c protein with the virion envelope. *Virology* **185:**911–917.

Liu, D. X., Cavanagh, D., Green, P., and Inglis, S. C. (1991). A polycistronic mRNA specified by the coronavirus infectious bronchitis virus. *Virology* **184:**531–544.

Liu, D. X., Shen, S., Xu, H. Y., and Wang, S. F. (1998). Proteolytic mapping of the coronavirus infectious bronchitis virus 1b polyprotein: Evidence for the presence of four cleavage sites of the 3C-like proteinase and identification of two novel cleavage products. *Virology* **246:**288–297.

Liu, Q., Yu, W., and Leibowitz, J. L. (1997). A specific host cellular protein binding element near the 3′ end of mouse hepatitis virus genomic RNA. *Virology* **232:**74–85.

Liu, Q., Johnson, R. F., and Leibowitz, J. L. (2001). Secondary structural elements within the 3′ untranslated region of mouse hepatitis virus strain JHM genomic RNA. *J. Virol.* **75:**12105–12113.

Liu, S., Xiao, G., Chen, Y., He, Y., Niu, J., Escalante, C. R., Xiong, H., Farmar, J., Debnath, A. K., Tien, P., and Jiang, S. (2004). Interaction between heptad repeat 1 and 2 regions in spike protein of SARS-associated coronavirus: Implications for virus fusogenic mechanism and identification of fusion inhibitors. *Lancet* **363:**938–947.

Lomniczi, B. (1977). Biological properties of avian coronavirus RNA. *J. Gen. Virol.* **36:**531–533.

Lomniczi, B., and Kennedy, I. (1977). Genome of infectious bronchitis virus. *J. Virol.* **24:**99–107.

Lomniczi, B., and Morser, J. (1981). Polypeptides of infectious bronchitis virus. I. Polypeptides of the virion. *J. Gen. Virol.* **55:**155–164.

Lontok, E., Corse, E., and Machamer, C. E. (2004). Intracellular targeting signals contribute to the localization of coronavirus spike proteins near the virus assembly site. *J. Virol.* **78:**5913–5922.

Lu, Y., and Denison, M. R. (1997). Determinants of mouse hepatitis virus 3C-like proteinase activity. *Virology* **230:**335–342.

Lu, Y., Lu, X., and Denison, M. R. (1995). Identification and characterization of a serine-like proteinase of the murine coronavirus MHV-A59. *J. Virol.* **69:**3554–3559.

Luo, Z., and Weiss, S. R. (1998). Roles in cell-to-cell fusion of two conserved hydrophobic regions in the murine coronavirus spike protein. *Virology* **244:**483–494.

Luo, Z., Matthews, A. M., and Weiss, S. R. (1999). Amino acid substitutions within the leucine zipper domain of the murine coronavirus spike protein cause defects in oligomerization and the ability to induce cell-to-cell fusion. *J. Virol.* **73:**8152–8159.

Luytjes, W., Sturman, L. S., Bredenbeek, P. J., Charite, J., van der Zeijst, B. A., Horzinek, M. C., and Spaan, W. J. M. (1987). Primary structure of the glycoprotein E2 of coronavirus MHV-A59 and identification of the trypsin cleavage site. *Virology* **161:**479–487.

Luytjes, W., Bredenbeek, P. J., Noten, A. F., Horzinek, M. C., and Spaan, W. J. M. (1988). Sequence of mouse hepatitis virus A59 mRNA 2: Indications for RNA recombination between coronaviruses and influenza C virus. *Virology* **166:**415–422.

Luytjes, W., Gerritsma, H., and Spaan, W. J. M. (1996). Replication of synthetic interfering RNAs derived from coronavirus mouse hepatitis virus-A59. *Virology* **216:**174–183.

Luytjes, W., Gerritsma, H., Bos, E., and Spaan, W. (1997). Characterization of two temperature-sensitive mutants of coronavirus mouse hepatitis virus strain A59 with maturation defects in the spike protein. *J. Virol.* **71:**949–955.

Machamer, C. E., and Rose, J. K. (1987). A specific transmembrane domain of a coronavirus E1 glycoprotein is required for its retention in the Golgi region. *J. Cell. Biol.* **105:**1205–1214.

Machamer, C. E., Mentone, S. A., Rose, J. K., and Farquhar, M. G. (1990). The E1 glycoprotein of an avian coronavirus is targeted to the cis Golgi complex. *Proc. Natl. Acad. Sci. USA* **87:**6944–6948.

Macnaughton, M. R., Davies, H. A., and Nermut, M. V. (1978). Ribonucleoprotein-like structures from coronavirus particles. *J. Gen. Virol.* **39:**545–549.

Maeda, J., Maeda, A., and Makino, S. (1999). Release of E protein in membrane vesicles from virus-infected cells and E protein-expressing cells. *Virology* **263:**265–272.

Maeda, J., Repass, J. F., Maeda, A., and Makino, S. (2001). Membrane topology of coronavirus E protein. *Virology* **281:**163–169.

Makino, S., Fujioka, N., and Fujiwara, K. (1985). Structure of the intracellular defective viral RNAs of defective interfering particles of mouse hepatitis virus. *J. Virol.* **54:**329–336.

Makino, S., Keck, J. G., Stohlman, S. A., and Lai, M. M. C. (1986). High-frequency RNA recombination of murine coronaviruses. *J. Virol.* **57:**729–737.

Makino, S., Fleming, J. O., Keck, J. G., Stohlman, S. A., and Lai, M. M. C. (1987). RNA recombination of coronaviruses: Localization of neutralizing epitopes and neuropathogenic determinants on the carboxyl terminus of peplomers. *Proc. Natl. Acad. Sci. USA* **84:**6567–6571.

Makino, S., Shieh, C.-K., Keck, J. G., and Lai, M. M. C. (1988). Defective interfering particles of murine coronavirus: Mechanism of synthesis of defective viral RNAs. *Virology* **163:**104–111.

Makino, S., Yokomori, K., and Lai, M. M. C. (1990). Analysis of efficiently packaged defective interfering RNAs of murine coronavirus: Localization of a possible RNA-packaging signal. *J. Virol.* **64:**6045–6053.

Makino, S., Joo, M., and Makino, J. K. (1991). A system for the study of coronavirus mRNA synthesis: A regulated expressed subgenomic defective interfering RNA results from intergenic site insertion. *J. Virol.* **65:**6031–6041.

Marra, M. A., Jones, S. J., Astell, C. R., Holt, R. A., Brooks-Wilson, A., Butterfield, Y. S., Khattra, J., Asano, J. K., Barber, S. A., Chan, S. Y., Cloutier, A., Coughlin, S. M. *et al.* (2003). The genome sequence of the SARS-associated coronavirus. *Science* **300:**1399–1404.

Martin, J. P., Koehren, F., Rannou, J. J., and Kirn, A. (1988). Temperature-sensitive mutants of mouse hepatitis virus type 3 (MHV-3): Isolation, biochemical and genetic characterization. *Arch. Virol.* **100:**147–160.

Marzi, A., Gramberg, T., Simmons, G., Moller, P., Rennekamp, A. J., Krumbiegel, M., Geier, M., Eisemann, J., Turza, N., Saunier, B., Steinkasserer, A., Becker, S. *et al.* (2004). DC-SIGN and DC-SIGNR interact with the glycoprotein of Marburg virus and the S protein of severe acute respiratory syndrome coronavirus. *J. Virol.* **78:**12090–12095.

Masters, P. S. (1992). Localization of an RNA-binding domain in the nucleocapsid protein of the coronavirus mouse hepatitis virus. *Arch. Virol.* **125:**141–160.

Masters, P. S. (1999). Reverse genetics of the largest RNA viruses. *Adv. Virus Res.* **53:**245–264.

Masters, P. S., and Rottier, P. J. M. (2005). Coronavirus reverse genetics by targeted RNA recombination. *Curr. Top. Microbiol. Immunol.* **287:**133–159.

Masters, P. S., Koetzner, C. A., Kerr, C. K., and Heo, Y. (1994). Optimization of targeted RNA recombination and mapping of a novel nucleocapsid gene mutation in the coronavirus mouse hepatitis virus. *J. Virol.* **68:**328–337.

Matsuyama, S., and Taguchi, F. (2002). Receptor-induced conformational changes of murine coronavirus spike protein. *J. Virol.* **76:**11819–11826.

Matsuyama, S., Ujike, M., Morikawa, S., Tashiro, M., and Taguchi, F. (2005). Protease-mediated enhancement of severe acute respiratory syndrome coronavirus infection. *Proc. Natl. Acad. Sci. USA* **102:**12543–12547.

Mayer, T, Tamura, T, Falk, M, and Niemann, H. (1988). Membrane integration and intracellular transport of the coronavirus glycoprotein E1, a class III membrane glycoprotein. *J. Biol. Chem.* **263:**14956–14963.

Mazumder, R., Iyer, L. M., Vasudevan, S., and Aravind, L. (2002). Detection of novel members, structure-function analysis and evolutionary classification of the 2H phosphoesterase superfamily. *Nucleic Acids Res.* **30:**5229–5243.

McIntosh, K. (1974). Coronaviruses. A comparative review. *Curr. Top. Microbiol. Imunol.* **63:**85–129.

Mendez, A., Smerdou, C., Izeta, A., Gebauer, F., and Enjuanes, L. (1996). Molecular characterization of transmissible gastroenteritis coronavirus defective interfering genomes: Packaging and heterogeneity. *Virology* **217:**495–507.

Miura, H. S., Nakagaki, K., and Taguchi, F. (2004). N-terminal domain of the murine coronavirus receptor CEACAM1 is responsible for fusogenic activation and conformational changes of the spike protein. *J. Virol.* **78:**216–223.

Mizutani, T., Repass, J. F., and Makino, S. (2000). Nascent synthesis of leader sequence-containing subgenomic mRNAs in coronavirus genome-length replicative intermediate RNA. *Virology* **275:**238–243.

Molenkamp, R., and Spaan, W. J. M. (1997). Identification of a specific interaction between the coronavirus mouse hepatitis virus A59 nucleocapsid protein and packaging signal. *Virology* **239:**78–86.

Moore, M. J., Dorfman, T., Li, W., Wong, S. K., Li, Y., Kuhn, J. H., Coderre, J., Vasilieva, N., Han, Z., Greenough, T. C., Farzan, M., and Choe, H. (2004). Retroviruses pseudotyped with the severe acute respiratory syndrome coronavirus spike protein efficiently infect cells expressing angiotensin-converting enzyme 2. *J. Virol.* **78:**10628–10635.

Mortola, E., and Roy, P. (2004). Efficient assembly and release of SARS coronavirus-like particles by a heterologous expression system. *FEBS Lett.* **576:**174–178.

Mossel, E. C., Huang, C., Narayanan, K., Makino, S., Tesh, R. B., and Peters, C. J. (2005). Exogenous ACE2 expression allows refractory cell lines to support severe acute respiratory syndrome coronavirus replication. *J. Virol.* **79:**3846–3850.

Motokawa, K., Hohdatsu, T., Hashimoto, H., and Koyama, H. (1996). Comparison of the amino acid sequence and phylogenetic analysis of the peplomer, integral membrane and nucleocapsid proteins of feline, canine and porcine coronaviruses. *Microbiol. Immunol.* **40:**425–433.

Mounir, S., and Talbot, P. J. (1993). Human coronavirus OC43 RNA 4 lacks two open reading frames located downstream of the S gene of bovine coronavirus. *Virology* **192:**355–360.

Nal, B., Chan, C., Kien, F., Siu, L., Tse, J., Chu, K., Kam, J., Staropoli, I., Crescenzo-Chaigne, B., Escriou, N., van der Werf, S., Yuen, K.-Y. *et al.* (2005). Differential maturation and subcellular localization of severe acute respiratory syndrome coronavirus surface proteins S, M and E. *J. Gen. Virol.* **86:**1423–1434.

Nanda, S. K., and Leibowitz, J. L. (2001). Mitochondrial aconitase binds to the 3′ untranslated region of the mouse hepatitis virus genome. *J. Virol.* **75:**3352–3362.

Nanda, S. K., Johnson, R. F., Liu, Q., and Leibowitz, J. L. (2004). Mitochondrial HSP70, HSP40, and HSP60 bind to the 3′ untranslated region of the Murine hepatitis virus genome. *Arch. Virol.* **149:**93–111.

Napthine, S., Liphardt, J., Bloys, A., Routledge, S., and Brierley, I. (1999). The role of RNA pseudoknot stem 1 length in the promotion of efficient −1 ribosomal frameshifting. *J. Mol. Biol.* **288:**305–320.

Narayanan, K., and Makino, S. (2001). Cooperation of an RNA packaging signal and a viral envelope protein in coronavirus RNA packaging. *J. Virol.* **75:**9059–9067.

Narayanan, K., Maeda, A., Maeda, J., and Makino, S. (2000). Characterization of the coronavirus M protein and nucleocapsid interaction in infected cells. *J. Virol.* **74:**8127–8134.

Narayanan, K., Chen, C. J., Maeda, J., and Makino, S. (2003a). Nucleocapsid-independent specific viral RNA packaging via viral envelope protein and viral RNA signal. *J. Virol.* **77:**2922–2927.

Narayanan, K., Kim, K. H., and Makino, S. (2003b). Characterization of N protein self-association in coronavirus ribonucleoprotein complexes. *Virus Res.* **98:**131–140.

Nash, T. C., and Buchmeier, M. J. (1996). Spike glycoprotein-mediated fusion in biliary glycoprotein-independent cell-associated spread of mouse hepatitis virus infection. *Virology* **223:**68–78.

Nash, T. C., and Buchmeier, M. J. (1997). Entry of mouse hepatitis virus into cells by endosomal and nonendosomal pathways. *Virology* **233:**1–8.

Navas, S., Seo, S. H., Chua, M. M., Sarma, J. D., Lavi, E., Hingley, S. T., and Weiss, S. R. (2001). Murine coronavirus spike protein determines the ability of the virus to replicate in the liver and cause hepatitis. *J. Virol.* **75:**2452–2457.

Nedellec, P., Dveksler, G. S., Daniels, E., Turbide, C., Chow, B., Basile, A. A., Holmes, K. V., and Beauchemin, N. (1994). Bgp2, a new member of the carcinoembryonic antigen-related gene family, encodes an alternative receptor for mouse hepatitis viruses. *J. Virol.* **68:**4525–4537.

Nelson, G. W., and Stohlman, S. A. (1993). Localization of the RNA-binding domain of mouse hepatitis virus nucleocapsid protein. *J. Gen. Virol.* **74:**1975–1979.

Nelson, G. W., Stohlman, S. A., and Tahara, S. M. (2000). High affinity interaction between nucleocapsid protein and leader/intergenic sequence of mouse hepatitis virus RNA. *J. Gen. Virol.* **81:**181–188.

Ng, M. L., Lee, J. W., Leong, M. L., Ling, A. E., Tan, H. C., and Ooi, E. E. (2004). Topographic changes in SARS coronavirus-infected cells at late stages of infection. *Emerg. Infect. Dis.* **10:**1907–1914.

Nguyen, V.-P., and Hogue, B. (1997). Protein interactions during coronavirus assembly. *J. Virol.* **71:**9278–9284.

Niemann, H., and Klenk, H.-D. (1981). Coronavirus glycoprotein E1, a new type of viral glycoprotein. *J. Mol. Biol.* **153:**993–1010.

Niemann, H., Boschek, B., Evans, D., Rosing, M., Tamura, T., and Klenk, H.-D. (1982). Post-translational glycosylation of coronavirus glycoprotein E1: Inhibition by monensin. *EMBO J.* **1:**1499–1504.

Nomura, R., Kiyota, A., Suzaki, E., Kataoka, K., Ohe, Y., Miyamoto, K., Senda, T., and Fujimoto, T. (2004). Human coronavirus 229E binds to CD13 in rafts and enters the cell through caveolae. *J. Virol.* **78:**8701–8708.

Norman, J. O., McClurkin, A. W., and Bachrach, H. L. (1968). Infectious nucleic acid from a transmissible agent causing gastroenteritis in pigs. *J. Comp. Pathol.* **78:**227–235.

O'Connor, J. B., and Brian, D. A. (1999). The major product of porcine transmissible gastroenteritis coronavirus gene 3b is an integral membrane glycoprotein of 31 kDa. *Virology* **256:**152–161.

Oh, J. S., Song, D. S., and Park, B. K. (2003). Identification of a putative cellular receptor 150 kDa polypeptide for porcine epidemic diarrhea virus in porcine enterocytes. *J. Vet. Sci.* **4:**269–275.

Ohtsuka, N., and Taguchi, F. (1997). Mouse susceptibility to mouse hepatitis virus infection is linked to viral receptor genotype. *J. Virol.* **71:**8860–8863.

Ohtsuka, N., Yamada, Y. K., and Taguchi, F. (1996). Difference in virus-binding activity of two distinct receptor proteins for mouse hepatitis virus. *J. Gen. Virol.* **77:**1683–1692.

Ontiveros, E., Kuo, L., Masters, P. S., and Perlman, S. (2001). Inactivation of expression of gene 4 of mouse hepatitis virus strain JHM does not affect virulence in the murine CNS. *Virology* **289:**230–238.

Opstelten, D.-J., de Groote, P., Horzinek, M. C., Vennema, H., and Rottier, P. J. M. (1993). Disulfide bonds in folding and transport of mouse hepatitis coronavirus glycoproteins. *J. Virol.* **67:**7394–7401.

Opstelten, D.-J. E., Raamsman, M. J. B., Wolfs, K., Horzinek, M. C., and Rottier, P. J. M. (1995). Envelope glycoprotein interactions in coronavirus assembly. *J. Cell Biol.* **131:**339–349.

Ortego, J., Escors, D., Laude, H., and Enjuanes, L. (2002). Generation of a replication-competent, propagation-deficient virus vector based on the transmissible gastroenteritis coronavirus genome. *J. Virol.* **76:**11518–11529.

Ortego, J., Sola, I., Almazan, F., Ceriani, J. E., Riquelme, C., Balasch, M., Plana, J., and Enjuanes, L. (2003). Transmissible gastroenteritis coronavirus gene 7 is not essential but influences *in vivo* virus replication and virulence. *Virology* **308:**13–22.

Oshiro, L. (1973). Coronaviruses. *In* "Ultrastructure of Animal Viruses and Bacteriophages: An Atlas" (A. J. Dalton and F. Haguenau, eds.), pp. 331–343. Academic Press, New York.

Ozdarendeli, A., Ku, S., Rochat, S., Williams, G. D., Senanayake, S. D., and Brian, D. A. (2001). Downstream sequences influence the choice between a naturally occurring noncanonical and closely positioned upstream canonical heptameric fusion motif during bovine coronavirus subgenomic mRNA synthesis. *J. Virol.* **75:**7362–7374.

Patel, J. R., Davies, H. A., Edington, N., Laporte, J., and Macnaughton, M. R. (1982). Infection of a calf with the enteric coronavirus strain Paris. *Arch. Virol.* **73:**319–327.

Parker, M. M., and Masters, P. S. (1990). Sequence comparison of the N genes of five strains of the coronavirus mouse hepatitis virus suggests a three domain structure for the nucleocapsid protein. *Virology* **179:**463–468.

Parker, S. E., Gallagher, T. M., and Buchmeier, M. J. (1989). Sequence analysis reveals extensive polymorphism and evidence of deletions within the E2 glycoprotein gene of several strains of murine hepatitis virus. *Virology* **173:**664–673.

Pasternak, A. O., van den Born, E., Spaan, W. J. M., and Snijder, E. J. (2001). Sequence requirements for RNA strand transfer during nidovirus discontinuous subgenomic RNA synthesis. *EMBO J.* **20:**7220–7228.

Pasternak, A. O., van den Born, E., Spaan, W. J. M., and Snijder, E. J. (2003). The stability of the duplex between sense and antisense transcription-regulating sequences is a crucial factor in arterivirus subgenomic mRNA synthesis. *J. Virol.* **77:**1175–1183.

Pasternak, A. O., Spaan, W. J. M., and Snijder, E. J. (2004). Regulation of relative abundance of arterivirus subgenomic mRNAs. *J. Virol.* **78:**8102–8113.

Peiris, J. S. M., Lai, S. T., Poon, L. L., Guan, Y., Yam, L. Y., Lim, W., Nicholls, J., Yee, W. K., Yan, W. W., Cheung, M. T., Cheng, V. C., Chan, K. H. *et al.* (2003). Coronavirus as a possible cause of severe acute respiratory syndrome. *Lancet* **361:**1319–1325.

Peng, D., Koetzner, C. A., and P. S. Masters, P. S. (1995a). Analysis of second-site revertants of a murine coronavirus nucleocapsid protein deletion mutant and construction of nucleocapsid protein mutants by targeted RNA recombination. *J. Virol.* **69:**3449–3457.

Peng, D., Koetzner, C. A., McMahon, T., Zhu, Y., and Masters, P. S. (1995b). Construction of murine coronavirus mutants containing interspecies chimeric nucleocapsid proteins. *J. Virol.* **69:**5475–5484.

Pensiero, M. N., Dveksler, G. S., Cardellichio, C. B., Jiang, G. S., Elia, P. E., Dieffenbach, C. W., and Holmes, K. V. (1992). Binding of the coronavirus mouse hepatitis virus A59 to its receptor expressed from a recombinant vaccinia virus depends on posttranslational processing of the receptor glycoprotein. *J. Virol.* **66:**4028–4039.

Penzes, Z., Tibbles, K., Shaw, K., Britton, P., Brown, T. D. K., and Cavanagh, D. (1994). Characterization of a replicating and packaged defective RNA of avian coronavirus infectious bronchitis virus. *Virology* **203:**286–293.

Peti, W., Johnson, M. A., Herrmann, T., Neuman, B. W., Buchmeier, M. J., Nelson, M., Joseph, J., Page, R., Stevens, R. C., Kuhn, P., and Wuthrich, K. (2005). Structural genomics of the severe acute respiratory syndrome coronavirus: Nuclear magnetic resonance structure of the protein nsP7. *J. Virol.* **79:**12905–12913.

Pewe, L., Zhou, H., Netland, J., Tangudu, C., Olivares, H., Shi, L., Look, D., Gallagher, T., and Perlman, S. (2005). A severe acute respiratory syndrome-associated coronavirus-specific protein enhances virulence of an attenuated murine coronavirus. *J. Virol.* **79:**11335–11342.

Phillips, J. J., Chua, M. M., Lavi, E., and Weiss, S. R. (1999). Pathogenesis of chimeric MHV4/MHV-A59 recombinant viruses: The murine coronavirus spike protein is a major determinant of neurovirulence. *J. Virol.* **73:**7752–7760.

Pinon, J. D., Mayreddy, R. R., Turner, J. D., Khan, F. S., Bonilla, P. J., and Weiss, S. R. (1997). Efficient autoproteolytic processing of the MHV-A59 3C-like proteinase from the flanking hydrophobic domains requires membranes. *Virology* **230:**309–322.

Plant, E. P., Perez-Alvarado, G. C., Jacobs, J. L., Mukhopadhyay, B., Hennig, M., and Dinman, J. D. (2005). A three-stemmed mRNA pseudoknot in the SARS coronavirus frameshift signal. *PLoS Biol.* **3:**1012–1023.

Poon, L. L. M., Chu, D. K. W., Chan, K. H., Wong, O. K., Ellis, T. M., Leung, Y. H. C., Lau, S. K. P., Woo, P. C. Y., Suen, K. Y., Yuen, K. Y., Guan, Y., and Peiris, J. S. M. (2005). Identification of a novel coronavirus in bats. *J. Virol.* **79:**2001–2009.

Popova, R., and Zhang, X. (2002). The spike but not the hemagglutinin/esterase protein of bovine coronavirus is necessary and sufficient for viral infection. *Virology* **294:**222–236.

Prentice, E., Jerome, W. G., Yoshimori, T., Mizushima, N., and Denison, M. R. (2004a). Coronavirus replication complex formation utilizes components of cellular autophagy. *J. Biol. Chem.* **279:**10136–10141.

Prentice, E., McAuliffe, J., Lu, X., Subbarao, K., and Denison, M. R. (2004b). Identification and characterization of severe acute respiratory syndrome coronavirus replicase proteins. *J. Virol.* **78:**9977–9986.

Putics, A., Filipowicz, W., Hall, J., Gorbalenya, A. E., and Ziebuhr, J. (2005). ADP-ribose-1′-monophosphatase: A conserved coronavirus enzyme that is dispensable for viral replication in tissue culture. *J. Virol.* **79:**12721–12731.

Raamsman, M. J. B., Krijnse Locker, J., de Hooge, A., de Vries, A. A. F., Griffiths, G., Vennema, H., and Rottier, P. J. M. (2000). Characterization of the coronavirus mouse hepatitis virus strain A59 small membrane protein E. *J. Virol.* **74:**2333–2342.

Racaniello, V. R., and Baltimore, D. (1981). Cloned poliovirus cDNA is infectious in mammalian cells. *Science* **214:**916–919.

Raman, S., and Brian, D. A. (2005). Stem-loop IV in the 5′ untranslated region is a cis-acting element in bovine coronavirus defective interfering RNA replication. *J. Virol.* **79:**12434–12446.

Raman, S., Bouma, P., Williams, G. D., and Brian, D. A. (2003). Stem-loop III in the 5′ untranslated region is a cis-acting element in bovine coronavirus defective interfering RNA replication. *J. Virol.* **77:**6720–6730.

Ramos, F. D., Carrasco, M., Doyle, T., and Brierley, I. (2004). Programmed −1 ribosomal frameshifting in the SARS coronavirus. *Biochem. Soc. Trans.* **32:**1081–1083.

Rao, P. V., Kumari, S., and Gallagher, T. M. (1997). Identification of a contiguous 6–residue determinant in the MHV receptor that controls the level of virion binding to cells. *Virology* **229:**336–348.

Regl, G., Kaser, A., Iwersen, M., Schmid, H., Kohla, G., Strobl, B., Vilas, U., Schauer, R., and Vlasak, R. (1999). The hemagglutinin-esterase of mouse hepatitis virus strain S is a sialate-4-O-acetylesterase. *J. Virol.* **73:**4721–4727.

Rest, J. S., and Mindell, D. P. (2003). SARS associated coronavirus has a recombinant polymerase and coronaviruses have a history of host-shifting. *Infect. Genet. Evol.* **3:**219–225.

Ricard, C. S., Koetzner, C. A., Sturman, L. S., and Masters, P. S. (1995). A conditional-lethal murine coronavirus mutant that fails to incorporate the spike glycoprotein into assembled virions. *Virus Res.* **39:**261–276.

Rice, C. M., Grakoui, A., Galler, R., and Chambers, T. J. (1989). Transcription of infectious yellow fever RNA from full-length cDNA templates produced by *in vitro* ligation. *New Biologist* **1:**285–296.

Risco, C., Anton, I. M., Sune, C., Pedregosa, A. M., Martin-Alonso, J. M., Parra, F., Carrascosa, J. L., and Enjuanes, L. (1995). Membrane protein molecules of transmissible gastroenteritis coronavirus also expose the carboxy-terminal region on the external surface of the virion. *J. Virol.* **69:**5269–5277.

Risco, C., Anton, I. M., Enjuanes, L., and Carrascosa, J. L. (1996). The transmissible gastroenteritis coronavirus contains a spherical core shell consisting of M and N proteins. *J. Virol.* **70:**4773–4777.

Robb, J. A., Bond, C. W., and Leibowitz, J. L. (1979). Pathogenic murine coronaviruses. III. Biological and biochemical characterization of temperature-sensitive mutants of JHMV. *Virology* **94:**385–399.

Robbins, S. G., Frana, M. F., McGowan, J. J., Boyle, J. F., and Holmes, K. V. (1986). RNA-binding proteins of coronavirus MHV: Detection of monomeric and multimeric N protein with an RNA overlay-protein blot assay. *Virology* **150:**402–410.

Roseto, A., Bobulesco, P., Laporte, J., Escaig, J., Gaches, D., and Peries, J. (1982). Bovine enteric coronavirus structure as studied by a freeze-drying technique. *J. Gen. Virol.* **63:**241–245.

Rota, P. A., Oberste, M. S., Monroe, S. S., Nix, W. A., Campagnoli, R., Icenogle, J. P., Penaranda, S., Bankamp, B., Maher, K., Chen, M. H., Tong, S., Tamin, A. *et al.* (2003). Characterization of a novel coronavirus associated with severe acute respiratory syndrome. *Science* **300:**1394–1399.

Rottier, P. J. M. (1995). *In* "The Coronaviridae" (S. G. Siddell, ed.), pp. 115–139. Plenum, New York.

Rottier, P. J. M., and Rose, J. K. (1987). Coronavirus E1 protein expressed from cloned cDNA localizes in the Golgi region. *J. Virol.* **61:**2042–2045.

Rottier, P. J. M., Horzinek, M. C., and van der Zeijst, B. A. M. (1981). Viral protein synthesis in mouse hepatitis virus strain A59-infected cells: Effects of tunicamycin. *J. Virol.* **40:**350–357.

Rottier, P., Brandenburg, D., Armstrong, J., van der Zeijst, B., and Warren, G. (1984). Assembly *in vitro* of a spanning membrane protein of the endoplasmic reticulum: The E1 glycoprotein of coronavirus mouse hepatitis virus A59. *Proc. Natl. Acad. Sci. USA* **81:**1421–1425.

Rottier, P. J. M., Welling, G. W., Welling-Wester, S., Niesters, H. G. M., Lenstra, J. A., and van der Zeijst, B. A. M. (1986). Predicted membrane topology of the coronavirus protein E1. *Biochemistry* **25:**1335–1339.

Rowe, C. L., Baker, S. C., Nathan, M. J., and Fleming, J. O. (1997). Evolution of mouse hepatitis virus: Detection and characterization of spike deletion variants during persistent infection. *J. Virol.* **71:**2959–2969.

Rowland, R. R. R., Chauhan, V., Fang, Y., Pekosz, A., Kerrigan, M., and Burton, M. D. (2005). Intracellular localization of the severe acute respiratory syndrome coronavirus nucleocapsid protein: Absence of nucleolar accumulation during infection and after expression as a recombinant protein in Vero cells. *J. Virol.* **79:**11507–11512.

Saif, L. J. (2004). Animal coronaviruses: What can they teach us about the severe acute respiratory syndrome? *Rev. Sci. Tech.* **23:**643–660.

Sainz, B., Jr., Rausch, J. M., Gallaher, W. R., Garry, R. F., and Wimley, W. C. (2005). Identification and characterization of the putative fusion peptide of the severe acute respiratory syndrome-associated coronavirus spike protein. *J. Virol.* **79:**7195–7206.

Sanchez, C. M., Jimenez, G., Laviada, M. D., Correa, I., Sune, C., Bullido, M. J., Gebauer, F., Smerdou, C., Callebaut, P., Escribano, J. M., and Enjuanes, L. (1990). Antigenic homology among coronaviruses related to transmissible gastroenteritis virus. *Virology* **174:**410–417.

Sanchez, C. M., Izeta, A., Sanchez-Morgado, J. M., Alonso, S., Sola, I., Balasch, M., Plana-Duran, J., and Enjuanes, L. (1999). Targeted recombination demonstrates that the spike gene of transmissible gastroenteritis coronavirus is a determinant of its enteric tropism and virulence. *J. Virol.* **73:**7607–7618.

Sapats, S. I., Ashton, F., Wright, P. J., and Ignjatovic, J. (1996). Novel variation in the N protein of avian infectious bronchitis virus. *Virology* **226:**412–417.

Sawicki, D., Wang, T., and Sawicki, S. (2001). The RNA structures engaged in replication and transcription of the A59 strain of mouse hepatitis virus. *J. Gen. Virol.* **82:**385–396.

Sawicki, S. G., and Sawicki, D. L. (1986). Coronavirus minus strand RNA synthesis and effect of cycloheximide on coronavirus RNA synthesis. *J. Virol.* **57:**328–334.

Sawicki, S. G., and Sawicki, D. L. (1990). Coronavirus transcription: Subgenomic mouse hepatitis virus replicative intermediates function in RNA synthesis. *J. Virol.* **64:**1050–1056.

Sawicki, S. G., and Sawicki, D. L. (1998). A new model for coronavirus transcription. *Adv. Exp. Med. Biol.* **440:**215–219.

Sawicki, S. G., and Sawicki, D. L. (2005). Coronavirus transcription: A perspective. *Curr. Top. Microbiol. Immunol.* **287:**31–55.

Schaad, M. C., and Baric, R. S. (1994). Genetics of mouse hepatitis virus transcription: Evidence that subgenomic negative strands are functional templates. *J. Virol.* **68:**8169–8179.

Schaad, M. C., Stohlman, S. A., Egbert, J., Lum, K., Fu, K., Wei, T., Jr., and Baric, R. S. (1990). Genetics of mouse hepatitis virus transcription: Identification of cistrons which may function in positive and negative strand RNA synthesis. *Virology* **177:**634–645.

Schelle, B., Karl, N., Ludewig, B., Siddell, S. G., and Thiel, V. (2005). Selective replication of coronavirus genomes that express nucleocapsid protein. *J. Virol.* **79:**6620–6630.

Schickli, J. H., Zelus, B. D., Wentworth, D. E., Sawicki, S. G., and Holmes, K. V. (1997). The murine coronavirus mouse hepatitis virus strain A59 from persistently infected murine cells exhibits an extended host range. *J. Virol.* **71:**9499–9507.

Schickli, J. H., Thackray, L. B., Sawicki, S. G., and Holmes, K. V. (2004). The N-terminal region of the murine coronavirus spike glycoprotein is associated with the extended host range of viruses from persistently infected murine cells. *J. Virol.* **78:**9073–9083.

Schiller, J. J., Kanjanahaluethai, A., and Baker, S. C. (1998). Processing of the coronavirus MHV-JHM polymerase polyprotein: Identification of precursors and proteolytic products spanning 400 kilodaltons of ORF1a. *Virology* **242:**288–302.

Schochetman, G., Stevens, R. H., and Simpson, R. W. (1977). Presence of infectious polyadenylated RNA in coronavirus avian bronchitis virus. *Virology* **77:**772–782.

Schultze, B., Gross, H. J., Brossmer, R., and Herrler, G. (1991). The S protein of bovine coronavirus is a hemagglutinin recognizing 9-O-acetylated sialic acid as a receptor determinant. *J. Virol.* **65:**6232–6237.

Schwarz, B., Routledge, E., and Siddell, S. G. (1990). Murine coronavirus nonstructural protein ns2 is not essential for virus replication in transformed cells. *J. Virol.* **64:**4784–4791.

Senanayake, S. D., Hofmann, M. A., Maki, J. L., and Brian, D. A. (1992). The nucleocapsid protein gene of bovine coronavirus is bicistronic. *J. Virol.* **66:**5277–5283.

Sethna, P. B., Hung, S. L., and Brian, D. A. (1989). Coronavirus subgenomic minus-strand RNAs and the potential for mRNA replicons. *Proc. Natl. Acad. Sci. USA* **86:**5626–5630.

Sethna, P. B., Hofmann, M. A., and Brian, D. A. (1991). Minus-strand copies of replicating coronavirus mRNAs contain antileaders. *J. Virol.* **65:**320–325.

Seybert, A., Hegyi, A., Siddell, S. G., and Ziebuhr, J. (2000). The human coronavirus 229E superfamily 1 helicase has RNA and DNA duplex-unwinding activities with 5′-to-3′ polarity. *RNA* **6:**1056–1068.

Shen, S., Law, Y. C., and Liu, D. X. (2004). A single amino acid mutation in the spike protein of coronavirus infectious bronchitis virus hampers its maturation and incorporation into virions at the nonpermissive temperature. *Virology* **326:**288–298.

Shen, X., and Masters, P. S. (2001). Evaluation of the role of heterogeneous nuclear ribonucleoprotein A1 as a host factor in murine coronavirus discontinuous transcription and genome replication. *Proc. Natl. Acad. Sci. USA* **98:**2717–2722.

Shi, S. T., Schiller, J. J., Kanjanahaluethai, A., Baker, S. C., Oh, J. W., and Lai, M. M. C. (1999). Colocalization and membrane association of murine hepatitis virus gene 1 products and *De novo*-synthesized viral RNA in infected cells. *J. Virol.* **73:**5957–5969.

Shi, S. T., Huang, P., Li, H.-P., and Lai, M. M. C. (2000). Heterogeneous nuclear ribonucleoprotein A1 regulates RNA synthesis of a cytoplasmic virus. *EMBO J.* **19:**4701–4711.

Shi, S. T., Yu, G. Y., and Lai, M. M. C. (2003). Multiple type A/B heterogeneous nuclear ribonucleoproteins (hnRNPs) can replace hnRNP A1 in mouse hepatitis virus RNA synthesis. *J. Virol.* **77:**10584–10593.

Siddell, S. G., (ed.) (1995). "The Coronaviridae." Plenum, New York.

Siddell, S. G., Barthel, A., and Ter Meulen, V. (1981). Coronavirus JHM: A virion-associated protein kinase. *J. Gen. Virol.* **52:**235–243.

Simmons, G., Reeves, J. D., Rennekamp, A. J., Amberg, S. M., Piefer, A. J., and Bates, P. (2004). Characterization of severe acute respiratory syndrome-associated coronavirus (SARS-CoV) spike glycoprotein-mediated viral entry. *Proc. Natl. Acad. Sci. USA* **101:**4240–4245.

Sims, A. C., Ostermann, J., and Denison, M. R. (2000). Mouse hepatitis virus replicase proteins associate with two distinct populations of intracellular membranes. *J. Virol.* **74:**5647–5654.

Skinner, M. A., Ebner, D., and Siddell, S. G. (1985). Coronavirus MHV-JHM mRNA 5 has a sequence arrangement which potentially allows translation of a second, downstream open reading frame. *J. Gen. Virol.* **66:**581–592.

Smith, A. L., Cardellichio, C. B., Winograd, D. F., de Souza, M. S., Barthold, S. W., and Holmes, K. V. (1991). Monoclonal antibody to the receptor for murine coronavirus MHV-A59 inhibits viral replication *in vivo*. *J. Infect. Dis.* **163:**879–882.

Smits, S. L., Gerwig, G. J., van Vliet, A. L., Lissenberg, A., Briza, P., Kamerling, J. P., Vlasak, R., and de Groot, R. J. (2005). Nidovirus sialate-O-acetylesterases: Evolution and substrate specificity of coronaviral and toroviral receptor-destroying enzymes. *J. Biol. Chem.* **280:**6933–6941.

Snijder, E. J., and Horzinek, M. C. (1993). Toroviruses: Replication, evolution and comparison with other members of the coronavirus-like superfamily. *J. Gen. Virol.* **74:**2305–2316.

Snijder, E. J., and Meulenberg, J. J. (1998). The molecular biology of arteriviruses. *J. Gen. Virol.* **79:**961–979.

Snijder, E. J., den Boon, J. A., Bredenbeek, P. J., Horzinek, M. C., Rijnbrand, R., and Spaan, W. J. M. (1990). The carboxy-terminal part of the putative Berne virus polymerase is expressed by ribosomal frameshifting and contains sequence motifs which indicate that toro- and coronaviruses are evolutionarily related. *Nucleic Acids Res.* **18:**4535–4542.

Snijder, E. J., den Boon, J. A., Horzinek, M. C., and Spaan, W. J. M. (1991). Comparison of the genome organization of toro- and coronaviruses: Evidence for two non-homologous RNA recombination events during Berne virus evolution. *Virology* **180:**448–452.

Snijder, E. J., Bredenbeek, P. J., Dobbe, J. C., Thiel, V., Ziebuhr, J., Poon, L. L. M., Guan, Y., Rozanov, M., Spaan, W. J. M., and Gorbalenya., A. E. (2003). Unique and conserved features of genome and proteome of SARS coronavirus, an early split-off from the coronavirus group 2 lineage. *J. Mol. Biol.* **331:**991–1004.

Soe, L. H., Shieh, C. K., Baker, S. C., Chang, M. F., and Lai, M. M. C. (1987). Sequence and translation of the murine coronavirus 5′-end genomic RNA reveals the N-terminal structure of the putative RNA polymerase. *J. Virol.* **61:**3968–3976.

Sola, I., Moreno, J. L., Zuniga, S., Alonso, S., and Enjuanes, L. (2005). Role of nucleotides immediately flanking the transcription-regulating sequence core in coronavirus subgenomic mRNA synthesis. *J. Virol.* **79:**2506–2516.

Somogyi, P., Jenner, A. J., Brierley, I., and Inglis, S. C. (1993). Ribosomal pausing during translation of an RNA pseudoknot. *Mol. Cell. Biol.* **13:**6931–6940.

Song, H. C., Seo, M. Y., Stadler, K., Yoo, B. J., Choo, Q. L., Coates, S. R., Uematsu, Y., Harada, T., Greer, C. E., Polo, J. M., Pileri, P., Eickmann, M. *et al.* (2004). Synthesis and characterization of a native, oligomeric form of recombinant severe acute respiratory syndrome coronavirus spike glycoprotein. *J. Virol.* **78:**10328–10335.

Spagnolo, J. F., and Hogue, B. G. (2000). Host protein interactions with the 3′ end of bovine coronavirus RNA and the requirement of the poly(A) tail for coronavirus defective genome replication. *J. Virol.* **74:**5053–5065.

Sperry, S. M., Kazi, L., Graham, R. L., Baric, R. S., Weiss, S. R., and Denison, M. R. (2005). Single-amino-acid substitutions in open reading frame (ORF) 1b-nsp14 and ORF 2a proteins of the coronavirus mouse hepatitis virus are attenuating in mice. *J. Virol.* **79:**3391–3400.

Stanhope, M. J., Brown, J. R., and Amrine-Madsen, H. (2004). Evidence from the evolutionary analysis of nucleotide sequences for a recombinant history of SARS-CoV. *Infect. Genet. Evol.* **4:**15–19.

Stauber, R., Pfleiderera, M., and Siddell, S. (1993). Proteolytic cleavage of the murine coronavirus surface glycoprotein is not required for fusion activity. *J. Gen. Virol.* **74:**183–191.

Stavrinides, J., and Guttman, D. S. (2004). Mosaic evolution of the severe acute respiratory syndrome coronavirus. *J. Virol.* **78:**76–82.

Stern, D. F., and Sefton, B. M. (1982). Synthesis of coronavirus mRNAs: Kinetics of inactivation of infectious bronchitic virus RNA synthesis by UV light. *J. Virol.* **42:**755–759.

Stern, D. F., and Sefton, B. M. (1982). Coronavirus proteins: Structure and function of the oligosaccharides of the avian infectious bronchitis virus glycoproteins. *J. Virol.* **44:**804–812.

Stohlman, S. A., and Lai, M. M. C. (1979). Phosphoproteins of murine hepatitis virus. *J. Virol.* **32:**672–675.

Stohlman, S. A., Fleming, J. O., Patton, C. D., and Lai, M. M. C. (1983). Synthesis and subcellular localization of the murine coronavirus nucleocapsid protein. *Virology* **130:**527–532.

Stohlman, S. A., Baric, R. S., Nelson, G. N., Soe, L. H., Welter, L. M., and Deans, R. J. (1988). Specific interaction between coronavirus leader RNA and nucleocapsid protein. *J. Virol.* **62:**4288–4295.

Sturman, L. S. (1977). Characterization of a coronavirus: I. Structural proteins: Effect of preparative conditions on the migration of protein in polyacrylamide gels. *Virology* **77:**637–649.

Sturman, L. S., and Holmes, K. V. (1983). The molecular biology of coronaviruses. *Adv. Virus Res.* **28:**35–111.

Sturman, L. S., Holmes, K. V., and Behnke, J. (1980). Isolation of coronavirus envelope glycoproteins and interaction with the viral nucleocapsid. *J. Virol.* **33:**449–462.

Sturman, L. S., Ricard, C. S., and Holmes, K. V. (1985). Proteolytic cleavage of the E2 glycoprotein of murine coronavirus: Activation of cell-fusing activity of virions by trypsin and separation of two different 90K cleavage fragments. *J. Virol.* **56:**904–911.

Sturman, L. S., Eastwood, C., Frana, M. F., Duchala, C., Baker, F., Ricard, C. S., Sawicki, S. G., and Holmes, K. V. (1987). Temperature-sensitive mutants of MHV-A59. *Adv. Exp. Med. Biol.* **218:**159–168.

Sturman, L. S., Ricard, C. S., and Holmes, K. V. (1990). Conformational change of the coronavirus peplomer glycoprotein at pH 8.0 and 37 degrees C correlates with virus aggregation and virus-induced cell fusion. *J. Virol.* **64:**3042–3050.

Sugiyama, K., and Amano, Y. (1981). Morphological and biological properties of a new coronavirus associated with diarrhea in infant mice. *Arch. Virol.* **67:**241–251.

Sui, J., Li, W., Murakami, A., Tamin, A., Matthews, L. J., Wong, S. K., Moore, M. J., Tallarico, A. S., Olurinde, M., Choe, H., Anderson, L. J., Bellini, W. J. *et al.* (2004). Potent neutralization of severe acute respiratory syndrome (SARS) coronavirus by a human mAb to S1 protein that blocks receptor association. *Proc. Natl. Acad. Sci. USA* **101:**2536–2541.

Supekar, V. M., Bruckmann, C., Ingallinella, P., Bianchi, E., Pessi, A., and Carfi, A. (2004). Structure of a proteolytically resistant core from the severe acute respiratory syndrome coronavirus S2 fusion protein. *Proc. Natl. Acad. Sci. USA* **101:**17958–17963.

Sutton, G., Fry, E., Carter, L., Sainsbury, S., Walter, T., Nettleship, J., Berrow, N., Owens, R., Gilbert, R., Davidson, A., Siddell, S., Poon, L. L. *et al.* (2004). The nsp9 replicase protein of SARS-coronavirus, structure and functional insights. *Structure* **12:**341–353.

Suzuki, H., and Taguchi, F. (1996). Analysis of the receptor-binding site of murine coronavirus spike protein. *J. Virol.* **70:**2632–2636.

Swift, A. M., and Machamer, C. E. (1991). A Golgi retention signal in a membrane-spanning domain of coronavirus E1 protein. *J. Cell Biol.* **115:**19–30.

Taguchi, F. (1993). Fusion formation by the uncleaved spike protein of murine coronavirus JHMV variant cl-2. *J. Virol.* **67:**1195–1202.

Taguchi, F. (1995). The S2 subunit of the murine coronavirus spike protein is not involved in receptor binding. *J. Virol.* **69:**7260–7263.

Taguchi, F., Ikeda, T., Makino, S., and Yoshikura, H. (1994). A murine coronavirus MHV-S isolate from persistently infected cells has a leader and two consensus sequences between the M and N genes. *Virology* **198:**355–359.

Tahara, S. M., Dietlin, T. A., Bergmann, C. C., Nelson, G. W., Kyuwa, S., Anthony, R. P., and Stohlman, S. A. (1994). Coronavirus translational regulation: Leader affects mRNA efficiency. *Virology* **202:**621–630.

Tahara, S. M., Dietlin, T. A., Nelson, G. W., Stohlman, S. A., and Manno, D. J. (1998). Mouse hepatitis virus nucleocapsid protein as a translational effector of viral mRNAs. *Adv. Exp. Med. Biol.* **440:**313–318.

Tan, K., Zelus, B. D., Meijers, R., Liu, J. H., Bergelson, J. M., Duke, N., Zhang, R., Joachimiak, A., Holmes, K. V., and Wang, J. H. (2002). Crystal structure of murine sCEACAM1a[1,4]: A coronavirus receptor in the CEA family. *EMBO J.* **21:**2076–2086.

Thackray, L. B., and Holmes, K. V. (2004). Amino acid substitutions and an insertion in the spike glycoprotein extend the host range of the murine coronavirus MHV-A59. *Virology* **324:**510–524.

Thackray, L. B., Turner, B. C., and Holmes, K. V. (2005). Substitutions of conserved amino acids in the receptor-binding domain of the spike glycoprotein affect utilization of murine CEACAM1a by the murine coronavirus MHV-A59. *Virology* **334:**98–110.

Thiel, V., and Siddell, S. G. (1994). Internal ribosome entry in the coding region of murine hepatitis virus mRNA5. *J. Gen. Virol.* **75:**3041–3046.

Thiel, V., and Siddell, S. G. (2005). Reverse genetics of coronaviruses using vaccinia virus vectors. *Curr. Top. Microbiol. Immunol.* **287:**199–227.

Thiel, V., Rashtchian, A., Herold, J., Schuster, D. M., Guan, N., and Siddell, S. G. (1997). Effective amplification of 20–kb DNA by reverse transcription PCR. *Anal. Biochem.* **252:**62–70.

Thiel, V., Herold, J., Schelle, B., and Siddell, S. G. (2001a). Infectious RNA transcribed *in vitro* from a cDNA copy of the human coronavirus genome cloned in vaccinia virus. *J. Gen. Virol.* **82:**1273–1281.

Thiel, V., Herold, J., Schelle, B., and Siddell, S. G. (2001b). Viral replicase gene products suffice for coronavirus discontinuous transcription. *J. Virol.* **75:**6676–6681.

Thiel, V., Ivanov, K. A., Putics, A., Hertzig, T., Schelle, B., Bayer, S., Weissbrich, B., Snijder, E. J., Rabenau, H., Doerr, H. W., Gorbalenya, A. E., and Ziebuhr, J. (2003a). Mechanisms and enzymes involved in SARS coronavirus genome expression. *J. Gen. Virol.* **84:**2305–2315.

Thiel, V., Karl, N., Schelle, B., Disterer, P., Klagge, I., and Siddell, S. G. (2003b). Multigene RNA vector based on coronavirus transcription. *J. Virol.* **77:**9790–9798.

Thorp, E. B., and Gallagher, T. M. (2004). Requirements for CEACAMs and cholesterol during murine coronavirus cell entry. *J. Virol.* **78:**2682–2692.

Tooze, J., Tooze, S. A., and Warren, G. (1984). Replication of coronavirus MHV-A59 in Sac- cells: Determination of the first site of budding of progeny virions. *Eur. J. Cell Biol.* **33:**281–293.

Tooze, S. A., Tooze, J., and Warren, G. (1988). Site of addition of N-acetyl-galactosamine to the E1 glycoprotein of mouse hepatitis virus-A59. *J. Cell Biol.* **106:**1475–1487.

Torres, J., Wang, J., Parthasarathy, K., and Liu, D. X. (2005). The transmembrane oligomers of coronavirus protein E. *Biophys. J.* **88:**1283–1290.

Towler, P., Staker, B., Prasad, S. G., Menon, S., Tang, J., Parsons, T., Ryan, D., Fisher, M., Williams, D., Dales, N. A., Patane, M. A., and Pantoliano, M. W. (2004). ACE2 X-ray structures reveal a large hinge-bending motion important for inhibitor binding and catalysis. *J. Biol. Chem.* **279:**17996–18007.

Tresnan, D. B., Levis, R., and Holmes, K. V. (1996). Feline aminopeptidase N serves as a receptor for feline, canine, porcine, and human coronaviruses in serogroup I. *J. Virol.* **70:**8669–8674.

Tripet, B., Howard, M. W., Jobling, M., Holmes, R. K., Holmes, K. V., and Hodges, R. S. (2004). Structural characterization of the SARS-coronavirus spike S fusion protein core. *J. Biol. Chem.* **279:**20836–20849.

Tsunemitsu, H., el-Kanawati, Z. R., Smith, D.R, Reed, H. H., and Saif, L. J. (1995). Isolation of coronaviruses antigenically indistinguishable from bovine coronavirus from wild ruminants with diarrhea. *J. Clin. Microbiol.* **33:**3264–3269.

van der Hoek, L., Pyrc, K., Jebbink, M. F., Vermeulen-Oost, W., Berkhout, R. J. M., Wolthers, K. C., Wertheim-van Dillen, P. M. E., Kaandorp, J., Spaargaren, J., and Berkhout, B. (2004). Identification of a new human coronavirus. *Nat. Med.* **10:**368–373.

van der Meer, Y., Snijder, E. J., Dobbe, J. C., Schleich, S., Denison, M. R., Spaan, W. J. M., and Locker, J. K. (1999). Localization of mouse hepatitis virus nonstructural proteins and RNA synthesis indicates a role for late endosomes in viral replication. *J. Virol.* **73:**7641–7657.

van der Most, R. G., and Spaan, W. J. M. (1995). *In* "The Coronaviridae" (S. G. Siddell, ed.), pp. 11–31. Plenum, New York.

van der Most, R. G., Bredenbeek, P. J., and Spaan, W. J. M. (1991). A domain at the 3′ end of the polymerase gene is essential for encapsidation of coronavirus defective interfering RNAs. *J. Virol.* **65:**3219–3226.

van der Most, R. G., Heijnen, L., Spaan, W. J. M., and de Groot, R. J. (1992). Homologous RNA recombination allows efficient introduction of site-specific mutations into the genome of coronavirus MHV-A59 via synthetic co-replicating RNAs. *Nucleic Acids Res.* **20:**3375–3381.

van der Most, R. G., de Groot, R. J., and Spaan, W. J. M. (1994). Subgenomic RNA synthesis directed by a synthetic defective interfering RNA of mouse hepatitis virus: A study of coronavirus transcription initiation. *J. Virol.* **68:**3656–3666.

van der Most, R. G., Luytjes, W., Rutjes, S., and Spaan, W. J. M. (1995). Translation but not the encoded sequence is essential for the efficient propogation of defective interfering RNAs of the coronavirus mouse hepatitis virus. *J. Virol.* **69:**3744–3751.

van Marle, G., Luytjes, W., van der Most, R. G., van der Straaten, T., and Spaan, W. J. M. (1995). Regulation of coronavirus mRNA transcription. *J. Virol.* **69:**7851–7856.

van Marle, G., Dobbe, J. C., Gultyaev, A. P., Luytjes, W., Spaan, W. J. M., and Snijder, E. J. (1999). Arterivirus discontinuous mRNA transcription is guided by base pairing between sense and antisense transcription-regulating sequences. *Proc. Natl. Acad. Sci. USA* **96:**12056–12061.

van Vliet, A. L., Smits, S. L., Rottier, P. J. M., and de Groot, R. J. (2002). Discontinuous and non-discontinuous subgenomic RNA transcription in a nidovirus. *EMBO J.* **21:**6571–6580.

Vennema, H., Heijnen, L., Zijderveld, A., Horzinek, M. C., and Spaan, W. J. M. (1990). Intracellular transport of recombinant coronavirus spike proteins: Implications for virus assembly. *J. Virol.* **64:**339–346.

Vennema, H., Rijnbrand, R., Heijnen, L., Horzinek, M. C., and Spaan, W. J. M. (1991). Enhancement of the vaccinia virus/phage T7 RNA polymerase expression system using encephalomyocarditis virus 5′-untranslated region sequences. *Gene* **108:**201–209.

Vennema, H., Godeke, G.-J., Rossen, J. W. A., Voorhout, W. F., Horzinek, M. C., Opstelten, D.-J. E., and Rottier, P. J. M. (1996). Nucleocapsid-independent assembly of coronavirus-like particles by co-expression of viral envelope protein genes. *EMBO J.* **15:**2020–2028.

Vlasak, R., Luytjes, W., Spaan, W., and Palese, P. (1988a). Human and bovine coronaviruses recognize sialic acid-containing receptors similar to those of influenza C viruses. *Proc. Natl. Acad. Sci. USA* **85:**4526–4529.

Vlasak, R., Luytjes, W., Leider, J., Spaan, W., and Palese, P. (1988b). The E3 protein of bovine coronavirus is a receptor-destroying enzyme with acetylesterase activity. *J. Virol.* **62:**4686–4690.

von Grotthuss, M., Wyrwicz, L. S., and Rychlewski, L. (2003). mRNA cap-1 methyltransferase in the SARS genome. *Cell* **113:**701–702.

Wang, Y., and Zhang, X. (1999). The nucleocapsid protein of mouse hepatitis virus interacts with the cellular heterogeneous nuclear ribonucleoprotein A1 *in vitro* and *in vivo*. *Virology* **265:**96–109.

Wang, L., Junker, D., and Collisson, E. W. (1993). Evidence of natural recombination within the S1 gene of infectious bronchitis virus. *Virology* **192:**710–716.

Wang, L., Junker, D., Hock, L., Ebiary, E., and Collisson, E. W. (1994). Evolutionary implications of genetic variations in the S1 gene of infectious bronchitis virus. *Virus Res.* **34:**327–338.

Wang, P., Chen, J., Zheng, A., Nie, Y., Shi, X., Wang, W., Wang, G., Luo, M., Liu, H., Tan, L., Song, X., Wang, Z. *et al.* (2004). Expression cloning of functional receptor used by SARS coronavirus. *Biochem. Biophys. Res. Commun.* **315:**439–444.

Wege, H., Muller, A., and ter Meulen, V. (1978). Genomic RNA of the murine coronavirus JHM. *J. Gen. Virol.* **41:**217–227.

Weismiller, D. G., Sturman, L. S., Buchmeier, M. J., Fleming, J. O., and Holmes, K. V. (1990). Monoclonal antibodies to the peplomer glycoprotein of coronavirus mouse hepatitis virus identify two subunits and detect a conformational change in the subunit released under mild alkaline conditions. *J. Virol.* **64:**3051–3055.

Weiss, S. R., Zoltick, P. W., and Leibowitz, J. L. (1993). The ns 4 gene of mouse hepatitis virus (MHV), strain A 59 contains two ORFs and thus differs from ns 4 of the JHM and S strains. *Arch. Virol.* **129:**301–309.

Weisz, O. A., Swift, A. M., and Machamer, C. E. (1993). Oligomerization of a membrane protein correlates with its retention in the Golgi complex. *J. Cell Biol.* **122:**1185–1196.

Wentworth, D. E., and Holmes, K. V. (2001). Molecular determinants of species specificity in the coronavirus receptor aminopeptidase N (CD13): Influence of N-linked glycosylation. *J. Virol.* **75:**9741–9752.

Wessner, D. R., Shick, P. C., Lu, J. H., Cardellichio, C. B., Gagneten, S. E., Beauchemin, N., Holmes, K. V., and Dveksler, G. S. (1998). Mutational analysis of the virus and monoclonal antibody binding sites in MHVR, the cellular receptor of the murine coronavirus mouse hepatitis virus strain A59. *J. Virol.* **72:**1941–1948.

Wilbur, S. M., Nelson, G. W., Lai, M. M. C., McMillan, M., and Stohlman, S. A. (1986). Phosphorylation of the mouse hepatitis virus nucleocapsid protein. *Biochem. Biophys. Res. Commun.* **141:**7–12. Erratum 884.

Wilhelmsen, K. C., Leibowitz, J. L., Bond, C. W., and Robb, J. A. (1981). The replication of murine coronaviruses in enucleated cells. *Virology* **110:**225–230.

Williams, G. D., Chang, R. Y., and Brian, D. A. (1999). A phylogenetically conserved hairpin-type 3′ untranslated region pseudoknot functions in coronavirus RNA replication. *J. Virol.* **73:**8349–8355.

Williams, R. K., Jiang, G. S., Snyder, S. W., Frana, M. F., and Holmes, K. V. (1990). Purification of the 110–kilodalton glycoprotein receptor for mouse hepatitis virus (MHV)-A59 from mouse liver and identification of a nonfunctional, homologous protein in MHV-resistant SJL/J mice. *J. Virol.* **64:**3817–3823.

Williams, R. K., Jiang, G. S., and Holmes, K. V. (1991). Receptor for mouse hepatitis virus is a member of the carcinoembryonic antigen family of glycoproteins. *Proc. Natl. Acad. Sci. USA* **88:**5533–5536.

Wilson, L., McKinlay, C., Gage, P., and Ewart, G. (2004). SARS coronavirus E protein forms cation-selective ion channels. *Virology* **330:**322–331.

Wong, S. K., Li, W., Moore, M. J., Choe, H., and Farzan, M. (2004). A 193–amino acid fragment of the SARS coronavirus S protein efficiently binds angiotensin-converting enzyme 2. *J. Biol. Chem.* **279:**3197–3201.

Woo, K., Joo, M., Narayanan, K., Kim, K. H., and Makino, S. (1997). Murine coronavirus packaging signal confers packaging to nonviral RNA. *J. Virol.* **71:**824–827.

Woo, P. C. Y., Lau, S. K. P., Chu, C.-M., Chan, K.-H., Tsoi, H.-W., Huang, Y., Wong, B. H. L., Poon, R. W. S., Cai, J. J., Luk, W.-K., Poon, L. L. M., Wong, S. S. Y. *et al.* (2005). Characterization and complete genome sequence of a novel coronavirus, coronavirus HKU1, from patients with pneumonia. *J. Virol.* **79:**884–895.

Wu, H. Y., Guy, J. S., Yoo, D., Vlasak, R., Urbach, E., and Brian, D. A. (2003). Common RNA replication signals exist among group 2 coronaviruses: Evidence for *in vivo* recombination between animal and human coronavirus molecules. *Virology* **315:**174–183.

Wurm, T., Chen, H., Hodgson, T., Britton, P., Brooks, G., and Hiscox, J. A. (2001). Localization to the nucleolus is a common feature of coronavirus nucleoproteins, and the protein may disrupt host cell division. *J. Virol.* **75:**9345–9356.

Xiao, X., Chakraborti, S., Dimitrov, A. S., Gramatikoff, K., and Dimitrov, D. S. (2003). The SARS-CoV S glycoprotein: Expression and functional characterization. *Biochem. Biophys. Res. Commun.* **312:**1159–1164.

Xu, H. Y., Lim, K. P., Shen, S., and Liu, D. X. (2001). Further identification and characterization of novel intermediate and mature cleavage products released from the ORF 1b region of the avian coronavirus infectious bronchitis virus 1a/1b polyprotein. *Virology* **288:**212–222.

Xu, Y., Liu, Y., Lou, Z., Qin, L., Li, X., Bai, Z., Pang, H., Tien, P., Gao, G. F., and Rao, Z. (2004a). Structural basis for coronavirus-mediated membrane fusion. Crystal structure of mouse hepatitis virus spike protein fusion core. *J. Biol. Chem.* **279:**30514–30522.

Xu, Y., Lou, Z., Liu, Y., Pang, H., Tien, P., Gao, G. F., and Rao, Z. (2004b). Crystal structure of severe acute respiratory syndrome coronavirus spike protein fusion core. *J. Biol. Chem.* **279:**49414–49419.

Yamada, Y. K., Yabe, M., Ohtsuki, T., and Taguchi, F. (2000). Unique N-linked glycosylation of murine coronavirus MHV-2 membrane protein at the conserved O-linked glycosylation site. *Virus Res.* **66:**149–154.

Yang, H., Yang, M., Ding, Y., Liu, Y., Lou, Z., Zhou, Z., Sun, L., Mo, L., Ye, S., Pang, H., Gao, G. F., Anand, K. *et al.* (2003). The crystal structures of severe acute respiratory

syndrome virus main protease and its complex with an inhibitor. *Proc. Natl. Acad. Sci. USA* **100:**13190–13195.

Yang, Z.-Y., Huang, Y., Ganesh, L., Leung, K., Kong, W.-P., Schwartz, O., Subbarao, K., and Nabel, G. J. (2004). pH-dependent entry of severe acute respiratory syndrome coronavirus is mediated by the spike glycoprotein and enhanced by dendritic cell transfer through DC-SIGN. *J. Virol.* **78:**5642–5650.

Ye, R., Montalto-Morrison, C., and Masters, P. S. (2004). Genetic analysis of determinants for spike glycoprotein assembly into murine coronavirus virions: Distinct roles for charge-rich and cysteine-rich regions of the endodomain. *J. Virol.* **78:**9904–9917.

Yeager, C. L., Ashmun, R. A., Williams, R. K., Cardellichio, C. B., Shapiro, L. H., Look, A. T., and Holmes, K. V. (1992). Human aminopeptidase N is a receptor for human coronavirus 229E. *Nature* **357:**420–422.

Yokomori, K., and Lai, M. M. C. (1991). Mouse hepatitis virus S RNA sequence reveals that nonstructural proteins ns4 and ns5a are not essential for murine coronavirus replication. *J. Virol.* **65:**5605–5608.

Yokomori, K., and Lai, M. M. C. (1992). Mouse hepatitis virus utilizes two carcinoembryonic antigens as alternative receptors. *J. Virol.* **66:**6194–6199.

Yokomori, K., La Monica, N., Makino, S., Shieh, C. K., and Lai, M. M. C. (1989). Biosynthesis, structure, and biological activities of envelope protein gp65 of murine coronavirus. *Virology* **173:**683–691.

Youn, S., Leibowitz, J. L., and Collisson, E. W. (2005). *In vitro* assembled, recombinant infectious bronchitis viruses demonstrate that the 5a open reading frame is not essential for replication. *Virology* **332:**206–215.

Yount, B., Curtis, K. M., and Baric, R. S. (2000). Strategy for systematic assembly of large RNA and DNA genomes: Transmissible gastroenteritis virus model. *J. Virol.* **74:**10600–10611.

Yount, B., Denison, M. R., Weiss, S. R., and Baric, R. S. (2002). Systematic assembly of a full-length infectious cDNA of mouse hepatitis virus strain A59. *J. Virol.* **76:**11065–11078.

Yount, B., Curtis, K. M., Fritz, E. A., Hensley, L. E., Jahrling, P. B., Prentice, E., Denison, M. R., Geisbert, T. W., and Baric, R. S. (2003). Reverse genetics with a full-length infectious cDNA of severe acute respiratory syndrome coronavirus. *Proc. Natl. Acad. Sci. USA* **100:**12995–13000.

Yu, W., and Leibowitz, J. L. (1995a). Specific binding of host cellular proteins to multiple sites within the 3′ end of mouse hepatitis virus genomic RNA. *J. Virol.* **69:**2016–2023.

Yu, W., and Leibowitz, J. L. (1995b). A conserved motif at the 3′ end of mouse hepatitis virus genomic RNA required for host protein binding and viral RNA replication. *Virology* **214:**128–138.

Yu, X., Bi, W., Weiss, S. R., and Leibowitz, J. L. (1994). Mouse hepatitis virus gene 5b protein is a new virion envelope protein. *Virology* **202:**1018–1023.

Zakhartchouk, A. N., Viswanathan, S., Mahony, J. B., Gauldie, J., and Babiuk, L. A. (2005). Severe acute respiratory syndrome coronavirus nucleocapsid protein expressed by an adenovirus vector is phosphorylated and immunogenic in mice. *J. Gen. Virol.* **86:**211–215.

Zelus, B. D., Schickli, J. H., Blau, D. M., Weiss, S. R., and Holmes, K. V. (2003). Conformational changes in the spike glycoprotein of murine coronavirus are induced at 37 degrees C either by soluble murine CEACAM1 receptors or by pH 8. *J. Virol.* **77:**830–840.

Zhai, Y., Sun, F., Li, X., Pang, H., Xu, X., Bartlam, M., and Rao, Z. (2005). Insights into SARS-CoV transcription and replication from the structure of the nsp7–nsp8 hexadecamer. *Nat. Struct. Mol. Biol.* **12:**980–986.

Zhang, X., and Lai, M. M. C. (1995). Interactions between the cytoplasmic proteins and the intergenic (promoter) sequence of mouse hepatitis virus RNA: Correlation with the amounts of subgenomic mRNA transcribed. *J. Virol.* **69:**1637–1644.

Zhang, X., Liao, C.-L., and Lai, M. M. C. (1994). Coronavirus leader RNA regulates and initiates subgenomic mRNA transcription both in *trans* and in *cis*. *J. Virol.* **68:**4738–4746.

Zhang, X., Li, H.-P., Xue, W., and Lai, M. M. C. (1999). Formation of a ribonucleoprotein complex of mouse hepatitis virus involving heterogeneous nuclear ribonucleoprotein A1 and transcription-regulatory elements of viral RNA. *Virology* **264:**115–124.

Zhang, X. M., Herbst, W., Kousoulas, K. G., and Storz, J. (1994). Biological and genetic characterization of a hemagglutinating coronavirus isolated from a diarrhoeic child. *J. Med. Virol.* **44:**152–161.

Zhao, X., Shaw, K., and Cavanagh, D. (1993). Presence of subgenomic mRNAs in virions of coronavirus IBV. *Virology* **196:**172–178.

Zhou, M., and Collisson, E. W. (2000). The amino and carboxyl domains of the infectious bronchitis virus nucleocapsid protein interact with 3′ genomic RNA. *Virus Res.* **67:**31–39.

Zhou, M., Williams, A. K., Chung, S. I., Wang, L., and Collisson, E. W. (1996). The infectious bronchitis virus nucleocapsid protein binds RNA sequences in the 3′ terminus of the genome. *Virology* **217:**191–199.

Ziebuhr, J. (2005). The coronavirus replicase. *Curr. Top. Microbiol. Immunol.* **287:**57–94.

Ziebuhr, J., and Siddell, S. G. (1999). Processing of the human coronavirus 229E replicase polyproteins by the virus-encoded 3C-like proteinase: Identification of proteolytic products and cleavage sites common to pp1a and pp1ab. *J. Virol.* **73:**177–185.

Ziebuhr, J., Snijder, E. J., and Gorbalenya, A. E. (2000). Virus-encoded proteinases and proteolytic processing in the Nidovirales. *J. Gen. Virol.* **81:**853–879.

Ziebuhr, J., Thiel, V., and Gorbalenya, A. E. (2001). The autocatalytic release of a putative RNA virus transcription factor from its polyprotein precursor involves two paralogous papain-like proteases that cleave the same peptide bond. *J. Biol. Chem.* **276:**33220–33232.

Zuniga, S., Sola, I., Alonso, S., and Enjuanes, L. (2004). Sequence motifs involved in the regulation of discontinuous coronavirus subgenomic RNA synthesis. *J. Virol.* **78:**980–994.

ADVANCES IN VIRUS RESEARCH, VOL 66

CHLORELLA VIRUSES

Takashi Yamada,* Hideki Onimatsu,* and James L. Van Etten†

*Department of Molecular Biotechnology
Graduate School of Advanced Sciences of Matter
Hiroshima University, Higashi-Hiroshima 739-8530, Japan
†Department of Plant Pathology and Nebraska Center for Virology
University of Nebraska, Lincoln, Nebraska 68583-0722

ABSTRACT

Chlorella viruses or chloroviruses are large, icosahedral, plaque-forming, double-stranded-DNA–containing viruses that replicate in certain strains of the unicellular green alga *Chlorella*. DNA sequence analysis of the 330-kbp genome of *Paramecium bursaria chlorella virus 1* (PBCV-1), the prototype of this virus family (*Phycodnaviridae*), predict ~366 protein-encoding genes and 11 tRNA genes. The predicted gene products of ~50% of these genes resemble proteins of known function, including many that are completely unexpected for a virus.

0065-3527/06 $35.00
DOI: 10.1016/S0065-3527(06)66006-5

In addition, the chlorella viruses have several features and encode many gene products that distinguish them from most viruses. These products include: (1) multiple DNA methyltransferases and DNA site-specific endonucleases, (2) the enzymes required to glycosylate their proteins and synthesize polysaccharides such as hyaluronan and chitin, (3) a virus-encoded K^+ channel (called Kcv) located in the internal membrane of the virions, (4) a SET domain containing protein (referred to as vSET) that dimethylates Lys27 in histone 3, and (5) PBCV-1 has three types of introns; a self-splicing intron, a spliceosomal processed intron, and a small tRNA intron. Accumulating evidence indicates that the chlorella viruses have a very long evolutionary history. This review mainly deals with research on the virion structure, genome rearrangements, gene expression, cell wall degradation, polysaccharide synthesis, and evolution of PBCV-1 as well as other related viruses.

I. Introduction

Members, including the chlorella viruses, and prospective members of the family *Phycodnaviridae* constitute a genetically diverse, but morphologically similar, group of viruses with eukaryotic algal hosts from both fresh and marine waters. The family name derives from two distinguishing characteristics: (1) "phyco" from their algal hosts and (2) "dna" because all of these viruses have dsDNA genomes (Wilson *et al.*, 2005b). The phycodnaviruses have some of the largest virus genomes known, ranging in size from ~170 to 560 kb and contain several hundred protein-encoding genes.

The phycodnaviruses are among the virioplankton recognized as important ecological elements in aqueous environments. They, along with other viruses, play important roles in the dynamics of algal blooms, nutrient cycling, algal community structure, and possibly gene transfer between organisms. The discovery phase of aquatic viruses, including the phycodnaviruses, is just beginning with new viruses continually being discovered as more environmental samples are examined. Ongoing metagenomic studies involving massive DNA sequencing reveal a greater viral diversity than could have been imagined just a few years ago (Hambly and Suttle, 2005; Wommack and Colwell, 2000). The genetic diversity that exists in the phycodnaviruses, albeit with only a few genomes sequenced, is enormous. To illustrate this diversity, viruses in three genera of the phycodnaviruses have been sequenced and

each of these viruses encodes several hundred genes. However, only 14 of these genes are common to all three viruses (Dunigan *et al*., 2006). Thus, there are more than 1000 unique genes in just these three viruses.

Accumulating evidence also indicates that the phycodnaviruses are probably very old viruses. The phycodnaviruses together with the poxviruses, iridoviruses, asfarviruses, and the recently discovered 1.2-Mb Mimivirus probably have a common evolutionary ancestor, perhaps arising at the time eukaryotes separated from prokaryotes, approximately 3 billion years ago (Raoult *et al*., 2004; Villarreal, 2005; Villarreal and DeFilippis, 2000). All of these viruses share 9 gene products, and 33 more gene products are present in at least two of these five viral families (Iyer *et al*., 2001; Raoult *et al*., 2004). Collectively, these viruses are referred to as nucleocytoplasmic large DNA viruses (NCLDV) (Iyer *et al*., 2001).

This review focuses on the chlorella viruses that constitute one genus in the family *Phycodnaviridae*. Phycodnaviruses are large (mean diameter of 160 ± 60 nm) icosahedrons and, where known, the viruses have an internal membrane that is required for infection. Phylogenetic analyses of the δ-DNA polymerases from the phycodnaviruses indicate that they are more closely related to each other than to other dsDNA viruses and that they form a monophyletic group, consistent with a common ancestor (Wilson *et al*., 2005b). However, the viruses fall into six clades which correlate with their hosts and each has been given genus status. Often the genera can be distinguished by additional properties for example, lytic versus lysogenic life styles or linear versus circular genomes (Wilson *et al*., 2005b). Members of the genus *Chlorovirus* (chlorella viruses) infect fresh water algae, whereas members of the other five genera (*Coccolithovirus*, *Phaeovirus*, *Prasinovirus*, *Prymnesiovirus*, and *Raphidovirus*) infect marine algae.

The type chorella virus is *Paramecium bursaria chlorella virus 1* (PBCV-1). Because there have been several reviews on the phycodnaviruses and the chlorella viruses (Dunigan *et al*., 2006; Kang *et al*., 2005; Van Etten, 2003; Van Etten and Meints, 1999; Van Etten *et al*., 1991, 2002), this review deals mainly with research on virion structure, infection cycle, genome rearrangements, gene expression, cell wall degradation, and polysaccharide synthesis. Additional information, including a complete list of chlorella virus publications and additional images of the viruses, is available on the "World of Chlorella Viruses" Web site at: http://www.ianr.unl.edu/plantpath/facilities/Virology/index.htm/. The general history of the algal viruses and ecological aspects of these fascinating viruses can be found in other reviews (Brussaard, 2004;

Dodds, 1979; Fuhrman, 1999; Lemke, 1976; Müller *et al.*, 1998; Suttle, 2000, 2005; Wommack and Colwell, 2000).

II. Research History, Classification, and Specific Features

A. History and Classification of Viruses and their Hosts

In 1978, Kawakami and Kawakami (1978) described the appearance of large (~180 nm in diameter) icosahedral, lytic viruses in zoochlorellae of the protozoan *Paramecium bursaria* (designated zoochlorella cell virus [ZCV]) after the algae were released from the paramecium. No virus particles were detected in zoochlorellae growing symbiotically inside the paramecium cells, although ZCV particles were present in the depressions of the pellicle, between the cilia, and in the food vacuole of the paramecium. ZCV infected the zoochlorella by adsorption and digestion of the cell wall and virus particles accumulated in the algal cytoplasm. After cell lysis, progeny viruses were released into the medium.

Independently, a few years later, similar lytic viruses were described in zoochlorellae isolated from the green coelenterate *Hydra viridis* (Meints *et al.,* 1981; Van Etten *et al.*, 1981) and also from *P. bursaria* (Van Etten *et al.*, 1982). A laboratory infection system for these viruses was developed using exsymbiotic zoochlorella strains as hosts, including *Chlorella* NC64A that was originally isolated from a *P. bursaria* (Van Etten *et al.*, 1983a). This system allows chlorella viruses to be produced in large quantities and the viruses can be assayed by plaque formation using standard bacteriophage techniques (Van Etten *et al.*, 1983a). Since these early studies, literally hundreds of chlorella viruses have been isolated from natural sources.

Chlorella viruses included in the genus *Chlorovirus* (Wilson *et al.*, 2005b) currently consist of three species: (i) Viruses that infect *Chlorella* NC64A (NC64A viruses). (ii) Viruses that infect *Chlorella* Pbi (Pbi viruses). NC64A viruses neither infect nor attach to *Chlorella* Pbi, and vice versa. (iii) Viruses that infect symbiotic zoochlorella in the coelenterate *Hydra viridis*. Hydra zoochlorella have not been cultured free of virus, so these viruses can only be isolated from chlorella cells freshly released from hydra. Recently, a virus that infects zoochlorella of the heliozoon *Acanthocystis turfacea* was described (Bubeck and Pfitzner, 2005). These viruses, designated ATCV-1 and ATCV-2, infect *Chlorella* SAG 3.83, a symbiont of *A. turfacea* but do not infect either *Chlorella* SAG 211–6, a host for the NC64A viruses, or *Chlorella* SAG 241–80, a host for the Pbi viruses.

NC64A viruses have been isolated from fresh water collected in the United States (Van Etten *et al*., 1985a), South America, Japan (Yamada *et al*., 1991), China (Zhang *et al*., 1988), South Korea (Cho *et al*., 2002), Australia, Israel, and Italy (Van Etten *et al*., 2002). Pbi viruses initially were discovered in fresh water collected in Europe (Reisser *et al*., 1988) and more recently in water collected in Australia, Canada, and the northern United States or at higher elevations in the western United States (Van Etten, J. L., and Nelson, M., unpublished results). The most important factors influencing the distribution of NC64A and Pbi viruses are probably latitude and altitude. *Chlorella* NC64A and *Chlorella* Pbi were originally isolated from American and European isolates of *P. bursaria*, respectively. The component sugars in the cell walls of *Chlorella* NC64A and *Chlorella* Pbi differ considerably (Kapaun *et al*., 1992). Because the viruses can distinguish the two chlorella isolates, it seemed likely that the host receptor for the viruses might also serve as the recognition factor for becoming a symbiont in the paramecia. However, *Chlorella* NC64A and *Chlorella* Pbi each established a stable symbiotic relationship with both American and European isolates of *P. bursaria* (Reisser *et al*., 1991).

18S rRNA sequence analyses of zoochlorella from American and European paramecia have been conducted (Hoshina *et al*., 2004, 2005). Zoochlorella 18S rRNAs separate into two lineages; NC64A (USA), Syngen 2-3 (USA), Cs2 (China), MRBG1 (Australia), and strains from Japan belong to the American type, whereas PB-SW1 (Germany) and CCAP 1660/11 (UK) strains belong to the European type. The American type symbionts have three group-I introns in the 18S rRNA genes, whereas a single group-I intron, located at a different position, exists in the European symbionts. Likewise, the 18S rRNA sequence distinguishes the two groups: (1) Cs2, MRBG1, and strains from Japan and (2) PB-SW1 and CCAP 1660/11. The American type and European type of zoochlorellae correspond to the hosts for NC64A viruses and Pbi viruses, respectively. It will be interesting to determine where *Chlorella* SAG3.83, which is the host for new chlorella viruses, fits into this scheme (Bubeck and Pfitzner, 2005).

B. Specific Features of the Chlorella Viruses

The chlorella viruses have many interesting properties. Most of these studies have been conducted on PBCV-1 and its related NC64A viruses such as chlorella virus Kyoto 2 (CVK2) (Van Etten and Meints, 1999; Van Etten *et al*., 1991; Yamada *et al*., 1991). Some of these features are summarized as follows:

i. The virus genomes are large linear dsDNAs (315–380 kbp) with cross-linked hairpin termini.
ii. The viruses infect host cells by a bacteriophage-like mechanism.
iii. Chlorella viruses often encode multiple type II DNA methyltransferases and DNA site-specific (restriction) endonucleases (Nelson *et al.*, 1993, 1998).
iv. Unlike other glycoprotein-containing viruses, chlorella viruses encode most, if not all, of the components required to glycosylate their proteins (Graves *et al.*, 2001; Markine-Goriaynoff *et al.*, 2004; Wang *et al.*, 1993).
v. Chlorella viruses were the first viruses discovered to have more than one type of intron: PBCV-1 has a self-splicing intron in a transcription factor TFIIS-like gene (Li *et al.*, 1995; Yamada *et al.*, 1994), a spliceosomal-processed intron in its DNA polymerase gene (Grabherr *et al.*, 1992; Zhang *et al.*, 2001), and a small intron in one of its tRNA genes (Nishida *et al.*, 1999a).
vi. Many chlorella virus encoded proteins are either the smallest or among the smallest proteins of their class and some may represent the minimal catalytic unit.
vii. Some translational components, such as tRNAs (Li *et al.*, 1997; Nishida *et al.*, 1999a), and elongation factor EF-3 (Yamada *et al.*, 1993) are virus encoded and expressed during the infection cycle.
viii. Chlorella viruses encode a functional K^+ channel protein called Kcv. Kcv was the first virus encoded K^+ channel to be discovered, and it is the smallest protein known to form a functional K^+ selective channel (Gazzarrini *et al.*, 2003; Kang *et al.*, 2003; Plugge *et al.*, 2000).

III. Virion Structure

PBCV-1 virions have a sedimentation coefficient of about 2300 S in sucrose density gradients (Van Etten *et al.*, 1983b) and an estimated molecular mass of 1×10^9 Da (Yonker *et al.*, 1985). The virion contains 64% protein, 21–25% DNA, and 5–10% lipid (Skrdla *et al.*, 1984). The PBCV-1 virion contains more than 100 virion-encoded proteins (Skrdla *et al.*, 1984; Dunigan, D. D. *et al.*, unpublished results) including two DNA restriction endonucleases, DNA binding proteins and protein kinases (Yamada *et al.*, 1996). The PBCV-1 54 kDa major capsid protein Vp54 is a glycoprotein and comprises ~40% of the virus

protein. Vp54 has been crystallized and consists of 2 eight-stranded, antiparallel β-barrel, "jelly-roll" domains related by a pseudo-sixfold rotation (Nandhagopal *et al*., 2002).

Ultrastructural studies have been conducted on both intact and disrupted chlorella virus virions using either negative staining (Becker *et al*., 1993) or cryo-electron microscopy with three-dimensional image reconstructions (26 Å resolution) (Yan *et al*., 2000). The latter study was complemented and extended by fitting the structure of the major capsid protein Vp54 to the cryo-electron microscopy density maps of PBCV-1 (Simpson *et al*., 2003). The outer glycoprotein capsid is icosahedral and surrounds a lipid bilayer membrane. The membrane is connected to the outer shell by regularly spaced proteins. Disruption of the membrane destroys PBCV-1 infectivity (Skrdla *et al*., 1984). The outer diameter of the viral capsid varies from a minimum of 1650 Å along the two- and threefold axes to a maximum of 1900 Å along the fivefold axes. The capsid shell consists of 1680 donut-shaped trimeric capsomers plus 12 pentameric capsomers at each icosahedral vertex. The trimeric capsomers are arranged into 20 trisymmetrons (each containing 66 trimers) and 12 pentasymmetrons (each containing 30 trimers and 1 pentamer at the icosahedral vertices) (Fig. 1). Assuming all the trimeric capsomers are identical, the outer capsid of the virus contains 5040 copies of the major capsid protein Vp54. The triangulation number (T) for the virus is 169 ($h = 7, k = 8$) and the virus has a right handed, skew class of T lattice (Caspar and Klug, 1962).

Most of the trimeric capsomers have a central, concave depression surrounded by three protuding towers. The trimeric capsomers are 72 Å in diameter and $\sim$75 Å high. The capsomers interconnect at their bases in a contiguous shell that is 20–25 Å thick. Twelve pentamer capsomers, each $\sim$70 Å in diameter, exist at the virus fivefold vertices and probably consist of a different protein. Each pentamer has a cone-shaped axial channel at its base. One or more proteins appear below the axial channel and outside the inner membrane (Fig. 1B). This protein(s) may be responsible for digesting the host cell wall during infection. Presumably contact between the virus and its host receptor alters the channel sufficiently to release the wall-degrading enzyme(s).

Complementary information about the PBCV-1 virion structure was obtained by atomic force microscopy (AFM) (Kuznetsov *et al*., 2005). Since AFM is not dependent on symmetry averaging as is cryo-electron microscopy, it can reveal unique properties of individual particles. From the response of the AFM tip in contact with the particles, the virus particles appear somewhat soft and are readily deformed. The individual trimeric capsomers appear to have a small hole in their

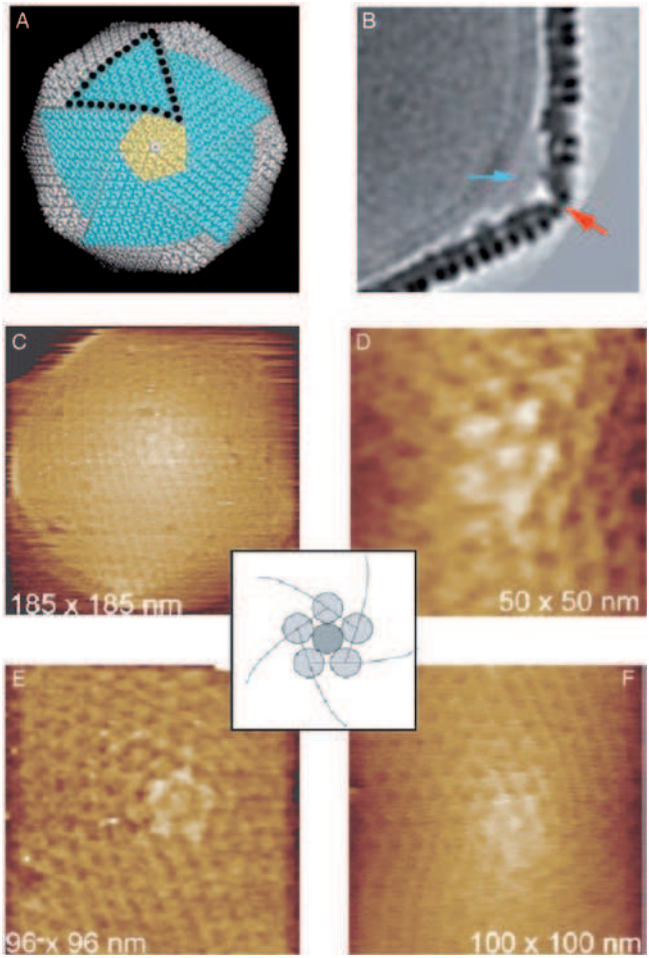

FIG 1. Three-dimensional image reconstruction of chlorella virus PBCV-1 from cryo-electron micrographs and atomic force micrographs. (A) The virion capsid consists of 12 pentasymmetrons and 20 trisymmetrons. Five trisymmetrons are highlighted in the reconstruction (blue) and a single pentasymmetron is colored yellow. A pentavalent capsomer (white) lies at the center of each pentasymmetron. Each pentasymmeton consists of one pentamer plus 30 trimers. Eleven capsomers form the edge of each trisymmetron (black dots) and therefore each trisymmetron has 66 trimers (Yan *et al.*, 2000). (B) Dense material (blue arrow) (cell wall digesting enzyme(s)?) is present at each vertex (red arrow) between the vertex and the membrane. (C–F) Atomic force microscopy images of the surfaces of PBCV-1 virions showing the pentameric arrangements of proteins around the fivefold vertices, with a unique protein on the vertex (Kuznetsov *et al.*, 2005).

center and a distinctive triangular shape that is more angular and accentuated than the "doughnut" shape deduced from the cryo-electron microscopy (Yan *et al*., 2000). The pentagonal vertices are formed by five copies of a different protein, and this has yet another unique protein in its center (Fig. 1D and E). The central protein exhibits some unusual behavior when subjected to AFM tip pressure; it disappears into the virion interior, leaving a distinct hole. When the AFM tip pressure is decreased, it returns to its original position. Virion degradation is accompanied by the appearance of many small, uniform, spherical, and virus-like particles (VLP) consistent with $T = 1$ or 3 icosahedral products (Kuznetsov *et al*., 2005).

IV. Virus Life Cycle

PBCV-1 infects its host by attaching rapidly, specifically, and irreversibly to the external surface of the algal cell wall (Meints *et al*., 1984). Attachment always occurs at a virus vertex, possibly with hair-like appendages (Van Etten *et al*., 1991) and is followed by degradation of the host wall at the attachment point. The determinants for host range are associated with attachment. Onimatsu *et al*. (2004) reported that a virion protein Vp130 from *Chlorovirus* CVK2 binds specifically to the host *Chlorella* cell wall. Vp130 is a homolog of PBCV-1 protein A140/145R and consists of 1126 amino acid residues (predicted mol wt, 121,257 and pI, 10.76). The Vp130 N-terminus is blocked by some unknown structure and the C-terminus consists of 23 tandem PAPK repeats. Internally, Vp130 contains seven repeats of 70–73 amino acids, each copy of which is separated by several PAPK sequences. This protein is well conserved among the NC64A viruses. Because externally added Vp130 competes with CVK2 in binding to host cells, Vp130 is most likely a host-recognizing protein in the virion (Onimatsu *et al*., 2004). Immune electron microscopy using Vp130 antibody established that the protein is localized specifically at the vertices of the CVK2 virion (Onimatsu, H. *et al*., manuscript in preparation).

Attachment of the virion to the host cell wall probably alters the virion structure slightly, allowing release of a virion-packaged wall digesting enzyme(s). Following host cell wall degradation, the internal membrane of the virus probably fuses with the host membrane resulting in entry of the viral DNA and virion-associated proteins. An empty capsid is left on the cell surface. Infection results in rapid depolarization of the host membrane (Frohns *et al*., 2006; Mehmel *et al*., 2003), and

we hypothesize that this rapid depolarization is caused by a virus-encoded K^+ channel (called Kcv) located in the internal membrane. This depolarization may aid in the release of DNA into the cell and/or limit subsequent infection by additional viruses.

Circumstantial evidence indicates that the PBCV-1 DNA and suspected virion-associated proteins quickly move to the nucleus where early transcription is detected within 5–10 min postinfection (pi) (Kawasaki *et al.*, 2004; Schuster *et al.*, 1986). Experimental results indicate that host chromosomal DNA begins to be degraded, possibly due to two restriction endonucleases that are packaged in the PBCV-1 virion, within minutes of infection (Agarkova, I. V. *et al.*, submitted for publication; Dunigan, D. D. *et al.*, unpublished results).

In the immediate-early phase of infection, the host is reprogrammed to transcribe viral RNAs. Very little is known about how this occurs, but chromatin remodeling may be involved. PBCV-1 encodes a 119 amino acid SET domain containing protein (referred to as vSET) that dimethylates Lys27 in histone 3 (Manzur *et al.*, 2003). vSET is packaged in the PBCV-1 virion, and accumulating evidence indicates that vSET is involved in repression of host transcription following PBCV-1 infection (Manzur, K. L. *et al.*, manuscript in preparation).

PBCV-1 DNA replication begins 60–90 min pi and is followed by transcription of late virus genes (Schuster *et al.*, 1986; Van Etten *et al.*, 1984). Ultrastructural studies of PBCV-1 infected chlorella suggest that the nuclear membrane remains intact, at least during the early stages of virus replication (Meints *et al.*, 1986). However, a functional host nucleus is not required for virus replication since PBCV-1 can replicate, albeit poorly and with a small burst size, in UV-irradiated cells (Van Etten *et al.*, 1986). Approximately 2–3 hpi, assembly of virus capsids begins in localized regions in the cytoplasm, called virus assembly centers, which become prominent at 3–4 hpi (Meints *et al.*, 1986). By 5 hpi, the cytoplasm is filled with infectious progeny virus particles ($\sim$1000 particles/cell) and by 6–8 hpi localized lysis of the host cell releases progeny virions. Of the progeny released, 25–50% of the particles are infectious; that is, each infected cell yields $\sim$350 plaque-forming units (PFU) (Van Etten *et al.*, 1983b). Intact infectious PBCV-1 particles accumulate inside the host 30–40 min before release. Other chlorella viruses have longer replication cycles than PBCV-1. For example, NC64A virus NY-2A requires approximately 18 h for replication and consequently forms smaller plaques.

Some virion proteins are processed by specific proteinase activities (Songsri *et al.*, 1997). One of them is a signal peptidase-like activity

and removes the N-terminal 25–33 amino acids of target proteins that contain a highly hydrophobic sequence of 17 amino acid residues. Lysine with an acidic amino acid on the N-side always precedes the cleavage site. Proteins A168R, A203R, and A532L are targets of this activity. These results lead to the following questions: (1) what enzymes (either of viral or host origin) are responsible for processing the virion proteins? (2) When, where, and how does processing occur in the course of *Chlorovirus* replication? (3) What are the biological effects of processing?

Thus, progress has been made on characterization of the viral structural proteins as well as the whole virion architecture. However, many fundamental questions remain to be answered about the assembly of such a large, complex virus particles in the host cells. Like poxviruses, iridoviruses, and African swine fever virus (ASFV), *Chlorovirus* assembly occurs in localized regions in the cytoplasm, referred to as virus assembly centers (Van Etten *et al*., 1991). (1) Where and how is the virus assembly center determined? (2) What is the origin of the virus internal membrane? Is it derived from the ER, like other membrane-containing viruses (Cobbold *et al*., 1996; Wolf *et al*., 1998)? (3) What is the role of the membrane in assembling the virion (e.g., does it function as a scaffold)? (4) How is genomic DNA packaged into an empty preformed capsid? (5) How are the more than 100 component proteins specifically assembled into a virion?

V. Virus Gene Expression: Immediate Early and Late Gene Expression

The PBCV-1 genome does not encode either a recognizable RNA polymerase or RNA polymerase subunit (Van Etten and Meints, 1999). The lack of a virus-encoded RNA polymerase suggests that the infecting viral DNA is targeted to the cell nucleus and that a host RNA polymerase initiates viral transcription, possibly in conjunction with virus-packaged transcription factors. Consistent with this possibility, PBCV-1 encodes at least four transcription factor-like elements, TFIIB, TFIID, TFIIS, and VLTF-2. PBCV-1 also encodes two enzymes involved in forming the mRNA cap structure, an RNA triphosphatase (Ho *et al*., 2001) and an RNA guanylyltransferase (Ho *et al*., 1996). However, there is no evidence that any of these proteins are packaged in the virion. The size, amino acid sequence, and biochemical properties of the PBCV-1 capping enzymes resemble yeast capping enzymes

more than the multifunctional poxvirus and ASFV RNA capping enzymes (Gong and Shuman, 2002). PBCV-1 also encodes an active RNase III that presumably is involved in processing either virus mRNAs and/or tRNAs (Zhang *et al.*, 2003). In addition, PBCV-1 encodes two proteins that contain sequence elements of superfamily II helicases. Superfamily II helicases are involved in transcription (Tanner and Linder, 2001).

Two studies (Schuster *et al.*, 1986, 1990) which examined PBCV-1 RNA synthesis reached the following conclusions:

i. Viral infection rapidly inhibits host RNA synthesis.
ii. Chloroplast rRNAs but not cytoplasmic rRNAs are degraded beginning at about 30 min pi.
iii. PBCV-1 transcription is temporally programmed, and the first transcripts appear within 5–10 min pi (immediate early transcription). A few, but not all, early virus transcripts are synthesized in the absence of *de novo* protein synthesis. The synthesis of late transcripts that occurs after 60–90 min pi (late transcription) requires translation of an early virus gene(s).
iv. Early and late virus genes are interspersed throughout the PBCV-1 genome.
v. Full length gene probes often hybridize to mRNA transcripts that are 40–60% larger than the gene itself.
vi. Transcription mapping of seven PBCV-1 genes revealed that the virus has mRNAs with 5′ untranslated regions as small as 14 nucleotides and as large as 149 nucleotides. Transcripts often extend beyond the translational stop codon (Graves and Meints, 1992; Hiramatsu *et al.*, 1999; Kawasaki *et al.*, 2004; Schuster *et al.*, 1990).

A study (Kawasaki *et al.*, 2004) has produced some new insights into immediate early expressed genes. They isolated and characterized 23 *Chlorovirus* PBCV-1 and CVK2 genes expressed in host cells as early as 5–10 min pi. Some of these immediate early gene products resembled transcriptional factors and mRNA-processing proteins including, TFIIB, helicases, mRNA capping enzyme (RNA guanylyltransferase), nucleolin, and a bean transcription factor. Other immediate early genes encoded factors influencing translation such as possible aminoacyl tRNA synthetases, possible ribosomal proteins and unknown proteins. Enzymes involved in polysaccharide synthesis were also found. All of these gene transcripts had a poly(A) tail, which decreased in size by 20 min pi, possibly caused by an exonuclease. A typical TATA-box and a common 5′-ATGACAA element were present in the promoter

region of all 23 immediate early genes, which may be recognized by host RNA polymerase and transcription factors. As suggested by the presence of the poly(A) tail, all of the immediate early genes contain a typical poly(A) addition signal 5′-AATAAA-3′, 10–90 bp downstream of the translational stop codon.

At 40 min pi, a dramatic change occurs in the transcription of the *Chlorovirus* genes. The immediate early genes gradually decreased in size, suggesting some weakening or cessation of poly(A) polymerase activity. Concurrently, some larger transcripts began to appear. These larger transcripts are due to readthrough from an upstream ORF and/or into a downstream ORF. These results indicate that promoter selection changes around 40 min pi by some mechanism, possibly involving regulatory proteins encoded by some of the immediate early transcripts. In other organisms, transcription termination signals in a gene are recognized by a series of RNA-binding proteins and RNA-processing enzymes including cleavage stimulation factor F (CstF), cleavage and polyadenylation specific factor (CPSF), and poly(A) polymerase; but these factors may not function well after 40 min pi, resulting in elongated or unprocessed transcripts. Once in the cytosol, the poly(A) tail of mRNA is gradually shortened by an exonuclease (deadenylation nuclease called DAN) that digests the tail in the 3′–5′ direction. Once the size of the poly(A) tail reaches a critical threshold, the mRNA 5′ cap is removed (decapping) and the RNA is rapidly degraded. Therefore, a 3′-extension of each transcript by readthrough might serve as an alternate way to protect a coding region from degradation by 3′-exonuclease. This is a unique feature of chloroviruses contrasting to similar large viruses such as vaccinia and ASFV, both of which encode a functional poly(A) polymerase and mRNAs are polyadenylated (Johnson *et al*., 1993; Yanez *et al*., 1995).

A poly(A) tail is also involved in initiation of translation. Efficient translation requires the mRNA poly(A) tail to bind to poly(A)-binding proteins, which, in turn, interact with translation initiation factor eIF-4G. Poly(A)-deficient mRNAs formed 40 min pi might require an internal ribosome entry site (IRES)-dependent mechanism in order to be translated (Sachs, 2000).

A conserved nucleotide sequence has been identified in the promoter region of genes expressed late in PBCV-1 infected cells. Kang *et al*. (2004a) reported that an AAAAATAnTT element or a subset of this sequence is located 6–30 nucleotides upstream of the ATG start codon of seven late-expressed PBCV-1 genes.

However, many fundamental questions regarding *Chlorovirus* gene transcription remain to be answered including: (1) what kind of RNA

polymerase and its related factors are involved? (2) How are transcription initiation and termination regulated? (3) What mechanism switches transcription from early to late? (4) What DNA elements are responsible for the promoter function? (5) What trans-acting factors are involved in the regulation?

VI. Virus Protein Synthesis, Modification, and Degradation

Some early virus-encoded proteins appear within 15 min pi. Since cycloheximide, but not chloramphenicol, inhibits viral replication, PBCV-1 proteins are synthesized on cytoplasmic ribosomes and not organellar ribosomes (Skrdla *et al.*, 1984). How the virus takes over the host translational machinery forcing it to translate virus mRNAs is unknown. However, some of the factors involved in this process are expected to be virus encoded. Therefore, studying the chlorella virus system may reveal new insights into the regulation of eukaryotic protein synthesis.

The chlorella viruses are the first known viruses to encode a translation elongation factor (EF) (Yamada *et al.*, 1993). The gene for a putative EF-3 is highly conserved in all *Chlorovirus* isolates examined so far. The EF-3 proteins from CVK2 and PBCV-1 (94% amino acid identity) have ~45% amino acid identity to an EF-3 protein from fungi (Belfield and Tuite, 1993; Chakraburtty, 2001). The fungal protein stimulates EF-1α-dependent binding of aminoacyl-tRNA to the A site of the ribosome. Like fungal EF-3 proteins, the CVK2 and PBCV-1 proteins have an ABC transporter family signature and two ATP/GTP binding-site motifs.

PBCV-1 and CVK2 codon usages are biased to codons ending in XXA/U (63%) over those ending in XXC/G (37%) (Nishida *et al.*, 1999a; Schuster *et al.*, 1990). This bias is expected because PBCV-1 DNA is 40% G + C (CVK2, 41% G + C), whereas host nuclear DNA is 67% G + C (Van Etten *et al.*, 1985b). Therefore, finding that PBCV-1 encodes 11 tRNA genes may not be surprising: 3 for Lys, 2 each for Asn and Leu, and 1 each for Ile, Tyr, Arg, and Val. Similarly CVK2 encodes 14 tRNA genes: 3 for Lys, 2 each for Asn and Leu, and 1 each for Arg, Asp, Gly, Gln, Ile, Tyr, and Val (Nishida *et al.*, 1999a). None of the tRNAs have a CCA sequence encoded at the 3′ end of the acceptor stem. Typically these three nucleotides are added separately to tRNAs. Some chlorella viruses encode as many as 16 tRNAs (Cho *et al.*, 2002; Nishida *et al.*, 1999a). There is a strong correlation between the abundance of virus encoded tRNAs and the virus gene codon use (Lee *et al.*, 2005; Nishida *et al.*, 1999a).

The virus encoded tRNAs contain internal A and B boxes characteristic of RNA polymerase III promoter elements, suggesting the tRNAs might be transcribed individually by RNA polymerase III (Nishida *et al*., 1999a). However, the tRNA genes are transcribed as a large precursor RNA and processed via intermediates to mature tRNAs at both early and late stages of virus replication. Some, if not all, of the tRNAs are aminoacylated *in vivo*, suggesting they probably function in viral protein synthesis (Nishida *et al*., 1999a). Possibly, the virus-encoded EF-3 in combination with the virus encoded tRNAs alter the host protein synthetic machinery to preferentially translate viral mRNAs.

PBCV-1 has several genes encoding proteins that are involved in posttranslational modification. In addition to putative glycosyltransferases (see in a later section), PBCV-1 encodes 7 Ser/Thr-protein kinases (Valbuzzi, P. *et al*., unpublished results), one putative Tyr-protein kinase and a putative Tyr phosphatase. Three protein kinases are packaged in the chlorella virus CVK2 virion (Yamada *et al*., 1996). PBCV-1 also encodes several enzymes involved in posttranslational modification, such as an ERV/ALR protein, which functions as a protein thiol oxidoreductase (Senkevich *et al*., 2000), a putative protein disulfide isomerase and a prolyl 4-hydroxylase that converts Pro-containing peptides into hydroxyl-Pro-containing peptides (Eriksson *et al*., 1999). Moreover, PBCV-1 encodes two putative proteins that interact with ubiquitin, a ubiquitin C-terminal hydrolase and a Skp1 protein. Skp1 proteins belong to the SCF-E3 ubiquitin ligase family that targets cell cycle proteins and other regulatory factors for degradation (Deshaies, 1999). Finally, PBCV-1 encodes at least one putative serine proteinase.

VII. Diversity of Chlorella Virus Genomes

The PBCV-1 genome is a linear 330,744-bp nonpermuted dsDNA molecule with covalently closed hairpin termini (Rohozinski *et al*., 1989). The termini consist of 35-nucleotide-long covalently closed hairpin loops that exist in one of two forms; the two forms are complementary when the 35-nucleotide sequences are inverted (flip-flop) (Zhang *et al*., 1994). Identical 2221-bp inverted repeats are adjacent to each hairpin end (Strasser *et al*., 1991). The remainder of the PBCV-1 genome contains primarily single-copy DNA (Girton and Van Etten, 1987). These features can be compared with those of other chloroviruses because the genomic sequences of three more chlorella

viruses have been completed—viruses NY-2A and AR158 which, like PBCV-1, infect *Chlorella* NC64A and virus MT325 which infects *Chlorella* Pbi. These sequences are available on the Web site http://greengene.uml.edu, which represents work in progress; the sequences have not yet been published or deposited in the public databases. Some comparative data are listed in Table I. PBCV-1 and all other NC64A virus genomes are ~40% G + C, which is significantly lower than the 67% G + C of the host *Chlorella* NC64A nuclear DNA (Van Etten *et al.*, 1985b). Chlorovirus MT325 that is a Pbi virus has a slightly higher G + C content (~45%). The newly sequenced genomes vary from 315 (MT325) to 369 kbp (NY-2A), reflecting a difference in the number of genes (~330–~400).

Some of the additional proteins encoded by NY-2A genes include ubiquitin, chitin synthase, *N*-acetylglucosaminyl transferase, 6 transposases, and 43 homing endonucleases. Furthermore, inteins exist in two of the NY-2A gene products, the α-subunit of ribonucleotide reductase and a putative helicase (Fitzgerald, L. A. *et al.*, manuscript in preparation). Not all chlorovirus genes are required for virus replication in the laboratory. For example, extended deletions can occur in the chlorovirus genomes; 27–37-kbp deletions in PBCV-1 (Landstein *et al.*, 1995) and 30–42-kbp deletions in CVK1 (Songsri *et al.*, 1995) are located in the left terminus of the genome. A detailed comparison of the gene contents between viruses should identify a set of highly conserved genes and variable or dispensable genes.

TABLE I
COMPARISON OF THE GENOME ORGANIZATION AMONG SEVERAL CHLORELLA VIRUSES

Viruses	Genome size (bp)	G + C content (%)	Size of terminal inverted repeats (kbp)	No. of protein-encoding genes	No. of tRNA encoding genes
PBCV-1	330,744	39.6	2.2	367	11
NY-2A	368,683*	40.3	2.4	~420	7
A158R	344,690*	40.4	0.27†	~400	6
MT325	314,335*	44.9	ND	~330	10
CVK2	~350,000‡	ND	2.4	ND	14

† Tentative size to be verified.
‡ Tentative size based on pulsed-field gel electrophoresis (PFGE)-estimation.
ND, Not determined. * Unpublished results, can be seen at Web site http://greengene.uml.edu.

A. Hairpin Ends and Inverted Terminal Repeats

The 35-nucleotide sequence of the PBCV-1 hairpin end differs considerably from the hairpin loop sequence (43 nucleotides) of *Chlorovirus* CVK2 (Hiramatsu, S., and Yamada, T., unpublished result) (Fig. 2). It is interesting that a single base change in the most distal position of the CVK2 sequence reduces the loop to 33 nucleotides. A region of 15–16 bp immediately adjacent to the hairpin end in the inverted terminal repeats also differs between PBCV-1 and CVK2; however beyond this region, the inverted repeat sequences are nearly identical between the two viruses.

The terminal inverted repeats are 2.2–2.4 kbp in size (Table II). Although the inverted repeats of PBCV-1 and CVK2 are similar, this is not true for all viruses. The PBCV-1 inverted repeat region was hybridized to 36 other NC64A viruses. Twenty-eight hybridized very well to the probe, however, eight did not hybridize at all, indicating sequence differences. Such rearrangements may be mediated by numerous short repeated sequences that frequently occur at the junctions between the inverted repeats and the single copy region (Yamada and Higashiyama, 1993). Comparison of the nucleotide sequence of the inverted repeats among chloroviruses PBCV-1, CVK2, NY-2A, and AR158 indicated no significant identity in the terminal inverted repeats sequences except for occasional homology islands, a ~600-bp region next to the hairpin loop and a 400~600-bp region immediately adjacent to the single copy region (Nishida *et al*., 1999b).

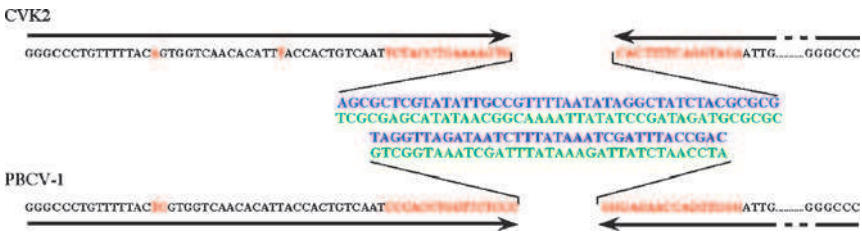

FIG 2. Comparison of the nucleotide sequences at the PBCV-1 and CVK2 terminal hairpin ends. The most distal portions of the terminal inverted repeats (shown by arrows) are relatively similar between PBCV-1 and CVK2 DNAs (unidentical bases are shown in red), whereas the sequences of the covalently closed hairpin loops (35 nucleotides for PBCV-1 and 43 nucleotides for CVK2) are completely different. The hairpin loops exist in one of two forms (shown in blue and green); the two forms are complementary when the sequences are inverted (flip-flop) (Zhang *et al*., 1994).

TABLE II

REPRESENTATIVE ORFS ENCODED BY CHLORELLA VIRUS PBCV-1*

DNA replication, recombination and repair		**Signaling, ion channels and protein kinases**	
DNA polymerase (δ)	*A185R* (913)	Potassium ion channel protein	*A250R* (94)†
DNA primase	*A468R* (443)†	Ligand-gated channel protein	*A162L* (411)
ATP-dependent DNA ligase	*A544R* (298)†		*A163R* (433)
DNA topoisomerase II	*A583L* (1061)†	Ser/Thr protein kinase	*A34R* (308)†
PCNA	*A193L* (262)		*A248R* (308)†
	A574L (264)		*A277L* (303)†
RNase H	*A399R* (194)		*A278L* (610)†
Replication factor C (Archae large subunit)	*A417L* (429)		*A282L* (569)†
			A289L (283)†
Helicase (superfamily III)	*A456L* (654)		*A614L* (577)†
Exonuclease	*A166R* (268)†	Tyr-protein kinase	*A617R* (321)
Pyrimidine dimmer-specific glycosylae	*A50L* (141)†	Tyr-protein phosphatase	*A305L* (204)
DNA packaging ATPase	*A392R* (258)		
DNA methyltransferase and site-specific endonucleases			
Adenine DNA methylase	*A251R* (326)†	**Nucleotide metabolism**	
	A581R (265)†	Aspartate transcabamylase	*A169R* (323)†
Cytosine DNA methylase	*A517L* (344)†	Ribonucleotide reductase large subunit	*A629R* (771)
	A530R (335)†	Ribonucleotide reductase small subunit	*A476* (324)
	A683L (367)	Thioredoxin	*A427L* (119)

DNA site-specific endonuclease	*A252R* (342)†
	A579L (183)†
Insertion and transposition	
Transposase	*A625R* (433)
Homing endonuclease (GIY-YIG)	*A163L* (165)
	A287R (251)
	A315L (246)
	A351L (358)
	A495R (221)
	A539R (173)
	A651L (230)
Homing endonuclease (HNH)	*A87R* (456)
	A267L (314)
	A422R (342)
	A478L (310)
	A490L (310)
Transcription	
Transcription factor IIB	*A107L* (290)
Transcription factor IID	*A552R* (270)
Transcription factor IIS	*A125L* (180)
VLTF2-type transcription factor	*A482R* (215)
RNA triphosphatase	*A449R* (193)†
RNA guanylyltransferase	*A103R* (330)†
Glutaredoxin	*A438* (78)†
dUTP pyrophosphatase	*A551L* (141)†
dCMP deaminase	*A596R* (142)†
Thymidylate kinase	*A416R* (188)
Nucleotide triphosphatase	*A326L* (209)
Cytidine deaminase	*A200R* (118)
Thymidylate synthase X	*A674R* (216)†
ATPase	*A392R* (258)
ATPase	*A554L* (271)
Sugar manipulation enzymes	
Glucose dehydrogenase	*A609L* (389)†
Glucosamine synthase	*A100R* (595)†
Hyaluronan synthase	*A98R* (568)†
Fucose synthase	*A295L* (317)†
GDP-D-mannose dehydratase	*A118R* (345)†
Mannosyltransferase	*A64R* (638)
Fucosyltransferase	*A114R* (485)
Glycosyltransferase	*A111R* (389)
	A222/226R (432)
	A328L (355)
	A473L (517)
	A546L (321)

(*continues*)

TABLE II *(continued)*

Helicase (superfamily II)	*A153R* (459)		
	A363R (811)	**Cell wall digestion**	
SWI/SNF helicase	*A548L* (458)	Chitinase	*A181/182R* (830)†
Ski1 helicase	*A241R* (725)		*A260R* (484)†
RNase III	*A464R* (245)†	Chitosanase	*A292L* (328)†
Histone H3, Lys 27 dimethylase	*A612L*†	β-1,3-Glucanase	*A94L* (364)†
Protein synthesis, modification, and degradation		Polysaccharide lyase	*A215L* (321)
Translation elongation factor III	*A666L* (918)		
Prolyl-4-hydroxylase	*A85R* (242)†	**Lipid manipulation enzymes**	
Protein disulfide isomerase	*A448L* (106)	Glycerphosphoryl diesterase	*A49L* (219)
Thiol oxidoreductase	*A465R* (118)	2-Hydroxyacid dehydrogenase	*A53R* (363)
Ubiquitin C-terminal hydrolyase	*A105L* (284)	Lysophospholipase	*A271L* (159)
SKP-1 protein	*A39L* (151)	*N*-Acetyltransferase	*A654L* (197)
Zn metallopeptidase	*A604L* (134)		

* ORFs for structural proteins including the major capsid protein Vp54 (A430L, 437 aa) and its related proteins are not listed. The number in brackets refers to the number of codons in the ORF.

† A dagger means that the recombinant protein has been produced and shown to have the expected activity.

Yamada and Higashiyama (1993) detected a site-specific nick in the inverted repeat region of *Chlorovirus*, CVK1. This nick might serve as the initiation point for DNA replication.

B. PBCV-1 Genes

In the initial report describing the sequence of the PBCV-1 genome, 702 ORFs of 65 codons or larger were identified and 377 of them were predicted to encode proteins (Kutish *et al*., 1996; Li *et al*., 1995, 1996; Lu *et al*., 1995, 1996). However, mistakes are being detected in the original sequence; often two adjacent ORFs consist of a single ORF. Currently we believe that PBCV has 691 ORFs of 65 codons or larger, of which 366 are protein-encoding. PBCV-1 protein-encoding genes were identified initially by the following criteria: (1) A minimal size of 65 codons initiated by an ATG codon. (2) The largest ORF was chosen when competing ORFs overlapped. (3) ORFs with AT-rich (>70%) sequences in the 50 nucleotides upstream of the putative initiation codons. To date, most of the protein-encoding genes have met these criteria.

Unlike the poxviruses, in which genes near the terminal regions are transcribed toward the termini (Moss, 1996), the 366 PBCV-1 putative protein-encoding genes are evenly distributed on both strands and, with one exception, intergenic space is minimal. In fact, 275 ORFs are separated by less than 100 nucleotides. The exception is a 1788 nucleotide sequence near the middle of the genome. This DNA region, which contains many stop codons in all reading frames, encodes 11 tRNA genes. The 2.2-kb inverted terminal repeat region of the PBCV-1 genome contains four ORFs, which are duplicated (Lu *et al*., 1995). Approximately 50% of the 366 PBCV-1 gene products have been tentatively identified, including some that seem irrelevant to virus replication. Some PBCV-1 genes are closely related to genes of bacteria and their viruses, whereas other PBCV-1 genes appear eukaryotic in origin. Consequently, the chlorella virus genomes contain an interesting mosaic of prokaryotic and eukaryotic genes. Some of the PBCV-1 gene products are listed in Table II. Additional comments on these genes can be found in other reviews (Van Etten, 2003; Van Etten and Meints, 1999; Van Etten *et al*., 2002).

C. Linearity of Gene Arrangements in the Chlorella Viruses

To understand the fundamental organization of the chlorovirus genomes and to identify essential genes for viral replication, it will be

necessary to separate highly conserved regions from variable and/or dispensable regions. Nishida *et al*. (1999b) compared the gene arrangement between PBCV-1 and CVK2. Four major variations were detected: (1) insertion of an approximately 20-kbp sequence near the left end of CVK2, (2) a duplication of the gene for the major capsid protein in CVK2, (3) deletions/insertions of some ORFs, and (4) a divergence in the terminal inverted repeat sequences. Despite these changes, colinearity was maintained for most of the PBCV-1 and CVK2 genes.

The recent sequencing of three more chlorella viruses make it possible to compare gene arrangements over their entire genomes. Figure 3 compares the positions of 22 randomly chosen genes among four chlorella viruses. Although a few minor rearrangements occur (Section VII.D.2), in general, colinearity exists among the NC64A viruses (Fig. 3A). In contrast, there is almost no colinearity between the genomes of PBCV-1 and MT325, a Pbi virus (Fig. 3B). Some PBCV-1 genes that are absent in NY-2A and AR158, such as *A245R* and *A646L*, are present in MT325, whereas the genes for A544R and A604L that are conserved in NC64A-viruses are missing in MT325. A detailed comparison of the gene contents and the genome architecture between the two major groups of chloroviruses is in progress (Fitzgerald, L. A. *et al*., manuscript in preparation).

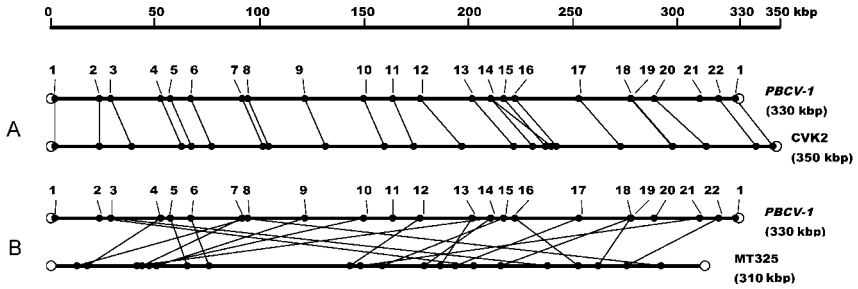

FIG 3. Comparison of the location of 22 genes in four *Chlorovirus* genomes: between PBCV-1 and CVK2 (A), and PBCV-1 and MT325 (Pbivirus) (B). Corresponding gene positions are connected by lines. PBCV-1 genes used as landmarks are: (1) *A3R*, (2) *A35L*, (3) *A50L*, (4) *A100R*, (5) *A107L*, (6) *A125L*, (7) *A181R*, (8) *A185R*, (9) *A245R*, (10) *A292L*, (11) tRNA genes, (12) *A357L*, (13) *A413L*, (14) *A430L*, (15) *A448L*, (16) *A464R*, (17) *A533R*, (18) *A575L*, (19) *A577L*, (20) *A604L*, (21) *A646L*, and (22) *A666L*. Some PBCV-1 genes are duplicated or missing in the other virus genomes. Although a few minor rearrangements occur (ex. a large insertion between (2) and (3) in CVK2), in general, colinearity exists among the NC64A viruses (A). In contrast, there is almost no colinearity between the genomes of PBCV-1 and MT325 (B). Unpublished sequence data for NY-2A and MT325 (J. L. Van Etten and M. V. Graves) are used in the comparison.

D. Patterns of Gene Rearrangement

1. Large Deletions/Insertions

The CVK2 genome is approximately 20 kbp larger than the PBCV-1 genome, primarily because of an extra 22.2-kbp sequence close to the left terminus (Fig. 3A) (Chuchird *et al.,* 2002). This 22.2-kbp region has five gene copies of the Vp260-like protein, a possible viral-surface glycoprotein. Although none of these copies occur in the corresponding region in the PBCV-1 genome, four and three copies of the Vp260-like protein-encoding genes are also located together at almost the same position in the NY-2A and AR158 genomes. These rearrangements do not appear to be mere insertions/deletions but more complicated gene replacement events (Chuchird *et al*., 2002).

Four PBCV-1 spontaneously derived antigenic variants were isolated that contain 27–37-kbp deletions at the left end of the 330-kbp genome (Landstein *et al*., 1995). Two of these mutants had deletions that began at nucleotide positions 4.9 or 16 kb and ended at position 42 kb. The two deletions probably resulted from recombination at a repeated sequence. The other two mutants, which probably arose from nonhomologous recombination, lacked the entire left-terminal 37 kb of the PBCV-1 genome, including the 2.2-kbp terminal inverted repeats. The deleted left terminus was replaced by the transposition of an inverted 7.7- or 18.5-kbp copy from the right end of the PBCV-1 genome. Similar 30–45-kbp deletions were also obtained with NC64A virus CVK1 after exposure of CVK1-infected cells to UV radiation (Songsri *et al*., 1995; Yamada and Higashiyama, 1993). These deletions also occurred in the left terminal portion of the virus genome, possibly by homologous recombination. These experiments indicate that 40–45 kbp (12–13% of the total genome) at the left end of PBCV-1 and CVK2 genomes are unnecessary for viral replication in the laboratory. Similar deletion mutants occur in the poxviruses (Turner and Moyer, 1990) and ASFV (Blasco *et al*., 1989a, b); these virus genomes also have inverted terminal repeats and hairpin ends like the chloroviruses. The generation of chlorovirus deletions may be explained by the models proposed for deletions/transpositions in the poxvirus genomes (Shchelkunov and Totmenin, 1995; Turner and Moyer, 1990).

2. Small Deletions/Insertions

Small DNA deletions/insertions also often occur in chlorella virus genomes. Typically these events consist of one or two genes. An example is seen at the ORF *A430L*(Vp54)-*A431L-432L* region in the PBCV-1

genome. The entire *A431L*-like sequence is missing from this gene cluster in the CVK2 genome, leaving a two-gene cluster *A430L-432L* (Nishida *et al.*, 1999b). In addition a duplicate copy of A430L (A430L′) is inserted in the CVK2 genome at the region corresponding to PBCV-1 ORF *A452L-A454L*, resulting in a cluster of *A452L-A430L′-A454L* (Nishida *et al.*, 1999b). In this case, short 5′GTTTT or 5′CAAAA sequences are located at the rearrangement points and are assumed to be involved in the rearrangements. Similarly, a region surrounding the PBCV-1 A250R (Kcv) gene serves as an example of such rearrangements; this region was sequenced in 17 NC64A viruses. In PBCV-1 the genes for A251R and A252R are located immediately downstream of *A250R*; however, these genes are absent in 12 of the 17 NC64A viruses (Kang *et al.*, 2004a). In addition, two of the viruses had an extra ORF inserted between *A248R* and *A250R*. Many other examples of small insertions/deletions occur in the chlorella viruses. For example, virus NY-2A encodes 18 DNA methyltransferases whereas PBCV-1 has 5 DNA methyltransferases and 7 DNA restriction/modification enzymes (Fitzgerald, L. A. *et al.*, manuscript in preparation).

3. Gene Amplification

Eighty-four of the PBCV-1 ORFs resemble one or more other PBCV-1 ORFs forming 26 families. Thirteen families have two members, eight families have three members, three families have six members, and two families have eight members. One six-member family contains multiple ankyrin-like repeats (Peters and Lux, 1993). Five members in another family encode proteins that resemble the PBCV-1 major capsid protein Vp54, although these genes do not hybridize to one another on Southern blots. These observations suggest some gene amplification mechanisms probably exist in the PBCV-1 genome. Additional examples of gene amplification in other chloroviruses, such as Vp260, are described in an earlier section. It will be interesting to identify the regions in the 370-kbp NY-2A genome that are expanded as compared to the 330-kbp PBCV-1 genome. However, it is known that the region corresponding to *A292R-A330R* in PBCV-1 contains genes that are amplified extensively in NY-2A; *A328L* (two times), *A154L* (5 times), *A354R* (10 times), and *A315L* (12 times). These amplified genes are at least one reason that the NY-2A genome is larger than PBCV-1.

4. Gene Replacements

Comparison of the gene arrangements between chloroviruses has also revealed gene replacements. In the CVK2 genome, a single ORF (corresponding to PBCV-1 *A330R*) is replaced with a 5-kbp sequence

containing the genes encoding chitin synthase (*chs*), UDP-glucose dehydrogenase (*ugdh*), and two other ORFs (Ali *et al*., 2005). In PBCV-1, the hyaluronan synthase gene (*has*, A98R) is located at nucleotide positions 51–53 kbp in a cluster of A93L-A94L (β-1,3-glucanase)-A98R (hyaluronan synthase)-A100R (glucosamine synthase) (Li *et al*., 1995). A similar gene cluster occurs at the corresponding region in the CVK2 genome; however, the two internal ORFs are replaced with different genes, *bgl2* encoding another β-1,3-glucanase and *chs2* encoding another chitin synthase. The latter arrangement is also found in the NY-2A and AR158 genomes (Ali *et al*., 2005).

Often these rearrangement events include a set of genes, and it is certainly possible that the set may have genes whose products are functionally related, for example, like restriction endonucleases and their companion DNA methyltransferases. In fact, the ORF immediately adjacent to *chs2* described previously resembles a chitin deacetylase (Ali *et al*., 2005).

To summarize, the different sizes of the *Chlorovirus* genomes as well as their large and small deletions and insertions suggest that dynamic and frequent rearrangements of virus genomes occur in natural environments. These variations probably result from several mechanisms. The fact that the left end of the *Chlorovirus* genome is tolerant to deletions/insertions/rearrangements suggests that a recombinational "hotspot(s)" in this region allows viruses to exchange genes among themselves and possibly with their host(s). However, despite these differences, the location of most PBCV-1 genes, many of which are probably housekeeping genes, is nearly colinear in the 330–370-kb NC64A viruses, suggesting similar overall genome organization between these *Chlorovirus* isolates. Given the fact that the chlorella viruses often encode multiple transposases and homing endonucleases, one might expect the virus genomes to be unstable. However, this does not appear to be the case, at least in the laboratory.

VIII. Cell Wall Digestion: Chitinase, Chitosanase, Polysaccharide Lyase, and β-1,3-Glucanase

In a normal lytic cycle, PBCV-1 attaches to the surface of host chlorella cells and degrades the cell wall at the point of attachment; the viral core is then released into the host cytoplasm, leaving an empty capsid on the cell wall (Meints *et al*., 1984). Within 6–8 hpi, nascent viruses exit the cells after cell lysis. Thus, both the initial and final stages of the PBCV-1 replication cycle require cell wall-digesting

activities. A common characteristic of virus-sensitive chlorella strains is a rigid cell wall containing glucosamine in addition to other sugars; glucosamine comprises 7–17% of the total sugars in the cell wall (Kapaun and Reisser, 1995; Kapaun *et al*., 1992; Meints *et al*., 1988; Takeda, 1988, 1995). The presence of glucosamine suggests that enzymes degrading polymers of glucosamine, like chitin (β-1,4-linked polymer of *N*-acetyl-D-glucosamine) and chitosan (β-1,4-linked polymer of D-glucosamine with various degrees of *N*-acetylation), might be involved in the viral infection process. In fact, when *Chlorovirus* CVK2 proteins are separated into the capsid and core particle fractions (Songsri *et al*., 1997; Yamada *et al*., 1997), and assayed by SDS-PAGE with chitosan or chitin as a substrate in the gel matrix (Yamada *et al*., 1997), several enzymatically active proteins with molecular masses ranging from 35 to 70 kDa are detected in the core fraction. Of these, a 65-kDa protein has the most chitosanase activity and a few 50–60-kDa proteins have chitinase activities. Moreover, three PBCV-1 ORFs have significant amino acid sequence identities with bacterial chitinases and chitosanases (Lu *et al*., 1996). Yamada *et al*. (1997) chracterized a chitosanase (*vChta-1*) gene from virus CVK2. This gene, which corresponds to PBCV-1 ORF *A292L*, encodes two functional chitosanase proteins with apparently different roles in virus replication. The larger 65-kDa chitosanase is packaged in the virion and presumably functions during infection. In contrast, the smaller 37-kDa enzyme remains in the host cytoplasm, where it most likely aids in cell wall digestion during viral release. The enzymatic characterization of the PBCV-1 A292L protein has also been described (Sun *et al*., 1999).

As for the chitinase genes, a PBCV-1 ORF (A181/182R) encodes an active chitinase with two catalytic domains; the enzyme belongs to the family 18 glycosyl hydrolases (Sun *et al*., 1999). A A181/182R homolog is present in CVK2 (Hiramatsu *et al*., 1999, 2000). The first catalytic domain resembles a catalytic sequence from *Saccharopolyspora* (*Streptomyces*) *erythraeus* (30% identity) chitinase, whereas the second domain resembles a chitinase from *Ewingelle americana* (34.7% identity). The two catalytic domains are linked by a short, proline rich sequence. This structure suggests that the two vChti-1 chitinase domains might have independent origins (Hiramatsu *et al*., 1999). A C-terminal–truncated derivative of vChti-1, containing the first catalytic domain, produced chitobiose from either chitotetraose, chitohexaose, or high-molecular mass chitin; this product is typical of an exochitinase. In contrast, an N-terminal–truncated derivative of vChti-1 produced *N*-acetylglucosamine from chitobiose

as well as chitooligosaccharides. Therefore, this domain possessed *N*-acetylglucosaminidase activity as well as endochitinase activity. The presence of two catalytic domains with different enzymatic properties in the viral enzyme may allow natural substrates to be hydrolyzed in a cooperative fashion (Hiramatsu *et al*., 2000).

The CVK2 chitinase gene (*vChti-1*) is expressed in virus-infected cells beginning at 120 min pi. However, the 94-kDa protein product is not incorporated into virions but remains in the medium after cell lysis (Hiramatsu *et al*., 1999). Similar results were reported for the PBCV-1 A181R/A182R protein (Sun *et al*., 1999). Another PBCV-1 ORF, A260R, also resembles a chitinase (Sun *et al*., 1999). This gene is expressed late in infection, and the 55-kDa protein is enzymatically active and packaged in PBCV-1 virions. All of these chitinase and chitosanase genes are widely conserved in the chlorella viruses, suggesting their importance in viral replication.

However, *Chlorella* NC64A cells do not exhibit any drastic morphological changes when treated with vChti-1 and/or vChta-1 chitosanase (Hiramatsu *et al*., 1999; Yamada *et al*., 1999). Therefore, additional virus encoded enzymes are probably involved in host cell wall digestion. To detect such cell wall-degrading activities, *E. coli* lysates expressing virus CVK2 genes were assayed by monitoring halo-forming activity using *Chlorella* NC64A cells as a substrate. These expreriments revealed two algal-lytic activities (vAL-1 and vAL-2) (Sugimoto *et al*., 2000). *Val-1* transcription and translation products appear at 60 and 90 min pi, respectively. The vAL-1 protein is not incorporated into the viral particles but remains in the cell lysate, suggesting it is involved in cell wall digestion during viral release. *Chlorella* NC64A cell walls are digested by vAL-1 under physiological conditions. TLC and MALDI-TOF mass spectrometric analyses of the degradation products (oligosaccharides) revealed that the major oligosaccharides had unsaturated D-glucuronic acid (GlcA) (C4 = C5) at the reducing terminus, and a side chain attached at C2 or C3 of GlcA (C4 = C5). The side chain consisted primarily of Ara, GlcNAc, and Gal. These results indicate that vAL-1 is a novel polysaccharide lyase, cleaving chains of either β- or α-1,4-linked GlcAs (Sugimoto *et al*., 2004). In addition to *Chlorella* NC64A, vAL-1 lysed cells of four *C. vulgaris* isolates as well as *Chlorella* SAG-241–80 (Chuchird *et al*., 2001; Sugimoto *et al*., 2000). A PBCV-1 ORF (*A94L*) encodes a protein with 26–30% amino acid identity with family 16 endo-β-1,3-glucanases from several bacteria. A94L also has the critical amino acids in the catalytic site of family 16 endo-β-1,3- and endo-β-1,3–1,4-glucanases. The A94L recombinant protein hydrolyzed the β-1,3-glucan laminarin

and had slightly less hydrolytic activity on β-1,3–1,4-glucan lichenan and barley β-glucan (Sun *et al.*, 2000). The *a94l* gene is expressed early in PBCV-1 infection. Furthermore, the A94R protein appears early during PBCV-1 replication but then disappears by 120 min pi. The biological function of this β-1,3-glucanase is unknown as approximately 50% of chlorella viruses lack this gene. However, some chlorella viruses lacking A94L homologs contain another gene encoding an endo-β-1,3-glucanase (*bgl2*) (Ali *et al.*, 2005). The functions of these genes and their products are unknown.

The chlorella viruses may be a good source of polysaccharide digesting enzymes because cell wall polysaccharides can differ significantly among chlorella isolates (Yamada and Sakaguchi, 1982). Thus one predicts that some virual enzymes may have some unique activities.

At the same time, the origin and evolution of the genes encoding the polysaccharide-degrading enzymes in the chloroviruses are intriguing. A gene encoding a chitinase, that shares significant amino acid sequence identity with vChti-1, was discovered in host *Chlorella* NC64A (Ali, A. M. *et al.*, manuscipt in preparation). Comparison of the structure, nature and function of this gene product with vChti-1 may reveal information on the origin and evolution of the viral genes.

IX. Glycosyltransferases and Synthesis of Polysaccharides and Fucose

A. Glycosylation of the Virus Structural Proteins

Virus PBCV-1 contains six possible glycosyltransferase encoding genes, *a64r*, *a111/114r*, *a222/226r*, *a328l*, *a473l*, and *a546l* (Van Etten, 2003; Van Etten *et al.*, 2002). None of these putative glycosyltransferases have an identifiable signal peptide that would target them to the endoplasmic reticulum (ER) or Golgi. Furthermore, the cellular protein localization program PSORT predicts that four of these proteins are located in the cytoplasm and two have a transmembrane domain (Van Etten, 2003). The *a64r* gene encodes a 638 amino acid protein that has four motifs conserved in "Fringe type" glycosyltransferases. Analysis of 13 PBCV-1 antigenic variants, with differences in the major capsid protein Vp54 glycans, have mutations in *a64r* that correlated with specific antigenic variations. Dual infection experiments with different antigenic variants established that wild-type PBCV-1 could be formed by complementation and recombination of the variants. These results led to the conclusion that *a64r* encodes a glycosyltransferase associated with Vp54 glycan synthesis (Graves

et al., 2001). Typically, viral proteins are glycosylated by host-encoded glycosyltransferases located in the ER and Golgi (Doms *et al*., 1993; Knipe, 1996; Olofsson and Hansen, 1998). Consequently, the glycan portion of virus glycoproteins is host specific. Therefore, glycosylation of PBCV-1 major capsid proteinVp54 differs from this paradigm. Additional experiments to support this statement are provided in a review (Markine-Goriaynoff *et al*., 2004).

These findings lead to several questions including: are the Vp54 glycan precursors attached to a lipid carrier such as undecaprenol-phosphate which serves as an intermediate in bacterial peptidoglycan synthesis (Raetz and Whitfield, 2002) or dolichol diphosphate which serves the same function in eukaryotic cells (Reuter and Gabius, 1999)? Could Vp54 glycosylation reflect an ancestral pathway that existed prior to the ER and Golgi formation?

B. Extracellular Polysaccharide Synthesis

The chloroviruses are also unusual because they encode enzymes involved in the biosynthesis of the linear polysaccharides hyaluronan (also called hyaluronic acid) and/or chitin. Typically, hyaluronan is only found in the extracellular matrix of vertebrates and capsules of a few pathogenic bacteria (DeAngelis, 1999, 2002). It is composed of $\sim$20,000 alternating β-1,4-glucuronic acid and β-1,3-*N*-acetylglucosamine residues (DeAngelis, 1999). Unexpectedly, virus PBCV-1 contains genes encoding hyaluronan synthase (HAS) (DeAngelis *et al*., 1997) and two other enzymes involved in the synthesis of hyaluronan precursors, glutamine:fructose-6-phosphate amidotransferase and UDP-glucose dehydrogenase (Landstein *et al*., 1998). All three genes are expressed early during PBCV-1 infection. These results led to the discovery that hyaluronan lyase-sensitive, hair-like fibers begin to accumulate on the surface of PBCV-1 infected host cells by 15 min pi (Graves *et al*., 1999). By 4 hpi, the infected cells are covered with a dense fibrous hyaluronan network.

The *has* gene is present in many, but not all, chloroviruses isolated from diverse geographical regions (Graves *et al*., 1999), suggesting that not all chloroviruses encode hyaluronan. Surprisingly, many chloroviruses that lack a *has* gene, have a gene encoding a functional chitin synthase (CHS). Furthermore, cells infected with these viruses produce chitin fibers on their external surface (Kawasaki *et al*., 2002). Chitin, an insoluble linear homopolymer of β-1,4-linked *N*-acetylglucosamine residues, is a common component of insect exoskeletons, shells of crustaceans, and fungal cell walls (Gooday *et al*., 1986).

Some chloroviruses contain both *has* and *chs* genes, and form both hyaluronan and chitin on the surface of the infected cells (Kawasaki *et al.*, 2002; Yamada and Kawasaki, 2005). Finally, a few chloroviruses probably lack both genes because no extracellular polysaccharides are formed on the host surface of cells infected with these viruses (Graves *et al.*, 1999).

The fact that many chloroviruses encode enzymes involved in extracellular polysaccharide biosynthesis suggests that the polysaccharides are important in the virus life cycle. At present this function is unknown; however, we have considered three possibilities. (1) The polysaccharides prevent uptake of virus-infected chlorella by the paramecium. Presumably, such infected algae would lyse inside the paramecium, and the released virions would be digested by the protozoan. This scenario would be detrimental to virus survival. (2) The viruses have another host that acquires the virus by taking up the polysaccharide-covered algae. (3) Virus-infected cells aggregate, presumably due to the extracellular polysaccharide. This aggregation, which could trap uninfected cells, might aid the virus in finding its next host. However, a complicating factor in understanding the biological role of these two polysaccharides is that some viruses apparently lack both genes.

Ali *et al.* (2005) investigated the genetic relationship between "hyaluronan-synthesizing" and "chitin-synthesizing" viruses by characterizing two genomic regions in the chitin-synthesizing virus CVK2 and comparing them to PBCV-1. One region surrounds the CVK2 *chs* region and the other corresponds to the region containing PBCV-1 *has*. A single PBCV-1 ORF (A330R) is replaced in the CVK2 genome with a 5-kb region containing *chs*, *ugdh2* (a second gene encoding UDP-glucose dehydrogenase) and two other ORFs. In CVK2 the location of the PBCV-1 *has* gene is replaced with another *chs* gene (described in Section VII.C.4). Some chloroviruses lack *ugdh*. These results suggest that chloroviruses change from "*has* viruses" to "*chs* viruses" or from "*chs* viruses" to "*has* viruses" by exchanging genes (Fig. 4).

These observations also indicate that there is no functional incompatibility between the two genes or their gene products, that is, hyaluronan and chitin. These conclusions are interesting because it has been suggested that the *has* gene in vertebrates evolved from chitin synthase or cellulose synthase through the addition of a β-1-3 glycosyltransferase activity to a preexisting β-1-4 glycosyltransferase enzyme and that the ability to synthesize hyaluronan occurred relatively recently in metazoan evolution (Lee and Spicer, 2000). Another *chs*-like gene was reported to be encoded by the 336-kbp *Ectocarpus*

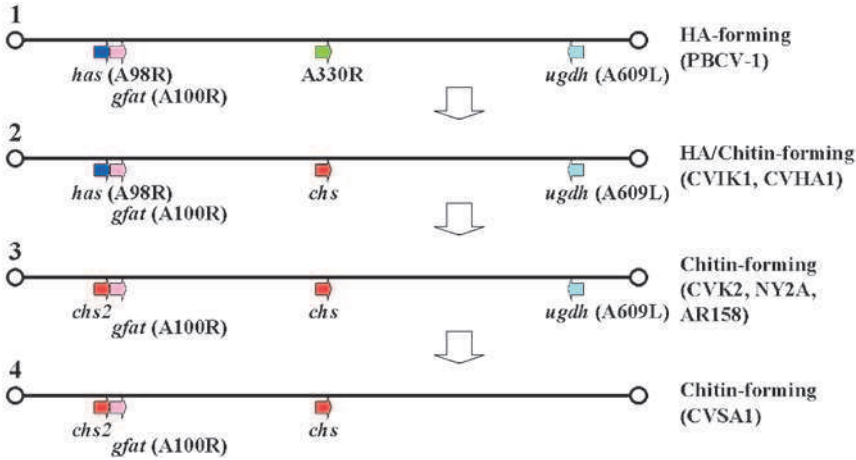

FIG 4. A diagram illustrating the genetic differences between HA and/or chitin synthesizing chloroviruses (Ali *et al*., 2005). Line 1 shows the location of three PBCV-1 genes involved in the synthesis of HA. Viruses CVIK1 and CVHA1 that synthesize both HA and chitin (Line 2) have a chitin synthesizing gene inserted in the position of the PBCV-1 A330R ORF. Viruses that only synthesize chitin have two *chs* genes. These viruses may still have a *ugdh* gene (viruses CVK2, NY-2A, and AR158 in Line 3) or lose it (virus CVSA1 in Line 4). It is equally likely that the events depicted could occur in reverse order, that is, from Line 4 to Line 1.

siliculosus virus EsV-1 (Delaroque *et al*., 2001). EsV-1 also belongs to the *Phycodnaviridae* but is lysogenic, in contrast to the lytic chlorella viruses. No information is available on the expression or function of the EsV-1 *chs*-like gene.

The discovery of viral encoded enzymes involved in polysaccharide synthesis leads to many questions such as: (1) what is the function of these extracellular polysaccharides? (2) Why do infected cells expend huge amounts of energy on these processes when they are going to lyse in a few hours? (3) How were these genes acquired by the viruses? (4) Which was the original form of viral-encoded polysaccharides, hyaluronan or chitin? (5) How are hyaluronan and chitin polymers synthesized in the host cells and translocated through the cell wall?

C. Fucose Synthesis

PBCV-1 also encodes enzymes involved in nucleotide sugar metabolism. Two enzymes encoded by PBCV-1, GDP-D-mannose 4,6 dehydratase (GMD) and the bifunctional GDP-4-keto-6-deoxy-D-mannose epimerase/

reductase (GMER) comprise the highly conserved pathway that converts GDP-D-mannose to GDP-L-fucose. *In vitro* reconstruction of the biosynthetic pathway using recombinant PBCV-1 GMD and GMER produced in *E. coli* synthesized GDP-L-fucose (Tonetti *et al.*, 2003). Unexpectedly, however, the PBCV-1 GMD, which has been crystallized recently (Rosano *et al.*, 2005), also catalyzes the NADPH-dependent reduction of the intermediate GDP-4-keto-6-deoxy-D-mannose, forming GDP-D-rhamnose. Similar results were obtained with GMD and GMER encoded by virus CVK2 (Isono, K. *et al.*, unpublished data). Both fucose and rhamnose are constituents of the glycans attached to the PBCV-1 major capsid protein Vp54; therefore, the virus might encode the enzymes to meet this need. However, both sugars are also components of the uninfected host cell wall (Meints *et al.*, 1988).

X. Relationship of Chloroviruses to Other Viruses

As mentioned in the introduction, the phycodnaviruses are members of the superfamily of viruses referred to as NCLDVs and that accumulating evidence indicates that the phycodnaviruses have a long evolutionary history, possibly beginning at the time eukaryotes separated from prokaryotes (over 3 billion years ago). The evidence includes: (1) Phylogenetic analyses of DNA polymerases place the algal virus enzymes near the root of all eukaryotic δ-DNA polymerases (Villarreal and DeFilippis, 2000). (2) Phylogenetic analyses of other PBCV-1 encoded proteins often place the proteins near the root of their eukaryotic counterparts, for example, the K^+ channel protein Kcv (Plugge *et al.*, 2000) and ornithine decarboxylase (Shah *et al.*, 2004). (3) Many *Chlorovirus* encoded proteins are either the smallest or among the smallest proteins in their class. Examples include the type II DNA topoisomerase (Dickey *et al.*, 2005), Kcv (Plugge *et al.*, 2000), ornithine decarboxylase (Shah *et al.*, 2004), and lysine di-methyltransferase (Manzur *et al.*, 2003). These proteins could represent progenitors of their more complex relatives. (4) Some PBCV-1-encoded enzymes are more flexible than those from higher eukaryotic organisms. For example, some virus enzymes carry out two functions whereas more "advanced" organisms require two separate enzymes to accomplish the same tasks. One interpretation of this observation is that these virus proteins may be progenitor enzymes and thus more precocious than their highly evolved counterparts in higher eukaryotes, where two separate enzymes carry out the function of one virus enzyme. This

dual functionality in the PBCV-1 enzymes does not result from gene fusion. Examples include: (a) ornithine decarboxylase which decarboxylates arginine more efficiently than ornithine (Shah *et al*., 2004). (b) dCMP deaminase which also deaminates dCTP and dCDP, as well as the expected dCMP (Zhang, Y. *et al*., manuscript in preparation). (c) GDP-D-mannose 4,6 dehydratase not only catalyzes the formation of GDP-4-keto-6-deoxy-D-mannose, which is an intermediate in the synthesis of GDP-L-fucose, the enzyme also reduces the same intermediate to GDP-D-rhamnose (Tonetti *et al*., 2003). (5) Even though PBCV-1 encodes both prokaryotic- and eukaryotic-like proteins, the 40% G + C content is fairly uniform throughout the genome. This pattern suggests that most of the genes have existed together in the virus for a long time. (6) The major coat protein from several dsDNA viruses that infect all three domains of life, including bacteriophage PRD1, human adenoviruses, and a virus STIV infecting the Archaea, *Sulfolobus solfataricus*, are structurally similar to that of PBCV-1. This finding led Benson *et al*. (2004) to suggest that all these viruses may have a common evolutionary ancestor, even though there is no significant amino acid sequence similarity among their proteins. (7) Finally, one of the earliest eukaryotic cells could have resembled a single celled alga (Yoon *et al*., 2004).

Some evolutionary biologists have suggested that NCLDVs may be the origin of the nucleus in eukaryotic cells (Bell, 2001; Pennisi, 2004; Villarreal, 2005), whereas other biologists (Raoult *et al*., 2004) have suggested that Mimivirus, and by inference the NCLDVs, may represent a fourth domain of life. This later hypothesis resulted from a phylogenetic tree of life derived from the concatenated sequences of seven universally conserved proteins sequences: arginyl-tRNA synthetase, methionyl-tRNA synthetase, tyrosyl-tRNA synthetase, RNA polymerase II largest subunit, RNA polymerase II second largest subunit, PCNA, and 5′–3′ exonuclease. Mimivirus formed a branch near the origin of the Eukaryotic domain.

Continuing with this hypothesis, perhaps the NCLDVs originally arose from a more complex ancestor and this progenitor ancestor (virus) became associated with different organisms that evolved into various eukaryotic lineages. These lineages placed various demands on the evolving NCLDVs resulting in the loss of some genes, either by donating genes to their hosts or the genes were no longer required for replication of the evolving viruses. The net result is that the NCLDVs now only have nine common genes. Of course over 3 billion years of evolution the viruses also acquired selected genes from their hosts that were necessary for survival.

Eight of the 10 viruses with the largest sequenced genomes are NCLDVs and 6 of them are members of the *Phycodnaviridae* (http://giantvirus.org). The largest algal virus genome sequenced to date infects *Emiliania huxleyi* and has a genome of 407 kb that contains ~470 protein-encoding genes (Wilson *et al*., 2005a). However, larger algal virus genomes exist; examples include lytic viruses specific for *Phaeocystis pouchetii* (PpV) (Jacobsen *et al*., 1996), *Chrysochromulina ericina* (CeV-01B) (Sandaa *et al*., 2001), and *Pyramimonas orientalis* (PoV-01B) (Sandaa *et al*., 2001), which have genomes of approximately 485, 510, and 560 kb, respectively. To put the size of these viral genomes into perspective, the smallest bacterium, *Mycoplasma genitalium* has a genome of 580 kb that contains ~470 protein-encoding genes (Fraser *et al*., 1995) and the smallest Archaea, *Nanoarchaeum equitans*, has a 490-kb genome that contains ~550 protein-encoding genes (Waters *et al*., 2003). Estimates of the minimum genome size required to support life are ~250 protein-encoding genes (e.g., Itaya, 1995; Mushegian and Koonin, 1996). The Mimivirus genome is actually larger than 25 microbial genomes currently in the databases (http://giantvirus.org). Thus a big question is: what differentiates large complex DNA viruses from small obligate intracellular microorganisms? It is also obvious that metagenomic sequencing projects are identifying many more genes associated with large dsDNA viruses (Breibart *et al*., 2002; Tyson *et al*., 2004; Venter *et al*., 2004). Without doubt many of these will be algal infecting viruses (Suttle, 2005).

The presumed long evolutionary history of the NCLDVs can also explain why the phycodnaviruses are so diverse. Of the six genera in the family *Phycodnaviridae*, members of two genera in addition to the chlorella viruses have been sequenced, the circular *Emiliania huxleyi* virus (EhV-1) 407-kb genome (Wilson *et al*., 2005a) and the linear *Ectocarpus siliculosus* virus (EsV-1) 335-kb genome (Delaroque *et al*., 2001). Including PBCV-1, each of these three viruses codes for several hundred proteins (Dunigan *et al*., 2006). However, it is truly amazing that only 14 protein-encoding genes are common to all three viruses. This means that just these three viruses contain more than a 1000 unique protein-encoding genes. Despite the large genetic diversity in these three sequenced phycodnaviruses, phylogenetic analyses of their δ-DNA polymerases (Chen and Suttle, 1996; Wilson *et al*., 2005a) and a superfamily of archeao-eukaryotic primases (Iyer *et al*., 2005) indicate that the phycodnaviruses fall into a monophyletic clade within the NCLDVs.

The long evolutionary history can also explain the diversity among viruses that infect *Chlorella* NC64A or *Chlorella* Pbi. The amino acid sequence of protein homologs between *Chlorella* NC64A infecting viruses can differ by as much as 25%. This difference can be ~50% between homologs from NC64A and Pbi viruses. This diversity can be used to identify amino acid substitutions that alter the functional properties of proteins, for example as has been done with the chlorovirus encoded K^+ channels (Gazzarrini *et al*., 2004; Kang *et al*., 2004b).

In addition to the genomic sequence of PBCV-1, sequences of several other chlorella virus geneomes are now available, and they make it possible to determine a pan-genome of chlorella virus, which consists of a core genome shared by all isolates and a dispensable genome consisting of partially shared and isolate-specific genes. The core genes, which are highly conserved among different viral isolates, reflect their importance in the basic infection cycle. The variable genes are related to recent growth history and the range of infection of individual virus isolates. One outcome of this diversity is that the total number of *Chlorovirus* protein-encoding genes is much larger than that from any one virus.

XI. Perspectives

It has been ~25 years since the first chloroviruses were described. Sequencing the 330-kb PBCV-1 genome about 10 years ago revealed, and is continuing to reveal, many unexpected genes such as genes encoding proteins involved in polysaccharide biosynthesis, polyamine biosynthesis, and ion transport proteins. The discovery of these genes, and the fact that many of their gene products are easy to work with, has led to an expansion in the number of investigators who are studying chloroviruses and their genes. However, many fundamental events in chlorovirus replication have only begun to be studied as indicated by some of the questions posed in this review. The biggest handicap facing studies on the chloroviruses, as well as all of the phycodnaviruses, is the lack of a functional molecular genetic system. However, new tools are coming into play with the chlorella viruses. For example, microarrays containing all of the putative PBCV-1 protein-encoding genes are now being used to study PBCV-1 gene expression, proteinomic studies are identifying all of the virion-encoded proteins packaged in the virion, and the USA Department of Energy has agreed to sequence the PBCV-1 host *Chlorella* NC64A. These new tools should

lead to a greater understanding of virus-host relationships in the near future.

Acknowledgments

This work was supported in part by a grant from Nagase Science and Technology Foundation. Research in the Van Etten laboratory has been supported in part by Public Health Service grant GM32441 from the National Institute of General Medical Sciences, the National Science Foundation grant EF-0333197, and grant P20-RR15635 from the COBRE program of the National Center for Research Resources.

References

Ali, M. M. A., Kawasaki, T., and Yamada, T. (2005). Genetic rearrangements on the chlorovirus genome that switch between hyaluronan synthesis and chitin synthesis. *Virology* **342:**102–110.

Becker, B., Lesenmann, D. E., and Reisser, W. (1993). Ultrastructural studies on a chlorella virus from Germany. *Arch. Virol.* **130:**145–155.

Belfield, G. P., and Tuite, M. F. (1993). Translation elongation factor 3: A fungus-specific translation factor? *Mol. Microbiol.* **9:**411–418.

Bell, P. J. (2001). Viral eukaryogenesis: Was the ancestor of the nucleus a complex DNA virus. *J. Mol. Evol.* **53:**251–256.

Benson, S. D., Bamford, J. K. H., Bamford, D. H., and Burnett, R. M. (2004). Does common architechture reveal a virus lineage spanning all three domains of life? *Mol. Cell* **16:**673–685.

Blasco, R., Aguero, M., Almendral, J. M., and Vinuela, E. (1989). Variable and constant regions in African swine fever virus DNA. *Virology* **168:**330–338.

Blasco, R., De La Dega, I., Almazan, F., Aguero, M., and Vinuela, E. (1989). Genetic variation of African swine fever virus: Variable regions near the ends of the viral DNA. *Virology* **173:**251–257.

Breibart, M., Salamon, P., Andresen, B., Mahaffy, J. M., Segall, A. M., Mead, D., Azam, F., and Rohwer, F. (2002). Genomic analysis of uncultured marine communities. *Proc. Natl. Acad. Sci. USA* **99:**14250–14255.

Brussaard, C. P. D. (2004). Viral control of phytoplankton populations: A review. *J. Eukarot Microbiol.* **51:**125–138.

Bubeck, J. A., and Pfitzner, A. J. (2005). Isolation and characterization of a new type of chlorovirus that infects an endosymbiotic chlorella strain of the heliozoon *Acanthocystis turfacea*. *J. Gen. Virol.* **86:**2871–2877.

Caspar, D. L. D., and Klug, A. (1962). Physical principles in the construction of regular viruses. *Cold Spring Harb. Symp. Quant. Biol.* **27:**1–24.

Chakraburtty, K. (2001). Translational regulation by ABC systems. *Res. Microbiol.* **152:**391–399.

Chen, F., and Suttle, C. A. (1996). Evolutionary relationships among large double-stranded DNA viruses that infect microalgae and other organisms as inferred from DNA polymerase genes. *Virology* **219:**170–178.

Cho, H. H., Park, H. H., Kim, J. O., and Choi, T. J. (2002). Isolation and characterization of chlorella viruses from freshwater sources in Korea. *Mol. Cells* **14:**168–176.

Chuchird, N., Hiramatsu, S., Sugimoto, I., Fujie, M., Usami, S., and Yamada, T. (2001). Digestion of *Chlorella* cells by chlorovirus-encoded polysaccharide degrading enzymes. *Microbes and Environment* **16:**197–205.

Chuchird, N., Nishida, K., Kawasaki, T., Fujie, M., Usami, S., and Yamada, T. (2002). A variable region on the chlorovirus CVK2 genome contains five copies of the gene for Vp260, a viral-surface glycoprotein. *Virology* **295:**289–298.

Cobbold, C., Whittle, J. T., and Wileman, T. (1996). Involvement of the endoplasmic reticulum in the assembly and envelopment of African swine fever virus. *J. Virol.* **70:**8382–8390.

DeAngelis, P. L. (1999). Hyaluronan synthases: Fascinating glycosyltransferases from vertebrates, bacterial pathogens, and algal viruses. *Cell Mol. Life Sci.* **56:**670–682.

DeAngelis, P. L. (2002). Evolution of glycosaminoglycans and their glycosyltransferases: Implications for the extracellular matrices of animals and the capsules of pathogenic bacteria. *Anat. Rec.* **268:**317–326.

DeAngelis, P. L., Jing, W., Graves, M. V., Burbank, D. E., and Van Etten, J. L. (1997). Hyaluronan synthase of chlorella virus PBCV-1. *Science* **278:**1800–1803.

Delaroque, N., Müller, D. G., Bothe, G., Pohl, T., Knippers, R., and Boland, W. (2001). The complete DNA sequence of the *Ectocarpus siliculosus* virus genome. *Virology* **287:**112–132.

Deshaies, R. J. (1999). SCF and Cullin/RING H2-based ubiquitin ligases. *Annu. Rev. Cell Dev. Biol.* **15:**435–467.

Dickey, J. S., Choi, T.-J., Van Etten, J. L., and Osheroff, N. (2005). Chlorella virus Marburg topoisomerase II: High DNA cleavage activity as a characteristic of chlorella virus type II enzymes. *Biochemistry* **44:**3899–3908.

Dodds, J. A. (1979). Viruses of marine algae. *Experientia* **35:**440–442.

Doms, R. W., Lamb, R. A., Rose, J. K., and Helenius, A. (1993). Folding and assembly of viral membrane proteins. *Virology* **193:**545–562.

Dunigan, D. D., Fitzgerald, L. A., and Van Etten, J. L. (2006). Phycodnaviruses: A peak at genetic diversity. *Virus Research* **117:**119–132.

Eriksson, M., Myllyharju, J., Tu, H., Hellman, M., and Kivirikko, K. I. (1999). Evidence for 4-hydroxyproline in viral proteins: Characterization of a viral prolyl 4-hydroxylase and its peptide substrates. *J. Biol. Chem.* **274:**22131–22134.

Fraser, C. M., Gocayne, J. D., White, O., Adams, M. D., Clayton, R. A., Fleischmann, R. D., Bult, C. J., Kerlavage, A. R., Sutton, J. M., Kelley, G., Fritchman, J. L., Weidman, J. F. *et al.* (1995). The minimal gene complement of *Mycoplasma genitalium*. *Science* **270:**397–403.

Frohns, F., Käsmann, A., Schäfer, B., Kramer, D., Mehmel, M., Kang, M., Van Etten, J. L., Gazzarrini, S., Moroni, A., and Thiel, G. (2006). Potassium ion channels of chorella viruses cause rapid depolarization of host cells during infection. *J. Virol.* **80:**2437–2444.

Fuhrman, J. A. (1999). Marine viruses and their biogeochemical and ecological effects. *Nature* **399:**541–548.

Gazzarrini, S., Severino, M., Morandi, M., Lombardi, M., DiFrancesco, D., Van Etten, J. L., Thiel, G., and Moroni, A. (2003). The viral K^+ channel Kcv: Structural and functional features. *FEBS Lett.* **552:**12–16.

Gazzarrini, S., Kang, M., Van Etten, J. L., Tayefeh, S., Kast, S. M., DiFrancesco, D., Thiel, G., and Moroni, A. (2004). Long distance interactions within the potassium channel pore are revealed by molecular diversity of viral proteins. *J. Biol. Chem.* **279:**28443–28449.

Girton, L., and Van Etten, J. L. (1987). Restriction site map of the chlorella virus PBCV-1 genome. *Plant Mol. Biol.* **9:**247–257.

Gong, C., and Shuman, S. (2002). Chlorella virus RNA triphosphatase: Mutational analysis and mechanism of inhibition by tripolyphosphate. *J. Biol. Chem.* **277:**15317–15324.

Gooday, G. W., Humphreys, A. M., and McIntosh, W. H. (1986). Role of chitinases in fungal growth. *In* "Chitin in Nature and Technology" (R. Muzzarelli, C. Jeuniaux, and G. W. Gooday, eds.), pp. 83–91. Plenum Press, New York.

Grabherr, R., Strasser, P., and Van Etten, J. L. (1992). The DNA polymerase gene from chlorella viruses PBCV-1 and NY-2A contains an intron with nuclear splicing sequences. *Virology* **188:**721–731.

Graves, M. V., and Meints, R. H. (1992). Characterization of the gene encoding the most abundant *in vitro* translation product from virus-infected chlorella-like algae. *Gene* **113:**149–155.

Graves, M. V., Burbank, D. E., Roth, R., Heuser, J., DeAngelis, P. L., and Van Etten, J. L. (1999). Hyaluronan synthesis in virus PBCV-1 infected chlorella-like green algae. *Virology* **257:**15–23.

Graves, M. V., Bernadt, C. T., Cerny, R., and Van Etten, J. L. (2001). Molecular and genetic evidence for a virus-encoded glycosyltransferase involved in protein glycosylation. *Virology* **285:**332–345.

Hambly, E., and Suttle, C. A. (2005). The viriosphere, diversity, and genetic exchange within phage communities. *Curr. Opin. Microbiol.* **8:**444–450.

Hiramatsu, S., Ishihara, M., Fujie, M., Usami, S., and Yamada, T. (1999). Expression of a chitinase gene and lysis of the host cell wall during chlorella virus CVK2 infection. *Virology* **260:**308–315.

Hiramatsu, S., Fujie, M., Usami, S., Sakai, K., and Yamada, T. (2000). Two catalytic domains of chlorella virus CVK2 chitinase. *J. Biosci. Bioeng.* **89:**252–257.

Ho, C. K., Van Etten, J. L., and Shuman, S. (1996). Expression and characterization of an RNA capping enzyme encoded by chlorella virus PBCV-1. *J. Virol.* **70:**6658–6664.

Ho, C. K., Gong, C., and Shuman, S. (2001). RNA triphosphatase component of the mRNA capping apparatus of *Paramecium bursaria Chlorella* virus 1. *J. Virol.* **75:**1744–1750.

Hoshina, R., Kamako, S., and Imamura, N. (2004). Phylogenetic position of endosymbiotic green algae in *Paramecium bursaria* Ehrenberg from Japan. *Plant Biol.* **6:**447–453.

Hoshina, R., Kato, Y., Kamako, S., and Imamura, N. (2005). Genetic evidence of "American" and "European" type symbiotic algae of *Paramecium bursaria* Ehrenberg. *Plant Biol.* **7:**526–532.

Itaya, M. (1995). An estimation of minimal genome size required for life. *FEBS Lett.* **362:**257–260.

Iyer, L. M., Aravind, L., and Koonin, E. V. (2001). Common origin of four diverse families of large eukaryotic DNA viruses. *J. Virol.* **75:**11720–11734.

Iyer, L. M., Koonin, E. V., Leipe, D. D., and Aravind, L. (2005). Origin and evolution of the archaeo-eukaryotic primase superfamily and related palm-domain proteins: Structural insights and new members. *Nucleic Acids Res.* **33:**3875–3896.

Jacobsen, A., Bratbak, G., and Heldal, M. (1996). Isolation and characterization of a virus infecting *Phaeocystis pouchetii* Prymnesiophyceae. *J. Phycol.* **32:**923–927.

Johnson, G. P., Goebel, S. J., and Paoletti, E. (1993). An update on the vaccinia virus genome. *Virology* **196:**381–401.

Kang, M., Moroni, A., Gazzarrini, S., and Van Etten, J. L. (2003). Are algal viruses a rich source of ion channel genes? *FEBS Lett.* **18:**2–6.

Kang, M., Graves, M., Mehmel, M., Moroni, A., Gazzarrini, S., Thiel, G., Gurnon, J. R., and Van Etten, J. L. (2004a). Genetic diversity in chlorella viruses flanking *kcv*, a gene that encodes a potassium ion channel protein. *Virology* **326:**150–159.

Kang, M., Moroni, A., Gazzarrini, S., DiFrancesco, D., Thiel, G., Severino, M., and Van Etten, J. L. (2004b). Small potassium ion channel proteins encoded by chlorella viruses. *Proc. Natl. Acad. Sci. USA* **101:**5318–5324.

Kang, M., Dunigan, D. D., and Van Etten, J. L. (2005). Chlorovirus: A genus of Phycodnaviridae that infects certain chlorella-like green algae. *Mol. Plant Pathol.* **6:**212–224.

Kapaun, E., and Reisser, W. (1995). A chitin-like glycan in the cell wall of a *Chlorella* sp. Chlorococcales, Chlorophyceae. *Planta* **197:**577–582.

Kapaun, E., Loos, E., and Reisser, W. (1992). Cell wall composition of virus-sensitive symbiotic chlorella species. *Phytochemistry* **31:**3103–3104.

Kawakami, H., and Kawakami, N. (1978). Behavior of a virus in a symbiotic system. *Paramecium bursaria*-zoochlorella. *J. Protozool.* **25:**217–225.

Kawasaki, T., Tanaka, M., Fujie, M., Usami, S., Sakai, K., and Yamada, T. (2002). Chitin synthesis in chlorovirus CVK2-infected *Chlorella* cells. *Virology* **302:**123–131.

Kawasaki, T., Tanaka, M., Fujie, M., Usami, S., and Yamada, T. (2004). Immediate early genes expressed in chlorovirus infection. *Virology* **318:**214–223.

Knipe, D. M. (1996). Virus-host cell interactions. *In* "Fields Virology" (B. N. Fields, D. M. Knipe, P. M. Howley, R. M. Chanock, J. L. Melnick, T. P. Monath, B. Roizman, and S. E. Straus, eds.), 3rd edn., pp. 273–299. Lippincott-Raven Publication, Philadephia.

Kutish, G. F., Li, Y., Lu, Z., Furuta, M., Rock, D. L., and Van Etten, J. L. (1996). Analysis of 76 kb of the chlorella virus PBCV-1 330-kb genome: Map positions 182 to 258. *Virology* **223:**303–317.

Kuznetsov, Y. G., Gurnon, J. R., Van Etten, J. L., and McPherson, A. (2005). Atomic force microscopy investigation of a chlorella virus, PBCV-1. *J. Struct. Biol.* **149:**256–263.

Landstein, D., Burbank, D. E., Nietfeldt, J. W., and Van Etten, J. L. (1995). Large deletions in antigenic variants of the chlorella virus PBCV-1. *Virology* **214:**413–420.

Landstein, D., Graves, M. V., Burbank, D. E., DeAngelis, P., and Van Etten, J. L. (1998). Chlorella virus PBCV-1 encodes functional glutamine: Fructose-6-phosphate amidotransferase and UDP-glucose dehydrogenase enzymes. *Virology* **250:**388–396.

Lee, D. A., Graves, M. V., Van Etten, J. L., and Choi, T.-J. (2005). Functional implication of the tRNA genes encoded in the chlorella virus PBCV-1 genome. *Plant Pathol. J.* **21:**334–342.

Lee, J. Y., and Spicer, A. P. (2000). Hyaluronan: A multifunctional megaDalton, stealth molecule. *Curr. Opin. Cell Biol.* **12:**581–586.

Lemke, P. A. (1976). Viruses of eucaryotic microorganisms. *Annu. Rev. Microbiol.* **30:**105–145.

Li, Y., Lu, Z., Burbank, D. E., Kutish, G. F., Rock, D. L., and Van Etten, J. L. (1995). Analysis of 43 kb of the chlorella virus PBCV-1 330 kb genome: Map position 45 to 88. *Virology* **212:**134–150.

Li, Y., Lu, Z., Sun, L., Ropp, S., Kutish, G. F., Rock, D. L., and Van Etten, J. L. (1997). Analysis of 74 kb of DNA located at the right end of the 330-kb chlorella virus PBCV-1 genome. *Virology* **237:**360–377.

Lu, Z., Li, Y., Zhang, Y., Kutish, G. F., Rock, D. L., and Van Etten, J. L. (1995). Analysis of 45 kb of DNA located at the left end of the chlorella virus PBCV-1 genome. *Virology* **206:**339–352.

Lu, Z., Li, Y., Que, Q., Kutish, G. F., Rock, D. L., and Van Etten, J. L. (1996). Analysis of 94 kb of the chlorella virus PBCV-1 330-kb genome: Map positions 88 to 182. *Virology* **216:**102–123.

Manzur, K. L., Farooq, A., Zeng, L., Plotnikova, O., Koch, A. W., Sachchidanand, and Zhou, M.-M. (2003). A dimeric viral SET domain methyltransferase specific to Lys^{27} of histone H3. *Nat. Struct. Mol. Biol.* **10:**187–196.

Markine-Goriaynoff, N., Gillet, L., Van Etten, J. L., Korres, H., Verma, N., and Vanderplasschen, A. (2004). Glycosyltransferases encoded by viruses. *J. Gen. Virol.* **85:**2741–2754.

Mehmel, M., Rothermel, M., Meckel, T., Van Etten, J. L., Moroni, A., and Thiel, G. (2003). Possible function for virus encoded K^+ channel Kcv in the replication of chlorella virus PBCV-1. *FEBS Lett.* **552:**7–11.

Meints, R. H., Van Etten, J. L., Kuczmarski, D., Lee, K., and Ang, B. (1981). Viral infection of the symbiotic chlorella-like alga present in *Hydra viridis*. *Virology* **113:**698–703.

Meints, R. H., Lee, K., Burbank, D. E., and Van Etten, J. L. (1984). Infection of a chlorella-like alga with the virus, PBCV-1: Ultrastructural studies. *Virology* **138:**341–346.

Meints, R. H., Lee, K., and Van Etten, J. L. (1986). Assembly site of the virus PBCV-1 in a chlorella-like green alga: Ultrastructural studies. *Virology* **154:**240–245.

Meints, R. H., Burbank, D. E., Van Etten, J. L., and Lamport, D. T. A. (1988). Properties of the chlorella receptor for the virus PBCV-1. *Virology* **164:**15–21.

Moss, B. (1996). Poxviridae: The viruses and their replication. *In* "Fields Virology" (B. N. Fields, D. M. Knipe, P. M. Howley, R. M. Chanock, J. L. Melnick, T. P. Monath, B. Roizman, and S. E. Straus, eds.), pp. 2637–2671. Lippincott-Raven, Philadelphia.

Müller, D. G., Kapp, M., and Knippers, R. (1998). Viruses in marine brown algae. *Adv. Virus Res.* **50:**49–67.

Mushegian, A. R., and Koonin, E. V. (1996). A minimal gene set for cellular life derived by comparison of complete bacterial genomes. *Proc. Natl. Acad. Sci. USA* **93:**10268–10273.

Nandhagopal, N., Simpson, A., Gurnon, J. R., Yan, X., Baker, T. S., Graves, M. V., Van Etten, J. L., and Rossmann, M. G. (2002). The structure and evolution of the major capsid protein of a large, lipid-containing DNA virus. *Proc. Natl. Acad. Sci. USA* **99:**14758–14763.

Nelson, M., Zhang, Y., and Van Etten, J. L. (1993). DNA methyltransferases and DNA site-specific endonucleases encoded by chlorella viruses. *In* "DNA Methylation: Molecular Biology and Biological Significance" (J. P. Jost and H. P. Saluz, eds.), pp. 186–211. Birkhauser Verlag, Basel.

Nelson, M., Burbank, D.E, and Van Etten, J. L. (1998). Chlorella viruses encode multiple DNA methyltransferases. *Biol. Chem.* **379:**423–428.

Nishida, K., Kawasaki, T., Fujie, M., Usami, S., and Yamada, T. (1999a). Aminoacylation of tRNAs encoded by chlorella virus CVK2. *Virology* **263:**220–229.

Nishida, K., Kimura, Y., Kawasaki, T., Fujie, M., and Yamada, T. (1999b). Genetic variation of chlorella viruses: Variable regions localized on the CVK2 genomic DNA. *Virology* **255:**376–384.

Olofsson, S., and Hansen, J. E. S. (1998). Host cell glycosylation of viral glycoproteins ? A battlefield for host defence and viral resistance. *Scand. J. Infect. Dis.* **30:**435–440.

Onimatsu, H., Sugimoto, I., Fujie, M., Usami, S., and Yamada, T. (2004). Vp130, a chloroviral surface protein that interacts with the host *Chlorella* cell wall. *Virology* **319:**71–80.

Pennisi, E. (2004). Evolutionary biology. The birth of the nucleus. *Science* **305:**1641–1644.

Peters, L. L., and Lux, S. E. (1993). Ankyrins: Structure and function in normal cells and hereditary spherocytes. *Semin. Hematol.* **30:**85–118.

Plugge, B., Gazzarrini, S., Nelson, M., Cerana, R., Van Etten, J. L., Derst, C., DiFrancesco, D., Moroni, A., and Thiel, G. (2000). A potassium channel protein encoded by chlorella virus PBCV-1. *Science* **287:**1641–1644.

Raetz, C. R., and Whitfield, C. (2002). Lipopolysaccharide endotoxins. *Annu. Rev. Biochem.* **71:**635–700.

Raoult, D., Audic, S., Robert, C., Abergel, C., Renesto, P., Ogata, H., La Scola, B., Suzan, M., and Claverie, J.-M. (2004). The 1.2-megabase genome sequence of mimivirus. *Science* **306:**1344–1350.

Reisser, W., Burbank, D. E., Meints, S. M., Meints, R. H., Becker, B., and Van Etten, J. L. (1988). A comparison of viruses infecting two different chlorella-like green algae. *Virology* **167:**143–149.

Reisser, W., Burbank, D. E., Meints, R. H., Becker, B., and Van Etten, J. L. (1991). Viruses distinguish symbiotic *Chlorella* spp. of *Paramecium bursaria*. *Endocytobiosis Cell Res.* **7:**245–251.

Reuter, G., and Gabius, H. J. (1999). Eukaryotic glycosylation: Whim of nature or multipurpose tool. *Cell. Mol. Life Sci.* **55:**368–422.

Rohozinski, J., Girton, L. E., and Van Etten, J. L. (1989). Chlorella viruses contain linear nonpermuted double stranded DNA genomes with covalently closed hairpin ends. *Virology* **168:**363–369.

Rosano, C., Zuccotti, S., Sturla, L., Fruscione, F., Tonetti, M., and Bolognesi, M. (2005). Quaternary assembly and crystal structure of GDP-D-mannose 4,6 dehydratase from *Paramecium bursaria* chlorella virus. *Biochem. Biophys. Res. Comm.* **339:**191–195.

Sachs, A. (2000). Cell cycle-dependent translation initiation: IRES elements prevail. *Cell* **101:**243–245.

Sandaa, R. A., Heldal, M., Catsberg, T., Thyrhaug, R., and Bratbak, G. (2001). Isolation and characterization of two viruses with large genome size infecting *Chrysochromulina ericina* (Prymnesiophyceae) and *Pyramimonas orientalis* (Prasinophyceae). *Virology* **290:**272–280.

Schuster, A. M., Girton, L., Burbank, D. E., and Van Etten, J. L. (1986). Infection of a chlorella-like alga with the virus PBCV-1: Transcriptional studies. *Virology* **148:**181–189.

Schuster, A. M., Graves, M., Korth, K., Ziegelbein, M., Brumbaugh, J., Grone, D., and Meints, R. H. (1990). Transcription and sequence studies of a 4.3 kbp fragment from a dsDNA eukaryotic algal virus. *Virology* **176:**515–523.

Senkevich, T. G., White, C. L., Koonin, E. V., and Moss, B. (2000). A viral member of the ERV1/ALR protein family participates in a cytoplasmic pathway of disulfide bond formation. *Proc. Natl. Acad. Sci. USA* **97:**12068–12073.

Shah, R., Coleman, C. S., Mir, K., Baldwin, J., Van Etten, J. L., Grishin, N. V., Pegg, A. E., Stanley, B. A., and Phillips, M. A. (2004). *Paramecium bursaria* chlorella virus-1 encodes an unusual arginine decarboxylase that is a close homolog of eukaryotic ornithine decarboxylases. *J. Biol. Chem.* **279:**35760–35767.

Shchelkunov, S. N., and Totmenin, A. V. (1995). Two types of deletions in orthopoxvirus genomes. *Virus Genes* **9:**231–245.

Simpson, A. A., Nandhagopal, N., Van Etten, J. L., and Rossmann, M. G. (2003). Structural analysis of Phycodnaviridae and Iridoviridae. *Acta Crystallorgr.* **D59:**2053–2959.

Skrdla, M. P., Burbank, D. E., Xia, Y., Meints, R. H., and Van Etten, J. L. (1984). Structural proteins and lipids in a virus, PBCV-1, which replicates in a chlorella-like alga. *Virology* **135:**308–315.

Songsri, P., Hamazaki, T., Ishikawa, Y., and Yamada, T. (1995). Large deletions in the genome of chlorella virus CVK1. *Virology* **214:**405–412.

Songsri, P., Hiramatsu, M., Fujie, M., and Yamada, T. (1997). Proteolytic processing of chlorella virus CVK2 capsid proteins. *Virology* **227:**252–254.

Strasser, P., Zhang, Y. P., Rohozinski, J., and Van Etten, J. L. (1991). The termini of the chlorella virus PBCV-1 genome are identical 2.2-kbp inverted repeats. *Virology* **180:**763–769.

Suda, K., Tanji, Y., Hori, K., and Unno, H. (1999). Evidence for a novel chlorella virus encoded alginate lyase. *FEMS Microbiol. Lett.* **180:**45–53.

Sugimoto, I., Hiramatsu, S., Murakami, D., Fujie, M., Usami, S., and Yamada, T. (2000). Algal-lytic activities encoded by chlorella virus CVK2. *Virology* **277:**119–126.

Sugimoto, I., Onimatsu, H., Fujie, M., Usami, S., and Yamada, T. (2004). vAL-1, a novel polysaccharide lyase encoded by chlorovirus CVK2. *FEBS Lett.* **559:**51–56.

Sun, L., Adams, B., Gurnon, J. R., Ye, Y., and Van Etten, J. L. (1999). Characterization of two chitinase genes and one chitosanase gene encoded by chlorella virus PBCV-1. *Virology* **263:**376–387.

Sun, L., Gurnon, J. R., Adams, B. J., Graves, M. V., and Van Etten, J. L. (2000). Characterization of a ß-1,3-glucanase encoded by chlorella virus PBCV-1. *Virology* **276:**27–36.

Suttle, C. A. (2000). Ecological, evolutionary, and geochemical consequences of viral infection of cyanobacteria and eukaryotic algae. *In* "Viral Ecology" (C. Hurst, ed.), pp. 247–296. Academic Press, New York.

Suttle, C. A. (2005). Viruses in the sea. *Nature* **437:**356–361.

Takeda, H. (1988). Classification of *Chlorella* strains by cell wall sugar composition. *Phytochemistry* **27:**3822–3826.

Takeda, H. (1995). Cell wall composition and taxonomy of symbiotic chlorella from paramecium and acanthocystis. *Phytochemistry* **40:**457–459.

Tanner, N. K., and Linder, P. (2001). DexD/H box RNA helicases: From generic motors to specific dissociation functions. *Mol. Cell* **8:**251–262.

Tonetti, M., Zanardi, D., Gurnon, J. R., Fruscione, F., Armirotti, A., Damonte, G., Sturla, L., De Flora, A., and Van Etten, J. L. (2003). Chlorella virus PBCV-1 encodes two enzymes involved in the biosynthesis of GDP-L-frucose and GDP-D-rhamnose. *J. Biol. Chem.* **278:**21559–21565.

Turner, P. C., and Moyer, R. W. (1990). The molecular pathogenesis of poxviruses. *Curr. Top. Microbiol. Immunol.* **163:**125–151.

Tyson, G. W., Chapman, J., Hugenholtz, P., Allen, E. E., Ram, R. J., Richardson, R. M., Solovyev, V. V., Rubin, E. M., Rokhsar, D. S., and Banfield, J. F. (2004). Community structure and metabolism through reconstruction of microbial genomes from the environment. *Nature* **428:**37–43.

Van Etten, J. L. (2003). Unusual life style of giant chlorella viruses. *Annu. Rev. Genet.* **37:**153–195.

Van Etten, J. L., and Meints, R. H. (1999). Giant viruses infecting algae. *Ann. Rev. Microbiol.* **53:**447–494.

Van Etten, J. L., Meints, R. H., Burbank, D. E., Kuczmarski, D., Cuppels, D. A., and Lane, L. C. (1981). Isolation and characterization of a virus from the intracellular green alga symbiotic with *Hydra viridis*. *Virology* **113:**704–711.

Van Etten, J. L., Meints, R. H., Kuczmarski, D., Burbank, D. E., and Lee, K. (1982). Viruses of symbiotic chlorella-like algae isolated from *Paramecium bursaria* and *Hydra viridis*. *Proc. Natl. Acad. Sci. USA* **79:**3867–3871.

Van Etten, J. L., Burbank, D. E., Kuczmarski, D., and Meints, R. H. (1983). Virus infection of culturable chlorella-like algae and development of a plaque assay. *Science* **219:**994–996.

Van Etten, J. L., Burbank, D. E., Xia, Y., and Meints, R. H. (1983). Growth cycle of a virus, PBCV-1, that infects chlorella-like algae. *Virology* **126:**117–125.

Van Etten, J. L., Burbank, D. E., Joshi, J., and Meints, R. H. (1984). DNA synthesis in a chlorella-like alga following infection with the virus PBCV-1. *Virology* **134:**443–449.

Van Etten, J. L., Burbank, D. E., Schuster, A. M., and Meints, R. H. (1985). Lytic viruses infecting a chlorella-like alga. *Virology* **140:**135–143.

Van Etten, J. L., Schuster, A. M., Girton, L., Burbank, D. E., Swinton, D., and Hattman, S. (1985). DNA methylation of viruses infecting a eukaryotic chlorella-like green alga. *Nucleic Acids Res.* **13:**3471–3478.

Van Etten, J. L., Burbank, D. E., and Meints, R. H. (1986). Replication of the algal virus PBCV-1 in UV-irradiated chlorella. *Intervirology* **26:**115–120.

Van Etten, J. L., Lane, L. C., and Meints, R. H. (1991). Viruses and virus like particles of eukaryotic algae. *Microbiol. Rev.* **55:**586–620.

Van Etten, J. L., Graves, M. V., Muller, D. G., Boland, W., and Delaroque, N. (2002). *Phycodnaviridae* — large DNA algal viruses. *Arch. Virol.* **147:**1479–1516.

Venter, J. C., Remington, K., Heidelberg, J. F., Halpern, A. L., Rusch, D., Eisen, J. E., Wu, D., Paulsen, I., Nelson, K. E., Nelson, W., Fouts, D. E., Levy, S. *et al.* (2004). Environmental genome shotgun sequencing of the Sargasso Sea. *Science* **304:**66–74.

Villarreal, L. P. (2005). *In* "Viruses and the Evolution of Life," p. 395. American Society of Microbiology Press, Washington D.C.

Villarreal, L. P., and DeFilippis, V. R. (2000). A hypothesis for DNA viruses as the origin of eukaryotic replication proteins. *J. Virol.* **74:**7079–7084.

Wang, I.-N., Li, Y., Que, Q., Bhattacharya, M., Lane, L. C., Chaney, W. G., and Van Etten, J. L. (1993). Evidence for virus-encoded glycosylation specificity. *Proc. Natl. Acad. Sci. USA* **90:**3840–3844.

Waters, E., Hohn, M. J., Ahel, I., Graham, D. E., Adams, M. D., Barnstead, M., Beeson, K. Y., Bibbs, L., Bolanos, R., Keller, M., Kretz, K., Lin, X. *et al.* (2003). The genome of *Nanoarchaeum equitans*: Insights into early archaeal evolution and derived parasitism. *Proc. Natl. Acad. Sci. USA* **100:**12984–12988.

Wilson, W. H., Schroeder, D. C., Allen, M. J., Holden, M. T., Parkhill, J., Barrell, B. G., Churcher, C., Hamlin, N., Mungall, K., Norbertczak, H., Quail, M. A., Price, C. *et al.* (2005a). Complete genome sequence and lytic phase transcription profile of a Coccolithovirus. *Science* **309:**1090–1092.

Wilson, W. H., Van Etten, J. L., Schroeder, D. S., Nagasaki, K., Burssaard, C., Delaroque, N., Bratbak, G., and Suttle, C. (2005b). Phycodnaviridae. *In* "Virus Taxonomy, VIIIth Report of the ICTV" (C. M. Fauquet, M. A. Mayo, J. Maniloff, U. Desselberger, and L. A. Ball, eds.), pp. 163–175. Elsevier/Academis Press, London.

Wolf, S., Maier, I., Katsaros, C., and Müller, D. G. (1998). Virus assembly in *Hincksia hincksiae* (Ecocarpales, Phaeophyceae). An electron and fluorescence microscopic study. *Protoplasma* **203:**153–167.

Wommack, K. E., and Colwell, R. R. (2000). Virioplankton: Viruses in aquatic ecosystems. *Microbiol. Mol. Biol. Revs.* **64:**69–114.

Yamada, T., and Higashiyama, T. (1993). Characterization of the terminal inverted repeats and their neighboring tantem repeats in the chlorella CVK1 virus genome. *Mol. Gen. Genet.* **241:**554–563.

Yamada, T., and Kawasaki, T. (2005). Microbial synthesis of hyaluronan and chitin: New approaches. *J. Biosci. Bioeng.* **99:**521–528.

Yamada, T., and Sakaguchi, K. (1982). Comparative studies on chlorella cell walls: Induction of protoplast formation. *Arch. Microbiol.* **132:**10–13.

Yamada, T., Higashiyama, T., and Fukuda, T. (1991). Screening of natural waters for viruses which infect chlorella cells. *Appl. Environ. Microbiol.* **57:**3433–3437.

Yamada, T., Fukuda, T., Tamura, K., Furukawa, S., and Songsri, P. (1993). Expression of the gene encoding a translational elongation factor 3 homolog of chlorella virus CVK2. *Virology* **97:**742–750.

Yamada, T., Tamura, K., Aimi, T., and Songsri, P. (1994). Self-splicing group I introns in eukaryotic viruses. *Nucleic Acids Res.* **22:**2532–2537.

Yamada, T., Furukawa, S., Hamazaki, T., and Songsri, P. (1996). Characterization of DNA-binding proteins and protein kinase activities in chlorella virus CVK2. *Virology* **219:**395–406.

Yamada, T., Hiramatsu, S., Songsri, P., and Fujie, M. (1997). Alternative expression of a chitosanase gene produces two different proteins in cells infected with chlorella virus CVK2. *Virology* **230:**361–368.

Yamada, T., Chuchird, N., Kawasaki, T., Nishida, K., and Hiramatsu, S. (1999). *Chlorella* virus as a source of novel enzymes. *J. Biosci. Bioeng.* **88:**353–361.

Yan, X., Olson, N. H., VanEtten, J. L., Bergoin, M., Rossmann, M. G., and Baker, T. S. (2000). Structure and assembly of large, lipid-containing, dsDNA viruses. *Nat. Struct. Biol.* **7:**101–103.

Yanez, R. J., Rodriguez, J. M., Nogal, M. L., Yuste, L., Enriquez, C., Rodriguez, J. F., and Vinuela, E. (1995). Anaylsis of the complete nucleotide sequence of African swine fever virus. *Virology* **208:** 249–278.

Yonker, C. R., Caldwell, K. D., Giddings, J. C., and Van Etten, J. L. (1985). Physical characterization of PBCV virus by sedimentation field flow fractionation. *J. Virol. Methods* **11:**145–160.

Yoon, H. S., Hackett, J. D., Cinigliz, C., Pinto, G., and Bhattacharya, D. (2004). A molecular timeline for the origin of photosynthetic eukaryotes. *Mol. Biol. Evol.* **21:**809–818.

Zhang, Y., Burbank, D. E., and Van Etten, J. L. (1988). Chlorella viruses isolated in China. *Appl. Environ. Microbiol.* **54:**2170–2173.

Zhang, Y., Strasser, P., Grabherr, R., and Van Etten, J. L. (1994). Hairpin loop structure at the termini of the chlorella virus PBCV-1 genome. *Virology* **202:**1079–1082.

Zhang, Y., Adams, B., Sun, L., Burbank, D. E., and Van Etten, J. L. (2001). Intron conservation in the DNA polymerase gene encoded by chlorella viruses. *Virology* **285:**313–321.

Zhang, Y., Calin-Jageman, I., Gurnon, J. R., Choi, T.-J., Adams, B., Nicholson, A. W., and Van Etten, J. L. (2003). Characterization of a chlorella virus PBCV-1 encoded ribonuclease III. *Virology* **317:**73–83.

ADVANCES IN VIRUS RESEARCH, VOL 66

MESSENGER RNA TURNOVER AND ITS REGULATION IN HERPESVIRAL INFECTION

Britt A. Glaunsinger and Donald E. Ganem

Howard Hughes Medical Institute, Departments of Microbiology and Medicine
University of California, San Francisco, California 94143

ABSTRACT

The ability to regulate cellular gene expression is a key aspect of the lifecycles of a diverse array of viruses. In fact, viral infection often results in a global shutoff of host cellular gene expression; such inhibition serves not only to ensure maximal viral gene expression without competition from the host for essential machinery and substrates but also aids in evasion of immune responses detrimental to successful viral replication and dissemination. Within the herpesvirus family, host shutoff is a prominent feature of both the α- and γ-herpesviruses. Intriguingly, while both classes of herpesviruses block cellular gene expression by inducing decay of messenger RNAs, the viral factors responsible for this phenotype as well as the mechanisms by which it

0065-3527/06 $35.00
DOI: 10.1016/S0065-3527(06)66007-7

is achieved are quite distinct. However, data suggest that the host shutoff functions of α- and γ-herpesviruses are likely achieved both through the activity of virally encoded nucleases as well as via modulation of cellular RNA degradation pathways. This review highlights the processes governing normal cellular messenger RNA decay and then details the mechanisms by which herpesviruses promote accelerated RNA turnover. Parallels between the viral and cellular degradation systems as well as the known interactions between viral host shutoff factors and the cellular RNA turnover machinery are highlighted.

I. Introduction

In eukaryotic gene expression, many factors influence the levels of individual mRNAs creating a controlled environment that permits continuous expression of certain transcripts while allowing the expression of others to occur only at specified times. While discussion of this regulation once focused exclusively on transcriptional regulation, the important role of posttranscriptional controls in the regulation of gene expression is now widely accepted. A central pillar in the edifice of posttranscriptional regulation is the control of mRNA stability, which is governed by a complex and sophisticated machinery that acts via several different biochemical pathways. Given the importance of this regulation for cells to function appropriately under "normal" and stressful conditions, it is not surprising that several viruses have evolved means to modulate this cellular regulatory system to facilitate their own replication and immune evasion strategies.

The first portion of this review will focus on our current understanding of regulated mRNA turnover in mammalian cells. We will then detail how various members of the herpesvirus family promote widespread turnover of cellular mRNA, both via the action of virally encoded ribonucleases and through the presumed deregulation of cellular mRNA turnover pathways.

II. Regulation of Cytoplasmic mRNA Turnover in Mammalian Cells

A. Overview

The lion's share of our current knowledge of eukaryotic mRNA turnover comes from extensive research in yeast, although the last several years have shown a significant increase in the identification

and characterization of the parallel pathways in mammalian cells. Eukaryotic mRNA molecules are protected at their 5′ end by the presence of a m^7GpppN cap and at their 3′ end by a poly(A) tail. Each of these structures is in turn bound by several cellular proteins that contribute to mRNA stability and translation; a cap-binding complex includes the cap-associated eIF4E, which in turn associates with the translation initiation factor eIF4G; the poly(A) tail is protected by the poly A binding protein (PABP). PABP also interacts with eIF4G, effectively circularizing the mRNA and further protecting the ends from exonucleolytic attack (Munroe and Jacobson, 1990; Wells *et al*., 1998). Events that disrupt these stabilizing interactions, such as (1) translation or (2) recruitment of specific RNA binding proteins to messages with instability elements (see later) trigger degradation of the mRNAs. Thus, protein complexes engaged by the mRNA termini are essential for the control of message fate in cells.

In yeast, normal cellular mRNA decay initiates with the removal of the poly(A) tail by deadenylation enzymes in what is often the rate-limiting step of the turnover (Meyer *et al.*, 2004; Parker and Song, 2004; Wilusz *et al.*, 2001). Cellular decapping enzymes (including Dcp1/Dcp2 and the Lsm complex) then remove the 5′ m^7GpppN cap, thereby permitting access of the 5′ end of the RNA to the Xrn1p 5′–3′ ribonuclease that degrades the body of the message. In addition, yeast also possess a secondary pathway that promotes degradation in the 3′–5′ direction by the yeast exosome, an enzymatic complex that includes numerous 3′–5′ RNases, as well as additional proteins involved in RNA binding and helicase activity (Raijmakers *et al.*, 2004). Many of these RNA degradation components have been shown to localize within discreet cytoplasmic foci termed P bodies or cytoplasmic bodies, suggesting that these may represent sites of mRNA turnover in cells (Sheth and Parker, 2003).

Turnover of mRNA in mammalian cells appears to proceed similarly to yeast, in that it involves deadenylation, decapping, and exonucleolytic decay (Fig. 1). Many of the mammalian mRNA degradation components were identified based on homology to their yeast counterparts. However, a key difference between mammalian and yeast turnover lies in the relative importance of the 5′–3′ and 3′–5′ exonucleolytic decay pathways; in mammalian cells, the exosome-mediated 3′–5′ pathway appears to predominate. However, the majority of evidence supporting this view has been acquired via *in vitro* studies, and it is not unlikely that this view may undergo revision in the future. For example, there does exist a mammalian homolog of the 5′–3′ Xrn1 RNase, a strong indication that this pathway likely plays some role in mammalian

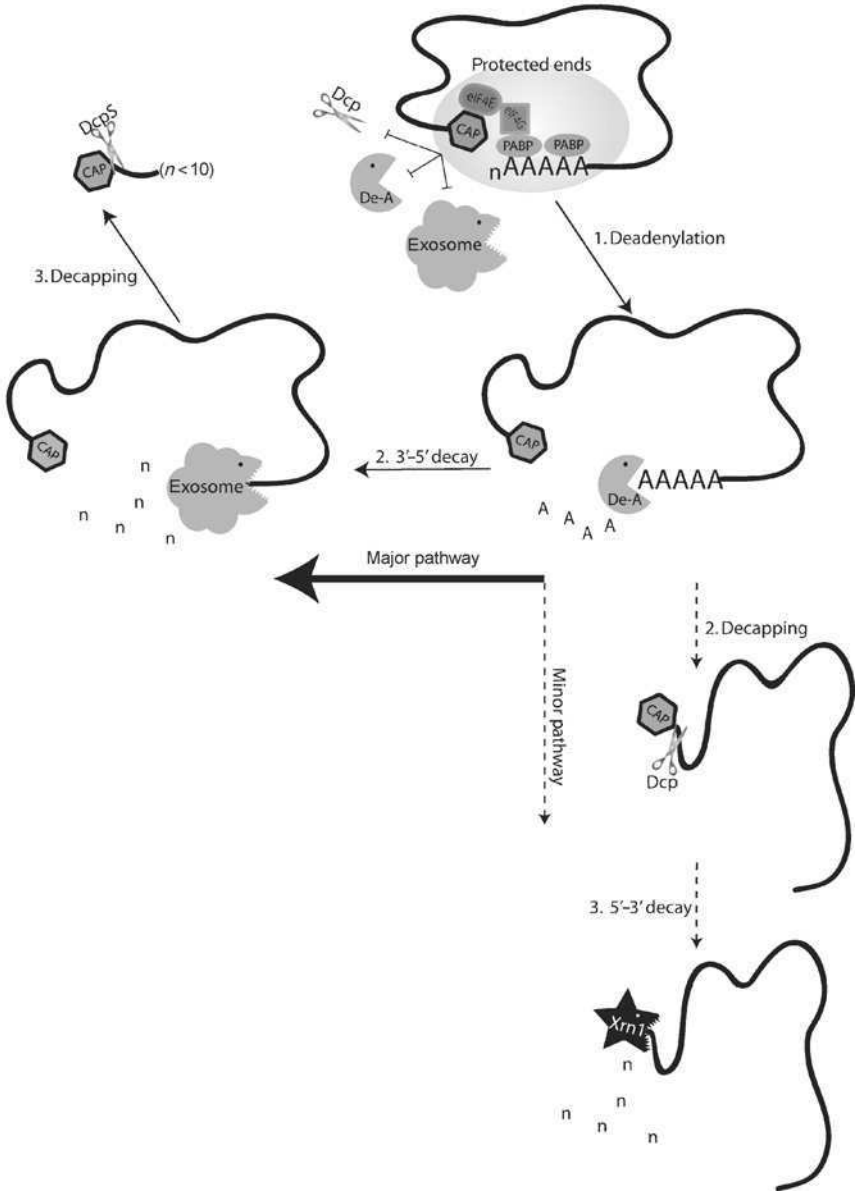

FIG 1. Pathways of mammalian mRNA turnover. The 3′ and 5′ ends of mRNAs are normally protected via their interactions with PABP and the cap-binding complex. However, events that disrupt these associations lead to exposure of the ends to cellular exonucleases. The first step of mammalian mRNA turnover involves deadenylation of the

systems as well (Bashkirov *et al*., 1997; Meyer *et al.*, 2004). Nearly all of these factors have roles in both the nucleus and the cytoplasm, although the mRNA turnover function correlates primarily with their cytoplasmic localization. Several mRNA degradation enzymes, as well as the cap binding protein eIF4E, have been shown to colocalize with the RNA binding protein GW182 in cytoplasmic bodies (also called P bodies, GW bodies); it is postulated that these sites represent domains of posttranslational mRNA decay (Andrei *et al*., 2005; Cougot *et al.*, 2004; Eystathioy *et al*., 2002, 2003; Ingelfinger *et al*., 2002; van Dijk *et al*., 2002). As the majority of regulated cellular mRNA turnover occurs in the cytoplasm of cells, this review will focus on the cytoplasmic pathways and their control. The following sections will describe the current state of knowledge regarding each stage of regulated mammalian mRNA turnover.

B. Deadenylation

Shyu *et al*. (1991) used transcriptional pulse-chase experiments to show that deadenylation of the c-fos mRNA occurred prior to degradation of the body of the message. Couttet *et al*. (1997) subsequently measured a variety of liver mRNA poly(A) tail lengths using an RT-PCR approach and confirmed that shortening of mammalian mRNA poly(A) tails from 100 to 300 nucleotides (nt) to approximately 30–60 nt precedes decapping and decay of the remainder of the message. It is now established that deadenylation represents the first step of cytoplasmic mRNA turnover. Several deadenylases have been identified in mammals: poly(A)-specific exoribonuclease (PARN, previously called DAN), the CCR4-NOT complex, the poly(A) nuclease complex (hPan2/Pan3), and nocturnin.

PARN, the best characterized deadenylase in mammalian cells, was originally identified as a deadenylating activity in HeLa cell extracts (Astrom *et al.*, 1991) and was subsequently purified to homogeneity from calf thymus (Korner and Wahle, 1997; Martinez *et al*., 2000). PARN exists as a homo-oligomer (perhaps trimer) that specifically degrades poly(A) located at the 3′ end of messages in a processive

poly(A) tail by deadenylases such as PARN or hPan. The majority of deadenylated RNAs then undergo 3′–5′ degradation by the exosome, followed by cap removal by the scavenger decapping enzyme DcpS. Alternatively, rather than undergoing exosomal decay, some deadenylated RNAs are first decapped by the Dcp1/2 decapping complex (assisted by the Lsm proteins; not shown) then degraded in a 5′–3′ manner by the Xrn1 nuclease.

manner is dependent on divalent cations (preferably Mg^{2+}) and is inhibited by the presence of PABP on the poly(A) tail (Ford *et al.*, 1997; Martinez *et al.*, 2000). The human PARN cDNA was shown to exhibit homology to RNase D-like enzymes of the DEDD superfamily family of 3′ RNA and DNA exonucleases, and site-directed mutational analyses confirmed that four conserved amino acids in PARN aligning with the RNase D motifs involved in catalysis (Asp-28, Glu-30, Asp-292, Asp-382) are essential for PARN activity via binding of divalent metal ions (Korner *et al.*, 1998; Ren *et al.*, 2002, 2004). Western blots and immunofluorescence assays demonstrate that, in HeLa cells, PARN is a predominantly cytoplasmic protein of approximately 75 kDa. PARN appears to have homologs in a diverse range of organisms including plants and *Caenorhabditis elegans* but not in yeast. The development of a HeLa S100-based *in vitro* degradation system that faithfully reproduced regulated mRNA turnover (Ford and Wilusz, 1999) facilitated subsequent analyses of the mechanism of PARN activity at the molecular level. The observation that immunodepletion of PARN from HeLa extracts greatly reduced deadenylation of substrate RNAs suggested that PARN represented the major deadenylase, at least *in vitro* (Gao *et al.*, 2000). Significantly, in HeLa and *Xenopus* oocyte extracts, PARN also associates with the 5′ cap on mRNAs in a manner that is blocked by eIF4E and stimulated by the poly(A) tail, and this interaction enhances its deadenylation activity (Dehlin *et al.*, 2000; Gao *et al.*, 2000). Thus, PARN appears to interact simultaneously with both the 5′ and 3′ ends of mRNA. Martinez *et al.* (2001) demonstrated that PARN activity is stimulated by cap structures provided in *cis* (attached to the 5′ end of the mRNA) or in *trans* at low concentrations, but it is inhibited by high concentrations of cap analog added in *trans* (Martinez *et al.*, 2001). They propose a model whereby trimeric PARN associates with the poly(A) tail and one subunit also binds the 5′ cap; following that interaction, a conformational change in that subunit which would serve to activate the remaining two subunits and enhance the processivity of the enzyme. Low concentrations of cap analog could stimulate the enzyme by helping recruit PARN to uncapped messages, whereas high concentrations might inhibit it by either inactivating or blocking necessary interactions of the other subunits (Martinez *et al.*, 2001).

Collectively, these observations suggest that the 5′ and 3′ terminal interactions of a translatable mRNA protect the message from PARN-induced deadenylation; however, disruption of these associations, for example, during the process of ribosome scanning and translation, permits PARN access to the message. Additionally, PARN-mediated

deadenylation can occur in a translation-independent manner during decay of mRNAs containing destabilizing elements in their coding region or 3′ untranslated regions (UTRs), as discussed in a subsequent section of this review. It is important to note that the contribution of PARN to *in vivo* mRNA turnover has yet to be confirmed in mammalian cells. However, Seal *et al*. (2005) have shown that serum deprivation of human liver Hep G2 cells results in enhanced mRNA turnover that correlates with a decrease in cap-associated eIF4E and an increase in cap binding by PARN. Furthermore, they demonstrate that under these conditions PARN phosphorylation is increased whereas phosphorylation of the cellular cap binding proteins was diminished; thus, PARN-mediated deadenylation in mammalian cells may be regulated, at least in part, by this posttranslational modification.

The major deadenylase in yeast is the CCR4-NOT complex, a group of proteins including Ccr4p, Pop2p/Caf1p, Caf40p, Caf130p, and Not1-5p that were originally identified as transcriptional repressors (Chen *et al*., 2001b; Collart, 2003). The Ccr4p component of the complex exhibits homology to *Escherichia coli* exonuclease III and the Pop2p/Caf1p subunit is a member of the RNase D-like DEDD family of nucleases. Yeast deletion mutants lacking Ccr4p, Pop2/Caf1p, or Not2, -3, -4, or -5 exhibit a deadenylation defect phenotype, suggesting that these are all important for the *in vivo* function of the complex (Meyer *et al.*, 2004). This deadenylase appears to be inhibited by Pab1p in yeast, similar to mammalian PARN (Tucker *et al*., 2002). Human homologs of the CCR4-NOT complex have been identified and appear to be ubiquitously expressed in human tissues (Albert *et al*., 2000). The ability of hNot3 and hNot4 to partially complement yeast Not3/4 mutants suggests that these enzymes are functionally conserved. Furthermore, recombinant human Caf1 and Pop2 purified from *E. coli* exhibit *in vitro* deadenylase activity and have been shown to interact with Ccr4 family members (Bianchin *et al*., 2005; Dupressoir *et al*., 2001). Significantly, experiments using small interfering RNAs (siRNAs) to knock down Ccr4 in NIH 3T3 cells have shown that in the absence of this factor deadenylation of c-fos reporter mRNAs in cells occurs with reduced rate (Yamashita *et al*., 2005). Thus, the available data are consistent with the idea that these deadenylases retain some functional similarities to their yeast counterparts and additionally may play a prominent role in mammalian mRNA turnover.

The human cytoplasmic poly(A) nuclease complex (hPan) was identified based on its homology to the yeast Pan deadenylase (Uchida *et al.*, 2004). As in yeast, hPan is composed of two proteins, the hPan2 catalytic subunit and the hPan3 regulatory subunit. hPan2

is an Mg^{2+}-dependent 3′–5′ distributive exonuclease with homology to RNase D; mutation of a conserved residue in the hPan2 RNase D catalytic domain abrogated its nuclease activity *in vitro*. In contrast to the other eukaryotic deadenylases, in yeast Pan activity is stimulated rather than repressed by Pab1p (Sachs and Deardorff, 1992). This is believed to play a role in its putative function in the shortening or trimming of poly(A) tails just after their synthesis (Brown *et al*., 1996). In accord with its activity in yeast, hPan3 has been shown to directly bind PABP in a manner that stimulates the activity of the hPan enzyme. Substrates from which PABP had been immunodepleted were degraded with significantly reduced efficiency, although they were rapidly deadenylated upon addition of recombinant PABP in an hPan3-dependent manner (Uchida *et al.*, 2004). The fact that Pan activity is enhanced by the presence of PABP and does not require the presence of a 5′ cap suggests that this enzyme may be able to promote deadenylation during or prior to translation (Uchida *et al.*, 2004).

The most recently identified mammalian deadenylase is nocturnin, a Ccr4 homolog located in the photoreceptor cells of *Xenopus laevis*, where it is specifically expressed at night and contributes to the regulation of circadian rhythm (Baggs and Green, 2003; Chen *et al.*, 2002; Green and Besharse, 1996). As with PARN, no nocturnin orthologs have been found in yeast, although murine nocturnin was shown to be expressed in a circadian pattern in numerous mouse tissues (Wang *et al*., 2001).

Why would a cell require multiple independent enzymes to perform a single function? Although the answer to this question is not really known, it is postulated that the multitude of deadenylases allows for multiple tiers of regulation. Since deadenylation is the first and likely rate-limiting step of turnover, it makes sense that the cell would impose layers of redundancy to ensure timely and accurate deadenylase activity and fine-tuning of its regulation.

C. 3′–5′ Decay by the Exosome

After deadenylation, the bulk of the mRNA body is degraded in a 3′–5′ manner by the mammalian exosome. The exosome is a multienzyme complex present in all eukaryotes that has both nuclear and cytoplasmic functions. While the nuclear exosome functions in processing rRNAs, snRNAs, and snoRNAs as well as digests improperly processed pre-mRNAs (Butler, 2002), the cytoplasmic exosome is involved in mRNA turnover (Raijmakers *et al.*, 2004). In agreement with these functions, the exosome is localized to the cytoplasm, nucleoplasm, and nucleolus. It is assumed to be assembled in the cytoplasm and subsequently

transported into the necessary nuclear compartments, an event perhaps mediated by the putative nuclear localization signals located on the PM/Scl-100, Rrp41p, and PM/Scl-75 subunits (Raijmakers *et al*., 2003, 2004). The events dictating how the fully or partially assembled exosomes are parceled to a specific nuclear compartment or retained in the cytoplasm are not yet known.

The core of the human exosome is composed of nine proteins that can be grouped into two basic subunit types: (1) those with sequence similarity to the RNase PH domains of *E. coli* polynucleotide phosphorylase (PNPase) (Rrp41, Rrp42, Rrp46, PM/Scl-75, Mtr3, OIP2/Rrp43); and (2) those with S1/KH RNA binding domains (Rrp4, Rrp40, Csl4) (Allmang *et al*., 1999; Chen *et al*., 2001a; Mitchell *et al*., 1997). The complex also associates with several accessory factors, including the RNA helicase hSki2w, MPP6, which is a protein of unknown function that is phosphorylated during mitosis, and PM/Scl-100, a protein with homology to RNase D (Chen *et al*., 2001a; Matsumoto-Taniura *et al*., 1996). In humans, the exosome was originally identified as a group of proteins that coprecipitate with PM/Scl-75 and PM/Scl-100, antigens to which patients with the autoimmune disease polymyositis-scleroderma overlap syndrome (PM/Scl) develop autoantibodies (Alderuccio *et al.*, 1991; Ge *et al*., 1992; Gelpi *et al*., 1990; Reimer, 1990). These factors were later discovered to be the human counterparts to the yeast exosome components (Allmang *et al*., 1999; Brouwer *et al*., 2001).

Prokaryotic PNPase, which forms the core of the degradosome (the prokaryotic counterpart to the exosome), is composed of amino- and carboxyl-terminal RNase PH domains and forms a "trimer of dimers" core ring structure with a central channel believed to accommodate the RNA substrate (Symmons *et al*., 2002). The fact that the eukaryotic exosome contains six RNase PH domain-containing subunits has lead to the hypothesis that it forms a similar hexameric ring core structure (Fig. 2). Several lines of evidence support this notion; extensive yeast and mammalian 2-hybrid analyses of interactions between all known human exosomal proteins showed that these six subunits associate with each other in an unambiguous order that is further bolstered by data from the crystallization of the archaeal exosome core (Lehner and Sanderson, 2004; Lorentzen *et al*., 2005; Raijmakers *et al*., 2002). These components all exhibit sequence homology to known 3′–5′ exonucleases, and several (e.g., hRrp46, PM/Scl-75, OIP2) have had nuclease activity experimentally demonstrated. Of this group of core components, human Rrp41 and Rrp44 can complement the corresponding yeast mutants suggesting functional conservation (Brouwer *et al*., 2001; Estevez *et al.*, 2001; Mitchell *et al*., 1997; Shiomi *et al*., 1998).

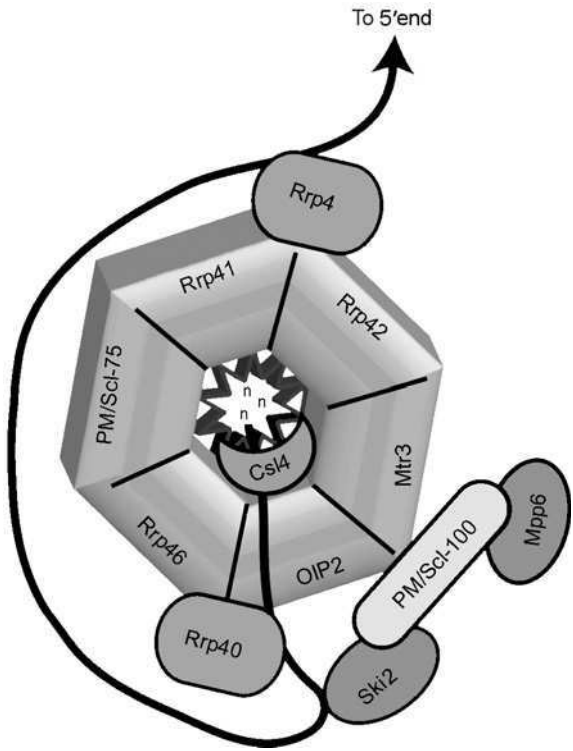

FIG 2. The mammalian exosome. The core of the exosome is composed of six ribonuclease subunits (Rrp41, Rrp42, Mtr3, OIP2, Rrp46, and PM/Scl-75) believed to associate in a ring-like structure with a central core to accomodate the mRNA, similar to the prokaryotic PNPase. It is also bound by three proteins with S1/KH RNA binding domains (Rrp4, Rrp40, and Csl4) that are likely involved in recognition of the mRNA substrate, as well as several accessory factors (e.g., Ski2, PM/Scl-100, Mpp6).

As mentioned earlier, the mammalian exosome is also composed of three core proteins (Rrp4, Rrp40, and Csl4) with homology to the ribosomal S1/KH RNA binding domain. These factors have each been shown to interact with specific RNase PH domain subunits and are proposed to be located on the outer surface of the core hexameric ring (Lehner and Sanderson, 2004; Raijmakers *et al*., 2002). Thus, they may have a role in RNA substrate recognition whereas the other six main subunits would encompass the enzymatic core. It is notable that, at least in yeast, inactivation of individual exosomal subunits of both types (with RNase PH domains or with S1/KH RNA binding domains)

inhibits both the nuclear and cytoplasmic functions of the exosome. This suggests that all the subunits are required to form one active enzymatic complex in cells, rather than the enzymes functioning individually on the substrate RNAs (Allmang *et al*., 1999; Anderson and Parker, 1998; Mitchell *et al*., 1997). Thus, although individual recombinant yeast exosome components are quite active as nucleases *in vitro*, the RNase function of the exosome complex purified from yeast is diminished (Mitchell *et al*., 1997). This suggests that the accessory factors present in cells but not associated with the purified exosome are required for *in vivo* activity of the multienzyme complex (Mitchell and Tollervey, 2000).

D. Decapping and 5′–3′ Exoribonucleolytic Decay

Wang and Kiledjian (2001) identified a novel scavenger decapping activity (DcpS) in HeLa cell extracts that followed 3′–5′ exosomal decay. DcpS, which represents a major decapping pathway in mammals, is a pyrophosphatase that releases m^7GMP upon cap cleavage. Purified DcpS was shown to be a 40 kDa protein with a histidine triad (HIT) pyrophosphatase motif found in nucleotide binding proteins that hydrolize pyrophosphate bonds (Liu *et al*., 2002). Mutations within this motif inactivate DcpS, indicating its importance in DcpS catalytic function. DcpS shows a strong preference for hydrolyzing free cap analog or caps attached to RNAs less than 10 nt in length (e.g., products created by 3′–5′ exosomal decay); in fact, DcpS has been shown to associate with the exosome in co-immunoprecipitation experiments (Wang and Kiledjian, 2001). The amino terminus of the protein has been demonstrated to be involved in cap binding, and analogous to its catalytic activity DcpS associates with free cap much more efficiently than longer capped mRNAs (Liu *et al*., 2004b). Crystallization of DcpS, revealed it to be an asymmetrical dimer that shifts between an open (inactive) or closed (active) structure upon a 30 Å conformational change (Chen *et al*., 2005; Gu *et al*., 2004). Based on its structure, it has been proposed that the reason DcpS binds longer capped mRNAs so inefficiently is related to the increased entropy present on larger RNA molecules that could block cap binding or prevent the enzyme from adopting the active closed structure (Gu *et al*., 2004). DcpS is able to effectively compete with eIF4E for binding of free cap but not capped mRNA, suggesting a cellular mechanism to prevent eIF4E sequestration by degraded mRNAs (Liu *et al*., 2004b). Although hydrolysis of normal mRNA cap structure following exosomal decay occurs in the cytoplasm, a significant fraction of DcpS resides in the nucleus, suggesting additional roles

for this enzyme perhaps in the decapping of aberrant transcripts degraded prior to nuclear export (Liu *et al.*, 2004b).

As mentioned earlier, after deadenylation the major decay pathway in yeast is decapping followed by 5′–3′ turnover mediated by the Xrn1 ribonuclease. A mammalian Xrn1 homolog has been cloned and although its activity has been detected in cell extracts this appears to be a less important pathway in mammalian cells (Bashkirov *et al.*, 1997; Gao *et al.*, 2001; van Dijk *et al.*, 2003; Wang and Kiledjian, 2001). The presence of Xrn1 in mammalian P bodies may suggest, however, that this enzyme is involved in mRNA decay at these sites (Kedersha *et al.*, 2005). In HeLa cell extracts, the deadenylation-dependent decapping activity mimicked that in yeast, in that it was regulated by both cap binding proteins and repressed by PABP, and yielded m^7GDP product (distinct from the m^7GMP product of DcpS) (Gao *et al.*, 2001).

Mammalian homologs to the yeast deadenylation-dependent decapping enzymes Dcp1 and Dcp2 (hDcp1a, hDcp1b, and hDcp2) were cloned in 2002 and, analogous to their yeast counterparts, hDcp1a and hDcp2 were shown to interact to form a functional enzyme localized to the cytoplasm of cells (Lykke-Andersen, 2002; Wang *et al.*, 2002). hDcp1b appears to be expressed at much lower levels and its role in this decapping complex is not yet clear. hDcp2, the catalytic subunit, possesses a nucleotide diphosphate linked to X moiety (NUDIX) pyrophosphatase motif that mutational analysis has shown to be essential for its activity. In contrast to DcpS, hDcp2 cannot hydrolize free cap but instead acts on capped deadenylated mRNAs targeted for degradation by the 5′–3′ decay system (Piccirillo *et al.*, 2003). hDcp2 activity is inhibited by PABP, which has been shown to bind directly to the cap of mRNAs (but not free cap) after eIF4E removal (Khanna and Kiledjian, 2004). hDcp1a (also called SMIF) is believed to play more of a regulatory role, although it has also been shown to bind Smad4 and transloctate to the nucleus upon TGFβ stimulation and is thus possibly involved in modulating multiple cellular pathways (Bai *et al.*, 2002). The events dictating whether an mRNA is degraded by the exosome followed by DcpS-mediated decapping or instead first decapped by hDcp1a/Dcp2 then turned over by hXrn1 have yet to be revealed.

E. Endoribonucleolytic Decay

In *E. coli*, the major mRNA turnover pathways initiate with endoribonucleolytic cleavage that involves the recognition of sequence or structural elements within the target mRNA (Kushner, 2004). Endonuclease-mediated decay also plays an important role in the turn-

over of many eukaryotic messages, particularly those whose expression is regulated by extracellular and/or developmental stimuli. For example, this type of turnover is involved in the stability of apolipoprotein II (Binder *et al*., 1989), groα (Stoeckle, 1992), maternal homeodomain proteins (Brown and Harland, 1990; Brown *et al.*, 1993), albumin (Pastori *et al.*, 1991b), transferrin receptor (Tf R) (Binder *et al*., 1994), IGF II (Meinsma *et al*., 1991; Scheper *et al*., 1995), c-myc (Ioannidis *et al*., 1996; Lee *et al.*, 1998), and the globin genes (Albrecht *et al*., 1984; Lim and Maquat, 1992; Wang and Kiledjian, 2000a). Specific sequence or structural elements on the target messages likely are very important in recruiting endonucleases to mediate turnover (Fig. 3). In several cases, these elements are bound by protective factors under certain conditions although alternative stimuli cause them to disassociate and allow en-

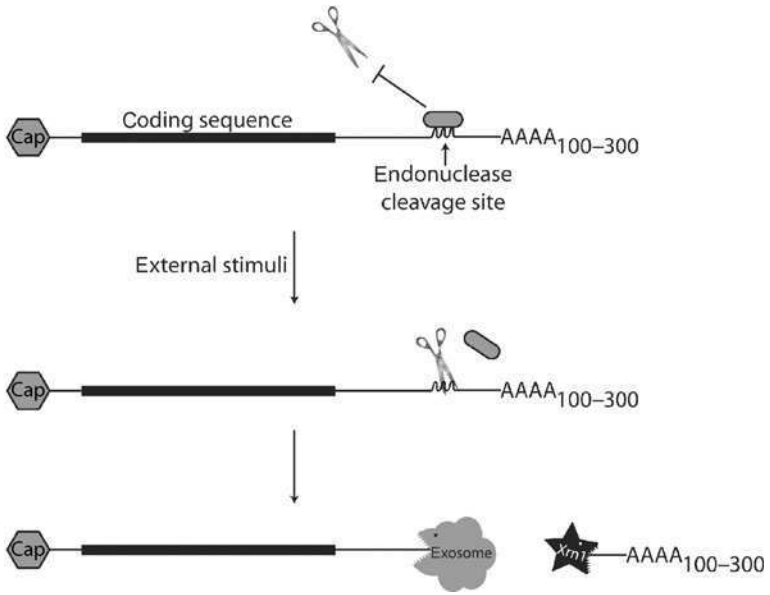

FIG 3. Endonucleolytic decay. mRNAs whose stability is regulated by endonuclease-mediated cleavage frequently contain either sequence or strucural elements that serve as endonuclease recognition sites. Often, these elements are bound by one or more protective factors under conditions requiring stabilization of the message. However, specific external stimuli can induce dissociation of these protective factors and/or activation of the appropriate endonuclease, leading to cleavage of the transcript. An endonucleolytic cleavage event will produce new unprotected 5′ and 3′ termini, which render the RNA susceptible to rapid turnover by other cellular exonucleases such as the exosome and Xrn1.

donucleolytic cleaveage. Notable examples of such regulation are the TfR and α-globin messages. The 3′ UTR of TfR contains a five stem-loop structure that is protectively bound by the iron regulatory protein under conditions of low iron. However, upon increased iron concentrations, this binding is destabilized, resulting in endonucleolytic cleavage of the message within the stem-loop structures (Binder *et al.*, 1994; Casey *et al.*, 1989; Seiser *et al.*, 1995). Rather than stem-loop elements, α-globin messages contain three cytosine-rich elements in their 3′ UTR that associate with an mRNP complex including poly C binding proteins, the AU-rich element associated protein AUF-1, and PABP, which stabilizes the message from endonucleolytic cleavage within the C-rich element by the erythroid cell-enriched endonuclease (ErEN) (Waggoner and Liebhaber, 2003). In addition, AU-rich instability elements (described later) have been shown to be sites of endonucleolytic cleavage on certain messages (Hua *et al.*, 1993; Kowalski and Denhardt, 1989; Wennborg *et al.*, 1995). Deadenylation is not a prerequisite for endonucleolytic activity on the majority of targets analyzed thus far (Binder *et al.*, 1994; Cunningham *et al.*, 2001). One interesting exception is the ErEN nuclease involved in α-globin decay, as it has been shown to be inhibited by PABP and the poly(A) tail (Wang and Kiledjian, 2000b).

In general, endonucleolytic decay has been difficult to characterize due to the extremely rapid rate of degradation of the cleavage products; thus, only a few vertebrate endonucleases have been identified. One of the best studied is polysomal ribonuclease I (PMR1), whose activation upon estrogen stimulation of *Xenopus* hepatocytes has been shown to result in degradation of the majority of serum protein mRNAs (Pastori *et al.*, 1991a,b). PRM1 activity has also been demonstrated in COS-1 and murine erythroleukemia cells (Bremer *et al.*, 2003; Yang *et al.*, 2004). Unlike many of the eukaryotic decapping and exonucleolytic decay enzymes, PRM1 is not located in P bodies or in nuclei but rather is distributed diffusely throughout the cytoplasm (Yang and Schoenberg, 2004). It has no RNA binding domains and therefore does not appear to bind its mRNA substrates directly; it is, however, associated with mRNAs on the translating mRNP complex (Cunningham *et al.*, 2001; Yang and Schoenberg, 2004). Thus, PRM1 is likely to be recruited to its substrates by other mRNA binding proteins, whereupon it associates with the mRNP complex until it is activated by external stimuli (e.g., estrogen) to cleave the mRNA. It is of note that a single endonucleolytic cleavage event would effectively disrupt the protective circular mRNA structure thereby providing immediate access to the 5′ and 3′ ends of the message by exonucleases; thus, this

type of cleavage should result in more rapid mRNA inactivation and degradation than deadenylation-mediated decay.

Of course, the most famous endonucleolytic events are those induced by the RNAi pathway to cleave double stranded RNA molecules. As this topic has been the subject of numerous reviews, it will only be briefly summarized herein. The pathway is initiated by the RNase III-like enzyme Dicer-induced degradation of double stranded RNAs into siRNAs duplexes characterized by an ~20-nt duplex region and 2 nucleotide 3′ overhang region. These siRNAs are then incorporated into the RNA-induced silencing complex (RISC) that directs endonucleolytic cleavage of complementary mRNAs at the specific domain homologous to the RNA oligo (Elbashir *et al.*, 2001; Martinez *et al.*, 2002; Nykanen *et al.*, 2001). In mammals, the endonuclease function of RISC is carried out by Argonaute 2 (AGO-2) (Hammond *et al.*, 2001; Liu *et al.*, 2004a; Rand *et al.*, 2004; Tabara *et al.*, 1999). AGO-2 contains a central PAZ domain responsible for binding the 3′ end of substrate RNAs as well as recognition of the siRNA oligo 3′ overhangs and a carboxyl-terminal Piwi domain believed to fold into an RNase H-like catalytic core (Lingel *et al.*, 2003, 2004; Liu *et al.*, 2004a; Ma *et al.*, 2004; Song *et al.*, 2003, 2004; Yan *et al.*, 2003). After an RNA has been cleaved by RISC, evidence in *Drosophila* cells indicates that the resulting molecules are degraded by the 5′–3′ Xrn1 and 3′–5′ exosomal pathways described for normal mRNA turnover (Orban and Izaurralde, 2005). In agreement with this idea, AGO-2 has been shown to colocalize with the mRNA degradation machinery in cytoplasmic P bodies (Sen and Blau, 2005).

F. AU-Rich Instability Elements

Controlling the rate of mRNA degradation is an important mechanism to regulate expression of proteins in response to a variety of cellular stimuli. Thus, many mRNAs contain specific *cis*-acting sequences that associate with *trans*-acting factors involved in regulating their stability. The most widespread and best characterized of these are instability elements (Bonnieu *et al.*, 1990; Caput *et al.*, 1986; Peng *et al.*, 1996; Shyu *et al.*, 1989) although stabilizing sequences also exist (Stefanovic *et al.*, 1997). AU-rich elements (ARE), found in the 3′ UTR of a number of tightly regulated cellular genes, are the most common instability determinants in mammalian cells. Three classes of AREs have been described (Chen and Shyu, 1995; Peng *et al.*, 1996; Xu *et al.*, 1997). Class I AREs contain one to three copies of the AUUUA penta-

nucleotide with a nearby U-rich sequence; these AREs are most often found in early response genes such as transcription factors (e.g., *c-fos*) and some cytokines (e.g., interleukin 4 and 6 [IL-4, IL-6]). Class II AREs contain multiple copies (five to six) of the AUUUA sequence that cluster together as well as a 20–30 nucleotide AU-rich region 5′ to these clusters; these are frequently found in cytokines (e.g., GM-CSF, TNFα, IL-3). Finally, class III AREs do not possess the pentanucleotide sequence but rather contain stretches of U residues and a U-rich domain (e.g., *c-jun*). The decay of these different types of AREs is likely to occur via distinct mechanisms, as it has been observed that deadenylation of class I and III messages occurs with distributive kinetics whereas class II ARE-containing messages are deadenylated in a processive manner (Chen and Shyu, 1995; Xu *et al*., 1997).

A variety of ARE-binding proteins (AUBPs) have been described that either promote ARE message turnover (e.g., TTP, KSRP, AUF1) or stabilize such mRNAs (e.g., HuR) (described later). AUBP-mediated mRNA turnover is believed to occur by a number of different mechanisms, including recruitment of the exosome (Chen *et al*., 2001a), stimulation of decapping (Gao *et al*., 2001), and promoting deadenylation either via direct activation of PARN or perhaps by disrupting interactions between PABP/poly(A) tail and/or the cap-binding complex/5′ end (Gao *et al*., 2000; Lai *et al*., 2003; Wilusz *et al*., 2001). The observations that immunodepletion of the exosome resulted in stabilization of ARE mRNAs and that several AUBPs were associated with the exosome in UV cross-linking and co-immunoprecipitation experiments emphasize the importance of the exosome in ARE-mRNA turnover (Chen *et al*., 2001a; Mukherjee *et al*., 2002). Collectively, these data suggest that multiple distinct degradative pathways may be activated independently during ARE-mediated decay. Since AUBPs appear to be critical mediators of this process, we now review the known contributions of several of the best characterized of these proteins.

1. Tristetraprolin

Tristetraprolin (TTP), the most extensively studied AUBP, is one of three members (along with *b*utyrate-*r*esponsive *f*actors 1 and 2 [BRF1, BRF2]) of the Tis11 family of CCCH tandem zinc-finger proteins, which have been shown to associate with ARE-containing mRNAs (preferentially class II) and mediate their destabilization (Carballo *et al*., 1998). It is a nuclear/cytoplasmic shuttling protein whose export to the cytosol is induced by stimuli, such as serum, growth factors, or phorbol esters, and results in its association with AREs (Phillips *et al*., 2002; Taylor *et al*., 1996b). TTP knockout mice exhibit a severe inflam-

matory phenotype that includes polyarticular erosive arthritis, myeloid hyperplasia, and autoimmunity; these defects were shown to be due to increased levels of TNFα and GM-CSF, whose mRNAs contain AREs targeted by TTP (Carballo *et al*., 1997). Both BRF1 and BRF2 are essential for mouse development (Ramos *et al*., 2004; Stumpo *et al*., 2004; Taylor *et al*., 1996a) and, like TTP, are involved in destabilization of ARE-containing mRNAs (Lai *et al*., 2000; Stoecklin *et al*., 2002).

Lai *et al*. (2003) used a cell free system to show that TTP activates PARN to degrade class II ARE messages. The mechanism of this activation is still unclear, as the two proteins do not appear to interact (at least directly). Thus, TTP may recruit PARN indirectly via other associations or, alternatively, may displace protective factors from the mRNA 3′ end that normally prevent PARN access. In addition to stimulating deadenylation, Lykke-Anderson and Wagner demonstrated co-immunoprecipitation of TTP and BRF1 with multiple mRNA turnover enzymes, including hDcp1a, hDcp2, hXrn1, hCCR4, hRrp4, and Pm/Scl-75 in a non-RNA–dependent manner (Lykke-Andersen and Wagner, 2005). Although TTP appears to contain both amino- and carboxyl-terminal activation domains, the amino-terminal domain alone is necessary and sufficient for these interactions. They further showed that overexpression of hDcp2 in HeLa cells stably expressing a β-globin-GM-CSF ARE chimeric reporter mRNA significantly increased the rate of turnover of this message but not that of stable non-ARE mRNAs, suggesting that decapping may be a limiting step of ARE decay. Although the significance of other interactions has yet to be revealed, these data indicate that the TTP family may be involved in recruiting and perhaps activating numerous pathways of mRNA turnover to facilitate ARE degradation.

Control of TTP activity is a subject of some controversy. TTP is phosphorylated by several kinases in a manner that is believed to regulate its activity (Carballo *et al*., 2001; Mahtani *et al*., 2001; Taylor *et al*., 1995; Zhu *et al*., 2001). Stoecklin *et al*. (2004) reported that p38 MAPK/MK2-mediated phosphorylation of TTP induced binding to 14-3-3 proteins that resulted in inhibition of its ability to degrade ARE mRNAs and excluded it from stress granules (cytoplasmic foci containing complexes of translationally stalled mRNAs that accumulate in response to environmental stress). Furthermore, it has been shown that activation of the p38 MAPK/MK2 pathway together with overexpression of the ARE stabilizing protein HuR inhibited TTP function, and that PKB-mediated phosphorylation of the TTP-related protein BRF1 resulted in its association with 14-3-3 proteins and inactivation (Ming *et al*., 2001; Schmidlin *et al*., 2004). However, Rigby

et al. *(2005) failed to detect an association of 14-3-3 with TTP and found that MK2 activation did not affect TTP function. Additional studies of TTP-mediated destabilization of the β4GalT1 gene in resting HUVECs also found no role for MK2 in the association of 14-3-3 with TTP but instead described an interaction between the 14-3-3β isoform and TTP that resulted in retention of TTP in the cytoplasm and facilitation of TTP-induced turnover (Gringhuis* et al.*, 2005). One possibility is that TTP phosphorylation by different signaling pathways may lead to distinct regulatory outcomes. Additionally, the seemingly contradictory data regarding 14-3-3 binding may be at least partially reconciled by the possibility that the different isoforms of 14-3-3 may have divergent effects on TTP function. In any case, it seems clear that more research is required to deconstruct the complexity of the regulation of this important AUBP.*

2. AUF1

AUF1 (also called hnRNP D) exists in four isoforms—p37, p40, p42, and p45—that are generated by alternative pre-mRNA splicing and have distinct *in vitro* ARE binding affinities (p37 > p42 > p45 > p40) (Wagner *et al*., 1998). Although the majority of data describe roles for AUF1 in ARE-containing mRNA turnover, the observations that it is also part of the α-globin mRNA stability complex (Kiledjian *et al*., 1997) and is involved in the major coding determinant-directed decay of *c-fos* (Grosset *et al*., 2000) indicate that this factor likely has multiple roles in mRNA stability. The bulk of data regarding the effect of AUF1 isoforms on ARE-mediated decay comes from analyzing their overexpression in various cell lines, which have not always produced congruous results. Loflin *et al*. (1999) demonstrated that the hemin-induced stabilization of β-globin-GM-CSF ARE and β-globin-c-fos ARE reporter constructs in the K562 human erythroleukemic cell line was reversed by overexpression of the p37 and p42 (and to a lesser extent p40 and p45) isoforms, indicating a role for these factors in mRNA destabilization. It was subsequently reported that all four isoforms promoted stabilization of class II ARE mRNAs in NIH 3T3 cells, with p37 exhibiting the strongest effect (Chen *et al*., 2004; Xu *et al*., 2001). However, these findings were not supported in experiments performed by Sarkar *et al*. (2003), who instead observed that overexpression of p37 and, to some extent, p40, promoted destabilization of a β-Gal-GM-CSF reporter in 293, NIH 3T3, HeLa, and COS cells. It has been suggested that control of ARE messages may be regulated, at least in part, by the relative abundance of each AUF1 isoform (Raineri *et al*.,

2004); thus, one possibility is that this may be a confounding factor in interpretations of overexpression data.

AUF1 has been shown to complex with several cellular factors, including hsc70-hsp70, eIF4G, and PABP, and to be regulated by ubiquitin-mediated proteasomal decay (Laroia *et al*., 1999). Degradation of GM-CSF ARE messages correlated both with release of eIF4G and proteosomal decay of AUF1; proteasome inhibition resulted in the relocalization of AUF1 from the nucleus and cytoplasm to the perinuclear region and nucleus and stabilization of GM-CSF. The ubiquitination appeared to be specific for the p37 and p40 isoforms of the protein (Laroia and Schneider, 2002; Laroia *et al*., 2002). AUF1 may also be regulated by phosphorylation, as dephosphorylation of p40 on ser83 and ser87 by TPA treatment of THP-1 leukemia cells resulted in the stabilization of IL-1β and TNFα mRNAs (Wilson *et al*., 2003). Finally, siRNA-mediated knockdown of p40/p45 (but not all four isoforms) stabilized both a GFP-ARE reporter and endogenous GM-CSF RNAs in HT1080-derived cells (Raineri *et al*., 2004). Collectively, these data indicate that AUF1 is involved in the turnover of a variety of ARE-containing messages, although the regulation of the activity of each isoform and how they cooperatively contribute to this function is likely to be regulated on multiple levels—the majority of which have yet to be clarified.

3. TIA-1/TIAR

TIA-1 and the TIA-related protein TIAR are members of the RNA recognition motif (RRM) family of RNA binding proteins and each have three amino-terminal RRM domains that mediate their interaction with U-rich sequences (Dember *et al*., 1996). They are both shuttling proteins involved in the regulation of stress-induced translational arrest through the recruitment of mRNAs into stress granules to prevent translation initiation (Kedersha *et al*., 1999). TIA-1 associates with the ARE of TNFα and COX-2 mRNAs, and expression of both factors is increased in TIA-1 null cells (Dixon *et al*., 2003; Piecyk *et al*., 2000). However, unlike most other AUBPs, it appears as though TIA-1-mediated repression of these proteins occurs at the level of translation rather than mRNA stability.

4. KSRP

K homology splicing regulatory protein (KSRP; also called FBP2) was identified as an AUBP from Jurkat cell extracts that associated with the IL-2 3′ UTR as well as with the exosome (Chen *et al*., 2001a). Gherzi *et al*. (2004) solidified the role of KSRP in ARE-mediated decay

by showing that either immunodepleting it from Jurkat, HeLa, or HT1080 cell extracts or abrogating its expression from HeLa cells by siRNA methodology resulted in stabilization of CAT reporter RNAs fused to AREs of all three classes. They further showed that it associated simultaneously with the exosome and PARN, interactions that required the central of its four KH domain RNA binding motifs. Thus, it appears as though KSRP may mediate ARE mRNA turnover by recruiting specific RNA turnover enzymes to the RNA. Although this ARE-mediated turnover occurs in the cytoplasm of cells, KSRP also has established roles in splicing (Min *et al.*, 1997) and in accordance with the latter function appears to localize strongly to the nucleus of HeLa cells (Hall *et al.*, 2004). Thus, as yet unidentified stimuli may be required to recruit this protein into the cytoplasm to fulfill its role in that locale.

5. HuR

HuR is a ubiquitously expressed member of the ELAV family of RNA binding proteins (Ma *et al.*, 1996) and, unlike the vast majority of other AUBPs described, mediates stabilization rather than turnover of ARE-containing messages. It contains three RRM domains, the first two are involved in ARE binding whereas the third mediates association with the poly(A) tail (Chung *et al.*, 1996; Ma *et al.*, 1997). In addition, HuR possesses a novel HNS shuttling sequence that mediates its transport from the nucleus, where it is predominantly located, to the cytoplasm (Fan and Steitz, 1998a). Translocation of HuR to the cytoplasm upon treatment of cells with various stimuli correlates with ARE mRNA stabilization (Wang *et al.*, 2000b; Yaman *et al.*, 2002). In overexpression experiments, HuR has been shown to bind and stabilize a number of p38 MAPK-regulated messages, including GM-CSF, TNFa, IL-3, and COX-2, suggesting a role for this pathway in HuR function (Dean *et al.*, 2001; Fan and Steitz, 1998b; Ming *et al.*, 2001; Sully *et al.*, 2004). However, the observation that it was not responsible for IL-8 stabilization during p38/MK2 activation and IL-8 sequences required for HuR-mediated stabilization were distinct from those involved in p38/MK2 responsiveness indicate that the mechanisms of p38/MK2 and HuR stabilization do not completely overlap (Winzen *et al.*, 2004). Antisense or siRNA-mediated HuR depletion experiments have confirmed its involvement in the protection of several ARE-containing mRNAs, including VEGF, cyclin A, cyclin B, p21, urokinase, and urokinase receptor (Levy *et al.*, 1998; Tran *et al.*, 2003; Wang *et al.*, 2000a,b).

III. Introduction to Herpesvirus-Induced Host Shutoff

A number of viruses have been shown to potently inhibit cellular gene expression to facilitate their own replication. Such host shutoff can occur via a variety of mechanisms; transcription, RNA splicing and nuclear export, mRNA decay, and translation are all cellular events targeted for disruption during viral infection. Viruses frequently induce host shutoff to avoid competition from cellular transcripts during the mass-production of their own proteins and, additionally, to prevent expression of cellular factors involved in stimulating an immune response to infection.

The herpesvirus family encompasses a large group of enveloped, double-stranded DNA viruses that infect a wide array of metazoans. All herpesviruses are characterized by their ability to engage in two alternative genetic programs, latency and lytic replication. In latency, the viral genome is maintained in the nucleus at low-copy number, and expression of the genome is highly restricted—of the 100–200 viral genes, only a handful are typically expressed in latency. As a result, no virus production ensues; latency represents, in effect, a persistent cryptic state. However, because the entire genome is retained, the potential for reactivation of lytic infection exists. During lytic infection, the majority of viral genes are expressed in a temporally regulated cascade; viral DNA replicates to high-copy number and infectious progeny are produced with death of the host cell.

Taxonomically, herpesviruses are subdivided into α, β, and γ subfamilies, which differ in their genomic organization, lytic cycle kinetics, and the cell types in which latency is established. Although lytic replication of some β-herpesviruses does not block cellular gene expression, members of both the α- and γ-herpesvirus subfamilies exhibit a prominent host shutoff phenotype during virus production. In both cases, the viruses encode proteins that promote the selective degradation of mRNA within the cell. In the next sections we review current knowledge of herpesvirus-induced mRNA turnover, with emphasis on its complex relationship to cellular mRNA decay pathways.

IV. α-Herpesvirus–Induced mRNA Decay

A. Overview

Herpes simplex type 1 (HSV-1) is the prototypic member of the neurotropic α-herpesvirus family, and both HSV-1 and HSV-2 are ubiquitous human pathogens associated with a variety of diseases

(Roizman and Knipe, 2001). α-Herpesvirus infection initiates at mucosal surfaces, where the viruses undergo lytic replication in the surrounding epithelial cells, then subsequently enter the nearby sensory nerve termini. There, they exploit retrograde axoplasmic flow to travel to the nuclei of sensory ganglia, where they establish a life-long latent infection. Subsequently, the latent viruses can experience periodic lytic reactivation; reactivated virus travels back down axon termini to cutaneous epithelial cells, where further lytic spread results in lesion formation and transmission to new hosts. Lytic α-herpesvirus infection induces a global shutoff of host cell gene expression and directs production of three temporal classes of viral mRNAs. The α or immediate early class of genes encodes regulatory proteins required for the expression of the second β (early) class of genes, which play key roles in viral replication. The final group of viral genes expressed is the γ (late) messages encoding structural proteins for assembly of the virion. In addition to the newly transcribed viral genes, α-herpesviruses package a number of important regulatory factors into the virion tegument that are then delivered directly into the newly infected cells for immediate activity. One such factor is vhs, a protein responsible for degradation of cellular mRNAs resulting in widespread host shutoff during the early stages of infection. As discussed later, vhs activity plays integral roles both in facilitating the transition between stages of viral gene expression as well as in evasion of the host immune response.

The ability of HSV to promote mRNA turnover in infected cells was first observed in the mid 1970s, although it was known that HSV infection caused a decrease in cellular protein synthesis a decade earlier (Fenwick, 1984; Sydiskis and Roizman, 1967). Early observations that a protein synthesis decline occurred even upon infection with UV-inactivated virus (Nishioka and Silverstein, 1978), as well as in the presence of cyclohexamide or actinomycin D and in enucleated cytoplasts (Fenwick and Walker, 1978; Fenwick *et al.*, 1979), suggested that a virion component could promote the effect in the cytoplasm of infected cells in the absence of viral protein synthesis. This shutoff of cellular protein synthesis was originally linked to mRNA abundance using polyoma virus-transformed BHK cells infected with HSV. Monitoring of the levels of polyoma virus mRNA in the cells before and during HSV infection revealed that within 5 h of HSV infection these levels had declined to 20% of those in uninfected cells (Pizer and Beard, 1976). Similar experiments using adenovirus-transformed cells showed a significant decline in adenoviral mRNA early upon HSV-1 infection (Spector and Pizer, 1978). A preferential decline in messenger RNA as opposed to other types of RNA in

HSV-infected cells was demonstrated by a reduced ability of cDNA probes to anneal to poly(A) RNA but not nonadenylated RNA (Nakai *et al.*, 1982). Furthermore, it was shown that pseudorabies virus (PRV) infection resulted in a decline in "functional" mRNA that could be *in vitro* transcribed and translated into protein (McGrath and Stevely, 1980). The ability of HSV to promote a rapid turnover of mRNA was shown in a number of different cell types (Mayman and Nishioka, 1985; Nakai *et al.*, 1982; Nishioka and Silverstein, 1977; Schek and Bachenheimer, 1985). These data described the effect of α-herpesvirus infection at early times after viral entry (primary shutoff); however, a subsequent and distinct secondary shutoff occurred at later times during infection that required viral gene expression (Fenwick and Clark, 1982; Nishioka and Silverstein, 1978; Read and Frenkel, 1983). This secondary shutoff phenotype is caused by the product of the α27 ORF (ICP27), which blocks pre-mRNA splicing in infected cells and also affects nuclear–cytoplasmic mRNA transport and other posttranscriptional processes (Hardwicke and Sandri-Goldin, 1994; Sandri-Goldin, 1998).

Key to identifying the virion-associated factor required for the primary shutoff was the isolation of 6 HSV-1 mutants capable of infecting cells but unable to block cellular gene expression in the presence of actinomycin D (Read and Frenkel, 1983). These mutants were accordingly termed *vhs-1*$\rightarrow$ *6*, for their lack of *v*irion *h*ost *s*hutoff activity, and their ability to replicate to near wild-type levels in tissue culture demonstrated that the shutoff function was not essential for virus growth *in vitro*. However, analysis of viral polypeptide synthesis during the *vhs* mutant infections revealed abnormally high levels of the α(immediate early) proteins, providing the first indication that this primary shutoff function played an additional role in regulating certain aspects of viral gene expression. Significantly, infection with the *vhs* mutants still induced the secondary shutoff in the absence of actinomycin D, providing compelling evidence that the primary and secondary shutoff functions are carried out by distinct viral polypeptides (Read and Frenkel, 1983). Subsequent analysis of the *vhs-1* mutant virus showed it to be defective in promoting enhanced turnover of both cellular and viral mRNAs (Kwong and Frenkel, 1987; Oroskar and Read, 1989; Strom and Frenkel, 1987). *Vhs-1* mapped to a single base mutation within the UL41 open reading frame (ORF) of HSV-1 (Kwong and Frenkel, 1989; Kwong *et al.*, 1988).

Shortly after mapping *vhs* mutations to HSV-1 UL41, peptide antisera were used to show that this ORF encoded a 58 kDa phosphoprotein expressed late in infection, which, as predicted from the shutoff

activity of UV-inactivated virus, was a component of the viral tegument (McLauchlan *et al.*, 1992; Smibert *et al.*, 1992). Evidence indicates that vhs protein present in the virions is released into the cytoplasm of newly infected cells, where it promotes a widespread degradation of mRNA. Vhs homologs are found in all α-herpesviruses, including HSV-1, HSV-2, varicella-zoster virus (VZV), PRV, bovine herpesvirus 1 (BHV-1), and equine herpesvirus 1 (EHV-1) but not in β- or γ-herpesviruses (Berthomme *et al.*, 1993). In addition, all vhs homologs have been shown to possess RNase activity in cells, albeit with differing efficiencies; for example, the HSV-2 vhs is 40–50-fold more active than that of HSV-1, whereas VZV and EHV-1 vhs display significantly reduced activity (Everly and Read, 1997; Lin *et al.*, 2004a; Sato *et al.*, 2002). As described in the following section, over the past 20 years significant advances have been made toward understanding vhs biology and the mechanisms by which it promotes degradation of cellular and viral mRNAs as well as facilitates the sharp transition between α, β, and γ viral gene expression.

B. Vhs as a Ribonuclease

The development of *in vitro* assays to analyze vhs activity greatly facilitated the dissection of its RNase function (Smiley *et al.*, 2001). Krikorian and Read were the first to describe such a system and using HeLa cytoplasmic extracts they showed that GAPDH and TK mRNAs were rapidly degraded in extracts from wt HSV-1 but not *vhs-1* mutant-infected cells (Krikorian and Read, 1991). The mRNA degradation proceeded even after treatment with RNasin to inactivate nonspecific cellular RNases but was inhibited by proteinase K digestion, exposure to high temperature, or high K^+ concentrations (>7 mM). Furthermore, this activity was strongly dependent on the presence of Mg^{2+} (optimally 20 mM). Additional evidence that the HSV-associated RNase activity derived from vhs rather than a contaminating cellular component came from Zelus *et al.* (1996), who showed that ^{32}P-labeled β-globin mRNA was effectively degraded upon incubation with purified wt but not *vhs-1* or ΔSma [a truncation mutant of vhs (Read *et al.*, 1993)] mutant virion extract; preclearing of the extract with anti-vhs antibodies blocked the mRNA turnover. The observations that *in vitro* translated vhs protein from rabbit reticulocyte lysates (RRL) similarly degraded exogenously added mRNA and that reporter gene expression was blocked in cells transiently transfected with a vhs-expressing plasmid demonstrated that vhs RNase activity did not require

additional viral components (Jones *et al*., 1995; Pak *et al*., 1995; Zelus *et al*., 1996).

These *in vitro* degradation systems for vhs also allowed a number of questions regarding the mechanism of its RNA turnover function to be addressed. For example, the fact that vhs promotes widespread mRNA turnover but spares rRNA and tRNA suggests that mRNA molecules may possess a specific feature(s) that renders them susceptible to decay. However, the most obvious distinguishing elements on mRNAs, their 5′ cap and 3′ poly(A) tail, were shown to be dispensable for RNA turnover by RRL-translated vhs (Elgadi *et al.*, 1999; Zelus *et al*., 1996). Precise analysis of the degradative intermediates of a labeled SRPα RNA revealed multiple endonucleolytic cleavage events by vhs, which appeared to cluster toward the 5′ end of the transcript (Elgadi *et al*., 1999). Additional experiments measuring degradation intermediates of the TK mRNA in infected HeLa cells confirmed a more rapid decay of the 5′ mRNA segment over the 3′ end (Karr and Read, 1999). Vhs remained active in the RRL system after removal of the ribosomes by centrifugation, arguing against the idea that vhs is directed to mRNAs undergoing translation (Elgadi *et al*., 1999). Addition of an EMCV or poliovirus IRES element into reporter mRNAs in multiple positions resulted in a strong preference for endonucleolytic cleavage just downstream of the IRES, indicating that these elements can somehow influence vhs activity (Elgadi and Smiley, 1999). Unexpectedly, the *vhs-1* mutant, which fails to degrade non-IRES containing mRNAs, was still able to promote endonucleolytic cleavage specifically after the ECMV IRES element *in vitro* (Lu *et al.*, 2001). After the initial IRES-dependent cleavage event, the *vhs-1* mutant failed to subsequently promote degradation of the resulting RNA fragments, however, suggesting that perhaps wt vhs promotes multiple types of mRNA degradation and that the *vhs-1* mutant is defective in only select aspects of the enzymatic function.

Vhs displays weak homology to the cellular fen-1 nucleases (Doherty *et al.*, 1996), a family of enzymes with roles in DNA replication and repair. In addition, a BLAST search followed by hidden Markov modeling revealed similarities between vhs and a larger family of nucleases from humans, yeast, and *E. coli*, including XPG, RAD2, and Pol I (Everly *et al*., 2002). Vhs proteins within the α-herpesvirus family display significant homology in three conserved regions of the protein (Berthomme *et al.*, 1993; Everly and Read, 1997; Jones *et al.*, 1995), and the first two conserved vhs domains exhibit homology to critical residues within the catalytic sites of the aforementioned cellular nucleases. Significantly, mutation of several vhs amino acids

corresponding to catalytic residues in the homologous cellular nucleases reduced or abrogated vhs nuclease activity, providing further genetic evidence that vhs is a nuclease (Everly *et al.*, 2002).

Although all of the previously mentioned experiments strongly suggest that vhs possesses RNase activity, without directly purifying the protein the possibility that vhs does not act alone cannot be excluded. For example, vhs could activate a host nuclease or could represent an essential subunit of a cellular RNase complex; alternatively, vhs might require a cellular cofactor to activate its own latent nuclease function or to direct it to its mRNA targets. Several lines of evidence suggest that in fact vhs likely requires at least one mammalian factor to achieve efficient cellular mRNA turnover. Although vhs retains some nuclease activity in yeast, degradation of reporter RNAs in this system is markedly less efficient than in mammalian extracts and there is no global turnover of mRNA in vhs-expressing yeast (Doepker *et al.*, 2004; Lu *et al.*, 2001). In addition, vhs-mediated degradation in yeast produces a different mRNA decay pattern and cleavage after IRES elements is not observed, suggesting that yeast lack one or more mammalian factors required for proper targeting of vhs to mRNAs. Supporting this notion is the observation that addition of RRL to the vhs-expressing yeast lysates both enhances vhs activity and restores targeting of vhs to IRES elements (Doepker *et al.*, 2004). Furthermore, extracts of partially purified HSV virions exhibit a vhs-induced RNA degradation pattern that lacks the specificity observed *in vivo* and in RRL, in that non-mRNAs do not escape degradation, and the vhs-induced turnover does not occur at the 5′ RNA sites preferred in both the RRL and HeLa cell systems (Zelus *et al.*, 1996). These data suggest that the virion extracts lack one or more components necessary to target vhs appropriately to its substrates.

It is intriguing that sites of vhs-mediated endonucleolytic cleavage are at the 5′ end of mRNAs and directly after IRES elements, given that these are regions associated with mRNA translation initiation. Although neither translational inhibitors nor the absence of a 5′ cap appear to interfere with vhs-mediated turnover, it remains possible that vhs associates with a translation initiation factor that directs it to these sites on the mRNA (Elgadi and Smiley, 1999; Elgadi *et al.*, 1999; Schek and Bachenheimer, 1985; Strom and Frenkel, 1987). After all, such an event would not require actual translation initiation or elongation but could nonetheless provide the specificity exhibited by vhs for mRNAs *in vivo*. In support of this idea, vhs was shown to interact with the mammalian translation initiation factor eIF4H and the RNA helicase eIF4AII in a yeast 2-hybrid system and in mammalian cell co-immunoprecipitations and also with eIF4B *in vitro* (Doepker *et al.*,

2004; Feng *et al.*, 2001, 2005). Several vhs mutants with defective RNase activity failed to bind eIF4H in GST pulldown assays, suggesting that this interaction may be important for vhs-mediated mRNA turnover. eIF4H functions early in translation initiation, where it is believed to assist in mRNA unwinding and scanning of the small ribosomal subunit (Hershey and Merrick, 2000). eIF4B is the sequence paralog of eIF4H and assists eIF4H with the helicase activity of eIF4A (Richter *et al.*, 1999; Rogers *et al.*, 2001). The observation that eIF4AII (one of the three eIF4A isoforms) associates directly with both eIF4H and vhs provides a link between vhs and the eIF4A/eIF4G/eIF4E cap binding complex (Feng *et al.*, 2005). Vhs mutants, such as T214I, which cannot bind eIF4H but retain binding to eIF4AII and are defective for turnover of mRNAs translated by scanning, indicating that interactions of vhs with both proteins may be required for appropriate mRNA targeting and cleavage. Thus, one attractive model is that these factors direct vhs to sites of translation initiation on mRNAs, perhaps thereby providing both the specificity for mRNAs and explaining the preferential endonucleolytic cleavage by vhs within the 5′ quadrant of these molecules. This notion is supported by the fact that addition of partially purified eIF4H or eIF4B to vhs-expressing yeast extracts enhances the turnover of reporter mRNAs. However, neither of these proteins can restore vhs-mediated targeting to IRES elements in the yeast system, suggesting that additional mammalian factors (likely eIF4A, and perhaps others) are involved in directing vhs-mediated turnover and/or contributing to its enzymatic activity (Doepker *et al.*, 2004). The eIF4H-vhs interaction may also help resolve the issue of whether vhs is itself an RNase by facilitating purification of the vhs protein. The major impediment to definitively calling vhs a nuclease has been the inability to generate highly purified protein due to its insoluble nature. However, Everly *et al.* (2002) revealed that co-expression with eIF4H significantly enhanced the solubility of vhs in *E. coli*, and their purified vhs from this system retained nuclease activity (although additional protein bands were present in the vhs fractions).

From these data it can be seen that the vhs endonucleolytic activity may parallel that of cellular endonucleases, such as PMR1, in that it appears to be similarly targeted to specific sites on target mRNAs via other RNA or cap binding factors and/or structural elements (Fig. 4). However, the fact that mammalian endonucleolytic cleavage is reserved for select messages whereas vhs promotes global mRNA turnover would indicate that the proteins and/or structural elements which recruit or activate vhs are much more widespread than those involved in the selective mammalian endonucleolytic decay. The observed interactions between vhs and eIF4 proteins fit this prediction as these

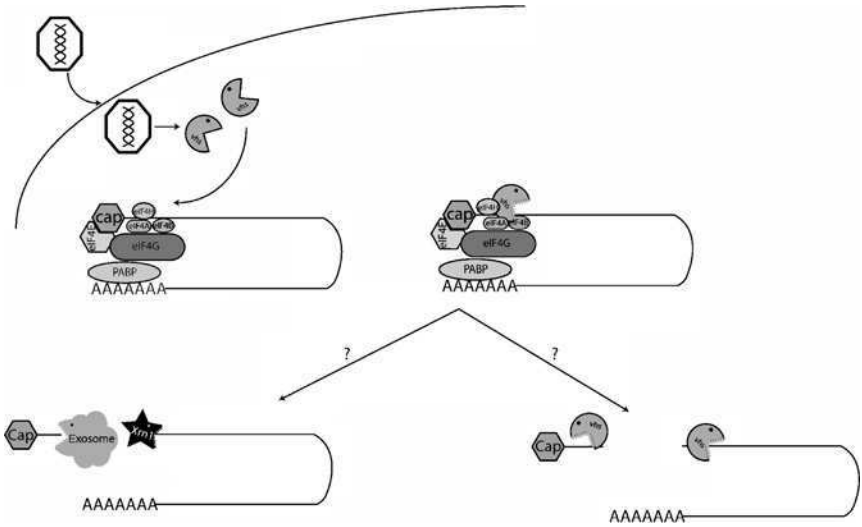

FIG 4. Model for vhs targeting to mRNAs. Vhs is packaged into the viral particles, and is thus present in the cell immediately after infection, where it promotes rapid turnover of mRNAs. Vhs preferentially cleaves near the 5′ end of messages, and is likely targeted to these sites via its interactions with the translation initiation factors eIF4H, eIF4A, and eIF4B. Vhs-mediated endonucleolytic cleavage then produces exposed and unprotected 5′ and 3′ termini, which would be susceptible to rapid turnover by cellular exonucleases and/or additional cleavages by vhs.

factors should associate with a large pool of mRNAs. An additional interesting issue is whether decay of vhs-cleaved messages proceeds via the Xrn1 and exosomal pathways as is likely the case for mRNAs targeted by mammalian endonucleases, or whether vhs itself completes the degradation. One or a few vhs-mediated cleavage events would effectively inactivate a message and render it susceptible to immediate degradation by cellular exonucleases. Although purified virion extract does promote turnover of labeled substrate RNAs, the mRNA half-lives were shortened substantially in the presence of cytosol, suggesting that the cleavage products are targets of cellular nucleases (Zelus *et al*., 1996).

C. Degradation of ARE-Containing Cellular Messages

DNA microarray analysis has identified a number of cellular genes that are upregulated during HSV infection, even in the face of host shutoff (Taddeo *et al.*, 2002). Several of these genes were noted to

contain AREs within their 3′ UTRs, characteristic of tightly regulated unstable messages such as cytokines and growth factors. As discussed earlier in this review, inactivation of ARE-containing messages is assisted by several cellular ARE binding proteins, including TTP, TIA-1, and TIAR. Cells infected with HSV-1 exhibited an increase in TTP expression at both the mRNA and protein level (Esclatine *et al*., 2004). Furthermore, the TTP in infected cells was localized diffusely within the cytoplasm whereas it was predominantly nuclear in uninfected cells [except upon mitogen stimulation (Taylor *et al*., 1996b)]. Although neither TIA-1 nor TIAR were upregulated by HSV-1, both proteins were similarly present in the cytoplasm of infected cells, reflective of an activated state (Esclatine *et al*., 2004). It is unlikely that vhs is directly responsible for the TTP upregulation given that TTP was not induced upon infection with a $\Delta\alpha 4$ virus that contains active vhs. However, infection of HEp-2 or HFF cells with a vhs mutant virus ($\Delta U_L 41$) similarly failed to induce TTP, suggesting that vhs is somehow involved in TTP accumulation. Supporting this hypothesis is the observation that vhs interacts with TTP in coimmunoprecipitations from infected cells. In addition, $\Delta U_L 41$-infected cells displayed an aggregate pattern of TIA-1/TIAR staining in the cytoplasm reminiscent of stress granules rather than the diffuse staining observed during wild type HSV-1 infection. Thus, interactions of these factors may be altered in the absence of vhs leading to the divergent localizations.

The outcome of the upregulation and/or cytoplasmic relocalization of these AUBPs with respect to the stability of HSV-induced ARE-containing cellular mRNAs is currently controversial. Taddeo *et al*. (2003) examined the expression of one such mRNA, the stress-inducible cellular gene *IEX-1*, throughout infection of cells with HSV-1 or $\Delta U_L 41$. They reported that although early in infection *IEX-1* mRNA was upregulated and translated into protein, at later times the message existed in partially degraded forms lacking 3′ sequences and was therefore incapable of producing protein product. These degradation products were not seen in $\Delta U_L 41$ infections, suggesting that vhs was responsible for their cleavage. Esclatine *et al*. (2004) extended these results to show that similar degradation products accumulated in a vhs-dependent manner for the ARE-containing c-fos and IκBα mRNAs but not for GADD45β and TTP mRNAs that lack AREs. The authors argue for a model whereby the induction of ARE-containing cellular genes that may be detrimental to viral infection or immune evasion is quenched by a selective and sequence-specific degradation of the

mRNAs by vhs, perhaps assisted by the AUBPs TTP and TIA-1/TIAR (Esclatine *et al.*, 2004; Taddeo *et al.*, 2003, 2004).

However, this hypothesis has been contested by data from Hsu *et al.* (2005), who failed to detect any increased degradation of *IEX-1* mRNA during infection. While they did observe the degradation intermediates described earlier during HSV-1 infection, they also found them in cells infected with vhs-deficient virus as well as in uninfected cells. In addition, they measured the half-life of *IEX-1* mRNA by actinomycin D chase assays and found it to be stabilized both in cells infected with wild-type and vhs-null virus relative to uninfected cells. Thus, rather than stimulating selective degradation of *IEX-1*, their data suggest that HSV-1 infection stabilizes this message even in the presence of vhs. They present the possibility that the vhs–TTP interaction may contribute to this effect by disrupting the normal turnover of select ARE-containing messages in infected cells (Hsu *et al.*, 2005).

Although more research is required to resolve this issue, in either case the tantalizing link between vhs and cellular ARE-mediated mRNA decay is anticipated to reveal novel aspects of vhs-mediated as well as perhaps cellular turnover of this important class of messages. It will also be of considerable interest to determine how the group of non-ARE containing messages upregulated early in HSV infection is evading degradation by vhs.

D. Regulation of Vhs During HSV Infection

It is well established that the nuclease activity of vhs plays an integral role in facilitating the sharp transition from immediate early (α) to early (β) and late (γ) viral gene expression, due to the fact that vhs delivered into the cytoplasm from infecting virions degrades both cellular and immediate early viral mRNAs. In the absence of other viral factors vhs readily degrades β and γ mRNAs as well, although during infection these genes are expressed to high levels. Thus, it seemed likely that one or more viral factors might exert a temporal control of vhs activity to protect delayed-early (β) and late (γ) viral transcripts from turnover. A candidate vhs regulatory factor was revealed when Smibert *et al.* (1994) showed that VP16, a viral structural protein involved in the transcriptional activation of the α-genes (Batterson and Roizman, 1983; Campbell *et al.*, 1984), interacted with vhs. VP16 is a highly abundant tegument protein, which, like vhs, is delivered directly into cells by infecting virions. It is composed of a C-terminal acidic activation domain and a DNA binding domain that targets it to α-gene promoters via interactions with the host

factors Oct1 and HCF (Herr, 1998; Herr and Cleary, 1995). The significance of the VP16–vhs interaction became evident upon the observation that infection with a VP16 null mutant virus (8MA) resulted in drastically reduced levels of viral protein synthesis, suggesting that VP16 was required for the maintenance of viral intermediate and late protein levels (Lam *et al*., 1996). This reduction was not due to the absence of VP16 transcriptional activation activity, as neither infection with a VP16 truncation mutant lacking the activation domain but retaining its vhs binding capability nor with a VP16–vhs double knockout (8MA/ΔSma) resulted in a viral protein synthesis decline.

The interaction domains of these factors were mapped to amino acids 310–330 of vhs and a nonlinear VP16 motif (making precise mapping difficult), although isolation of a VP16 L344 point mutant defective for vhs binding but retaining its other functions demonstrated these activities of VP16 are separable (Knez *et al.*, 2003; Schmelter *et al*., 1996). Deletion of the 20-amino acid VP16 binding domain of vhs does not affect its ability to degrade reporter RNAs in transient transfection assays, in agreement with the fact that the binding domain is located outside of the region required for nuclease activity (Strand and Leib, 2004). However, in the context of a viral infection this mutant displayed several unexpected properties. First, in cells infected with the VP16 binding domain mutant virus (Δ20) vhs Δ20 retained the ability to interact with virally expressed VP16. Thus, the interaction of vhs with VP16 that occurs in yeast 2-hybrid assays and in co-immunoprecipitations from RRLs does not mimic their association during a viral infection. Secondly, despite the ability of vhs Δ20 to bind VP16 during infection, this mutant virus lacked vhs activity upon infection in the presence of actinomycin D, although it exhibited wild-type levels of vhs activity in the absence of actinomycin D. Thus, while the newly made vhs Δ20 was active, the vhs Δ20 derived from the tegument was not. Furthermore, this Δ20 virus was attenuated in mice, although not to the extent of a vhs null virus. Collectively, these data indicate that this 20 amino acid region plays a critical role in tegument-derived vhs function, perhaps as a site of a specific phosphorylation event or other posttranslational modification required for release from the virus particle in an active form.

Although the mechanism whereby VP16 modulates vhs activity is not yet known, the simplest model is that VP16 binds and inactivates newly synthesized vhs, for example, by preventing other necessary cellular interactions or sequestering vhs within the nucleus. There are many more copies of VP16 in the tegument than there are of vhs, yet tegument-derived vhs is not inactivated by the incoming VP16.

One possibility is that VP16 is complexed with other factors in the virion that preclude its ability to bind vhs or, alternatively, upon entry into cells VP16 preferentially interacts with its cellular binding partners and is titrated away from the vhs molecules. The vhs-induced host shutoff could then be envisioned to eliminate these cellular binding competitors and free up VP16 to associate with and inactivate vhs.

E. Vhs Activity In Vivo

Although deletion of vhs has only minimal effects on HSV replication in cell culture, it has a profound influence on viral pathogenicity and clearance in mice and inhibits establishment of latency as well as reactivation (Leib *et al*., 1999; Strelow and Leib, 1995, 1996; Strelow *et al.*, 1997). This is presumably due to the ability of vhs to block host immune responses via downregulation of key immunomodulatory molecules. As these data are the subject of a review (Smiley, 2004), they will only be briefly summarized herein.

Initiation of an *in vivo* antiviral immune response requires the activity of dendritic cells (DCs), potent antigen presenters that acquire antigens from peripheral tissues then migrate to the lymph nodes where they mature and stimulate naïve T cells (Banchereau and Steinman, 1998). Infection with HSV-1 has been shown to inhibit the maturation and T cell stimulatory capacity of DCs as well as downregulate several cell surface markers, thus evading this integral arm of the immune system (Kruse *et al*., 2000; Salio *et al*., 1999). Significantly, Samady *et al*. (2003) subsequently demonstrated that deletion of the *vhs* gene from HSV releases the block to DC activation thereby permitting T cell stimulation, suggesting that early host shutoff plays a role in escaping T cell-mediated antiviral responses of the host. However, that HSV-1 infection of DCs induces several changes that are not dependent on vhs, including the downregulation of CCR7 and CXCR4 that results in migration defects (Prechtel *et al*., 2005). α-Herpesviruses also evade cytotoxic T lymphocyte (CTL) responses by interfering with cell surface MHC I expression through both a reduction in the overall levels of MHC I synthesis and by ICP47-mediated inhibition of TAP peptide transport (Fruh *et al*., 1995; Hill *et al*., 1994, 1995; York *et al*., 1994). In addition, HSV-1 infection of glioblastoma cells results in a shutoff of MHC class II synthesis and cell surface expression (Trgovcich *et al.*, 2002). The activity of the corresponding viral vhs proteins has been shown to contribute to the general decrease in both MHC class I and class II expression (although other mechanisms are involved in the specific surface downregulation of these factors); thus,

vhs likely contributes to viral evasion of T cell responses (Gopinath *et al*., 2002; Koppers-Lalic *et al*., 2001; Tigges *et al*., 1996).

Evidence suggests that HSV-2 vhs plays a role in viral evasion of innate immunity as well via modulation of the α interferon (IFN) response. IFN release from infected cells triggers a signal transduction cascade resulting in expression of an array of IFN-stimulated genes (*ISG*s) that block protein synthesis, degrade RNA, and inhibit viral replication (Taniguchi and Takaoka, 2002). Unlike many other viruses, HSV infection is quite resistant to the effects of this response (Harle *et al*., 2002; Leib *et al*., 1999; Mossman *et al.*, 2000). HSV-2 vhs mutants were severely attenuated for replication and pathogenesis in wild-type 129 mice but not in IFN-α receptor knockouts, suggesting that vhs may be a key player in HSV-2-mediated IFN resistance (Murphy *et al*., 2003). In contrast, an HSV-1 vhs mutant remained defective in both types of mice, in agreement with previous data showing that IFN resistance in HSV-1 mapped to viral factors other than vhs (Leib *et al*., 1999; Murphy *et al*., 2003). Additional data however suggest that HSV-1 vhs may instead cooperate with ICP0 to dampen the effects of direct ISG stimulation by IRF-3 and IRF-7 in the absence of IFN activity, thereby contributing to HSV-1-mediated evasion of the innate immune response (Lin *et al*., 2004b). Furthermore, Suzutani *et al*. (2000) showed in a mouse encephalitis model that an HSV-1 vhs-deficient mutant inoculated into the mouse brain had severe virulence defects unless the mouse was subjected to γ-ray irradiation thereby eliminating sensitive cells such as lymphocytes and neutrophils (Suzutani *et al*., 2000). They suggest that vhs therefore may be involved in viral evasion of these host defense mechanisms, and support this hypothesis with the observation that cells infected with the vhs null virus expressed significantly higher levels of IL-1β, IL-8, and MIP-1α.

Collectively, these data indicate that in addition to facilitating virus replication and gene expression in infected cells, vhs likely plays a critical immune evasion role *in vivo* by contributing to the suppression of both specific and nonspecific host immune responses.

V. γ-Herpesvirus–Induced mRNA Decay

A. Overview

γ-Herpesviruses comprise a group of lymphotropic viruses containing two members—Kaposi's sarcoma-associated herpesvirus (KSHV) and Epstein-Barr virus (EBV)—that cause human disease. KSHV is

the most recently identified human tumor virus and is associated with several proliferative disorders, the most common being Kaposi's sarcoma (KS) (Moore and Chang, 2001). Although originally described as a rare tumor found predominantly in elderly Mediterranean or African men, with the onset of the AIDS epidemic KS became the most common neoplasm associated with untreated human immunodeficiency virus (HIV) infection. KS lesions are characterized by proliferation of spindle-shaped endothelial cells, infiltration by host inflammatory cells, and striking neoangiogenesis. Although still incompletely understood, KS pathogenesis is thought to involve high-level production of growth factors, inflammatory cytokines, and angiogenic factors by one or more of the cellular components of the lesion. In addition to KS, KSHV is associated with two rare lymphoproliferative disorders, primary effusion lymphoma (PEL) and multicentric Castleman's disease (MCD).

Similar to herpes simplex viruses, EBV is nearly ubiquitous in the human population; nearly 90% of the world is infected with this virus (Kieff, 1996). The majority of infected people remain asymptomatic, although EBV is linked to several human cancers including Burkitt's lymphoma, Hodgkin's disease, and nasopharyngeal carcinoma. It is also the causative agent of infectious mononucleosis, which can arise in persons whose primary exposure does not occur until adolescence. In immunocompromised hosts, such as AIDS patients and transplant recipients, the virus can induce fatal B-cell lymphoproliferative disease. EBV establishes a latent and lifelong infection in B lymphocytes and, as with KSHV, only a small subpopulation of infected cells undergoes lytic replication.

The question of whether γ-herpesviruses induce a host shutoff upon lytic infection had lain neglected largely because of technical difficulties. For EBV and KSHV, typical stimuli that induce lytic reactivation do so inefficiently, resulting in induction of only 5–20% of latently infected cells. Under such circumstances, continued host gene expression in the majority latent population would obscure any shutoff in the lytic population. However, within the last few years it has become possible to bypass these experimental difficulties, and with this has come the realization that, like their α-herpesvirus counterparts, several γ-herpesviruses also promote a global shutoff of cellular gene expression at the level of mRNA stability. Though, these viruses have no vhs homolog and instead utilize a completely different viral gene product to promote cellular mRNA turnover. Furthermore, data suggest that the mechanism(s) by which the shutoff is achieved at least during KSHV infection are likely to be quite unique.

Unlike most α-herpesviruses, the default pathway for KSHV infection is latency, during which only a restricted subset of viral genes required for maintenance of the viral episome and promoting cell growth are expressed (Dupin *et al*., 1999; Friborg *et al*., 1999; Radkov *et al.*, 2000). However, there is also a small subpopulation of infected cells undergoing spontaneous lytic induction; this lytic cycle can be more efficiently induced by ectopic expression of the viral major lytic transactivator RTA (Cannon *et al*., 2000; Gradoville *et al*., 2000; Lukac *et al*., 1998; Miller *et al*., 1996). By optimizing the efficiency of lytic induction, as well as by developing single-cell assays for shutoff, Glaunsinger and Ganem (2004b) showed that a robust shutoff of host protein synthesis initiated early in infection was not blocked by the viral DNA replication inhibitor PFA and continued until cell death (Glaunsinger and Ganem, 2004b). Moreover, analysis of several cellular messages by northern blotting and nuclear runoff assays showed that while cellular genes were efficiently transcribed in infected cells, total mRNA levels were drastically reduced by 12 h post reactivation. Overall, these data indicated that lytic KSHV infection promotes degradation of cellular mRNAs. Similar results were subsequently obtained from experiments analyzing EBV-induced changes to host gene expression during lytic reactivation of EBV-positive AKBM cells (Ressing *et al*., 2005; Ressing, M. E., and Wiertz, E., in preparation). These cells exhibited an EBV-induced reduction in total cellular protein synthesis that did not require late viral gene expression. Moreover, RT PCR analyses of several cellular transcripts showed that, similar to KSHV, this shutoff manifested at the level of mRNA. As discussed in the next section, a screen of KSHV lytic genes for the ability to promote shutoff revealed a single viral factor, encoded by ORF 37 (termed SOX), to be responsible for this phenotype; its EBV homolog (BGLF5) was shown to possess a parallel function (Ressing, M. E., Glaunsinger, B., Ganem, D., and Wiertz, E., in preparation).

B. Effectors of γ-Herpesvirus–Induced Host Shutoff

A screen of KSHV genes for their ability to promote turnover of a GFP reporter protein in 293 cells lead to the identification of ORF37 as a candidate host shutoff factor (Glaunsinger and Ganem, 2004b). In agreement with this function as well as its activity as a DNase (discussed later), the protein was named SOX (*s*hut*o*ff and e*x*onuclease). SOX expression initiates at approximately 8 h post lytic reactivation, precisely concordant with the onset of host shutoff. Unlike vhs, SOX is not packaged into the virion (Bechtel and Ganem, unpublished

observations) and therefore cannot promote host shutoff immediately upon KSHV entry. Co-expression of this gene with a GFP reporter message resulted in disappearance of the GFP mRNA, despite the fact that transcription of the gene was unaffected as were the levels of GFP DNA. It was subsequently shown that SOX significantly reduced the half-life of the GFP message. SOX-induced mRNA turnover was also shown for several additional cellular messages, confirming that its activity paralleled the shutoff phenotype observed during KSHV lytic infection described earlier (Glaunsinger and Ganem, 2004b; Glaunsinger *et al*., 2005). Finally, siRNA-mediated knockdown of SOX during KSHV replication effectively blocked turnover of the cellular messages, demonstrating that it is the dominant effector of KSHV-induced host shutoff.

Surprisingly, the gene encoding SOX is conserved across the entire herpesvirus family, where it is known to function as an alkaline exonuclease (AE) on viral DNA (Goldstein and Weller, 1998; Martinez *et al*., 1996). In addition, it has been revealed that the HSV-1 AE homolog (UL12) exhibits strand exchange activity *in vitro* and acts in conjunction with the single stranded DNA binding protein ICP8 as a recombinase (Reuven and Weller, 2005; Reuven *et al*., 2003, 2004). These functions are believed to be important for resolution of branched structures in newly replicated viral DNA, as HSV-1 UL12 mutants accumulate highly structured DNA in the nucleus leading to poor packaging of the genome and inefficient nuclear egress of the progeny virions (Shao *et al*., 1993). Although the HSV AE protein exhibits both 5′ and 3′ exonuclease activity and limited endonuclease activity on DNA, it does not possess any RNA turnover activity (Glaunsinger and Ganem, 2004b; Knopf and Weisshart, 1990; Sheaffer *et al*., 1997). Furthermore, the AE proteins have no role in host shutoff in either α- or β-herpesviruses. KSHV SOX does retain the conserved DNase activity of its homologs—as would be expected considering both the essential nature of that function and the conservation of regions known to be required for DNase activity. Thus, it appears as though evolution has endowed KSHV SOX with a novel mRNA degradation function.

In accordance with its established functions, HSV-1 AE has been shown to exhibit a strictly nuclear cellular localization. In contrast, SOX localization mapped to both the nucleus and cytoplasm of cells (Glaunsinger *et al*., 2005). SOX mutants lacking the putative nuclear localization signal (NLS) lost the majority of their nuclear staining and were no longer active in DNase assays but retained wild-type host shutoff function. These data suggest that it is the cytoplasmic fraction

of SOX that is involved in cellular mRNA turnover. In agreement with this hypothesis, Northern blotting of nuclear and cytoplasmic RNA fractions in SOX-expressing cells demonstrated a selective reduction in the cytoplasmic messages (Glaunsinger *et al.*, 2005).

Extensive mutagenesis of the SOX protein led to the identification of multiple single-function mutants that retained either the DNase or the shutoff function, thereby demonstrating that these activities are genetically separable (Glaunsinger *et al.*, 2005). The fact that shutoff-deficient mutations are distributed across the SOX protein indicates that they are likely part of one or more nonlinear motifs required for RNA turnover (Fig. 5A). The mutant that selectively lost DNase activity mapped to conserved residues of the protein, whereas the mutants that lost RNA shutoff activity mapped to numerous nonconserved residues. These observations lend further credence to the hypothesis that KSHV SOX has evolved a novel function not present outside the γ-herpesvirus family.

Given the similarity of the EBV-induced host shutoff phenotype to that of KSHV and the conservation of several residues involved in SOX-induced shutoff, it seemed likely that the viral effector of the EBV-induced mRNA turnover would be the EBV homolog of SOX, BGLF5. It has been shown that upon co-expression with BGLF5 the levels of a GFP reporter message are drastically reduced in 293T cells and mRNA half-life experiments confirmed that this reduction is due to BGLF5-induced mRNA instability (Ressing, M. E., Glaunsinger, B., Ganem, D., and Wiertz, E., in preparation). The ability of BGLF5 to promote a global host shutoff was demonstrated by infecting Sf9 insect cells with a BGLF5-expressing recombinant baculovirus; metabolic labeling showed a significant reduction in total protein synthesis in the BGLF5-expressing cells compared with uninfected cells or cells infected with a control EBNA1-expressing baculovirus (Ressing, M. E., Glaunsinger, B., Ganem, D., and Wiertz, E. J., in preparation).

C. SOX and the Exosome

Regarding the mechanism of SOX function, the simplest explanation would be that SOX has evolved an RNase activity (similar to HSV vhs) in addition to its preexisting DNase activity. However, such an activity has yet to be consistently detected using a variety of *in vitro* systems (Glaunsinger and Ganem, unpublished observations). Thus, either SOX is an RNase but requires one or more cellular cofactors not present in the assay conditions examined thus far or, alternatively, SOX is not an RNase but instead modulates or redirects the activity of

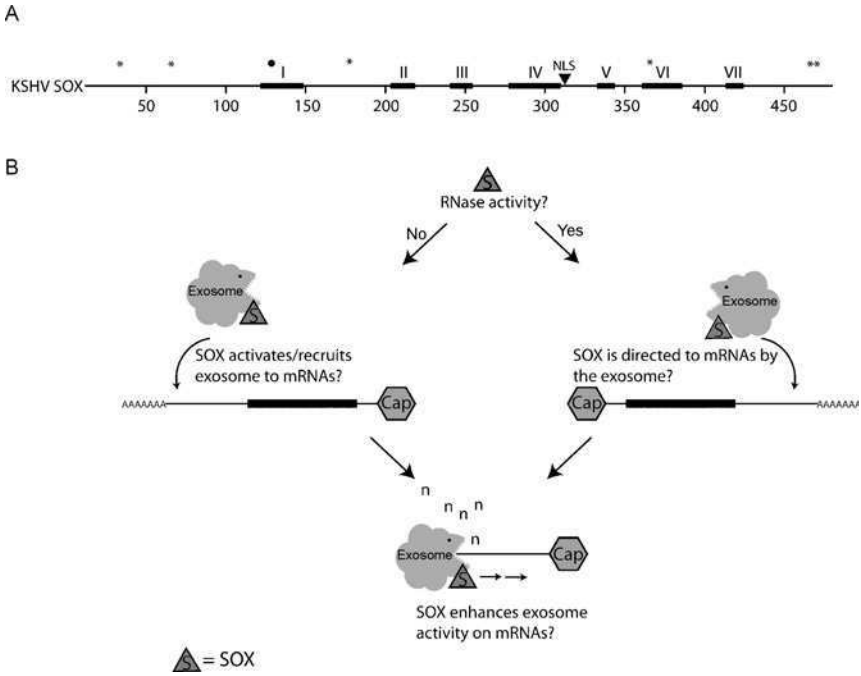

FIG 5. Organization of the SOX protein and models for its function. (A) SOX is a 486-amino acid protein containing 7 motifs present in all herpesvirus homologs that are believed to be involved in the conserved AE function (black boxes), as well as a centrally located NLS. The location of single-function SOX mutations that retain either only the DNase activity (asterisks) or only the RNA turnover function (black circle) is indicated above. (B) Possible functions of the SOX–exosome interaction. The association of SOX with several members of the mammalian exosome suggests that this group of exonucleases may assist in host shutoff, although the means by which this might occur have yet to be determined. Possible models include activation of the exosomal enzymes and/or recruitment of the exosome to mRNAs by SOX (this scenario does not require an RNase activity for SOX itself), usage of the exosome as a vechicle for SOX to access cellular mRNAs (e.g., if SOX possessed RNase activity), or SOX-induced enhancement of exosomal activity (which could occur whether or not SOX functions as an RNase).

one or more cellular mRNA degradation enzymes. Intriguingly, SOX has been shown to interact with several members of the mammalian exosome (Glaunsinger, and Ganem, unpublished observations). These interactions occur even in RNase A-treated lysates, demonstrating that they are indeed protein–protein interactions rather than nonspecific associations occuring via RNA binding. Furthermore, binding reactions using recombinant proteins purified from *E. coli* revealed

that SOX binds at least one of these enzymes (PM/Scl-100) directly, and perhaps recruits other members of the exosomal machinery via indirect interactions. This preliminary data hints that the mechanism of SOX action may involve the appropriation of one or more cellular mRNA turnover pathways (Fig. 5B). Whether these interactions result in activation of the exonucleases, or SOX-mediated recruitment of the exosome to target mRNAs is unknown. Alternatively, if SOX indeed proves to have nuclease activity, such interactions may exist to direct SOX to the normal mRNA targets of the exosome—in this model, it is the exosome that is the targeting device, not SOX.

An interaction between SOX and the PARN or hPan deadenylases has not been observed, which may suggest that SOX associates with a different deadenylase or can stimulate RNA degradation in the absence of the prior deadenylation required in normal mammalian mRNA turnover (such a model might be applied if SOX indeed has nuclease function). Alternatively, the observation that several members of distinct mRNA degradation pathways have been shown to interact with each other could provide a means for SOX to simultaneously recruit deadenylation and/or decapping enzymes via more indirect associations. It could also be envisioned to recruit the exosome to mRNAs already bound by deadenylase enzymes. Cytoplasmic SOX does not appear to localize to the punctate P bodies associated with cellular mRNA decay (Glaunsinger *et al.*, 2005). Thus, it seems unlikely that SOX activity manifests at these sites, although it is not established whether any P body components are recruited elsewhere during KSHV lytic infection. Clearly, much remains to be learned about the biochemistry of SOX-mediated mRNA turnover.

D. Escape from SOX-Induced Turnover

Although KSHV lytic infection imparts a widespread shutoff to host gene expression, expression profiling of infected TIME cells revealed that a small group of cellular mRNAs remains upregulated throughout the KSHV lytic cycle and therefore must escape SOX-mediated degradation (Glaunsinger and Ganem, 2004a). These genes are anticipated to play key roles in the KSHV lifecycle. One such transcript encodes human IL-6, a factor whose expression is common to several KSHV-associated neoplasms, including multicentric Castleman's disease and PEL (Asou *et al.*, 1998; Oksenhendler *et al.*, 2002). Another is HIF-1α, a transcription factor stabilized during hypoxia whose targets include a number of cellular factors frequently involved in tumorigenesis (Safran and Kaelin, 2003). Hypoxia can induce lytic reactivation of

KSHV and several viral lytic promoters contain hypoxia-responsive elements, perhaps indicating that HIF-1α may be involved in the expression of select viral genes (Davis *et al*., 2001; Haque *et al*., 2003). Transient co-transfection of SOX with each of the escapees reveals that these RNAs can evade SOX-mediated degradation even in uninfected cells, under conditions in which control RNAs are rapidly degraded (Glaunsinger and Ganem, 2004a). This suggests that *cis*-acting sequences (or secondary structures) in some cellular transcripts can rescue their RNA from the SOX-mediated degradative pathway.

It is of note that nearly all of the host shutoff escapees possess AREs within their 3′ UTRs, perhaps suggesting that this element somehow mediates resistance to SOX activity (Glaunsinger and Ganem, 2004a). This theory is supported by the observation that addition of the IL-6 3′ UTR to GFP confers stability to the GFP message in SOX-expressing cells (Glaunsinger and Ganem, unpublished data). In addition, our finding that SOX co-immunoprecipitates with the AUBP TTP in cells provides a tantalizing connection between these instability elements and SOX (Glaunsinger and Ganem, unpublished data). These observations are also intriguing given the similar escape of ARE-containing messages from HSV-mediated host shutoff and the association between HSV-1 vhs and TTP (Esclatine *et al*., 2004; Hsu *et al.*, 2005; Taddeo *et al*., 2002). One possibility is that these viruses although possessing distinct effectors and mechanisms of imposing host shutoff have somehow evolved similar means of protecting select cellular transcripts. It is important to keep in mind, however, that there are numerous ARE-containing messages that do not escape KSHV-mediated host shutoff and are susceptible to SOX activity, indicating that if the ARE plays a role in resistance, it is not the sole factor mediating escape (Glaunsinger and Ganem, 2004a).

VI. Future Directions and Concluding Remarks

Historically, viruses have proven to be excellent teachers of the biology of eukaryotic gene expression—virus-encoded regulators like HIV tat and rev have opened whole pathways of posttranscriptional control to experimental view. We believe that the herpesviral regulators of mammalian mRNA turnover have the potential for imparting similar lessons. Although our understanding of how the viral modulators of RNA turnover work is still fragmentary, we anticipate that the next few years will yield exciting advances in this field. In particular, the connections between ARE-containing messages, ARE-binding

proteins, and viral effectors of host shutoff should be a major focus of research. Elucidation of the precise elements and proteins responsible for directing these viral effectors of host shutoff to their mRNA targets, as well as defining how select messages (including viral ones!) escape degradation are also issues of significant interest that will likely advance our knowledge of targeted cellular mRNA decay as well.

Acknowledgments

We thank M. E. Ressing, E. J. Wiertz, and J. Bechtel for allowing us to present their unpublished results. B. G. is supported by an American Cancer Society postdoctoral fellowship.

References

Albert, T. K., Lemaire, M., van Berkum, N. L., Gentz, R., Collart, M. A., and Timmers, H. T. (2000). Isolation and characterization of human orthologs of yeast CCR4-NOT complex subunits. *Nucleic Acids Res.* **28**(3)**:**809–817.

Albrecht, G., Krowczynska, A., and Brawerman, G. (1984). Configuration of beta-globin messenger RNA in rabbit reticulocytes. Identification of sites exposed to endogenous and exogenous nucleases. *J. Mol. Biol.* **178**(4)**:**881–896.

Alderuccio, F., Chan, E. K., and Tan, E. M. (1991). Molecular characterization of an autoantigen of PM-Scl in the polymyositis/scleroderma overlap syndrome: A unique and complete human cDNA encoding an apparent 75-kD acidic protein of the nucleolar complex. *J. Exp. Med.* **173**(4)**:**941–952.

Allmang, C., Petfalski, E., Podtelejnikov, A., Mann, M., Tollervey, D., and Mitchell, P. (1999). The yeast exosome and human PM-Scl are related complexes of 3′→5′ exonucleases. *Genes Dev.* **13**(16)**:**2148–2158.

Anderson, J. S., and Parker, R. P. (1998). The 3′ to 5′ degradation of yeast mRNAs is a general mechanism for mRNA turnover that requires the SKI2 DEVH box protein and 3′ to 5′ exonucleases of the exosome complex. *EMBO J.* **17**(5)**:**1497–1506.

Andrei, M. A., Ingelfinger, D., Heintzmann, R., Achsel, T., Rivera-Pomar, R., and Luhrmann, R. (2005). A role for eIF4E and eIF4E-transporter in targeting mRNPs to mammalian processing bodies. *RNA* **11**(5)**:**717–727.

Asou, H., Said, J. W., Yang, R., Munker, R., Park, D. J., Kamada, N., and Koeffler, H. P. (1998). Mechanisms of growth control of Kaposi's sarcoma-associated herpes virus-associated primary effusion lymphoma cells. *Blood* **91**(7)**:**2475–2481.

Astrom, J., Astrom, A., and Virtanen, A. (1991). *In vitro* deadenylation of mammalian mRNA by a HeLa cell 3′ exonuclease. *EMBO J.* **10**(10)**:**3067–3071.

Baggs, J. E., and Green, C. B. (2003). Nocturnin, a deadenylase in *Xenopus laevis* retina: A mechanism for posttranscriptional control of circadian-related mRNA. *Curr. Biol.* **13**(3)**:**189–198.

Bai, R. Y., Koester, C., Ouyang, T., Hahn, S. A., Hammerschmidt, M., Peschel, C., and Duyster, J. (2002). SMIF, a Smad4-interacting protein that functions as a co-activator in TGFbeta signalling. *Nat. Cell Biol.* **4**(3)**:**181–190.

Banchereau, J., and Steinman, R. M. (1998). Dendritic cells and the control of immunity. *Nature* **392**(6673)**:**245–252.

Bashkirov, V. I., Scherthan, H., Solinger, J. A., Buerstedde, J. M., and Heyer, W. D. (1997). A mouse cytoplasmic exoribonuclease (mXRN1p) with preference for G4 tetraplex substrates. *J. Cell Biol.* **136**(4)**:**761–773.

Batterson, W., and Roizman, B. (1983). Characterization of the herpes simplex virion-associated factor responsible for the induction of alpha genes. *J. Virol.* **46** (2)**:**371–377.

Berthomme, H., Jacquemont, B., and Epstein, A. (1993). The pseudorabies virus host-shutoff homolog gene: Nucleotide sequence and comparison with alphaherpesvirus protein counterparts. *Virology* **193**(2)**:**1028–1032.

Bianchin, C., Mauxion, F., Sentis, S., Seraphin, B., and Corbo, L. (2005). Conservation of the deadenylase activity of proteins of the Caf1 family in human. *RNA* **11**(4)**:**487–494.

Binder, R., Hwang, S. P., Ratnasabapathy, R., and Williams, D. L. (1989). Degradation of apolipoprotein II mRNA occurs via endonucleolytic cleavage at 5′-AAU-3′/5′-UAA-3′ elements in single-stranded loop domains of the 3′-noncoding region. *J. Biol. Chem.* **264**(28)**:**16910–16918.

Binder, R., Horowitz, J. A., Basilion, J. P., Koeller, D. M., Klausner, R. D., and Harford, J. B. (1994). Evidence that the pathway of transferrin receptor mRNA degradation involves an endonucleolytic cleavage within the 3′ UTR and does not involve poly(A) tail shortening. *EMBO J.* **13**(8)**:**1969–1980.

Bonnieu, A., Roux, P., Marty, L., Jeanteur, P., and Piechaczyk, M. (1990). AUUUA motifs are dispensable for rapid degradation of the mouse c-myc RNA. *Oncogene* **5** (10)**:**1585–1588.

Bremer, K. A., Stevens, A., and Schoenberg, D. R. (2003). An endonuclease activity similar to Xenopus PMR1 catalyzes the degradation of normal and nonsense-containing human beta-globin mRNA in erythroid cells. *RNA* **9**(9)**:**1157–1167.

Brouwer, R., Allmang, C., Raijmakers, R., van Aarssen, Y., Egberts, W. V., Petfalski, E., van Venrooij, W. J., Tollervey, D., and Pruijn, G. J. (2001). Three novel components of the human exosome. *J. Biol. Chem.* **276**(9)**:**6177–6184.

Brown, B. D., and Harland, R. M. (1990). Endonucleolytic cleavage of a maternal homeo box mRNA in Xenopus oocytes. *Genes Dev.* **4**(11)**:**1925–1935.

Brown, B. D., Zipkin, I. D., and Harland, R. M. (1993). Sequence-specific endonucleolytic cleavage and protection of mRNA in Xenopus and Drosophila. *Genes Dev.* **7** (8)**:**1620–1631.

Brown, C. E., Tarun, S. Z., Jr., Boeck, R., and Sachs, A. B. (1996). PAN3 encodes a subunit of the Pab1p-dependent poly(A) nuclease in *Saccharomyces cerevisiae*. *Mol. Cell. Biol.* **16**(10)**:**5744–5753.

Butler, J. S. (2002). The yin and yang of the exosome. *Trends Cell Biol.* **12**(2)**:**90–96.

Campbell, M. E., Palfreyman, J. W., and Preston, C. M. (1984). Identification of herpes simplex virus DNA sequences which encode a trans-acting polypeptide responsible for stimulation of immediate early transcription. *J. Mol. Biol.* **180**(1)**:**1–19.

Cannon, J. S., Ciufo, D., Hawkins, A. L., Griffin, C. A., Borowitz, M. J., Hayward, G. S., and Ambinder, R. F. (2000). A new primary effusion lymphoma-derived cell line yields a highly infectious Kaposi's sarcoma herpesvirus-containing supernatant. *J. Virol.* **74** (21)**:**10187–10193.

Caput, D., Beutler, B., Hartog, K., Thayer, R., Brown-Shimer, S., and Cerami, A. (1986). Identification of a common nucleotide sequence in the 3′-untranslated region of mRNA molecules specifying inflammatory mediators. *Proc. Natl. Acad. Sci. USA* **83** (6)**:**1670–1674.

Carballo, E., Gilkeson, G. S., and Blackshear, P. J. (1997). Bone marrow transplantation reproduces the tristetraprolin-deficiency syndrome in recombination activating gene-2 (-/-) mice. Evidence that monocyte/macrophage progenitors may be responsible for TNFalpha overproduction. *J. Clin. Invest.* **100**(5)**:**986–995.

Carballo, E., Lai, W. S., and Blackshear, P. J. (1998). Feedback inhibition of macrophage tumor necrosis factor-alpha production by tristetraprolin. *Science* **281** (5379)**:**1001–1005.

Carballo, E., Cao, H., Lai, W. S., Kennington, E. A., Campbell, D., and Blackshear, P. J. (2001). Decreased sensitivity of tristetraprolin-deficient cells to p38 inhibitors suggests the involvement of tristetraprolin in the p38 signaling pathway. *J. Biol. Chem.* **276** (45)**:**42580–42587.

Casey, J. L., Koeller, D. M., Ramin, V. C., Klausner, R. D., and Harford, J. B. (1989). Iron regulation of transferrin receptor mRNA levels requires iron-responsive elements and a rapid turnover determinant in the 3′ untranslated region of the mRNA. *EMBO J.* **8**(12)**:**3693–3699.

Chen, C. Y., and Shyu, A. B. (1995). AU-rich elements: Characterization and importance in mRNA degradation. *Trends Biochem. Sci.* **20**(11)**:**465–470.

Chen, C. Y., Gherzi, R., Ong, S. E., Chan, E. L., Raijmakers, R., Pruijn, G. J., Stoecklin, G., Moroni, C., Mann, M., and Karin, M. (2001a). AU binding proteins recruit the exosome to degrade ARE-containing mRNAs. *Cell* **107**(4)**:**451–464.

Chen, C. Y., Xu, N., Zhu, W., and Shyu, A. B. (2004). Functional dissection of hnRNP D suggests that nuclear import is required before hnRNP D can modulate mRNA turnover in the cytoplasm. *RNA* **10**(4)**:**669–680.

Chen, J., Rappsilber, J., Chiang, Y. C., Russell, P., Mann, M., and Denis, C. L. (2001b). Purification and characterization of the 1.0 MDa CCR4-NOT complex identifies two novel components of the complex. *J. Mol. Biol.* **314**(4)**:**683–694.

Chen, J., Chiang, Y. C., and Denis, C. L. (2002). CCR4, a 3′-5′ poly(A) RNA and ssDNA exonuclease, is the catalytic component of the cytoplasmic deadenylase. *EMBO J.* **21** (6)**:**1414–1426.

Chen, N., Walsh, M. A., Liu, Y., Parker, R., and Song, H. (2005). Crystal structures of human DcpS in ligand-free and m7GDP-bound forms suggest a dynamic mechanism for scavenger mRNA decapping. *J. Mol. Biol.* **347**(4)**:**707–718.

Chung, S., Jiang, L., Cheng, S., and Furneaux, H. (1996). Purification and properties of HuD, a neuronal RNA-binding protein. *J. Biol. Chem.* **271**(19)**:**11518–11524.

Collart, M. A. (2003). Global control of gene expression in yeast by the Ccr4-Not complex. *Gene* **313:**1–16.

Cougot, N., Babajko, S., and Seraphin, B. (2004). Cytoplasmic foci are sites of mRNA decay in human cells. *J. Cell Biol.* **165**(1)**:**31–40.

Couttet, P., Fromont-Racine, M., Steel, D., Pictet, R., and Grange, T. (1997). Messenger RNA deadenylylation precedes decapping in mammalian cells. *Proc. Natl. Acad. Sci. USA* **94**(11)**:**5628–5633.

Cunningham, K. S., Hanson, M. N., and Schoenberg, D. R. (2001). Polysomal ribonuclease 1 exists in a latent form on polysomes prior to estrogen activation of mRNA decay. *Nucleic Acids Res.* **29**(5)**:**1156–1162.

Davis, D. A., Rinderknecht, A. S., Zoeteweij, J. P., Aoki, Y., Read-Connole, E. L., Tosato, G., Blauvelt, A., and Yarchoan, R. (2001). Hypoxia induces lytic replication of Kaposi sarcoma-associated herpesvirus. *Blood* **97**(10)**:**3244–3250.

Dean, J. L., Wait, R., Mahtani, K. R., Sully, G., Clark, A. R., and Saklatvala, J. (2001). The 3′ untranslated region of tumor necrosis factor alpha mRNA is a target of the mRNA-stabilizing factor HuR. *Mol. Cell. Biol.* **21**(3)**:**721–730.

Dehlin, E., Wormington, M., Korner, C. G., and Wahle, E. (2000). Cap-dependent deadenylation of mRNA. *EMBO J.* **19**(5):1079–1086.

Dember, L. M., Kim, N. D., Liu, K. Q., and Anderson, P. (1996). Individual RNA recognition motifs of TIA-1 and TIAR have different RNA binding specificities. *J. Biol. Chem.* **271**(5):2783–2788.

Dixon, D. A., Balch, G. C., Kedersha, N., Anderson, P., Zimmerman, G. A., Beauchamp, R. D., and Prescott, S. M. (2003). Regulation of cyclooxygenase-2 expression by the translational silencer TIA-1. *J. Exp. Med.* **198**(3):475–481.

Doepker, R. C., Hsu, W. L., Saffran, H. A., and Smiley, J. R. (2004). Herpes simplex virus virion host shutoff protein is stimulated by translation initiation factors eIF4B and eIF4H. *J. Virol.* **78**(9):4684–4699.

Doherty, A. J., Serpell, L. C., and Ponting, C. P. (1996). The helix-hairpin-helix DNA-binding motif: A structural basis for non-sequence-specific recognition of DNA. *Nucleic Acids Res.* **24**(13):2488–2497.

Dupin, N., Fisher, C., Kellam, P., Ariad, S., Tulliez, M., Franck, N., van Marck, E., Salmon, D., Gorin, I., Escande, J. P., Weiss, R. A., Alitalo, K., *et al.* (1999). Distribution of human herpesvirus-8 latently infected cells in Kaposi's sarcoma, multicentric Castleman's disease, and primary effusion lymphoma. *Proc. Natl. Acad. Sci. USA* **96**(8):4546–4551.

Dupressoir, A., Morel, A. P., Barbot, W., Loireau, M. P., Corbo, L., and Heidmann, T. (2001). Identification of four families of yCCR4- and Mg2+-dependent endonuclease-related proteins in higher eukaryotes, and characterization of orthologs of yCCR4 with a conserved leucine-rich repeat essential for hCAF1/hPOP2 binding. *BMC Genomics* **2**(1):9.

Elbashir, S. M., Lendeckel, W., and Tuschl, T. (2001). RNA interference is mediated by 21- and 22-nucleotide RNAs. *Genes Dev.* **15**(2):188–200.

Elgadi, M. M., and Smiley, J. R. (1999). Picornavirus internal ribosome entry site elements target RNA cleavage events induced by the herpes simplex virus virion host shutoff protein. *J. Virol.* **73**(11):9222–9231.

Elgadi, M. M., Hayes, C. E., and Smiley, J. R. (1999). The herpes simplex virus vhs protein induces endoribonucleolytic cleavage of target RNAs in cell extracts. *J. Virol.* **73**(9):7153–7164.

Esclatine, A., Taddeo, B., Evans, L., and Roizman, B. (2004). The herpes simplex virus 1 UL41 gene-dependent destabilization of cellular RNAs is selective and may be sequence-specific. *Proc. Natl. Acad. Sci. USA* **101**(10):3603–3608.

Estevez, A. M., Kempf, T., and Clayton, C. (2001). The exosome of Trypanosoma brucei. *EMBO J.* **20**(14):3831–3839.

Everly, D. N., Jr., and Read, G. S. (1997). Mutational analysis of the virion host shutoff gene (UL41) of herpes simplex virus (HSV): Characterization of HSV type 1 (HSV-1)/HSV-2 chimeras. *J. Virol.* **71**(10):7157–7166.

Everly, D. N., Jr., Feng, P., Mian, I. S., and Read, G. S. (2002). mRNA degradation by the virion host shutoff (Vhs) protein of herpes simplex virus: Genetic and biochemical evidence that Vhs is a nuclease. *J. Virol.* **76**(17):8560–8571.

Eystathioy, T., Chan, E. K., Tenenbaum, S. A., Keene, J. D., Griffith, K., and Fritzler, M. J. (2002). A phosphorylated cytoplasmic autoantigen, GW182, associates with a unique population of human mRNAs within novel cytoplasmic speckles. *Mol. Biol. Cell* **13**(4):1338–1351.

Eystathioy, T., Jakymiw, A., Chan, E. K., Seraphin, B., Cougot, N., and Fritzler, M. J. (2003). The GW182 protein colocalizes with mRNA degradation associated proteins hDcp1 and hLSm4 in cytoplasmic GW bodies. *RNA* **9**(10):1171–1173.

Fan, X. C., and Steitz, J. A. (1998a). HNS, a nuclear-cytoplasmic shuttling sequence in HuR. *Proc. Natl. Acad. Sci USA* **95**(26)**:**15293–15298.

Fan, X. C., and Steitz, J. A. (1998b). Overexpression of HuR, a nuclear-cytoplasmic shuttling protein, increases the *in vivo* stability of ARE-containing mRNAs. *EMBO J.* **17**(12)**:**3448–3460.

Feng, P., Everly, D. N., Jr., and Read, G. S. (2001). mRNA decay during herpesvirus infections: Interaction between a putative viral nuclease and a cellular translation factor. *J. Virol.* **75**(21)**:**10272–10280.

Feng, P., Everly, D. N., Jr., and Read, G. S. (2005). mRNA decay during herpes simplex virus (HSV) infections: Protein-protein interactions involving the HSV virion host shutoff protein and translation factors eIF4H and eIF4A. *J. Virol.* **79**(15)**:**9651–9664.

Fenwick, M. L. (1984). The effect of herpesviruses on cellular macromolecule synthesis. *In* "Comprehensive Virology" (H. Fraenkel-Conrat and R. K. Wagner, eds.), Vol. 19, pp. 359–390. Plenum Press, New York.

Fenwick, M. L., and Clark, J. (1982). Early and delayed shut-off of host protein synthesis in cells infected with herpes simplex virus. *J. Gen. Virol.* **61**(Pt. 1)**:**121–125.

Fenwick, M. L., and Walker, M. J. (1978). Suppression of the synthesis of cellular macromolecules by herpes simplex virus. *J. Gen. Virol.* **41:**37–51.

Fenwick, M. L., Morse, L. S., and Roizman, B. (1979). Anatomy of HSV DNA. XI. Apparent clustering of functions effecting rapid inhibition of host DNA and protein synthesis. *J. Virol.* **29:**825.

Ford, L. P., and Wilusz, J. (1999). An *in vitro* system using HeLa cytoplasmic extracts that reproduces regulated mRNA stability. *Methods* **17**(1)**:**21–27.

Ford, L. P., Bagga, P. S., and Wilusz, J. (1997). The poly(A) tail inhibits the assembly of a 3′-to-5′ exonuclease in an *in vitro* RNA stability system. *Mol. Cell. Biol.* **17**(1)**:**398–406.

Friborg, J., Jr., Kong, W., Hottiger, M. O., and Nabel, G. J. (1999). p53 inhibition by the LANA protein of KSHV protects against cell death. *Nature* **402**(6764)**:**889–894.

Fruh, K., Ahn, K., Djaballah, H., Sempe, P., van Endert, P. M., Tampe, R., Peterson, P. A., and Yang, Y. (1995). A viral inhibitor of peptide transporters for antigen presentation. *Nature* **375**(6530)**:**415–418.

Gao, M., Fritz, D. T., Ford, L. P., and Wilusz, J. (2000). Interaction between a poly(A)-specific ribonuclease and the 5′ cap influences mRNA deadenylation rates *in vitro*. *Mol. Cell* **5**(3)**:**479–488.

Gao, M., Wilusz, C. J., Peltz, S. W., and Wilusz, J. (2001). A novel mRNA-decapping activity in HeLa cytoplasmic extracts is regulated by AU-rich elements. *EMBO J.* **20** (5)**:**1134–1143.

Ge, Q., Frank, M. B., O'Brien, C., and Targoff, I. N. (1992). Cloning of a complementary DNA coding for the 100-kD antigenic protein of the PM-Scl autoantigen. *J. Clin. Invest.* **90**(2)**:**559–570.

Gelpi, C., Alguero, A., Angeles Martinez, M., Vidal, S., Juarez, C., and Rodriguez-Sanchez, J. L. (1990). Identification of protein components reactive with anti-PM/Scl autoantibodies. *Clin. Exp. Immunol.* **81**(1)**:**59–64.

Gherzi, R., Lee, K. Y., Briata, P., Wegmuller, D., Moroni, C., Karin, M., and Chen, C. Y. (2004). A KH domain RNA binding protein, KSRP, promotes ARE-directed mRNA turnover by recruiting the degradation machinery. *Mol. Cell* **14**(5)**:**571–583.

Glaunsinger, B., and Ganem, D. (2004a). Highly selective escape from KSHV-mediated host mRNA shutoff and its implications for viral pathogenesis. *J. Exp. Med.* **200**(3)**:**391–398.

Glaunsinger, B., and Ganem, D. (2004b). Lytic KSHV infection inhibits host gene expression by accelerating global mRNA turnover. *Mol. Cell* **13**(5)**:**713–723.

Glaunsinger, B., Chavez, L., and Ganem, D. (2005). The exonuclease and host shutoff functions of the SOX protein of Kaposi's sarcoma-associated herpesvirus are genetically separable. *J. Virol.* **79**(12)**:**7396–7401.

Goldstein, J. N., and Weller, S. K. (1998). *In vitro* processing of herpes simplex virus type 1 DNA replication intermediates by the viral alkaline nuclease, UL12. *J. Virol.* **72** (11)**:**8772–8781.

Gopinath, R. S., Ambagala, A. P., Hinkley, S., and Srikumaran, S. (2002). Effects of virion host shut-off activity of bovine herpesvirus 1 on MHC class I expression. *Viral Immunol.* **15**(4)**:**595–608.

Gradoville, L., Gerlach, J., Grogan, E., Shedd, D., Nikiforow, S., Metroka, C., and Miller, G. (2000). Kaposi's sarcoma-associated herpesvirus open reading frame 50/Rta protein activates the entire viral lytic cycle in the HH-B2 primary effusion lymphoma cell line. *J. Virol.* **74**(13)**:**6207–6212.

Green, C. B., and Besharse, J. C. (1996). Identification of a novel vertebrate circadian clock-regulated gene encoding the protein nocturnin. *Proc. Natl. Acad. Sci. USA* **93** (25)**:**14884–14888.

Gringhuis, S. I., Garcia-Vallejo, J. J., van Het Hof, B., and van Dijk, W. (2005). Convergent actions of I(kappa)B kinase beta and protein kinase C(delta) modulate mRNA stability through phosphorylation of 14–3-3beta complexed with tristetraprolin. *Mol. Cell. Biol.* **25**(15)**:**6454–6463.

Grosset, C., Chen, C. Y., Xu, N., Sonenberg, N., Jacquemin-Sablon, H., and Shyu, A. B. (2000). A mechanism for translationally coupled mRNA turnover: Interaction between the poly(A) tail and a c-fos RNA coding determinant via a protein complex. *Cell* **103** (1)**:**29–40.

Gu, M., Fabrega, C., Liu, S. W., Liu, H., Kiledjian, M., and Lima, C. D. (2004). Insights into the structure, mechanism, and regulation of scavenger mRNA decapping activity. *Mol. Cell* **14**(1)**:**67–80.

Hall, M. P., Huang, S., and Black, D. L. (2004). Differentiation-induced colocalization of the KH-type splicing regulatory protein with polypyrimidine tract binding protein and the c-src pre-mRNA. *Mol. Biol. Cell* **15**(2)**:**774–786.

Hammond, S. M., Boettcher, S., Caudy, A. A., Kobayashi, R., and Hannon, G. J. (2001). Argonaute2, a link between genetic and biochemical analyses of RNAi. *Science* **293** (5532)**:**1146–1150.

Haque, M., Davis, D. A., Wang, V., Widmer, I., and Yarchoan, R. (2003). Kaposi's sarcoma-associated herpesvirus (human herpesvirus 8) contains hypoxia response elements: Relevance to lytic induction by hypoxia. *J. Virol.* **77**(12)**:**6761–6768.

Hardwicke, M. A., and Sandri-Goldin, R. M. (1994). The herpes simplex virus regulatory protein ICP27 contributes to the decrease in cellular mRNA levels during infection. *J. Virol.* **68**(8)**:**4797–4810.

Harle, P., Sainz, B., Jr., Carr, D. J., and Halford, W. P. (2002). The immediate-early protein, ICP0, is essential for the resistance of herpes simplex virus to interferon-alpha/beta. *Virology* **293**(2)**:**295–304.

Herr, W. (1998). The herpes simplex virus VP16-induced complex: Mechanisms of combinatorial transcriptional regulation. *Cold Spring Harbor Symp. Quant. Biol.* **63:**599–607.

Herr, W., and Cleary, M. A. (1995). The POU domain: Versatility in transcriptional regulation by a flexible two-in-one DNA-binding domain. *Genes Dev.* **9**(14)**:**1679–1693.

Hershey, J. W. B., and Merrick, W. C. (2000). Pathway and mechanism of initiation of protein synthesis. *In* "Translational Control of Gene Expression" (N. Sonenberg, J. W. B. Hershey, and M. B. Mathews, eds.), pp. 33–89. Cold Spring Harbor Press, Cold Spring Harbor, New York.

Hill, A. B., Barnett, B. C., McMichael, A. J., and McGeoch, D. J. (1994). HLA class I molecules are not transported to the cell surface in cells infected with herpes simplex virus types 1 and 2. *J. Immunol.* **152**(6)**:**2736–2741.

Hill, A., Jugovic, P., York, I., Russ, G., Bennink, J., Yewdell, J., Ploegh, H., and Johnson, D. (1995). Herpes simplex virus turns off the TAP to evade host immunity. *Nature* **375** (6530)**:**411–415.

Hsu, W. L., Saffran, H. A., and Smiley, J. R. (2005). Herpes simplex virus infection stabilizes cellular IEX-1 mRNA. *J. Virol.* **79**(7)**:**4090–4098.

Hua, J., Garner, R., and Paetkau, V. (1993). An RNasin-resistant ribonuclease selective for interleukin 2 mRNA. *Nucleic Acids Res.* **21**(1)**:**155–162.

Ingelfinger, D., Arndt-Jovin, D. J., Luhrmann, R., and Achsel, T. (2002). The human LSm1-7 proteins colocalize with the mRNA-degrading enzymes Dcp1/2 and Xrnl in distinct cytoplasmic foci. *RNA* **8**(12)**:**1489–1501.

Ioannidis, P., Havredaki, M., Courtis, N., and Trangas, T. (1996). *In vivo* generation of 3′ and 5′ truncated species in the process of c-myc mRNA decay. *Nucleic Acids Res.* **24** (24)**:**4969–4977.

Jones, F. E., Smibert, C. A., and Smiley, J. R. (1995). Mutational analysis of the herpes simplex virus virion host shutoff protein: Evidence that vhs functions in the absence of other viral proteins. *J. Virol.* **69**(8)**:**4863–4871.

Karr, B. M., and Read, G. S. (1999). The virion host shutoff function of herpes simplex virus degrades the 5′ end of a target mRNA before the 3′ end. *Virology* **264**(1)**:**195–204.

Kedersha, N., Stoecklin, G., Ayodele, M., Yacono, P., Lykke-Andersen, J., Fitzler, M. J., Scheuner, D., Kaufman, R. J., Golan, D. E., and Anderson, P. (2005). Stress granules and processing bodies are dynamically linked sites of mRNP remodeling. *J. Cell Biol.* **169**(6)**:**871–884.

Kedersha, N. L., Gupta, M., Li, W., Miller, I., and Anderson, P. (1999). RNA-binding proteins TIA-1 and TIAR link the phosphorylation of eIF-2 alpha to the assembly of mammalian stress granules. *J. Cell Biol.* **147**(7)**:**1431–1442.

Kedersha, N., Stoecklin, G., Ayodele, M., Yacono, P., Lykke-Andersen, J., Fitzler, M. J., Scheuner, D., Kaufman, R. J., Golan, D. E., and Anderson, P. (2005). Stress granules and processing bodies are dynamically linked sites of mRNP remodeling. *J. Cell Biol.* **169**(6)**:**871–884.

Khanna, R., and Kiledjian, M. (2004). Poly(A)-binding-protein-mediated regulation of hDcp2 decapping *in vitro*. *EMBO J.* **23**(9)**:**1968–1976.

Kieff, E. (1996). Epstein-Barr virus and its replication. *In* "Fields Virology" (B. N. Fields, D. M. Knipe, and P. M. Howley, eds.), 3rd edn., pp. 2343–2396. Lippincott-Raven, Philidelphia.

Kiledjian, M., DeMaria, C. T., Brewer, G., and Novick, K. (1997). Identification of AUF1 (heterogeneous nuclear ribonucleoprotein D) as a component of the alpha-globin mRNA stability complex. *Mol. Cell. Biol.* **17**(8)**:**4870–4876.

Knez, J., Bilan, P. T., and Capone, J. P. (2003). A single amino acid substitution in herpes simplex virus type 1 VP16 inhibits binding to the virion host shutoff protein and is incompatible with virus growth. *J. Virol.* **77**(5)**:**2892–2902.

Knopf, C. W., and Weisshart, K. (1990). Comparison of exonucleolytic activities of herpes simplex virus type-1 DNA polymerase and DNase. *Eur. J. Biochem.* **191**(2)**:**263–273.

Koppers-Lalic, D., Rijsewijk, F. A., Verschuren, S. B., van Gaans-Van den Brink, J. A., Neisig, A., Ressing, M. E., Neefjes, J., and Wiertz, E. J. (2001). The UL41-encoded virion host shutoff (vhs) protein and vhs-independent mechanisms are responsible for down-regulation of MHC class I molecules by bovine herpesvirus 1. *J. Gen. Virol.* **82** (Pt. 9)**:**2071–2081.

Korner, C. G., and Wahle, E. (1997). Poly(A) tail shortening by a mammalian poly(A)-specific 3′-exoribonuclease. *J. Biol. Chem.* **272**(16)**:**10448–10456.

Korner, C. G., Wormington, M., Muckenthaler, M., Schneider, S., Dehlin, E., and Wahle, E. (1998). The deadenylating nuclease (DAN) is involved in poly(A) tail removal during the meiotic maturation of Xenopus oocytes. *EMBO J.* **17**(18)**:**5427–5437.

Kowalski, J., and Denhardt, D. T. (1989). Regulation of the mRNA for monocyte-derived neutrophil-activating peptide in differentiating HL60 promyelocytes. *Mol. Cell. Biol.* **9**(5)**:**1946–1957.

Krikorian, C. R., and Read, G. S. (1991). *In vitro* mRNA degradation system to study the virion host shutoff function of herpes simplex virus. *J. Virol.* **65**(1)**:**112–122.

Kruse, M., Rosorius, O., Kratzer, F., Stelz, G., Kuhnt, C., Schuler, G., Hauber, J., and Steinkasserer, A. (2000). Mature dendritic cells infected with herpes simplex virus type 1 exhibit inhibited T-cell stimulatory capacity. *J. Virol.* **74**(15)**:**7127–7136.

Kushner, S. R. (2004). mRNA decay in prokaryotes and eukaryotes: Different approaches to a similar problem. *IUBMB Life* **56**(10)**:**585–594.

Kwong, A. D., and Frenkel, N. (1987). Herpes simplex virus-infected cells contain a function(s) that destabilizes both host and viral mRNAs. *Proc. Natl. Acad. Sci. USA* **84**(7)**:**1926–1930.

Kwong, A. D., and Frenkel, N. (1989). The herpes simplex virus virion host shutoff function. *J. Virol.* **63**(11)**:**4834–4839.

Kwong, A. D., Kruper, J. A., and Frenkel, N. (1988). Herpes simplex virus virion host shutoff function. *J. Virol.* **62**(3)**:**912–921.

Lai, W. S., Carballo, E., Thorn, J. M., Kennington, E. A., and Blackshear, P. J. (2000). Interactions of CCCH zinc finger proteins with mRNA. Binding of tristetraprolin-related zinc finger proteins to Au-rich elements and destabilization of mRNA. *J. Biol. Chem.* **275**(23)**:**17827–17837.

Lai, W. S., Kennington, E. A., and Blackshear, P. J. (2003). Tristetraprolin and its family members can promote the cell-free deadenylation of AU-rich element-containing mRNAs by poly(A) ribonuclease. *Mol. Cell. Biol.* **23**(11)**:**3798–3812.

Lam, Q., Smibert, C. A., Koop, K. E., Lavery, C., Capone, J. P., Weinheimer, S. P., and Smiley, J. R. (1996). Herpes simplex virus VP16 rescues viral mRNA from destruction by the virion host shutoff function. *EMBO J.* **15**(10)**:**2575–2581.

Laroia, G., and Schneider, R. J. (2002). Alternate exon insertion controls selective ubiquitination and degradation of different AUF1 protein isoforms. *Nucleic Acids Res.* **30**(14)**:**3052–3058.

Laroia, G., Cuesta, R., Brewer, G., and Schneider, R. J. (1999). Control of mRNA decay by heat shock-ubiquitin-proteasome pathway. *Science* **284**(5413)**:**499–502.

Laroia, G., Sarkar, B., and Schneider, R. J. (2002). Ubiquitin-dependent mechanism regulates rapid turnover of AU-rich cytokine mRNAs. *Proc. Natl. Acad. Sci. USA* **99**(4)**:**1842–1846.

Lee, C. H., Leeds, P., and Ross, J. (1998). Purification and characterization of a polysome-associated endoribonuclease that degrades c-myc mRNA *in vitro*. *J. Biol. Chem.* **273**(39)**:**25261–25271.

Lehner, B., and Sanderson, C. M. (2004). A protein interaction framework for human mRNA degradation. *Genome Res.* **14**(7)**:**1315–1323.

Leib, D. A., Harrison, T. E., Laslo, K. M., Machalek, M. A., Moorman, N. J., and Virgin, H. W. (1999). Interferons regulate the phenotype of wild-type and mutant herpes simplex viruses *in vivo*. *J. Exp. Med.* **189**(4)**:**663–672.

Levy, N. S., Chung, S., Furneaux, H., and Levy, A. P. (1998). Hypoxic stabilization of vascular endothelial growth factor mRNA by the RNA-binding protein HuR. *J. Biol. Chem.* **273**(11)**:**6417–6423.

Lim, S. K., and Maquat, L. E. (1992). Human beta-globin mRNAs that harbor a nonsense codon are degraded in murine erythroid tissues to intermediates lacking regions of exon I or exons I and II that have a cap-like structure at the 5′ termini. *EMBO J.* **11** (9)**:**3271–3278.

Lin, H. W., Chang, Y. Y., Wong, M. L., Lin, J. W., and Chang, T. J. (2004a). Functional analysis of virion host shutoff protein of pseudorabies virus. *Virology* **324**(2)**:** 412–418.

Lin, R., Noyce, R. S., Collins, S. E., Everett, R. D., and Mossman, K. L. (2004b). The herpes simplex virus ICP0 RING finger domain inhibits IRF3- and IRF7-mediated activation of interferon-stimulated genes. *J. Virol.* **78**(4)**:**1675–1684.

Lingel, A., Simon, B., Izaurralde, E., and Sattler, M. (2003). Structure and nucleic-acid binding of the Drosophila Argonaute 2 PAZ domain. *Nature* **426**(6965)**:**465–469.

Lingel, A., Simon, B., Izaurralde, E., and Sattler, M. (2004). Nucleic acid 3′-end recognition by the Argonaute2 PAZ domain. *Nat. Struct. Mol. Biol.* **11**(6)**:**576–577.

Liu, H., Rodgers, N. D., Jiao, X., and Kiledjian, M. (2002). The scavenger mRNA decapping enzyme DcpS is a member of the HIT family of pyrophosphatases. *EMBO J.* **21** (17)**:**4699–4708.

Liu, J., Carmell, M. A., Rivas, F. V., Marsden, C. G., Thomson, J. M., Song, J. J., Hammond, S. M., Joshua-Tor, L., and Hannon, G. J. (2004a). Argonaute2 is the catalytic engine of mammalian RNAi. *Science* **305**(5689)**:**1437–1441.

Liu, S. W., Jiao, X., Liu, H., Gu, M., Lima, C. D., and Kiledjian, M. (2004b). Functional analysis of mRNA scavenger decapping enzymes. *RNA* **10**(9)**:**1412–1422.

Loflin, P., Chen, C. Y., and Shyu, A. B. (1999). Unraveling a cytoplasmic role for hnRNP D in the *in vivo* mRNA destabilization directed by the AU-rich element. *Genes Dev.* **13** (14)**:**1884–1897.

Lorentzen, E., Walter, P., Fribourg, S., Evguenieva-Hackenberg, E., Klug, G., and Conti, E. (2005). The archaeal exosome core is a hexameric ring structure with three catalytic subunits. *Nat. Struct. Mol. Biol.* **12**(7)**:**575–581.

Lu, P., Saffran, H. A., and Smiley, J. R. (2001). The vhs1 mutant form of herpes simplex virus virion host shutoff protein retains significant internal ribosome entry site-directed RNA cleavage activity. *J. Virol.* **75**(2)**:**1072–1076.

Lukac, D. M., Renne, R., Kirshner, J. R., and Ganem, D. (1998). Reactivation of Kaposi's sarcoma-associated herpesvirus infection from latency by expression of the ORF 50 transactivator, a homolog of the EBV R protein. *Virology* **252**(2)**:**304–312.

Lykke-Andersen, J. (2002). Identification of a human decapping complex associated with hUpf proteins in nonsense-mediated decay. *Mol. Cell. Biol.* **22**(23)**:**8114–8121.

Lykke-Andersen, J., and Wagner, E. (2005). Recruitment and activation of mRNA decay enzymes by two ARE-mediated decay activation domains in the proteins TTP and BRF-1. *Genes Dev.* **19**(3)**:**351–361.

Ma, W. J., Cheng, S., Campbell, C., Wright, A., and Furneaux, H. (1996). Cloning and characterization of HuR, a ubiquitously expressed Elav-like protein. *J. Biol. Chem.* **271**(14)**:**8144–8151.

Ma, W. J., Chung, S., and Furneaux, H. (1997). The Elav-like proteins bind to AU-rich elements and to the poly(A) tail of mRNA. *Nucleic Acids Res.* **25**(18)**:**3564–3569.

Ma, J. B., Ye, K., and Patel, D. J. (2004). Structural basis for overhang-specific small interfering RNA recognition by the PAZ domain. *Nature* **429**(6989)**:**318–322.

Mahtani, K. R., Brook, M., Dean, J. L., Sully, G., Saklatvala, J., and Clark, A. R. (2001). Mitogen-activated protein kinase p38 controls the expression and posttranslational modification of tristetraprolin, a regulator of tumor necrosis factor alpha mRNA stability. *Mol. Cell. Biol.* **21**(19)**:**6461–6469.

Martinez, R., Sarisky, R. T., Weber, P. C., and Weller, S. K. (1996). Herpes simplex virus type 1 alkaline nuclease is required for efficient processing of viral DNA replication intermediates. *J. Virol.* **70**(4)**:**2075–2085.

Martinez, J., Ren, Y. G., Thuresson, A. C., Hellman, U., Astrom, J., and Virtanen, A. (2000). A 54-kDa fragment of the poly(A)-specific ribonuclease is an oligomeric, processive, and cap-interacting poly(A)-specific 3′ exonuclease. *J. Biol. Chem.* **275**(31)**:**24222–24230.

Martinez, J., Ren, Y. G., Nilsson, P., Ehrenberg, M., and Virtanen, A. (2001). The mRNA cap structure stimulates rate of poly(A) removal and amplifies processivity of degradation. *J. Biol. Chem.* **276**(30)**:**27923–27929.

Martinez, J., Patkaniowska, A., Urlaub, H., Luhrmann, R., and Tuschl, T. (2002). Single-stranded antisense siRNAs guide target RNA cleavage in RNAi. *Cell* **110**(5)**:**563–574.

Matsumoto-Taniura, N., Pirollet, F., Monroe, R., Gerace, L., and Westendorf, J. M. (1996). Identification of novel M phase phosphoproteins by expression cloning. *Mol. Biol. Cell* **7**(9)**:**1455–1469.

Mayman, B. A., and Nishioka, Y. (1985). Differential stability of host mRNAs in Friend erythroleukemia cells infected with herpes simplex virus type 1. *J. Virol.* **53**(1)**:**1–6.

McGrath, B. M., and Stevely, W. S. (1980). The characteristics of the cell-free translation of mRNA from cells infected with the herpes virus pseudorabies virus. *J. Gen. Virol.* **49**(2)**:**323–332.

McLauchlan, J., Addison, C., Craigie, M. C., and Rixon, F. J. (1992). Noninfectious L-particles supply functions which can facilitate infection by HSV-1. *Virology* **190**(2)**:**682–688.

Meinsma, D., Holthuizen, P. E., Van den Brande, J. L., and Sussenbach, J. S. (1991). Specific endonucleolytic cleavage of IGF-II mRNAs. *Biochem. Biophys. Res. Commun.* **179**(3)**:**1509–1516.

Meyer, S., Temme, C., and Wahle, E. (2004). Messenger RNA turnover in eukaryotes: Pathways and enzymes. *Crit. Rev. Biochem. Mol. Biol.* **39**(4)**:**197–216.

Miller, G., Rigsby, M. O., Heston, L., Grogan, E., Sun, R., Metroka, C., Levy, J. A., Gao, S. J., Chang, Y., and Moore, P. (1996). Antibodies to butyrate-inducible antigens of Kaposi's sarcoma-associated herpesvirus in patients with HIV-1 infection. *N. Engl. J. Med.* **334**(20)**:**1292–1297.

Min, H., Turck, C. W., Nikolic, J. M., and Black, D. L. (1997). A new regulatory protein, KSRP, mediates exon inclusion through an intronic splicing enhancer. *Genes Dev.* **11**(8)**:**1023–1036.

Ming, X. F., Stoecklin, G., Lu, M., Looser, R., and Moroni, C. (2001). Parallel and independent regulation of interleukin-3 mRNA turnover by phosphatidylinositol 3-kinase and p38 mitogen-activated protein kinase. *Mol. Cell. Biol.* **21**(17)**:**5778–5789.

Mitchell, P., and Tollervey, D. (2000). Musing on the structural organization of the exosome complex. *Nat. Struct. Biol.* **7**(10)**:**843–846.

Mitchell, P., Petfalski, E., Shevchenko, A., Mann, M., and Tollervey, D. (1997). The exosome: A conserved eukaryotic RNA processing complex containing multiple 3′ → 5′ exoribonucleases. *Cell* **91**(4)**:**457–466.

Moore, P., and Chang, Y. (2001). Kaposi's sarcoma-associated herpesvirus. *In* "Fields Virology" (D. M. Knipe and P. M. Howley, eds.), Vol. 2, pp. 2803–2833. Lippincott Williams and Wilkins, Philadelphia.

Mossman, K. L., Saffran, H. A., and Smiley, J. R. (2000). Herpes simplex virus ICP0 mutants are hypersensitive to interferon. *J. Virol.* **74**(4)**:**2052–2056.

Mukherjee, D., Gao, M., O'Connor, J. P., Raijmakers, R., Pruijn, G., Lutz, C. S., and Wilusz, J. (2002). The mammalian exosome mediates the efficient degradation of mRNAs that contain AU-rich elements. *EMBO J.* **21**(1–2)**:**165–174.

Munroe, D., and Jacobson, A. (1990). mRNA poly(A) tail, a 3′ enhancer of translational initiation. *Mol. Cell. Biol.* **10**(7)**:**3441–3455.

Murphy, J. A., Duerst, R. J., Smith, T. J., and Morrison, L. A. (2003). Herpes simplex virus type 2 virion host shutoff protein regulates alpha/beta interferon but not adaptive immune responses during primary infection *in vivo*. *J. Virol.* **77**(17)**:**9337–9345.

Nakai, H., Maxwell, I. H., and Pizer, L. I. (1982). Herpesvirus infection alters the steady-state levels of cellular polyadenylated RNA in polyoma virus-transformed BHK cells. *J. Virol.* **42**(3)**:**1131–1134.

Nishioka, Y., and Silverstein, S. (1977). Degradation of cellular mRNA during infection by herpes simplex virus. *Proc. Natl. Acad. Sci. USA* **74**(6)**:**2370–2374.

Nishioka, Y., and Silverstein, S. (1978). Requirement of protein synthesis for the degradation of host mRNA in Friend erythroleukemia cells infected with herpes simplex virus type 1. *J. Virol.* **27**(3)**:**619–627.

Nykanen, A., Haley, B., and Zamore, P. D. (2001). ATP requirements and small interfering RNA structure in the RNA interference pathway. *Cell* **107**(3)**:**309–321.

Oksenhendler, E., Boulanger, E., Galicier, L., Du, M. Q., Dupin, N., Diss, T. C., Hamoudi, R., Daniel, M. T., Agbalika, F., Boshoff, C., Clauvel, J. P., Isaacson, P. G., *et al.* (2002). High incidence of Kaposi sarcoma-associated herpesvirus-related non-Hodgkin lymphoma in patients with HIV infection and multicentric Castleman disease. *Blood* **99** (7)**:**2331–2336.

Orban, T. I., and Izaurralde, E. (2005). Decay of mRNAs targeted by RISC requires XRN1, the Ski complex, and the exosome. *RNA* **11**(4)**:**459–469.

Oroskar, A. A., and Read, G. S. (1989). Control of mRNA stability by the virion host shutoff function of herpes simplex virus. *J. Virol.* **63**(5)**:**1897–1906.

Pak, A. S., Everly, D. N., Knight, K., and Read, G. S. (1995). The virion host shutoff protein of herpes simplex virus inhibits reporter gene expression in the absence of other viral gene products. *Virology* **211**(2)**:**491–506.

Parker, R., and Song, H. (2004). The enzymes and control of eukaryotic mRNA turnover. *Nat. Struct. Mol. Biol.* **11**(2)**:**121–127.

Pastori, R. L., Moskaitis, J. E., Buzek, S. W., and Schoenberg, D. R. (1991a). Coordinate estrogen-regulated instability of serum protein-coding messenger RNAs in *Xenopus laevis*. *Mol. Endocrinol.* **5**(4)**:**461–468.

Pastori, R. L., Moskaitis, J. E., and Schoenberg, D. R. (1991b). Estrogen-induced ribonuclease activity in Xenopus liver. *Biochemistry* **30**(43)**:**10490–10498.

Peng, S. S., Chen, C. Y., and Shyu, A. B. (1996). Functional characterization of a non-AUUUA AU-rich element from the c-jun proto-oncogene mRNA: Evidence for a novel class of AU-rich elements. *Mol. Cell. Biol.* **16**(4)**:**1490–1499.

Phillips, R. S., Ramos, S. B., and Blackshear, P. J. (2002). Members of the tristetraprolin family of tandem CCCH zinc finger proteins exhibit CRM1-dependent nucleocytoplasmic shuttling. *J. Biol. Chem.* **277**(13)**:**11606–11613.

Piccirillo, C., Khanna, R., and Kiledjian, M. (2003). Functional characterization of the mammalian mRNA decapping enzyme hDcp2. *RNA* **9**(9)**:**1138–1147.

Piecyk, M., Wax, S., Beck, A. R., Kedersha, N., Gupta, M., Maritim, B., Chen, S., Gueydan, C., Kruys, V., Streuli, M., and Anderson, P. (2000). TIA-1 is a translational silencer that selectively regulates the expression of TNF-alpha. *EMBO J.* **19** (15)**:**4154–4163.

Pizer, L. I., and Beard, P. (1976). The effect of herpesvirus infection on mRNA in polyoma virus-transformed cells. *Virology* **75:**477.

Prechtel, A. T., Turza, N. M., Kobelt, D. J., Eisemann, J. I., Coffin, R. S., McGrath, Y., Hacker, C., Ju, X., Zenke, M., and Steinkasserer, A. (2005). Infection of mature dendritic cells with herpes simplex virus type 1 dramatically reduces lymphoid chemokine-mediated migration. *J. Gen. Virol.* **86**(Pt. 6)**:**1645–1657.

Radkov, S. A., Kellam, P., and Boshoff, C. (2000). The latent nuclear antigen of Kaposi sarcoma-associated herpesvirus targets the retinoblastoma-E2F pathway and with the oncogene Hras transforms primary rat cells. *Nat. Med.* **6**(10)**:**1121–1127.

Raijmakers, R., Egberts, W. V., van Venrooij, W. J., and Pruijn, G. J. (2002). Protein-protein interactions between human exosome components support the assembly of RNase PH-type subunits into a six-membered PNPase-like ring. *J. Mol. Biol.* **323**(4)**:**653–663.

Raijmakers, R., Egberts, W. V., van Venrooij, W. J., and Pruijn, G. J. (2003). The association of the human PM/Scl-75 autoantigen with the exosome is dependent on a newly identified N terminus. *J. Biol. Chem.* **278**(33)**:**30698–30704.

Raijmakers, R., Schilders, G., and Pruijn, G. J. (2004). The exosome, a molecular machine for controlled RNA degradation in both nucleus and cytoplasm. *Eur. J. Cell Biol.* **83**(5)**:**175–183.

Raineri, I., Wegmueller, D., Gross, B., Certa, U., and Moroni, C. (2004). Roles of AUF1 isoforms, HuR and BRF1 in ARE-dependent mRNA turnover studied by RNA interference. *Nucleic Acids Res.* **32**(4)**:**1279–1288.

Ramos, S. B., Stumpo, D. J., Kennington, E. A., Phillips, R. S., Bock, C. B., Ribeiro-Neto, F., and Blackshear, P. J. (2004). The CCCH tandem zinc-finger protein Zfp36l2 is crucial for female fertility and early embryonic development. *Development* **131**(19)**:**4883–4893.

Rand, T. A., Ginalski, K., Grishin, N. V., and Wang, X. (2004). Biochemical identification of Argonaute 2 as the sole protein required for RNA-induced silencing complex activity. *Proc. Natl. Acad. Sci. USA* **101**(40)**:**14385–14389.

Read, G. S., and Frenkel, N. (1983). Herpes simplex virus mutants defective in the virion-associated shutoff of host polypeptide synthesis and exhibiting abnormal synthesis of alpha (immediate early) viral polypeptides. *J. Virol.* **46**(2)**:**498–512.

Read, G. S., Karr, B. M., and Knight, K. (1993). Isolation of a herpes simplex virus type 1 mutant with a deletion in the virion host shutoff gene and identification of multiple forms of the vhs (UL41) polypeptide. *J. Virol.* **67**(12)**:**7149–7160.

Reimer, G. (1990). Autoantibodies against nuclear, nucleolar, and mitochondrial antigens in systemic sclerosis (scleroderma). *Rheum. Dis. Clin. North Am.* **16**(1)**:**169–183.

Ren, Y. G., Martinez, J., and Virtanen, A. (2002). Identification of the active site of poly (A)-specific ribonuclease by site-directed mutagenesis and Fe(2+)-mediated cleavage. *J. Biol. Chem.* **277**(8)**:**5982–5987.

Ren, Y. G., Kirsebom, L. A., and Virtanen, A. (2004). Coordination of divalent metal ions in the active site of poly(A)-specific ribonuclease. *J. Biol. Chem.* **279**(47)**:**48702–48706.

Ressing, M. E., van Leeuwen, D., Verreck, F. A., Keating, S., Gomez, R., Franken, K. L., Ottenhoff, T. H., Spriggs, M., Schumacher, T. N., Hutt-Fletcher, L. M., Rowe, M., and Wiertz, E. J. (2005). Epstein-Barr virus gp42 is posttranslationally modified to produce soluble gp42 that mediates HLA class II immune evasion. *J. Virol.* **79**(2)**:**841–852.

Reuven, N. B., and Weller, S. K. (2005). Herpes simplex virus type 1 single-strand DNA binding protein ICP8 enhances the nuclease activity of the UL12 alkaline nuclease by increasing its processivity. *J. Virol.* **79**(14)**:**9356–9358.

Reuven, N. B., Staire, A. E., Myers, R. S., and Weller, S. K. (2003). The herpes simplex virus type 1 alkaline nuclease and single-stranded DNA binding protein mediate strand exchange *in vitro*. *J. Virol.* **77**(13)**:**7425–7433.

Reuven, N. B., Willcox, S., Griffith, J. D., and Weller, S. K. (2004). Catalysis of strand exchange by the HSV-1 UL12 and ICP8 proteins: Potent ICP8 recombinase activity is revealed upon resection of dsDNA substrate by nuclease. *J. Mol. Biol.* **342**(1)**:**57–71.

Richter, N. J., Rogers, G. W., Jr., Hensold, J. O., and Merrick, W. C. (1999). Further biochemical and kinetic characterization of human eukaryotic initiation factor 4H. *J. Biol. Chem.* **274**(50)**:**35415–35424.

Rigby, W. F., Roy, K., Collins, J., Rigby, S., Connolly, J. E., Bloch, D. B., and Brooks, S. A. (2005). Structure/function analysis of tristetraprolin (TTP): p38 stress-activated protein kinase and lipopolysaccharide stimulation do not alter TTP function. *J. Immunol.* **174**(12)**:**7883–7893.

Rogers, G. W., Jr., Richter, N. J., Lima, W. F., and Merrick, W. C. (2001). Modulation of the helicase activity of eIF4A by eIF4B, eIF4H, and eIF4F. *J. Biol. Chem.* **276** (33)**:**30914–30922.

Roizman, B., and Knipe, D. M. (2001). Herpes simplex viruses and their replication. *In* "Fields Virology" (D. M. Knipe, P. M. Howley, D. E. Griffin, R. A. Lamb, M. A. Martin, B. Roizman, and S. E. Strauss, eds.), 4th edn., pp. 2381–2398. Lippincott Williams & Wilkins, Philadelphia.

Sachs, A. B., and Deardorff, J. A. (1992). Translation initiation requires the PAB-dependent poly(A) ribonuclease in yeast. *Cell* **70**(6)**:**961–973.

Safran, M., and Kaelin, W. G., Jr. (2003). HIF hydroxylation and the mammalian oxygen-sensing pathway. *J. Clin. Invest.* **111**(6)**:**779–783.

Salio, M., Cella, M., Suter, M., and Lanzavecchia, A. (1999). Inhibition of dendritic cell maturation by herpes simplex virus. *Eur. J. Immunol.* **29**(10)**:**3245–3253.

Samady, L., Costigliola, E., MacCormac, L., McGrath, Y., Cleverley, S., Lilley, C. E., Smith, J., Latchman, D. S., Chain, B., and Coffin, R. S. (2003). Deletion of the virion host shutoff protein (vhs) from herpes simplex virus (HSV) relieves the viral block to dendritic cell activation: Potential of vhs-HSV vectors for dendritic cell-mediated immunotherapy. *J. Virol.* **77**(6)**:**3768–3776.

Sandri-Goldin, R. M. (1998). ICP27 mediates HSV RNA export by shuttling through a leucine-rich nuclear export signal and binding viral intronless RNAs through an RGG motif. *Genes Dev.* **12**(6)**:**868–879.

Sarkar, B., Xi, Q., He, C., and Schneider, R. J. (2003). Selective degradation of AU-rich mRNAs promoted by the p37 AUF1 protein isoform. *Mol. Cell. Biol.* **23** (18)**:**6685–6693.

Sato, H., Callanan, L. D., Pesnicak, L., Krogmann, T., and Cohen, J. I. (2002). Varicella-zoster virus (VZV) ORF17 protein induces RNA cleavage and is critical for replication of VZV at 37 degrees C but not 33 degrees C. *J. Virol.* **76**(21)**:**11012–11023.

Schek, N., and Bachenheimer, S. L. (1985). Degradation of cellular mRNAs induced by a virion-associated factor during herpes simplex virus infection of Vero cells. *J. Virol.* **55** (3)**:**601–610.

Scheper, W., Meinsma, D., Holthuizen, P. E., and Sussenbach, J. S. (1995). Long-range RNA interaction of two sequence elements required for endonucleolytic cleavage of human insulin-like growth factor II mRNAs. *Mol. Cell. Biol.* **15**(1)**:**235–245.

Schmelter, J., Knez, J., Smiley, J. R., and Capone, J. P. (1996). Identification and characterization of a small modular domain in the herpes simplex virus host shutoff protein sufficient for interaction with VP16. *J. Virol.* **70**(4)**:**2124–2131.

Schmidlin, M., Lu, M., Leuenberger, S. A., Stoecklin, G., Mallaun, M., Gross, B., Gherzi, R., Hess, D., Hemmings, B. A., and Moroni, C. (2004). The ARE-dependent mRNA-destabilizing activity of BRF1 is regulated by protein kinase B. *EMBO J.* **23** (24)**:**4760–4769.

Seal, R., Temperley, R., Wilusz, J., Lightowlers, R. N., and Chrzanowska-Lightowlers, Z. M. (2005). Serum-deprivation stimulates cap-binding by PARN at the expense of eIF4E, consistent with the observed decrease in mRNA stability. *Nucleic Acids Res.* **33** (1)**:**376–387.

Seiser, C., Posch, M., Thompson, N., and Kuhn, L. C. (1995). Effect of transcription inhibitors on the iron-dependent degradation of transferrin receptor mRNA. *J. Biol. Chem.* **270**(49)**:**29400–29406.

Sen, G. L., and Blau, H. M. (2005). Argonaute 2/RISC resides in sites of mammalian mRNA decay known as cytoplasmic bodies. *Nat. Cell Biol.* **7**(6)**:**633–636.

Shao, L., Rapp, L. M., and Weller, S. K. (1993). Herpes simplex virus 1 alkaline nuclease is required for efficient egress of capsids from the nucleus. *Virology* **196**(1)**:**146–162.

Sheaffer, A. K., Weinheimer, S. P., and Tenney, D. J. (1997). The human cytomegalovirus UL98 gene encodes the conserved herpesvirus alkaline nuclease. *J. Gen. Virol.* **78**(Pt. 11)**:**2953–2961.

Sheth, U., and Parker, R. (2003). Decapping and decay of messenger RNA occur in cytoplasmic processing bodies. *Science* **300**(5620)**:**805–808.

Shiomi, T., Fukushima, K., Suzuki, N., Nakashima, N., Noguchi, E., and Nishimoto, T. (1998). Human dis3p, which binds to either GTP- or GDP-Ran, complements *Saccharomyces cerevisiae* dis3. *J. Biochem. (Tokyo)* **123**(5)**:**883–890.

Shyu, A. B., Greenberg, M. E., and Belasco, J. G. (1989). The c-fos transcript is targeted for rapid decay by two distinct mRNA degradation pathways. *Genes Dev.* **3**(1)**:**60–72.

Shyu, A. B., Belasco, J. G., and Greenberg, M. E. (1991). Two distinct destabilizing elements in the c-fos message trigger deadenylation as a first step in rapid mRNA decay. *Genes Dev.* **5**(2)**:**221–231.

Smibert, C. A., Johnson, D. C., and Smiley, J. R. (1992). Identification and characterization of the virion-induced host shutoff product of herpes simplex virus gene UL41. *J. Gen. Virol.* **73**(Pt. 2)**:**467–470.

Smibert, C. A., Popova, B., Xiao, P., Capone, J. P., and Smiley, J. R. (1994). Herpes simplex virus VP16 forms a complex with the virion host shutoff protein vhs. *J. Virol.* **68**(4)**:**2339–2346.

Smiley, J. R. (2004). Herpes simplex virus virion host shutoff protein: Immune evasion mediated by a viral RNase? *J. Virol.* **78**(3)**:**1063–1068.

Smiley, J. R., Elgadi, M. M., and Saffran, H. A. (2001). Herpes simplex virus vhs protein. *Methods Enzymol.* **342:**440–451.

Song, J. J., Liu, J., Tolia, N. H., Schneiderman, J., Smith, S. K., Martienssen, R. A., Hannon, G. J., and Joshua-Tor, L. (2003). The crystal structure of the Argonaute2 PAZ domain reveals an RNA binding motif in RNAi effector complexes. *Nat. Struct. Mol. Biol.* **10**(12)**:**1026–1032.

Song, J. J., Smith, S. K., Hannon, G. J., and Joshua-Tor, L. (2004). Crystal structure of Argonaute and its implications for RISC slicer activity. *Science* **305**(5689)**:**1434–1437.

Spector, D., and Pizer, L. I. (1978). Herpesvirus infection modified adenovirus RNA metabolism in adenovirus type 5-transformed cells. *J. Virol.* **27:**1.

Stefanovic, B., Hellerbrand, C., Holcik, M., Briendl, M., Aliebhaber, S., and Brenner, D. A. (1997). Posttranscriptional regulation of collagen alpha1(I) mRNA in hepatic stellate cells. *Mol. Cell. Biol.* **17**(9)**:**5201–5209.

Stoeckle, M. Y. (1992). Removal of a 3′ non-coding sequence is an initial step in degradation of gro alpha mRNA and is regulated by interleukin-1. *Nucleic Acids Res.* **20** (5)**:**1123–1127.

Stoecklin, G., Colombi, M., Raineri, I., Leuenberger, S., Mallaun, M., Schmidlin, M., Gross, B., Lu, M., Kitamura, T., and Moroni, C. (2002). Functional cloning of BRF1, a regulator of ARE-dependent mRNA turnover. *EMBO J.* **21**(17)**:**4709–4718.

Stoecklin, G., Stubbs, T., Kedersha, N., Wax, S., Rigby, W. F., Blackwell, T. K., and Anderson, P. (2004). MK2-induced tristetraprolin:14–3-3 complexes prevent stress granule association and ARE-mRNA decay. *EMBO J.* **23**(6)**:**1313–1324.

Strand, S. S., and Leib, D. A. (2004). Role of the VP16-binding domain of vhs in viral growth, host shutoff activity, and pathogenesis. *J. Virol.* **78**(24)**:**13562–13572.

Strelow, L., Smith, T., and Leib, D. (1997). The virion host shutoff function of herpes simplex virus type 1 plays a role in corneal invasion and functions independently of the cell cycle. *Virology* **231**(1)**:**28–34.

Strelow, L. I., and Leib, D. A. (1995). Role of the virion host shutoff (vhs) of herpes simplex virus type 1 in latency and pathogenesis. *J. Virol.* **69**(11)**:**6779–6786.

Strelow, L. I., and Leib, D. A. (1996). Analysis of conserved domains of UL41 of herpes simplex virus type 1 in virion host shutoff and pathogenesis. *J. Virol.* **70**(8)**:**5665–5667.

Strom, T., and Frenkel, N. (1987). Effects of herpes simplex virus on mRNA stability. *J. Virol.* **61**(7)**:**2198–2207.

Stumpo, D. J., Byrd, N. A., Phillips, R. S., Ghosh, S., Maronpot, R. R., Castranio, T., Meyers, E. N., Mishina, Y., and Blackshear, P. J. (2004). Chorioallantoic fusion defects and embryonic lethality resulting from disruption of Zfp36L1, a gene encoding a CCCH tandem zinc finger protein of the tristetraprolin family. *Mol. Cell. Biol.* **24** (14)**:**6445–6455.

Sully, G., Dean, J. L., Wait, R., Rawlinson, L., Santalucia, T., Saklatvala, J., and Clark, A. R. (2004). Structural and functional dissection of a conserved destabilizing element of cyclo-oxygenase-2 mRNA: Evidence against the involvement of AUF-1 [AU-rich element/poly(U)-binding/degradation factor-1], AUF-2, tristetraprolin, HuR (Hu antigen R) or FBP1 (far-upstream-sequence-element-binding protein 1). *Biochem. J.* **377** (Pt. 3)**:**629–639.

Suzutani, T., Nagamine, M., Shibaki, T., Ogasawara, M., Yoshida, I., Daikoku, T., Nishiyama, Y., and Azuma, M. (2000). The role of the UL41 gene of herpes simplex virus type 1 in evasion of non-specific host defence mechanisms during primary infection. *J. Gen. Virol.* **81**(Pt. 7)**:**1763–1771.

Sydiskis, R. J., and Roizman, B. (1967). The degradation of host polyribosomes in productive and abortive infection with herpes simplex virus. *Virology* **32:**678–686.

Symmons, M. F., Williams, M. G., Luisi, B. F., Jones, G. H., and Carpousis, A. J. (2002). Running rings around RNA: A superfamily of phosphate-dependent RNases. *Trends Biochem. Sci.* **27**(1)**:**11–18.

Tabara, H., Sarkissian, M., Kelly, W. G., Fleenor, J., Grishok, A., Timmons, L., Fire, A., and Mello, C. C. (1999). The rde-1 gene, RNA interference, and transposon silencing in *C. elegans*. *Cell* **99**(2)**:**123–132.

Taddeo, B., Esclatine, A., and Roizman, B. (2002). The patterns of accumulation of cellular RNAs in cells infected with a wild-type and a mutant herpes simplex virus 1 lacking the virion host shutoff gene. *Proc. Natl. Acad. Sci. USA* **99**(26)**:**17031–17036.

Taddeo, B., Esclatine, A., Zhang, W., and Roizman, B. (2003). The stress-inducible immediate-early responsive gene IEX-1 is activated in cells infected with herpes simplex virus 1, but several viral mechanisms, including 3′ degradation of its RNA, preclude expression of the gene. *J. Virol.* **77**(11)**:**6178–6187.

Taddeo, B., Esclatine, A., and Roizman, B. (2004). Post-transcriptional processing of cellular RNAs in herpes simplex virus-infected cells. *Biochem. Soc. Trans.* **32** (Pt. 5)**:**697–701.

Taniguchi, T., and Takaoka, A. (2002). The interferon-alpha/beta system in antiviral responses: A multimodal machinery of gene regulation by the IRF family of transcription factors. *Curr. Opin. Immunol.* **14**(1)**:**111–116.

Taylor, G. A., Thompson, M. J., Lai, W. S., and Blackshear, P. J. (1995). Phosphorylation of tristetraprolin, a potential zinc finger transcription factor, by mitogen stimulation in intact cells and by mitogen-activated protein kinase *in vitro*. *J. Biol. Chem.* **270** (22)**:**13341–13347.

Taylor, G. A., Carballo, E., Lee, D. M., Lai, W. S., Thompson, M. J., Patel, D. D., Schenkman, D. I., Gilkeson, G. S., Broxmeyer, H. E., Haynes, B. F., and Blackshear, P. J. (1996a). A pathogenetic role for TNF alpha in the syndrome of cachexia, arthritis, and autoimmunity resulting from tristetraprolin (TTP) deficiency. *Immunity* **4**(5)**:**445–454.

Taylor, G. A., Thompson, M. J., Lai, W. S., and Blackshear, P. J. (1996b). Mitogens stimulate the rapid nuclear to cytosolic translocation of tristetraprolin, a potential zinc-finger transcription factor. *Mol. Endocrinol.* **10**(2)**:**140–146.

Tigges, M. A., Leng, S., Johnson, D. C., and Burke, R. L. (1996). Human herpes simplex virus (HSV)-specific CD8+ CTL clones recognize HSV-2-infected fibroblasts after treatment with IFN-gamma or when virion host shutoff functions are disabled. *J. Immunol.* **156**(10)**:**3901–3910.

Tran, H., Maurer, F., and Nagamine, Y. (2003). Stabilization of urokinase and urokinase receptor mRNAs by HuR is linked to its cytoplasmic accumulation induced by activated mitogen-activated protein kinase-activated protein kinase 2. *Mol. Cell. Biol.* **23** (20)**:**7177–7188.

Trgovcich, J., Johnson, D., and Roizman, B. (2002). Cell surface major histocompatibility complex class II proteins are regulated by the products of the gamma(1)34.5 and U(L) 41 genes of herpes simplex virus 1. *J. Virol.* **76**(14)**:**6974–6986.

Tucker, M., Staples, R. R., Valencia-Sanchez, M. A., Muhlrad, D., and Parker, R. (2002). Ccr4p is the catalytic subunit of a Ccr4p/Pop2p/Notp mRNA deadenylase complex in *Saccharomyces cerevisiae*. *EMBO J.* **21**(6)**:**1427–1436.

Uchida, N., Hoshino, S., and Katada, T. (2004). Identification of a human cytoplasmic poly(A) nuclease complex stimulated by poly(A)-binding protein. *J. Biol. Chem.* **279** (2)**:**1383–1391.

van Dijk, E., Cougot, N., Meyer, S., Babajko, S., Wahle, E., and Seraphin, B. (2002). Human Dcp2: A catalytically active mRNA decapping enzyme located in specific cytoplasmic structures. *EMBO J.* **21**(24)**:**6915–6924.

van Dijk, E., Le Hir, H., and Seraphin, B. (2003). DcpS can act in the 5′-3′ mRNA decay pathway in addition to the 3′-5′ pathway. *Proc. Natl. Acad. Sci. USA* **100**(21)**:**12081–12086.

Waggoner, S. A., and Liebhaber, S. A. (2003). Regulation of alpha-globin mRNA stability. *Exp. Biol. Med. (Maywood)* **228**(4)**:**387–395.

Wagner, B. J., DeMaria, C. T., Sun, Y., Wilson, G. M., and Brewer, G. (1998). Structure and genomic organization of the human AUF1 gene: Alternative pre-mRNA splicing generates four protein isoforms. *Genomics* **48**(2)**:**195–202.

Wang, W., Caldwell, M. C., Lin, S., Furneaux, H., and Gorospe, M. (2000a). HuR regulates cyclin A and cyclin B1 mRNA stability during cell proliferation. *EMBO J.* **19** (10)**:**2340–2350.

Wang, W., Furneaux, H., Cheng, H., Caldwell, M. C., Hutter, D., Liu, Y., Holbrook, N., and Gorospe, M. (2000b). HuR regulates p21 mRNA stabilization by UV light. *Mol. Cell. Biol.* **20**(3)**:**760–769.

Wang, Y., Osterbur, D. L., Megaw, P. L., Tosini, G., Fukuhara, C., Green, C. B., and Besharse, J. C. (2001). Rhythmic expression of Nocturnin mRNA in multiple tissues of the mouse. *BMC Dev. Biol.* **1**(1)**:**9.

Wang, Z., Jiao, X., Carr-Schmid, A., and Kiledjian, M. (2002). The hDcp2 protein is a mammalian mRNA decapping enzyme. *Proc. Natl. Acad. Sci. USA* **99** (20)**:**12663–12668.

Wang, Z., and Kiledjian, M. (2000a). Identification of an erythroid-enriched endoribonuclease activity involved in specific mRNA cleavage. *EMBO J.* **19**(2)**:**295–305.

Wang, Z., and Kiledjian, M. (2000b). The poly(A)-binding protein and an mRNA stability protein jointly regulate an endoribonuclease activity. *Mol. Cell. Biol.* **20**(17)**:** 6334–6341.

Wang, Z., and Kiledjian, M. (2001). Functional link between the mammalian exosome and mRNA decapping. *Cell* **107**(6)**:**751–762.

Wells, S. E., Hillner, P. E., Vale, R. D., and Sachs, A. B. (1998). Circularization of mRNA by eukaryotic translation initiation factors. *Mol. Cell* **2**(1)**:**135–140.

Wennborg, A., Sohlberg, B., Angerer, D., Klein, G., and von Gabain, A. (1995). A human RNase E-like activity that cleaves RNA sequences involved in mRNA stability control. *Proc. Natl. Acad. Sci. USA* **92**(16)**:**7322–7326.

Wilson, G. M., Lu, J., Sutphen, K., Sun, Y., Huynh, Y., and Brewer, G. (2003). Regulation of A + U-rich element-directed mRNA turnover involving reversible phosphorylation of AUF1. *J. Biol. Chem.* **278**(35)**:**33029–33038.

Wilusz, C. J., Wormington, M., and Peltz, S. W. (2001). The cap-to-tail guide to mRNA turnover. *Nat. Rev. Mol. Cell Biol.* **2**(4)**:**237–246.

Winzen, R., Gowrishankar, G., Bollig, F., Redich, N., Resch, K., and Holtmann, H. (2004). Distinct domains of AU-rich elements exert different functions in mRNA destabilization and stabilization by p38 mitogen-activated protein kinase or HuR. *Mol. Cell. Biol.* **24**(11)**:**4835–4847.

Xu, N., Chen, C. Y., and Shyu, A. B. (1997). Modulation of the fate of cytoplasmic mRNA by AU-rich elements: Key sequence features controlling mRNA deadenylation and decay. *Mol. Cell. Biol.* **17**(8)**:**4611–4621.

Xu, N., Chen, C. Y., and Shyu, A. B. (2001). Versatile role for hnRNP D isoforms in the differential regulation of cytoplasmic mRNA turnover. *Mol. Cell. Biol.* **21**(20)**:** 6960–6971.

Yaman, I., Fernandez, J., Sarkar, B., Schneider, R. J., Snider, M. D., Nagy, L. E., and Hatzoglou, M. (2002). Nutritional control of mRNA stability is mediated by a conserved AU-rich element that binds the cytoplasmic shuttling protein HuR. *J. Biol. Chem.* **277** (44)**:**41539–41546.

Yan, K. S., Yan, S., Farooq, A., Han, A., Zeng, L., and Zhou, M. M. (2003). Structure and conserved RNA binding of the PAZ domain. *Nature* **426**(6965)**:**468–474.

Yang, F., and Schoenberg, D. R. (2004). Endonuclease-mediated mRNA decay involves the selective targeting of PMR1 to polyribosome-bound substrate mRNA. *Mol. Cell* **14** (4)**:**435–445.

Yang, F., Peng, Y., and Schoenberg, D. R. (2004). Endonuclease-mediated mRNA decay requires tyrosine phosphorylation of polysomal ribonuclease 1 (PMR1) for the targeting and degradation of polyribosome-bound substrate mRNA. *J. Biol. Chem.* **279** (47)**:**48993–49002.

Yamashita, A., Chang, T. C., Yamashita, Y., Zhu, W., Zhong, Z., Chen, C., and Shyu, A. B. (2005). Concerted action of poly(A) nucleases and decapping enzyme in mammalian mRNA turnover. *Nat. Struct. Mol. Biol.* **12**(12)**:**1054–1063.

York, I. A., Roop, C., Andrews, D. W., Riddell, S. R., Graham, F. L., and Johnson, D. C. (1994). A cytosolic herpes simplex virus protein inhibits antigen presentation to CD8+ T lymphocytes. *Cell* **77**(4)**:**525–535.

Zelus, B. D., Stewart, R. S., and Ross, J. (1996). The virion host shutoff protein of herpes simplex virus type 1: Messenger ribonucleolytic activity *in vitro*. *J. Virol.* **70**(4)**:** 2411–2419.

Zhu, W., Brauchle, M. A., Di Padova, F., Gram, H., New, L., Ono, K., Downey, J. S., and Han, J. (2001). Gene suppression by tristetraprolin and release by the p38 pathway. *Am. J. Physiol. Lung Cell. Mol. Physiol.* **281**(2)**:**L499–L508.

INDEX

A

B

C

D

E

F

G

H

I

J

K

L

M

N

O

P

R

S

T

U

V

W

X

Y

Z